

THE JOURNAL OF PHYSICAL CHEMISTRY

(Registered in U. S. Patent Office)

CONTENTS

G. P. Haight, Jr., and Alice Carroll Swift: Kinetics of the Oxidation of Molybdenum(V) by Hydroxylamine.	1921	William Seaman: Effects of High Energy Radiation on Some Inclusion Compounds of Urea, Thiourea and Hydroquinone.	2029
J. T. MacQueen, F. R. Meeks and O. K. Rice: The Effect of an Impurity on the Phase Transition in a Binary Liquid System as a Surface Phenomenon.	1925	Stig R. Erlander: Determination of Molecular Weights of Charged Polymers from Equilibrium Ultracentrifugations.	2033
George R. Hertel and Herbert M. Clark: Paramagnetic Resonance Behavior of Tetrachloroferrate Ion in Isopropyl Ether.	1930	J. Danon: Activity Coefficients of LiNO_3 , HNO_3 and NH_4NO_3 in Dowex-1 Anion-Exchange Resin.	2039
Gerald S. Golden and Herbert M. Clark: The Extraction of Ferric Bromide by Diethyl Ether.	1932	G. R. Argue, E. E. Mercer and J. W. Cobble: An Ultrasensitive Thermistor Microcalorimeter and Heats of Solution of Neptunium, Uranium and Uranium Tetrachloride.	2041
Edward Sturm: Quantitative Differential Thermal Analysis by Controlled Heating Rates.	1935	I. Warsaw and Rustum Roy: Polymorphism of the Rare Earth Sesquioxides.	2048
E. Hayon: The Photochemistry of Iodide Ion in Aqueous Solution.	1937	Theodore L. Brown, J. G. Verkade and T. S. Piper: The Dipole Moments of Some Phosphite Esters and their Derivatives.	2051
J. O'M. Bockris and D. F. A. Koch: Comparative Rates of the Electrolytic Evolution of Hydrogen and Deuterium on Iron, Tungsten and Platinum.	1941	R. Bruce Martin: A Complete Ionization Scheme for Citric Acid.	2053
W. J. Wosten: The Vapor Pressure of Cadmium Selenide.	1949	M. W. Shafer: High Temperature Phase Relations in the Ferrite Region of the Ni-Fe-O System.	2055
R. A. Osteryoung, C. Kaplan and D. L. Hill: Solubility and Complex Ion Formation of Silver Chloride in Molten Nitrates.	1951	D. T. Peterson and V. G. Fattore: Calcium-Calcium Hydride Phase System.	2062
R. A. Robinson and R. H. Stokes: Activity Coefficients in Aqueous Solutions of Sucrose, Mannitol and their Mixtures at 25°.	1954	Benton B. Owen, Robert C. Miller, Clifford E. Milner and Harold L. Cogan: The Dielectric Constant of Water as a Function of Temperature and Pressure.	2065
F. J. Kelly, R. A. Robinson and R. H. Stokes: The Thermodynamics of the Ternary System Mannitol-Sodium Chloride-Water at 25° from Solubility and Vapor Pressure Measurements.	1958	J. J. Fritz, P. E. Field and Ingmar Grenthe: The Low Temperature Magnetic Properties and Magnetic Energy Levels of Some Rare Earth Chelates of Acetylacetone and Ethylenediaminetetraacetic Acid.	2070
Richard J. Bearman: On the Molecular Basis of Some Current Theories of Diffusion.	1961	Robert E. Connick and E. Diane Stover: Rate of Elimination of Water Molecules from the First Coordination Sphere of Paramagnetic Cations as Detected by Nuclear Magnetic Resonance Measurements of O^{17} .	2075
S. Ainsworth: Spectrophotometric Analysis of Reaction Mixtures.	1968	Ralph P. Seward and Harry W. Otto: The Rate of Dissociation of Perchlorate Ion in Fused Sodium Hydroxide.	2078
O. K. Rice: On the Relation between an Equilibrium Constant and the Nonequilibrium Rate Constants of Direct and Reverse Reactions.	1972	W. B. Frank: Thermodynamic Considerations in the Aluminum-Producing Electrolyte.	2081
Bernard J. Wood and Henry Wise: Kinetics of Hydrogen Atom Recombination on Surfaces.	1976	Richard M. Badger and Ralph C. Greenough: The Association of Phenol in Water Saturated Carbon Tetrachloride Solutions.	2088
W. R. Krigbaum, J. E. Kurz and P. Smith: The Conformation of Polymer Molecules. IV. Poly-(1-butene).	1984	C. D. Ritchie: The Transmission and Additivity of Polar Effects.	2091
F. Ascoli, C. Botré and A. M. Liquori: On the Polyelectrolyte Behavior of Heparin. I. Binding of Sodium Ions.	1991	R. M. Wallace and E. K. Dukas: A Spectrophotometric Study of the Reaction between Ferric Ion and Hydrozoic Acid.	2094
P. J. Proll and L. H. Sutcliffe: Species of Cobalt(II) in Acetic Acid. Part II. Cobalt(II) in the Presence of Lithium Bromide, Lithium Chloride and Ammonium Thiocyanate.	1993	Assa Lipshitz and B. Perlmutter-Hayman: The Kinetics of the Hydrolysis of the Bichromate Ion.	2098
E. Blomgren, J. O'M. Bockris and C. Jesch: The Adsorption of Butyl, Phenyl and Naphthyl Compounds at the Interface Mercury-Aqueous Acid Solution.	2000	NOTES	
Joseph R. Ligenza: Effect of Crystal Orientation on Oxidation Rates of Silicon in High Pressure Steam.	2011	Guenter Ahlers and James F. Hornig: Molecular Orbital Calculations for Cyclooctatetraene.	2102
J. E. McDonald and J. W. Cobble: The Heat of Formation of the Hypobromite Ion.	2014	Jerome L. Rosenberg and Donald J. Shombert: A New Method for Studying Pore Sizes by the Use of Dye Luminescence.	2103
Fred M. Snell and Esther B. Nielsen: A Theoretical Treatment of the Solubility of Polyvalent Ampholytes Binding Other Molecules.	2015	P. S. Aggarwal and A. Goswami: An Oxide of Tervalent Nickel.	2105
D. Fiat, M. Folman and U. Garbatski: Dielectric Polarization and Hydrogen Bonding of Adsorbate: Methanol and Isobutane on Porous Vapor Glass.	2018	M. H. J. Wijnen: Primary Steps in the Photolysis of Methyl Carbonate.	2105
John R. Merrill: Measurements of Intramolecular Hydrogen Bonding by Nuclear Magnetic Resonance and Infrared Spectroscopy.	2023	Lloyd H. Dreger and John L. Margrave: Vapor Pressures of Platinum Metals. II. Rhodium.	2106
William A. Barber and Carol L. Sloan: Solubility of Calcium Carbide in Fused Salt Systems.	2026	W. F. O'Hara and L. G. Hepler: Thermodynamics of Ionization of Aqueous <i>meta</i> -Chlorophenol.	2107

THE JOURNAL OF PHYSICAL CHEMISTRY

(Registered in U. S. Patent Office)

W. ALBERT NOYES, JR., EDITOR

ALLEN D. BLISS

ASSISTANT EDITORS

A. B. F. DUNCAN

EDITORIAL BOARD

A. O. ALLEN
C. E. H. BAWN
J. BIGEISEN
D. D. ELEY

D. H. EVERETT
S. C. LIND
F. A. LONG
K. J. MYSELS

J. E. RICCI
R. E. RUNDLE
W. H. STOCKMAYER
A. R. UBBELOHDE

E. R. VAN ARTSDALEN
M. B. WALLENSTEIN
W. WEST
EDGAR F. WESTRUM, JR.

Published monthly by the American Chemical Society at 20th and Northampton Sts., Easton, Pa.

Second-class mail privileges authorized at Easton, Pa. This publication is authorized to be mailed at the special rates of postage prescribed by Section 131.122.

The *Journal of Physical Chemistry* is devoted to the publication of selected symposia in the broad field of physical chemistry and to other contributed papers.

Manuscripts originating in the British Isles, Europe and Africa should be sent to F. C. Tompkins, The Faraday Society, 6 Gray's Inn Square, London W. C. 1, England.

Manuscripts originating elsewhere should be sent to W. Albert Noyes, Jr., Department of Chemistry, University of Rochester, Rochester 20, N. Y.

Correspondence regarding accepted copy, proofs and reprints should be directed to Assistant Editor, Allen D. Bliss, Department of Chemistry, Simmons College, 300 The Fenway, Boston 15, Mass.

Business Office: Alden H. Emery, Executive Secretary, American Chemical Society, 1155 Sixteenth St., N. W., Washington 6, D. C.

Advertising Office: Reinhold Publishing Corporation, 430 Park Avenue, New York 22, N. Y.

Articles must be submitted in duplicate, typed and double spaced. They should have at the beginning a brief Abstract, in no case exceeding 300 words. Original drawings should accompany the manuscript. Lettering at the sides of graphs (black on white or blue) may be pencilled in and will be typeset. Figures and tables should be held to a minimum consistent with adequate presentation of information. Photographs will not be printed on glossy paper except by special arrangement. All footnotes and references to the literature should be numbered consecutively and placed in the manuscript at the proper places. Initials of authors referred to in citations should be given. Nomenclature should conform to that used in *Chemical Abstracts*, mathematical characters be marked for italic, Greek letters carefully made or annotated, and subscripts and superscripts clearly shown. Articles should be written as briefly as possible consistent with clarity and should avoid historical background unnecessary for specialists.

Notes describe fragmentary or incomplete studies but do not otherwise differ fundamentally from articles and are subjected to the same editorial appraisal as are articles. In their preparation particular attention should be paid to brevity and conciseness. Material included in Notes must be definitive and may not be republished subsequently.

Communications to the Editor are designed to afford prompt preliminary publication of observations or discoveries whose value to science is so great that immediate publication is imperative. The appearance of related work from other laboratories is in itself not considered sufficient justification for the publication of a Communication, which must in addition

meet special requirements of timeliness and significance. Their total length may in no case exceed 1000 words or their equivalent. They differ from Articles and Notes in that their subject matter may be republished.

Symposium papers should be sent in all cases to Secretaries of Divisions sponsoring the symposium, who will be responsible for their transmittal to the Editor. The Secretary of the Division by agreement with the Editor will specify a time after which symposium papers cannot be accepted. The Editor reserves the right to refuse to publish symposium articles, for valid scientific reasons. Each symposium paper may not exceed four printed pages (about sixteen double spaced typewritten pages) in length except by prior arrangement with the Editor.

Remittances and orders for subscriptions and for single copies, notices of changes of address and new professional connections, and claims for missing numbers should be sent to the American Chemical Society, 1155 Sixteenth St., N. W., Washington 6, D. C. Changes of address for the *Journal of Physical Chemistry* must be received on or before the 30th of the preceding month.

Claims for missing numbers will not be allowed (1) if received more than sixty days from date of issue (because of delivery hazards, no claims can be honored from subscribers in Central Europe, Asia, or Pacific Islands other than Hawaii), (2) if loss was due to failure of notice of change of address to be received before the date specified in the preceding paragraph, or (3) if the reason for the claim is "missing from files."

Subscription rates (1961): members of American Chemical Society, \$12.00 for 1 year; to non-members, \$24.00 for 1 year. Postage to countries in the Pan-American Union \$0.80; Canada, \$0.40; all other countries, \$1.20. Single copies, current volume, \$2.50; foreign postage, \$0.15; Canadian postage, \$0.10; Pan-American Union, \$0.10. Back volumes (Vol. 56-64) \$30.00 per volume; foreign postage, per volume \$1.20, Canadian, \$0.40; Pan-American Union, \$0.80. Single copies: back issues, \$3.00; for current year, \$2.50; postage, single copies: foreign, \$0.15; Canadian, \$0.10; Pan-American Union, \$0.10.

The American Chemical Society and the Editors of the *Journal of Physical Chemistry* assume no responsibility for the statements and opinions advanced by contributors to THIS JOURNAL.

The American Chemical Society also publishes *Journal of the American Chemical Society*, *Chemical Abstracts*, *Industrial and Engineering Chemistry*, International Edition of *Industrial and Engineering Chemistry*, *Chemical and Engineering News*, *Analytical Chemistry*, *Journal of Agricultural and Food Chemistry*, *Journal of Organic Chemistry*, *Journal of Chemical and Engineering Data*, *Chemical Reviews*, *Chemical Titles* and *Journal of Chemical Documentation*. Rates on request.

J. A. Knight, R. L. McDaniel, R. C. Palmer and Fred Sicilio: H ₂ and C ₁ -C ₇ Yields from the Radiolysis of 2,2,4-Trimethylpentane.....	2109
E. B. Weronki: On Polarographic and Coulometric Investigations of the Reduction Rate of Cobalt Ions in the Presence of Some Amino Acids and Proteins....	2110

COMMUNICATIONS TO THE EDITOR	
Jürg Hoigné and Tino Gäumann: On a Possible Track Réaction in the Radiolysis of Toluene.....	2111
Clifford E. Myers: Heat of Dissociation of Boron Phosphide, BP(s).....	2111
Eugene Shilov and S. Solodushenkov: On the Morris Mechanism of Hydrolysis of Chlorine.....	2112

THE JOURNAL OF PHYSICAL CHEMISTRY

(Registered in U. S. Patent Office) (© Copyright, 1961, by the American Chemical Society)

VOLUME 65

DECEMBER 6, 1961

NUMBER 11

KINETICS OF THE OXIDATION OF MOLYBDENUM(V) BY HYDROXYLAMINE¹

By G. P. HAIGHT, JR., AND ALICE CARROLL SWIFT

Department of Chemistry, Swarthmore College, Swarthmore, Pennsylvania

Received July 22, 1960

The kinetics of the oxidation of Mo(V) by hydroxylamine have been studied in hydrochloric acid. In concentrated (12.0 *M*) acid there is no reaction. In 3.0 *M* acid there is essentially complete reaction. $2\text{Mo(V)} + \text{NH}_2\text{OH}^+ = 2\text{Mo(VI)} + \text{NH}_4^+$. The rate law for the reaction is $d[\text{Mo(V)}]/dt = k[\text{Mo(V)}][\text{NH}_2\text{OH}^+][\text{H}^+]^2$ in solutions 3.0 molar in chloride ion. The rate constant, k , is 4.0×10^{-6} at 25° and 1.20×10^{-4} at 35° if concentrations are expressed in moles per liter and time in seconds. The energy of activation is 23 kcal. and the entropy of activation is 4.8 e.u. A side reaction which might have interfered with colorimetric analysis of Mo(V) was observed. A color forming reaction between Mo(VI) and hydroxylamine was examined but found not to be the side reaction in question. The side reaction apparently involves complex formation between hydroxylamine and Mo(V).

Introduction

A study of the molybdate-catalyzed reduction of hydroxylamine carried out in this Laboratory suggested to one of the authors the need for a study of the direct oxidation of Mo(V) by hydroxylamine. This reaction was postulated as a possible key step in the catalytic process. The rate of the reaction is too slow and its activation energy too high for it to be directly involved in the catalysis. However, the kinetics and mechanism of the reaction have proved to be of sufficient interest to constitute the subject of a separate report. We have examined the stoichiometry and kinetics of the oxidation of Mo(V) by hydroxylamine in 3.0 molar hydrochloric acid, examined the nature of an observed side reaction, and deduced a possible mechanism for the reaction.

Experimental

Reagent grade materials were used without further purification. Hydroxylamine solutions were prepared by dissolving hydroxylamine hydrochloride in hydrochloric acid so that the final concentration of chloride ion was 3.0 molar. Sodium molybdate was dissolved in 3.0 *M* hydrochloric acid, reduced to Mo(V) with mercury, and stored over mercury in an atmosphere of nitrogen. Nitrogen, scrubbed with chromous sulfate solution, was bubbled through reagent flasks containing Mo(V) whenever they were opened for sampling.

Hydrochloric acid solutions were standardized with sodium carbonate, using methyl orange as indicator. Hydroxylamine solutions were standardized by the method of

Bray, Simpson and McKenzie.² Mo(V) solutions were standardized by diluting 40-fold in dilute sulfuric acid and titrating with permanganate and also by measuring their absorbance at 410 *mμ* with a Beckman D.U. Spectrophotometer.

The rate of the reaction of Mo(V) with hydroxylamine was determined by observing the decrease in absorbance due to Mo(V) at 410 *mμ*. A secondary reaction appeared during the latter half of runs containing high excesses of hydroxylamine which produced an interfering yellow color. Therefore, a second analytical method was employed. Five ml. samples of reaction mixture were withdrawn and quenched in 200 ml. of a solution of ferric sulfate in dilute sulfuric acid. The solution was boiled, cooled and then titrated with standard potassium permanganate. The procedure is essentially that of Bray, Simpson and McKenzie for hydroxylamine. However, in this case both the Mo(V) and hydroxylamine reduce ferric ions to ferrous ions. The permanganate titer is thus a measure of the sum of Mo(V) and hydroxylamine present. Two equivalents of ferrous ion are produced per mole of hydroxylamine and one per gram atom of Mo(V) present. The method was useful only when neither Mo(V) nor hydroxylamine was present in excess. The two analytical methods gave identical rate laws with rate constants that agreed within experimental errors. Only initial portions of colorimetric runs involving excess hydroxylamine were used.

Qualitative observations were made on the oxidation of Mo(V) and the reduction of Mo(VI) by hydroxylamine in concentrated (12 *M*) hydrochloric acid by observing the change in absorbance of solutions due to green,³ monomeric⁴ Mo(V) at 720 *mμ*.

(2) Wm. C. Bray, M. E. Simpson and A. A. McKenzie, *J. Am. Chem. Soc.*, **41**, 1362 (1919).

(3) C. F. Hiskey and V. W. Meloche, *ibid.*, **62**, 1819 (1940); **63**, 964 (1941).

(4) L. Sacconi and R. Cini, *ibid.*, **76**, 4239 (1954).

(1) Presented at Delaware Valley Regional Meeting of the American Chemical Society, Philadelphia, 1960.

Results

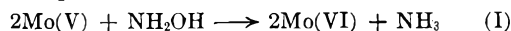
Stoichiometry of the Oxidation of Mo(V) by Hydroxylamine.—Tables of oxidation potentials⁵ and other potentiometric data⁶ indicate that hydroxylamine is thermodynamically capable of reducing Mo(VI) as well as oxidizing Mo(V). It was imperative, therefore, to determine whether the oxidation of Mo(V) could be studied without interference from the reduction of Mo(VI) or not.

Mixtures of Mo(V) and hydroxylamine in 3.0 *M* hydrochloric acid reacted as follows:

a. If Mo(V) were present in excess, absorbance at 410 *mμ* decreased until the number of moles of Mo(V) consumed was equal to twice the number of moles of hydroxylamine initially present.

b. If hydroxylamine were present in excess, the absorbance of solutions at 410 *mμ* decreased until 50 to 80% of the Mo(V) had disappeared, then slowly increased due to a secondary reaction. The total Mo(V) plus hydroxylamine concentration continued to decrease, however, until the reducing power of the solution toward ferric ions corresponded to a hydroxylamine value which would be left if all the Mo(V) had been consumed along with one mole of hydroxylamine for each two moles of Mo(V).

It thus appeared that in the time needed to observe the reaction, the only significant oxidation-reduction process to occur was the reaction



Moreover, solutions of Mo(VI) and hydroxylamine in 3.0 *M* hydrochloric acid and in water showed no change in reducing power toward ferric ions over a period of five days despite the fact that complicated color changes were observed. Thus, except for the secondary color forming reaction which does not involve oxidation-reduction, reaction I appears to be the only process occurring during the time of observation under the conditions employed.

Kinetics of the Oxidation of Mo(V) by Hydroxylamine.—Runs which were analyzed by decreasing absorbance at 410 *mμ* gave the following results.

a. For runs in which $[\text{Mo(V)}] = 2[\text{NH}_2\text{OH}]$, the change in absorbance with time followed the law

$$dA/dt = \frac{k_{\text{obs}}A^2}{2\epsilon^2} \quad (1)$$

where *A* is the measured absorbance, ϵ is the molar absorbance of Mo(V) in 3.0 *M* hydrochloric acid at 410 *mμ*, and k_{obs} is the observed bimolecular rate constant.

b. When a high excess of hydroxylamine was used, the change in absorbance with time initially followed the law

$$dA/dt = k_{\text{obs}}A[\text{NH}_2\text{OH}]/\epsilon \quad (2)$$

In case 2, k_{obs} was lower than in case 1. This was later found to be caused by the decrease in hydrogen ion concentration resulting from the use of high hydroxylamine concentrations while main-

taining a constant chloride ion concentration of 3.0.

Although the results in each case agreed with the rate law

$$d[\text{Mo(V)}]/dt = k_{\text{obs}}[\text{Mo(V)}][\text{NH}_2\text{OH}] \quad (3)$$

the change in absorption spectrum at the end of runs containing a large excess of hydroxylamine led us to use the titrimetric procedure outlined in the Experimental portion of the paper. The results obtained by this procedure were analyzed as follows.

Since both hydroxylamine and Mo(V) reduce ferric ion to ferrous ion, the concentration of reducing equivalents (*r*) is given by

$$r = [\text{Mo(V)}] + 2[\text{NH}_2\text{OH}]$$

For the case in which $[\text{Mo(V)}] = 2[\text{NH}_2\text{OH}]$, we find that

$$dr/dt = 2 d[\text{Mo(V)}]/dt = \frac{k_{\text{obs}}r^2}{4} \quad (4)$$

if the rate law given by equation 3 is correct. For the case in which $[\text{Mo(V)}] \neq 2[\text{NH}_2\text{OH}]$, we define

$$b = 2[\text{NH}_2\text{OH}] - [\text{Mo(V)}]$$

where *b* is a constant during any given run, but may vary from run to run. The quantity *b* may be either positive or negative. The rate law of equation 3 requires that

$$dr/dt = \frac{k_{\text{obs}}(r - b)^2}{4} \quad (5)$$

The integrated forms of equations 4 and 5 give straight line plots for the functions of *r* vs. time in the cases where they apply. The values of k_{obs} calculated from the slopes of the lines are in agreement with the values obtained spectrophotometrically within limits of experimental error.

Effect of Changing Hydrogen Ion Concentration on k_{obs} .—In order to account for low results in k_{obs} obtained with high concentrations of hydroxylamine, the hydrogen ion concentration was varied between 1.5 and 3.0 molar by substitution of lithium chloride for hydrochloric acid. No further variation in the medium of reaction was attempted. Mo(V) species are very sensitive to changes in hydrogen ion or chloride ion concentrations.^{2,3} Over the narrow range of hydrogen ion concentration employed k_{obs} was found to be directly proportional to the square of the hydrogen ion concentration. Thus the rate law finally obtained is

$$d[\text{Mo(V)}]/dt = k[\text{Mo(V)}][\text{NH}_2\text{OH}][\text{H}^+]^2 \quad (6)$$

Effect of Changing Temperature on Reaction Rates.—Results obtained at 25 and 35° using each analytical method are summarized in Tables I and II. Temperature control was somewhat better for runs analyzed by the titration procedure, the results of which are to be preferred. The activation energy for the reaction as determined from the results at two temperatures is 23.0 kcal. and the entropy of activation is 4.8 e.u. The activation energy was checked by performing a run at 19.5°. The rate constant found was 1.45×10^{-5} vs. 1.50×10^{-5} calculated.

Effect of Reaction Products on Reaction Rates.—Neither sodium molybdate nor ammonium ion in concentrations comparable to those of Mo(V)

(5) W. M. Latimer, "Oxidation Potentials," 2nd Ed., Prentice-Hall, Inc., New York, N. Y., 1952.

(6) N. H. Furman and W. Murray, *J. Am. Chem. Soc.*, **58**, 1689 (1936).

TABLE I
 RESULTS OF RUNS AT 25°

Run number	[Mo(V)] ₀ , ^a mole/l.	[NH ₂ OH] ₀ , mole/l.	[H ⁺] ₀ , mole/l.	$k \times 10^6$, l. ³ mole ⁻² sec. ⁻¹	Method of analysis ^b
1	0.010	0.1	2.90	3.64	A
2	.010	.25	2.75	3.39	A
3	.010	.05	2.95	4.05	A
4	.010	.005	2.99	3.18	A
5	.017	.433	2.57	3.48	A
6	.036	.030	2.97	4.00	T
7	.050	.025	2.95	3.78	T
8	.040	.020	2.96	4.08	T
9	.040	.020	2.96	4.13	T

$$k = 3.75 \pm 0.30 \times 10^{-5} \text{ l.}^3 \text{ mole}^{-2} \text{ sec.}^{-1}$$

$$k = 4.00 \pm 0.20 \times 10^{-5} \text{ for runs 6-9}$$

^a Measured as though Mo(V) were monomeric. ^b A for light absorbance (initial slopes where NH₂OH was in excess); T for titration (most reliable). T control poor 0.3 to 0.5° below 25°.

 TABLE II
 RESULTS OF RUNS AT 35°

Run	[Mo(V)] ₀ , ^a mole/l.	[NH ₂ OH] ₀ , mole/l.	[H ⁺] ₀ , mole/l.	$k \times 10^4$, l. ³ mole ⁻² sec. ⁻¹	Analysis
1	0.040	0.020	2.96	1.16	T
2	.050	.025	2.50	1.23	T
3	.050	.025	2.00	1.21	T
4	.050	.025	1.50	1.35	T
5	.010	.250	2.75	1.20	A
6	.020	.100	2.90	1.14	A
7	.010	.050	2.95	1.39	A
8	.020	.020	2.98	1.06	A
9	.010	.010	2.99	1.11	A

^a See Table I. $k = 1.20 \pm 0.19 \times 10^{-4} \text{ l.}^3 \text{ mol.}^{-2} \text{ sec.}^{-1}$.
 $E_a = 23 \text{ kcal.}, S^* = 4.8 \text{ e.u.}$

or hydroxylamine produced any measurable effect on the rate of reaction.

Mechanism of Oxidation of Mo(V) by Hydroxylamine. Nature of Reactants in 3.0 M Hydrochloric Acid.—Hydroxylamine is certainly completely protonated to give hydroxylammonium ion in 3.0 M acid. The species of Mo(V) is not known. It is a diamagnetic dimer³ probably containing oxygen or hydroxide bridges between the two molybdenum atoms. Compounds prepared by James and Wardlaw⁷ from dilute hydrochloric acid indicate that there are probably two chloride ions per molybdenum atom in the complex species. The rest of the octahedral coordination sphere probably is filled out with water molecules and hydroxide ions. However, a mechanism that is reasonable can be proposed without exact knowledge of the structure of the Mo(V) dimer.

Formation of the Activated Complex.—Hydroxylamine, like water and hydrogen peroxide, probably can coordinate through its oxygen atom with molybdenum in its higher oxidation states. Such coordination to an atom of high positive charge should serve to weaken the N-O bond. The single bond energy for N-O is estimated to be over 30 kcal. per mole from the N-N and O-O single bond energies and the electronegativity values given by Pauling.⁸ The activated complex for

(7) R. G. James and W. Wardlaw, *J. Chem. Soc.*, 2145 (1927).

(8) L. Pauling, "The Nature of the Chemical Bond," 3rd Ed., Cornell University Press, Ithaca, N. Y., 1960.

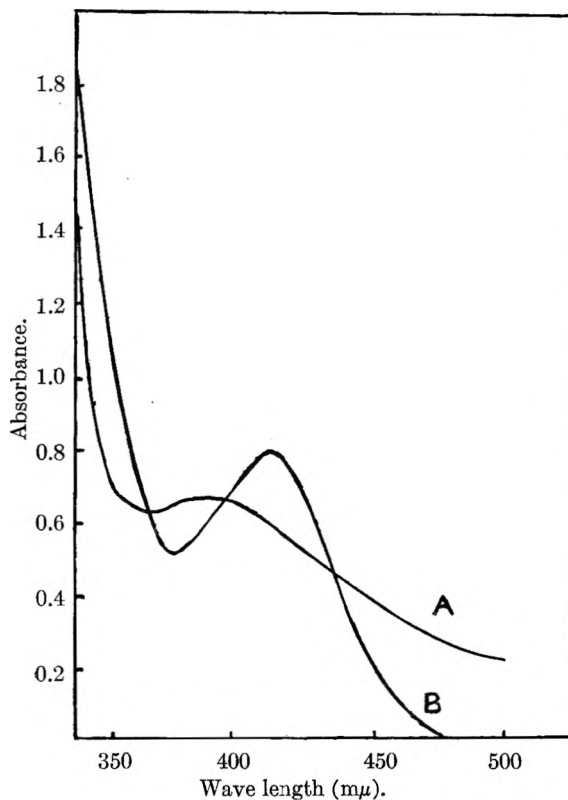
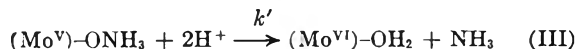
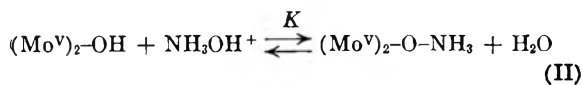


Fig. 1.—Absorption curves for 0.01 M Mo(V) in 3.0 M hydrochloric acid (A), and for 0.05 M Mo(V) plus 0.25 M hydroxylamine in 3.0 M hydrochloric acid after 23 hours (B).

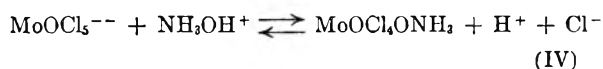
the reaction under study must be such as to weaken the N-O bond since the activation energy of the reaction is only 23.0 kcal. We therefore suggest a mechanism involving an equilibrium step in which hydroxylamine displaces an hydroxide ion (or water) in the coordination sphere of dimeric Mo(V). The complex formed then breaks up with the aid of hydrogen ions to form Mo(VI) and ammonia. Comparing this mechanism with



the empirical rate law, it is evident that the empirical rate constant k is equal to the product of K and k' , which are the equilibrium constant and rate constant for the first and second steps in the mechanism, respectively. The ammonia and Mo(VI) species resulting from the break up of the activated complex will react rapidly with the solvent to achieve their final equilibrium forms—ammonium ion and some unidentified chloromolybdate species. The fact that neither ammonium ion nor molybdate ion affects the reaction rate indicates that these final equilibrium forms must be produced in steps subsequent to the break up of the activated complex. The role indicated for hydrogen ion is only one of many possible and indistinguishable roles.

Reactions of Mo(V) and Mo(VI) with Hydroxylamine in 12 M Hydrochloric Acid.—For

purposes of comparison reactions were attempted in concentrated hydrochloric acid where mixtures of Mo(V) and hydroxylamine showed no decrease in absorbance due to Mo(V) at 720 $m\mu$ over a period of one week. On the other hand mixtures of hydroxylamine and Mo(VI) in concentrated hydrochloric acid slowly became green indicating formation of Mo(V). The latter reaction was by no means quantitative, however, even after standing for several weeks. In concentrated hydrochloric acid Mo(V) probably is the ion MoOCl_5^{--} . An equilibrium similar to reaction (IV) would be forced



far to the left by the high concentrations of hydrogen ion and chloride ion. In addition it is probably easier for dimeric Mo(V) to undergo direct divalent oxidation by hydroxylamine than for monomeric Mo(V) to undergo univalent oxidation with the production of radicals such as NH_3^+ or NH_2 .

Nature of the Side Reaction Interfering with Colorimetric Detection of Mo(V).—Figure 1 shows the change in absorption spectrum accompanying the appearance of an interfering yellow color during the latter portion of runs containing excess hydroxylamine. The Mo(V) concentration at the time of observation of curve B would be less than 1.0 millimolar according to the observed reaction rates.

Two possible origins of species giving rise to curve B were investigated qualitatively. The fact that Mo(V) was being destroyed by oxidation suggested that the new color might result from a reaction between Mo(VI) and hydroxylamine. Such a reaction producing a yellow color was indeed found to occur. It was too slow to cause interference with most of the kinetic observations and involved no oxidation of hydroxylamine or reduction of Mo(VI) for several days. In addition, the spectrum of the yellow color produced showed only general absorption increasing toward the ultraviolet, with no peak at 420 $m\mu$ as observed in curve B. Furthermore, color formation between Mo(VI) and hydroxylamine is inhibited by high concentrations of hydroxylamine rather than enhanced. It is clear that this color forming reaction between

Mo(VI) and hydroxylamine is *not* responsible for the interference in the kinetic studies.

The failure of the reaction of Mo(VI) and hydroxylamine to account for the color-giving curve B in Fig. 1, forced us to consider the possible formation of a more intensely colored Mo(V) species than that normally observed in 3.0 *M* hydrochloric acid. The form of the absorption curve B in Fig. 1 is very similar to that observed for Mo(V) in 4.0 *M* hydrochloric acid.³ It appears that hydroxylamine may have a similar effect to hydrochloric acid in displacing water or hydroxide from the coordination sphere of Mo(V). We believe that a strong enhancement of the peak at 420 $m\mu$ occurs when hydrochloric acid causes breaking of an oxygen bridge in the Mo(V) dimer while leaving a second bridge intact. If hydroxylamine could accomplish the same effect as hydrochloric acid, but at a much slower rate, the species giving curve B in Fig. 1 would be accounted for. This explanation is very speculative on present evidence, being offered merely as an hypothesis to explain the similar effects of hydroxylamine and hydrochloric acid on the spectrum of Mo(V). This explanation would allow a required distinction between reactions leading to the species giving curve B and reaction II leading to formation of the activated complex. In reaction II hydroxylamine replaces a peripheral oxygen in the Mo(V) dimer, while in the reaction giving the species responsible for curve B of Fig. 1 hydroxylamine becomes bound at a site left vacant by the breaking of an oxygen bridge, the latter process being very slow.

In conclusion, the reaction between Mo(V) and hydroxylamine to give Mo(VI) and ammonia (reaction I) has been shown to proceed quantitatively though at a very slow rate in 3.0 *M* hydrochloric acid. No reaction occurs in 12.0 *M* hydrochloric acid. The kinetics of reaction I and a possible mechanism have been described. A side reaction producing a change in the Mo(V) spectrum was observed and shown not to be the same as a color forming reaction between Mo(VI) and hydroxylamine.

Acknowledgment.—The authors wish to thank the Faculty Research Committee of Swarthmore College for a grant, and the Office of Ordnance Research, U. S. Army, for use of the spectrophotometer.

THE EFFECT OF AN IMPURITY ON THE PHASE TRANSITION IN A BINARY LIQUID SYSTEM AS A SURFACE PHENOMENON¹

BY J. T. MACQUEEN, F. R. MEEKS AND O. K. RICE

Department of Chemistry, University of North Carolina, Chapel Hill, North Carolina

Received November 7, 1960

The effect of small quantities of water on the transition temperature (one phase to two phases) of the cyclohexane-aniline system has been studied at two concentrations in or near the critical concentration range. Water increases the temperature at which a second phase separates from a given cyclohexane-aniline mixture. Furthermore, the water is more effective in increasing the transition temperature the greater the cyclohexane concentration, the effectiveness rising more rapidly than the cyclohexane concentration. It is inferred that, in coexisting phases, the water/aniline ratio is greater in the aniline-rich phase. These data offer new possibilities for a thermodynamic treatment. It is known that any impurity much more soluble in one of the constituents raises the coexistence curve, and, in particular, the critical temperature. Because the critical temperature is the temperature at which the interfacial tension vanishes, it is also possible to consider this as a surface phenomenon. Since the impurity raises the critical temperature and since the interfacial tension has a negative temperature coefficient, the impurity must raise the interfacial tension; therefore it must be negatively adsorbed at the interface. This situation can be discussed by combining the Gibbs-Duhem equation and the Gibbs adsorption isotherm, using the known temperature dependence of the interfacial tension of the cyclohexane-aniline system. The adsorption per unit area is found to be of the order of one-tenth the difference in concentration of water between phases times the thickness of the interface; the latter changes with temperature, but may be assumed to be a few ångströms, well below the critical temperature. It is thus possible to interpret the data in a way which gives information about the interface, and at the same time allows one to assess the reasonableness of the quantities involved.

In general, a slightly soluble third component, which is much more insoluble in one of the constituents of a binary liquid mixture than the other, tends to make these constituents separate. An example of such a third component is water in the cyclohexane-aniline system, water being much less soluble in cyclohexane than it is in aniline. This effect was measured by Atack and Rice² by adding small quantities of water to a cyclohexane-aniline mixture and observing the effect on the separation temperature for the mixture. Another type of measurement was made by Meeks, Gopal and Rice,³ who introduced a mixture of Li_2SO_4 and $\text{Li}_2\text{SO}_4\text{-H}_2\text{O}$ into a cyclohexane-aniline mixture, thereby maintaining the water at a definite activity. When there is no water present the coexistence curve of the cyclohexane-aniline system appears to be truncated,⁴⁻⁶ having a flat portion at the top (at the critical temperature). With the $\text{Li}_2\text{SO}_4\text{-Li}_2\text{SO}_4\text{-H}_2\text{O}$ mixture added the critical temperature is raised from 29.597 to 29.885°, and the flat portion practically disappears. The coexistence curve gives, in this case, the composition of the cyclohexane-aniline mixtures which are in equilibrium with each other when the salt mixture is present. It is, of course, a projection from the ternary diagram on the cyclohexane-aniline-temperature plane. In Fig. 1 we show two constant-temperature ternary diagrams, one for a temperature just below T_c , the critical temperature of the cyclohexane-aniline binary mixture, the other for T_c' , the critical temperature with the salt mixture present ($T_c' > T_c$). These diagrams are not drawn to scale, partly because the solubilities of cyclohexane and aniline in water are too

low to be shown readily to scale. At $T < T_c$ there are three one-phase regions at the corners. The tie-line w' shown in each of the diagrams represents (though not placed to scale) the one for which the activity of the water is that determined by the $\text{Li}_2\text{SO}_4\text{-Li}_2\text{SO}_4\text{-H}_2\text{O}$ mixture; projected on the cyclohexane-aniline-temperature plane it connects points on the coexistence curve with the salt mixture present. At $T = T_c'$ two of the one-phase regions have coalesced, and this region is bounded in part by the tie-line w' , which has become very short (perhaps vanishingly short). At all temperatures above this, the concentration of water having this activity will lie in the one-phase region.

As the temperature is increased the two tie-lines a and c will draw closer together, and eventually the three-phase region will disappear. Since the one-phase region near W is very small, the tie-lines a and c represent nearly constant cyclohexane-aniline ratios. If we have a mixture in the three-phase region containing sufficient water so that as the temperature is raised, the tie-line c or a crosses the point representing the composition of the mixture before the tie-line w crosses this point, then the cyclohexane- and aniline-rich phases will coalesce at the temperature of crossing and a second, water-rich phase will remain. Such a system may be said to be saturated with water.

Even in a system saturated with water the cyclohexane-aniline rich phase will always be very close to the lower edge of the diagram, and this is the situation with which we shall always deal in this paper. Therefore, it is justifiable for present purposes to consider that we are dealing with an impurity in a binary system.

The data which have been obtained so far have been insufficient to show how water is distributed between the coexisting cyclohexane-aniline phases. (This means that the positions of the tie-lines are not fixed, but since we treat water as an impurity, we prefer the other statement.) It was, therefore, decided to do some experiments, of the type first performed by Atack and Rice, at more than one composition, as by proper interpretation of these

(1) Work supported by the Office of Ordnance Research, U. S. Army. Presented at the Symposium on the Thermodynamics of Multicomponent and Multiphase Systems, Division of Industrial and Engineering Chemistry, A. C. S., St. Louis, Mo., December, 1960.

(2) D. Atack and O. K. Rice, *Disc. Faraday Soc.*, **15**, 210 (1953).

(3) F. R. Meeks, Ram Gopal and O. K. Rice, *J. Phys. Chem.*, **63**, 992 (1959).

(4) R. W. Rowden and O. K. Rice, in "Changements de Phases," *Compt. rend. 2^e réunion ann., soc. chim. phys., Paris*, **78** (1952).

(5) D. Atack and O. K. Rice, *J. Chem. Phys.*, **22**, 382 (1954).

(6) O. K. Rice, *ibid.*, **23**, 164 (1955).

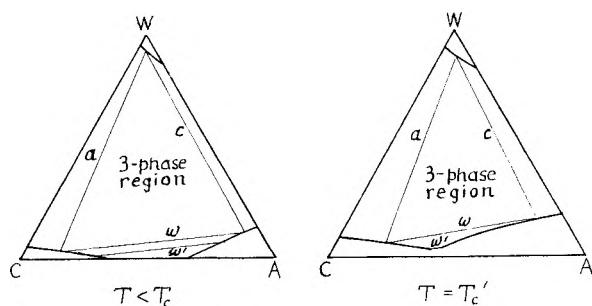


Fig. 1.—Schematic ternary diagrams for the cyclohexane-aniline-water system.

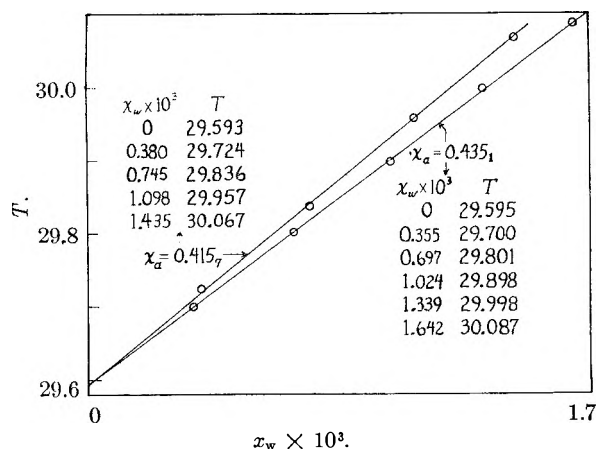


Fig. 2.—Transition temperatures as a function of composition. The tabulations give the experimental data for the points shown on the graph.

the desired information, which is important for the thermodynamic discussion of the data, can be obtained. It was found by Meeks, Gopal and Rice that with the lithium sulfate mixture present, a solution of about 0.417 mole fraction aniline was in equilibrium with one of mole fraction 0.436 at 29.883°. Accordingly, we decided to investigate solutions of approximately these concentrations by adding known amounts of water.

Experimental Details

A sample of well purified aniline, sample number A-1731, was obtained from the National Aniline Division of Allied Chemical and Dye Corporation. A portion of this was distilled three times from zinc dust under dry nitrogen at a pressure of 5.0 mm., using an efficient column and a reflux to take-off ratio of about eight to one. The portion retained was recrystallized twice by freezing, the first and last 10-cc. portions to freeze being discarded each time. The final portion from this process was distilled once more as described above.

The cyclohexane was sample 209a-25 from the National Bureau of Standards. It was used without purification except for drying as described below.

The purified aniline and the cyclohexane were introduced into separate parts of a vacuum system and dried by successive equilibrations with portions of calcined calcium oxide.⁴ These drying trains were connected by means of mercury valves to a bulb with a calibrated tube (stem of a microburet) attached, and this bulb to a manifold to which the sample tubes were sealed. The volume of liquid could thus be measured at a known temperature; account was taken of the vapor of cyclohexane above the liquid. It was thus possible to make up samples of 0.415₇ and 0.435₁ mole fraction aniline without again exposing the materials to the atmosphere. After the mixture was made up, it was distilled onto zinc dust, which removed mercury.

The separation temperatures of these samples were determined, the samples redried, and the separation tempera-

tures redetermined, constant values being obtained in each case differing by only 0.001° from the curve given by Meeks, Gopal and Rice. For all measurements the thermostat, resistance bridge and platinum thermometer used in their work were employed.

Known amounts of water vapor were added to the samples from a large volume, in which an ampoule containing a weighed amount of water had been broken, by a vapor sharing procedure employing a smaller volume with a ratio of 0.0202 to the larger. The portions of water from the small volume were condensed into the sample by freezing in liquid nitrogen. All the doses were aliquots of the same initial weight of water, 17% of it being sufficient. Although stopcocks were used in handling the water vapor, no stopcock ever came into contact with the cyclohexane-aniline mixture, even the vapor.

A correction was made for loss of water to the vapor phase in the following way. The vapor pressure of $\text{Li}_2\text{SO}_4 \cdot \text{H}_2\text{O}$ is known to be 2.25 mm. at the temperature at which the transition occurs when the salt is present⁷; we thus have about 1.4×10^{-6} mole of water in our vapor phase of about 12 cc. Since about 4.7×10^{-5} mole of water (about 1.0×10^{-3} mole fraction) was added to bring the 0.453₁ mixture to this transition point, we have lost about 3.0% to the vapor-phase. It was assumed that this was the same for all additions of water. The percentage of water in the vapor phase of the 0.415₇ mixture was 3.7. (Experiments made by saturating the system with water, performed after this paper was submitted, indicate that the correction may be considerably smaller.)

Results and General Discussion

The results are exhibited in Fig. 2, which shows the transition temperature, T , as a function of the mole fraction of water, x_w .

It will be observed that the water is less effective in raising the transition temperature of the mixture which is richer in aniline. Where these mixtures will be in equilibrium with each other, at about 29.9°, we can see that the mole fraction of water in the mixture with mole fraction 0.415₇ is 0.925×10^{-3} , while that in the mixture with mole fraction 0.435₁ is 1.025×10^{-3} . We observe that

$$\frac{(1.025 - 0.925)/1.025}{(0.4351 - 0.4157)/0.4351} = 2.17$$

Thus, if this may be generalized, we may say that a given relative increment in aniline concentration, as between two solutions which are in equilibrium with each other, is accompanied by about twice as great a relative increment of water concentration. This shows the effect of the greater solubility of water in the aniline, but must indicate also a tendency for more than one molecule of aniline to be associated with a given water molecule. If a single water molecule were attracted to a single aniline molecule, say by hydrogen bonding through the amine group, one would expect the water solubility to be merely proportional to the aniline concentration.

As noted at the beginning, this difference in solubility of water in aniline and cyclohexane has the effect of making the aniline and cyclohexane less soluble in each other. That this should be so, at least if the difference in solubility of the third component is great enough, has been shown on thermodynamic grounds by Prigogine⁸ and by

(7) H. Lescoeur, *Ann. chim. phys.*, **4**, 213 (1895); Y. Ueda, *Sci. Repts., Tohoku Imp. Univ.*, **22**, 879 (1933).

(8) See I. Prigogine and R. Defay (D. H. Everett, trans.), "Chemical Thermodynamics," Longmans, Green and Co., London, 1954, pp. 256 ff.

Rice.⁹ In more detail, a thermodynamic treatment¹⁰ shows that the aniline and cyclohexane are made less mutually soluble if the second derivative of the solubility of the third component with respect to concentration of aniline is positive.

Rice^{9,11} has suggested another way of regarding the situation. Since the interfacial tension vanishes at the critical temperature, a tendency to increase the interfacial tension will result in an increase in the critical temperature, hence a decrease in the mutual solubility of the cyclohexane and aniline. This must mean that there is negative adsorption of water at the interface. Use of Gibbs' adsorption equation will enable us to gain some quantitative information on this point, and this in turn can be related to the structure of the interface. This point of view seems especially appropriate if the coexistence curve is truncated, as it appears to be in the cyclohexane-aniline system, for this means that the phases are still different from each other even at the critical temperature, and that the latter is reached solely because the interfacial tension vanishes, so that the stability of the interface cannot be maintained. Though this idea already has been developed to some extent, the present data offer an opportunity for its application and extension.

Thermodynamics

Our considerations will be based upon the Gibbs-Duhem equations for the two phases and the Gibbs adsorption equation. We shall use the usual designations: chemical potential, μ ; mole fraction, x ; adsorption per unit area, Γ . To indicate the three constituents we shall use subscripts, as follows: cyclohexane, c ; aniline, a ; water, w . We shall use a prime to indicate the phase rich in cyclohexane, a double-prime for the phase rich in aniline. Then we may write the Gibbs-Duhem equations for the two phases in equilibrium, as

$$\begin{aligned} x_c' d\mu_c + x_a' d\mu_a + x_w' d\mu_w &= 0 \\ x_c'' d\mu_c + x_a'' d\mu_a + x_w'' d\mu_w &= 0 \end{aligned} \quad (1)$$

where $d\mu_c' = d\mu_c'' = d\mu_c$, etc. We may solve for $d\mu_c$ and $d\mu_a$ in terms of $d\mu_w$, obtaining

$$d\mu_c = \frac{x_a' x_w'' - x_a'' x_w'}{x_c' x_a'' - x_c'' x_a'} d\mu_w \quad (2)$$

and

$$d\mu_a = \frac{x_c' x_w'' - x_c'' x_w'}{x_a' x_c'' - x_a'' x_c'} d\mu_w \quad (3)$$

Now by definition

$$\begin{aligned} x_c' &> x_c'' \\ x_a'' &> x_a' \end{aligned} \quad (4)$$

We have found, experimentally, that not only is

$$x_w'' > x_w' \quad (5)$$

but

$$x_w''/x_a'' > x_w'/x_a' \quad (6)$$

When we add a small amount of water to a solution, we naturally have $d\mu_w > 0$. If we add small amounts x_w' and x_w'' to the two phases, previously containing no water, we will increase the vapor

pressure, or better the fugacity f_w , of water proportionally to x_w' and x_w'' . Since

$$d\mu_w = RT d \ln f_w = RT df_w/f_w \quad (7)$$

We will have

$$d\mu_w = RT dx_w'/x_w' = RT dx_w''/x_w'' \quad (8)$$

If we substitute these expressions into eq. 2 and 3 and integrate over a small range, where x_w' goes from 0 to a final value x_w' and x_w'' from 0 to x_w'' , with the other mole fractions not changing appreciably, we can write (2) and (3) in the approximate forms

$$\Delta\mu_c = \frac{x_a' x_w'' - x_a'' x_w'}{x_c' x_a'' - x_c'' x_a'} RT > 0 \quad (9)$$

and

$$\Delta\mu_a = \frac{x_c' x_w'' - x_c'' x_w'}{x_a' x_c'' - x_a'' x_c'} RT < 0 \quad (10)$$

the inequalities following from (4), (5) and (6). It is seen that the water has a "salting-out" effect on the cyclohexane, and a "salting-in" effect on the aniline.

These equations can be combined with the Gibbs adsorption equation to yield further information. At fixed temperature the change in surface tension σ upon change of composition will be given by

$$d\sigma = -\Gamma_c d\mu_c - \Gamma_a d\mu_a - \Gamma_w d\mu_w \quad (11)$$

The adsorption of any constituent is of course measured with respect to an arbitrary dividing surface placed in or near the interface, and in each case is the excess of the particular constituent over what would be present were the concentration on each side of the dividing surface constant up to the dividing surface. The position of the dividing surface is quite arbitrary if the surface is planar and has no effect on the validity of eq. 11, but in practice it is chosen to be in the region of the concentration gradient. It is to be noted that the concentrations, say in moles per cc., (for which we will use the symbol c) are directly concerned, rather than mole fractions, for the Γ 's are excess amounts (moles, if the μ 's are molal chemical potentials) per unit area. If we plot c_a and c_c against a distance r , normal to the interface, and increasing in the direction of the aniline-rich phase, the diagram would look something as shown in Fig. 3. We might imagine the dividing surface placed somewhere near the broken line. If we can place the dividing surface so that Γ_c and Γ_a are both zero, then eq. 11 becomes

$$d\sigma = -\Gamma_w d\mu_w \quad (12)$$

It was suggested previously that this could be done approximately^{2,11} and it should certainly be very nearly possible if the partial molal densities of cyclohexane and aniline are similar and the water is in sufficiently low concentration. But even if one cannot find a surface for which both Γ_c and Γ_a are precisely zero, it is always possible to place the surface somewhere close to the broken line of Fig. 3, where the composition is changing, so that

$$\Gamma_c d\mu_c + \Gamma_a d\mu_a = 0$$

and hence with this dividing surface eq. 12 is exact. If eq. 12 is to hold, we see from eq. 2 and 3 that we must have

(9) O. K. Rice, *Chem. Revs.*, **44**, 69 (1949).

(10) C. Wagner, *Z. Physik. Chem.*, **132**, 273 (1928).

(11) O. K. Rice, *J. Phys. Colloid Chem.*, **54**, 1293 (1950).

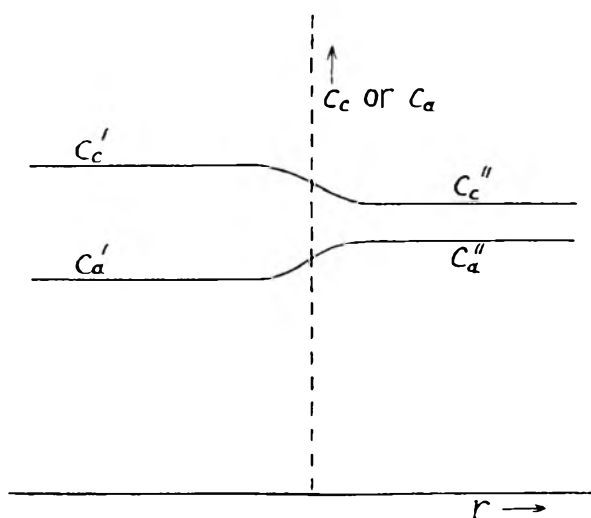


Fig. 3.—Compositions as function of the distance normal to the interface (schematic).

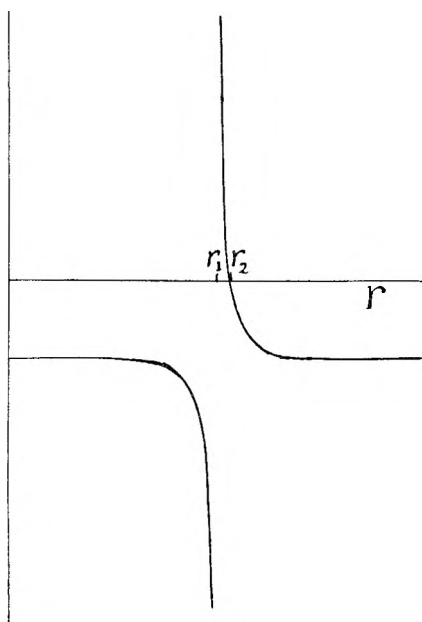


Fig. 4.— Γ_c/Γ_a as a function of the position of the dividing surface (schematic).

$$\frac{\Gamma_c}{\Gamma_a} = \frac{x_c' x_w'' - x_c'' x_w'}{x_a' x_w'' - x_a'' x_w'} \quad (13)$$

From (4), (5) and (6), we see that this ratio is positive. If we should set the dividing surface far to the left in Fig. 3 we would have

$$\frac{\Gamma_c}{\Gamma_a} = \frac{c_c' - c_c''}{c_a' - c_a''} \cong \frac{x_c' - x_c''}{x_a' - x_a''} \quad (14)$$

a negative value; if the dividing surface were far to the right Γ_c/Γ_a would have the same value. If the concentrations were actually strictly proportional to the mole fractions and if x_w were negligible, then we would expect Γ_a and Γ_c to vanish together. But if one vanishes at a slightly lower value of r than the other, the ratio Γ_c/Γ_a will go through every possible value in the region of the interface. Let us suppose that Γ_a vanishes first, at r_1 . The ratio then will become negatively infinite, then positively infinite as Γ_a changes sign, decreasing to

zero at the point r_2 where Γ_c becomes zero, and changing sign again, as shown in Fig. 4. Somewhere between r_1 and r_2 , the ratio Γ_c/Γ_a will have the value given by eq. 13. Through this point we will pass the dividing surface.

Let us now consider the situation at the critical temperature, where the interfacial tension remains zero as x_w is changed. We may write

$$d\sigma = (\partial\sigma/\partial T)_{x_w} dT + (\partial\sigma/\partial x_w)_T dx_w = 0 \quad (15)$$

whence

$$(\partial T/\partial x_w)_\sigma = -(\partial\sigma/\partial x_w)_T/(\partial\sigma/\partial T)_{x_w} \quad (16)$$

Also

$$\begin{aligned} (\partial\sigma/\partial x_w)_T &= (\partial\sigma/\partial\mu_w)_T(\partial\mu_w/\partial x_w)_T \\ &= -RT\Gamma_w/x_w \end{aligned} \quad (17)$$

by eq. 8 and 12. By eq. 16 and 17

$$\Gamma_w/x_w = (RT)^{-1}(\partial\sigma/\partial T)_{x_w}(\partial T/\partial x_w)_\sigma$$

In general we will apply this equation for small values of x_w , so since x_w may be taken as proportional to the concentration c_w of water, this equation also may be written

$$\Gamma_w/c_w = (RT)^{-1}(\partial\sigma/\partial T)_{c_w}(\partial T/\partial c_w)_\sigma \quad (18)$$

This equation was originally derived by Attack and Rice.² We will replace $(\partial\sigma/\partial T)_{x_w}$ by $d\sigma/dT$ for the pure cyclohexane-aniline system.

If the coexistence curve has a flat top, so that there is a range of critical concentrations, and so that there are two phases in equilibrium at (or infinitesimally below) the critical temperature, the water will distribute itself between the phases, as we have seen, and c_w will be different for these two phases. However $(\partial c_w/\partial T)_\sigma$ will be correspondingly different for the two phases and the same value of Γ_w will result in any case. Indeed, if we choose to consider $(\partial c_w/\partial T)_\sigma$ at some composition intermediate to those of the two coexisting phases, the effect will simply be to average c_w and $(\partial c_w/\partial T)_\sigma$ in the same way, so Γ_w shows no ambiguity.

There is, however, considerable difficulty in applying eq. 18 at the critical temperature because of the difficulty of measuring $d\sigma/dT$ there. It seems probable that σ varies about^{2,12,13} as $(T_c - T)^{2/3}$, where T_c is the critical temperature, except very close to T_c , if the concentration difference, say $x_a'' - x_a'$, varies as $(T_c - T)^{1/3}$. The latter relationship holds approximately, empirically, but the coexistence curve being truncated it seems more accurate to set, below the temperature of truncation,⁶ (which of course, is actually T_c)

$$x_a'' - x_a' = a(T_c - T + \tau)^{1/3} \quad (19)$$

with a constant, where $T_c + \tau$ would be the critical temperature if the truncation did not occur, *i.e.*, if the cube-root law held all the way to the critical point. This being the case it suggests itself that we set

$$\sigma = \kappa(T_c - T + \tau)^{2/3} \quad (20)$$

where κ is another constant, if $T_c - T \gg \tau$. At T_c , of course, σ vanishes, the behavior being somewhat as shown in Fig. 5. This figure suggests that $d\sigma/dT$ at T_c is slightly larger than what one

(12) J. W. Cahn and J. E. Hilliard, *J. Chem. Phys.*, **28**, 258 (1958).

(13) O. K. Rice, *J. Phys. Chem.*, **64**, 976 (1960).

would get by differentiating eq. 20 and setting $T = T_c$. Thus we get, rounding off

$$(d\sigma/dT)_{T=T_c} \cong -2\kappa\tau^{1/2} \quad (21)$$

Now we might expect Γ_w to be proportional to the difference in concentration of water in the two phases, namely $c_w'' - c_w' = \Delta c_w$, and to the thickness Δl of the transition layer between phases. From our experimental results we might expect $(x_w'' - x_w')/x_w''$ to be about 2.17 $(x_a'' - x_a')/x_a''$ so that at $T = T_c$ we get from eq. 19

$$\Delta x_w = x_w'' - x_w' = 2.17a\tau^{1/2}x_w''/x_a''$$

or, in view of the proportionality between x_w and c_w

$$\Delta c_w = 2.17a\tau^{1/2}c_w''/x_a'' \quad (22)$$

Thus, using eq. 21 and 22 in eq. 18 we obtain

$$\Gamma_w/\Delta c_w = -0.92(RT)^{-1}(\kappa/a)\tau^{1/2}x_a''(\partial T/\partial c_w)_\sigma \quad (23)$$

Discussion of Δl will be postponed briefly. The constants κ and a can be evaluated from the work of Attack and Rice.^{2,5,6} They turn out to be 0.0217 dynes cm.⁻¹ deg.^{-3/2} and 0.327 deg.^{-1/3}, respectively. From the present work it is found (noting that the density of a cyclohexane solution of 0.435 mole fraction aniline is 0.863 g./cc. and its mean molecular weight 88) that $(\partial T/\partial c_w)_\sigma$ is equal to 3.0×10^4 deg. cc. mole⁻¹. According to Attack and Rice $\tau = 0.005^\circ$; it will be seen that the dependence of eq. 23 on τ is weak. If these data be put into eq. 23 we obtain

$$\Gamma_w/\Delta c_w = -1.3 \times 10^{-8} \text{ cm.}$$

This means that the amount of adsorption (negative) in the interface is equal to the amount of water in a portion 1 cm.² in area and 1.3×10^{-8} cm. thick of the aniline-rich phase minus the amount of water in a similar portion of the cyclohexane-rich phase. In other words, one might say that the increase of concentration of the water does not begin until one is slightly within the transition layer to the aniline-rich phase. It has been shown¹³ that the thickness Δl of the transition layer may be expected to be proportional to $(T_c - T)^{-1/6}$ if σ is proportional to $(T_c - T)^{3/2}$ and $x_a'' - x_a'$ proportional to $(T_c - T)^{1/2}$. This being the case, it seems reasonable to suppose that in our case the thickness is proportional to $(T_c - T + \tau)^{-1/6}$. If the thickness is about 5×10^{-8} cm. at $T_c - T = 5^\circ$ then at $T = T_c$ it will be about 1.5×10^{-7} , about ten times $\Gamma_w/\Delta c_w$. From this point of view $\Gamma_w/\Delta c_w$ seems reasonable¹⁴; in any case, one would not expect $\Gamma_w/\Delta c_w$ to depart too far from molecular dimensions. The fact that there is a negative adsorption would indicate that the solubility of water in cyclohexane-aniline mixture should exhibit a curvature, as indicated in Fig. 6,

(14) We may, perhaps, note that the smaller τ is, the smaller our calculated value of $\Gamma_w/\Delta c_w$ and the larger Δl . So the reasonableness of our conclusions may, perhaps, be some verification for the value of τ . In view of the small powers involved, however, it is by no means sensitive to τ . There is some uncertainty in the interpretation because the theoretical discussion¹³ of Δl does not allow for the flat top and the existence of τ .

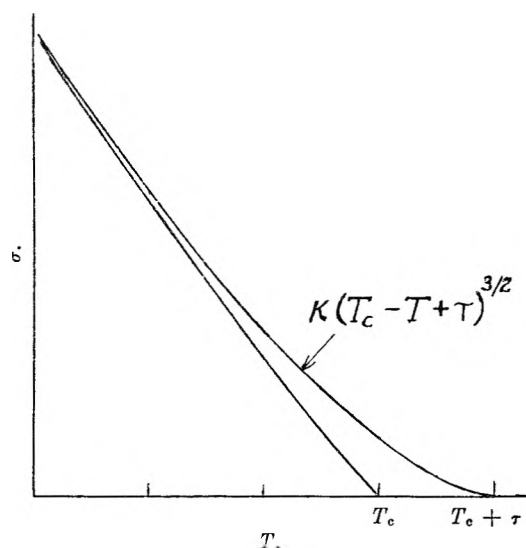


Fig. 5.—Surface tension as a function of temperature.

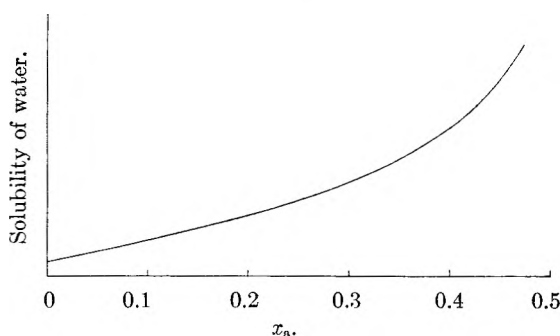


Fig. 6.—Estimated solubility of water as a function of composition.

which is consistent with the equation of Wagner.¹⁰ If the average solubility over the range of compositions differed from the mean of that at 0.42 and that at 0.47 mole fraction aniline (the approximate limits of the critical region for the pure cyclohexane-aniline system) by as much as 10% of the difference between the latter solubilities this could account for the result. This curvature is fairly large and Fig. 6, which we have attempted to draw roughly to scale, indicates that if this interpretation is correct we are in the sensitive concentration region. However, the fact that the curvature is large means that the concentration of water would increase more between mole fractions 0.42 and 0.47 than would be calculated from the experimental results over the smaller range of mole fractions, 0.4157 to 0.4351. This would indicate that the numerical factor in eq. 22 should be increased and that in eq. 23 decreased. We have tried to allow for this in constructing Fig. 6 and the figure implies that $\Gamma_w/\Delta c_w$ at the critical point is actually about -0.9×10^{-8} cm. It is suggested that an investigation of the solubility of water in cyclohexane-aniline mixtures of varying composition would be the next step in the elucidation of the situation.

PARAMAGNETIC RESONANCE BEHAVIOR OF TETRACHLOROFERRATE ION IN ISOPROPYL ETHER¹

By GEORGE R. HERTEL² AND HERBERT M. CLARK

Department of Chemistry, Rensselaer Polytechnic Institute, Troy, New York

Received December 16, 1960

The iron complex extracted into isopropyl ether from aqueous solutions of FeCl_3 in 6 *M* HCl was investigated by means of electron-paramagnetic-resonance (e.p.r.). Spectra of anhydrous FeCl_3 and the extracted complex are similar and consist of Lorentz-shaped lines centered at $g = 2.013$, indicating a tetrahedral configuration for FeCl_4^- . The marked differences between these spectra and that of $\text{FeCl}_3 \cdot 6\text{H}_2\text{O}$ is taken as evidence that the water in ether extracts containing the hydrated tetrachloroferric acid is not closely associated with the iron. The variation of the e.p.r. line width with ethereal iron concentration is interpreted as evidence of a varying relaxation phenomenon attributed to an association of the tetrachloroferric acid at concentrations greater than about 0.005 *M*.

Introduction

The extraction of ferric chloride from hydrochloric acid solution by isopropyl ether has been the subject of several investigations. With respect to the extractable species, it is generally accepted that the iron is extracted as tetrachloroferric acid, HFeCl_4 .³ On the basis of phase distribution, spectral and electrolysis studies^{3,4} there is evidence that the acid is hydrated and that it is the proton rather than the tetrachloroferrate ion which is hydrated. In addition, the well known dependence of the distribution ratio on iron concentration has been explained in terms of an activity or self-salting out effect in the aqueous layer⁵ and in terms of polymerization⁶ or ion-association^{7,8} or clustering⁹ of the extracted iron complex. These explanations of the deviations from the Nernst distribution law have been based on phase distribution, spectral, isopiestic, conductance and e.m.f. studies of the extracted species.

In this paper an account is given of an investigation in which the iron complex extracted by isopropyl ether was studied by means of an electron-paramagnetic-resonance (e.p.r.) spectrometer. The paramagnetic resonance behavior of iron salts has been reported previously by several investigators for salts in the solid state^{10,11} and in aqueous solution.¹²⁻¹⁴

Experimental

A Varian Model V-4500 Spectrometer and a Varian Model V-4007 Six-Inch Electromagnet System were used. The magnetic field was linearly variable from zero to over 6000 gauss. In the Varian equipment a microwave bridge circuit is employed in order to attain high sensitivity and a favorable signal to noise ratio. An AFC (automatic frequency control) circuit "locks" the klystron to the fixed resonant frequency of the cavity, which is located in the air gap of the magnet and makes up one arm of the bridge circuit. The bridge is balanced under conditions of no resonance. As the magnetic field is varied through resonance conditions, the sample absorbs energy causing the bridge to unbalance, thus producing a signal at the crystal detector in the bridge. The microwave power level is held constant throughout any one scan.

A Numar Model M-2 precision gaussmeter was used to measure field strength. The cavity resonance frequency (approximately 9500 Mc.) was measured by zero-beating the klystron signal with a harmonic of a frequency delivered by a Hewlett-Packard Model 450A transfer oscillator. Oscillator frequencies were measured by a Hewlett-Packard Model 524B electronic counter standardized by zero-beating with radio station WWV, Washington, D. C. The Varian Model V4500-30 rectangular microwave cavity was used for the investigations made at room temperature. Low temperature experiments were made using a specially constructed rectangular cavity capable of being cooled to the temperature of liquid nitrogen. Quartz sample tubes were used to avoid interfering spectra caused by the impurities found in other materials.

Line widths, defined to be the separation of the peaks of the derivative curve, were taken from spectra recorded at a rate of approximately 25 gauss/minute and a response time of 3 seconds. Checks were made at different settings to ensure that no line broadening effects were present.

Line shapes were determined using the method described by Bloembergen, Purcell and Pound.¹⁵ The ratio of maximum positive to maximum negative slopes of the derivative is 2.2 for a line having Gaussian shape and 4 for a line having Lorentzian shape.

Experiments were conducted on solid anhydrous ferric chloride, anhydrous ferric chloride in isopropyl ether, solid hydrated ferric chloride, and the ether phase obtained by the isopropyl ether extraction of 0.2 *M* ferric chloride from 6 *M* hydrochloric acid solution.

Anhydrous samples were prepared in a dry argon atmosphere. Two samples of anhydrous ferric chloride and two 50 μ l aliquots of a saturated solution of anhydrous ferric chloride in anhydrous isopropyl ether (purified by shaking with an acidified ferrous sulfate solution, dried over calcium chloride and distilled over calcium hydride in a closed system) were sealed in sample tubes.

Ether extraction and dilutions were made following the procedure outlined by Campbell.⁷ Two 100-ml. samples of approximately 0.2 *M* ferric chloride solutions in 6 *M* hydrochloric acid were shaken with equal volumes of purified, dry isopropyl ether. The samples were allowed to equilibrate for 48 hours before the phases were separated.

(1) Part of a thesis submitted to Rensselaer Polytechnic Institute by George R. Hertel in partial fulfillment of the requirements for the degree of Master of Science.

(2) Experimental work reported herein was done at Knolls Atomic Power Laboratory, operated by the General Electric Company for the U. S. Atomic Energy Commission.

(3) H. L. Friedman, *J. Am. Chem. Soc.*, **74**, 5 (1952).

(4) A. H. Laurene, D. E. Campbell, S. F. Wiberley and H. M. Clark, *J. Phys. Chem.*, **60**, 901 (1956).

(5) N. H. Nachtrieb and R. E. Fryxell, *J. Am. Chem. Soc.*, **70**, 3552 (1948).

(6) R. J. Myers and D. E. Metzler, *ibid.*, **72**, 3772 (1950).

(7) D. E. Campbell, H. M. Clark and W. H. Bauer, *J. Phys. Chem.*, **62**, 506 (1958).

(8) J. Saldick, *ibid.*, **60**, 500 (1956).

(9) N. H. Nachtrieb and R. E. Fryxell, *J. Am. Chem. Soc.*, **74**, 897 (1952).

(10) D. M. S. Bagguley, B. Bleaney, J. H. E. Griffiths, R. P. Penrose and B. I. Plumptre, *Proc. Phys. Soc. (London)*, **61**, 542, 551 (1948).

(11) B. Bleaney and K. W. H. Stevens, *Repts. Progr. in Phys.*, **16**, 108 (1953).

(12) B. R. McGarvey, *J. Phys. Chem.*, **61**, 1232 (1957).

(13) N. S. Garif'yanov, *Soviet Phys. JETP*, **10**, 1101 (1960).

(14) V. I. Avvakumov, N. S. Garif'yanov, E. M. Kozyrev and P. G. Tishkov, *ibid.*, **10**, 1110 (1960).

(15) N. Bloembergen, E. M. Purcell and R. V. Pound, *Phys. Rev.*, **73**, 679 (1948).

The ether phases were analyzed for iron by a procedure based on a colorimetric method developed by Lawler.¹⁶ Dilutions of the ether phases were made with purified isopropyl ether which had been equilibrated over an equal volume of 6 *M* hydrochloric acid.

Results

Spectra of anhydrous FeCl_3 in anhydrous isopropyl ether, solid anhydrous FeCl_3 , hydrated FeCl_3 , and isopropyl ether extracts of the iron complex were obtained at 25 and -196° . The spectra did not change with temperature.

Careful search failed to reveal fine or hyperfine structure even at sweep amplitudes of less than 0.5 gauss, a sweep rate of 5 gauss/min., and a response time of 3 seconds.

The line width of anhydrous FeCl_3 was found to be 370 ± 3 gauss. For hydrated FeCl_3 a weak, extremely broad, asymmetric line (>1200 gauss wide) centered about $g = 2$ was observed. There was an indication of a second, very weak resonance at a very low field (Fig. 1).

The variations in line width, ΔH , of the ether extracts as the concentration of iron was decreased by dilution are illustrated graphically in Fig. 2.

Line shapes were Lorentzian in character, with one important exception. The center peak of the complex spectrum of hydrated ferric chloride had a definite Gaussian shape.

G-factor measurements for all spectra gave a value slightly higher (approx. 2.013 ± 0.006) than the free electron value of 2.0023. There appeared to be no significant deviations from this value in any of the spectra.

Discussion

The fact that spectra taken at different temperatures were identical is a strong indication that the spin-lattice relaxation time of the ferric ion in this system is long in comparison to the spin-spin relaxation time. As Van Vleck¹⁷ has shown, the shorter of the two relaxation times controls the width and shape of the line and the spin-lattice time is strongly temperature dependent, whereas the spin-spin time is not. The line shape is also consistent with the supposition that spin-spin relaxation is the dominant type in this system. In addition, the Lorentzian shape indicates strong exchange interactions between iron atoms.¹⁸ Garstens and Liebson¹⁹ have found exchange narrowing responsible for the decrease in the line width of the manganous spectrum of highly concentrated aqueous solutions ($> 6 M \text{ MnCl}_2$). The evidence in this work is that exchange narrowing is a dominant factor at concentrations as low as 0.02 *M* Fe(III). However, according to Van Vleck,²⁰ exchange narrowing does not occur unless similar paramagnetic ions are precessing about parallel axes. It is assumed that conditions favorable for exchange interaction are provided by a polymerization or clustering of the tetrachloroferric acid. The

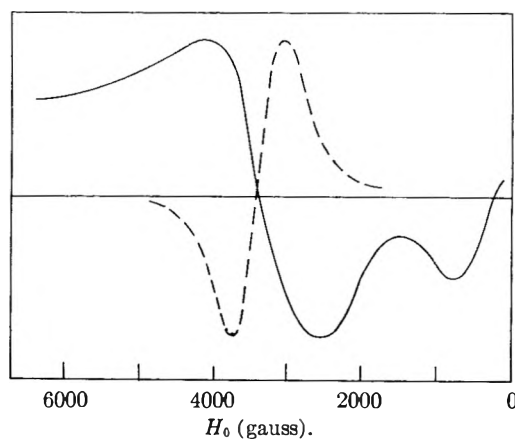


Fig. 1.—E.p.r. spectra of $\text{FeCl}_3 \cdot 6\text{H}_2\text{O}$ (solid curve) and anhydrous FeCl_3 (dotted curve).

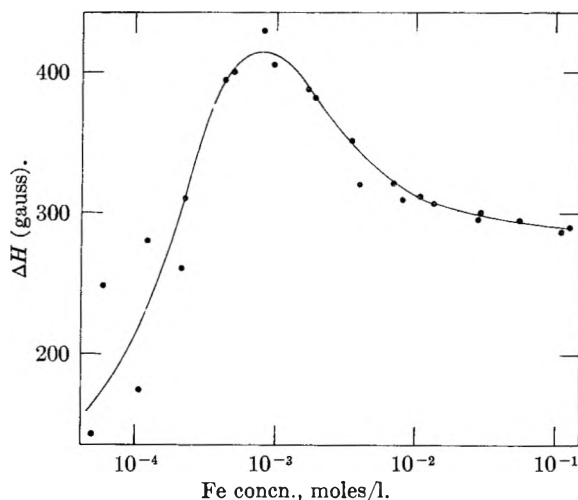


Fig. 2.—Dependence of e.p.r. line width on Fe(III) concentration in the isopropyl ether extract of FeCl_3 from 6 *M* HCl.

shape and width of the resonance line observed for ether extracts having iron concentrations in the range of 10^{-1} to $10^{-2} M$ are attributed to such polymerization. As the concentration is decreased, the clusters begin to break up, the dipole-dipole interactions become more important and the line width increases. With further dilution, the monomeric iron complex becomes the predominate species, the line-broadening dipole interactions are weakened, the spin-spin relaxation time is lengthened considerably and the line width decreases rapidly as shown in Fig. 2.

The proximity of the observed *g*-value of the ferric complex in the ether solutions to the free electron value of 2.0023 indicates that the five unpaired *d* electrons are relatively undisturbed by other ions. It is also a definite indication that none of the 3*d* orbitals is being used as a bonding orbital in the FeCl_4^- complex, for if any were, the special case of the half-filled shell would be destroyed and the spectrum altered. This is considered to be strong evidence that the FeCl_4^- ion has a tetrahedral sp^3 configuration.

The similarity of the spectra of anhydrous ferric chloride and of the ferric complex in the ether extracts and the distinct dissimilarities between these

(16) H. M. Lawler, MIT-1110, p. 33, March 10, 1953.

(17) J. H. Van Vleck, *Phys. Rev.*, **57**, 426 (1940).

(18) P. W. Anderson and P. R. Weiss, *Rev. Mod. Phys.*, **25**, 269 (1953).

(19) M. A. Garstens and S. H. Liebson, *J. Chem. Phys.*, **20**, 1647 (1952).

(20) J. H. Van Vleck, *Phys. Rev.*, **74**, 1168 (1948).

spectra and the spectrum of hydrated ferric chloride indicate that water is not closely connected to the tetrachloroferrate anion; *i.e.*, the anion resembles the anhydrous salt much more than the hydrated ferric chloride.

Acknowledgment.—The authors wish to express their gratitude to Dr. Norval J. Hawkins for his

instructive discussions concerning magnetic resonance phenomena. The iron analyses were performed by Carolyn J. McCoy and David A. Del Grosso. Certain materials used in this research were made available at Rensselaer Polytechnic Institute by the U. S. Atomic Energy Commission under Contract No. AT(30-1)-1663.

THE EXTRACTION OF FERRIC BROMIDE BY DIETHYL ETHER¹

By GERALD S. GOLDEN AND HERBERT M. CLARK

Department of Chemistry, Rensselaer Polytechnic Institute, Troy, New York

Received December 23, 1960

The extraction of Fe(III) from aqueous acidic bromide solutions into diethyl ether at 24.9° was studied as a function of the concentration of hydrobromic acid, iron and salting agents. Included in the study was an investigation of the extraction of hydrobromic acid into diethyl ether. Iron extracts as a strong acid, HFeBr₂, which forms ion clusters in the organic phase at high concentrations. The amount of water accompanying the extracting species into the ether decreases with an increase of the ionic strength of the aqueous phase. When the molar ratio of water to hydrogen ion in the ether phase reaches four, two ether phases form. With further increase in aqueous salt concentration, the ratio remains four in the lighter ether phase but continues to decrease approaching unity in the heavier phase.

Although many investigators have studied the solvent extraction of iron(III) as tetrachloroferric acid by various organic solvents, relatively few²⁻⁵ have studied the extraction of tetrabromoferric acid. In this paper the results of an investigation of the extraction of Fe(III) from acidic bromide solution by diethyl ether are described. The investigation included a study of the extraction of hydrobromic acid since it not only co-extracts with tetrabromoferric acid, but also largely controls the relative volumes of the equilibrated phases.

Experimental

Materials.—Reagent grade diethyl ether was treated to remove peroxides, dried over CaCl₂ and distilled over calcium hydride. The fraction boiling at 34.3 ± 0.2° was collected. Reagent grade 48% hydrobromic acid was distilled in a light-protected Pyrex column. The constant boiling fraction was collected and stored in low-actinic glass vessels. Ferric bromide stock solution (1 M) was prepared by dissolving C.P. ferric oxide in an excess of concentrated hydrobromic acid and stored in low-actinic glassware. Analysis showed less than 0.05% Fe(II). All other materials were reagent grade.

Procedure.—Equal volumes of an aqueous solution of the desired composition and of diethyl ether were mixed thoroughly in stoppered, low-actinic glass cylinders and allowed to equilibrate with intermittent shaking in a water-bath at a temperature of 24.9 ± 0.1° for at least 48 hours. This equilibration time was necessary in order to ensure that the small amount of non-extractable Fe(II) (approximately 0.1% of the total iron) formed in the ether phase migrated to the aqueous phase. Conductance measurements for ether extracts were made with a dipping-type cell having a cell constant of 0.100 cm.⁻¹. Absorption spectra were obtained with either a Beckman Model B spectrophotometer or a Perkin-Elmer Spectracord, Model 4000.

Methods of Analysis.—In the absence of iron, the HBr concentration in the aqueous phase was determined by titration with standard sodium hydroxide and that in the ether

phase by the Volhard method. The latter method was used also for the determination of bromide when iron was present.

In the ether phase, where all the iron was present as Fe(III), iron analyses were performed on the same aliquot used for the determination of bromide. After removal of the AgBr precipitate, the solution was acidified with HCl, the iron reduced by Zimmermann-Reinhardt procedure and titrated with Ce(IV) to the ferroin end-point. In the aqueous phase, the total iron concentration was determined by precipitation with ammonia, then dissolution in HCl and titration with ceric sulfate after a stannous chloride reduction. For very low iron concentrations aluminum was used as a carrier. The concentration of Fe(II) was found by adding an excess of AgNO₃ to an aliquot of the aqueous phase and titrating immediately with ceric sulfate. The aqueous Fe(III) concentration was found by difference.

In the ether phase the hydrogen ion concentration was calculated as the difference between the bromide ion concentration and three times the ferric ion concentration. Water in the ether phase was determined by the Karl Fischer method. In the presence of iron, the Laurene⁶ modification of the latter method was used.

Results and Discussion

Extraction of HBr.—The distribution of HBr is shown in Fig. 1. The data of Chalkely and Williams⁷ at 13° are included for comparison. Above 4 M initial aqueous HBr concentration the solubility of diethyl ether in the aqueous phase increases rapidly with resulting increase in the volume of the aqueous phase and decrease in the volume of the ether phase. Above 6.7 M HBr only one liquid phase remains after mixing.

Over the two-liquid-phase range of HBr concentration the equilibrium concentration of H₂O in the ether phase decreases with increasing initial HBr concentration from 0.444 M for water-saturated ether to 0.332 M at 3.01 M HBr and to 0.227 M at 6.17 M HBr. As the water in the aqueous phase becomes insufficient to fully solvate the proton, at the higher concentrations of HBr, water is withdrawn from the ether phase, the solubility of ether in the aqueous phase increases, and conditions become favorable for solvation of the

(1) Abstracted from a thesis presented by Gerald S. Golden to Rensselaer Polytechnic Institute in partial fulfillment of the requirements of the Ph.D. degree. This work was supported by the U. S. Atomic Energy Commission, Contract No. AT(30-1)-1663.

(2) I. Wada and R. Ishi, *Sci. Papers Inst. Phys. Chem. Research (Tokyo)*, **24**, 135 (1934).

(3) W. A. E. McBryde and J. H. Yoe, *Anal. Chem.*, **20**, 1094 (1948).

(4) R. Bock, H. Kusche and E. Bock, *Z. anal. Chem.*, **135**, 167 (1953).

(5) H. G. Richter, S.M. Thesis, Mass. Inst. of Tech., 1950.

(6) A. H. Laurene, *Anal. Chem.*, **24**, 1496 (1952).

(7) D. E. Chalkely and R. J. P. Williams, *J. Chem. Soc.*, 1920 (1955).

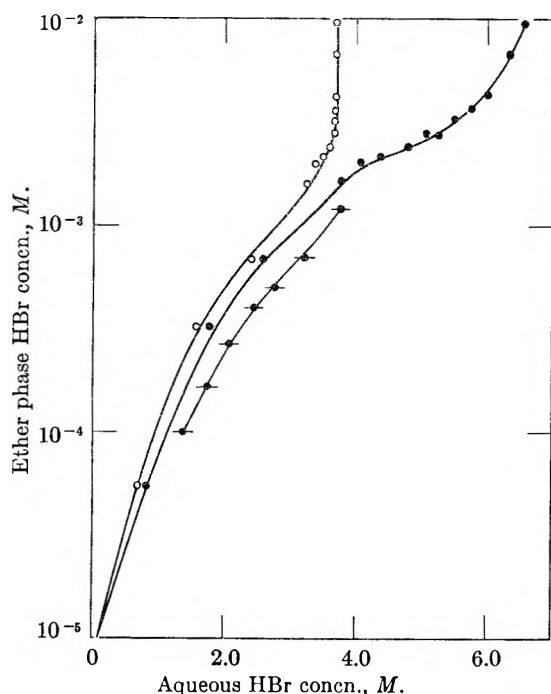


Fig. 1.—Extraction of HBr by diethyl ether: ●, initial aqueous HBr, *M*; ○, equilibrium aqueous HBr, *M*; ●, data of Chalkely and Williams⁷ at 13°, equilibrium aqueous HBr, *M*.

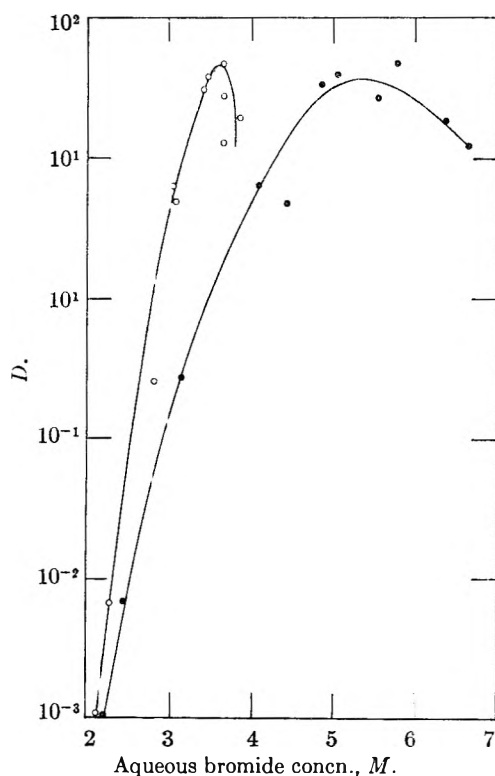


Fig. 3.—*D* for Fe(III) as a function of aqueous HBr concn.: ●, initial total bromide concn.; ○, equilibrium total bromide concn.

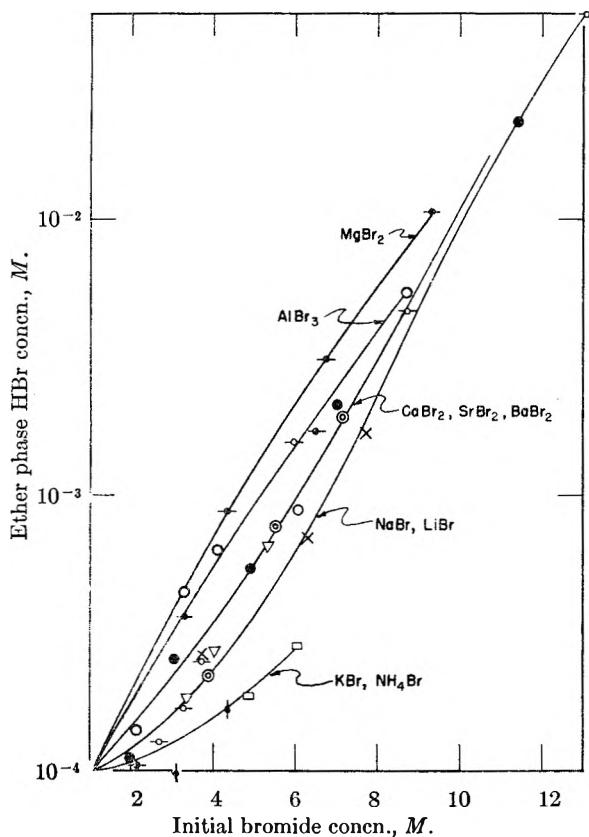


Fig. 2.—Effect of salts on the extraction of HBr by diethyl ether. Salts added to 1.06 *M* HBr: ○, AlBr₃; □, NH₄Br; ▽, BaBr₂; ●, CaBr₂; ⊙, LiBr; ●, MgBr₂; ●, KBr; ×, NaBr; ⊙, SrBr₂.

the proton by ether and formation of ion-paired or even molecular HBr.

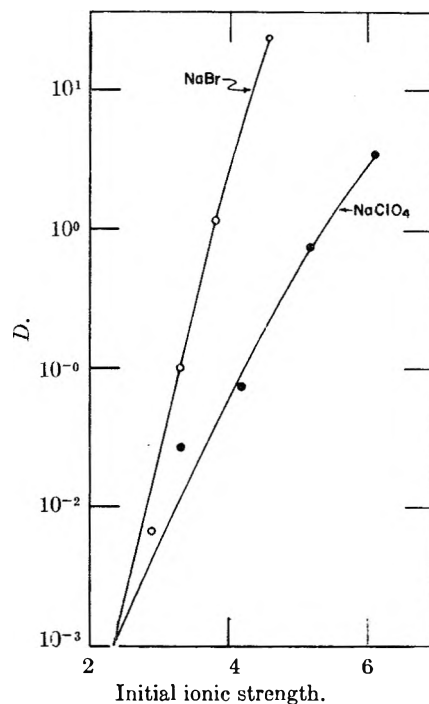


Fig. 4.—Effect of ionic strength on the extraction of Fe(III) into diethyl ether from solutions 0.2 *M* in Fe(III) and 1.1 *M* in HBr.

When salts are present in the aqueous phase, extraction increases as illustrated in Fig. 2 for solutions having an initial HBr concentration of 1.06 *M*. The over-all salt effect is in part a common-ion effect and in part a measure of the lowering of the activity of water in the aqueous

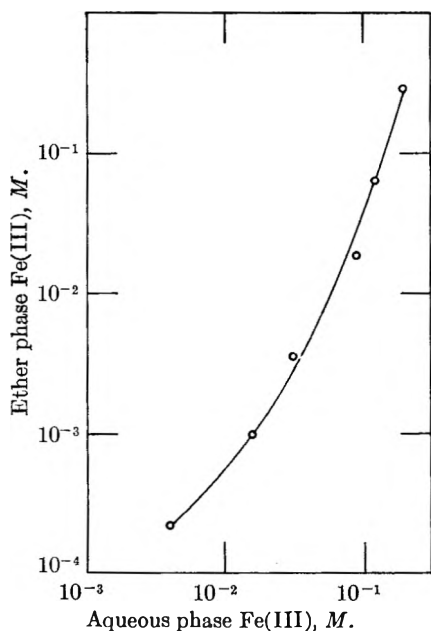


Fig. 5.—Dependence of extraction of Fe(III) on total iron concn.

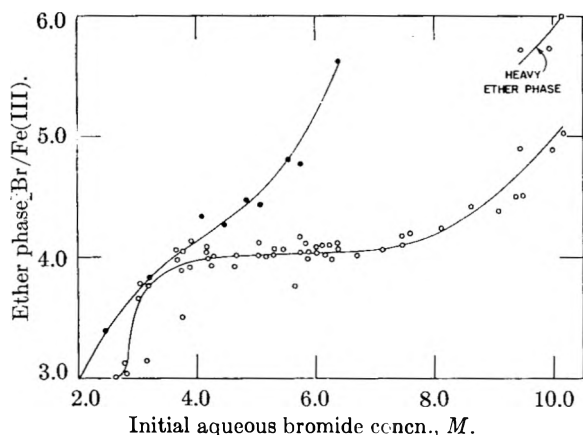


Fig. 6.—Variation of Br/Fe(III) in the ether phase with initial total bromide concentration: ●, HBr; ○, HBr, 1.1 *M* plus metal bromides.

phase. A general treatment of the salt effect has been given by Diamond.⁸

Extraction of Iron(III).—The variation of *D*, the distribution ratio, for Fe(III) with HBr concentration for extraction from aqueous phase initially 0.2 *M* in Fe(III) as bromide is represented in Fig. 3. *D* is plotted vs. both the total initial and the total equilibrium aqueous bromide concentration. Volume changes are the same as those for the extraction of HBr alone at corresponding acid concentrations. *D* becomes essentially constant when the equilibrium aqueous HBr concentration also becomes constant. If the aqueous bromide concentration is increased by adding a bromide salt at constant initial FeBr₃ and HBr concentrations (0.2 and 1.1 *M*, respectively), *D* increases reaching values of about 50 for 2.2 *M* alkaline earth bromides or 3.8 *M* lithium bromide. The extraction of Fe(III) increases with increasing salt concentration because (1) with increasing bromide concentration there is greater conversion

of Fe(III) to the extractable HFeBr₄ and (2) with increasing cation concentration there is a lowering of the water activity in the aqueous phase with resulting greater etheration and extraction of the proton. There is also greater conversion of various hydrated Fe(III) cations having a coordination number of six to FeBr₄⁻ having a coordination number of four. These common-ion and the diverse-ion salt effects are illustrated in Fig. 4.

Extraction increases with increasing concentration of Fe(III) as shown in Fig. 5, which is based on data obtained by varying the initial aqueous iron concentration from 0.02 to 0.5 *M* while holding the equilibrium aqueous concentrations of acid and bromide constant at 2.3 and 2.9 *M*, respectively, using HBr and NaBr. This behavior and the variation of the electrical conductance of extracts when diluted with ether are consistent with polymerization or ion-clustering in the ether phase and resemble those of the strong acid tetrachloroferic acid in isopropyl ether.⁹ The conductance per equivalent of iron as tetrabromoferrate ion decreases from 29.7 to a minimum of 4.29 and then increases to 18.1 for ethereal iron concentrations of 0.306, 0.00245 and 0.000098 *M*, respectively. Further evidence of clustering may be obtained by examining the concentration ratio of bromide to iron in the ether phase. In Fig. 6 the ratio, corrected for the bromide expected in the absence of iron, is plotted as a function of the initial aqueous bromide concentration corresponding to 0.2 *M* FeBr₃ and variable HBr concentration for one curve and to 0.2 *M* FeBr₃, 1.1 *M* HBr and variable bromide salt concentration for the other. The initial rise from three to four could result from a slight extraction of FeBr₃ at low aqueous bromide concentration. Values above four could be an indication of the extraction of higher anionic complexes, e.g., FeBr₅⁻, except that spectral measurements in the region 320–520 *mμ* show identical spectra for ether extracts over the entire range of aqueous bromide concentration studied. Values above four are attributed to increased solubility of hydrobromic acid in the ether phase resulting from the formation of mixed-ion clusters, i.e., Br⁻H⁺FeBr₄⁻ and H⁺FeBr₄⁻H⁺, in the ether phase at high aqueous bromide concentrations. There is, then, increased solubility of hydrobromic acid beyond that already ascribed to ion pair formation in the absence of iron.

The extent of hydration of the proton in ether extracts of tetrabromoferric acid varies with the conditions of extraction. Thus, the concentration ratio H₂O/H⁺ decreases from 8.45 to 5.99 for an increase of initial HBr concentration from 2.70 to 5.40 *M*. When LiBr is added to the system, initially 0.2 *M* in FeBr₃ and 1.1 *M* in HBr, the ratio decreases to four when the Li⁺ concentration is about 8 *M*. At higher aqueous Li⁺ concentrations two ether phases form. For the heavy ether phase in which mixed ion clustering favors an increase in the iron concentration with increasing aqueous lithium concentration, the ratio

(8) R. M. Diamond, *J. Phys. Chem.*, **63**, 659 (1959).

(9) D. E. Campbell, H. M. Clark and W. H. Bauer, *ibid.*, **62**, 506 (1958).

continues to decrease and approaches unity. For the light phase, however, the ratio remains essentially constant at four and the iron concentration decreases. Thus, there is no single value for the number of water molecules associated with the extracting species for all conditions of extraction.

The number varies with the aqueous acid or salt concentration, *i.e.*, with the activity of water in the aqueous phase. Similarly, the formation of two ether phases is governed by the activity of water in the system as controlled by non-extractable salts in the aqueous phase.

QUANTITATIVE DIFFERENTIAL THERMAL ANALYSIS BY CONTROLLED HEATING RATES¹

BY EDWARD STURM

Department of Geology, Texas Technological College, Lubbock, Texas

Received January 26, 1961

The determination of quantities of heat, associated with thermal changes occurring in a sample when investigated by the method of differential thermal analysis, requires difficult evaluations of experimental variables such as the thermal conductivity of the sample and the heat leakage through the thermocouple wires. The method suggested here is based on the experimental determination of the over-all thermal conductivity of the total sample. The over-all thermal conductivity is computed from data obtained when heating the sample at a rate resulting in a constant thermal gradient. The conductivity thus found is incorporated in a constant of proportionality which relates the heat of the reaction to the area under the differential thermal curve.

Introduction

The aim of quantitative differential thermal analysis is the evaluation of heat changes taking place in a substance while it undergoes an exothermic or endothermic reaction. In the conventional method, the sample substance and a thermally inert substance are heated at a constant rate. By means of a differential thermocouple, the e.m.f.'s developed by the two junctions embedded in the sample and inert substances can be continuously compared. The differential e.m.f., which is proportional to the differential temperature, is plotted against the temperature prevailing in the center of the inert reference substance by means of an X-Y recorder or two strip-chart recorders. Thermal changes occurring in the sample are recorded as deviations from the base line (Fig. 1). The area under the curve is approximately proportional to the amount of heat liberated or absorbed during the thermal reaction.²⁻⁵ The numerical relationship between the quantity of heat involved and the area under the curve may be expressed as

$$Q = \psi \int_{t_1}^{t_2} \theta dt \quad (1)$$

where

- Q = quantity of heat (cal.)
- θ = differential temperature (deg.)
- t_1, t_2 = initial and final time of the reaction (sec.)
- ψ = proportionality constant to be evaluated experimentally (cal./sec. deg.)

To evaluate the results of differential thermal analysis quantitatively, one must find the constant of proportionality for the given experimental conditions.

Several workers^{6,7} made use of the divergence theorem (Green theorem) to obtain an expression for the total heat. Boersma⁶ derived a general expression (2) for the total heat

$$Q'V = -k_s S \left[\frac{\partial}{\partial r} \int_{t_1}^{t_2} \theta dt \right] \quad (2)$$

where

- Q' = quantity of heat per unit volume (cal./cm.³)
- V = volume of sample (cm.³)
- S = surface of sample (cm.²)
- k_s = thermal conductivity of sample (cal./sec. cm. deg.)

For a sample holder of cylindrical shape, whose height (h) equals or exceeds twice its radius (r), Boersma⁶ derived the relationship

$$\int_{t_1}^{t_2} \theta dt = \frac{Q'}{k_s} \int_0^r \frac{V}{S} dr = \frac{Q'r^2}{4k_s} \quad (3)$$

where

- r = radius of the sample holder (cm.)

Although the lower limit of integration should be r = radius of the thermocouple bead, no significant error is introduced by making this limit equal zero. Further, since $Q = Q'V$, and $V = \pi r^2 h$

$$\psi = \frac{Q}{\int_{t_1}^{t_2} \theta dt} = k_s [4\pi h] \quad (4)$$

In practice, the conductivity, k_s , is the over-all conductivity of the total sample. This bulk conductivity, henceforth referred to as the effective conductivity, k_e , is a function of not only the material under test but also of the effects of the thermocouple wires and the sample holder.

The Effective Conductivity

In the conventional experimental arrangement, the thermocouple beads are embedded in the center of the sample and inert substances contained in

(1) This work was supported by a research grant from Texas Technological College, Lubbock, Texas.

(2) F. C. Kracek, *J. Phys. Chem.*, **34**, 225 (1930).

(3) L. G. Berg, *Compt. rend. Acad. Sci. U.R.S.S.*, **49**, 648 (1945).

(4) S. Speil, *et al.*, U. S. Bureau of Mines Tech. Paper 664, 1945.

(5) M. J. Vold, *Anal. Chem.*, **21**, 683 (1949).

(6) S. L. Boersma, *J. Am. Ceram. Soc.*, **38**, 281 (1955). Note: the symbols used here are different from those used by Boersma.

(7) C. M. A. deBruijn and W. Van der Marel, *Geol. en Mijnbouw*, **16**, 69 (1954).

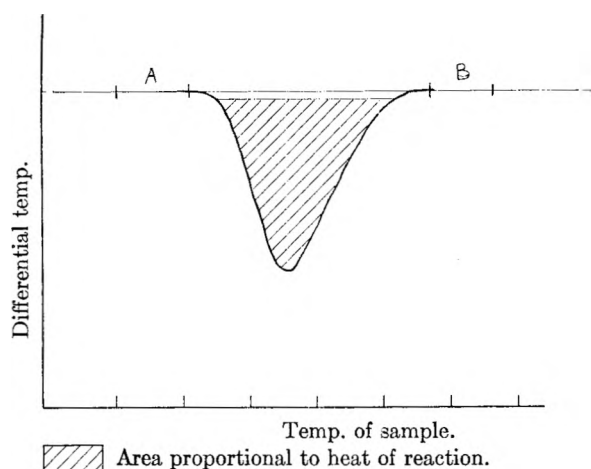


Fig. 1.—Thermogram of differential temperature versus temperature. Shaded area is the area proportional to heat of reaction.

sample holders of cylindrical shape. The temperature at the thermocouple bead is due to the heat flow through the sample material as well as that through the thermocouple wires. Ignoring the end effects, the radial heat flow through the sample, under steady-state conditions, may be described as

$$Q'_s = \frac{k_s 2\pi h [T_0 - T_i]}{\ln \frac{r}{r_0}} \quad (5)$$

where

- Q'_s = quantity of heat flowing through the sample per second (cal./sec.)
- h = height (or length) of the sample holder (cm.)
- $T_0 - T_i$ = the thermal gradient; that is, the difference between the furnace temperature and the temperature at the center of the sample (deg.)
- r_0 = the radius of a single, centrally located thermocouple wire whose cross-sectional area equals twice the cross-sectional area of the wire used, that is, $r_0 = r_w \sqrt{2}$, where r_w = the radius of the wire used (cm.)

In differential thermal analysis the thermocouple wires perform the double role of heat detection device and heat sink. Their presence has the effect of reducing the peak area by an amount related to the ratio of the heat flow through the sample material to that through the thermocouple wires. The evaluation of the variables affecting the area under the curve poses a number of experimental difficulties. To mention only one: The sample conductivity, k_s , is a function not only of the substance itself but also of its porosity which, in turn, is a function of its particle size distribution and the manner of sample packing. Further, the conductivity of the sample substance cannot be considered a constant in view of the fact that the composition of the sample changes during the thermal reaction.

In order to obtain a value for the over-all or effective conductivity, k_e , one may consider the sample powder, the sample holder, and the thermocouple wires a single, non-homogeneous cylindrical body. The total sample has an effective conductivity which is a function of the variables mentioned above and others related to the type of sample holder used and the geometry of the arrangement.

A value for the effective conductivity of the total sample can be found experimentally by heating the sample at a rate resulting in almost steady-state conditions of heat flow, that is, a rate at which the difference between the temperature prevailing outside the sample and that at the center of the sample ($T_0 - T_i$) remains constant.

Considering the sample holder, the sample, and the enclosed thermocouple wires a single, non-homogeneous sample, one may write $\ln(r)$ instead of $\ln(r/r_0)$, and k_e instead of k_s in equation 5. Equating two expressions for total heat, we obtain

$$Q = \frac{2\pi h k_e [T_0 - T_i] [t_2 - t_1]}{\ln r} = [m_s c_s + m_w c_w] [T_2 - T_1] \quad (6)$$

where

- $t_2 - t_1$ = the time interval (sec.)
- T_2, T_1 = furnace temperatures at times t_2 and t_1 , respectively (deg.)
- m_s, m_w = wt. of the sample and wt. of the portion of the thermocouple wire embedded in the sample (g.)
- c_s, c_w = specific heats of the sample and thermocouple wire, respectively (cal./g. deg.)
- k_e = over-all or effective conductivity (cal./sec. cm. deg.)

Determination of the Proportionality Constant ψ .—Solving equation 6 for k_e and substituting in equation 4, the expression (7) for ψ is now obtained.

$$\psi = M 2 \ln r \frac{[m_s c_s + m_w c_w] [T_2 - T_1]}{[t_2 - t_1] [T_0 - T_i]} \quad (7)$$

where

- M = an amplification factor depending on the signal amplification employed (pure number)

The proportionality constant must be evaluated for each analysis in order to allow for differences in sample packing, particle size distribution, and variables due to heat leakage through the thermocouple wires. Care should be taken to use approximately the same volume of sample material for each run. Another implicit assumption is that the thermocouple beads are well centered, and that the height of the sample be at least twice its radius.

Because many substances change significantly during the thermal reaction, it is necessary to determine ψ for temperature ranges before and after the reaction (A and B in Fig. 1) and to use the average value.

Excepting weight and specific heat determinations, all variable quantities required by equation 7 can be obtained from measurements made with the sample in the holder. This procedure assures that the conditions under which ψ is determined are the same as those prevailing during the reaction.

Suggested Experimental Procedure—In order to determine the required variables it is necessary to find the heating rate at which the thermal gradient ($T_0 - T_i$) remains constant for a period of approximately three to twenty minutes. The required heating rate can be found with the aid of a voltage divider placed between the furnace control and the furnace, and a third thermocouple placed between the sample holders. The furnace is allowed to reach a temperature within the range for which ψ is to be determined. The voltage divider then is set so that a low heating rate is obtained. When the thermal gradient begins to decrease, as observed on the recorder, the rate of heating

is slowly increased. The latter results in a decrease of the slope of the differential temperature curve. After the slope has been reduced to zero, the measurements of time ($t_2 - t_1$) and temperature ($T_2 - T_1$) and ($T_0 - T_1$) are made. Although the temperature measurements may be made with the aid of a potentiometer, no substantial loss in accuracy was found when using the recorder.

The method was tested by determining the known heats of fusion of KNO_3 , AgNO_3 , NaNO_3 and $\text{K}_2\text{Cr}_2\text{O}_7$. Considerable difficulty was encountered when attempting to find the heating rates at which the thermal gradient remained constant. The difficulty is due to the thermal inertia of

the system. Although the heating rate can be changed rapidly, the results of the change can be measured only after a time lag during which the system tends to reach a new state of equilibrium. At the present time, research efforts are directed toward finding a more convenient laboratory technique which either would simplify the procedure for finding the required heating rate or would obviate the need for finding the rate. No limits of accuracy can yet be given. The accuracy is of course also a function of the quality of the amplifying and recording equipment and the accuracy of instrument calibration and sample weighing.

THE PHOTOCHEMISTRY OF IODIDE ION IN AQUEOUS SOLUTION¹

BY E. HAYON²

Chemistry Department, Brookhaven National Laboratory, Upton, Long Island, New York

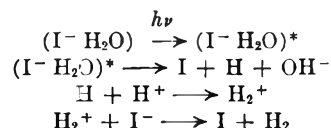
Received January 30, 1961

The quantum yield for the formation of I_2 on exposure of air-free aqueous solutions of iodide to 2537 Å. light is dependent upon the concentration of iodide and hydrogen ions, as was observed by other workers. In dilute solutions of iodide at $\text{pH} > 3$, ϕ_{I_2} is almost zero. Addition of acceptors for electrons or hydrogen atoms, such as H_2O_2 and KNO_3 , brings about an iodide-induced decomposition of these scavengers in neutral and alkaline solutions. This indicates, contrary to the postulates of Farkas and Farkas and of Platzman and Franck, that hydrogen ions *per se* are not essential in the primary photochemical process. The dependence of ϕ_{I_2} upon $[\text{H}^+]$ may be due to the formation of H_2^+ as proposed by Rigg and

Weiss, or to the scavenging of electrons by the hydrogen ions in solution $(\text{I}^- \text{H}_2\text{O}) \xrightarrow{h\nu} (\text{I}^- \text{H}_2\text{O})^*$ and $(\text{I}^- \text{H}_2\text{O})^* + \text{H}^+ \longrightarrow \text{I} + \text{H} + \text{H}_2\text{O}$.

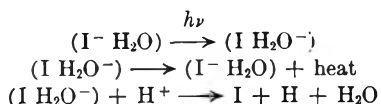
A number of mechanisms have been postulated for the primary photochemical processes occurring in the oxidation of iodide ions in aqueous solutions. As early as 1928 Franck and Scheibe³ characterized the absorption bands of iodides as "electron affinity spectra," and in 1931 Franck and Haber⁴ proposed that the absorption of energy by iodide ions resulted in the transfer of the electron from the anion to a water molecule on the hydration sphere. Farkas and Farkas,⁵ in order to explain

of the quantum yield upon H^+ and I^- concentrations by proposing the formation of H_2^+



More recently Platzman and Franck^{7,8} proposed a model for the excited complex in which the electron transfer process was based on the rate of collision between ionic species. To explain the decline in the quantum yield of iodine with decreasing hydrogen ion concentration, they presumed the photolytic process to result from a collision of a hydrogen ion with the entity formed by the absorption act.⁷ Smith and Symonds,⁹ in trying to explain the dependence of the absorption band of iodide on temperature and the nature of the solvent used, have suggested another model based on a modification of that proposed by Platzman and Franck.^{7,8}

the dependence of the photooxidation of iodides upon the hydrogen ion concentration, suggested that the transfer of the electron occurred from the hydration sphere to a hydrogen ion in solution.



Rigg and Weiss⁶ investigated the photochemistry of iodide solutions over a wide range of iodide and hydrogen ion concentrations, and observed that the quantum yield was dependent upon both H^+ and I^- concentrations. Since the Farkas and Farkas mechanism excluded a dependence of the quantum yield on iodide concentration, Rigg and Weiss postulated the formation of H and I atoms in aqueous solution, and explained the dependence

The experiments carried out in this work indicate that hydrogen ions are not essential in the primary photochemical process resulting in the oxidation of iodide ions, since such an oxidation was obtained in oxygen-free neutral or alkaline solutions of iodide in the presence of solutes which can themselves scavenge electrons or hydrogen atoms. The hydrogen ion can, however, play the same role as the other solutes used insofar as it too can scavenge electrons or hydrogen atoms, but with much lower efficiency. Recently, after the completion of

(1) Research performed under the auspices of the U. S. Atomic Energy Commission.

(2) Department of Physical Chemistry, Cambridge University, England.

(3) J. Franck and G. Scheibe, *Z. physik. Chem.*, **A139**, 22 (1928).

(4) J. Franck and F. Haber, *S. B. preuss. Akad. Wiss. (Phys. Math.)*, 250 (1931).

(5) A. Farkas and L. Farkas, *Trans. Faraday Soc.*, **34**, 1113 (1938).

(6) T. Rigg and J. Weiss, *J. Chem. Soc.*, 4198 (1952).

(7) R. Platzman and J. Franck, Research Council of Israel, Special Publication No. 1, Jerusalem, 1952, p. 21.

(8) R. Platzman and J. Franck, *Z. Physik*, **138**, 411 (1954).

(9) M. Smith and M. C. R. Symonds, *Trans. Faraday Soc.*, **54**, 346 (1958).

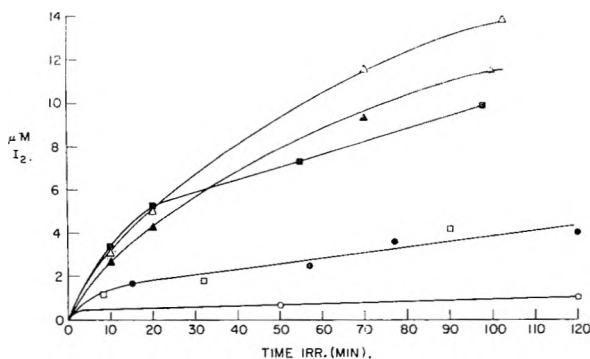


Fig. 1.—Iodine produced by illumination of potassium iodide solutions, N_2 atmosphere unless stated otherwise: \circ , 10^{-3} M KI, pH 5.7; \bullet , 10^{-1} M, pH 6.2; \square , 10^{-1} M, pH 9.2; \blacksquare , 1 M, pH 6.5; \triangle , 1.0 M, air-saturated; \blacktriangle , 1.0 M, air-saturated, lower light intensity.

this work, Dainton and Sills¹⁰ briefly reported experiments on the ultraviolet irradiation of aqueous solutions of iodide in the presence of nitrous oxide which yielded similar results.

Experimental

A low pressure mercury resonance lamp Hanovia SC-2537 was used, run from a 6000 volt transformer at 50 ma. in all cases except a few runs at lower intensity in which 20 ma. current was used. The radiation cells were cylindrical (of the type described by Saldick and Allen¹¹), 5×2.5 cm. diam., made of quartz glass with a Vycor window on the side incident to the light, such that all the 1849 Å. mercury resonance line was absorbed by the Vycor glass. The volumes used were about 22 to 25 cc. and the solutions were stirred magnetically. A water-lubricated stopcock and a quartz frit were sealed on at the bottom of the cell. The light from the lamp first passed through a Vycor condenser of 5 cm. internal diameter containing triply distilled water, before reaching the radiation cells. All experiments were done under conditions of complete absorption of the incident light by the iodide. The light input was measured by means of the ferric oxalate actinometer¹² ($\phi = 1.2$) under conditions identical to the experiments with iodide. The intensity at which almost all the work was done was 3.16×10^{-5} einsteins/l.-min.; the lower intensity used was 7.9×10^{-6} einsteins/l.-min.

The water used in preparing the solutions was triply distilled from acid dichromate, alkaline permanganate and a final distillation.¹³ Stock solutions of 2×10^{-3} M potassium iodide (Baker Analyzed reagent) were prepared weekly; solutions of iodide above 2×10^{-3} M were prepared just previous to irradiation. The solutions were de-aerated by bubbling prepurified nitrogen for about 20 min. through the quartz frit, while the solution was magnetically stirred. A small quartz stopper above displaced some of the solution so as to leave no air-space above the liquid.

Iodine in the irradiated solutions was measured directly as I_3^- at 350 m μ , whose concentration in 0.1 M I^- was 38.9 μ M per optical density unit. The sum of the yields of hydrogen peroxide and iodine was measured using Ghormley's iodide reagent¹⁴ which contains molybdate as catalyst. Blanks for the unirradiated solutions as well as for the iodide reagent were done simultaneously in all cases. Sulfuric acid or sodium hydroxide was used to adjust the pH. Nitrite was determined by the method of Shin,^{15a} and the procedure and extinction coefficient used were those of Schwarz and Allen.^{15b}

(10) F. S. Dainton and S. A. Sills, *Nature*, **186**, 879 (1960).

(11) J. Saldick and A. O. Allen, *J. Chem. Phys.*, **22**, 438 (1954).

(12) C. G. Hatchard and C. A. Parker, *Proc. Roy. Soc. (London)*, **235A**, 518 (1956).

(13) E. R. Johnson and A. O. Allen, *J. Am. Chem. Soc.*, **74**, 4147 (1952).

(14) C. J. Hochanadel, *J. Phys. Chem.*, **56**, 587 (1952).

(15) (a) M. B. Shin, *Ind. Eng. Chem., Anal. Ed.*, **13**, 33 (1941);

(b) H. A. Schwarz and A. O. Allen, *J. Am. Chem. Soc.*, **77**, 1324 (1955).

Results

In the photochemistry of 10^{-3} M neutral air-free solutions of iodide only a very small amount of iodine, and equivalent hydrogen as recently has been measured by Edgecombe and Norrish,¹⁶ is formed, as shown in Fig. 1. Increasing the iodide concentration produces an increase in the rate of formation of iodine both initially and at longer times. Addition of hydrogen peroxide to neutral air-free solutions of iodide brings about photo-induced changes in the concentration of the added solute (Fig. 2), and addition of nitrate to neutral air-free solutions of iodide increases the quantum yield for the photochemical oxidation of iodide (Fig. 3). The photochemical changes taking place are dependent on the nature as well as the concentration of the added substance. The amounts of H_2O_2 and NO_3^- added are relatively small and they absorb less than 2% of the incident light. In the absence of iodide the concentration of the added solutes remains unchanged on irradiation, under otherwise identical experimental conditions.

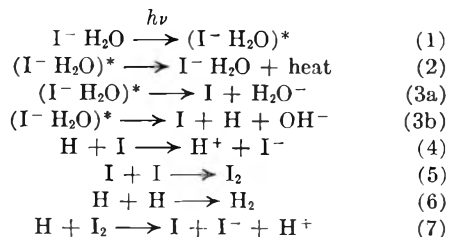
When H_2O_2 is added to neutral dilute iodide solutions, the amount of iodine formed is still very small ($< 1 \mu$ M) but hydrogen peroxide is decomposed, Fig. 2, with a yield independent of pH between 5.7 and 10.5, but dependent upon the concentration of initially added H_2O_2 (in 10^{-3} M KI, $\phi_{(-H_2O_2)} = 0.11$ and 0.05 for 222 and 54 μ M H_2O_2 solutions, respectively). Owing to the thermal reaction between I^- and H_2O_2 , which takes place even in neutral solution, the decomposition of H_2O_2 could not be investigated at high I^- concentration.

The addition of potassium nitrate to air-free neutral solutions of iodide results on illumination in the formation of substantial amounts of iodine and nitrite (Fig. 3). However, when H_2SO_4 is added to the mixture to bring the pH to 2.0, very little nitrite or iodine is formed. No reduction of nitrate takes place in the absence of iodide, indicating that the reduction of nitrate is photo-induced by the iodide.

Figure 4 shows the dependence of the yield of iodine upon $[H^+]$ and $[I^-]$.

Discussion

The processes resulting from the absorption of light by iodide ions, present in neutral air-free aqueous solutions, are



The effect of iodide concentration upon the formation of iodine ($\phi_{I_2} = 0.008$ and 0.016 for 0.1 and 1.0 M KI, respectively) from air-free neutral and

(16) F. H. C. Edgecombe and R. G. W. Norrish, *Proc. Roy. Soc. (London)*, **253A**, 154 (1959).

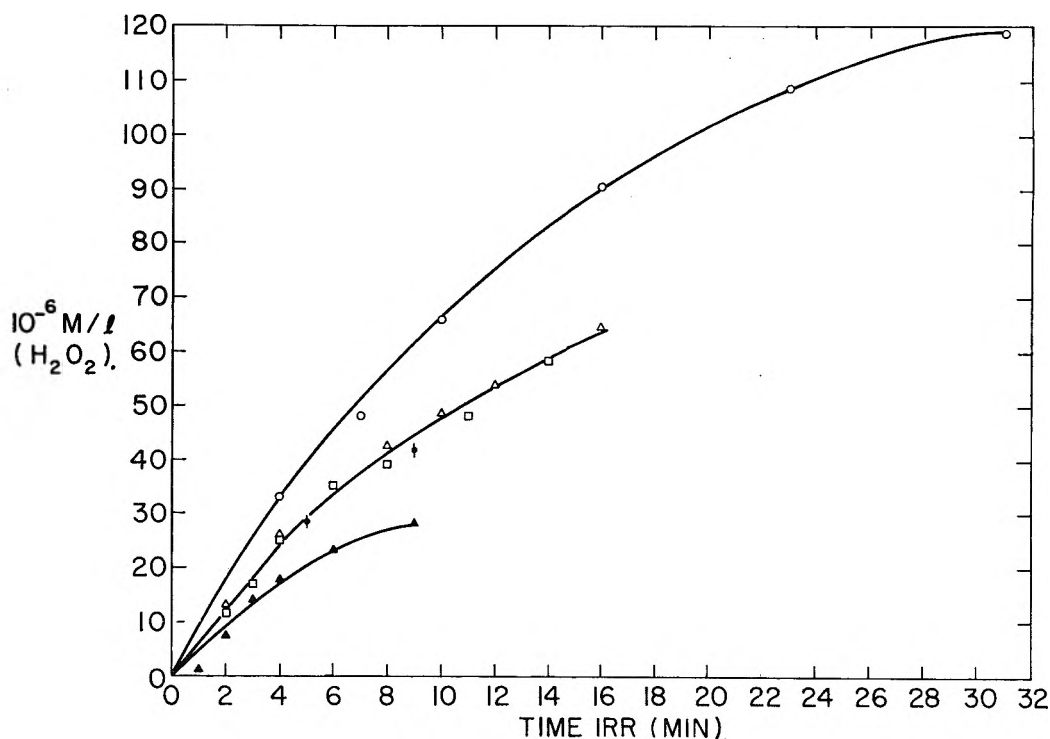
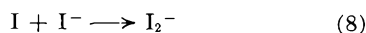
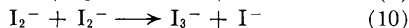
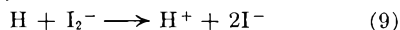


Fig. 2.—Photochemistry of KI ($2 \times 10^{-3} M$) in presence of H_2O_2 , N_2 atmosphere: \circ , $200 \mu M/l$, pH 5.7; \square , $110 \mu M/l$, pH 5.7; \blacktriangle , $47 \mu M/l$, pH 5.7; \triangle , $105 \mu M/l$, pH 9.4; \bullet , $95 \mu M/l$, pH 10.6.

alkaline iodide solutions (Fig. 1) can be explained as being a result of the formation of I_2^-



an unstable species whose absorption spectrum has been observed in flash photolysis of iodide solutions by Grossweiner and Matheson¹⁷ and Edgcombe and Norrish,¹⁶ and is believed to be the dihalide. The rate of disappearance of I_2^- was found¹⁷ to be independent of pH but to increase with a decrease in the iodide concentration. The effect of iodide concentration (Fig. 1) in the steady irradiation may be explained if one assumes that the rate constant for reaction 4 is greater than that for reaction 9 since the rate of reaction 5 is greater than that of (10)¹⁷



The minimum value for the rate constant of reaction 10 was found¹⁷ to be 1.2×10^4 and at the lowest $[I^-]$ used in these experiments, $10^{-3} M$, most I atoms will be present as I_2^- . It is also possible that the reduction of the trihalide I_3^- is less favorable than that of I_2 .

No iodine ($< 1 \mu M$) is formed on addition of H_2O_2 to neutral or alkaline dilute solutions of iodide, but hydrogen peroxide is decomposed (Fig. 2). In the absence of iodide the concentration of H_2O_2 remains unchanged on irradiation; furthermore Hunt and Taube¹⁸ showed that the photodecomposition of aqueous solutions of hydrogen peroxide is unaffected by the addition of halides. It follows therefore that the photodecomposition of H_2O_2 observed in neutral and alkaline air-free solutions

(17) L. I. Grossweiner and M. S. Matheson, *J. Phys. Chem.*, **61**, 1089 (1957).

(18) J. P. Hunt and H. Taube, *J. Am. Chem. Soc.*, **74**, 5999 (1952).

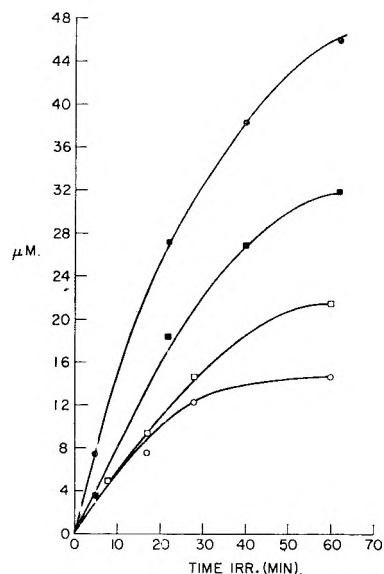
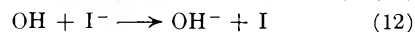
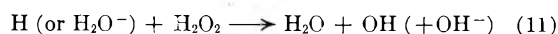


Fig. 3.—Formation of iodine and nitrite on illumination of neutral solutions of potassium iodide and potassium nitrate: \circ , I_2 and \square , NO_2^- found in a solution of $10^{-3} M$ KI and $10^{-4} M$ KNO_3 ; \bullet , I_2 and \blacksquare , NO_2^- in $10^{-2} M$ KI and $10^{-4} M$ KNO_3 .

of iodide must be induced by the iodide which absorbs more than 98% of the incident light. The following known^{19,20} reactions take place



(19) (a) M. G. Evans, N. S. Hush and N. Uri, *Quart. Revs.*, **6**, 186 (1952); E. J. Hart and C. B. Senvar, *Second Intl. Conf. Peaceful Uses of Atomic Energy*, Geneva (1958); (b) A. O. Allen and H. A. Schwarz, *J. Chem. Phys.*, **29**, 30 (1958).

(20) E. Hayon and A. O. Allen, to be published.

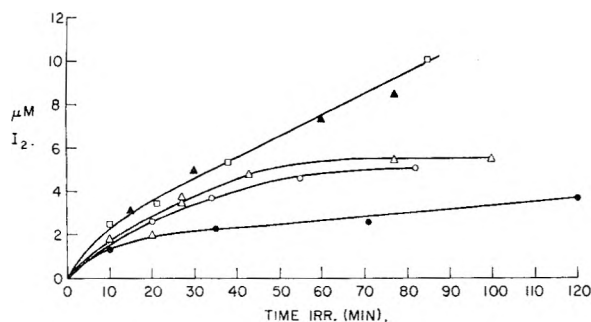
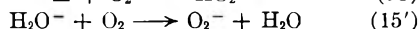
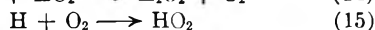
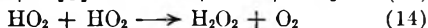
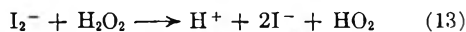


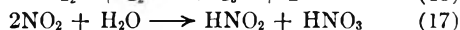
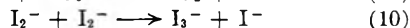
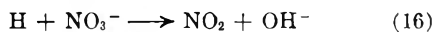
Fig. 4.—Iodine produced by illumination of KI in acid solutions, N_2 atmosphere: ●, $10^{-3} M$ KI, pH 1.2; ○, $10^{-2} M$, pH 2.0; △, $10^{-1} M$, pH 2.9; □, $10^{-1} M$, pH 2.2; ▲, $10^{-2} M$, pH 1.4.



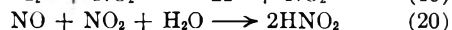
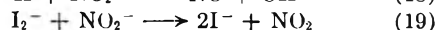
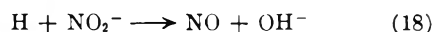
The competition between reactions 11 and 15 or 15' accounts for the departure from linearity of $(-H_2O_2)$ as a function of time of illumination (Fig. 2). It was shown^{19b} in radiation chemistry that $[k(15)/k(11)]$ for neutral solutions is 1.85 and the results in Fig. 2 are within $\pm 10\%$, in good agreement with this value. It is not possible from the above experiments to distinguish categorically whether the entities which reduce H_2O_2 are H atoms or H_2O^- . The effect of H_2O_2 , however, is to reduce the back reactions which take place in the absence of added scavengers, reactions 4-7.

On irradiation of $10^{-3} M$ KI in the presence of $60 \mu M$ H_2O_2 at pH 2.9 to 4.3, iodine is formed and an equivalent amount of H_2O_2 decomposed. These results are in agreement with the finding in the radiation chemistry²⁰ of I^-/H_2O_2 solutions that reaction 13 does not take place, *i.e.*, is reversed in acid solution. At pH below 2.9, $2-3 \mu M$ I_2 only is formed and the concentration of H_2O_2 remains unchanged. This shows that the H species formed at low pH in the photochemistry of iodide (reaction 3) are relatively unreactive toward hydrogen peroxide, as was observed in the radiation chemistry under similar conditions.¹⁴ It appears therefore that the reducing species formed in the radiation chemistry of water are similar to those formed in the photochemistry of aqueous solutions of iodide.

The addition of NO_3^- ions to air-free neutral solutions of iodide results in the formation of I_2 and reduction of nitrate to nitrite (Fig. 3). Initially the mechanism of formation of I_2 and NO_2^- is probably

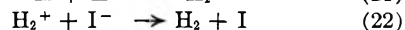
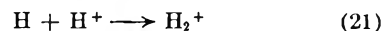


Secondary reactions, however, take place and the ensuing steps are not clear. The irradiation of $10^{-3} M$ KI and $10^{-4} M$ KNO_2 in neutral air-free solution results in no net oxidation of nitrite and no formation of iodine. This is explained as a result of the reaction of hydrogen and iodine atoms with nitrite, followed by reaction 20



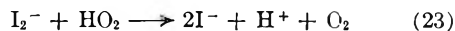
Reactions 16-20 already have been postulated.²¹

The dependence of the quantum yield of iodine upon hydrogen ion concentration (Fig. 4) may be due to one or both of the following possibilities: (i) A result of formation of hydrogen molecule ions, H_2^+ , as postulated by Rigg and Weiss,⁶ which would account for the increase in ϕ_{I_2} with I^- and H^+ concentrations

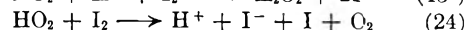
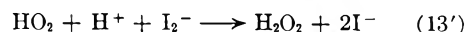


(ii) The dependence on hydrogen ion concentration may be similar to that of hydrogen peroxide or nitrate in the photochemistry of neutral iodide solutions, *i.e.*, hydrogen ions react with the H atom precursor, the hydrated electrons, in the primary photochemical process ($H_2O^- + H^+ \rightarrow H + H_2O$) and no H_2^+ formation need be considered. The effect of the $[I^-]$ in both cases would be to stabilize the I atom as an I_2^- , and reduce the back reactions 4 and 5. It does not seem at present possible to differentiate between the two alternatives.

In the photochemistry of neutral air-saturated $10^{-3} M$ solutions of iodide no H_2O_2 is formed and only traces ($<1 \mu M$) of I_2 . This can be explained by reactions 15, 14, 13 and 23 taking place. The



photochemistry of aerated solutions of iodide at low pH also was investigated, and I_2 and H_2O_2 were found to be formed in exactly the same yields. These yields were found right from the smallest doses to be markedly dependent upon pH and iodide concentration, the yields increasing with increase in $[H^+]$ and $[I^-]$. The initial ϕ_{I_2} formation in air-saturated solution is about five times greater than that in air-free solutions for $10^{-3} M$ KI, pH 1.2 ($\phi_{I_2} = 0.028$ and 0.005 , respectively). Addition of small amounts of H_2O_2 previous to irradiation causes no changes, but addition of a few μM of I_2 reduces the quantum yield of I_2 and H_2O_2 formation. As was postulated in the radiation chemistry of aerated acidified solutions of iodide,²⁰ reactions 13' and 24 probably also occur in the photochemistry of iodide, and account for the increased yields. Reaction 13' as written



is stoichiometric and does not preclude intermediate steps. In addition, oxygen may be increasing the photooxidation of iodide by scavenging the electrons or hydrogen atoms formed in the primary photochemical process (reactions 15 and 15').

Acknowledgment.—The author wishes to thank Dr. A. O. Allen for reading the manuscript and suggesting some changes.

(21) H. A. Schwarz and A. J. Salzman, *Radiation Research*, **9**, 502 (1958).

COMPARATIVE RATES OF THE ELECTROLYTIC EVOLUTION OF HYDROGEN AND DEUTERIUM ON IRON, TUNGSTEN AND PLATINUM

By J. O'M. BOCKRIS AND D. F. A. KOCH

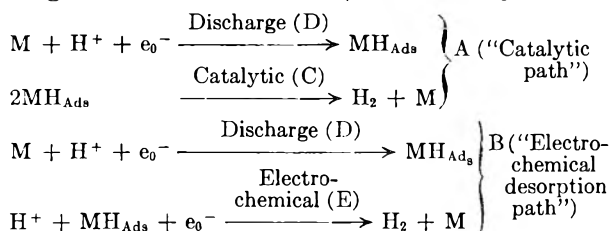
John Harrison Laboratory of Chemistry, University of Pennsylvania, Philadelphia 4, Pennsylvania

Received February 24, 1961

Methods previously described for the determination of the mechanism of hydrogen evolution and dissolution do not allow the slow electrochemical desorption step to be distinguished from that of proton transfer. The fact that theory indicates a ratio of $(i_0)_{\text{H}_2\text{O}^+}/(i_0)_{\text{D}_2\text{O}^+}$ characteristic of mechanism is used in this study. The exchange current density for hydrogen evolution has been determined in 0.5 M HCl dissolved in H₂O and in 0.5 M DCl dissolved in D₂O under conditions of high purity. The ratio of the exchange current densities is 4 for Fe, 8 for W and 3 for Pt. Tafel slopes are the same for both isotopes. The concentrations of the relevant entities present in D-containing solutions are calculated. Equations are derived from which $(i_0)_{\text{D}_2\text{O}^+}$ can be obtained from the apparent exchange current density in D solution containing a few molecular per cent. of water. Relations are derived for the dependence of the separation factor, S , on the $c_{\text{D}}/c_{\text{H}}$ ratio in solution. Limiting values of S exist as $c_{\text{D}}/c_{\text{H}}$ tends to zero and to infinity, in which S is simply related to $(i_0)_{\text{H}_2\text{O}^+}/(i_0)_{\text{D}_2\text{O}^+}$. Discussion of available values of S , and the exchange current density ratio, gives information on mechanisms following the rate-determining reaction. The theoretical values of exchange current density ratios arising from assumption of a given mechanism depend on the differences in the heat of adsorption of H and D on the metal. Two methods of estimating this are given. The evidence favors a choice of 0.2 kcal. mole⁻¹ for all metals. The results are consistent with rate-controlling proton transfer to iron, electrochemical desorption from tungsten and atomic combination of platinum.

I. Introduction

In recent years only two paths have been considered as probable (but *cf.* Horiuti¹) for the hydrogen evolution reaction (h.e.r.) and the reverse hydrogen dissolution reaction (h.d.r.). They are



The behavior theoretically expected for some specific mechanisms is given in Table I² (with the experimentally well supported assumption of a symmetry factor of 1/2). When the rate-determining reaction is the second reaction in a consecutive series, the preceding reaction is assumed to be in virtual equilibrium except for mechanisms (4)_c, (2)_e, (1)_a and (3)_a; when the rate-determining step is the first one in a consecutive series, the succeeding is assumed *not* to be in equilibrium except for (1)_c, (3)_c, (2)_a and (4)_a. (Earlier calculations³ neglected mechanisms in which following fast reactions were in equilibrium; and distinguishing criteria which arise only if data on the little examined h.d.r. are available.)

Inspection of Table II shows that unique identification of all mechanisms stated can be made in systems in which the experimental quantities of the table can be experimentally determined. The usefulness of the pressure coefficients becomes apparent (Table II, 3rd column). Column 4 of Table II has the significance that if the experimentally determined values of the coefficients there stated coincide with any unique values (Table I) for these coefficients, the mechanism is thereby determined. However, the unique values are characteristic of a mechanism at a given coverage; if a unique value is not found corresponding to a certain mechanism and coverage, the mechanism

may clearly occur at some other conditions (*e.g.*, of current density) on the given metal.

A main difficulty in evaluating a mechanism by application of the results of Table II lies in the fact that distinction between (3)_c and (4)_c demands θ determinations. These often can be made in alkaline solution,⁴ but difficulties are associated with their measurement in acid solution,⁵ except for the noble metals.⁶ Additional methods for distinction between (3)_c and (4)_c are hence desirable.⁷ It has been suggested that the plot of $\log i_0$ decreases with increase of $\Delta H_{\text{Ads,H}}$ for a series of metals if (4)_c is the mechanism but increases if (3)_c is effective.⁸ An alternative method for distinction has been suggested by Gerischer and Mehl,⁹ but the mechanism-indicating section of the current density-time relation, which is diagnostic at sufficiently low times, may be obscured by the rise time of the apparatus. (The method assumes, further, a negligible H concentration on the electrode at the commencement of the cathodic current-time transient.) It may be possible to distinguish between (3)_c and (4)_c by suitable analysis¹⁰ of galvanostatic transients, where the problem of sufficiently fast rise times is less severe.

In addition to the difficulty of the θ determinations, certain coefficients of Tables I and II are difficult to determine in many practical systems.

(i) **Stoichiometric Number (ν) Determinations.**—These depend upon the absence of reac-

(3) J. O'M. Bockris and E. C. Potter, *J. Electrochem. Soc.*, **99**, 169 (1952).

(4) M. A. V. Devarathan, J. O'M. Bockris and W. Mehl, *J. Electroanal. Chem.*, **1**, 143 (1959/1960).

(5) A recent theoretical analysis¹⁰ of transient data shows the possibility of making determinations of coverage with H even on corroding metals.

(6) M. Breiter, H. Kammermaier and C. A. Knorr, *Z. Elektrochem.*, **60**, 37 (1956).

(7) (3)_c is rate determined by discharge, with following fast electrochemical desorption; (4)_c is rate determined by the electrochemical desorption with preceding fast discharge.

(8) J. O'M. Bockris and B. E. Conway, *J. Chem. Phys.*, **26**, 532 (1957).

(9) H. Gerischer and W. Mehl, *Z. Elektrochem.*, **59**, 1049 (1955).

(10) J. O'M. Bockris and H. Kita, *J. Electrochem. Soc.*, **108**, 676 (1961).

(1) J. Horiuti, *Z. physik. Chem.*, **18**, 162 (1958).

(2) J. O'M. Bockris and H. Mauser, *Can. J. Chem.*, **37**, 475 (1959).

TABLE I
CRITERIA OF MECHANISM IN THE HYDROGEN EVOLUTION AND DISSOLUTION REACTIONS

Mechanism	Cathodic						Anodic					
	$\theta_H \rightarrow 0$		ν	$\theta_H \rightarrow 1$		ν	$\theta_H \rightarrow 0$		ν	$\theta_H \rightarrow 1$		ν
$\frac{\partial \eta}{\partial \ln i_c}$	$\frac{\partial \eta}{\partial \ln p_{H_2}}$	$\frac{\partial \eta}{\partial \ln i_c}$		$\frac{\partial \eta}{\partial \ln p_{H_2}}$	$\frac{\partial \eta}{\partial \ln i_a}$		$\frac{\partial \eta}{\partial \ln p_{H_2}}$	$\frac{\partial \eta}{\partial \ln i_c}$		$\frac{\partial \eta}{\partial \ln p_{H_2}}$	$\frac{\partial \eta}{\partial \ln i_a}$	
Slow D—Fast C	(1 _c) _c $-\frac{2RT}{F}$	$\frac{RT}{2F}$	2	(1 _c) _c $-\frac{2RT}{F}$	$-\frac{RT}{2F}$	2	(1 _a) _a $\frac{2RT}{F}$	$-\frac{RT}{2F}$	2	(1 _a) _a $\frac{2RT}{F}$	$\frac{RT}{2F}$	2
Slow C—Fast D	(2 _c) _c $-\frac{RT}{2F}$	$\frac{RT}{2F}$	1	(2 _c) _c ∞	$\frac{RT}{2F}$	1	(2 _a) _a ∞	$\frac{RT}{2F}$	1	(2 _a) _a $\frac{RT}{2F}$	0	1
Slow D—Fast E	(3 _c) _c $-\frac{2RT}{F}$	$\frac{RT}{2F}$	1	(3 _c) _c $-\frac{2RT}{3F}$	$-\frac{RT}{6F}$	1	(3 _a) _a $\frac{2RT}{3F}$	$-\frac{RT}{6F}$	1	(3 _a) _a $\frac{2RT}{F}$	$\frac{RT}{2F}$	1
Slow E—Fast D	(4 _c) _c $-\frac{2RT}{3F}$	$\frac{RT}{2F}$	1	(4 _c) _c $-\frac{2RT}{F}$	$\frac{RT}{2F}$	1	(4 _a) _a $\frac{2RT}{F}$	$-\frac{RT}{2F}$	1	(4 _a) _a $\frac{2RT}{3F}$	$-\frac{RT}{6F}$	1

TABLE II

MINIMUM EXPERIMENTAL QUANTITIES NEEDED TO IDENTIFY CERTAIN MECHANISMS IN HYDROGEN EVOLUTION

Mechanism	Cathodic Min. quantities needed for identification	Mechanism	Anodic Min. quantities needed for identification	Most diagnostic quantities if both cathodic and anodic data available	Uniquely diagnostic quantities for reaction mechanism
(1 _c) _c	ν with $\frac{\partial \eta}{\partial \ln p_{H_2}}$ or ν with θ	(1 _a) _a	$\frac{\partial \eta}{\partial \ln p_{H_2}}$ or ν and θ	$1_c \left(\frac{\partial \eta}{\partial \ln p_{H_2}} \right)$ anodic	
(1 _c) _c	$\frac{\partial \eta}{\partial \ln p_{H_2}}$; or ν with θ	(1 _a) _a	$\frac{\partial \eta}{\partial \ln p_{H_2}}$ and ν or ν + θ	$1_a \left(\frac{\partial \eta}{\partial \ln p_{H_2}} \right)$ cathodic	
(2 _c) _c	$\frac{\partial \eta}{\partial \ln i}$	(2 _a) _a	$\frac{\partial \eta}{\partial \ln i}$	$2_0 \left(\frac{\partial \eta}{\partial \ln i} \right)$ cathodic or anodic	$\left(\frac{\partial \eta}{\partial \ln p_{H_2}} \right)$ cathodic
(2 _c) _c	$\frac{\partial \eta}{\partial \ln i}$	(2 _a) _a	$\frac{\partial \eta}{\partial \ln i}$ or $\frac{\partial \eta}{\partial \ln p_{H_2}}$	$2_1 \left(\frac{\partial \eta}{\partial \ln i} \right)$ cathodic or anodic	
(3 _c) _c	$\frac{\partial \eta}{\partial \ln i}$	(3 _a) _a	$\frac{\partial \eta}{\partial \ln p_{H_2}}$ and θ	$3_0 \left(\frac{\partial \eta}{\partial \ln p_{H_2}} \right)$ + θ anodic	$\left(\frac{\partial \eta}{\partial \ln p_{H_2}} \right)$ anodic
(3 _c) _c	$\frac{\partial \eta}{\partial \ln p_{H_2}}$	(3 _a) _a	$\frac{\partial \eta}{\partial \ln i}$; $\frac{\partial \eta}{\partial \ln p_{H_2}}$	$3_1 \left(\frac{\partial \eta}{\partial \ln p_{H_2}} \right)$ cathodic	
(4 _c) _c	$\frac{\partial \eta}{\partial \ln i}$ with either $\frac{\partial \eta}{\partial \ln p_{H_2}}$ or θ	(4 _a) _a	$\frac{\partial \eta}{\partial \ln p_{H_2}}$	$4_0 \left(\frac{\partial \eta}{\partial \ln p_{H_2}} \right)$ anodic	$\left(\frac{\partial \eta}{\partial \ln p_{H_2}} \right)$ anodic
(4 _c) _c	$\frac{\partial \eta}{\partial \ln i}$; $\frac{\partial \eta}{\partial \ln p_{H_2}}$ and θ	(4 _a) _a	$\frac{\partial \eta}{\partial \ln p_{H_2}}$; ν and θ $\frac{\partial \eta}{\partial \ln i}$	$4_1 \left(\frac{\partial \eta}{\partial \ln i}, \nu \text{ and } \theta \right)$ $\frac{\partial \eta}{\partial \ln p_{H_2}}$	

tions (e.g., due to adventitious entities which undergo reactions which compete with the reaction under examination), a condition difficult to achieve at c.d.'s $< 10^{-8}$ amp. cm.⁻². In acid solution, most metals dissolve at low c.d.'s, making determinations impossible if the dissolution rate is comparable with $(i_0)_H$.

(ii).—Pressure effects are difficult to make because it may not be feasible to obtain cathodic pressure coefficients at c.d.'s sufficiently low so that bubbles (at $p_{H_2} = 1$ atm.) are not formed. In the anodic direction, difficulties associated with dissolution of the metal and passivation arise, particularly for those metals where the data is most needed.

Determinations of mechanism in alkaline solutions are easier than those in acid solutions, because the shift of the reversible H_2 potential to more negative regions decreases the tendency of the metal to dissolve. Stoichiometric number determinations then become practical;¹¹ the double pulse galvanostatic method⁴ can be used to obtain θ , and pressure effects can be obtained.

Measurements of the velocity of permeation of

H through metal foils¹² distinguish reaction (1_c)_c from (3_c)_c and (4_c)_c (but do not distinguish between (3_c)_c and (4_c)_c). This method has the advantage that it is applicable at potentials sufficiently cathodic to be outside the corrosion region. Were it practical to obtain foils thin enough so that the r.d.s. had become the passage from surface to bulk, then the dependence of permeation upon temperature would give the heat of activation for this process, whereupon an order of magnitude calculation of the rate constant for the process $H \xrightarrow{\text{surface}} H_{\text{bulk}}$ would be obtainable, and this, together with the experimental permeation rate, would allow calculation of an order of magnitude value of θ .

In this paper, use is made of the fact that $(i_0)_H / (i_0)_D$ can be shown theoretically to depend markedly upon the r.d.s. assumed and the experimental ratios compared with theoretical ones for various r.d.s.'s.

II. Experimental Methods

(a) Apparatus.—The electrolysis cell was essentially as described.¹¹ The volume of H_2O or D_2O used per run (including washings) was 100 ml. and the working volume in the cathode compartment, 10 ml. The polarizing current

(11) N. Pentland, J. O'M. Bockris and E. Sheldon, *J. Electrochem Soc.*, **104**, 182 (1957).

(12) R. Thacker, O.N.E. Report Dec. 1959.

was supplied by a Dresden-Barnes Regulated Supply. Currents from 10^{-2} to 10^{-5} amp. were measured with a microammeter and from 10^{-8} to 10^{-9} amp. on an electrometer. Potential measurements were made to ± 1 mv. (tube potentiometer).

(b) **Preparation of Cell and Solution.**—The electrolysis cell was in contact with a 1:1 mixture of nitric-sulfuric acid for three hours after each run, and then was washed successively with many changes of distilled and conductance water before the next run. Conductance water of $K < 10^{-6}$ mhos cm.^{-1} was refluxed for three hours in helium and distilled into the anode compartment. The specific conductance was then less than 5×10^{-7} mhos cm.^{-1} . When D_2O was used, the washing procedure was the same as above but was followed by three washings with D_2O distilled into the cell in helium.

The acid strength was obtained by passing HCl or DCl gas in helium into the anode compartment and measuring the conductance of the solution *in situ* by means of Pt probes. HCl was prepared by heating KCl to 400° for three hours in helium (eliminates traces of organic contaminants), and passing the gases evolved on additions of H_2SO_4 in helium through traps at -80° into the cell. DCl ($> 95\%$ D substituted) was held in a flask at 1 atm. pressure and passed in a stream of helium through the traps into the cell.

Helium used was purified by passing it through hopcalite, sodalime, copper on diatomaceous earth at 400° , anhydrous CaSO_4 , and three traps containing charcoal at liquid nitrogen temperatures. H_2 and D_2 were passed through a similar train, in which platinized asbestos was substituted for copper.

(c) **Preparation of Electrodes.**—All electrodes were prepared by heating a wire of the metal (0.05 cm. diam.) in H_2 , D_2 or He and sealing into a glass bulb¹³ which was broken in the cell immediately before the electrode was used. The electrodes were heated at 800° for 15 minutes in a wire-wound silica tube which was jointed onto the glass bulb through a graded seal and, after heating, the electrodes were drawn into position in the bulb with a magnet. (Iron wire was joined to platinum and tungsten electrodes.) The gases, He, H_2 and D_2 , used in electrode preparation were recycled through a purification train using a pulsating mercury pump. Liquid air traps and gold foil decreased the possibility of contamination with mercury vapor.

Spectroscopically pure iron wire was flame-welded to tungsten. The electrodes were electropolished in 1:3 phosphoric acid to remove oxide near the weld. A glass sheath was sealed onto the tungsten and extended over the joint. The electrodes then were treated as described above; platinum 99.95% was sealed to tungsten and then heated in H_2 or He. No significant difference in parameters was observed for surfaces prepared with either gas.

Tungsten electrodes were prepared by cleaning 99.95% W wire with molten sodium nitrite and then sealing a glass sheath over a section of the wire to provide a metal glass seal. The oxide formed in this step was removed by a further cleaning with sodium nitrite and the electrodes were then thoroughly washed in conductivity water and dried with filter paper prior to the heating in hydrogen or deuterium as described for iron.

The bulbs were sealed to tubes which fitted corresponding tubes in the head of the cathode compartment. They (five) were moved into solution when required.

(d) **Procedure.**—Part of the HCl or DCl solution was introduced from the anode to the cathode compartment; pre-electrolysis was carried out on an electrode (0.2 cm.^2 area) of the metal concerned at 3 ma. for 20 hours. Helium was bubbled through the anode and cathode compartments during pre-electrolysis and the gas was changed to hydrogen or deuterium 15 minutes prior to commencement of measurements. Solution from the cathode compartment was passed into the reference electrode (platinized Pt) compartment and H_2 or D_2 bubbled through this. Electrode bulbs were broken in hydrogen or deuterium at the top of the cathode compartment and introduced into solution with potential applied to prevent the electrode dissolving. The potential was read for a series of currents first with increasing c.d. in the case of Pt and W and then with decreasing current density. For iron, the first Tafel curve was with decreasing

c.d. to minimize surface changes due to dissolution. All electrode potentials showed a negative drift with time but two complete traverses of the current potential curves, taking 10 min., showed a drift of overpotential at a given current density of less than 5 mv. In some instances, a greater drift was noted for platinum and when this occurred only the first "up" curve was taken.

III. Results

Departure from linearity of the Tafel curves for hydrogen and deuterium evolution in 0.5 N acid on iron occurred when oxide was present, or when the temperature at which the surface had been prepared was raised over 800° . Parameters are in Table III.

Platinum electrodes prepared in helium or hydrogen showed a time-dependent overpotential and were irreproducible. The Tafel relations showed two slopes, one of about 0.04 at low c.d.'s ($< 10^{-2.5}$ amp. cm.^{-2}) and the other of about 0.13 at c.d.'s between $10^{-2.5}$ and $10^{-1.5}$. Reproducible values were obtained by anodic activation of the electrode at 10^{-2} amp. cm.^{-2} for 10 seconds (Table III). (This increase in reproducibility obtained by anodic activation was earlier reported by Bockris, Ammar and Huq¹⁴).

The $\log i - \eta$ curves for tungsten showed two slopes in both hydrogen and deuterium. The results in hydrogen are similar to those published by Bockris, Ammar and Huq¹⁴ except that the lower slope now recorded begins at a slightly higher overpotential than that formerly observed.

The $(i_0, \text{D})_M$ values were obtained by reference to the reversible deuterium electrode. Conway¹⁵ has given the potential difference between the normal reversible hydrogen and deuterium potentials as -0.009 v. after correcting for the liquid junction potential (Table IV).

IV. Discussion

(1) **Effect of Water Content on the Evaluation of $(i_0)_{\text{D}_3\text{O}^+}$.** (a) **Calculation of Species Present in Solutions.**—The weight per cent. of H in the mixture solutions used in the present work¹⁶ is 3, giving an atomic ratio (H to D) of 3/48.5. Using this value and the equilibrium constants (Kirchenbaum,¹⁷ Schwarzenbach¹⁸) shown above together with a total acid concentration of 0.5 N it is possible to calculate the concentrations of the individual species by successive approximation. The concentrations obtained in this manner are shown in Table V.

(b) **Evaluation of $(i_0)_{\text{D}_3\text{O}^+}$ from $(i_0, \text{D})_M$ in Deuterium-containing Solution.**—The measured value of i_0 in the deuterium oxide solutions, $(i_0, \text{D})_M$ cannot be directly compared with the $(i_0)_{\text{H}_3\text{O}^+}$ measured in the aqueous solutions, because the measured exchange current density represents the net effect of discharge from D_3O^+ , HOD_2^+ , DOH_2^+ , etc., whereas, to compare directly with $(i_0)_{\text{H}_3\text{O}^+}$, the $(i_0)_{\text{D}_3\text{O}^+}$ value must be evaluated from $(i_0, \text{D})_M$. The dependence of i_0 for a given ionic species upon the concentration of this species depends upon

(14) J. O'M. Bockris, I. A. Ammar and A. K. M. S. Huq, *J. Phys. Chem.*, **61**, 879 (1957).

(15) B. E. Conway, *Proc. Roy. Soc. (London)*, **A247**, 400 (1958).

(16) Determined by a mass spectrographic method.

(17) I. Kirchenbaum, "Physical Properties and Analysis of Heavy Water," McGraw-Hill Book Co., New York, N. Y., 1951, p. 54.

(18) G. Schwarzenbach, *Z. Electrochem.*, **44**, 47 (1938).

(13) J. O'M. Bockris and B. E. Conway, *J. Sci. Instr.*, **25**, 283 (1948).

TABLE III
TAFEL CONSTANTS AND CORROSION POTENTIAL IN HYDROGEN AND DEUTERIUM IN 0.5 N HCl OR DCl

	Fe		Pt	
	Hydrogen	Deuterium	Hydrogen	Deuterium
<i>b</i>	0.133 ± 0.004	0.134 ± 0.004	0.029 ± 0.003	0.026 ± 0.006
-log <i>i</i> ₀	5.18 ± .10	5.77 ± .14	3.33 ± .14	3.62 ± .45
corr.	0.203 ± .007	0.217 ± .004		
No. of Tafel lines	12	7	18	18
No. of electrodes	12	7	9	9

	W		W	
	Lower slope Hydrogen	Higher slope Hydrogen	Lower slope Deuterium	Higher slope Deuterium
<i>b</i>	0.070 ± 0.005	0.112 ± 0.009	0.069 ± 0.006	0.101 ± 0.004
-log <i>i</i> ₀	7.87 ± .31	6.30 ± .23	8.34 ± .27	7.10 ± .42
corr.				
No. of Tafel lines	13	13	8	12
No. of electrodes	7	7	4	6

TABLE IV
(*i*₀)_{H₂O*} AND (*i*₀)_M FOR Fe, Pt AND W

	(<i>i</i> ₀) _{H₂O*}	(<i>i</i> ₀) _M	<i>i</i> _{0H} / (<i>i</i> _{0D}) _M
Fe	6.5 ± 0.8 × 10 ⁻⁸	2.2 ± 0.8 × 10 ⁻⁸	3.0 ± 1.1
Pt	5.1 ± 1.7 × 10 ⁻⁴	2.6 ± 0.8 × 10 ⁻⁴	2.0 ± 0.9
W (Lower)	1.51 ± 0.45 × 10 ⁻⁸	4.37 ± 1.2 × 10 ⁻⁹	3.4 ± 1.0
W (Higher)	5.01 ± 1.15 × 10 ⁻⁷	7.94 ± 3.2 × 10 ⁻⁸	6.3 ± 2.80

TABLE V
CONCENTRATIONS OF H AND D SPECIES PRESENT
IN EXPERIMENTAL SOLUTIONS

HOD = 5.37 m./1000 g. D₂O⁺ = 0.368 m./1000 g.
H₂O = 0.179 m./1000 g. HD₂O⁺ = 0.108 m./1000 g.
D₂O = 42.91 m./1000 g. H₂DO⁺ = 0.0234 m./1000 g.
H₃O⁺ = 0.0015 m./1000 g.

the rate determining step effective. If this is (3)_c or (4)_c (Table I), then

$$i_0 = K a_{H^+} \exp\left(\frac{-\beta V_{RF}}{RT}\right) \quad (1)$$

Hence

$$i_0 = K' a_{H^+}^{(1-\beta)}$$

Or, if (2)_c is rate determining

$$i_0 = K' \quad (2)$$

(1) and (2) refer to systems which contain ions at concentrations sufficiently high to give $d\phi_{2-b}/d \ln a_{H^+} \rightarrow 0$, where ϕ_{2-b} is the potential of the Gouy-Helmholtz boundary, and to avoid the attaining of limiting current densities by any species for the current densities used in the measurements (this requirement is satisfied in the systems discussed here, except for H₃O⁺ in the deuterium-containing solutions; the contribution to *i*_{0,M} of the latter ion hence will be neglected).

Consider the discharge of a given isotopic ion, *i*, in a solution in which it is the only discharging species. Then, for a "standard" concentration of this ion, *c*_{s,i}, for which a "standard" value of *i*₀ is known

$$(i_{0,i})_{c_{s,i}} = k_i c_{s,i} \exp[-\beta \ln c_{s,i}] \quad (3)$$

Consider now the corresponding value of (*i*_{0,i})_{c_i} for a solution in which *i* has a concentration *c*_i, and in which are other isotopic species of concentrations *c*_j, *c*_k, etc. The standard reversible potentials for the reaction concerned being *V*_{0,i}, *V*_{0,j}, *V*_{0,k}, etc., respectively.

Then

$$(i_{0,i})_{c_i} = k_i c_i \exp[-\beta \ln (c_i + c_j + c_k + \dots)] \quad (4)$$

Hence, from (3) and (4)

$$(i_{0,i})_{c_i} = (i_{0,i})_{c_{s,i}} \frac{c_i}{(c_{s,i})^{1-\beta} (c_i + c_j + c_k + \dots)^\beta} \quad (5)$$

For $\beta = 1/2$

$$(i_{0,i})_{c_i} = \frac{(i_{0,i})_{c_{s,i}}}{(c_{s,i})^{1/2}} N_i (c_i + c_j + c_k + \dots)^{1/2} \quad (6)$$

where

$$N_i = \frac{c_i}{c_i + c_j + c_k + \dots}$$

and for dilute solutions is the ionic fraction of the isotopic series, *i*. (It easily can be shown that there is no effect of the partial pressures of gases arising from *i*_j, *i*_k, etc., on these equations.)

It is necessary to estimate *i*₀ values for HOD₂⁺ and DOH₂⁺, during H discharge and D discharge from each, respectively. Considering the discharge of H⁺ from HOD₂⁺, in terms of a potential energy profile diagram,¹⁹ it is clear that the potential energy profile for the final state for the reaction HOD₂⁺ + e₀⁻ → H_{Ads} + D₂O is the same as that for H₃O⁺ + e₀⁻ → H_{Ads} + H₂O. The potential energy curve of the initial state is changed only by a shift of the solvation energies, but this is compensated by an equal and opposite change¹⁵ in the zero point energies of the comparable ions, e.g., H₃O⁺, HOD₂⁺. The bond undergoing rupture in HOD₂⁺ + e₀⁻ → H_{Ads} + D₂O has the same zero point energy as that in H₃O⁺. Hence, the *i*₀ value for HOD₂⁺ discharging to give H should be almost the same as that for H₃O⁺ in a similar discharge, except that for HOD₂⁺ the proton has probability of discharge of 1/3rd of that in H₃O⁺.

Hence

$$(i_{0,H-HOD_2^+})_{c_s} = \frac{1}{3} (i_{0,H-H_3O^+})_{c_s} \quad (7)$$

Similarly

$$(i_{0,H-DOH_2^+})_{c_s} = \frac{2}{3} (i_{0,H-H_3O^+})_{c_s} \quad (8)$$

Also

$$(i_{0,D-HOD_2^+})_{c_s} = \frac{2}{3} (i_{0,D-D_2O^+})_{c_s} \quad (9)$$

(19) J. O'M. Bockris, "Modern Aspects of Electrochemistry," Vol. I, Butterworths Scientific Publications, 1954, p. 235.

$$(i_{0,D-D_2O^+})_{\infty} = \frac{1}{3} (i_{0,D-D_2O^+})_{c_s} \quad (10)$$

Further

$$c_{s,i} = c_i + c_j + c_k + \dots \quad (11)$$

and with $\beta = 1/2$, one has

$$(i_{0,D})_M = \frac{(i_0)_{D_2O^+}}{c_{s,i}} \left[c_{D_2O^+} + \frac{2}{3} c_{HD_2O^+} + \frac{1}{3} c_{H_2OD^+} \right] + \frac{(i_0)_{H_2O^+}}{c_{s,i}} \left[\frac{1}{3} c_{HOD_2^+} + \frac{2}{3} c_{H_2OD^+} + c_{H_2O^+} \right] \quad (12)$$

Taking $c_{s,i}$ as 0.5 M, the concentrations of the indicated species and the values of $(i_{0,D})_M$ and $(i_0)_{H_2O^+}$ for Fe from Table IV, one obtains

$$\frac{(i_0)_{H_2O^+}}{(i_0)_{D_2O^+}} = 3.6$$

which is not significantly different to the $(i_{0,D})_M / (i_0)_{H_2O^+}$ ratio given in Table IV so that the effect on entities other than D_2O in the case of Fe is negligible.

In the case of tungsten the measured ratio is

$$\frac{(i_0)_{H_2O^+}}{(i_{0,D})_M} = 6.33 \text{ (Table IV)}$$

Assuming a slow discharge mechanism as before we obtain

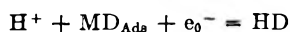
$$(i_0)_{D_2O^+} = 3.10 \times 10^{-8} \text{ amp. cm.}^{-2}$$

and hence

$$\frac{(i_0)_{H_2O^+}}{(i_0)_{D_2O^+}} = 16.20$$

which is much higher than any ratio predicted theoretically in the following section and also appears anomalous when it is remembered that the separation factors on tungsten are not very different from those on iron.²⁰

Correspondingly, without correction for the effect of H-containing ions, the value of $(i_0)_{H_2O^+} / (i_{0,D})_M = 6.33$ for tungsten leads to unlikely values for the difference in heats of adsorption of hydrogen and deuterium, if discharge is rate-determining. It is worthwhile therefore to consider the possibility of a slow electrochemical desorption mechanism in this case. The effect of proton concentration on $(i_{0,D})_M$ is here more complex than for simple discharge, since it is probable that H^+ discharges onto MD_{Ads} rather than HA_{Ads} from solutions containing D:H in the mole ratio 48.5:3. Consequently the rate of the H reaction would be that of



which will be expressed as $(i_0)_{H_2O^+ - D}$ and would be in magnitude between $(i_0)_{H_2O^+}$ and $(i_{0,D})_M$. Assuming $(i_0)_{H_2O^+ - D}$ is the mean of these two values

$$(i_0)_{H_2O^+ - D} \approx \frac{1}{2} (i_0)_{H_2O^+ - H}$$

$$\frac{(i_0)_{H_2O^+}}{(i_0)_{D_2O^+}} = 8.29$$

For systems in which the Tafel slope is $RT/2F$ the atomic combination reaction may be rate determining. The values of $(i_{0,i})_{c_s}$ required in the correction equation may be obtained as follows. In the deuterious solutions, the discharge of D_2O^+

is large compared with the contributions made to $(i_{0,D})_M$ by other species. Hence, the combination of discharged D, e.g., from HOD_2^+ , will be with D. Thus, the rate-determining reaction is identical with that for D from D_2O^+ , and therefore $(i_{0,D-HOD_2^+})_{c_s} = 2/3 (i_{0,D-D_2O^+})_{c_s}$. Other relations are as above.

For reactions in which the rate-determining reaction is $(2_0)_c$, the equation corresponding to (6) is

$$(i_{0,i})_{c_i} = (i_{0,i})_{\infty} N_i^2 \quad (13)$$

where N_i is the ionic fraction of the species i .

$$(i_{0,D})_M = \frac{(i_0)_{D_2O^+}}{c_s^2} \left(c_{D_2O^+} + \frac{2}{3} c_{HOD_2^+} \right) + \frac{(i_0)_{H_2O^+}}{c_s^2} \left(\frac{1}{3} c_{HOD_2^+} \right) \quad (14)$$

Terms dependent upon concentrations of H_2OD^+ may be neglected since they will be negligibly small when squared. Assuming $(i_0)_{H_2O^+ - H} = (i_0)_{H_2O^+ - D}$, and using the values of $(i_{0,D})_M$ and $(i_0)_{H_2O^+}$ in Table IV and concentration terms in Table V, equation 14 gives

$$(i_0)_{D_2O^+} = 2.1 \times 10^{-4}$$

Assuming $(i_0)_{H_2O^+ - D}$ for combination between H and D is the arithmetic mean of $(i_0)_{H_2O^+ - H}$ and $(i_{0,D})_M$

$$\frac{(i_0)_{H_2O^+}}{(i_0)_{D_2O^+}} = 2.3$$

Both corrections do not significantly alter the measured $(i_{0,D})_M / (i_0)_{H_2O^+}$ ratios for Pt.

(2) The Exchange Current Densities of Isotopic Ions and the Separation Factor.—The separation factor for H and D is defined by¹⁸

$$S = \frac{(c_H/c_D)_{gas}}{(c_H/c_D)_{soln}} = \left(\frac{c_D}{c_H} \right)_{soln} \frac{\sum_i i_{(H)}}{\sum_i i_{(D)}} \quad (15)$$

where c_i is the concentration of the given entity in the given phase (independent of the species in which it exists), and i_i is the total current density of evolutions of the indicated species.

Utilizing equation 6 which applies when the Tafel slope is $2RT/F$ and $\beta = 1/2$ one has

$$\frac{i_H}{i_D} = \frac{(i_0)_{H_2O^+} \left(c_{H_2O^+} + \frac{2}{3} c_{H_2DO^+} + \frac{1}{3} c_{H_2O^+} \right)}{(i_0)_{D_2O^+} \left(c_{D_2O^+} + \frac{2}{3} c_{HD_2O^+} + \frac{1}{3} c_{H_2DO^+} \right)}$$

and consequently

$$S = \left(\frac{c_D}{c_H} \right)_{soln} \frac{(i_0)_{H_2O^+} \left(c_{H_2O^+} + \frac{2}{3} c_{H_2DO^+} + \frac{1}{3} c_{H_2O^+} \right)}{(i_0)_{D_2O^+} \left(c_{D_2O^+} + \frac{2}{3} c_{HD_2O^+} + \frac{1}{3} c_{H_2DO^+} \right)} \quad (16)$$

For iron this gives

$$S_{Fe} = 6.9$$

and for tungsten, assuming

$$\frac{(i_0)_{H_2O^+ - D}}{(i_0)_{D_2O^+}} = \frac{1}{2} \frac{(i_0)_{H_2O^+ - H}}{(i_0)_{D_2O^+}}$$

$$S_w = 7.87$$

When the Tafel slope is $RT/2F$ we have from equation 13

(20) B. Topley and H. Eyring, *J. Chem. Phys.*, **2**, 217 (1934).

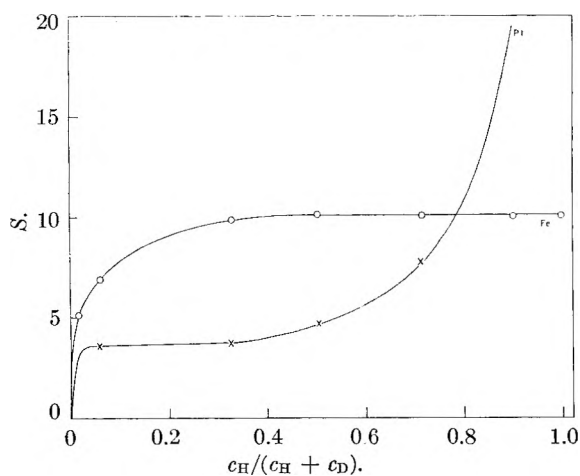


Fig. 1.—Calculated separation factor as a function of $c_H/c_H + c_D$. Fe values are based on a slow proton transfer mechanism and Pt values on a slow recombination mechanism.

$$S = \left(\frac{c_D}{c_H}\right)_{\text{soln}} \frac{(i_0)_{\text{H}_3\text{O}^+} \left(c_{\text{H}_3\text{O}^+} + \frac{2}{3} c_{\text{H}_2\text{DO}^+} + \frac{1}{3} c_{\text{HD}_2\text{O}^+} \right)}{(i_0)_{\text{D}_3\text{O}^+} \left(c_{\text{D}_3\text{O}^+} + \frac{2}{3} c_{\text{HD}_2\text{O}^+} + \frac{1}{3} c_{\text{H}_2\text{DO}^+} \right)} \quad (17)$$

and assuming

$$\frac{(i_0)_{\text{H}_3\text{O}^+ - \text{D}}}{(i_0)_{\text{D}_3\text{O}^+}} = \frac{1}{2} \frac{(i_0)_{\text{H}_3\text{O}^+ - \text{H}}}{(i_0)_{\text{D}_3\text{O}^+}}$$

$$S_{\text{Pt}} = 3.5$$

The separation factors here have all been calculated for a 0.5 M acid solution using the concentrations shown in Table V. In view of the appearance of the concentration terms in the expression for S it is of interest to determine the effect of c_H/c_D on S .

Let $c_H/c_D = R$. As R varies, the distribution of H and D among the various species varies and hence $\Sigma i_{(H)}/\Sigma i_{(D)}$ varies. Calculations have been carried out for $(c_H/c_D)_{\text{soln}}$ (mole ratios) from 0.01 to 100, the latter corresponding to water containing 1% D. Knowing R , the corresponding $c_{\text{H}_2\text{O}}$, $c_{\text{D}_2\text{O}}$ and c_{HOD} (moles l.⁻¹) can be calculated; thence, using the ratios of the equilibrium constants described in IV, 1, the concentrations of the various ions for a solution of given R can be calculated. Utilizing those values in (16) and (17), together with the $(i_0)_e$ values stated above, S has been evaluated as a function of R . Results are shown in Fig. 1.

The calculations of the limiting values of S for variations in R have been carried out using the exchange c.d.'s for Fe and Pt of this paper. However, the results are not sensitive to values of the exchange c.d., but upon the distribution of H and D among the various ionic species, and the relative exchange c.d.'s of H_3O^+ and D_3O^+ . The calculations are influenced by the dependence of $(i_0)_e$ upon c_i . Figure 1 has been calculated using (16) and (17). The separation factor for Fe is little dependent upon R for $c_H/c_H + c_D > 0.3$, in which range most experimental determinations have been made (a similar conclusion would be reached for W). The fair concordance of results for S determined in solutions without attention being paid to c_H/c_D is therefore understandable.

A sharp increase in S for $c_H/(c_H + c_D) < 0.4$ is observed on the curve for platinum (Fig. 1) calculated by equation 17. The concentration terms in this equation are squared so that any error in the values of the equilibrium constants would be magnified.

Condensing (16), it is clear that

$$S_{c_H/c_D \rightarrow \infty} = \frac{3i_{0,\text{H}_3\text{O}^+}}{i_{0,\text{D}_3\text{O}^+}} \quad (18)$$

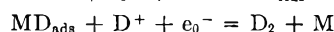
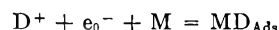
$$S_{c_H/c_D \rightarrow 0} = \frac{i_{0,\text{H}_3\text{O}^+}}{3i_{0,\text{D}_3\text{O}^+}} \quad (19)$$

It can be seen from the values of $(i_0)_{\text{H}_3\text{O}^+}/(i_0)_{\text{D}_3\text{O}^+}$ that S lies between 1.2–10.8, 1.3–12, and 0–∞ for iron, tungsten and platinum, respectively. The exchange c.d.'s determined in nearly pure D_2O and nearly pure H_2O are, therefore, consistent with the experimental data measured in mixtures of H_2O and D_2O containing excess H_2O .^{21–23}

From (18) and (19), it can be seen that separation factor determinations in limitingly high R values give $(i_0)_{\text{D}_3\text{O}^+}$ directly, $(i_0)_{\text{H}_3\text{O}^+}$ being known.

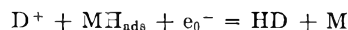
The results of Post and Hiskey²³ for $i_{0\text{H}}/i_{0\text{D}}$ on mercury is 3. This is in fair agreement with the slow discharge mechanism. The separation factor, however, is also 3 and the calculations shown above indicate that for slow discharge in solutions of low D content, $S = 3(i_{0\text{H}}/i_{0\text{D}})$. These calculations however assumed that the discharge of protons and deuterons occurred by the same mechanism both in pure and mixed solutions of H and D. This is not necessarily the case and it will now be shown that the reaction path may determine $(i_{0\text{H}})/i_{0\text{D}}$ in mixed solution.

(a) **Slow Discharge—Fast Electrochemical.**—In a pure solution the reaction steps for D_2 evolution are



and analogous steps would apply to hydrogen evolution.

In a solution containing an excess of H over D, however, the deuterons would discharge more rapidly onto an adsorbed hydrogen atom than onto the bare metal (remembering that the electrochemical step is faster than discharge). Consequently the relevant value of $i_{0\text{D}}$ would be that for the reaction



and therefore

$$\left(\frac{i_{0\text{H}}}{i_{0\text{D}}}\right)_{\text{pure soln}} > \left(\frac{i_{0\text{H}}}{i_{0\text{D}}}\right)_{\text{mixed soln}}$$

so that

$$S < \frac{3i_{0\text{H}}}{i_{0\text{D}}}$$

a result consistent with that on mercury.

(b) **Slow Discharge—Fast Catalytic.**—In this case if the discharge reaction is faster than a possible electrochemical step (the effect of heating

(21) H. A. Smith, C. O. Thomas and J. C. Posey, *J. Electrochem. Soc.*, **106**, 576 (1959).

(22) Y. Takahashi, S. Oka and M. Oikawa, *Bull. Chem. Soc. Japan*, **31**, 220 (1958).

(23) B. Post and C. F. Hiskey, *J. Am. Chem. Soc.*, **72**, 4203 (1950).

on iron already discussed suggests this) the rate ratio in pure solutions would apply to mixed solutions since the rate-determining step for both H and D would be discharge in both cases, *i.e.*

$$\left(\frac{i_{0H}}{i_{0D}}\right)_{\text{pure soln}} = \left(\frac{i_{0H}}{i_{0D}}\right)_{\text{mixed soln}}$$

and

$$S = 3 \left(\frac{i_{0H}}{i_{0D}}\right)$$

as has been shown for iron.

Consequently the determination of the separation factor at undetermined c_H/c_D is not diagnostic of the r.d.s. but together with (i_{0H}/i_{0D}) , which is diagnostic, may show both the slow step pure solution and the reaction path.

3. Numerical Values Consistent with the Ratios of Exchange c.d. for h.e.r. and d.e.r. as a Function of Mechanism.—A crude approximation to a calculation of the ratio of i_0 's of isotopic species was carried out by Bockris.¹⁹ Conway and Bockris²⁴ pointed out later that this ratio would depend significantly on the mechanism assumed and detailed numerical calculations were carried out by Conway.¹⁵ In the present work, a $\Delta\Delta H_{\text{Ads}}$ (where $\Delta\Delta H_{\text{Ads}}$ is the difference in heats of adsorption of H and D on the metal) value of 0.2 kcal. mole⁻¹ was assumed and, taking into account the increase in the difference of heats of activation for the isotopic reaction due to a difference in the shapes of the Morse curves of the M-H and M-D molecules (ratio of Morse constants a_{M-H}/a_{M-D} is calculated to be 1.017), $(i_0)_{\text{H}_3\text{O}^+}/(i_0)_{\text{D}_3\text{O}^+}$ was found to be 6 for the slow discharge mechanism.

In the case of the electrochemical desorption mechanism, the same method of calculation as that of Conway²⁴ was used except as follows:

(i) differences in the shapes of the Morse curves for H₂ and D₂ were taken into account. The data²⁵ show that $a_{\text{H}_2}/a_{\text{D}_2} = 1.005$ and taking this factor into account appreciably reduces the theoretically expected value of $(i_0)_{\text{H}_3\text{O}^+}/(i_0)_{\text{D}_3\text{O}^+}$ (*e.g.*, from 26 to 20 for $\Delta\Delta H = 0.2$ kcal. mole⁻¹).

(ii) The two cases in which H on the surface is mobile or immobile are distinguished, since if H and D on the electrode surface are mobile the value of the partition function ratio is 2 and if immobile it is 1. H adsorbed from the gas phase in W is mobile.²⁵ The introduction of adsorbed water on the surface will tend to reduce the mobility. Conversely, the effective M-H bond strength will be weakened and mobility thus made more likely.

A summary of calculated $(i_0)_{\text{H}_3\text{O}^+}/(i_0)_{\text{D}_3\text{O}^+}$ for an arbitrary value of $\Delta\Delta H_{\text{Ads}}$ (see below) is shown in Table VI.

TABLE VI

THEORETICAL $(i_0)_{\text{H}_3\text{O}^+}/(i_0)_{\text{D}_3\text{O}^+}$ FOR VARIOUS MODELS	
$\Delta\Delta H_{\text{Ads}} = 0.2$ kcal. mole ⁻¹	
Slow discharge 6	
Slow electrochemical immobile	7
mobile	13
Slow catalytic	3

(24) B. E. Conway and J. O'M. Bockris, *Can. J. Chem.*, **35**, 1124 (1957).

(25) O. Beeck, *Advances in Catalysis*, **2**, 151 (1950).

4. Effect of Heat of Adsorption of H and D on Theoretical Values.—The values of the theoretical ratio to be expected can be calculated with significance depending on the chosen model only.

Limits to the value of $\Delta\Delta H_{\text{Ads}}$ may be estimated theoretically, upon the basis of alternative extreme assumption concerning the degree of coverage. Such estimates are orientive only.

(i) If the interaction in the surface is neglected, an absolute upper limit, for the heat of adsorption of H or D on the metal may be calculated. This is given by⁸

$$\Delta H_{M-H} = \frac{1}{2}(D_{H-H^0} + D_{M-M^0}) + 23.06(X_M - X_H)^2 \quad (20)$$

where D^0 is the heat of dissociation and X the electronegativity. Since X is the same for isotopes

$$\Delta H_{M-H} - \Delta H_{M-D} = \frac{1}{2}(D_{H_2^0} - D_{D_2^0}) = 0.9 \text{ kcal. mole}^{-1} \quad (21)$$

(ii) A more realistic model for the surface must take into account interactions between the adsorbed atoms. It may be assumed that

$$\Delta H_{\theta-\theta} \propto (1 - \theta) \quad (22)$$

where $\Delta H_{\theta-\theta}$ is the heat of adsorption when the degree of coverage is θ .

Then

$$\Delta H_{\theta-\theta} = \Delta H_{\theta=0} [1 - \theta] \quad (23)$$

$$\therefore (\Delta H_{\theta})_H - (\Delta H_{\theta})_D = \frac{1}{2}(1 - \theta)(D_{H_2^0} - D_{D_2^0}) \quad (24)$$

For all mechanisms of the h.e.r. the surface is covered with either water or H. It appears therefore that the appropriate value for θ used here is $\theta \rightarrow 1$ in all cases. Thus $(\Delta H_{\theta})_H - (\Delta H_{\theta})_D \rightarrow 0$.

Thus, the theoretical estimates allow a variation of $\Delta\Delta H$ from 0.0 to 0.9. A decision as to the choice within these limits may be made by reference to the experimental work of Rozenthal, Dolin and Erschler,²⁶ who measured $\Delta\Delta H$ by means of A.C. measurements on Pt. On the basis of a Langmuir adsorption isotherm, a value of 0.2 kcal. mole⁻¹ is obtained from their results for $\Delta\Delta H_{\text{ads}}$. The use of a Langmuir adsorption isotherm would be consistent with the assumption of a fairly low (*i.e.*, < 10%) degree of coverage with H on Pt and this is consistent with the values measured by Breiter²⁷ for smooth Pt.

5. Mechanistic Conclusions.—Comparison of the theoretical expectation in Table VI with the results for Pt is consistent with slow combination as a rate determining step. This conclusion is consistent with $\Delta\Delta H$ values of about 0.5 or less.

It is widely agreed that the mechanism on Pt in aqueous acid solutions ($b = 0.029$) involves a r.d.s. of the combination reaction and it seems reasonable therefore to allow the assumption of this mechanism, together with the observed value of $(i_0)_{\text{H}_3\text{O}^+}/(i_0)_{\text{D}_3\text{O}^+}$, to suggest a $\Delta\Delta H$ of about 0.2 (*cf.* the

(26) K. I. Rozenthal, P. I. Dolin and B. V. Erschler, *Acta Physicochim. U. R. S. S.*, **13**, 74 (1940).

(27) M. Breiter, "Symposium on Electrode Kinetics," Philadelphia, May 1959.

Russian value of 0.2). One would expect this to be largely unchanged for the other metals. The $\Delta\Delta H$ value expected from bond strength data (which refers effectively to an empty surface) is about 0.5–0.8 kcal. mole⁻¹ for a number of metals, and the reduction to the value of about 0.2 would arise from the effect of adsorbed water in lowering the adsorption heats. This effect would be expected to be about the same for all metals.

The present results are not consistent with the view that the h.e.r. on noble metals measured under the conditions used here is controlled by diffusion of molecular H₂ away from the electrode surface.⁶ The rate of the diffusion of H₂ and D₂ in aqueous solution would depend upon interaction with the solvent, and not involve vibrational states in H₂ and D₂, so that no isotopic effects would be expected (*cf.* Table VI).

The experimental value of the ratio of the i_0 's for Fe of 4 is in fair agreement with slow discharge control if the $\Delta\Delta H$ value is about 0.2, when $i_{0H}/i_{0D} = 6$. The values for Fe are inconsistent with the requirements of electrochemical discharge with mobile H, and are consistent only with the unlikely case of immobile H.

The observed ratio for W of 8.3 is in reasonable agreement with the expectations of the electrochemical rate control for $\Delta\Delta H$ of about 0.2 (which indicates a ratio of 13 for a rate-determining electrochemical mechanism and mobile H).

The present results offer clear evidence against the tunnelling of protons as a rate-controlling mechanism as the h.e.r. Thus, the Tafel slope expected from this mechanism would differ for the H and D evolutions,²⁸ but no such difference is observed on the three metals studied.

The conclusion concerning the mechanism on Fe is at variance with that suggested earlier for the mechanism on this metal from a consideration of the $\log i_0 - \Delta H_{ads}$ relation,⁸ when the apparent trend of the $\log i_0$ values for a number of metals to decrease with increase of ΔH_{ads} was interpreted to indicate the rate-determining electrochemical desorption for metals showing this behavior. W fell upon a section of the proposed relation corresponding to relatively high $\Delta H_{ads,H}$ values and it may be that the position of certain of the metals in the intermediate part of the $\log i_0 - \Delta H_{ads}$ graph is better interpreted as an extension of the section of the $\log i_0 - \Delta H_{ads}$ corresponding to the $\log i_0 - \Delta H_{ads,H}$ relation.

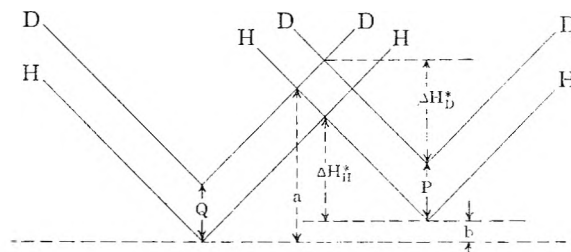
Acknowledgments.—The authors wish to acknowledge the support of the U. S. Air Force

(28) B. E. Conway, *Can. J. Chem.*, **37**, 178 (1959).

under Contract AF 33(616)-5681, SA No. 6, and discussion with Dr. R. Barton of the Wright Air Base. They are grateful to Dr. M. Enyo for theoretical discussion, to Mr. N. Nordin for help with the experimental work on Fe and Pt, to Mrs. V. Drazic and Mr. S. Srinivasan for carrying out a major portion of the experimental work on W, and to the Executive of the C.S.I.R.O. (Australia) for granting leave of absence to one of us (D.F.A.K.).

Appendix

Calculation of $\Delta H_{0,D}^* - \Delta H_{0,H}^*$ from Potential Energy Diagrams.—The initial and final state potential energy curves for H and D are shown schematically in the following figure



In order to calculate the relative rates for H₂ and D₂ evolution it is necessary to know the differences in activation energies for these two processes ($\Delta H_{0D}^* - \Delta H_{0H}^*$).

In the first instance, neglecting the zero point energy differences of the initial state, the following geometric relationships can be obtained from the above figure.

$$\Delta H_H^* = a - b - \beta Q$$

$$\Delta H_D^* = a - b + \beta P - P = a - b - (1 - \beta)P$$

where β is the symmetry factor and Q and P are the differences between the minima of the PE curves of hydrogen and deuterium species for the final and initial states, respectively. Thus $\Delta H_D^* - \Delta H_H^* = \beta Q + (\beta - 1)P$ and with $\beta = 1/2$.

$$\Delta H_D^* - \Delta H_H^* = 1/2(Q - P)$$

Now correcting for the zero point energy of the initial state the required activation energies are

$$\Delta H_{0H}^* = \Delta H_H^* - (\text{z.p.e.})_H$$

$$\Delta H_{0D}^* = \Delta H_D^* - (\text{z.p.e.})_D$$

$$\Delta H_{0,H}^* - \Delta H_{0,D}^* = 1/2(Q - P) + (\text{z.p.e.})_H - (\text{z.p.e.})_D$$

This value has been corrected for the difference in slope of the H and D curves by the appropriate "a" constant of the Morse curve as described in the paper.

THE VAPOR PRESSURE OF CADMIUM SELENIDE

BY W. J. WÖSTEN

Physics Laboratory of the National Defence Research Organization T.N.O., The Hague, Netherlands

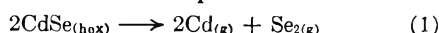
Received February 27, 1961

The vapour pressure of CdSe was measured between 740 and 900° by Regnault's method.¹ The result is $\log p_{\text{Cd}} \times p_{\text{Se}_2}$ (atm.³) = $\log K_p = - (34.400) (1/T) + 20.9$ for CdSe of the Wurtzite structure. The standard heat of sublimation of CdSe (25°) is 39.1 kcal./mole, the standard heat of formation—37.5 kcal./mole. The entropy of CdSe (hex) at 25° is 18.6 cal./deg. mole.

Introduction

CdSe has important photo-electric properties. Measurement of the vapor pressure will be useful for the preparation of photo-conductive layers by evaporation or growing of crystals from the vapor.

CdSe dissociates in the vapor



$$\log K_p = \log p_{\text{Cd}}^2 p_{\text{Se}_2} (\text{atm.}^3) = -\Delta H/2.3RT + \Delta S_{(p=1)}/2.3R \quad (2)$$

and if the vapor is stoichiometric: ($p_{\text{Cd}} = 1/2 p_{\text{Se}_2}$)

$$\log p_{\text{Cd}} = -\Delta H/6.9RT + \Delta S_{p=1}/6.9R + 0.1 \quad (3)$$

We have measured the vapor pressure by an indirect method.^{1,2} A nitrogen stream is passed over the vaporizing CdSe at constant temperature and total pressure (P_{tot}).

The gases are assumed ideal and the flowing gas is saturated with CdSe vapor of stoichiometric composition. $P_{(\text{tot})}$ is proportional to the number of gaseous molecules present (n_t). For each component i in the gas the partial pressure p_i is proportional to n_i and by Dalton's law, the partial pressure of cadmium will be

$$\frac{p_{\text{Cd}}}{p_{\text{tot}}} = \frac{n_{\text{Cd}}}{n_t} = \frac{n_{\text{Cd}}}{n_{\text{N}_2} + n_{\text{Cd}} + n_{\text{Se}_2}} \quad (4)$$

$$p_{\text{CdSe}} = p_{\text{Cd}} + p_{\text{Se}_2} = 1.5 p_{\text{Cd}} \quad (5)$$

Experimental (see Fig. 1)

Oxygen was removed from the nitrogen stream by a copper heater. The gas was dried in a liquid air trap. The flow rate of 45 cm.³/minute was kept constant. The saturation of the nitrogen gas with CdSe was proved by lowering the flow rate. The volume and temperature of gas in E (Fig. 1) and the atmospheric pressure (P) were measured to calculate n_{N_2} (Table I).

The nitrogen pressure in E was found by subtracting the saturated vapor pressure of water of the temperature in E from the atmospheric pressure. The furnace was regulated to constant temperature and measured with a calibrated Pt-Pt-10% Rh thermocouple in B (Fig. 1). The temperature differences over a length of 30 cm. in the center of the furnace were $\pm 2^\circ$.

The CdSe was prepared from the elements (99.995% pure). The reaction between these elements is complicated by the low solubility of CdSe in the molten components.

A layer of CdSe is formed between the components and Cd vapor cannot escape because the vapor pressure of selenium is higher than the Cd pressure.

The vapors of the elements react violently with each other. About 100 g. of CdSe was prepared in an evacuated quartz ampoule (diam 4 cm., length 20 cm.) from the elements in stoichiometric quantities. By partially heating the tube in a horizontal furnace at 800° high pressures are prevented.

First the selenium evaporates to the colder parts of the ampoule. When the cadmium begins to evaporate the reaction with selenium proceeds rapidly. The non-reacting portions of the elements evaporate to the colder parts of the ampoule. Then the ampoule is reversed. This is repeated

(1) Regnault, *Ann. Chim. (Paris)* **15**, 1 (1845).

(2) K. Jellinek and G. A. Rosner, *Z. physik. Chem.*, **143**, 51 (1929).

TABLE I

No.	T, °K.	SATURATED VAPOR PRESSURE OF CdSe					
		n_{N_2} , mg. mole	$n_{\text{Cd}} \times 10^4$ mg. at	P, mm.	$p'_{\text{Cd}} \times 10^5$, atm.	$p_{\text{CdSe}} \times 10^5$, atm.	
1	1016	258	13.7	771.2	5.39	8.08	
2	1033	253	20.6	761.4	8.16	12.2	
3	1037	255	26.2	764.1	10.3	15.4	
4	1037	250	29.8	756.8	11.9	17.8	
5	1050	257	29.6	766.7	11.6	17.4	
6	1054	256	42.3	768.6	16.7	25.1	
7	1060	252	34.9	760.1	13.9	20.8	
8	1069	251	57.4	758.7	22.8	34.2	
9	1080	255	57.4	768.4	22.7	34.0	
10	1081	251	74.1	759.3	29.5	44.2	
11	1083	249	69.7	756.2	27.9	41.9	
12	1094	255	98.7	767.1	39.1	58.6	
13	1096	252	106.0	766.0	42.5	63.7	
14	1113	253	143	767.0	57.2	85.9	
15	1116	254	150	766.2	59.3	89.0	
16	1123	252	199	761.4	79.0	118	
17	1128	255	207	766.5	81.9	123	
18	1137	258	232	766.4	90.7	136	
19	1151	254	325	766.0	129	193	
20	1157	250	362	746.1	142	213	
21	1157	249	324	748.7	128	192	
22	1157	249	382.5	749.9	152	228	
23	1160	251	337	759.7	134	201	
24	1160	253	338	759.5	133	200	
25	1162	248	363	749.7	144	216	
26	1166	254	414	751.4	161	242	
27	1168	250	406	759.4	162	243	
28	1170	198	372	744.8	184	276	

until the reaction has gone to completion. The CdSe was powdered and heated to 800° in a nitrogen stream to evaporate any excess of the components. Owing to the large difference in volatility the CdSe and any excess of Cd and Se were deposited on different places in the tube C (Fig. 1) during the measurement. So the stoichiometric composition of the vapor could be ascertained visually after a measurement. It also was proved by chemical analysis of the deposit.

If the nitrogen gas is not oxygen-free, some free selenium will be formed by the reaction: $2\text{CdSe} + \text{O}_2 \rightarrow 2\text{CdO} + \text{Se}_2$.

Chemical Analysis.—The CdSe in the quartz tube C was dissolved in 10 M HNO₃ and evaporated to dryness after adding conc. H₂SO₄. The residue was dissolved in a few drops of HCl. The Cd concentration is measured in 1 M NH₄Cl-0.5 M NH₄OH-0.0001% gelatine with a polarograph at 25°.

The quantity of Cadmium (n_{Cd}) has been calculated from these measurements.

Calculations.—The method of least squares was used to express the measurements of Table I in equations 2 and 3. See Fig. 2.

$$\log K_{\text{CdSe}} = \log p_{\text{Cd}}^2 \times p_{\text{Se}_2} = -\frac{34.440}{T} + 20.88 (740-900^\circ) \quad (2a)$$

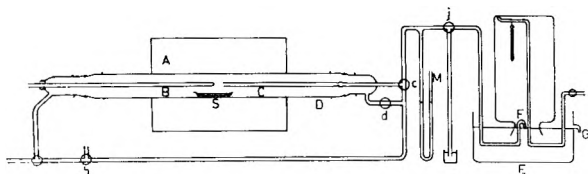


Fig. 1.—A = electric furnace; B = thermocouple tube; C = CdSe collecting tube; S = boat with CdSe; M = manometer; E = nitrogen collecting flask; B-C-D-S = quartz; a-b-c-d-j- are glass taps to control the gas stream.

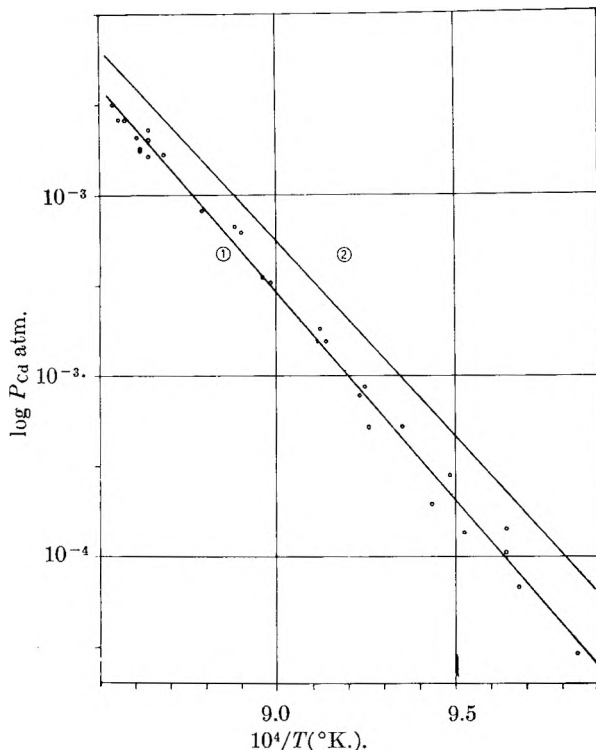


Fig. 2.—Dependence of the vapor pressure of CdSe on $1/T$: 1, our measurements of $\log p_{Cd}$; 2, extrapolated and corrected values of $\log p_{Cd}$ of Kroneeva, *et al.*⁷

$$\log p_{Cd} = -\frac{11.480}{T} + 7.06 \quad (740-900^\circ) \quad (2b)$$

and from (2a)

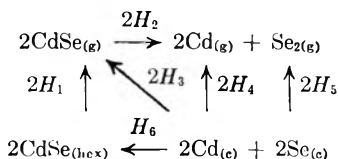
$$\Delta H_{1100} = (157.4 \pm 2.7) \text{ kcal.}$$

$$\Delta S_{1100} = (95.5 \pm 2.5) \text{ kcal./deg.}$$

A value of $\Delta c_p = -6$ cal./deg. mole was estimated for the reaction $2\text{CdSe}_{(s)} \rightarrow 2\text{Cd}_{(g)} + \text{Se}_{2(g)}$ by comparison with similar compounds ($\text{ZnS} - \text{CdS}$).¹¹

$$\Delta H_{298} = 157.4 + \int_{298}^{1100} \Delta c_p dT = (162.2 \pm 3) \text{ kcal.}$$

$$(\Delta S)_{298} = 95.5 + c_p \ln T'/298 = 103.2 \pm 3 \text{ cal./deg.}$$



H_1 = standard heat of sublimation of CdSe

H_2 = standard heat of dissociation of CdSe in Cd and Se_2 vapor

H_3 = standard heat of formation of CdSe vapor = 1.6 kcal./mole³

H_4 = standard heat of formation of Cd vapor = 26.97 kcal./mole³

H_5 = standard heat of formation of Se_2 vapor = 33.14 kcal./mole³

H_6 = standard heat of formation of CdSe (hex)

$$H_2 = H_4 + \frac{1}{2}H_5 - H_3 = 41.94 \text{ kcal./mole}$$

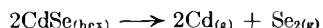
Evaluation of the experimental results gives

$$\Delta H = -2H_6 + 2H_4 + H_5 = 2H_1 + 2H_2 = (162.2 \pm 3) \text{ kcal.}$$

$$H_1 = (39.1 \pm 1.5) \text{ kcal./mole}$$

$$H_6 = (37.5 \pm 1.5) \text{ kcal./mole}$$

The standard entropy of CdSe (hex), $S^{\circ}_{\text{CdSe}}(25^\circ)$ is calculated from



S°_{Cd} = standard entropy of Cd vapor = 40.07 cal./deg. mole³

$S^{\circ}_{\text{Se}_2}$ = standard entropy of Se_2 vapor = 60.22 cal./deg. mole³

$$S = 2S^{\circ}_{\text{Cd}} + S^{\circ}_{\text{Se}_2} - 2S^{\circ}_{\text{CdSe}} = (103 \pm 3) \text{ cal./deg.}$$

$$S^{\circ}_{\text{CdSe}} = (18.6 \pm 1.5) \text{ cal./deg. mole}$$

Discussion

(1) The assumption that CdSe dissociates was proved by heating CdSe powder at 900° in N_2 or selenium or cadmium atmosphere of equal pressure (~ 0.1 atm.) Sublimation was suppressed with selenium or cadmium, not with nitrogen. We also mixed selenium vapor with the nitrogen stream in the apparatus of Fig. 1. The CdSe did not evaporate from the quartz boat at 800° .³ The fraction of Se_6 molecules can be neglected in our experiments.⁴

(2) The standard entropy of CdSe is not known. Specific heat data on CdSe are not available. Kireev⁵ calculated a value of (19.2 ± 2) cal./deg. mole for CdSe. This value agrees with our value (18.6 ± 1.5) cal./deg. mole. The heat of formation of CdSe has been measured by Fabre⁶ to 24 kcal./mole. Kubaschewski¹⁰ gives a value of (25 ± 4) kcal./mole.

(3) Korneeva,⁷ *et al.*, have measured the vapor pressure of CdSe by effusion in the range $540-740^\circ$ assuming CdSe molecules in the vapor

$$\log p'_{\text{CdSe}} = -\frac{10.957}{T} + 6.85 \quad (540-740^\circ) \quad \text{Fig. 2}$$

They calculated a heat of sublimation $(H_1)_{900^\circ\text{K}} = 50.1$ kcal./mole. Comparing their results with our value indicates that CdSe also is dissociated in the range $540-740^\circ$.

McCabe⁸ has given a correction that can be applied to data obtained by the Knudsen effusion method. This allows the pressure of CdSe_2 over CdSe to be calculated from Knudsen-cell data, assuming complete dissociation

$$p_{Cd} = p'_{\text{CdSe}} \frac{M_{\text{Cd}}^{1/3} M_{\text{Se}_2}^{1/6}}{(M_{\text{CdSe}})^{1/2}} \quad (M = \text{mol. weight})$$

$$p_{Cd} = 0.81p'_{\text{CdSe}}$$

and after correcting Korneeva's equation

$$\log p_{Cd} = -\frac{10.957}{T} + 6.736 \quad (540-740^\circ)$$

With formula 3

$$\Delta H_{910} = 150 \text{ kcal.} \quad \Delta S_{910} = 90.8 \text{ cal./deg. mole}$$

$$\Delta H^{\circ}_{298} = 150 + \Delta c_p(910-298) = 153.6 \text{ kcal.} \rightarrow H^{\circ}_{\text{CdSe}} = 33.3 \text{ kcal./mole}$$

(3) "Selected Values of Chemical Thermodynamic Properties," Circular of the National Bureau of Standards 500 (1952).

(4) G. Preuner, and I. Brockmüller, *Z. physik. Chem.*, **81**, 120 (1912).

(5) B. A. Kireev, *Zhur. Obshchei Khim.*, **16**, 1569 (1946).

(6) Fabre, *Ann. chim. phys.*, **6**, 505 (1877).

(7) I. V. Korneeva, V. V. Sokolov and A. V. Novoselova, *Zhur. Neorg. Khim.*, **5**, 241 (1960) (Russ.).

(8) C. L. McCabe, *Trans. Am. Inst. Mining Met. Engrs.*, **200**, 969 (1954).

$$\Delta S_{298} = 90.8 + \Delta c_p \ln \frac{910}{298} = 97.5 \text{ kcal.} \longrightarrow$$

$$S^{\circ}_{\text{CdSe}} = 21.4 \text{ cal./deg. mole}$$

(4) Drowart and Goldfinger⁹ have measured the vapor pressure of CdSe by mass spectrometry at 480°. Dissociation of CdSe is probable. Their value of 3×10^{-7} atm. for p_{Cd} (480–530°) is, however, too high.^{10,11}

(9) J. Drowart and P. Goldfinger, *J. Phys.*, **55**, [10] 721 (1958).

(10) O. Kubaschewski and E. L. Evans, "Metallurgical Thermodynamics," Pergamon Press, London, 1956.

(11) K. K. Kelley, Bull. U.S. Bur. Min., no. 476 (1949).

NOTE ADDED IN PROOF.—Recently Somorjai¹² also published the vapor pressure of CdSe. His values do not agree with ours. We have tested our apparatus with CdS and found complete agreement with the results of Pogoreleyi.¹³

Acknowledgment.—Thanks are due to Miss M. G. Geers for the experimental work, to prof. dr. G. A. M. Diepen and prof. dr. G. Meyer of the Technological University Delft for helpful discussions. Acknowledgment also is due to the chairman of the National Defence Research Organization T.N.O. for permission to publish this paper.

(12) G. A. Somorjai, *J. Chem. Phys.*, **65**, 1059 (1961).

(13) A. D. Pogoreleyi, *J. Phys. Chem. U.S.S.R.*, **22**, 731 (1948).

SOLUBILITY AND COMPLEX ION FORMATION OF SILVER CHLORIDE IN MOLTEN NITRATES

BY R. A. OSTERYOUNG,¹ C. KAPLAN AND D. L. HILL

Department of Chemistry, Rensselaer Polytechnic Institute, Troy, N. Y.

Received March 10, 1961

The solubility of silver chloride in the molten equimolar potassium nitrate–sodium nitrate solvent has been investigated at 280° in the presence of a varying excess of chloride ion. The results are interpreted in terms of the formation of the species AgCl and AgCl_2^- , and formation constants for these species are determined.

The solubility of silver halides in fused nitrates has been investigated recently by Flengas and Rideal,² and by Seward.³ The former authors utilized a potentiometric titration procedure to determine the solubility product, $K_{\text{sp}} = [\text{Ag}^+][\text{Cl}^-]$ of AgCl in an equimolar potassium nitrate–sodium nitrate solvent. Their K_{sp} values were determined for the most part with an excess of chloride ion present, and the K_{sp} remained constant with varying amounts of excess chloride. They obtained a K_{sp} value of 4.89×10^{-6} (moles/1000 g.)² at 248° and a ΔH of 18.3 kcal. Seward studied the solubility of AgCl in various nitrates and mixtures of nitrates. He found that in one system, a mixture of 90 mole % potassium nitrate and 10% potassium chloride, the solubility of AgCl increased relative to the solubility in the pure potassium nitrate. Earlier observations in this Laboratory had indicated that in a nitrate melt precipitated silver chloride would redissolve on addition of sufficient excess chloride.

These observations appear to be at variance with the constant solubility product obtained by Flengas and Rideal. The present work was undertaken, therefore, to study the solubility of silver chloride in a fused potassium nitrate–sodium nitrate solvent in the presence of limited amounts of excess chloride. All measurements in this solvent were made at 280°.

Experimental

All chemicals were reagent grade or prepared from reagent grade materials. The equimolar KNO_3 – NaNO_3 solvent was prepared by mixing the pure oven-dried salts in a bottle on a ball mill roller. Silver chloride was prepared by precipitation from silver nitrate and hydrochloric acid in aqueous solution. The furnace used was a Cenco–Cooley Crucible Furnace, powered by a variable transformer. Room tem-

perature was sufficiently stable so that the furnace temperature, on reaching equilibrium, could be held steady to within a degree of the desired value.

A solubility determination was made by placing a weighed amount of solvent, about 200 g., in a 250-ml. beaker, adding approximately 1 g. of AgCl , and the desired weighed amount of potassium chloride. The beaker then was placed in the furnace which was provided with a cover having two holes for the insertion of a mercury thermometer and a motor-driven glass stirrer. Equilibration was made at the selected temperature for periods of 1 to 4 hours, sometimes longer; then the stirrer was stopped and the undissolved AgCl permitted to settle to the bottom of the beaker for a half hour. Decantation of about half of the supernatant liquid was made by rapid pouring onto aluminum foil. The cooled solidified pieces of solvent were weighed, placed in water to leach the nitrates, and the insoluble silver chloride was determined by filtration through a previously weighed sintered glass crucible. As a check on this procedure, a determination of the solubility of AgCl in pure molten KNO_3 was performed, and the results were in good agreement with those reported by Seward.

Preliminary efforts to obtain reproducible data for the solubility of AgCl in the KNO_3 – NaNO_3 solvent by this procedure indicated that one hour equilibration at a temperature of 280° was insufficient and that it was preferable to allow at least three hours for the systems to equilibrate at the desired temperature. This point was further checked by preparing one sample of the molten nitrate solvent containing approximately 0.008 mole of dissolved AgNO_3 and a second sample containing the same number of moles of KCl . The two fused samples were mixed together, the precipitated AgCl was allowed to settle and then treated as indicated above. The results from this procedure were in good agreement with those from the longer period equilibration of the melts containing the solid AgCl . One other comment regarding an experimental observation is pertinent. Certain batches of solvent prepared from one manufacturer's reagent grade potassium nitrate were observed to form a brown precipitate, probably silver oxide, when the equilibration with the silver chloride was made. A similar precipitate formed on addition of silver nitrate to the same batch of solvent. It was concluded that this potassium nitrate contained sufficient impurity, probably oxide or hydroxide, to precipitate silver oxide, which was less soluble than the silver chloride. In all experimental results cited here the melt used was free of brownish precipitate on addition of the silver chloride.

(1) Atomics International, Canoga Park, California.

(2) S. N. Flengas and K. Rideal, *Proc. Roy. Soc. (London)*, **233**, 443 (1955).

(3) R. P. Seward, *J. Phys. Chem.*, **63**, 760 (1959).

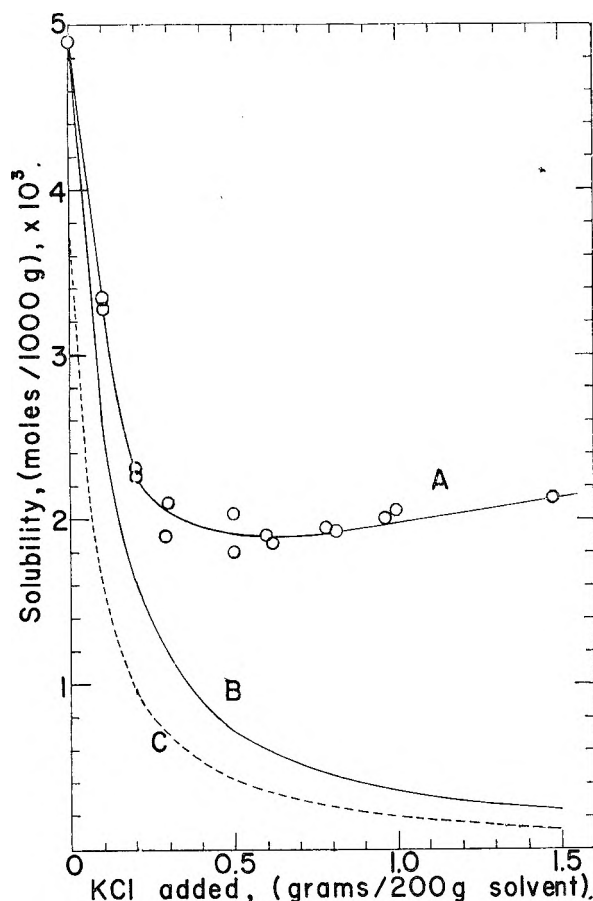


Fig. 1.—Solubility of AgCl as a function of added potassium chloride at 280°: A, experimental results; B, calculated curve from experimental solubility without added potassium chloride; C, calculated curve from extrapolated data of Flengas and Rideal.

Results and Discussion

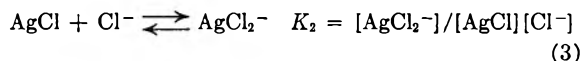
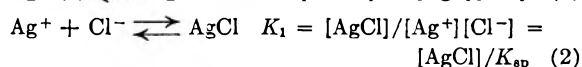
Figure 1 is a plot of the experimentally determined solubility, S , as moles of AgCl per 1,000 g. of solvent, at 280°, vs. the grams of KCl per 200 g. of solvent. The points at zero added KCl represent the solubility of AgCl in the pure solvent. Also on this figure is a calculated theoretical solubility curve, obtained by using the solubility value 4.9×10^{-3} moles AgCl/1,000 g. solvent as determined for no added chloride, calculating the apparent solubility product of silver chloride from this value, and then calculating the solubility of silver in excess chloride from the relation $[Ag^+] = K_s/[Cl^-]_T$. In these calculations the $[Cl^-] = [KCl] + [Ag^+]$, the second term on the right being important only at low concentrations of KCl. Also on Fig. 1 is a similar theoretical solubility plot calculated from the data of Flengas and Rideal at 248° and their experimentally determined ΔH of 18.3 kcal. Figure 2 shows the calculated apparent solubility product K_{sp} from the present work, plotted against the concentration of chloride. The straight line indicates the 280° value extrapolated from the data of Flengas and Rideal. The apparent K_{sp} for this work was calculated from the data as indicated on Fig. 1, and from the relations

$$\begin{aligned} [Ag^+] &= S \\ [Cl^-] &= S + [KCl] \end{aligned}$$

It is obvious that there is a significant disagreement between the experimentally determined solubility curve and either the theoretical curve calculated from our data with no added chloride, or the data of Flengas and Rideal.

It is now necessary to attempt an explanation for the lack of agreement of these data with those of Flengas and Rideal and also to explain the deviation of the solubility relation from the theoretical. The latter explanation will be attempted first.

The existence of AgCl complex ions in aqueous solution is well known.⁴ Several studies of this system have been made: the one by Jonte and Martin may serve as an example.⁵ The deviation of the experimental solubility from the theoretical may be explained by postulating the existence in the nitrate melt of undissociated AgCl and $AgCl_2^-$ in addition to free silver ions. These are the same two species presumed to exist in aqueous solutions by Jonte and Martin. Consider the equilibria



and, from (2)

$$[AgCl] = K_1 K_{sp} = \text{constant at a given temperature}$$

If it now is assumed that Flengas and Rideal measured the K_{sp} expressed by (1), a point to be discussed later, then it is reasonable to assume that the difference between the solubility measured here (4.9×10^{-3} moles AgCl/1,000 g. of solvent) and that (3.7×10^{-3} moles AgCl/1,000 g. of solvent) calculated from the data of Flengas and Rideal (extrapolated to 280°, $K_{sp} = 1.36 \times 10^{-6}$ (moles AgCl/1,000 g. of solvent)²) may be taken as the concentration of the undissociated AgCl in solution. It is further assumed that with no added chloride in excess, the concentration of $AgCl_2^-$ will be negligible. Then

$$[AgCl] = 4.9 \times 10^{-3} - 3.7 \times 10^{-3} = 1.2 \times 10^{-3} \quad (4)$$

and, from (2)

$$K_1 = [AgCl]/K_{sp} = 1.2 \times 10^{-3}/1.36 \times 10^{-6} = 88 \quad (5)$$

If the solubility of AgCl now is expressed in terms of all the postulated silver species in solution

$$S = [Ag^+] + [AgCl] + [AgCl_2^-] \quad (6)$$

and substituting from (1), (3) and (4) above

$$S = K_{sp}/[Cl^-] + 1.2 \times 10^{-3} + 1.2 \times 10^{-3}[Cl^-]K_2 \quad (7)$$

As a test of this hypothesis, values of K_2 may be calculated from the measured solubility, S , at a given concentration of total chloride, and the K_{sp} value of Flengas and Rideal. As a first approximation, it may be assumed that the concentration of chloride is due solely to the KCl added, the net sum of other additions of chloride (additions as AgCl solubility, and subtractions as AgCl or $AgCl_2^-$) being small compared to the amount of

(4) I. M. Kolthoff and E. Sandell, "Textbook of Quantitative Inorganic Analysis," 3rd edition, The Macmillan Co., New York, N. Y., 1952, p. 63.

(5) J. H. Jonte and D. S. Martin, *J. Am. Chem. Soc.*, **74**, 2052 (1952).

KCl. The results of this calculation are indicated in the first three columns of Table I, the data being taken from a smoothed curve drawn through the experimental points. The constancy of K_2 indicates the plausibility of the model.

TABLE I
SOLUBILITY DATA, K_2 AND F -FUNCTION VALUES

Moles Cl ⁻ per kg. solvent × 10 ³	$S \times 10^3$ moles per kg. ^a	K_2^b	Grams KCl per 200 g. solvent	F_0^c	F_1^c	F_2^c
0	4.9	..	0
6.71	3.29	7.5	.1	6.62	92.5	626
13.41	2.30	5.3	.2	2.27	94.6	469
20.10	2.04	6.8	.3	3.02	101	647
26.82	1.95	7.5	.4	3.84	106	671
33.52	1.90	7.3	.5	4.68	110	657
40.23	1.90	7.5	.6	5.63	115	671
47.04	1.90	7.3	.7	6.57	118	637
53.64	1.92	7.3	.8	7.57	123	652
60.34	1.95	7.2	.9	8.65	127	647
67.05	1.98	7.2	1.0	9.76	131	641
100.6	2.13	6.6	1.5	15.90	149	607

^a Solubility of AgCl (moles per 1000 g. solvent 10³) taken from smoothed curve A in Fig. 1 at concentration of KCl or Cl⁻ as indicated in columns 4 and 1. ^b Values of K_2 calculated from eq. 7 using $K_{sp} = 1.36 \times 10^{-6}$ (moles AgCl/1000 g. solvent)², as extrapolated from Flengas and Rideal to 280°. ^c F_0 , F_1 and F_2 calculated from equations 8, 9 and 10.

A slightly different analysis of the data may be made by a slope-intercept procedure similar to that utilized by Hume and DeFord.⁶ A function F_0 may be defined by rewriting equation 6 and substituting from equations 1, 2 and 3

$$F_0 = \frac{S}{[Ag^+]} = 1 + K_1[Cl^-] + K_1K_2[Cl^-]^2 \quad (8)$$

where S is the measured solubility at a given concentration of chloride, and it again is assumed that the equilibrium concentration of chloride is that due to the added potassium chloride only. The $[Ag^+]$ is calculated from the K_{sp} data of Flengas and Rideal and the concentration of added potassium chloride.

Two additional functions now can be defined

$$F_1 = \frac{(F_0 - 1)}{[Cl^-]} = K_1 + K_1K_2[Cl^-] \quad (9)$$

and

$$F_2 = \frac{(F_1 - K_1)}{[Cl^-]} = K_1K_2 \quad (10)$$

and if F_1 is plotted against the concentration of chloride, a straight line should result whose intercept is K_1 and whose slope is K_1K_2 . A plot of F_2 against concentration of chloride should be a straight line independent of chloride concentration. Values for F_0 , F_1 and F_2 determined from data taken from a smoothed curve through the experimental points (A in Fig. 1) are given in Table I. A plot of the F_1 function was linear in chloride. From the slope of the F_1 plot, 640, and using K_1 as previously determined (eq. 5), a value of K_2 of 7.3 is found.

An examination of the method used by Flengas and Rideal in the calculations of K_{sp} would now be of interest. These authors demonstrated, with a concentration cell represented by

(6) D. D. DeFord and D. N. Hume, *J. Am. Chem. Soc.*, **73**, 5021 (1951).

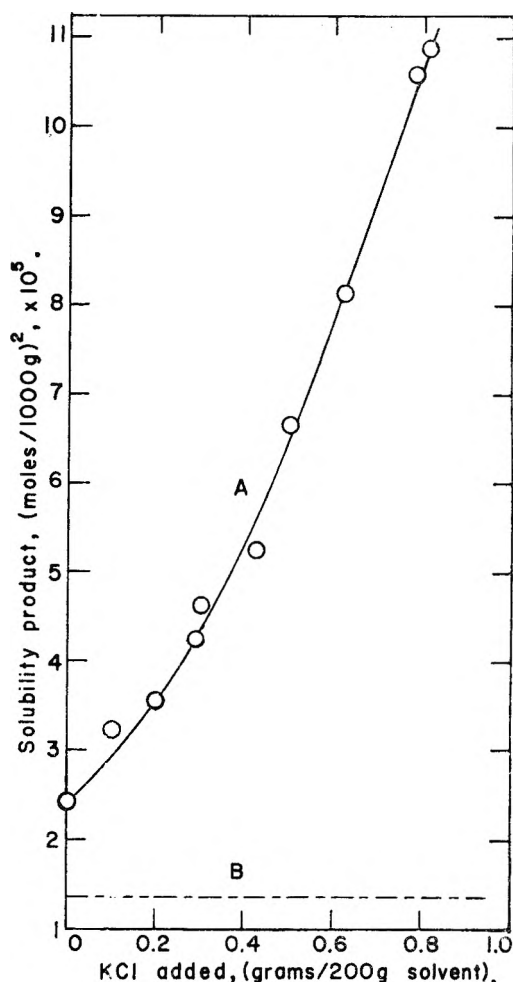
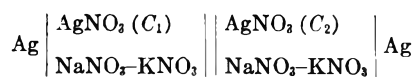


Fig. 2.—Solubility product of AgCl as a function of added potassium chloride: A, calculated apparent K_{sp} from experimental results at 280°; B, extrapolated from data of Flengas and Rideal.



that a plot of $\log C_2/C_1$ vs. E gave a straight line of theoretical slope 2.3 (RT/F). They then measured the e.m.f. of this cell as potassium chloride was added to the right hand side of the cell above and used this measured e.m.f. to determine the concentration of silver ion. Since they knew how much $AgNO_3$ was present initially, and how much KCl had been added, the calculations could be made

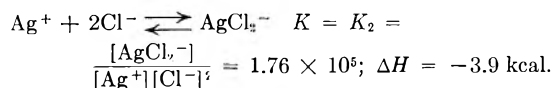
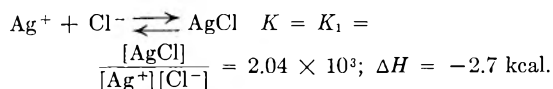
$[Ag^+]$ — determined from the e.m.f. of the above cell by the Nernst equation

$$[Cl^-] = [KCl] - [AgNO_3] + [Ag^+] \quad (11)$$

The present work indicates that a small extra term, to account for the chloride tied up as a complex ion, $AgCl_2^-$, should be subtracted from the right-hand side of (11). However, this term is negligible compared to the sum of the three terms on the right side of (11) as written above, although it would be sizable compared to the last term of (11). Hence, since the e.m.f. measurements indicated the concentration of free silver ion, Ag^+ , their calculations represent the actual solubility product of AgCl as in equation 1. The solubility measurements as carried out in the present work, however,

directly measure the solubility of all silver species in solution.

Jonto and Martin obtained data in aqueous solution at 25° for 2 and 3 reactions.



Extrapolation of these data to 280° yields a K_1 of 251 and a K_2 of 34 compared to K_1 of 88 and K_2 of 7.3 determined in this work. Although certainly not identical, the order of magnitude of the constants is such as to indicate that the complex formation is not too greatly affected by differences in the solvent media.

The above treatment offers an explanation for the apparent discrepancy between the constant values of the ionic product obtained by Flengas

and Rideal and the variable values indicated by the work of Seward and the present authors. No direct comparison can be made between the results of the above treatment and those from the elegant work of Blander and co-workers,⁷ who have recently proposed a quasi-lattice model treatment of similar molten reciprocal salt systems. It is hoped that current work in this Laboratory based on the present approach in the same systems studied by Blander will enable a direct comparison to be made, at least for the value of K .

Acknowledgment.—One author (C.K.) would like to acknowledge support under a National Science Foundation Research Participation Program for High School Teachers. This work also was supported, in part, under U. S. Atomic Energy Commission Contract AT (30-3)-241.

(7) (a) M. Blander, F. F. Blankenship and R. F. Newton, *J. Phys. Chem.*, **63**, 1259 (1959); (b) M. Blander, *ibid.*, **63**, 1262 (1959); (c) J. Braunstein and M. Blander, *ibid.*, **64**, 10 (1960); (d) D. G. Hill, J. Braunstein and M. Blander, *ibid.*, **64**, 1038 (1960).

ACTIVITY COEFFICIENTS IN AQUEOUS SOLUTIONS OF SUCROSE, MANNITOL AND THEIR MIXTURES AT 25°

BY R. A. ROBINSON¹ AND R. H. STOKES

Department of Chemistry of the University of New England, Armidale, N.S.W., Australia

Received March 13, 1961

Isopiestic vapor pressure measurements are reported for sucrose and mannitol solutions and for sucrose-mannitol in mixed solutions. Some improvements in the technique of manipulating the isopiestic dishes are described, giving a reproducibility of 0.03%. A new method of calculating activity coefficients in the mixed solutions is developed, and equations for the activity coefficients at all compositions are derived. Each solute is "salted-out" by the other.

Introduction

The isopiestic vapor pressure method has been widely applied to solutions of single electrolytes and has been used for a few pairs of mixed electrolytes.² A recent paper from this Laboratory³ gave data for the sodium chloride-potassium chloride-water system, and other studies shortly to be reported deal with the systems sodium chloride-mannitol-water and sodium chloride-sucrose-water, which are of interest in connection with diffusion studies in ternary systems. Here we deal with the simpler system sucrose-mannitol-water, which is as far as we know the first system of two non-electrolytes to be examined by this method.

Notation.

- γ_B, γ_C = molal activity coefficients of B and C, resp., in a soln. containing component B at a molality m_B and component C at a molality m_C
 ϕ = molal osmotic coefficient of this soln.
 γ_B^0 = activity coefficient of B in a soln. containing B only at a molality m_B
 ϕ_B^0 = molal osmotic coefficient of this soln.
 γ_C^0 = activity coefficient of C in a soln. containing C only at a molality m_C
 ϕ_C^0 = molal osmotic coefficient of this soln.

(1) Present address: National Bureau of Standards, Washington 25, D. C.

(2) R. A. Robinson and R. H. Stokes, "Electrolyte Solutions," Second Edition, Butterworths Scientific Publications, London, 1959, pp. 443-449.

(3) R. A. Robinson, *J. Phys. Chem.*, **65**, 662 (1961).

In this work, B = sucrose, C = mannitol. It should be noted that γ_B^0 and γ_C^0 were used with a different meaning in an earlier paper.³

Experimental

The sucrose was supplied by the Colonial Sugar Refining Company; it had been twice recrystallized from the "standard sucrose" used as their laboratory standard. A sample of sucrose obtained from the National Bureau of Standards, Washington, gave identical isopiestic results. The sucrose was dried *in vacuo* over calcium chloride at room temperature. Mannitol was four times recrystallized from the Colonial Sugar Refining Company's commercial product and dried in the same way. Solutions were made up in conductance water.

The isopiestic apparatus used in this work and in that described in an earlier paper³ consisted of glass vacuum desiccators of the "old-fashioned" design, with a cylindrical body and a conical base, which is more readily mounted on the rocking stand than the modern nearly spherical pattern. Each contained a silver-plated copper block, 15 cm. in diameter and 2.5 cm. thick. A round the circumference of this block, eleven silver dishes could be placed, leaving a clear central space 8.5 cm. in diameter. The dishes were 3 cm. in diameter and 2 cm. deep. In the central space was placed a device made of tinned copper wire and sheet, shown in Fig. 1. At the start of the run, the hinged lids of the dishes were held open by the upper circle of wire. At the end of the run, the ground joint in the desiccator lid, carrying the tap, was slowly rotated through 360°. The glass inlet-tube of the tap unit, engaged between the flat plates at the top of the device, caused it to rotate on the copper block, and as it did so the gap in the wire circle allowed each dish lid in turn to fall into the closed position. The vacuum was then broken, and the dishes were removed, wiped dry, and

weighed. The lids fitted so closely that evaporation losses during weighing were not more than 0.1 mg.

Another source of error in isopiestic measurements is the formation of air or vapor bubbles in the liquid in the dishes during the initial evacuation; in breaking, these sometimes cause droplets of solution to be lost. Evacuation on a water-pump often will cause this trouble if the room temperature is higher than that of the water supply. To eliminate it, we adopted the practice of cooling the copper block to about 0° in the refrigerator before setting the dishes in position. Small drops of the sodium chloride reference solution were placed on the block to ensure good thermal contact between the block and each dish. Equilibration periods in the 25° thermostat were from two to five days; temperature control was $\pm 0.005^\circ$, and the desiccators were rocked through an angle of 15° once every five seconds.

Scatchard, Hamer and Wood⁴ reported that they used no sucrose solution which had been made up for more than a week. We agree that this precaution is essential and, indeed, because of the possibility of microbial action, the sucrose and mannitol solutions were made up freshly for each run. Attempts to run sucrose solutions for periods longer than four or five days often led to poor reproducibility, which was attributed to such microbial action. Similarly, the dilution or concentration of a set of solutions which already had been equilibrated seldom gave a good result. All weighings were made on a semi-micro balance, and corrected to vacuum.

Activity and Osmotic Coefficients of Sucrose and Mannitol as Single Solutes.—Table I gives molalities of isopiestic pairs of sodium chloride and sucrose solutions. Each sodium chloride concentration is the mean of triplicate dishes and each of the non-electrolytes the mean of duplicate or triplicate dishes. The extreme difference in triplicates was not more than 0.05% in the molality and duplicates agreed within 0.03%. Table II gives similar results for sodium chloride and mannitol solutions.

TABLE I

ISOPIESTIC SOLUTIONS OF SODIUM CHLORIDE AND SUCROSE^a

m_{NaCl}	m_{B}	m_{NaCl}	m_{B}	m_{NaCl}	m_{B}
0.2100	0.3770	1.0694	1.7330	2.1469	3.2504
.2855	.5065	1.1088	1.7887	2.2481	3.3928
.4193	.7293	1.1597	1.8618	2.7365	4.0731
.4246	.7372	1.1808	1.8914	2.8807	4.2796
.4984	.8572	1.1951	1.9123	2.9604	4.3947
.5277	.9045	1.5042	2.3547	3.1524	4.6631
.5761	.9824	1.8013	2.7706	3.3733	4.9876
.7051	1.1852	1.8637	2.8576	3.4556	5.1056
.9001	1.4819	1.9349	2.9588	3.9149	5.7951
.9558	1.5657				

^a B = Sucrose.

TABLE II

ISOPIESTIC SOLUTIONS OF SODIUM CHLORIDE AND MANNITOL^a

m_{NaCl}	m_{C}	m_{NaCl}	m_{C}	m_{NaCl}	m_{C}
0.1165	0.2164	0.3732	0.6846	0.5608	1.0264
.1623	.3002	.4146	.7598	.5761	1.0545
.2100	.3875	.4246	.7788	.6048	1.1063
.2808	.5163	.4812	.8799	.6768	1.2376
.2855	.5248	.4984	.9120	.7000	1.2807

^a C = Mannitol.

The osmotic coefficients of mannitol calculated from these data are well represented (*i.e.*, with a maximum deviation of 0.0013 and a mean deviation of 0.0005 in φ_{C}^0) by

$$\varphi_{\text{C}}^0 = 1 + 0.0034m_{\text{C}} + 0.0042m_{\text{C}}^2 \quad (1)$$

whence the activity coefficient is given by

$$\log \gamma_{\text{C}}^0 = 0.00295m_{\text{C}} + 0.00274m_{\text{C}}^2 \quad (2)$$

(4) G. Scatchard, W. J. Hamer and S. E. Wood, *J. Am. Chem. Soc.*, **60**, 3061 (1938).

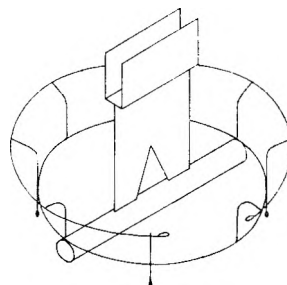


Fig. 1.—Device for closing lids of isopiestic dishes with desiccator under vacuum.

Up to 2 *M* the osmotic coefficient of sucrose can be represented with a maximum deviation of 0.0009 and a mean deviation of 0.0004 in φ_{B}^0 by

$$\varphi_{\text{B}}^0 = 1 + 0.0740m_{\text{B}} + 0.0100m_{\text{B}}^2 \quad (3)$$

with the corresponding equation

$$\log \gamma_{\text{B}}^0 = 0.0643m_{\text{B}} + 0.0065m_{\text{B}}^2 \quad (4)$$

But to describe the results over the entire concentration range, a more extended equation is necessary

$$\varphi_{\text{B}}^0 = 1 + 0.07028m_{\text{B}} + 0.01847m_{\text{B}}^2 - 0.004045m_{\text{B}}^3 + 0.000228m_{\text{B}}^4 \quad (5)$$

This represents the experimental data within 0.001 in φ_{B}^0 . The corresponding equation for the activity coefficient is

$$\log \gamma_{\text{B}}^0 = 0.06105m_{\text{B}} + 0.01203m_{\text{B}}^2 - 0.002343m_{\text{B}}^3 + 0.000124m_{\text{B}}^4 \quad (6)$$

The osmotic coefficients of sucrose given previously⁵ were collated from three sources^{4,5} and our present results give somewhat lower osmotic coefficients in the more dilute solutions. The new coefficients are lower by 0.004 at 1 *M*, 0.006 at 1.5 *M* and 0.003 at 2.5 *M*; at higher concentrations there is no significant difference.

The System Sucrose–Mannitol–Water.—In making these measurements, three of the dishes contained the reference sodium chloride solution and usually there were eight dishes containing four pairs of mixed sucrose–mannitol solutions (or one pair containing sucrose solutions and three pairs containing mixed sucrose–mannitol solutions). Table III gives the mean molalities of the triplicate reference solutions and of the mixed solutions. Also included are the quantity Δ defined by equation 15 and values of $\Delta/(m_{\text{B}}m_{\text{C}})$. φ_{ref} , the osmotic coefficient of the reference solution, was interpolated from tables⁷; the osmotic coefficient φ_{B}^0 of a solution of sucrose alone at the same molality as that of sucrose in the mixed solution was calculated by equations 3 or 5; φ_{C}^0 , the corresponding quantity for the mannitol component, by equation 1.

Discussion of the Sucrose–Water and Mannitol–Water Systems.—Scatchard⁸ has drawn attention to the fact that much of the behavior of a sucrose solution in water can be explained by ascribing a hydration number between 4 and 5 to the solute.

(5) Ref. 2, Appendix 8.6, p. 478.

(6) (a) R. A. Robinson and D. A. Sinclair, *J. Am. Chem. Soc.*, **56**, 1830 (1934); (b) R. A. Robinson, P. K. Smith and E. R. B. Smith, *Trans. Faraday Soc.*, **38**, 63 (1942).

(7) Ref. 2, Appendix 8.3, p. 476.

(8) G. Scatchard, *J. Am. Chem. Soc.*, **43**, 2406 (1921).

TABLE III
THE SYSTEM: SUCROSE-MANNITOL-WATER^a

<i>m</i> _{ref.}	<i>m</i> _B	<i>m</i> _C	Δ	$\frac{\Delta}{m_B m_C}$	Equation 23— Δ	%
0.4475	0.6227	0.1604	0.0096	0.0961	0.0094	-0.03
	.4597	.3332	.0139	.0908	.0143	+ .05
	.3139	.4880	.0131	.0855	.0139	+ .10
0.5490	.1555	.6559	.0081	.0794	.0088	+ .09
	.7561	.1947	.0145	.0985	.0146	+ .01
	.5594	.4057	.0219	.0967	.0220	+ .01
0.8495	.3828	.5953	.0207	.0908	.0216	+ .09
	.1900	.8014	.0138	.0906	.0137	+ .01
	1.1776	.2528	.0311	.1045	.0318	+ .04
0.9987	0.9443	.5105	.0501	.1039	.0511	+ .06
	.7117	.7682	.0557	.1019	.0570	+ .08
	.5015	1.0008	.0510	.1016	.0509	+ .01
1.0694	1.2411	0.4342	.0598	.1110	.0591	- .04
1.1808	1.1848	.6191	.0793	.1081	.0813	+ .10
	1.0509	.7692	.0883	.1092	.0895	+ .06
1.1951	1.6151	.3172	.0574	.1120	.0570	- .02
	1.3081	.6653	.0999	.1148	.0981	- .09
	1.0148	1.0012	.1150	.1132	.1144	- .03
1.8637	1.5970	0.3594	.0665	.1159	.0640	- .11
	1.4767	.4971	.0839	.1143	.0824	- .07
	1.1259	.8979	.1130	.1118	.1142	+ .04
2.4226	2.5321	.3874	.1092	.1113	.1075	- .05
	2.2820	.6829	.1795	.1152	.1784	- .03
	1.9707	1.0494	.2485	.1202	.2469	- .04
3.7186	3.4904	0.1760	.0593	.0965	.0588	- .01
	3.3738	.3224	.1040	.0956	.1077	+ .07
	3.2571	.4637	.1507	.0998	.1543	+ .07
3.7186	3.0949	.6557	.2169	.1069	.2161	- .02
	5.2913	.2669	.1093	.0774	.1005	- .11
	5.1174	.4889	.1980	.0791	.1887	- .11
	4.9530	.7051	.2710	.0776	.2783	+ .09

^a The reference solute was sodium chloride.

We propose to examine to what extent this postulate can be used to explain not only the properties of mannitol and sucrose solutions but also those of the mixed solutions.

If hydration is the only cause for departure from ideality of an aqueous non-electrolyte solution, the water activity of the solution is given by

$$a_w = \frac{1 - 0.018hm}{1 - 0.018(h-1)m} \quad (7)$$

By expanding $\ln a_w$ in a series and converting to the osmotic coefficient, we obtain

$$\begin{aligned} -55.51 \ln a_w &= m + 0.018 \left(h - \frac{1}{2} \right) m^2 + \\ & 0.018^2 \left(h^2 - h + \frac{1}{3} \right) m^3 \\ \varphi_B^0 &= 1 + 0.018 \left(h - \frac{1}{2} \right) m + \\ & 0.018^2 \left(h^2 - h + \frac{1}{3} \right) m^2 \quad (8) \end{aligned}$$

neglecting terms with higher powers of m . Putting $0.018(h_B^{-1/2}) = 0.0740$ for sucrose gives $h_B = 4.61$ whence the last term of equation 8 should have a coefficient of 0.0055. Clearly there is a contribution of $0.0045m_B^2$ to φ_B^0 which cannot be accounted for by hydration. Nevertheless, the hydration hypothesis can be used to calculate, for example, $\varphi_B^0 = 1.1700$ at 2 M against 1.1880 calculated by equation 3. Thus the major deviation of the solution from ideality can be ascribed, up to 2 M at least, to hydration.

Equation 3 represents the data for sucrose only up to 2 M . To fit the results up to higher concentrations, the extended equation 5 must be used.

Nevertheless, equation 8 predicts $\varphi_B^0 = 1.5075$ at 5 M . Equation 5 gives $\varphi_B^0 = 1.4501$ so that even at 5 M hydration can still account for a major part of the deviation from ideality.

Similarly, the mannitol data are satisfied by $h_C = 0.69$ with a negligibly small term in m_C^2 ; equation 1 shows that there is a contribution of $0.0042m_C^2$ to φ_C^0 which cannot be accounted for by hydration.

Thermodynamic Theory for 3-Component Non-electrolyte Systems.—The value in ternary systems of the cross-differentiation relations

$$\left(\frac{\partial \ln a_B}{\partial m_C} \right)_{m_B} = \left(\frac{\partial \ln a_C}{\partial m_B} \right)_{m_C}, \text{ etc.} \quad (9)$$

has been pointed out by Guggenheim,⁹ while McKay¹⁰ has worked out in considerable detail the consequences for a solution containing two electrolytes. We now develop an alternative treatment which offers some advantages in convenience for non-electrolytes. The method gives the cross-differentials very directly. We assume that at all values of m_B and m_C the cross-differential can be represented by

$$\left(\frac{\partial \ln \gamma_B}{\partial m_C} \right)_{m_B} = f'(m_B) + F'(m_C) \quad (10)$$

where $f'(m_B)$ is a function of m_B only, and $F'(m_C)$ of m_C only. These functions are expressed as derivatives, their integrals with respect to m_B and m_C , respectively, being $f(m_B)$ and $F(m_C)$. The form (10) is fairly adaptable to special cases, no other restrictions except continuity being placed on the functions. However, we expressly exclude functions such as products of powers of m_B and m_C , for which the method is unsuitable. The case of two electrolytes, involving terms in $(m_B + m_C)^{1/2}$ is likewise excluded.

Integrating (10) at constant m_B between $m_C = 0$ and $m_C = m_C$ yields

$$\ln \gamma_B = \ln \gamma_B^0 + m_C f'(m_B) + F(m_C) - F(0) \quad (11)$$

Using the cross-differentiation relation

$$\left(\frac{\partial \ln \gamma_B}{\partial m_C} \right)_{m_B} = \left(\frac{\partial \ln \gamma_C}{\partial m_B} \right)_{m_C}$$

we obtain in a similar way

$$\ln \gamma_C = \ln \gamma_C^0 + m_B F'(m_C) + f(m_B) - f(0) \quad (12)$$

In practice $f(m_B)$ and $F(m_C)$ usually will be power series with leading terms in m_B and m_C , so that $F(0) = f(0) = 0$

The Gibbs-Duhem equation is

$$-55.51 d \ln a_w = m_B d \ln (m_B \gamma_B) + m_C d \ln (m_C \gamma_C) \quad (13)$$

which by equations 11 and 12 gives

$$\begin{aligned} -55.51 d \ln a_w &= dm_B + m_B d \ln \gamma_B^0 + dm_C + \\ & m_C d \ln \gamma_C^0 + m_B m_C f''(m_B) dm_B + m_B F''(m_C) dm_C + \\ & m_B f'(m_B) dm_C + m_B m_C F'''(m_C) dm_C + m_C f'(m_B) dm_B + \\ & m_C F''(m_C) dm_B = d(m_B \varphi_B^0) + d(m_C \varphi_C^0) + \\ & d[m_B m_C (f'(m_B) + F'(m_C))] \quad (14) \end{aligned}$$

We now define a quantity Δ by

$$\Delta = -55.51 \ln a_w - m_B \varphi_B^0 - m_C \varphi_C^0 \quad (15)$$

Let the composition of the reference sodium chlo-

(9) E. A. Guggenheim, "Thermodynamics, an Advanced Treatment for Chemists and Physicists," North-Holland Publishing Co., Amsterdam, 1949, p. 207.

(10) H. A. C. McKay, *Trans. Faraday Soc.*, **51**, 902 (1955); H. A. C. McKay and J. K. Perring, *ibid.*, **49**, 163 (1953).

ride solution in equilibrium with the mixed sucrose-mannitol solution be m_{ref} and its osmotic coefficient φ_{ref} . Then Δ is simply

$$\Delta = 2m_{ref}\varphi_{ref} - m_B\varphi_B^0 - m_C\varphi_C^0 \quad (16)$$

Equation 14 then may be integrated from infinite dilution of both components up to the composition m_B, m_C

$$\Delta = m_B m_C [f'(m_B) - F'(m_C)] \quad (17)$$

$$\text{or } \left(\frac{\partial \ln \gamma_B}{\partial m_C}\right)_{m_B} = \left(\frac{\partial \ln \gamma_C}{\partial m_B}\right)_{m_C} =$$

$$f'(m_B) + F'(m_C) = \frac{\Delta}{m_B m_C} \quad (18)$$

The remarkable feature of equation 18 is that (assuming that the vapor pressures of the single solute systems are known) a single measurement of the vapor pressure of the mixed solution yields directly the value of the cross-differential for that solution.

The result is obtained only on condition that the assumed form (10) is adequate to describe the cross-differential at all compositions from infinite dilution of both components up to the actual composition of the solution measured. It is thus likely to apply with good accuracy in the case of mixed aqueous non-electrolytes.

The following physical interpretations can be given to the quantity Δ .

(a) From equation (15)

$$\Delta = 55.51 \ln (p_B^0 p_C^0) / (p p_w)$$

where p_B^0 is the vapor pressure of water over a solution of sucrose alone at molality m_B ; p_C^0 is that over a solution of mannitol alone at molality m_C ; p is that over the mixed solution containing sucrose at molality m_B and mannitol at molality m_C ; and p_w is the vapor pressure of pure water.

(b) $-RT\Delta$ is the free energy change of the water in the following process: a solution of m_B moles of sucrose in 1 kg. of water is mixed isothermally with a solution of m_C moles of mannitol in 1 kg. of water; then 1 kg. of liquid water is isothermally separated *via* an osmotic membrane.

Discussion of the Sucrose-Mannitol-Water System.—The analog of equation 7 for a mixture is

$$a_w = \frac{1 - 0.18(h_B m_B + h_C m_C)}{1 - 0.18[(h_B - 1)m_B + (h_C - 1)m_C]} \quad (19)$$

$$\text{or } -55.51 \ln a_w = (m_B + m_C) + 0.018 \left[\left(h_B - \frac{1}{2} \right) m_B + \left(h_C - \frac{1}{2} \right) m_C \right] (m_B + m_C) + 0.018 \left[(h_B m_B + h_C m_C)^2 - (h_B m_B + h_C m_C)(m_B + m_C) + \frac{1}{2}(m_B + m_C)^2 \right] (m_B + m_C) \quad (20)$$

$$\text{and } \frac{\Delta}{m_B m_C} = 0.018 [h_B + h_C - 1] +$$

$$0.018^2 [m_B(h_B^2 + 2h_B h_C - 2h_B - h_C + 1) + m_C(h_C^2 + 2h_B h_C - 2h_C - h_B + 1)] \quad (21)$$

But we have already found that while hydration accounts for most of the departures from ideality of both sucrose and mannitol solutions, there is an additional small term in m^3 in the expression for $-55.51 \ln a_w$ or in m^2 for φ . Moreover, the coefficients of this term are almost the same: 0.0045 for sucrose and 0.0042 for mannitol. We therefore investigate the effect of adding a term

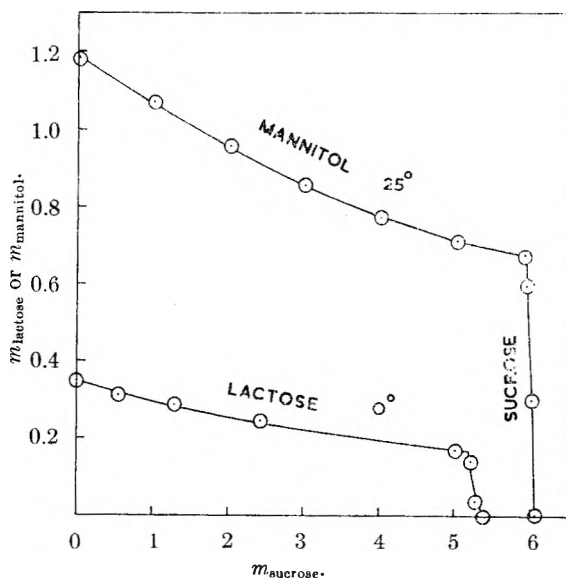


Fig. 2.—Solubility relations in the sucrose-mannitol-water and sucrose-lactose-water systems.

$0.0045(m_B + m_C)^3$ to equation 20. This is equivalent to adding a term $0.0135(m_B + m_C)$ to equation 21. Substituting $h_B = 4.61$, $h_C = 0.69$, we get

$$\frac{\Delta}{m_B m_C} = 0.0774 + 0.0195m_B + 0.0145m_C \quad (22)$$

Values of Δ calculated by this equation agree well with those found as recorded in the first 22 entries in the fourth column of Table III; the differences correspond to a mean error of 0.05% in the molality of the reference solutions.

This comparison cannot be valid above a total concentration of 2 M . However, equation 22 does suggest the form of a more extended equation: the first term on the right is the sum of the coefficients of the first terms on the right in equations 1 and 3. By analogy, equations 1 and 5 might give 0.0737 for the first term in an equation applicable to more concentrated solutions. As the mannitol concentration cannot be much greater than 1 M , it might be hoped that a term in the first power of m_C would suffice, but the appearance of m_B^4 terms in equation 5 suggests terms up to m_B^3 in our new equation. We therefore try

$$\frac{\Delta}{m_B m_C} = A + Bm_B + Cm_B^2 + Dm_B^3 + Em_C \quad (23)$$

and find that we can well represent the experimental data by putting

$$\begin{aligned} A &= 0.0737 & D &= 0.001194 \\ B &= 0.04096 & E &= 0.0107 \\ C &= -0.01425 \end{aligned}$$

The sixth column of Table III gives values of Δ

TABLE IV^a

SOLUBILITY OF MANNITOL IN SUCROSE SOLUTIONS							
m_B	0	1	2	3	4	5	5.902
$m_C(\text{sat.})$	1.186	1.075	0.960	0.860	0.779	0.718	0.672
SOLUBILITY OF SUCROSE IN MANNITOL SOLUTIONS							
m_C	0	0.3	0.6	0.672			
$m_B(\text{sat.})$	6.053	5.988	5.919	5.902			

^a The last column refers to solutions saturated with respect to both components.

TABLE V
MOLAL ACTIVITY COEFFICIENTS OF SUCROSE (B) AND MANNITOL (C) IN MIXED SOLUTION AT 25°^a

M_B	M_C	M_C						
		0	1	2	3	4	5	5.9
0	B	1.000	1.177	1.424	1.731	2.082	2.458	2.806
	C	1.000	1.094	1.216	1.351	1.485	1.606	1.707
0.3	B	1.023	1.214	1.471	1.785	2.138	2.513	2.862
	C	1.003	1.100	1.227	1.368	1.507	1.636	1.745
0.7	B	1.056	1.267	1.540	1.862	2.217	2.592	(2.943)
	C	1.008	1.110	1.244	1.393	1.541	1.681	(1.799)
1.0	B	1.082	1.310	(1.595)	(1.925)	(2.282)	(2.656)	(3.009)
	C	1.013	1.120	(1.259)	(1.414)	(1.569)	(1.717)	(1.843)

^a Values in parentheses refer to solutions supersaturated to mannitol.

calculated by equation 23 and the last column gives the percentage error in the molality of the reference solution necessary to account for the difference between the observed and calculated Δ values.

Activity Coefficients in the Sucrose-Mannitol-Water System.—Integration of equation 23 gives

$$\ln \gamma_B = \ln \gamma_B^0 + m_C \left[A + Bm_B + Cm_B^2 + Dm_B^3 + \frac{1}{2}Em_C \right] \quad (24)$$

for the activity coefficient of sucrose in the mixed solution, and

$$\ln \gamma_C = \ln \gamma_C^0 + m_B \left[A + \frac{B}{2}m_B + \frac{C}{3}m_B^2 + \frac{D}{4}m_B^3 + Em_C \right] \quad (25)$$

for the activity coefficient of mannitol in the mixture.

Solubility Relations.—The solubility of mannitol in sucrose solutions is determined by the condition

$$(m_C \gamma_C^0)_{\text{sat}} = (m_C \gamma_C)_{\text{sat}}$$

where the quantities on the left refer to a saturated solution in water and those on the right to saturated solutions containing sucrose. The saturated solution in water is known¹¹ to be 1.186 M ; at this

(11) J. M. Braham, *J. Am. Chem. Soc.* **41**, 1707 (1919).

molality, $\gamma_C^0 = 1.017$ and the solubility product is 1.207 mole kg.⁻¹. m_C now can be calculated for any given sucrose molality, γ_C being obtained by equation 25: a few successive approximations are needed. The solubility of sucrose in mannitol solutions likewise can be calculated, the saturated solution in water⁴ being 6.053 M . Table IV gives some solubilities calculated in this way.

No direct measurements of these solubilities are available but Fig. 2 compares the behavior of this system at 25° with that of the sucrose-lactose-water system¹² at 0°. The molal solubility of lactose in water at 25° is less than that of mannitol, and this difference is further enhanced by the lower temperature (0°) to which the data in Fig. 2 refer. It is clear that the relative magnitudes of the solubility lowering in the presence of sucrose are very similar.

Finally, Table V contains values of the activity coefficients of both mannitol and sucrose at round concentrations in mixed solutions. It will be noted that each component is "salted" out by the other.

We wish to thank the Colonial Sugar Refining Company for the supply of purified sucrose and for the gift of a semi-micro balance.

(12) P. N. Peter, *J. Phys. Chem.*, **32**, 1856 (1928).

THE THERMODYNAMICS OF THE TERNARY SYSTEM MANNITOL-SODIUM CHLORIDE-WATER AT 25° FROM SOLUBILITY AND VAPOR PRESSURE MEASUREMENTS

BY F. J. KELLY, R. A. ROBINSON¹ AND R. H. STOKES

Department of Chemistry, University of New England, Armidale, N.S.W., Australia

Received March 13, 1961

Isopiestic measurements on the ternary system mannitol-sodium chloride-water at 25° are used to derive equations for the activity coefficients of each solute. Solubilities of mannitol in sodium chloride solutions and of sodium chloride in mannitol solutions are measured and found to be in fair agreement with those computed by extrapolation of the activity data to the saturated solutions. Each solute is "salted-in" by the other.

Introduction

The activity coefficients of mannitol and sodium chloride in mixed solutions are required in connection with our current studies of diffusion in three-component systems. The data can be obtained from isopiestic measurements of the vapor pres-

ures of mixed solutions, and such measurements are reported in Table II. This method has the advantage of being in principle applicable at any composition of the mixture, but in practice experimental limitations confine its usefulness to cases where the total concentration of the two solutes is fairly large. The study of the solubility of one solute in the presence of varying concentrations of the other

(1) National Bureau of Standards, Washington 25, D. C.

yields the activity coefficient of the first more directly, but only over a limited range of molalities of the first solute, *viz.*, those of its saturated solutions.

Experimental

Mannitol was purified by three recrystallizations from conductance water, and dried *in vacuo* at room temperature.

Sodium chloride was of Analytical Reagent quality, dried at 400°.

Conductance water was used for all solutions.

I. Solubility of Sodium Chloride in Aqueous Mannitol Solutions.—Mannitol solutions of the compositions shown in Table I were made up by weight, and portions were sealed up in 6" × 1" Pyrex tubes along with excess sodium chloride. The tubes were rotated end over end in a 25° thermostat for several days. Without removing the lower part of the tube from the thermostat, the ends were opened and a

TABLE I

SOLUBILITIES IN THE SYSTEM MANNITOL-SODIUM CHLORIDE-WATER AT 25°^a

(a) Solus. satd. with mannitol (B)			(b) Solus. satd. with sodium chloride (C)		
Obsd.	Calcd.	<i>m_C</i>	<i>m_B</i>	Obsd.	Calcd.
1.185	(1.185)	0	0	6.147	(6.147)
1.206	1.205	1.549	0.4601	6.214	6.216
1.240	1.242	3.202	.8166	6.270	6.272
1.332	1.342	5.146	1.1947	6.322	6.334
1.381	1.395	5.772	1.3956	6.360	6.366
1.411	1.427	6.089			

^a Calculated values obtained by extrapolation from the isopiestic vapor pressure results on mixed solutions. *m* = moles solute/kg. water.

pipet, fitted with a sintered-glass filter tip, previously warmed to slightly above 25°, was used to withdraw a sample of the liquid phase. This was weighed and then analyzed gravimetrically for chloride as silver chloride. The results, expressed on the molality scale, are given in Table I. The value obtained for the solubility in water alone, 6.147 mole/kg., is in good agreement with published solubility data² and also agrees exactly to the fourth significant figure with unpublished measurements made by us by the isopiestic method described by Scatchard, Hamer and Wood.³

II. Solubility of Mannitol in Sodium Chloride Solutions.

—Because of the difficulty of precise chemical analysis for mannitol in the presence of large amounts of sodium chloride, the following technique, not involving analysis, was used. A sodium chloride solution of known molality was made up by weight. Six portions of this solution were weighed into sample tubes, and known weights of mannitol were added in regularly increasing amounts, so that the first tube would certainly form a solution unsaturated with mannitol, while the sixth tube would contain a readily visible excess of solid mannitol. The sealed tubes were rotated end over end in a glass-fronted water-thermostat at 25° until equilibrium was reached, the rotation being periodically stopped for visual inspection of the tubes. Thus the composition of the solution saturated to mannitol could be estimated as lying between the compositions of two successive tubes in the series, in one of which no excess solid was visible, while the next contained a small but visible amount. On the basis of this estimate a further set of six tubes was made up, in which the interval between the successive amounts of mannitol added was much smaller; this enabled the solubility to be bracketed within 0.2%. This method proved simple and reliable, a determination of the solubility of mannitol in water alone at 25° yielding 1.185 molal in good agreement with the value of 1.186 *M* calculated from the data of Braham.⁴ The method is of course applicable only to substances of relatively high solubility, since one can scarcely detect less than a milligram of excess solid visually. The results are given in Table I.

III. Isopiestic Measurements on the System Mannitol-Sodium Chloride-Water.—The experimental technique and

TABLE II^a

<i>m_{ref.}</i>	<i>m_B</i>	<i>m_C</i>	$\frac{\Delta}{m_{BmC}}$	Diff. %
0.7000	0.2465	0.5700	0.0164	+0.03
	.4871	.4400	.0107	— .03
	.8640	.2324	.0110	— .01
1.2616	.2297	1.1483	.0205	+ .08
	.4713	1.0259	.0172	+ .08
	.7159	0.8993	.0154	+ .08
	.9595	0.7702	.0138	+ .08
1.6178	.2756	1.4870	.0098	— .08
	.5337	1.3621	.0111	— .04
	.7391	1.2592	.0091	— .04
	.9070	1.1740	.0093	— .11
2.2253	.3091	2.0923	.0189	— .01
	.3946	2.0541	.0165	— .04
	.4391	2.0342	.0162	— .05
	.6672	1.9316	.0154	— .05
3.0957	.7362	1.9013	.0172	+ .02
	1.1344	1.7129	.0134	— .03
	0.2856	2.9900	.0248	— .04
	.5505	2.8905	.0264	+ .02
3.9788	.8125	2.7872	.0239	0
	1.0622	2.6857	.0224	+0.02
	0.2296	3.9097	.0409	+ .01
	.4713	3.8348	.0393	+ .02
5.1119	.6947	3.7631	.0378	+ .04
	.9377	3.6835	.0370	+ .09
	.2253	5.0613	.0567	— .04
	.4370	5.0142	.0581	— .02
5.3382	.6707	4.9609	.0586	+ .05
	.9096	4.9023	.0566	+ .04
	.2717	5.2843	.0671	0
	.5507	5.2249	.0641	+0.02
5.9544	.8191	5.1642	.0613	0
	1.1401	5.0904	.0604	+0.08
	0.2584	5.9159	.0822	+ .02
	.5026	5.8743	.0769	— .02
1.0482	.7285	5.8359	.0757	— .02
	5.7784	.0744	+ .01	

^a B = mannitol; C = NaCl; the reference solute was sodium chloride. Δ : defined by equation 1. "Diff. %": calculated by equations 1 and 5 with *a* = -0.0145, *b* = 0.00184, *c* = -0.0022, *e* = 0.0032.

the theory of the method for the case of two non-electrolyte solutes have been given in a previous paper from this Laboratory.⁵ When one solute (C), and the reference solution are 1:1 electrolytes, the only modification required is the introduction of a factor 2

$$\Delta = 2m_{ref} \varphi_{ref} - m_B \varphi_B^0 - 2m_C \varphi_C^0 \quad (1)$$

$$\frac{\Delta}{m_B m_C} = \left(\frac{\partial \ln \gamma_B}{\partial m_C} \right)_{m_B} = 2 \left(\frac{\partial \ln \gamma_C}{\partial m_B} \right)_{m_C} \quad (2)$$

Equation 2, as before, is valid subject to the condition that the cross-differentials may be adequately described by an equation of the form

$$\left(\frac{\partial \ln \gamma_B}{\partial m_C} \right)_{m_B} \equiv 2 \left(\frac{\partial \ln \gamma_C}{\partial m_B} \right)_{m_C} = f'(m_B) + F'(m_C) \quad (3)$$

Whether this holds must be determined experimentally in each case; with the present system, it does.

Table II gives *m_{ref.}*, the molality of the reference solution, sodium chloride, in equilibrium with mixed solutions of molalities *m_B* in mannitol and *m_C* in sodium chloride, and values of Δ defined by equation 1. In computing $\Delta_i \varphi_i^0$

(2) A. Seidell, "Solubilities of Inorganic and Metalorganic Compounds," 3rd ed., D. Van Nostrand, New York, N. Y., 1940.

(3) G. Scatchard, W. J. Hamer and S. E. Wood, *J. Am. Chem. Soc.*, **60**, 3061 (1938).

(4) J. M. Braham, *ibid.*, **41**, 1707 (1919).

(5) R. A. Robinson and R. H. Stokes, *J. Phys. Chem.*, **65**, 1954 (1961).

TABLE III

MOLAL ACTIVITY COEFFICIENTS OF MANNITOL (B) AND SODIUM CHLORIDE (C) IN MIXED SOLUTION AT 25°

M_B		M_C						
		0	1	2	3	4	5	6
0	B	1.000	0.986	0.969	0.946	0.914	0.868	0.809
	C	1.000	.6569	.6676	.7137	.7832	.8740	.9862
0.3	B	1.003	.989	.974	.952	.920	.875	.816
	C	0.9980	.6555	.6656	.7107	.7782	.8662	.9742
0.7	B	1.008	.996	.981	.960	.929	.885	.826
	C	0.9953	.6538	.6633	.7068	.7720	.8561	.9585
1.0	B	1.013	1.002	.988	.968	.938	.894	.835
	C	0.9936	0.6526	.6616	.7040	.7676	.8487	.9471

for sodium chloride was taken from standard tables,⁶ and φ_B^0 for mannitol was calculated⁵ by the equation

$$\varphi_B^0 = 1 + 0.0034m_B + 0.0042m_B^2 \quad (4)$$

Equations for the Activity Coefficients in the Mixed Solutions.—A three-dimensional graph was prepared on which the quantity $\Delta/(m_B m_C)$ was represented by metal rods of appropriate length, set into a wooden baseboard representing the m_B - m_C plane. Inspection of the surface so formed suggested the equation

$$\frac{\Delta}{m_B m_C} \equiv \left(\frac{\partial \ln \gamma_B}{\partial m_C} \right)_{m_B} \equiv \left(\frac{2 \partial \ln \gamma_C}{\partial m_B} \right)_{m_C} = a + bm_C + cm_C^2 + em_B \quad (5)$$

The constants a , b , c and e then were determined by the method of least squares to have the values shown in Table II. The final column of this table shows the accuracy with which the experimental results are reproduced by equation 5; the quantity "diff.%" is defined as follows

$$m_{\text{ref(calc)}} = (\varphi_B^0 m_B + 2\varphi_C^0 m_C + \Delta_{\text{calc}})/(2\varphi_{\text{ref}})$$

where Δ_{calc} is given by equation 5 and

$$\text{"Diff. \%"} = \frac{m_{\text{ref(obs)}} - m_{\text{ref(calc)}}}{m_{\text{ref(obs)}}} \times 100$$

The "difference" column of Table II therefore gives the percentage accuracy with which the molality of the reference solution in equilibrium with a given mixture can be predicted with the aid of equations 1 and 5. Alternatively, it may be regarded as giving the percentage difference between the calculated and observed vapor pressure *lowerings* of the mixed solution. The mean difference for the 37 solutions is $\pm 0.04\%$, which is well within the estimated accuracy of the measurements, since each value of $\Delta/(m_B m_C)$ really involves three measurements, one for each solute by itself and one for the mixture.

Integration of equation 5 and conversion to common logarithms yields the following expressions for the activity coefficients of each solute

$$\log \gamma_B = \log \gamma_B^0 + 0.4343m_C \left[a + \frac{1}{2}bm_C + \frac{1}{3}cm_C^2 + em_B \right] \quad (6)$$

$$\log \gamma_C = \log \gamma_C^0 + 0.21715m_B$$

(6) R. A. Robinson and R. H. Stokes, "Electrolyte Solutions," 2nd ed., Butterworths, London, 1959.

$$\left[a + bm_C + cm_C^2 + \frac{1}{2}em_B \right] \quad (7)$$

where $\log \gamma_B^0$ is obtainable from equation 4 by the Gibbs-Duhem equation and $\log \gamma_C^0$ from the standard tables for sodium chloride. Inserting the numerical values we have

$$\log \gamma_B = 0.00295m_B + 0.00274m_B^2 - m_C[0.00630 - 0.00040m_C + 0.000318m_C^2 - 0.00139m_B] \quad (8)$$

$$\log \gamma_C = \log \gamma_C^0 - m_B[0.00315 - 0.00040m_C + 0.000478m_C^2 - 0.00035m_B] \quad (9)$$

Calculation of Solubilities.—The solubility of mannitol in water being 1.185 molal, at which concentration the activity coefficient is 1.017, we can calculate its solubility in sodium chloride solutions (Table I) by the relation

$$\log m_{B(\text{sat})} = 0.0811 - \log \gamma_{B(\text{sat})} \quad (10)$$

where $\log \gamma_{B(\text{sat})}$ is given by equation 8 with m_C equal to the sodium chloride concentration of interest.

A first approximation for γ_B is obtained by using an estimated value of m_B in equation 8; this then is substituted in equation 10 to yield a better approximation to $m_{B(\text{sat})}$; this cycle is repeated, convergence being very rapid. Similar calculations from equation 9 give the solubility of sodium chloride in mannitol solutions. Since the solutes are mutually salted-in, the values of γ_B^0 and γ_C^0 in equations 6-9 must be extrapolated beyond the range of the experimental data for aqueous solutions of the pure substances. In the case of sodium chloride, the standard tables show that $\log \gamma_C^0$ is nearly linear in m_C in the 6 *M* aqueous solution, and the extrapolation was made by assuming the formula

$$1 + \log \gamma_C^0 = 0.9940 + 0.0545(m_C - 6)$$

Agreement between the measured and calculated solubilities is excellent. For mannitol, we have had to assume that the equation

$$\log \gamma_B^0 = 0.00295m_B + 0.00274m_B^2$$

(derived from equation 4 by the Gibbs-Duhem equation) remains valid above the saturation molality. This extrapolation is clearly less satisfactory than that for sodium chloride, and may be a reason for the discrepancies of the order of 1% between the measured and calculated mannitol solubilities at the higher concentrations of sodium chloride.

Table III gives activity coefficients for both components in the mixtures at round concentrations, calculated from equations 8 and 9.

ON THE MOLECULAR BASIS OF SOME CURRENT THEORIES OF DIFFUSION¹

BY RICHARD J. BEARMAN

Department of Chemistry, University of Kansas, Lawrence, Kansas

Received April 10, 1961

The equations of Eyring and his collaborators, of Hartley and Crank, and of Gordon for the concentration dependence of diffusion coefficients in liquid solutions are examined from the point of view of statistical mechanics. Although there are some ambiguities in the original derivations, the equations are basically equivalent and are valid for solutions which are regular. It is shown that the concept of "intrinsic" diffusion coefficient is unnecessary for the understanding of diffusion processes.

I. Introduction

Recently, we have been developing a unified statistical mechanical theory of transport processes in liquid solutions.² Since earlier theories of diffusion have been utilized extensively in the interpretation of experimental data, it is of value to compare their results with those of the statistical mechanical theory. In this paper we carry out this comparison and present it in a form suitable for those who are interested in the hypotheses and conclusions but not in complex mathematical details which, after all, are only a means to an end. We shall find that for a certain class of systems the new theory leads to old equations, clarifies their significance and derivations, and relates them in ways hitherto unrecognized. In this sense, the statistical mechanical theory provides the molecular basis for the earlier theories of diffusion.

At first sight, the statistical mechanical theory seems much more complicated and difficult than other approaches. However, once one adopts the more sophisticated outlook, one finds that in many ways it is simpler. Thus, it provides an overview of all transport processes, not only that of simple diffusion, and enables their systematic study. Moreover, it is not necessary to introduce parameters which have no clear meaning. In this paper we shall see in particular that one can dispense with the concept of "intrinsic diffusion coefficient," which we believe to be the cause of some confusion.

In the next section we present the hypotheses and results of the statistical mechanical theory. In the following sections we discuss the older theories of Eyring, Hartley and Crank, and Gordon in terms of the present results. Their familiar equations for the diffusion coefficients arise from the general theory when the solutions under consideration are regular; that is, when the different molecules have similar size, shape, and interaction potentials. Thus we would not expect their equations to hold for arbitrarily complex molecules even in the absence of chemical association. Additional complications are to be expected when association is present.³ The fact that no actual solutions are exactly regular

by no means implies that the simplified equations have little value. The situation is the same as that in the equilibrium thermodynamics of solutions. There, regular solution theory provides qualitative insight and serves as a starting point for further discussion. Furthermore, its equations are extremely useful for purposes of classification and of approximate prediction.

We close our introduction with a word concerning the possibility of future progress. The present series of papers enables the calculation of transport properties of non-electrolyte solutions in terms of their equilibrium properties. The situation is particularly simple for regular solutions where we have obtained explicit results. For more complicated solutions, it appears that it will not be possible to predict transport parameters precisely until there is an improvement in the status of the theory of the equilibrium state. At the present time, we believe that emphasis should be placed on experimental studies of simple solutions, especially those of the liquefied rare gases, with a view toward testing the present results. The thermodynamic behavior of these systems should be studied concurrently, for we should not expect regular solution theory to predict transport properties any more accurately than it predicts equilibrium thermodynamic properties.

II. The Statistical Mechanical Theory.—The mean frictional force acting on a molecule of species α in a ν component system undergoing one-dimensional, isothermal, isobaric diffusion may be denoted by $\bar{F}_\alpha^{(1, \nu)*}$. It is defined as follows in terms of distribution functions^{2b}

$$\bar{F}_\alpha^{(1, \nu)*} = 1/2 \sum_{\beta=1}^{\nu} \int c_\beta(\tau/r) \frac{dV_{\alpha\beta}}{dr} (g_{\alpha\beta}^{(2, \nu)} - g_{\beta\alpha}^{(2, \nu)}) d^3r \quad (1)$$

where c_β is the concentration of species β in units of molecules per unit volume. In eq. 1, $V_{\alpha\beta}$ is the potential of intermolecular force between molecules of species α and β . It is assumed to depend only upon the magnitude r of the vector distance \mathbf{r} separating the molecules and not upon the orientation of the molecules. The potential may be regarded as a smoothed potential in which effects of orientation and internal degrees of freedom, if present, have been averaged out. Thus, the present theory cannot account for such effects. A study of them (which would be of great value) is unnecessary in this communication, for we are here providing a rigorous basis to theories which make no pretense of accounting for complexities of molecular structure.

(1) This research was supported in part by a grant from the Office of Scientific Research of the U. S. Air Force to the University of Kansas.

(2) (a) R. J. Bearman, J. G. Kirkwood and M. Fixman, *Advances in Chem. Phys.*, **1**, 1 (1958); (b) R. J. Bearman and J. G. Kirkwood, *J. Chem. Phys.*, **28**, 136 (1958); (c) R. J. Bearman, *ibid.*, **29**, 1278 (1958); (d) *ibid.*, **30**, 835 (1959); (e) *ibid.*, **31**, 751 (1959); (f) *ibid.*, **32**, 1308 (1960); (g) R. J. Bearman and P. F. Jones, *ibid.*, **33**, 1432 (1960); (h) R. J. Bearman and V. S. Vaidyanathan, *ibid.*, **34**, 264 (1961).

(3) R. R. Irani and A. W. Adamson, *J. Phys. Chem.*, **64**, 199 (1960).

At equilibrium, the radial distribution function $g_{\alpha\beta}^{(2,0)}$ is an important determining factor in the behavior of thermodynamic systems.⁴ Its physical significance is that $-kT \ln g_{\alpha\beta}^{(2,0)} = W_{\alpha\beta}$, where $W_{\alpha\beta}$ is the potential of mean force acting on a molecule of species α near a molecule of species β , k is Boltzmann's constant, and T is the absolute temperature. The quantities $W_{\alpha\beta}$ and $g_{\alpha\beta}^{(2,0)}$ are in general composition dependent because the average force acting on the molecule of species α depends on the presence of other molecules in the system besides that of the fixed molecule. When the system is not at equilibrium the Boltzmann distribution law does not apply and the radial distribution function must be replaced by the pair correlation function $g_{\alpha\beta}^{(2)}$. Unlike the radial distribution function, it does not have spherical symmetry. The difference between the pair correlation function and the radial distribution function is the non-equilibrium perturbation, $g_{\alpha\beta}^{(2,1)}$, which appears in eq. 1. One of the objectives of the statistical mechanical theory is to determine $g_{\alpha\beta}^{(2,1)}$ insofar as possible in terms of $g_{\alpha\beta}^{(2,0)}$ and thereby express transport properties in terms of equilibrium functions of state.^{2b}

It is a mathematical consequence of eq. 1 that if we expand $g_{\alpha\beta}^{(2,1)}$ in a series of spherical harmonics, only the first harmonic contributes to the integral. Furthermore, in accordance with the phenomenological theory of transport, the perturbation should be a linear function of the velocities. We may meet these conditions by writing^{2b}

$$\frac{g_{\alpha\beta}^{(2,1)}}{g_{\alpha\beta}^{(2,0)}} = \psi_{\alpha\beta}^{(1)} \frac{\mathbf{r}}{r} \cdot (\mathbf{u}_\beta - \mathbf{u}_\alpha) + \text{harmonics of different order} \quad (2)$$

where \mathbf{u}_β and \mathbf{u}_α are the mean velocities of molecules of species β and α , respectively. These velocities are to be measured with respect to coordinates fixed in the laboratory. Thus, that contribution to $g_{\alpha\beta}^{(2,1)}$ which concerns us is proportional to the cosine of the angle between the vector separation, r , of the two molecules and the relative bulk velocities of species β and α . Now, eq. 2 is not the most general linear form for $g_{\alpha\beta}^{(2,1)}$ which is compatible with the above restrictions. Arguments in favor of eq. 2 are that it is in agreement with the Brownian motion theory of Kirkwood,⁵ that it agrees with some phenomenological considerations stressed especially by Laity,⁶ and that it leads readily to the Onsager reciprocal relations. Apart from questions concerning its general validity, it appears to be one of the assumptions implicit in the theories we are attempting to evaluate.

Shortly after a concentration gradient is established in a system, a quasi-stationary regime is reached in which the driving force for diffusion, the negative of the gradient of chemical potential, becomes sensibly equal in magnitude, but opposite in sign, to the frictional force.^{2c} From eq. 1 and 2, we then have

$$\frac{d\mu_\alpha}{dx} = \bar{F}_\alpha^{(1,1)*} = - \sum_{\beta=1}^r c_\beta \zeta_{\alpha\beta} (u_\alpha - u_\beta) \quad (3)$$

where μ_α is the chemical potential—the partial molecular Gibbs free energy—of species α and x is the dimension in the line of diffusion. The coefficients of friction $\zeta_{\alpha\beta}$ are defined by the relation

$$\zeta_{\alpha\beta} = \frac{1}{6} \int g_{\alpha\beta}^{(2,0)} \frac{dV_{\alpha\beta}}{dr} \{ \psi_{\alpha\beta}^{(1)} + \psi_{\beta\alpha}^{(1)} \} d^3r \quad (4)$$

The friction coefficients, which are ensemble averages, will in general depend upon composition. Since $V_{\beta\alpha} = V_{\alpha\beta}$ by definition and⁴ $g_{\alpha\beta}^{(2,0)} = g_{\beta\alpha}^{(2,0)}$, the friction coefficients obey the reciprocal relation $\zeta_{\alpha\beta} = \zeta_{\beta\alpha}$.

From eq. 3, Fick's law of mutual diffusion may be derived readily for a two component system. Several authors have emphasized the importance of the choice of a frame of reference with respect to which diffusion coefficients are measured.⁷ The choice is in some degree arbitrary but must always be specified. We select the volume frame because experimental data are often referred to it. However, our results may be readily converted to other frames if that is desirable. The volume velocity u^0 is defined to be $\sum_\alpha c_\alpha \bar{v}_\alpha u_\alpha$ and the diffusion flux of species α with respect to it, j_α^0 , is $c_\alpha (u_\alpha - u^0)$. The fluxes j_α^0 are not independent, for

$$\bar{v}_1 j_1^0 + \bar{v}_2 j_2^0 = 0 \quad (5a)$$

where \bar{v}_α is the partial molecular volume of species α .

In a two component system, eq. 3 reduces to

$$\begin{aligned} \frac{d\mu_1}{dx} &= -c_2 \zeta_{12} (u_1 - u_2), \\ \frac{d\mu_2}{dx} &= -c_1 \zeta_{12} (u_2 - u_1) \end{aligned} \quad (5b)$$

Adding and subtracting u^0 in eq. 5b and using eq. 5a, we have

$$\begin{aligned} j_1^0 &= -D \frac{dc_1}{dx}, \quad j_2^0 = -D \frac{dc_2}{dx} \\ D &\equiv \frac{\bar{v}_1 kT}{\zeta_{12}} \left[1 + \left(\frac{\partial \ln f_2}{\partial \ln c_2} \right)_{T,P} \right] \\ &\equiv \frac{\bar{v}_2 kT}{\zeta_{12}} \left[1 + \left(\frac{\partial \ln f_1}{\partial \ln c_1} \right)_{T,P} \right] \end{aligned} \quad (5c)$$

The equality of the diffusion coefficients D for the two fluxes follows from the Gibbs-Duhem equation and eq. 5a. The activity coefficients f_α are defined by the relations⁸

$$\begin{aligned} \mu_\alpha &= \mu_\alpha^0(T, P) + kT \ln a_\alpha \\ a_\alpha &= f_\alpha c_\alpha \end{aligned} \quad (6)$$

Molar units also may be used. We see from eq. 5c that the mutual diffusion coefficient D is related to the friction coefficient and therefore to the deviation $g_{12}^{(2,1)}$ of the pair correlation function $g_{12}^{(2)}$ from its equilibrium value.

Self-diffusion in a mixture is, in theory, the diffusion of a trace of a substance *identical* with one of the constituents. In practice, this is approximated by isotopic labeling techniques or similar methods. If we denote the labeled species by 1^* , we have from eq. 3

(7) J. G. Kirkwood, R. L. Baldwin, P. J. Dunlop, L. J. Gosting and G. Kegeles, *J. Chem. Phys.*, **33**, 1505 (1960).

(8) It is erroneously stated in ref. 2c that μ_α^0 is the chemical potential of pure α .

(4) J. G. Kirkwood, *J. Chem. Phys.*, **3**, 300 (1935).

(5) J. G. Kirkwood, *ibid.*, **14**, 180 (1946).

(6) R. W. Laity, *J. Phys. Chem.*, **63**, 80 (1959).

$$\frac{d\mu_1^*}{dx} = -(c_1 \zeta_{1*1} + c_2 \zeta_{1*2}) u_1^* \quad (7)$$

The terms involving u_1 and u_2 vanish because 1^* is present in such small quantity that it imparts no bulk velocity to species one and two. Since 1 and 1^* are identical we assume that we may replace ζ_{1*2} by ζ_{12} . We define ζ_{11} to be ζ_{1*1} . From eq. 7, we find that

$$\begin{aligned} j_1^* &= -D_1 \frac{dc_1^*}{dx} \\ D_1 &= kT/\zeta_1 \\ \zeta_1 &= c_1 \zeta_{11} + c_2 \zeta_{12} \end{aligned} \quad (8)$$

The gradient of the activity coefficient does not contribute to the flux in self-diffusion because the trace species moves through a uniform environment. D_1 is the self-diffusion coefficient of species one. The self-diffusion coefficient, D_2 , of species two is defined similarly. In a diffusing system, we then have three experimental diffusion coefficients D , D_1 , and D_2 corresponding to the three friction coefficients ζ_{12} , ζ_1 and ζ_2 . The diffusion coefficients may be measured separately and the friction coefficients determined from them. Both the friction coefficients and the diffusion coefficients depend in general on composition. At infinite dilution, the processes of mutual diffusion and of self-diffusion of the solute become physically identical. We might therefore expect the two diffusion coefficients to become equal in that limit. By eq. 5c and 8, the mutual diffusion coefficient does become equal to the self-diffusion coefficient provided that ζ_{12} remains finite or approaches infinity more slowly than the solute concentration approaches zero. This will be the case in the simple systems in which we are principally interested.

It is well-known that statistical mechanical predictions of thermodynamic properties of fluids involve considerations concerning the behavior of pairs of molecules.⁴ To predict transport properties we consider the motion of molecular pairs.² In particular, we use an analog of eq. 3 for the motion of a molecule in the presence of a second molecule. The analogous equation differs from Eq. (3) on both the left and right hand sides. The driving force for diffusion contains a term involving the gradient of the perturbation to the radial distribution function in addition to the one containing the gradient of chemical potential. The expression for the frictional force *must* take into account the fact that the average velocity of a molecule in the presence of another molecule differs from its velocity in the bulk. It also should take into account the dependence of the pair friction coefficient upon intermolecular separation. In practice it does not. With the hope that the dependence of the pair coefficient on intermolecular separation is not great, practical theories of transport phenomena, including the theory of interionic attraction, assume (implicitly or explicitly) that the pair coefficient may be replaced by $\zeta_{\alpha\beta}$, which it does approach asymptotically at large distances between the molecules. We, too, introduce this approximation. At present, it is not possible to evaluate the extent of its validity except insofar as its results agree with experiment, but its presence should not be forgotten. When the mathe-

matical details are carried through, we are able to obtain relations for the ratios of the friction coefficients, but not their absolute values.^{2f} For example

$$\frac{\zeta_{11} v k T}{x_1 \zeta_{11} + x_2 \zeta_{12}} = \frac{1}{6} \int \frac{d}{dr} V_{11} g_{11}^{(2,0)} \psi_{11} d^3 r \quad (9)$$

$$\psi_{11} \equiv \psi_{11}^{(1)} 2D_1$$

where v is the mean molecular volume (the molar volume divided by Avogadro's number) and x_1 and x_2 are mole fractions. The parameter ψ_{11} is determined by the equilibrium radial distribution function. Apparently, the calculation of the absolute values of diffusion coefficients requires their interpretation as autocorrelation functions. The autocorrelation theory may be joined with the present theory to provide a complete theory of transport coefficients.

Generally, the ratio on the left side of eq. 9 will depend upon composition. However, it is constant in the special case when (i) the radial distribution functions are independent of mole fraction at constant temperature and pressure and (ii) the volumes are additive; *i.e.*, $v = x_1 v_1 + x_2 v_2$, where v_1 and v_2 are the molecular volumes of the pure components. Such solutions are considered by Hildebrand and Scott in their treatise on nonelectrolytes⁹ in connection with the theory of regular solutions. For simplicity, we shall call these solutions "regular," although they may constitute a class of solutions slightly different from those with ideal entropies of mixing. The interpretation of $-kT \ln g_{\alpha\beta}^{(2,0)}$ as the potential of mean force suggests that the radial distribution function will never be *exactly* independent of composition unless species one and two are identical. However, one might expect that it is approximately constant whenever the molecules have similar size, shape and interaction potentials. When the ratios of friction coefficients are constant, it may be shown^{2f} that

$$\begin{aligned} \frac{D_1}{D_2} &= \frac{v_2}{v_1} \\ D &= D_1 \left[1 + \left(\frac{\partial \ln f_1}{\partial \ln c_1} \right)_{T,P} \right] \\ &= D_1 \left(\frac{\partial \ln a_1}{\partial \ln c_1} \right)_{T,P} \end{aligned} \quad (10)$$

But

$$\left(\frac{\partial \ln a_1}{\partial \ln c_1} \right)_{T,P} = \left(\frac{\partial \ln a_1}{\partial \ln x_1} \right)_{T,P} \frac{x_1 v_1 + x_2 v_2}{v_2} \quad (11)$$

so that

$$D = \left(\frac{\partial \ln a_1}{\partial \ln x_1} \right)_{T,P} \left[\frac{x_1 D_1 v_1}{v_2} + x_2 D_1 \right] \quad (12a)$$

$$= \left(\frac{\partial \ln a_1}{\partial \ln x_1} \right)_{T,P} [D_2 x_1 + D_1 x_2] \quad (12b)$$

The general theory also provides expressions for the coefficient of shear viscosity η .^{2g} Under the regular solution hypothesis, $D_1 \eta$ is independent of composition. If we multiply the second of eq. 10 by η and replace $D_1 \eta$ by $D^\infty \eta_2$, where D^∞ is the value of the mutual diffusion coefficient at infinite

(9) J. H. Hildebrand and R. L. Scott, "The Solubility of Nonelectrolytes," Reinhold Publ. Corp., New York, N. Y., 1950, 3rd ed., Chapt. VII.

dilution of species one (equal to D_1 at that concentration) and η_2 is the viscosity coefficient of pure species two, we find

$$D\eta = D^\infty\eta_2 \left[1 + \left(\frac{\partial \ln f_1}{\partial \ln c_1} \right)_{T,P} \right] \quad (13)$$

Multiplying the first eq. 12 by γ and replacing $D_1\eta$ by $D^\infty\eta_2$ we also have¹⁰

$$D\eta = \left[D^\infty\eta_2 \left(\frac{v_1}{v_2} - 1 \right) x_1 + D^\infty\eta_2 \right] \left(\frac{\partial \ln a_1}{\partial \ln x_1} \right)_{T,P} \quad (14)$$

Equations 10, 12a, 12b, 13 and 14 are alternative representations of the concentration dependence of the diffusion coefficients. They are all equally valid within the framework of the statistical mechanical theory. Equations 10–12 provide relationships between the mutual diffusion and self-diffusion coefficients in a mixture at a given composition. Equations 13 and 14 relate the product $D\eta$ at a given composition to its value at infinite dilution. Equation 12a follows from the second of eq. 10 by a purely equilibrium thermodynamic transformation, and hence the two are interchangeable. Likewise eq. 13 and 14 are thermodynamically equivalent. We shall see that eq. 10–14 are the precise statements of the Eyring, Hartley-Crank, and Gordon equations.

III. Comparison With Earlier Theories.¹¹ The Absolute Reaction Rate Theory.—This comprehensive theory of rate processes developed by Eyring and his collaborators is most completely discussed in the well-known monograph by Glasstone, Laidler and Eyring.¹² These authors adopt a quasi-crystalline model and consider separately diffusion in "ideal" and "non-ideal" solutions.

In the ideal case they compute the forward and reverse fluxes across a plane. The net flux is the difference between the two and is related by Fick's law to the diffusion coefficient D (their notation). Apart from the assumption that the flux is proportional to the jump length λ , which is not obvious to this critic, the principal hypothesis is that the rate constant k is the same for passage in both the forward and backward directions. On this basis they find that

$$D = \lambda^2 k \quad (15)$$

Glasstone, Laidler and Eyring emphasize that this relationship should hold only in ideal or dilute solutions. However, a more general interpretation of D is to suppose that it represents the self-diffusion coefficient of a species in any mixture. For, in self-diffusion, the diffusing molecule observes a uniform environment and *a priori* may move with equal likelihood in either direction. By this interpretation self-diffusion represents a purely statistical effect caused by the natural tendency towards maximum randomization. In this regard, we note that by eq. 3 whenever a gradient of chemical

potential exists a molecule does feel on the average a frictional force. The existence of this force, even in the ideal or dilute case when the surroundings are uniform, is connected with the so-called Gibbs' paradox of equilibrium thermodynamics: entropy or free energy changes may occur even when thermodynamic energy changes vanish. By comparison with the absolute reaction rate theory of viscosity, Glasstone, Laidler and Eyring suggest that

$$D\eta = \frac{\lambda_1 kT}{\lambda_2 \lambda_3}, \quad (16)$$

where k is Boltzmann's constant, λ_1 , λ_2 , and λ_3 are distances of the order of intermolecular separations and η is the coefficient of viscosity. We shall return to eq. 16 when we discuss diffusion in concentrated solutions.

Mutual diffusion in concentrated solutions differs from that in dilute solutions in that the probabilities of motion of a molecule in the forward and backward directions are no longer equal. Glasstone, Laidler and Eyring derive an expression (page 534) for this case starting with the equation

$$k = k_0 \frac{\gamma}{\gamma_\ddagger}, \quad (17)$$

where k is the specific rate for diffusion, k_0 is the specific rate in the "ideal" system, γ is the activity coefficient of the diffusing molecule in its initial state and γ_\ddagger is the activity coefficient in the activated state. The coefficients γ are mole fraction activity coefficients (*cf.* their page 410) defined by the relation

$$\begin{aligned} \mu_\alpha &= \mu_\alpha^\circ(T, P) + kT \ln a_\alpha' \\ a_\alpha' &= x_\alpha \gamma_\alpha \end{aligned} \quad (18)$$

From eq. 17, they find for the mutual diffusion coefficient D_1 of species one

$$\begin{aligned} D_1 &= \gamma^2 k \left[1 + \left(\frac{\partial \ln \gamma_1}{\partial \ln x_1} \right) \right] \\ &= D_1^0 \left[1 + \left(\frac{\partial \ln \gamma_1}{\partial \ln x_1} \right) \right] \end{aligned} \quad (19)$$

where D_1^0 is the diffusion coefficient in an "ideal" system and is to be identified with D of eq. 15. Glasstone, Laidler and Eyring multiply eq. 19 by η and then replace $D_1\eta$ by $\lambda_1 kT / \lambda_2 \lambda_3$ according to eq. 16. They then suggest that $\lambda_1 kT / \lambda_2 \lambda_3$ should be a linear function of mole fraction and thus $D_1\eta / [1 + (\partial \ln \gamma_1 / \partial \ln x_1)]$ should be a straight line when plotted *versus* mole fraction. Upon identification of their D_1 with the experimental diffusion coefficient (our D) they verify this for the system chloroform-ether.

So far, we have been considering the absolute reaction rate theory more or less within its own context. We now examine it in the light of the statistical mechanical theory. First, we observe that the statistical mechanical approach is more general, for, at the outset, the theory of absolute rates assumes a simplified quasi-crystalline model and a particular activated state mechanism for the diffusion process. However, it is entirely possible that a restricted approach leads to correct equations. It is with the object of exposing the valid aspects of the theory that we carry out our analysis.

(10) The derivations of eq. 12 and 14 from eq. 10 were communicated to the author by Dr. E. McLaughlin of The Imperial College of Science and Technology, and he has kindly permitted their publication here.

(11) In this discussion we shall attempt to retain the notation of the previous authors. Consequently, the same symbol may be used to represent different quantities and the same quantity may be represented at times by different symbols.

(12) S. Glasstone, K. J. Laidler and H. Eyring, "The Theory of Rate Processes," McGraw-Hill Book Co., Inc., New York, N. Y., 1941, Chapt. IX.

We have already identified the diffusion coefficients D of eq. 15 and 16 and D_1^0 of eq. 19 with the self-diffusion coefficient of a species in a mixture at a given composition. Equation 19 is therefore very similar to eq. 10 if the mutual diffusion coefficient D_1 is taken to be identical with the coefficient D of our theory (note that D of our theory is D_1 of Glasstone, Laidler and Eyring whereas our D_1 is their D or D_1^0 .) The principal difference between the two equations is that $\partial \ln j_1 / \partial \ln c_1$ appears in eq. 10 while $\partial \ln \gamma_1 / \partial \ln x_1$ occurs in eq. 19. Examination of the derivation of eq. 17 to be found on pages 187-90 and particularly 402-404 suggests that the concentration activity coefficient f_1 defined in our eq. 6 is more appropriate. The reason for this is that concentrations in units of molecules per unit volume are utilized in the derivations and therefore the original activities which the authors introduce are concentration activities. They hedge a little in order to switch to mole fraction activities. However, if that unnecessary change is not made, their derivations then lead to the modified form of eq. 19

$$D_1 = D_1^0 \left[1 + \left(\frac{\partial \ln f_1}{\partial \ln c_1} \right)_{T,P} \right] \quad (20)$$

With this correction, it appears that the two equations 10 and 19 are identical. Thus the coefficient D_1 of eq. 19 or 20 is actually the mutual diffusion coefficient (D in our notation) in the volume frame of reference. From the derivation of eq. 10, we see that implicit in the absolute rate theory is the assumption of the regularity of the solution. The diffusion coefficients of other solutions should not be expected to obey a simple formula.

We now investigate the basis of their suggestion (cf. eq. 19) that $D_1\eta/(1 + \partial \ln \gamma_1 / \partial \ln x_1)$ is linear in the mole fraction. According to our interpretation, $D_1^0\eta (= \lambda_1 kT / \lambda_2 \lambda_3$ in the absolute rate theory) is simply the product of the self-diffusion coefficient and the viscosity coefficient in the mixture at a given composition. We have seen that the statistical mechanical theory suggests that in a regular solution it is independent of composition. Glasstone, Laidler and Eyring suppose without justification that it is linear in mole fraction. The experimental measurements of Carman and Stein¹³ verify the near constancy of $D_1^0\eta$ in a simple system, ethyl iodide-*n*-butyl iodide. Why, then, should $D_1\eta/(1 + \partial \ln \gamma_1 / \partial \ln x_1)$ be linear in mole fraction? The answer is that it is eq. 20 or its thermodynamic equivalent, eq. 12a, which should be used and not eq. 19. The linearity of $D\eta/(1 + \partial \ln \gamma_1 / \partial \ln x_1)$ (here using our notation) follows from eq. 12a (or 14) when it is noted that by eq. 6 and 18

$$\left(\frac{\partial \ln a_1}{\partial \ln x_1} \right)_{T,P} = \left(\frac{\partial \ln a_1'}{\partial \ln x_1} \right)_{T,P} = 1 + \left(\frac{\partial \ln \gamma_1}{\partial \ln x_1} \right)_{T,P} \quad (21)$$

To obtain the linearity, we have assumed that the solution is regular. The importance of this limitation is borne out by experiment. Anderson, Hall and Babb¹⁴ examined a number of complex, strongly non-ideal systems and discovered that the ratio of $D\eta$ to the derivative of the logarithm of the ac-

tivity is not linear in general. For nearly ideal solutions, however, Caldwell and Babb¹⁵ found that the ratios are almost linear. The complexity of the friction coefficient ratio of eq. 9 in the general case also suggests that the condition of regularity may be necessary as well as sufficient.

We conclude that the absolute rate theory is compatible with the statistical mechanical theory. For the purposes of predicting the concentration dependence of diffusion coefficients, its principal virtue is that it provides a simple and understandable description of the diffusion process. Its defects are that: (i) the description is probably oversimplified in liquids, (ii) several important assumptions on the molecular level are concealed in the model, (iii) the physical significance of some of its parameters remain in doubt until determined from more detailed theories, and (iv) the intuitive reasoning involved in the derivations may lead to incorrect equations and misinterpretations of experimental data.

The Hartley-Crank Theory.—In the first five sections of their paper, Hartley and Crank¹⁶ consider the effect of choices of frames of reference and units of concentration upon the value of the diffusion coefficient. They define their frames of reference with respect to the walls of vessels which contain the diffusing systems. It seems to us that it is clearer to consider diffusion fluxes defined with respect to local mean velocities. Thus, the volume velocity u^0 at a point is defined to be $\sum c_\alpha \bar{v}_\alpha u_\alpha$

and the local fluxes j_1^0 and j_2^0 are $c_1(u_1 - u^0)$ and $c_2(u_2 - u^0)$, respectively, by definition. Fick's law then follows from the phenomenological equation (5)

$$j_1^0 = -D \partial c_1 / \partial x, \quad j_2^0 = -D \partial c_2 / \partial x \quad (22)$$

Here, the velocities u_1 and u_2 which determine u^0 are the bulk velocities of species one and two measured at a point fixed with respect to a Newtonian (laboratory) coordinate system. To be sure, u_1 and u_2 are not necessarily directly observable in a given experiment, but they are always well-defined on the molecular level as ensemble average velocities. The implications of Hartley and Crank to the contrary notwithstanding, eq. 22 are valid in a fluid whether or not u^0 is zero and whether or not the volumes are additive. Likewise, the definition of the volume velocity is unambiguous under all circumstances. The relationship of experimental data to the diffusion coefficient D may become complicated when u^0 is not zero. That, however, is a different problem involving the initial and boundary conditions, and, for the purpose of understanding the relationships among the various differential diffusion coefficients, it need not be considered. Hartley and Crank remark that a binary system undergoing mutual diffusion can be described by one diffusion coefficient, and alternative diffusion coefficients are thermodynamically related to each other. We heartily concur with this opinion, for, by eq. 5b, all mutual diffusion coefficients are simple functions of the friction coefficient. Unfor-

(13) P. C. Carman and L. H. Stein, *Trans. Faraday Soc.*, **52**, 619 (1956).

(14) D. K. Anderson, J. R. Hall and A. L. Babb, *J. Phys. Chem.*, **62**, 404 (1958). In this paper, the system chloroform-ether also is given further consideration.

(15) C. S. Caldwell and A. L. Babb, *ibid.*, **60**, 51 (1956).

(16) G. S. Hartley and J. Crank, *Trans. Faraday Soc.*, **45**, 801 (1949).

tunately, as we shall see in the following, Hartley and Crank do not maintain their position in a consistent way. The reason is that they do not use clear and straightforward fundamental definitions and equations.

In section six, Hartley and Crank discuss the physical nature of diffusion. They point out that diffusive motions of molecules are in general superimposed upon the mass flow of the system. They suggest that the volume frame diffusion coefficient, our D , does not properly separate effects of the mass flow from those due to diffusive flow. In this, they are in error: Phenomenologically, ordinary mutual diffusion in a binary system is described by eq. 5b, which concerns only the difference of the velocities of the two species and not the mass flow. When considering diffusion, it is often convenient to add and subtract a reference velocity and rewrite that equation as Fick's law. Since Fick's law comes from eq. 5b, the reference velocity and hence the mass flow effects cancel out. It thus makes no difference whether we use the volume velocity, the center of mass velocity, or any other reasonable reference velocity.¹⁷ They all describe the process of mutual diffusion equally well. Because of their fallacious notion that the volume frame diffusion coefficient does not adequately describe mutual diffusion, Hartley and Crank are led to the concept of "intrinsic" diffusion coefficient. We shall prove explicitly in the next paragraph that this concept adds nothing new to the description of mutual diffusion.

The seventh section of the paper by Hartley and Crank is concerned with the definition of "intrinsic" diffusion coefficients, \mathfrak{D}_A and \mathfrak{D}_B . These are defined with reference to a cross-section through which there is no net mass flow. For systems in which there is no volume change upon mixing, Hartley and Crank evaluate the net flow across a section moving with the mass velocity (which they never define precisely) and relate this to the net flux across a volume fixed section. They find for species A and B

$$D^V = v_{AC} (\mathfrak{D}_B - \mathfrak{D}_A) + \mathfrak{D}_A \quad (23)$$

Here D^V is our D , c_A is the concentration of species A (the authors use the symbol C_A^V but this change will cause no confusion), and v_A is its molar volume. The authors assert that \mathfrak{D}_A and \mathfrak{D}_B usually cannot be obtained separately. By relating \mathfrak{D}_A and \mathfrak{D}_B individually to D^V , we shall show that this is not the case. We shall show also that they are simply ordinary diffusion coefficients and thus occupy no special role from the molecular point of view. The exact definition of the "intrinsic" diffusion coefficient depends on which mass velocity is used. For our purposes, it is most convenient to use molar (or molecular) units. Thus we define the mass velocity u

$$cu = \sum_i c_i u_i \quad (24a)$$

$$\frac{1}{v} = c = \sum_i c_i$$

and the flux j_i

$$j_i = c_i (u_i - u). \quad i = A, B \quad (24b)$$

Evidently

$$j_A + j_B = 0 \quad (25)$$

Since, as usual, j_i at a point is equal to the number of moles per unit time per unit area crossing a plane moving with velocity u , eq. 25 states that the net number of moles crossing the plane is zero. Hence the velocity u may be used to represent a mass velocity in the sense of Hartley and Crank. Starting with the defining equations, eq. 5 and 24 for the fluxes and velocities, we derive expressions for \mathfrak{D}_A and \mathfrak{D}_B in terms of D^V

$$j_A - j_A^0 = c_A (u^0 - u) \quad (26)$$

But

$$u^0 - u = \sum_i c_i \bar{v}_i u_i - \sum_i \frac{c_i u_i}{c} = \frac{(\bar{v}_A - \bar{v}_B) x_A x_B}{v} (u_A - u_B) \quad (27)$$

To obtain the right-hand side, we have used the thermodynamic relations

$$c = 1/v, c_i = x_i/v, v = x_A \bar{v}_A + x_B \bar{v}_B \quad (28)$$

Because

$$u_A - u_B = (u_A - u^0) - (u_B - u^0) = j_A^0/c_A - j_B^0/c_B \quad (29)$$

and by eq. (5a)

$$\bar{v}_A j_A^0 + \bar{v}_B j_B^0 = 0 \quad (30)$$

eq. 26 and 27 reduce readily to

$$j_A = j_A^0 + \frac{x_A (\bar{v}_A - \bar{v}_B)}{\bar{v}_B} j_A^0 = \frac{j_A^0 v}{\bar{v}_B} \quad (31)$$

By symmetry

$$j_B = \frac{j_B^0 v}{\bar{v}_A} \quad (32)$$

From eq. 22 (recall D^V is our D), we then have

$$j_A = -\frac{D^V v}{\bar{v}_B} \frac{\partial c_A}{\partial x}, j_B = -\frac{D^V v}{\bar{v}_A} \frac{\partial c_B}{\partial x} \quad (33)$$

Thus \mathfrak{D}_A , which is the diffusion coefficient in the mass velocity frame of reference, must be equal to $D^V v / \bar{v}_B$ and \mathfrak{D}_B likewise is $D^V v / \bar{v}_A$. The "intrinsic" diffusion coefficients are therefore each determined directly by D^V . From this result, we may obtain the more complicated expression, eq. 23, of Hartley and Crank. For

$$\begin{aligned} D^V &\equiv D^V v \left[c_A + \frac{1 - c_A \bar{v}_A}{\bar{v}_B} \right] \\ &= D^V v \left[c_A - \frac{c_A \bar{v}_A}{\bar{v}_B} \right] + \frac{D^V v}{\bar{v}_B} \\ &= c_A \bar{v}_A \left[\frac{D^V v}{\bar{v}_A} - \frac{D^V v}{\bar{v}_B} \right] + \frac{D^V v}{\bar{v}_B} \\ &= c_A \bar{v}_A [\mathfrak{D}_B - \mathfrak{D}_A] + \mathfrak{D}_A \end{aligned} \quad (34)$$

Notice that we have not even found it necessary to assume that the volumes are additive. To derive eq. 33 and eq. 34 we have not used eq. 5 or the assumption of regularity or, indeed, any assumption of a molecular nature. We have proved that all phenomenological schemes which lead to Fick's law in the volume frame also lead to Fick's law in the mass frame, and conversely, with only one independent diffusion coefficient.¹⁸

(17) The criterion of reasonableness for a reference velocity is that it leads to Fick's law when substituted into eq. 5.

(18) One must not suppose from our discussion that we have uniquely determined the intrinsic diffusion coefficient. On p. 813, Hartley and

In the eighth and final section of their paper, Hartley and Crank present a "tentative quantitative theory." They first consider diffusion in ideal dilute solutions and by the usual arguments used in deriving the Stokes-Einstein relation find

$$D_A = \frac{RT}{N} \frac{1}{\sigma_A \eta} \quad (35)$$

where σ_A is a parameter with the dimensions of length, N is Avogadro's number, R is the gas constant, η is the viscosity, and D_A is the diffusion coefficient in the dilute solution. By a more abstruse argument, they discover for concentrated solutions

$$\mathfrak{D}_A = \frac{RT}{N} \frac{d \log x_A \gamma_A}{\sigma_A \eta d \log c_A} \quad (36)$$

[the authors use the symbol $N_A f_A$ and not $x_A \gamma_A$ but in this case it seems clear that they are referring to the activity of eq. 18]. It is by no means obvious from their derivation that \mathfrak{D}_A is identical with the "intrinsic" diffusion coefficient of the previous section. However, they insert eq. 36 into eq. 23 and discover

$$D^V = \frac{RT}{N} \frac{d \log x_A \gamma_A}{d \log x_A} \left(\frac{x_B}{\sigma_A \eta} + \frac{x_A}{\sigma_B \eta} \right) \quad (37)$$

In practical application the quantities $RT/N\sigma_A\eta$ and $RT/N\sigma_B\eta$ of eq. 37 have been replaced by the self-diffusion coefficients of A and B in the mixture.^{13,19} Generally, it does not appear possible to interpret eq. 36 and 37 in terms of the statistical mechanical theory. For regular solutions, a simple interpretation is possible. We first remark that the mutual diffusion coefficient, D_A of eq. 35 in the ideal dilute case is equal to the self-diffusion coefficient. But for regular solutions the statistical mechanical theory implies (without using the Stokes' equation) that the product of the self-diffusion coefficient and the viscosity is independent of composition. Thus $RT/N\sigma_A$ is $D_A\eta$ at any composition where D_A is the self-diffusion coefficient of A. Substituting this result into the right-hand side of eq. 36 and using eq. 6 and 18, we find

Crank define the intrinsic diffusion coefficient: "It is desirable to define new diffusion coefficients \mathfrak{D}_A and \mathfrak{D}_B in terms of the rate of transfer of A and B, respectively, across a section fixed so that no net mass flow occurs through it." The condition of no net mass flow is given by our eq. 25. By defining different mass velocities and using alternative units of mass, we may write down other "intrinsic" diffusion coefficients which obey this condition and also obey eq. 23. These, however, will all be mutually dependent, which leaves unaltered our conclusion that there exists only one independent mutual diffusion coefficient in a binary system. The multiplicity of possible intrinsic diffusion coefficients strengthens our conviction that there exists little need to introduce them. Hartley and Crank leave open the choice of the mass unit. For our present purposes of inter-relating the various theories, we have found it convenient to use the mole as our unit of mass. This by no means violates the spirit of their approach. One might inquire whether a perfectly general choice of the unit of mass would not also permit the volume frame diffusion coefficient to be regarded as an intrinsic diffusion coefficient. This would be logically correct, but we omit this possibility from consideration because Hartley and Crank clearly wish to distinguish the volume frame from the mass frame. We also wish to emphasize that the discussion in this section does not rely upon the general phenomenological equations but only upon the validity of Fick's law for mutual diffusion and the necessary definitions required to make the law precise. This comment appears necessary because some investigators [C. O. Bennett, *Chem. Eng. Sci.*, **9**, 45 (1958)] remain unconvinced that the usual phenomenological theory is correct in entirety.

(19) L. Miller and P. C. Carman, *Trans. Faraday Soc.*, **55**, 1831 (1959).

$$\mathfrak{D}_A = D_A \frac{d \log c_A f_A}{d \log c_A} \quad (38)$$

The right-hand side of eq. 38 is identical with that of eq. 10. Therefore, \mathfrak{D}_A is not the "intrinsic" diffusion coefficient, but is actually the mutual diffusion coefficient in the volume frame (D^V of Hartley and Crank). With this interpretation, eq. 36 is exactly eq. 10. It is still permissible to substitute eq. 36 into eq. 23 and obtain eq. 37 even though \mathfrak{D}_A and \mathfrak{D}_B are no longer the "intrinsic" diffusion coefficients, for eq. 23 is an obvious identity if $\mathfrak{D}_A = \mathfrak{D}_B = D^V$. Equation 37 is now identical with eq. 12b of the statistical mechanical theory, and hence the practical procedure of replacing $RT/N\sigma_A\eta$ and $RT/N\sigma_B\eta$ by the self-diffusion coefficients is justified. However, we may expect the equation to hold only when the solutions are regular.²⁰

The Gordon Equation.—In order to represent diffusion data in electrolyte solutions, Gordon²¹ proposed an empirical equation similar to eq. 13. Subsequently, the equation was restated for non-electrolyte solutions in exactly the form of eq. 13.²² Because the equation when it was originally formulated was empirical, we can have no critique of any previous derivation. We emphasize, however, that the derivation from statistical mechanics requires that the solution be regular. This requirement also fulfills a criterion set forth by Gordon²³ who pointed out that solutions which obey his equation also satisfy the relation

$$D_1^\infty \eta_2^0 / \bar{v}_2 = D_2^\infty \eta_1^0 / \bar{v}_1 \quad (39)$$

where D_1^∞ and D_2^∞ are the diffusion coefficients of one and two, respectively, at infinite dilution, and η_1^0 and η_2^0 are the viscosities of pure one and two. When the solutions are regular, eq. 39 follows from the first of eq. 10 and the constancy of the products $D_i \eta_i$.

IV. Conclusions

We have demonstrated that the equations of Eyring and his collaborators, of Hartley and Crank, and of Gordon, although superficially unrelated, are all of equivalent validity and may be derived from the more general equations of statistical mechanics. It has not been our objective to prove or disprove the equations, but rather we have elucidated the assumptions required in their derivations and have shed light on their exact statements and on their range of validity. The equations may be expected at best to apply accurately to that class of solutions for which the equilibrium radial distribution functions are independent of composition; that is, regular solutions. Although the equations have equivalent status on the molecular level, they may not necessarily fit empirical data with equal accuracy because they will apply only approxi-

(20) This paragraph must not be construed as a criticism of the treatment of Hartley and Crank. They proposed a "tentative" theory. We have shown that it is indeed possible to give a precise interpretation to their equations and to fit them into the framework of a more general theory.

(21) A. R. Gordon, *J. Chem. Phys.*, **5**, 522 (1937).

(22) (a) L. J. Gosting and M. S. Morris, *J. Am. Chem. Soc.*, **71**, 1998 (1949); (b) L. J. Gosting and D. F. Akeley, *ibid.*, **74**, 2059 (1952); (c) C. L. Sandquist and P. A. Lyons, *ibid.*, **76**, 4641 (1954).

(23) A. R. Gordon, *ibid.*, **72**, 4840 (1950).

mately to any real solution. It is our hope that in the near future there will exist experimental data on simple systems in sufficient abundance to provide thorough tests of the present equations and to suggest, perhaps, new equations of more general validity.

Appendix

A Glossary of Notation for the Diffusion Coefficients.—To aid the reader, we here present an index of notation together with our interpretation of the meaning of each of the symbols.

BEARMAN

D Mutual diffusion coefficient in the volume frame

$D_i, i = 1, 2, A, B$.. Self-diffusion (tracer diffusion) coefficient in the mixture

EYRING

D_1 Mutual diffusion coefficient in the volume frame

D, D_1^0 Self-diffusion coefficient in the mixture

HARTLEY-CRANK

D^v Mutual diffusion coefficient in the volume frame

$\mathfrak{D}_A, \mathfrak{D}_B$ Mutual diffusion coefficients in the mass frame (intrinsic diffusion coefficients) in their section seven. Mutual diffusion coefficients in the volume frame in their section eight

D_A, D_B Mutual diffusion coefficients at infinite dilution (equal to the corresponding self-diffusion coefficients)

SPECTROPHOTOMETRIC ANALYSIS OF REACTION MIXTURES¹

BY S. AINSWORTH

Department of Biochemistry, University of Sheffield, Sheffield, England

Received April 11, 1961

A method is described to give the number of absorbing species in a reaction mixture by employing spectrophotometric data in matrix form. Application of the method to various types of reactions is discussed and several test systems are examined.

Introduction

Sternberg, Stillo and Schwendeman² have described a least squares method in matrix form to fit the spectrum of a known mixture by the spectra of the pure components, the concentrations of which act as variables. They applied the method to determine the percentage composition of mixtures arising in the irradiation of ergosterol. Later, Reid and Pratt³ employed the same method in the analysis of ribonucleic acid.

In a recent paper, Weber⁴ has described another application of matrix analysis. The fluorescence of a mixture is excited at a number of wave lengths, n , and the emission observed at a further wave lengths, m . The nm observations are set out in a matrix, the rank of which gives the number of fluorescent components in the mixture.

This paper will describe a method, similar to that of Weber, to enumerate the absorbing species in a reaction mixture using spectrophotometric data. Prior knowledge of the spectra of the pure components is not required.

Enumeration of Components.—Assuming that the optical density, $d_{s,\lambda}$, at wave length λ of a mixture s , containing k components, is a function of its composition alone, we have

$$d_{s,\lambda} = c_{s1}\alpha_{\lambda 1} + c_{s2}\alpha_{\lambda 2} + \dots + c_{sk}\alpha_{\lambda k} \quad (1)$$

where c is the concentration of component k and α is its extinction coefficient at wave length λ .

For n such mixtures and m wave lengths, the nm optical density readings may be set out as an absorbance matrix, $A_{s,\lambda}$

$$A_{s,\lambda} = \begin{vmatrix} d_{11} & d_{21} & \dots & d_{n1} \\ \dots & \dots & \dots & \dots \\ d_{1m} & d_{2m} & \dots & d_{nm} \end{vmatrix} \quad (2)$$

The $A_{s,\lambda}$ matrix is the product, taken row by column, of two subsidiary matrices

$$A_{s,\lambda} = \begin{vmatrix} \alpha_{11} & \alpha_{12} & \dots & \alpha_{1k} \\ \dots & \dots & \dots & \dots \\ \alpha_{m1} & \alpha_{m2} & \dots & \alpha_{mk} \end{vmatrix} \begin{vmatrix} c_{11} & c_{21} & \dots & c_{n1} \\ \dots & \dots & \dots & \dots \\ c_{1k} & c_{2k} & \dots & c_{nk} \end{vmatrix} \quad (3)$$

In the same way, difference spectrum measurements may be used to set up a $D_{s,\lambda}$ matrix

$$\begin{vmatrix} d_{11} - d_{01} & \dots & d_{n1} - d_{01} \\ \dots & \dots & \dots \\ d_{1m} - d_{0m} & \dots & d_{nm} - d_{0n} \end{vmatrix} = \begin{vmatrix} c_{11} - c_{01} & \dots & c_{n1} - c_{01} \\ \dots & \dots & \dots \\ c_{1k} - c_{0k} & \dots & c_{nk} - c_{0k} \end{vmatrix} \alpha \quad (4)$$

where subscript 0 denotes some reference state of the system: the α matrix remains unchanged. Or, more shortly

$$D_{s,\lambda} = \begin{vmatrix} \Delta_1^1 & \Delta_2^1 & \dots & \Delta_n^1 \\ \dots & \dots & \dots & \dots \\ \Delta_1^k & \Delta_2^k & \dots & \Delta_n^k \end{vmatrix} \alpha \quad (5)$$

where Δ_n^k represents the change in concentration of component k between the state n and the chosen reference state.

By definition, a matrix is of order F if it contains at least one non-zero minor of order F , while all minors of order $F + 1$ are zero. In general, determinants derived from the α matrix are non-zero, irrespective of order, since, for absorbing species, each element has an arbitrary value. The possibility of a zero solution occurring by chance is small, and can be tested for by measurements at a further number of wave lengths. The ranks of the concentration matrices, therefore, determine the ranks of the corresponding $A_{s,\lambda}$ and $D_{s,\lambda}$ matrices, and operations performed on the one are equivalent to operations on the other.

Further, it is a standard theorem that if the matrix corresponding, for example, to the forms

(1) This work was supported in part by the Atomic Energy Commission.

(2) J. C. Sternberg, H. S. Stillo and R. H. Schwendeman, *Anal. Chem.*, **32**, 84 (1960).

(3) J. C. Reid and A. W. Pratt, *Biochem. Biophys. Research Commun.*, **3**, 337 (1960).

(4) G. Weber, *Nature*, **190**, 27 (1961).

$d_{s,\lambda}$ is of rank F , then these forms contain F linearly independent variables, any variables in excess of F being linearly dependent. Thus, for a given system, we have

$$\begin{aligned} P_A + F_A &= C \\ P_D + F_D &= C \end{aligned} \quad (6)$$

(depending on whether absolute or difference spectrum measurements are employed in the estimation of rank), where C enumerates the components in the system and P the relationships among them. Since the values of P and F depend on the type of system examined, these may now be defined.

1. Closed Systems.—In a closed system, the total concentration of the several components remains constant. Two main types of closed system may be distinguished.

(a) $A \rightarrow B$.—In this system, a complementary relationship exists between A and B, that is, $-\Delta_1^A = +\Delta_1^B$, and so on. The rank of the $D_{s,\lambda}$ matrix is therefore one

$$\left| \alpha \begin{vmatrix} \Delta_1^A & \Delta_2^A \\ \Delta_1^B & \Delta_2^B \end{vmatrix} \right| = 0 \quad (7)$$

indicating the presence of a single inter-relationship, $P_D = 1$. Nevertheless, the absolute concentrations of A and B remain arbitrary and the rank of the $A_{s,\lambda}$ matrix, F_A , is two, directly enumerating the components in the system. Similarly, the system $A \rightarrow B \rightarrow C$ has ranks, F_A and F_D , of 3 and 2, respectively.

(b) $aA + bB + \dots \rightarrow pP + qQ + \dots$.—In this system there is, in addition to the complementary relation discussed under (a), the possibility of further direct relations between two, or more, components. The effect of this is to reduce F_D , relative to C , by one unit for each such relationship. In the present example, $-\Delta_1^A/a = -\Delta_1^B/b = +\Delta_1^P/p = +\Delta_1^Q/q$, etc., and $F_D = 1$ (column or row multipliers do not affect the properties of a matrix).

The value of F_A depends on the initial state of the system. If the initial concentrations of the components are arbitrary, $F_A = C$. However, if $[A]_0/[B]_0 = a/b$ and $[P]_0/[Q]_0 = p/q$, $F_A = 2$ and there is a corresponding reduction in the value of F_A .

2. Open Systems.—In an open system, the concentrations of the components are varied arbitrarily. No inter-relationships are present between the different components and $F_A = F_D = C$.

3. Systems Containing Colorless Components.—(i.e. components that do not absorb at any of the m wave lengths employed to set up the matrix).—For the closed system, $A \rightarrow B \rightarrow C$, $F_A = 3$ and $F_D = 2$. However, if one of the components is colorless, the rank of both matrices is 2. The presence of the colorless component has produced, essentially, a two-component open system. Considered as a closed system, the situation is represented formally by inclusion of a column of zeros in the α matrix, with the consequent appearance of only two concentration terms in the $A_{s,\lambda}$ matrix. The appearance of additional colorless components in a closed system has no further effect on the rank.

4. Conversion of a Closed System to an Open System.—The conversion of a closed system to an open system, by permitting the independent enumeration of the absorbing species, could, in principle, provide additional information concerning the possible inter-relationships among the components of the closed system.

Application of Matrix Analysis to Reaction Systems.—It is suggested that the main use of the methods described above will be in the spectrophotometric investigation of reaction systems, i.e., closed systems in the above sense.

If the composition of the mixture varies as a function of time, the matrix can be set up by extinction measurements made after successive intervals. It is necessary, of course, to measure the several optical densities in a time short in comparison with the rate at which the system changes in composition; if this is not possible, measurements at different wave lengths can be made in successive runs.

For equilibrium systems, the composition of the mixture may be varied by alteration of such physical conditions as temperature or pressure or by control of the reactant and product concentrations. Similarly, photostationary states may be varied by alteration of the incident light intensity.

The conversion of a closed to an open system may be possible, in favorable cases, by stopping the reaction in several states followed by addition of components in arbitrary amounts.

Determination of Rank.—The rank of a matrix is determined as one less than the order of the lowest minor giving a zero solution. Estimation of the order of the first zero minor is subject to uncertainty arising from errors of measurement. Computational errors also may arise in the evaluation of the determinant since, in this process, numbers of the same order of magnitude are subtracted from one another. The consequent loss of leading significant figures may result in a solution less accurate than the given data. Assuming that computational error is guarded against (by carrying the calculation to more figures than the data), it is of interest to consider the effect of errors of measurement on a determinant as a function of its order, so that an objective test for a zero solution may be advanced.

Let S_n be the value of a determinant of order n with elements a_{ij} , and S_n' the value of the corresponding determinant in which the elements are subject to an error with standard deviation d . S_n' is the sum, having regard to sign, of $n!$ terms, each being the product of n elements from different columns of the determinant. Expanding

$$S_n' = \sum_{i \neq j} \pm \{(a_{1i} \pm d)(a_{2j} \pm d) \dots (a_{nx} \pm d)\} \quad (8)$$

the determinant and neglecting powers of d greater than one, we have

$$S_n' = \sum_{i \neq j} \pm (a_{1i} \dots a_{nx}) + \sum_{i \neq j} \pm (a_{1i} \dots a_{nx}) \left(\pm \frac{d}{a_{1i}} \dots \pm \frac{d}{a_{nx}} \right) \quad (9)$$

The signs in the second term are determined by the error, and therefore have equal probability.

But, as the probability of positive and negative signs as determined by the transposition rules is also equal, equation 9 may be rewritten as

$$S_n' = \sum_{i \neq j} \pm (a_{1i} \cdots a_{nx}) + d \sum_{i \neq j} \pm (a_{1i} \cdots a_{nx}) \left(+ \frac{1}{a_1} \cdots + \frac{1}{a_{nx}} \right) \quad (10)$$

$$\text{or } S_n' = S_n + d \sum_{i=1}^{n^2} \pm S_{mi} \quad (11)$$

The second term is the sum of n^2 minors of order $m = (n - 1)$, having random sign. If the values, S_{mi} , are randomly distributed about their average, the second term is equivalent to a random walk in one dimension of n^2 steps whose length is the root mean square of the minors.⁵ Hence, equation 11 becomes

$$S_n' = S_n \pm nd\sqrt{\bar{S}_{mi}^2} \quad (12)$$

Assuming that when $S_m \neq 0$, $S_m \approx S_{mi}'$ and employing the numerical average of the minors as an approximation to the root mean square, we have

$$\frac{S_n'}{\bar{S}_{mi}'} = \frac{S_n}{\bar{S}_m} \pm nd \quad (13)$$

This equation may be used as a test for a zero solution for, when $\bar{S}_n = 0$, $S_n'/\bar{S}_{mi}' = nd$.

However, to avoid chance effects, it is desirable to apply equation 13 to a significant sample of the minors of order n that can be obtained from the matrix of experimental results. In these circumstances, evaluation of all the possible minors of order m , required by equation 13, becomes too laborious: the selection of minors of order m is limited, therefore, to those arising in the expansions of S_n' . For this reason, an approximate solution of the ratio S_n/S_m , for non-zero determinants, in terms of the elements employed in the respective expansions is useful as a comparison to the value of nd .

We have

$$S_n = \sum_{i \neq j} \pm \mu_n^n \left\{ \left(1 + \frac{\sigma_{1i}}{\mu_n} \right) \cdots \left(1 + \frac{\sigma_{nx}}{\mu_n} \right) \right\} \quad (14)$$

where μ_n is the average numerical value of all the elements in S_n (negative rows or columns may be changed in sign without altering the properties of the determinant) and $(\mu_n + \sigma_{ij}) = a_{ij}$.

When this equation is expanded, terms in μ_n^n and μ_n^{n-1} disappear. The remaining terms have real sums, but, for $n \leq 4$ and $\sigma/\mu \gg 0.5$, only those in μ_n^{n-2} need be considered. If the variance, σ^2 , is employed as an approximation to the mean value of the products of residuals taken two at a time, we have

$$S_n = \sum_{i=1}^{\frac{n!n(n-1)}{2}} \pm (\mu_n^{n-2} \sigma_n^2)_i \quad (15)$$

Equation 15 represents a random walk and hence

$$S_n = \pm \sqrt{\frac{n!n(n-1)}{2}} \times \mu_n^{n-2} \sigma_n^2 \quad (16)$$

Substitution of equation 16 into equation 13 gives

(5) L. Brillouin, "Science and Information Theory," Academic Press, Inc., New York, N. Y., 1956, pp. 129-132.

$$\frac{\bar{S}_n'}{\bar{S}_m'} = \pm \frac{n}{\sqrt{n-2}} \times \frac{\bar{\mu}_n^{n-2} \bar{\sigma}_n^2}{\bar{\mu}_m^{m-2} \bar{\sigma}_m^2} \pm nd \quad (17)$$

where the equation is applied to the mean of a number of determinants of order n .

Since \bar{S}_m' represents all possible minors of \bar{S}_n'

$$\frac{\bar{\mu}_n^{n-2} \bar{\sigma}_n^2}{\bar{\mu}_m^{m-2} \bar{\sigma}_m^2} = \bar{\mu}_n$$

However, if the selection of minors of order m is limited to those obtained in the expansion of \bar{S}_n' the additional terms in equation 17 may be employed empirically as corrections, the subscripts defining the selection of elements included in the two expansions.

Equation 17 may be used as a test for a zero solution, thus

$$(a) \text{ If } \bar{S}_n'/\bar{S}_m' \leq 2nd, \bar{S}_n = 0$$

$$(b) \text{ If } \bar{S}_n'/\bar{S}_m' \approx \frac{n}{\sqrt{n-2}} \times \frac{\bar{\mu}_n^{n-2} \bar{\sigma}_n^2}{\bar{\mu}_m^{m-2} \bar{\sigma}_m^2}, \bar{S}_n \neq 0$$

the factor 2 being introduced to define the level of significance.

Application of Matrix Analysis to Model Systems. 1. Introduction.—A matrix of random numbers was used to test the validity of equations 16 and 17 in the absence of errors of measurement. The equations then were tested using artificial mixtures of dyes. Two real systems also were examined.

2. Experimental Methods and Results. Random Numbers.—A sequence of 32 random numbers less than 11 were obtained from statistical tables and arranged in a 4×8 matrix.

Dye Mixtures.—Three series of dye solutions were prepared containing 2, 3 and 4 components, respectively. Individual dyes were made up in alcohol (so as to prevent dimerization⁶) and the concentrations adjusted to give approximately equal optical densities at their absorption maxima. Mixtures of the dyes were prepared by replacing a given volume of one dye solution by an equal volume of the second, and so on. The two component system contained thionine and methylene blue. The 3-component system contained phenol red, acridine orange and di-iodo(R)fluorescein, with the addition in the 4-component system of rhodamine B. Optical densities at several wave lengths and for various proportions of the different components were measured and set out in matrices. Table I gives the results obtained with the 4-component system.

Cytochrome Oxidase Reaction.—A venom-solubilized preparation of cytochrome oxidase was reduced by dimercaptopropanol in the presence of catalytic amounts of cytochrome *c*. Optical density changes at different wave lengths occurring during the reaction of reduced cytochrome oxidase ($2 \times 10^{-6} M$ after mixing, pH 9, room temperature) with oxygen ($3 \times 10^{-6} M$ after mixing) were measured in a stopped flow apparatus. These results, which were kindly made available by Gibson and Greenwood,⁷ are given in Table II.

(6) E. Rabinowitch and L. F. Epstein, *J. Am. Chem. Soc.*, **63**, 69 (1941).

(7) Q. H. Gibson and C. Greenwood, private communication.

TABLE I
 OPTICAL DENSITIES $\times 10$ FOR MIXTURES OF FOUR DYES

Wave length, $m\mu$	Mixture									
	1	2	3	4	5	6	7	8	9	10
427	1.47	3.48	5.75	1.62	0.48	2.48	4.06	5.97	1.52	0.40
490	3.56	5.02	4.15	4.50	2.84	4.50	4.17	4.91	3.72	2.36
525	4.60	2.01	0.83	4.29	5.62	3.66	2.03	0.33	4.73	6.61
543	4.73	1.71	0.42	3.31	6.26	2.48	1.71	0.12	4.20	6.85

 TABLE II
 OPTICAL DENSITY CHANGES $\times 100$ MEASURED AT TIME t AFTER MIXING SOLUTIONS OF REDUCED CYTOCHROME OXIDASE AND OXYGEN (GIBSON AND GREENWOOD⁷)

The natural order of the table has been reduced so as to increase tetrad differences

t , msec.	Wave length, $m\mu$										
	415	435	445	425	405	430	395	440	450	420	400
23	2.0	-0.8	-5.1	4.3	2.0	1.8	1.4	-2.5	-4.6	2.8	1.4
3	6.3	-3.0	-10.2	7.2	6.1	2.6	3.3	-7.8	-8.5	6.6	4.6
33	1.4	-0.4	-3.7	3.8	1.5	1.6	0.9	-1.4	-3.8	2.0	1.0
13	3.6	-1.8	-7.3	5.6	3.7	2.0	2.0	-4.6	-6.0	4.1	2.8

Hemoglobin Mixtures.—Mixtures of oxyhemoglobin and reduced hemoglobin were prepared by the progressive deoxygenation of a dilute solution of oxyhemoglobin (pH 9, borate buffer) contained in a closed glass cuvette, in a side arm of which was placed a solution of reducing agent (anthraquinone- β -sulfonic acid and sodium dithionite in alkaline solution). Since reduction took place by diffusion of oxygen through the intervening gaseous phase, the rate of reaction was slow, and readings at a succession of wave lengths were easily made in a time during which no change in the composition of the solution occurred. Table III gives the results obtained.

 TABLE III
 OPTICAL DENSITIES $\times 10$ FOR MIXTURES OF HEMOGLOBIN AND OXYHEMOGLOBIN

The optical densities of mixtures 3, 4 and 5 were used in calculating the results given in Table IV.

Mixture	Wave length, $m\mu$								
	596	578	572	561	546	536	454	505 iso- bestic point	2.36
1	1.00	6.70	5.62	3.87	6.22	5.76	6.38	2.36	2.36
2	1.83	5.60	5.21	4.83	5.70	4.88	5.71	2.39	2.39
3	2.18	5.27	5.24	5.30	5.63	4.60	5.37	2.37	2.37
4	2.55	4.56	5.08	5.86	5.29	4.16	4.89	2.33	2.33
5	2.37	4.92	5.16	5.55	5.50	4.38	5.20	2.34	2.34

3. Evaluation of Determinants.— $N \times n$ determinants were expanded by minors. In every case, several such determinants were evaluated by moving crabwise along the matrix. The mean of the values thus obtained, together with mean values of the minors, are recorded in Table IV, where they are compared with values predicted by equations 16 and 17. The error term, \bar{d} , was calculated on the assumption that the extinction measurements were subject to a 2% error, to which was added a further 2% making up error in the case of the dye mixtures. Measurements of the cytochrome oxidase reaction were assumed subject to a 5% error.

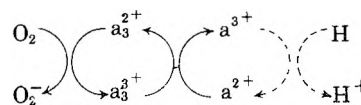
4. Discussion. Test Systems.—Table IV shows that, for a random system, the value of \bar{S}_D may be predicted within reasonable limits by

the use of equation 16. The predictions are less good for the dye systems, particularly for the 4-component system.

A similar comparison between the calculated and observed values of the ratio \bar{S}_n'/\bar{S}_m' gives better results, and application of the proposed test for a zero solution permits, in every example, an unequivocal estimation of rank.

The reduction in rank on passing from absorption spectra to difference spectra is illustrated in the three dye systems.

Cytochrome Oxidase Reaction.—The data in Table IV show that $F_D = 2$. This implies that at least three components contribute to the spectral changes occurring during the oxidation of reduced cytochrome oxidase. The simplest interpretation of this finding is that the system involves successive reactions of the type $A \rightarrow B \rightarrow C$. However, there is good evidence^{8,5} that cytochrome oxidase comprises two pigments, cytochromes a and a_3 , both of which participate in the transfer of electrons to oxygen



where the superscripts indicate the oxidation states of the two pigments. This system contains two independent variables for

$$-\Delta_n a_3^{2+} \neq -\Delta_n a_2^{2+} \text{ and } \Delta_n a_3^{2+} \neq \Delta_n a_2^{2+}$$

$$\text{but } -\Delta_n a_3^{3+} = \Delta_n a_3^{2+} \text{ and } -\Delta_n a_2^{3+} = \Delta_n a_2^{2+}$$

and is, therefore, consistent with the finding that $F_D = 2$.

Hemoglobin Mixtures.—Although it appears that the combination of hemoglobin with ligands, such as oxygen or carbon monoxide, takes place in four distinct stages, there is no spectral evidence to show the existence of the several intermediates.¹⁰ Many investigations, such as those of Nahas¹¹

(8) D. Keilin and E. F. Hartree, *Proc. Roy. Soc. (London)*, **B127**, 167 (1939).

(9) T. Yonetani, *J. Biol. Chem.*, **235**, 845 (1960); **235**, 3138 (1960).

(10) Q. H. Gibson and F. J. W. Roughton, *Proc. Roy. Soc. (London)*, **B146**, 206 (1957).

(11) G. G. Nahas, *Science*, **113**, 723 (1951).

TABLE IV
 DETERMINATION OF RANK

System	Matrix	S_1		S_2		S_3		S_4/S_1		S_1/S_2		Rank	
		Obsd.	Calcd.	Obsd.	Calcd.	Obsd.	Calcd.	Obsd.	Calcd.	$n\bar{d}$	Obsd.		Calcd.
1. Random numbers	4 × 8	27.1	12.3	184	140	2000	2060	10.9	14.7	..	6.8	11.4	..
2. 4 dyes— A_{θ}, λ	4 × 10	2.4	6.3	12.6	48.8	21.1	462	1.7	9.5	0.53	5.4	7.8	0.42
3. 4 dyes— D_{θ}, λ	4 × 10	2.0	8.4	7.8	55.1	5.1	1050	0.65	19.0	0.53	3.9	6.6	.42
4. 3 dyes— A_{θ}, λ	3 × 4	12.6	4.5	47.9	49.2	3.8	10.9	.46
5. 3 dyes— D_{θ}, λ	3 × 4	8.2	2.7	3.7	47.4	0.45	17.3	.46
6. 2 dyes— A_{θ}, λ	4 × 5	4.6	1.4	0.50	17.8	0.06	11	12.5
7. 2 dyes— D_{θ}, λ	4 × 5	0.14	0.91	0.01
8. Cytochrome oxidase— D_{θ}, λ	4 × 11	3.1	4.5	1.6	101	..	82	840	0.52	8.3	0.80	..	51
9. Hb/O ₂ Hb— A_{θ}, λ	3 × 7	1.5	1.5	0.12	21.8	08
10. Hb/O ₂ Hb— D_{θ}, λ	3 × 7	0.11	0.33

and Harboe,¹² have shown that the light absorption of a partially saturated hemoglobin solution at a given wave length is a linear function of its percentage saturation. It seemed worthwhile to check this result by the present method since it is independent of determinations of percentage saturation. Table IV shows that $F_A = 2$, thus confirming that the four haems of the hemoglobin molecule act independently in the absorption of light.

Chlorella Difference Spectra.—Coleman and Rabinowitch¹³ have presented difference spectra in

- (12) M. Harboe, *Scand. J. Clin. and Lab. Invest.*, **11**, 66 (1959).
 (13) J. W. Coleman and E. Rabinowitch, *J. Phys. Chem.*, **63**, 30 (1959).

which the light absorption of a suspension of *Chlorella* kept in the dark is compared with that of an identical suspension exposed to one of a range of light intensities. These spectra have been examined by the present method. Unfortunately, the available data are not extensive enough to reach reliable conclusions. However, matrix analysis, in principle, should permit enumeration of the species contributing to the various bands of the difference spectra.

Acknowledgment.—The author gratefully acknowledges the advice and criticism of Dr. G. Weber.

ON THE RELATION BETWEEN AN EQUILIBRIUM CONSTANT AND THE NONEQUILIBRIUM RATE CONSTANTS OF DIRECT AND REVERSE REACTIONS¹

By O. K. RICE

Department of Chemistry, University of North Carolina, Chapel Hill, North Carolina

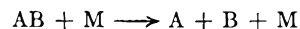
Received April 25, 1961

It is known that the rate of dissociation of a small molecule activated by an inert substance is affected by the fact that some of the excited states with energies close to the dissociation energy have less than their equilibrium population. It is shown that, in spite of this, the actual observed rates of dissociation and association will bear the same relation to the equilibrium constant as if equilibrium in all intermediate states were completely maintained. A similar conclusion can be extended to other types of reaction.

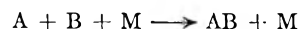
Recent calculations² have indicated that the rate of dissociation of small molecules activated by inert molecules may be affected, probably not by a very large factor but still appreciably, due to the fact that the energy states leading up to dissociation do not have their equilibrium population. A complementary effect would of course occur in the reverse association of the fragments in the presence of the same third body. Since the rates which are thus observed are not true equilibrium rates, it has been suggested by Nikitin and Sokolov,² by Pritchard,² by Widom,² and, by implication, by Ross and Mazur³ that it is not correct to set

$$k_{d,obs}/k_{a,obs} = K \quad (1)$$

where $k_{d,obs}$ is the observed rate constant for the dissociation, say,



with no A or B present, $k_{a,obs}$ is the observed rate constant for the association



with no AB present, and K is the equilibrium constant for



This is of some practical importance in connection with experiments on the association of atoms and the dissociation of diatomic molecules. For the most part experiments at low temperatures (usually using flash photolysis) give the rate of the association reaction, while experiments at high temperatures (usually using shock waves) give the rate of the dissociation reaction. It has been suggested that these experiments are not strictly comparable, because it has been supposed that one cannot calculate one rate from the other *via* the equilibrium constant.

In order to decide whether such a conclusion is

(1) Work assisted by the National Science Foundation.

(2) E. E. Nikitin and N. D. Sokolov, *J. Chem. Phys.*, **31**, 1371 (1959); J. C. Polanyi, *ibid.*, **31**, 1338 (1959); H. O. Pritchard, *J. Phys. Chem.*, **65**, 504 (1961); B. Widom, 139th meeting, Am. Chem. Soc., Paper No. 3, Div. of Phys. Chem. (March, 1961).

(3) J. Ross and P. Mazur, *J. Chem. Phys.*, **35**, 19 (1961).

correct or not it is necessary to consider the conditions under which eq. 1 might possibly be expected to hold. In the first place, a rather trivial condition is that the reactions must really be those written. This means that the concentration of M should be large compared to those of AB or A and B. This will avoid side reactions, such as



In practice it may be possible to make corrections for the presence of other third bodies, including the reacting species themselves, which is equivalent.

One matter which is of considerable importance is the relation between the relaxation time for redistribution of molecules AB among the various energy levels as compared to the time required for an appreciable amount of reaction to occur. This might be a matter of some concern in shock tubes, where the temperature becomes very high and the reaction becomes very fast. Smiley and Winkler⁴ have investigated relaxation times for the vibrational energy of Cl₂ at atmospheric pressure. These times decrease rapidly with temperature, and become of the order of 10⁻⁷ sec. at 1500°K. This probably may be fairly compared with the rate of dissociation of Br₂, which is about⁵ 5 × 10³ cc. mole⁻¹ sec.⁻¹ at 1500°K. At one atmosphere the concentration is about 8 × 10⁻⁶ mole cc.⁻¹, and the time of the reaction about 2.5 × 10⁻⁴ sec. It thus would seem reasonable to infer that the relaxation time would always be negligible. Palmer and Hornig also cited internal evidence that the relaxation time for Br₂ is negligible in the Br₂ dissociation. Indeed, this would be inferred from the fact that activation and reaction are in a sense the culmination of the relaxation process. (If the third body M is not relaxed, then, of course, the association and dissociation must be compared under similar conditions).

The fact that the relaxation time is so small has a number of important consequences. Let us fix our attention on the great bulk of the molecules in low energy levels which are much more highly populated than are those excited levels which are close to the transition state for dissociation. There will be relatively little attrition of these low levels due to reaction in the time of relaxation; therefore, they will be essentially in equilibrium. Only the energy levels near the transition state will depart appreciably from their equilibrium quota. Thus, as I have shown previously,⁶ the proper condition is set up for the population of *all* the levels to be in a *steady* state (it is true that a somewhat simplified mechanism was considered, as it would be impossible to treat the actual case in its full complexity). This being true, the *actual* rate at which the reaction will occur, regardless of the departure from equilibrium conditions in any of the energy levels, will be uniquely determined by the concentration and the temperature.

In view of the shortness of the relaxation time compared to the reaction time, we expect the elapsed time of the process of activation and reaction (or, inversely, for deactivation) to be small compared to the time required for any appreciable amount of

reaction to take place. Were this not so, we would observe an induction period of the same order of magnitude as the reaction time and we would not be able to determine a rate constant.

With these preliminaries established we may now proceed to a discussion of the validity of eq. 1. We make one further assumption, namely that the translational motion of the molecules is classical, so that we can follow the fate of any particular molecule. In order to fix the ideas we shall consider three separate situations which are related to each other in a definite way.

I. In this case we consider a system in which the concentration of AB is (AB)_I, that of M is (M), and those of A and B are zero. In a period of time δt , so small that a very small fraction of the material will react, the amount of reaction which will take place per unit volume will be equal to $k_{d,obs} (AB)_I (M) \delta t$.

II. We now consider a system in which M has the same concentration (M) as in case I, and A and B have concentration (A)_{II} and (B)_{II} such that

$$(A)_{II} (B)_{II} = K(AB)_I \quad (2)$$

but in which no AB is actually present. The amount of reaction per unit volume in the time δt will be, for this case, $k_{a,obs} (A)_{II} (B)_{II} (M) \delta t$.

At this point, and before considering case III, we need to pause in order to consider exactly what is meant by the "observed rate of reaction." In case I, no ambiguity is possible. Once an AB molecule is dissociated the fragments would, in the gas phase, be dissociated "forever"; they might, of course, react with other A and B molecules formed, but the number of such reactions within the small time δt would be negligible, and could not appreciably affect the rate of the back reaction.

In case II we remark that, as noted by Polani,² some excited molecules AB* might be formed which soon would be reactivated and dissociated again into A + B rather than being finally deactivated. At any given instant these molecules would be present in very small concentration, and would not be detected. If they redissociated they would not be included in the measured rate constant, $k_{a,obs}$. Only those that were finally deactivated would be included in the increase in the concentration of AB or the decrease in that of A + B. It is necessary to choose δt large enough to be greater than the time required for an AB* to be either redissociated or deactivated to the point where it would not react without starting the activation process *de novo*. At the same time, of course, δt must be small compared to the time of reaction, but in view of our discussion of the relaxation time it should be easy to reconcile these requirements.

III. Finally we consider a system in which all species A, B, AB and M are present in the concentrations (A)_{II}, (B)_{II}, (AB)_I and (M) noted in the above paragraphs, so that A, B and AB are in equilibrium. Suppose that we follow the behavior of the AB molecules originally present in the mixture. Their fate will, on the average, be exactly the same as it would have been in case I, when the A and B were not there, for the A and B are present in small enough concentration so that the collisions between AB and A or B can be neglected. If this

(4) E. F. Smiley and E. H. Winkler, *J. Chem. Phys.*, **22**, 2018 (1954).

(5) H. B. Palmer and D. F. Hornig, *ibid.*, **26**, 98 (1957).

(6) O. K. Rice, *J. Phys. Chem.*, **64**, 1851 (1960).

were not true it would mean a change in the environment of the AB molecules, which could indeed affect the rate of their decomposition, but not in a way essentially connected with lack of equilibrium.

In the same way, the rate of the association reaction would be the same in the equilibrium mixture III as it was in case II where the AB molecules were not present. The AB* would be formed, and would suffer the same fate as before. Thus the rate of association would not be changed.

Since with AB, A and B present in equilibrium concentrations the rate at which the AB's decompose and that at which A and B associate must be equal, we must have

$$k_{d,obs}(AB)_I(M)\delta t = k_{a,obs}(A)_I(B)_I(M)\delta t \quad (3)$$

Equation 1 follows immediately from eq. 2 and 3.

When A, B and AB are present in equilibrium quantities, every energy level must have its equilibrium population. If we include in the rate of decomposition the total contribution from every energy level of AB, regardless of its history (that is the contribution from every AB whose representative point crosses a certain surface in configuration space regardless of whether this system has just been formed from a pair of A and B), we will get a different rate constant, which we may call $k_{d,eq}$. This is the rate constant which one calculates from transition-state theory, unless a specific correction is made for states not in equilibrium. If, in the association reaction, we count all crossings of the surface in the configuration space regardless of whether or not they are soon reversed, we get the corresponding constant $k_{a,eq}$ and again we have, when (AB), (A) and (B) are equilibrium concentrations

$$k_{d,eq}(AB)(M)\delta t = k_{a,eq}(A)(B)(M)\delta t \quad (4)$$

and

$$k_{d,eq}/k_{a,eq} = \bar{X} \quad (5)$$

In this formulation we have specifically included in the rate of dissociation the redissociation of the molecules AB* which we have mentioned above, and have also included the rate of their formation in the rate of association. Since, in the system we are considering, the fate of a single AB molecule or a single pair of A and B molecules does not depend on the molecules present other than M's, it is legitimate to say that the observed rate of reaction (the rate which would actually be measured in an experiment in which no products were present) would differ from the equilibrium rate by an amount which is proportional to (AB) for the dissociation and proportional to the concentration of pairs or (A)(B), for the association. This is consistent with the expression obtained by subtracting eq. 3 from eq. 4, and shows that eq. 3 has the correct form. The change in the rate constant of the direct reaction due to lack of equilibrium is exactly compensated by the change in the reverse reaction.

It is of interest to note that near equilibrium the rate at which equilibrium is being approached will be given by the absolute value of $k_{d,obs}(AB)(M) - k_{a,obs}(A)(B)$. Thus, even in the immediate neighborhood of equilibrium the apparent observed rate of reaction will be measured by the "observed" rate constants rather than by the "equilibrium" rate constants. There will be no method by which

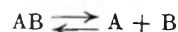
the experimental kineticist can determine the latter, for it is impossible to observe the elementary processes in which the molecules we have called AB* are formed or destroyed; only the accumulated increase of products or decrease in the reactants can be measured, but the observed rate constants will obey eq. 1.

It is, of course, possible to imagine special cases in which special manipulations are made, such as removing all molecules which appear in certain energies (say all energy levels belonging to AB, including those of AB*), which upset the applicability of eq. 1, but, lacking a Maxwell demon, it is hard to see how this could be done. One also could imagine a situation in which the relaxation time was comparable to the reaction time, but this would require the activation energy of the dissociation, compared to kT , to be rather low, and would probably preclude the possibility of making a measurement. If one could make a measurement, he would, as noted above, find an induction period of the order of magnitude of the reaction time, and the reaction rate constant would lose its significance. The activation energy for the association can be low, because the relaxation depends on binary collisions while the association depends on the much less frequent ternary collisions.

Our discussion can be considered to be, in a certain sense, an application of the law of microscopic reversibility, though a little more is involved. If only the dissociation is taking place, and some of the energy levels do not have their equilibrium quota, then the rate at which a given transition to a specific level is taking place may not be equal to the rate at which the reverse transition is taking place. This is not a violation of the law of microscopic reversibility, since equilibrium is not established. But when the reaction is occurring in the direction of association also, the products being present in equilibrium amounts, the difference in the direct and reverse transition rates is made up by contributions arising from molecules formed in the association reaction, these being independent of the contributions arising from the dissociation reaction. It is the independence of these contributions, demonstrated above, which is the element needed to supplement the law of microscopic reversibility. The law of microscopic reversibility says that for any portion of $k_{d,eq}$ which is excluded for purposes of calculating the "actual rate constant" for the reaction, there will be an exactly corresponding and balancing set of inverse processes which will not be included in the "actual rate constant" of the inverse reaction. The "law of independence or noninterference" says that these "actual rate constants" can be identified with $k_{d,obs}$ and $k_{a,obs}$, as determined when the system is not in equilibrium.

In the preceding discussion we have confined ourselves to an association-dissociation reaction in the gas phase. With the conditions described at the beginning of the article, the same conclusion can be extended to other cases. In particular, it is clear that it can be applied to other stoichiometries.

It will be of especial interest to consider the case of an association-dissociation reaction of solutes



in solution. Assuming first that the solution is dilute we may note that in this case it is in the association reaction, rather than in the dissociation reaction, that departures from equilibrium are likely to occur. In general, a pair of atoms which did not react would make several collisions in a short time interval before drifting apart. If they react on almost every collision, however, the pair of atoms will disappear at the first collision, its place being taken by a molecule. Thus there is a dearth of atoms close together. This results in a lowering of $k_{a,obs}$ —the well-known cage effect. But $k_{d,obs}$ will be lowered in the complementary manner—a molecule once dissociated may associate again in a relatively short time compared to the time of reaction. In general the behavior of any pair of atoms will be independent, in dilute solution, of the presence of AB molecules. Likewise the behavior of an AB molecule will be independent of A and B atoms, the probability being small that one of the atoms formed by the AB will react with another atom in the time it would take the pair to reassociate or to definitely dissociate. Also the number of A and B atoms in the intermediate state between association and dissociation will be small, and will not appreciably affect an observed rate. So exactly the same argument as given above will show that the equilibrium constant is given by $K = k_{d,obs}/k_{a,obs}$.

If the concentration of atoms is sufficiently large so that an atom does not in general have one nearest partner, and thus there is no cage effect, or a reduced one, a similar argument may be applied, at least in certain cases. Suppose the concentration of AB in equilibrium with $A + B$ was small compared to the concentrations of A and B. We then can imagine a case II in which AB was absent, and another case I in which AB was present in a concentration considerably greater than the equilibrium concentration, without appreciably changing the environment if the concentrations of A and B remained fixed. In case I we would observe the reaction $AB \rightarrow A + B$ proceeding at the rate $k_{d,obs}(AB)$; in case II we observe $A + B \rightarrow AB$ proceeding at the rate $k_{a,obs}(A)(B)$. The behavior of a given AB would be unaffected by the other AB's present. An atom, once formed, might react with other atoms already there, but this would simply merge in with the back reaction. Furthermore, the fate of any pair $A + B$ would be unaffected by the AB's present. We have thus fulfilled the condition that we always measure the same reactions. Therefore, at the equilibrium state obtained by properly fixing the concentration of AB, we again will have $k_{a,obs}(A)(B) = k_{d,obs}(AB)$, where $k_{a,obs}$ and $k_{d,obs}$ have the same values as before, and the usual relation between equilibrium and rate constants follows.

We will close by considering in some detail a special schematic mechanism suggested by Widom,⁷ which may be used to illustrate the assumptions made and the points involved. We suppose we have two substances A and B, which may exist in a total of four states, and that transitions may take place only between adjacent states



(7) B. Widom, private communication.

We suppose that A_2 and B_3 are activated states, which are present only in small numbers. The chemist will measure the quantities of A_1 and B_4 and will be essentially unaware of A_2 and B_3 . If the system is not in equilibrium the latter will not be present in their equilibrium quotas, but we can assume that they are in a steady state.⁸

If the whole system is in equilibrium we will have $k_{12}(A_1) = k_{21}(A_2)$, $k_{23}(A_2) = k_{32}(B_3)$, and $k_{34}(B_3) = k_{43}(B_4)$, where k_{ij} is the rate constant for the transition from state i to state j . For the equilibrium constant, then, we have

$$K = (B_4)/(A_1) = [(B_4)/(B_3)][(B_3)/(A_2)][(A_2)/(A_1)] = \frac{k_{12}k_{23}k_{34}}{k_{21}k_{32}k_{43}}$$

Now assuming that initially we have $A_4 = 0$, we can write for the forward rate constant

$$k_{f,obs} = -A_1^{-1}(dA_1/dt)$$

and the usual treatment of a steady state gives

$$k_{f,obs} = k_{12}k_{23}k_{34}/(k_{21}k_{32} + k_{23}k_{43} + k_{34}k_{21})$$

For the back reaction we have $A_1 = 0$ and

$$k_{b,obs} = -B_4^{-1}(dB_4/dt)$$

Simply by interchanging 1 and 4, and 2 and 3, in the expression for $k_{f,obs}$, we obtain

$$k_{b,obs} = k_{43}k_{32}k_{21}/(k_{23}k_{34} + k_{21}k_{34} + k_{31}k_{32})$$

Therefore

$$K = k_{f,obs}/k_{b,obs}$$

Let us now examine what has gone into this. In the first place the assumption that we are dealing always with the same reaction is embodied in the supposition that the k_{ij} are truly constant. The assumption that the relaxation time is small compared to the reaction time is implied in the assumption that, in a state of equilibrium, (A_2) and (B_3) are very small compared to either (A_1) or (B_4) . The time required for emptying of the state A_2 into A_1 , if the reverse reaction did not take place, would be of the order of k_{21}^{-1} . About the same amount of time would be required to fill the state A_2 if it started empty. Thus k_{21}^{-1} can be taken as the relaxation time, and we wish to show that $k_{31} \gg k_{f,obs}$. But it is obvious from the expression for $k_{f,obs}$ that it is less than k_{12} . Also since $(A_1)_{eq} \gg (A_2)_{eq}$ we know that $k_{21} \gg k_{12}$. Thus the necessary condition is fulfilled.

We may compare $k_{f,obs}$ with $k_{f,eq}$. At equilibrium the rate of "crossing of the surface in the phase space," would be just equal to

$$k_{23}(A_2)_{eq} = k_{22}[(A_2)_{eq}/(A_1)](A_1) = (k_{23}k_{12}/k_{21})(A_1)$$

Thus

$$k_{f,eq} = k_{23}k_{12}/k_{21}$$

and, similarly

$$k_{b,eq} = k_{32}k_{43}/k_{34}$$

It is seen that

$$K = k_{f,eq}/k_{b,eq}$$

though $k_{f,eq}$ and $k_{b,eq}$ are quite different from $k_{f,obs}$ and $k_{b,obs}$.

The general conclusions of this paper may, I

(8) Since writing the original version of this article, I have been informed by Dr. H. O. Pritchard that Dr. Norman Davidson demonstrated to him that an equation like eq. 1 would hold if all intermediate levels were in a steady state. This certainly is a necessary condition as we noted above, and we will use it directly in this example.

think, be fairly summarized by the statement that if unambiguous reaction rate constants can be found, then the quotient of the experimentally determined constants will give the equilibrium constant.

Without committing them to my views, I wish to thank Drs. Wendell Forst, Benjamin Widom, John Ross, and H. O. Pritchard for discussions and correspondence. In the light of their criticisms, the presentation has been considerably revised.

KINETICS OF HYDROGEN ATOM RECOMBINATION ON SURFACES¹

BY BERNARD J. WOOD AND HENRY WISE

Division of Chemical Physics, Stanford Research Institute, Menlo Park, California

Received April 17, 1961

The catalytic efficiencies of various solid surfaces for hydrogen atom recombination have been determined as a function of surface temperature. The values were derived from experiments in which atom concentration profiles in a cylindrical tube of finite length were measured with a movable catalytic probe. The experimental data were interpreted by means of a theoretical analysis which accounts for both radial and longitudinal atom diffusion. The applicability of the theory to the experimental arrangement and the limitations of the technique are evaluated. For such highly exothermic reactions as atom recombination, an interpretation of the catalytic properties must take into account energy transfer and dissipation in the solid. The effect of dissolved hydrogen on the catalytic activity of a metal is discussed.

Introduction

Numerous measurements of the catalytic efficiency of surfaces for heterogeneous atom recombination have been carried out. The methods employed varied widely in detail, but basically they may be differentiated according to the manner in which the gaseous atom density was estimated. Probe techniques involved measurements of the temperature rise²⁻⁶ or the heat input^{6,7-11} to a surface situated in a tube through which atoms migrated by diffusion or forced convection (or both) in order to estimate their concentration. Related techniques included the use of Wrede gages to estimate the change in concentration of hydrogen atoms along a cylindrical tube¹² and the photometric determination of the reduction of a molybdenum oxide layer by gaseous atomic hydrogen.¹³ More recently, electron paramagnetic resonance spectrometry has been applied to evaluate atom concentrations in a tube.^{11,14,15}

Many investigators saturated the molecular gas with water before admitting it to the discharge tube

employed for the production of hydrogen atoms. Some workers who used catalytic probes ignored the effect of this atom-measuring device upon the diffusional flow of atoms. Both of these factors may profoundly affect the results of the experiment and the interpretation of the data.

A comprehensive theoretical analysis of the diffusional flow of atoms in a cylindrical tube, as a result of heterogeneous recombination, has been developed.^{16,17} The theoretical model consists of a plane source of atoms situated at one end of the tube which is terminated at the opposite end by a plane closure. The wall of the tube has a uniform catalytic activity which may be identical with or different from that of the closure. The solutions to the steady-state diffusion equation yield the fractional atom concentrations to be expected at the closed ends of cylinders of various lengths, radii, and catalytic surface activities. By means of this analysis it is possible to use the experimental technique of Smith^{2a} to evaluate absolute atom recombination coefficients for the tube wall and the closure.

Experimental Procedure

A horizontal, water-jacketed Pyrex cylinder, closed by a flanged glass cap at one end, was joined at the open end to an electrodeless discharge tube. The effective length of the cylinder available to atomic species could be varied by means of a movable catalytic probe which effectively approximated a closure for the cylinder. Figure 1 is a schematic diagram of the apparatus. Gas was pumped through the discharge tube, which was at right angles to the axis of the cylinder, so that the flow of atoms within the cylinder was purely diffusional. The gas in the discharge tube was dissociated by means of the 17-megacycle signal from the radio transmitter.

The probe (Fig. 2) was a helix wound from fine wire of the metal whose catalytic activity was to be determined. It was affixed to a glass assembly which supported the filament in the center of the tube and which incorporated a glass-enclosed iron armature that permitted axial positioning of the probe from outside the tube by means of a large magnet. The filament was connected to flexible lead wires which did not interfere with the positioning of the probe, but which communicated with the outside through the cap at the end of the cylinder.

The decrease in electrical power from a battery required to maintain the filament at a constant resistance (and therefore

(1) This work was sponsored by Project Squid, which is supported by the Office of Naval Research, Department of the Navy, under Contract Nonr 1858(25) NR-098-038. Reproduction in full or in part is permitted for any use of the United States Government.

(2) (a) W. V. Smith, *J. Chem. Phys.*, **11**, 110 (1943); (b) V. V. Voevodski and G. K. Lavrovskaya, *Doklady Akad. Nauk, S.S.S.R.*, **63**, 151 (1948).

(3) S. Katz, G. B. Kistiakowsky and R. F. Steiner, *J. Am. Chem. Soc.*, **71**, 2258 (1949).

(4) K. Nakada, S. Sato and S. Shida, *Proc. Japan Acad.*, **31**, 449 (1955).

(5) J. W. Fox, A. C. H. Smith and E. J. Smith, *Proc. Phys. Soc.*, **73**, 553 (1959).

(6) K. Nakada, *Bull. Chem. Soc. Japan*, **32**, 809 (1959).

(7) S. Roginsky and A. Schechter, *Acta Physicochim. U.R.S.S.*, **1**, 318 (1934).

(8) R. Suhrmann and H. Csesch, *Z. physik. Chem.*, **B28**, 215 (1935).

(9) H. G. Poole, *Proc. Roy. Soc. (London)*, **A163**, 404 (1937).

(10) S. Sato, *J. Chem. Soc. Japan*, **76**, 1308 (1955).

(11) T. M. Shaw, *J. Chem. Phys.*, **30**, 1366 (1959).

(12) S. Sato, *J. Chem. Soc. Japan*, **77**, 940 (1956).

(13) H. W. Melville and J. C. Robb, *Proc. Roy. Soc. (London)*, **A196**, 479 (1949).

(14) S. Krongelb and M. W. P. Strandberg, *J. Chem. Phys.*, **31**, 1196 (1959).

(15) D. Hacker, S. A. Marshall and M. Steinberg, "Catalytic Surface Recombination of Atomic Oxygen," Quarterly Report ARF4203-3 (Armour Research Foundation, Chicago, Ill.).

(16) H. Wise and C. M. Ablow, *J. Chem. Phys.*, **29**, 634 (1958).

(17) H. Motz and H. Wise, *ibid.*, **32**, 1893 (1960).

constant temperature) in the presence of atomic species is related to the number of atoms recombining on the surface of the wire ($\Delta w \propto n$, where Δw is the power input to the filament due to atom recombination, and n is the gas phase concentration of atoms at the probe). The magnitude of this decrease was measured by incorporating the filament as one arm of a Wheatstone bridge (Fig. 3) and using a potentiometer to measure the voltage drop across the filament and the current through it. By this means changes in the power input to the filament as small as 0.01 microwatt could be detected.

The discharge tube and side arms were incorporated into a conventional vacuum system consisting of a mechanical fore pump, a mercury diffusion pump, and a refrigerated trap. A constant, steady-state pressure of gas in the apparatus was established by means of an adjustable leak.¹⁸ Pressure measurements were made with the McLeod gage and were corrected empirically for the pressure drop between the discharge tube and the gage.

Before entering the discharge tube Matheson prepurified-grade hydrogen (99.9% pure) was passed through a De-Oxo unit to remove oxygen and through a liquid nitrogen-cooled trap to remove water vapor. Emission spectrograms of the plasma demonstrated strong atomic hydrogen lines and gave no indication of OH, O, N or other foreign active species.

To avoid contamination of any part of the system by stopcock grease and its products of reaction with atomic hydrogen, all valves employed in the apparatus were made of brass.¹⁹ They were connected to the glass system by Kovar seals. The demountable caps at the ends of the side arms were equipped with Pyrex industrial glass pipe flanges which incorporated neoprene "O" rings to produce greaseless, vacuum-tight seals.

The experiments were carried out in a system in which the side tube wall and the gas were maintained near room temperature while the wire filament probes were heated electrically to higher temperatures. The total pressure in the system was maintained between 10 and 100 μ in order to minimize both the effect of the hot wire on gas transport properties and the contribution of homogeneous atom recombination, yet still remain in the regime of viscous flow.²⁰ Reported probe temperatures represent average temperatures which were calculated from the known dimensions of the filament and the published values of the resistivity of the metals,²¹ or were evaluated empirically. In all experiments the filaments were "cleaned" by flashing and heating them inside the hydrogen discharge plasma for periods of several hours.

With all the metals investigated, exposure of the filament to the gas containing atoms caused apparent changes of varying degrees in the resistivity of the wire. Upon extinguishment of the discharge, the wire reverted to its original state after an elapse of several hours. This phenomenon was attributed to absorption of hydrogen in the metal in the presence of gaseous atomic species. As a result, the probes were allowed to equilibrate in the vicinity of the plasma for several hours before any experimental measurements were made.

The heterogeneous recombination coefficients were evaluated from measurements of the change in steady-state atom concentration at the probe, n , relative to that at the atom source n_0 . In these experiments, the measure of the local atom density was the power, Δw , contributed to the filament by recombining atoms as the probe was moved to various positions along the tube. The change in this quantity relative to its value at the atom source Δw_0 was plotted as a function of the effective tube length (probe position) expressed as number of tube radii, L/R . By comparison with theoretical curves¹⁶ similar to those shown in Figs. 4 and 5, the catalytic activities of the tube wall and the probe were determined in terms of diffusion Reynolds numbers, δ and δ' , (primed symbols refer to the probe; unprimed, the wall). This dimensionless parameter is defined¹⁷

(18) A type "C" high vacuum valve, manufactured by Granville-Phillips, Pullman, Washington, was employed for this purpose.

(19) Packless high vacuum valves, manufactured by Voeco Vacuum Corp., New Hyde Park, Long Island, N. Y., were used.

(20) W. Gaede, *Ann. Physik*, **41**, 289 (1913).

(21) "International Critical Tables," Vol. 6, McGraw-Hill Book Co., Inc. New York, N. Y., 1929, p. 136.

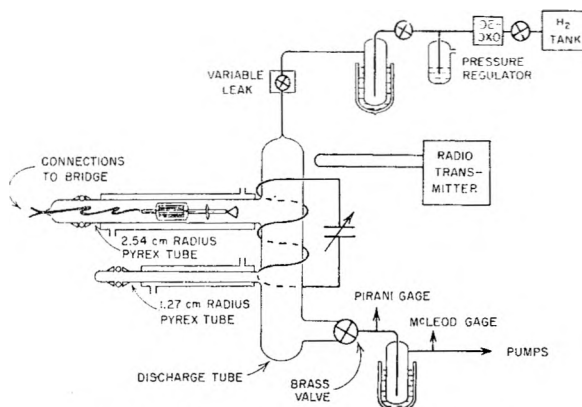


Fig. 1.—Schematic diagram of apparatus.

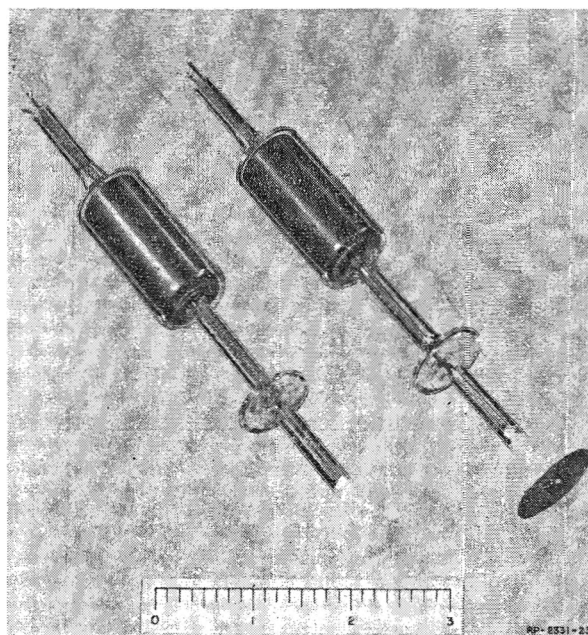


Fig. 2.—Typical filament probe assemblies.

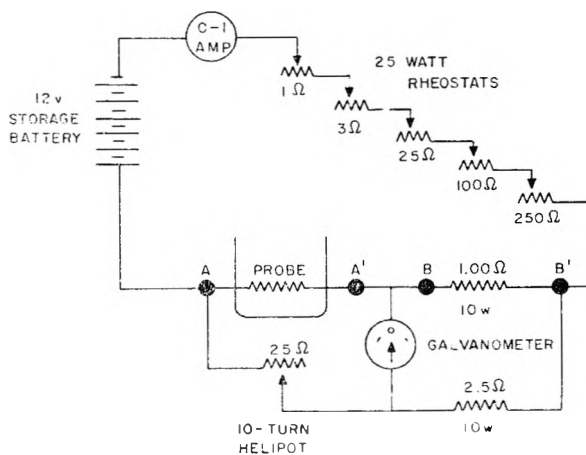


Fig. 3.—Wheatstone bridge circuit for measurement of power input to probe filament.

$$\delta = \frac{4D_{ij}(1 - \gamma/2)}{\gamma c_i R} \quad (1)$$

where D_{ij} is the interdiffusion coefficient for hydrogen atoms in molecular hydrogen, c_i is the mean atom velocity, R is the radius of the tube, and γ is the recombination coefficient.

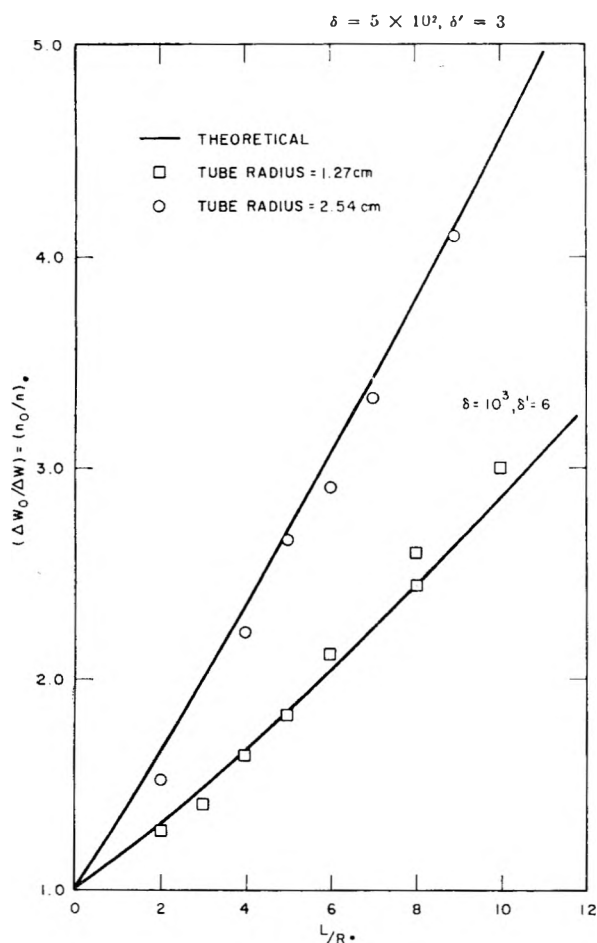


Fig. 4.—The variation of diffusion Reynolds number with tube radius; Pt probes, probe temperature 483 to 513°K.; total gas pressure 40 μ ; RF input 10 w.

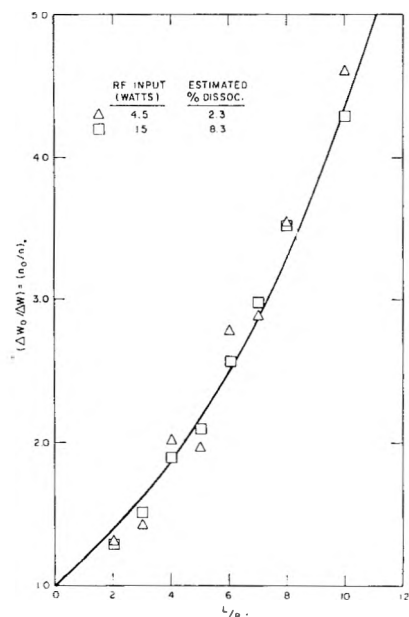


Fig. 5.—Relative atom concentration profile for two source concentrations of atoms; Pt probes, probe temperature 443 to 463°K.; tube radius 1.27 cm.; total gas pressure 70 μ .

To accurately determine δ' from experimental data for a particular probe surface, theoretical curves were constructed for specific values of L/R and δ , relating n_0/n to δ' . In

analyzing a particular experiment, a family of these curves representing a fixed value of δ was selected which gave the least scatter in δ' when the experimental values of $\Delta w_0/\Delta w$ (which are proportional to n_0/n) were plotted on the curves for their respective values of L/R . An example of this method of data analysis is given in Fig. 6. The recombination coefficients γ and γ' then were calculated by means of eq. 1, using Amdur's values of D_{ij} .²²

We may test the applicability of the theoretical analysis to the experimental technique by examining the variation of δ with tube radius and with total gas pressure. The results of such measurements are summarized in Figs. 4 and 7. It is observed that both δ and δ' are inversely proportional to pressure and to tube radius as required by eq. 1. A specific example of the independence of the diffusion Reynolds number on the atom concentration at the source is shown in Fig. 5.

In all the measurements reported the atom concentration did not exceed 10% of the total gas. A low atom concentration is desirable because the calorimetric procedure employed measures energy loss from the wire helix to the surroundings. Since the dissociation of a portion of the molecular hydrogen produces a change in the thermal conductivity of the gas, the magnitude of this change is kept small by limiting the fraction of gas dissociated to a few per cent. Also, the theoretical model ceases to be applicable at higher atom concentrations (>20%).^{17,23}

Some characteristics of the plasma source fundamentally important to these measurements have been evaluated. (cf. Appendix). The atom concentration in the source was not perturbed by the presence of the probe. This was demonstrated in an experiment in which identical platinum probes were located in each of the two side arms. It was observed that movement of the probe in one side arm closer to or farther from the source caused no significant steady-state change in the relative concentration seen by the probe in the other side arm. The uniformity of the source and an indication of its true location with respect to the side arm were established by observing the heat input to a probe which was moved in and through the plasma. The results demonstrated that the atom concentration in the plasma is uniform up to the juncture of the side arm and the discharge tube, within the experimental error of the technique. This juncture was employed as the source position ($L/R = 0$) in applying the analysis to the data. An estimate of the energy contribution to the probe from collisions by ionic or kinetically energetic species was made by substituting helium for hydrogen in the system. The heat input to the probe from the noble gas discharge was negligibly small compared to that observed in experiments with a hydrogen discharge. The absence of ions in the diffusion tube was examined by surrounding the cylindrical reactor with a magnet and examining the atom concentration profile with and without the magnetic field. In both cases identical results were obtained.

The theoretical model postulates a tube whose end is completely closed with a plate of uniform catalytic activity. It was found empirically for platinum and tungsten surfaces, however, that a probe with a surface area one-tenth that of the tube cross section approximated a true analog of the model. This was verified by performing duplicate experiments with two probes similar to those illustrated in Fig. 2. In one, the catalytically active surface consisted solely of a filament; in the other, it included also a disc of sheet metal, identical with the material of the filament, which effectively filled the entire cross section of the tube near the plane of the filament. The two experiments produced identical results.

Experimental Results

1. Platinum.—The data for platinum (Fig. 8) were obtained in a large variety of experiments in which such parameters as pressure, side arm radius, and filament dimensions were varied over wide limits. The average temperature of the filaments was varied between 338 and 1163°K. All filaments were fabricated from C.p. platinum wire.

The relatively large scatter in the data for the hydrogen-platinum system presented in this study

(22) I. Amdur, *J. Chem. Phys.*, **4**, 339 (1936).

(23) J. C. Greaves and J. W. Linnett, *Trans. Faraday Soc.*, **55**, 1338 (1959).

is attributed in large measure to some uncertainty involved in extrapolating the data to obtain Δw_0 . In the case of most of our experiments with a platinum probe in a Pyrex tube we assumed that the catalytic activity of the tube wall was so low, compared with the platinum, that the analytical treatment for the special case of a tube with non-catalytic wall could be applied near the atom source ($0 \leq L/R \leq 5$). For this condition the relationship between the concentration of atoms at the source (n_0) and the concentration at the probe (n) assumes the form¹⁶

$$1/n = (1/n_0) + L/(R \cdot n_0 \cdot \delta') \quad (2)$$

A plot of the reciprocal of atom concentration at the probe (or its equivalent, probe heat input) versus the position of the probe in terms of L/R is a straight line if the described conditions are fulfilled. In many experiments, the value of atom concentration at the source was established by an extrapolation of such a plot. An examination, however, of a number of these curves in which the atom concentration was evaluated with a probe at $L/R = 0$ indicated that under the experimental conditions one could not rely on the linearity of the curve near the origin.

An apparent activation energy of approximately 1000 cal./mole for the recombination process on

TABLE I
RECOMBINATION COEFFICIENTS OF HYDROGEN ATOMS ON VARIOUS METAL SURFACES AS A FUNCTION OF TEMPERATURE

Probe surface	Surface temp., °K.	γ'
W	353	0.065
	423	.055
	533	.068
	563	.062
	573	.055
	578	.054
	643	.059
	678	.062
	723	.057
	923	.062
1088	.067	
Cu	333	.14
	543	.10
	693	.10
Al	328	.29
	328	.32
	423	.21
	733	.27
Ti	308	.35
	308	.40
	335	.48
	421	.35
	558	.35
Ni	303	.25
	358	.13
	473	.19
	623	.17
	573	.14
Pd	448	.080
	448	.073
	673	.052
	763	.086

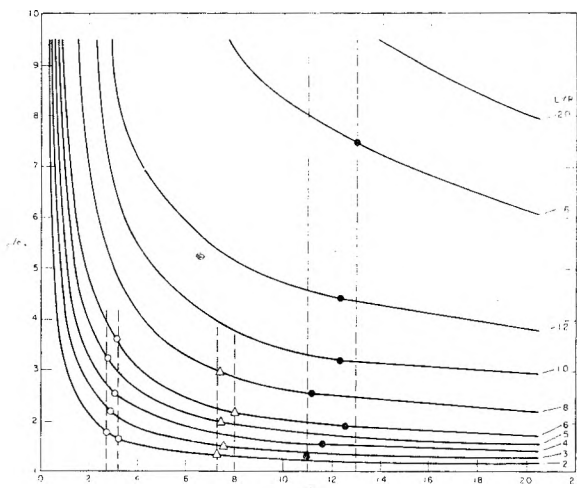


Fig. 6.—Fitting of experimental data to theoretical curves for the evaluation of diffusion Reynolds number. Solid lines are theoretical curves for $\delta = 100$; experimental points for probes of: ●, Pt; ○, Au; △, W; Pyrex tube.

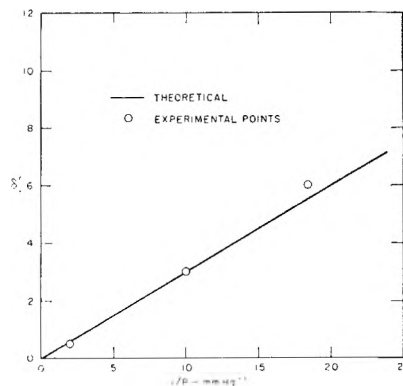


Fig. 7.—The variation of diffusion Reynolds number with total gas pressure; Pt probes, probe temperature 523 to 553°K., tube radius 1.27 cm.

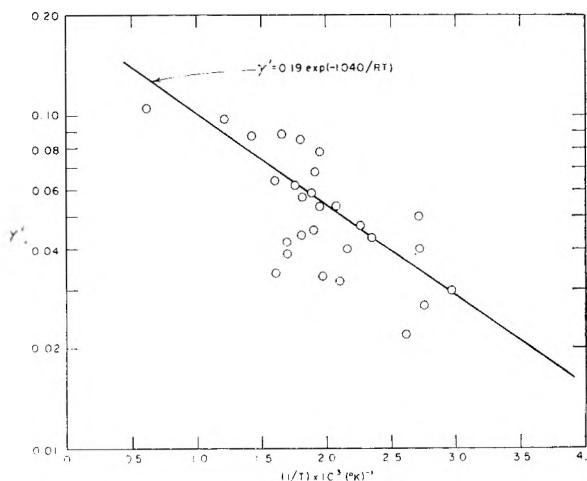


Fig. 8.—Recombination coefficient of hydrogen atoms on platinum as a function of temperature.

platinum is derived from the plot of $\log \gamma'$ versus $1/T$ (Fig. 8). Such a functional relationship is to be expected for a mobile adsorbate.

2. Tungsten.—Tungsten probes were fabricated from portions of filaments removed from

150-watt incandescent lamps.²⁴ The recombination coefficient was evaluated in the temperature range 353–1088°K. and found to be temperature-independent within the experimental error (Table I).

3. Copper.—A copper filament was wound from 1-mil thermocouple-grade, annealed copper wire. The recombination coefficient was measured in the temperature range 333–693°K. (Table I). Our data agree reasonably well with the experimental data of Sato,¹² both in magnitude and in the lack of a significant thermal effect. Sato estimates, from semiempirical energy considerations based on the assumption that the activated complex Cu...H...H has a linear configuration, that the activation energy for the heterogeneous recombination should be about 600 cal./mole. The existence of an energy of activation of this magnitude is not precluded by our data.

4. Aluminum.—Pure aluminum wire, obtained from Baker Platinum Division of Engelhard Industries, was used to construct a filament. The recombination coefficient was measured in the temperature range 328–733°K. and the data indicate that no appreciable activation energy for surface recombination is involved (Table I). The data represent, in all probability, the true recombination coefficient for hydrogen atoms on metallic aluminum, and not on aluminum oxide. The filament undoubtedly was covered with an oxide film at the outset since the wire was drawn, stored, and handled in air; but before any experimental data were recorded the filament was heated electrically and exposed to a hydrogen discharge plasma of high intensity. Under these conditions, complete removal of any oxide layer is to be expected.

5. Titanium.—Commercially pure, 10-mil wire was used to fabricate a titanium filament. This wire contained 0.029% C, 0.06% Fe, 0.01% N₂ and 0.013% H₂, and was oxide coated. As with aluminum, the titanium filament was exposed to atoms and ions in the hydrogen plasma for many hours before experimental data were taken. The appearance of the surface changed from dull, matte black to dull, lustrous silver-white during this cleaning operation. It is well known that titanium forms an alloy of somewhat variable composition with hydrogen.²⁵ Since the ratio of hydrogen to titanium in this alloy is highly temperature-dependent, it is impossible to state precisely what the surface configuration is in any given experiment. The recombination coefficient, however, appears to be constant and reproducible in the temperature range employed, 308–558°K. (Table I).

6. Nickel.—A filament was constructed from 5-mil diameter "A"-grade nickel wire which contained approximately 0.25% Mn, 0.15% Fe, and smaller quantities of C, Si, Cu and S as impurities. The recombination coefficient was determined in the temperature range 303–873°K. The data (Table I) possess appreciable scatter, but an examination of the sequence in which the experiments were run

indicates a gradual reduction of catalytic activity with exposure to hydrogen atoms. Such a phenomenon could be explained by progressive poisoning of the surface by impurities in the gas, but, since such an effect was not noted in any of the experiments with other metals, it seems unlikely. Probably the time-change in activity can be attributed to leaching of some of the inherent impurities by reaction with atomic hydrogen (carbon, silicon and sulfur form volatile hydrides when exposed to hydrogen atoms).²⁶

7. Palladium.—The recombination coefficient was determined in the temperature range 448–763°K. with filaments fabricated from 4-mil diameter pure palladium wire.²⁷ No significant activation energy was observed (Table I). It is well known that palladium readily dissolves hydrogen to form interstitial compounds, and the manifestation of this phenomenon caused the resistivity of the filaments to drift when large changes in the atomic concentration were made in the gas. By allowing the filament long periods of time to equilibrate, data of reasonable precision were obtained.

8. Gold.—Filaments of fine gold wire, 4 mils in diameter,²⁷ were used to measure recombination coefficients in the temperature range 448–838°K. The data (Fig. 9) indicate that the recombination of hydrogen atoms on gold involves an apparent activation energy of approximately 900 cal./mole.

9. Palladium-Gold Alloys.—Four-mil diameter wires of palladium-gold alloys containing 26.5, 44.5 and 62 atom % gold, respectively, were used to fabricate filaments.²⁷ The compositions of the alloys were verified by X-ray fluorescence analysis and by checking their resistivities against the values published by Geibel²⁸ for similar alloys. The 26.5 and 44.5 atom % gold alloys appear to exhibit activation energies for the recombination process, but the data demonstrate that a temperature coefficient for recombination is notably lacking in the case of the 62 atom % gold alloy (Fig. 10).

10. Pyrex.—A value for the recombination coefficient of hydrogen atoms on Pyrex was derived from a compendium of all the experiments reported herein, and represents the catalytic activity of the wall of the Pyrex tube of the apparatus. The temperature of the surface was in the range 288–303°K. The average value of the recombination coefficient is $5.8 \pm 1.8 \times 10^{-3}$. A thorough study has been made of the kinetics of hydrogen atom recombination on glass over a broad temperature range. This work is reported in a separate publication.²⁹

11. Thermocouple Probes.—The disparity in some cases between values of the recombination coefficients obtained with filament probes, and those derived earlier with thermocouple probes,³⁰ can be attributed to heat transfer variations associated with the latter. Changes in the rate of heat loss from the thermocouple probe as its tem-

(26) S. H. Inami and A. B. King, unpublished results; Kh. S. Bagdasaryan, *J. Phys. Chem. (U.S.S.R.)*, **10**, 389 (1937); *C. A.*, **32**, 1167 (1938).

(27) Palladium, gold and palladium-gold alloy wires were obtained from J. Bishop and Co., Malvern, Pa.

(28) W. Geibel, *Z. anorg. Chem.*, **69**, 38 (1911).

(29) B. J. Wood and H. Wise, to be published.

(30) B. J. Wood and H. Wise, *J. Chem. Phys.*, **29**, 1416 (1958).

(24) Manufactured by Sylvania Electric Products, Inc., Salem, Mass.

(25) D. T. Hurd, "An Introduction to the Chemistry of the Hydrides," John Wiley and Sons, Inc., New York, N. Y., 1952, pp. 181–183.

perature varied with L/R may have affected the shape of the experimental atom-decay curves and thus led to erroneous values of γ' . Evidence of such a perturbation was detected by comparing curves obtained from the thermocouple probes with those derived from filament probe experiments for the same metals, and in comparing data taken with a thermocouple probe in two temperature ranges. All data reported in this paper are derived from experiments made with filament probes.

Discussion

The results of our experiments agree, in general, with previously reported work^{2a,10,21,31} that the kinetics of heterogeneous atom recombination are first order with respect to gaseous atom concentration over the investigated ranges of temperature and pressure. Some investigators³²⁻³⁴ have noted a change to second-order kinetics at temperatures sufficiently high to produce a surface sparsely covered with adatoms, but evidence of such a phenomenon does not appear in our data. First-order kinetics could involve: (1) a slow adsorption step (at a rate proportional to gas-atom concentration) followed by rapid surface migration and recombination (Hinshelwood mechanism), or (2) reaction between an adsorbed atom on a fully covered surface and a gas atom (Rideal mechanism).

Although surface mobility of the adatoms probably prevails³⁵ under the conditions of our experiments, the Hinshelwood mechanism would exhibit activation energies comparable in magnitude to the energies of activation for surface diffusion (8-16 kcal./mole), which are from 10 to 20% of the binding energies of the chemisorbate.^{35,36} Our results, however, demonstrate much lower activation energies ($0 \leq E_a \leq 1$ kcal./mole) for the recombination process, which suggests that the Rideal mechanism is predominant. It has been demonstrated for the case of Pyrex glass²⁹ (H-surface bond energy $\cong 44$ kcal./mole) that adatom-adatom recombinations become kinetically significant above 500°K. Hence, because of the relatively greater stability of the bond between adatoms of hydrogen and a metal (60-80 kcal./mole), predominance of the Hinshelwood mechanism should appear only at temperatures of the order of 1300°K. or greater.

It is of interest to interpret the kinetics of heterogeneous hydrogen atom recombination from a microscopic point of view in terms of fundamental substrate and adsorbate characteristics. Numerous surface reactions involving hydrogen, such as hydrogen-deuterium exchange³⁷ and ortho-para-hydrogen conversion,³⁸ have been studied, and the observed reaction rates have been correlated with the electron distribution in the valence band of the substrate. The existence of a surface-adsorbed

(31) K. E. Shuler and K. J. Laidler, *J. Chem. Phys.*, **17**, 1212 (1949).

(32) F. Paneth and W. Lautsch, *Ber.*, **64B**, 2708 (1931).

(33) F. Paneth, W. Hofditz and A. Wunsch, *J. Chem. Soc.*, 372 (1935).

(34) N. Buben and A. Schechter, *Acta Physicochim. U.R.S.S.*, **10**, 371 (1939).

(35) R. Gomer, R. Wortman and R. Lundy, *J. Chem. Phys.*, **26**, 1147 (1957).

(36) R. Wortman, R. Gomer and R. Lundy, *ibid.*, **27**, 1099 (1957).

(37) G. K. Borekov and V. L. Kuchaev, *Doklady Akad. Nauk, S.S.S.R.*, **119**, 302 (1958); *Chem. Abstr.*, **52**, 16370a (1958).

(38) A. Couper and D. D. Eley, *Disc. Faraday Soc.*, **8**, 172 (1950).

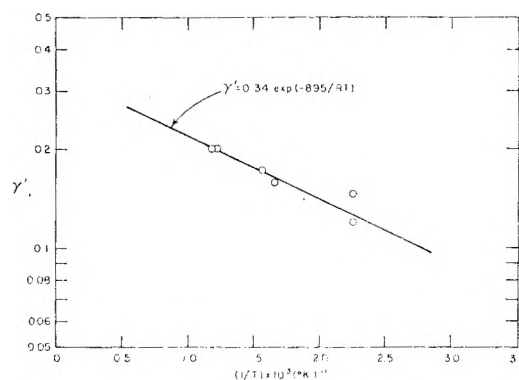


Fig. 9.—Recombination coefficient of hydrogen atoms on gold as a function of temperature.

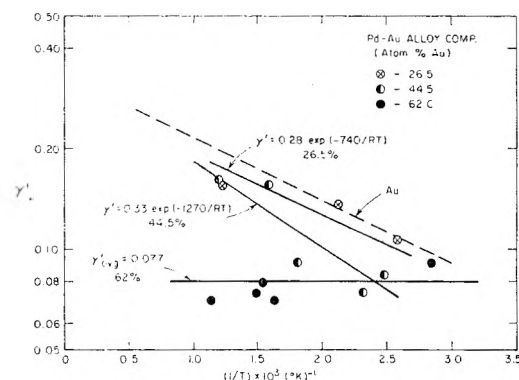


Fig. 10.—Recombination coefficients of hydrogen atoms on palladium-gold alloys as a function of temperature. (Au Values, cf. Fig. 9)

layer of hydrogen, however, may cause a modification of the electronic properties of the solid analogous to the changes produced by the formation of solid solutions composed of a combination of transition and non-transition metals (such as Pd and Au)³⁸ or Hume-Rothery alloys.³⁹ In the case of a transition metal lattice into which hydrogen atoms have diffused, the transfer of electrons from the hydrogen atom to the solid has been postulated to account for such phenomena as, for example, the decrease in magnetic susceptibility of the transition metal.⁴⁰ The extra electrons so furnished presumably decrease the number of positive holes in the d-band. A similar lowering of the susceptibility is demonstrated in the addition of gold to palladium.⁴¹ In our system, consisting of a transition metal in the presence of both atomic and molecular hydrogen, we may be dealing, therefore, with a solid of feebly paramagnetic or even diamagnetic properties because of the adsorption and absorption of hydrogen atoms. Such an explanation would account for the observed catalytic properties of palladium and the diamagnetic palladium-gold alloys (>55 atom % of gold).³⁸ As observed in our measurements of heterogeneous atom recombination, these two solids (in our case, palladium and a 62 atom % gold-palladium alloy) are identical in their catalytic efficiency, both in the absolute value of the recom-

(39) G. M. Schwaab, *Trans. Faraday Soc.*, **42**, 689 (1942).

(40) N. F. Mott and H. Jones, "The Theory of the Properties of Metals and Alloys," Dover Publ., New York, N. Y., 1958, p. 200.

(41) E. Vogt, *Ann. Physik*, **14**, 1 (1932).

bination coefficient and in the absence of an activation energy.

In view of the changes in electronic configuration of the solid brought about by chemisorbed hydrogen on the metal surface, no correlation is to be expected between the Pauling d-character or the degree of filling of holes in the d-band³⁸ and catalytic activity in metal-hydrogen systems where gas adsorption is appreciable.

The pronounced differences observed by us in the value of the recombination coefficients in a series of transition elements, such as that of Ti relative to that of Ni, and the high activity of non-transition metals, such as Al, must be due to some other cause. It appears that the presence of large amounts of hydrogen in the solid enhances the recombination process. Indeed, a qualitative correlation exists between our measured catalytic efficiency and the occlusive capacity of some of the metals as evidenced by solubility isobars for molecular hydrogen at 1 atmosphere.⁴² The importance of hydrogen dissolved in a catalyst has been established in numerous systems. Observations have been made of the decline of catalytic activity of Raney nickel by reduction of the hydrogen content of the solid⁴³; hydrogen dissolved in palladium was found to be quite important in the hydrogenation of ethylene⁴⁴ and benzene⁴⁵; the promoting effect of dissolved hydrogen in catalytic reactions also was reported by Roginsky.⁴⁶ An increasing amount of experimental evidence has pointed to the participation of lattice atoms in catalytic reactions. One example is the investigation of carbon monoxide oxidation on transition metal oxides by Garner,⁴⁷ from which he concluded that the process involves oxygen extraction from the solid, the oxide surface being alternately reduced by CO and oxidized by oxygen. For the recombination of oxygen atoms on oxide surfaces the formation of a gaseous molecule by the interaction of a gaseous oxygen atom with an oxygen atom supplied to the surface from the lattice has been considered.⁴⁸ The replacement of such a surface vacancy by an atom diffusing from the interior of the solid rather than by subsequent surface adsorption from the gas may be an important factor in catalysis.

In our experiments the presence of atomic hydrogen in the gas appears to alter completely the sorption characteristics of the metal surface. The relatively high catalytic activity we observed for gold, for example, which chemisorbs molecular hydrogen only at elevated temperatures,⁴⁹ may be attributed to the presence of gaseous atomic hydrogen which encounters no energy barrier for dissociative chemisorption. As a result, hydrogen atoms

may readily diffuse into the underlying crystal lattice. Such an effect has been demonstrated with a silicon surface⁵⁰ and probably explains the absorption behavior of the gold and palladium-gold alloys (>55 atom % Au) in which molecular hydrogen is reported to be insoluble.⁴¹

Another possible effect of the presence of dissolved gas in a solid which must be considered is the perturbation of the lattice dimensions by the occluded species. Whether such occlusions take the form of interstitial metal-hydrogen compounds or of hydrogen accumulation in "rifts" and other lattice dislocations has not been settled, but there is evidence for the displacement of metal lattice atoms on absorption of hydrogen.⁵¹ Such distortions of the crystal may lead to geometric dispositions of the lattice and the formation of additional electronic states which render the surface favorable for the recombination reaction.

The formation of a hydrogen molecule by heterogeneous recombination of hydrogen atoms is accompanied by the release of energy of a magnitude not commonly encountered in catalytic reactions. For the collisional transfer of kinetic energy between a gas atom and a solid in the absence of chemical reaction, energy dissipation by the spontaneous emission of phonons into the crystal has been considered in some detail.^{52,53} If the energy that goes into sound waves is carried away rapidly enough, thermal accommodation is to be expected. At the same time, the transfer of energy becomes less efficient above a critical value of the incident energy, and a more elastic collision takes place. In an exothermic heterogeneous atom reaction, partial energy accommodation may lead to the production of a molecule containing excess internal or kinetic energy. Indeed, recent observations^{54,55} have suggested the formation of electronically excited molecules formed by the recombination of atoms on solid surfaces. In the gas phase⁵⁶ for exothermic reactions of the type $A + BC \rightarrow AB + C$, one-half of the energy of reaction may appear as vibrationally excited AB^* , when C is massive with respect to A and B.

In analogy to the theoretical considerations for collisional energy transfer without chemical reaction, one may attempt to correlate our observed coefficients for atom recombination to some lattice property related to the propagation of lattice waves from the point of impact. As a first approximation, the Debye characteristic temperature θ_D may be considered since the normal mode frequency spectrum of the lattice has an upper limit at the Debye frequency. Such a model does not exclude the addition of many phonons of identical energy to the lattice. As the temperature is increased beyond θ_D the vibrational frequencies remain independent of temperature but the amplitude of vibrations

(42) D. P. Smith, "Hydrogen in Metals," Univ. of Chicago Press, Chicago, Ill., 1948, p. 35.

(43) R. J. Kokes and P. H. Emmett, *J. Am. Chem. Soc.*, **81**, 5032 (1959).

(44) D. Dobytschin and A. Frost, *Acta Physicochim. U.R.S.S.*, **5**, 111 (1936).

(45) A. A. Alekhudzhyan and M. A. Indzhikyan, *Zhur. Fiz. Khim.*, **33**, 983 (1959).

(46) S. F. Roginsky, *J. Phys. Chem. (U.S.S.R.)*, **15**, 1 (1941).

(47) W. E. Garner, F. S. Stone and P. F. Tiley, *Proc. Roy. Soc. (London)*, **A211**, 472 (1952).

(48) J. W. Linnett and D. J. H. Marsden, *ibid.*, **A234**, 504 (1956).

(49) B. M. W. Trapnell, *ibid.*, **A218**, 566 (1953).

(50) J. T. Law, *J. Chem. Phys.*, **30**, 1568 (1959).

(51) C. R. Cupp, edited by B. Chalmers, "Progress in Metal Physics," Pergamon Press, London, 1953, Chap. 3.

(52) N. Cabrera, *Discussions Faraday Soc.*, **28**, 16 (1959).

(53) R. W. Zwanzig, *J. Chem. Phys.*, **32**, 1173 (1960).

(54) R. R. Reeves, G. Manella and P. Harteck, *ibid.*, **32**, 946 (1960).

(55) P. Harteck, R. R. Reeves and G. Manella, *Can. J. Chem.*, **38**, 1648 (1960).

(56) F. T. Smith, *J. Chem. Phys.*, **31**, 1352 (1959).

may rise. A plot of the recombination coefficient γ' vs. the Debye characteristic temperature yields the curve shown in Fig. 11. A monotonic increase of γ' with θ_D is noted. Such a correlation suggests that high recombination efficiency of the solid may be associated with materials of low compressibility which exhibit high velocity of propagation of longitudinal and transverse lattice waves.

However, in the non-reactive interaction of a gas with a solid surface the quantity of kinetic energy that can be transferred in a collision with the lattice decreases with increasing lattice force constant⁵³ (which is related to the Debye characteristic temperature in a one-dimensional lattice). Such considerations lead to the conclusion that a solid may exhibit high efficiency for atom recombination but at the same time low energy accommodation.

Evidence of non-equilibrium distribution of energy between the surface and desorbing molecules has been observed in our experiments. The energy contributed by heterogeneous atom recombination to filaments of various metals situated in a hydrogen discharge of fixed intensity (and, therefore, uniform atom density at the source) was evaluated. From this measurement and from previously measured values of the recombination coefficients, the relative energy appearing as heat in the wires per mole of recombining atoms per unit geometric area of surface was calculated. These results suggest that there exists a wide variation in the ability of metals to thermally accommodate adsorbed species under such conditions. Further work is in progress in order to determine whether, in the case of hydrogen atom recombination, this energy appears as internal or/and kinetic energy of the desorbing molecule.

Appendix

The following specific facts demonstrate that the atom density, n_0 , of an atom source at $x = 0$ remains essentially constant during the course of an experiment.

1. An increase in power input into the R-F discharge produces a corresponding rise in atom

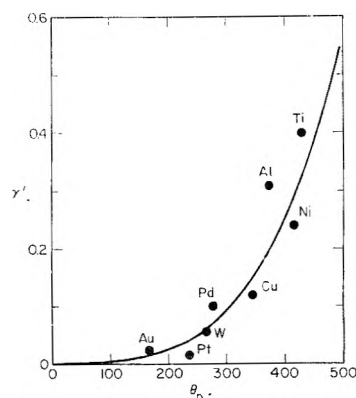


Fig. 11.—Variation of recombination coefficient with Debye characteristic temperature.

density. Although the atom density was varied by more than an order of magnitude in this manner, the relative atom density profile in the diffusion tube for a given catalytic surface remained unaffected by such changes in absolute atom concentration. This is to be expected for a first-order surface reaction.

2. Changes in radius of the diffusion tube resulted in appropriate changes of the diffusion Reynolds number δ' which is proportional to $(1/R)$.

3. Changes in total gas pressure P were reflected in corresponding changes in δ' which is proportional to $(1/P)$.

4. A filament traverse of the region near the atom source in the flow tube indicated a uniform atom concentration up to the juncture of the side arm and the discharge tube.

5. The activity of the Pyrex walls of the diffusion tube evaluated near the atom source, $0 \leq (L/R) \leq 10$, agrees well with the value obtained from measurements at much larger distances where the atom density curve approaches an exponential decay.

The experimental results point to a definite difference in the catalytic activity of the metals investigated, *i.e.*, different values of γ' .

THE CONFORMATION OF POLYMER MOLECULES.

IV. POLY-(1-BUTENE)

By W. R. KRIGBAUM, J. E. KURZ AND P. SMITH

*Department of Chemistry, Duke University, Durham, N. C.**Received April 19, 1961*

Poly-(1-butene) was separated into atactic and isotactic portions by extraction and these materials were individually fractionated. The two forms obeyed identical intrinsic viscosity-molecular weight relationships in good solvents; however, the isotactic modification exhibited lower values of the osmotic second virial coefficient for molecular weights below 7×10^5 . This type of behavior in good solvents has been reported by other workers for the two forms of polystyrene and polypropylene, and hence appears to be quite general. Precipitation temperature measurements in anisole gave a higher entropy parameter, ψ_1 , for the stereoregular poly-(1-butene), in agreement with the result reported by Kinsinger and Wessling for polypropylene in phenyl ether. On the other hand, the latter workers found a *lower* theta temperature for isotactic polypropylene, whereas we obtained a *higher* theta temperature for the stereoregular poly-(1-butene). Thus, atactic poly-(1-butene) is more soluble in anisole than its stereoregular counterpart for all molecular weights, whereas atactic polypropylene should be the form of lower solubility in phenyl ether for molecular weights above 39,000. Isotactic poly-(1-butene) appears to have a more highly extended molecular conformation than its atactic counterpart, as judged from unperturbed dimensions estimated from light scattering data obtained using a good solvent. Parameters are given which permit a comparison of the relative extensions of a number of polyolefins.

Introduction

The method of preparation and the physical properties of a number of linear, stereoregular polyolefins were described by Natta and co-workers in 1955.¹ Since that time there has been considerable interest in comparing the molecular dimensions and thermodynamic interactions of the isomeric forms of these polymers in solution. The majority of this work has involved the measurement of intrinsic viscosities, molecular sizes and second virial coefficients in thermodynamically good solvents.²⁻¹¹ The conclusions drawn from these investigations are that the perturbed molecular dimensions in good solvents are indistinguishable for the atactic and isotactic forms, but that the stereoregular polymers exhibit smaller second virial coefficients (at least for lower molecular weights) in these solvents. This latter conclusion is in agreement with the earlier work of Muthana and Mark,¹² who compared crystalline and amorphous samples of poly-(vinyl isobutyl ether). Finally, in the case of polystyrene the (\bar{r}_0^2/M) ratio estimated from values of the intrinsic viscosity and second virial coefficient measured in good solvents was reported to be 15 to 20% larger for the isotactic form.⁶

Much less information is available concerning the behavior of these polymers in thermodynamically poor solvents. Kinsinger and Wessling¹³

have reported precipitation temperature measurements for atactic and isotactic polypropylene in the theta solvent diphenyl ether. They found that the isotactic form exhibited a smaller theta temperature, but a larger entropy parameter, ψ_1 . This is rather surprising, since it means that for sufficiently high molecular weights the stereoregular polymer is *more* soluble in this solvent than its random counterpart, whereas most separations are based upon the *lower* solubility of the stereoregular polymer.

The foregoing studies have been performed upon polymers whose stereoregular isomers have high melting points. This necessitates the use of elevated temperatures to avoid molecular aggregation, which enhances the possibility of degradation. Poly-(1-butene) was chosen for the present study, since the isotactic isomer melts at a lower temperature, 130°, than either polypropylene (176°) or polystyrene (240°). Molecular weights and dimensions (as determined by osmotic pressure and light scattering measurements using good solvents), and precipitation temperature data in anisole, are reported.

Experimental

Polymer Extraction and Fractionation.—The atactic polymer was extracted from all of the poly-(1-butene) samples¹⁴ using boiling ethyl ether. This extraction yielded 19 g. having a density of 0.87 g./ml., which is in agreement with the value reported by Natta and co-workers¹ for the atactic form. This material is designated AB. The isotactic material, designated as series B, had a density of 0.92 g./ml. and a melting point of 131°.

The atactic sample was fractionated at 35° using the conventional precipitation method, while for the isotactic polymer a two-stage extraction-precipitation technique¹⁵ was used at 60°, beginning with 25 g. of polymer. In either case ligroin (b.p. 90-120°) was the solvent and absolute ethyl alcohol the precipitant. Although the initial phase separation for the isotactic polymer was reversible, some crystallization occurred overnight at 60°. The fractions were recovered by pouring the concentrated phase into a large quantity of alcohol, filtering and drying to constant weight in a vacuum oven at 60°. This procedure did not give complete recovery of some of the lower molecular weight atactic samples.

(14) The samples were generously donated by the Hercules Powder Company, Union Carbide Chemicals Company, Naugatuck Chemical Company, and E. I. du Pont de Nemours and Company.

(15) W. R. Krigbaum and A. M. Kotliar, *J. Polymer Sci.*, **32**, 323 (1958).

(1) G. Natta, P. Pino, P. Corradini, F. Danusso, E. Mantisa, G. Mazzanti and G. Moraglio, *J. Am. Chem. Soc.*, **77**, 1708 (1955); *J. Polymer Sci.*, **16**, 143 (1955); *Makromol. Chem.*, **16**, 77, 213 (1955).

(2) G. Natta, F. Danusso and G. Moraglio, *ibid.*, **20**, 37 (1956).

(3) F. W. Peaker, *J. Polymer Sci.*, **22**, 25 (1956).

(4) F. Danusso and G. Moraglio, *ibid.*, **24**, 161 (1957).

(5) F. Ang, *ibid.*, **25**, 126 (1957); F. Ang and H. Mark, *Monatsh. Chem.*, **88**, 427 (1957).

(6) W. R. Krigbaum, D. K. Carpenter and S. Newinan, *J. Phys. Chem.*, **62**, 1586 (1958).

(7) R. Chiang, *J. Polymer Sci.*, **28**, 235 (1958).

(8) F. Danusso and G. Moraglio, *Makromol. Chem.*, **28**, 250 (1958).

(9) J. B. Kinsinger and R. E. Hughes, *J. Phys. Chem.*, **63**, 2002 (1959).

(10) L. Trossarelli, E. Campi and G. Saini, *J. Polymer Sci.*, **35**, 205 (1959).

(11) P. Parrini, F. Sebastiano and G. Messina, *Makromol. Chem.*, **38**, 27 (1960).

(12) M. S. Muthana and H. Mark, *J. Polymer Sci.*, **4**, 531 (1949).

(13) J. B. Kinsinger and R. A. Wessling, *J. Am. Chem. Soc.*, **81**, 2908 (1959).

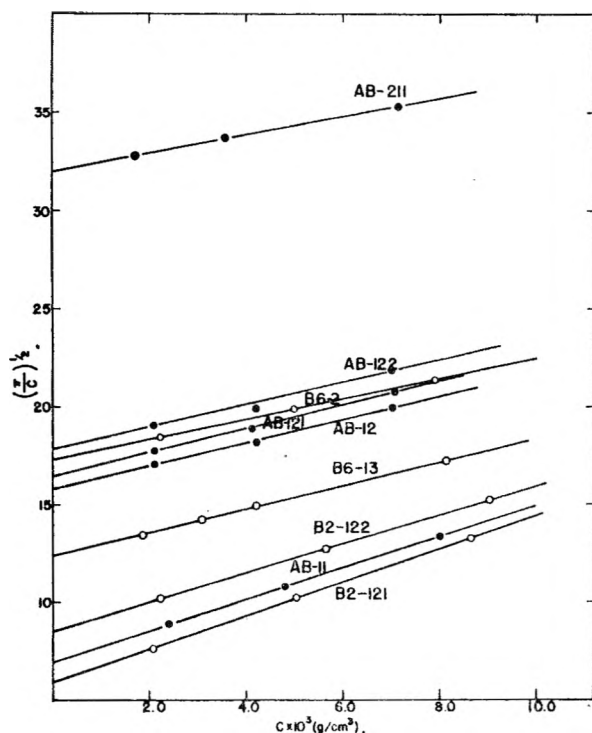


Fig. 1.—Osmotic data for atactic (●) and isotactic (○) poly-(1-butene) in toluene at 45°.

Viscosities.—Ubbelohde viscometers were employed. Kinetic energy corrections were applied, but the effect of shear rate was not investigated. Most of the aromatic impurities were removed^{16,17} from the ethylcyclohexene, and all of the solvents were dried and distilled shortly before use.

Osmometry.—Stabin high speed osmometers¹⁸ were employed with either Type 300 wet regenerated cellulose¹⁹ or dried 300 PUT-0²⁰ membranes. The latter were swollen in nearly boiling water for 24 hours before beginning the usual conditioning procedure.²¹ Static measurements were performed, and the Δh values were read to 0.01 mm. The capillaries were not perfectly matched, which necessitated small corrections to all the Δh values. The solvent, reagent grade toluene, was dried and distilled before use.

Light Scattering.—Measurements were performed over the angular range 45–135° using vertically polarized light of 436 m μ wave length. The instrument has been adequately described elsewhere.²² The inner cell, made according to the design of Dandliker and Kraut,²³ was thermostated by circulating oil through a double-walled brass jacket enclosing the outer cell.²⁴ The temperature was measured by a two junction thermocouple inserted in the solvent in the outer cell. A 0.5% toluene solution of the "Cornell standard" polystyrene, having for its excess scattering a Raleigh ratio $R_v = 4.20 \times 10^{-4} \text{ cm.}^{-1}$ at 436 m μ ,²² was used as the intensity standard. The instrument, when aligned, gave dissymmetry, z_{45} , of 1.18 to 1.19 for the standard polystyrene solution.

(16) R. W. Crowe and C. P. Smyth, *J. Am. Chem. Soc.*, **73**, 5406 (1951).

(17) S. A. Ashmore, *Analyst*, **72**, 206 (1947).

(18) J. V. Stabin and E. K. Immergut, *J. Polymer Sci.*, **14**, 209 (1954).

(19) Obtained from the Sylvania Division, American Viscose Corporation, Fredricksburg, Va.

(20) Obtained from E. I. du Pont de Nemours and Co., Wilmington, Del.

(21) W. R. Krigbaum and P. J. Flory, *J. Am. Chem. Soc.*, **75**, 1775 (1953).

(22) D. K. Carpenter and W. R. Krigbaum, *J. Chem. Phys.*, **24**, 1041 (1956).

(23) W. B. Dandliker and J. Kraut, *J. Am. Chem. Soc.*, **78**, 2380 (1956).

(24) W. R. Krigbaum and D. K. Carpenter, *J. Phys. Chem.*, **59**, 1166 (1955).

The solutions were clarified by centrifuging at 50,000 g for 30 to 40 minutes using a Spinco Model L preparative ultracentrifuge with a SW 25.1 swinging bucket rotor. The rotor was heated to 90° before centrifuging the isotactic solutions, and the temperature drop during centrifugation was always less than 10°.

The Brice-Phoenix differential refractometer was calibrated with sucrose solutions.²² The atactic and isotactic forms exhibited the same dn/dc values in n -nonane. These were 0.108 at 80° and 0.092 at 35° for 436 m μ light. Depolarization was negligible for both isomeric forms.

Phase Equilibria Measurements.—The apparatus and procedure for the determination of the critical miscibility temperatures was essentially that described by Shultz and Flory.²⁵ The temperature of the ethylene glycol bath was lowered at a rate of 0.1°/min. until the solutions became sufficiently cloudy to obscure a thermometer scale held behind them. The solvent, anisole, was washed with aqueous NaOH and water, dried with CaCl₂, and finally refluxed and fractionally distilled over sodium. The purity was 99.9 mole %, as ascertained using a freezing point depression apparatus²⁶ with a platinum resistance thermometer and Mueller Bridge.

Experimental Results

Osmotic Pressure and Light Scattering Measurements.—Osmotic pressure measurements were performed upon four isotactic fractions and five atactic fractions of poly-(1-butene) in toluene. Although the second virial coefficients indicate that toluene is a thermodynamically good solvent, solutions of the isotactic polymer exhibited phase separation within 24 hours at temperatures below 39°. The osmotic data therefore were obtained at 45°. The isotactic polymer appeared to be stable toward degradation, but some of the atactic fractions degraded in the bulk state. For this reason 3–5 mg. of Ionol²⁷ was added to the atactic poly-(1-butene) solutions.

Figure 1 shows the osmotic data plotted in accordance with the relation

$$(\pi/c)^{1/2} = (\pi/c)_0^{1/2} [1 + (\Gamma_2/2)c] \quad (1)$$

where π is the osmotic pressure. The second virial coefficient, A_2 , is given by $\Gamma_2/(M)_2$.

The solvent for the light scattering measurements was n -nonane. Solutions of the isotactic polymer exhibited a visually observable phase separation at temperatures below 50°, but the low angle scattering was found to increase with time at temperatures up to 70°. The isotactic polymer solutions therefore were studied at 80°, and were maintained above this temperature during clarification. Data were obtained for the atactic fractions at 35°, and 0.1% Ionol (which had no effect upon the scattered intensity) was added as an inhibitor to degradation. The atactic solutions were more difficult to clarify, and additional centrifugation was required in some cases. Dry weight measurements indicated that no polymer was lost by centrifugation, but occasionally the concentration had increased somewhat due to evaporation of the solvent.

All fractions examined gave linear plots of $c/I_v(\theta)$ vs. $\sin^2(\theta/2)$, where $I_v(\theta)$ is the scattering intensity, expressed in Rayleigh ratio units, as measured at an angle θ to the incident beam. An example appears in Fig. 2, which illustrates the

(25) A. R. Shultz and P. J. Flory, *J. Am. Chem. Soc.*, **74**, 4760 (1952).

(26) F. W. Schwab and E. R. Smith, *J. Research Natl. Bur. Standards*, **54**, 333 (1945).

(27) Obtained from Shell Chemical Co.

TABLE I
 OSMOTIC PRESSURE AND LIGHT SCATTERING RESULTS

Fraction	$10^{-5} \langle M \rangle_n$	$10^4 A_2$	$10^{-5} \langle M \rangle_w$	$10^4 A_2$	$10^{10} \langle r^2 \rangle_z$	$\frac{\langle M \rangle_w}{\langle M \rangle_n}$	$10^{16} \frac{\overline{r^2}}{M}$
AB-11	5.58	4.10	13.0	2.4	3.18	2.33	1.56
AB-121	0.997	7.35	(1.49) ^a				
AB-12	(1.08)	(6.88)	1.42	2.4	0.247	(1.7) ^b	1.23
AB-122	0.864	7.50	(0.966) ^a				
AB-211	0.263	10.8	(0.441) ^a				
B2-121	7.75	3.73	9.35	1.05	2.02	1.21	1.85
B2-122	3.72	4.66	4.12	3.56	0.810	1.11	1.78
B6-13	1.75	5.49	1.70	4.31	.270	~1.0	1.59
B6-2	0.901	6.57	1.05	6.02	.173	1.17	1.43

^a Molecular weights calculated from intrinsic viscosities.

^b Ratio estimated as described in the text.

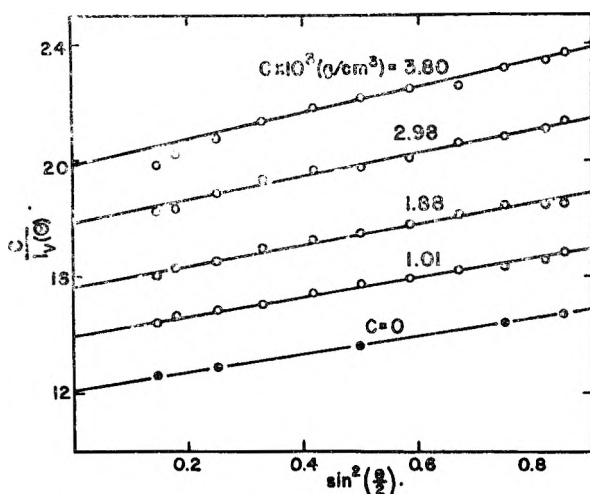


Fig. 2.—Light scattering results for isotactic fraction B6-13 in *n*-nonane at 80°.

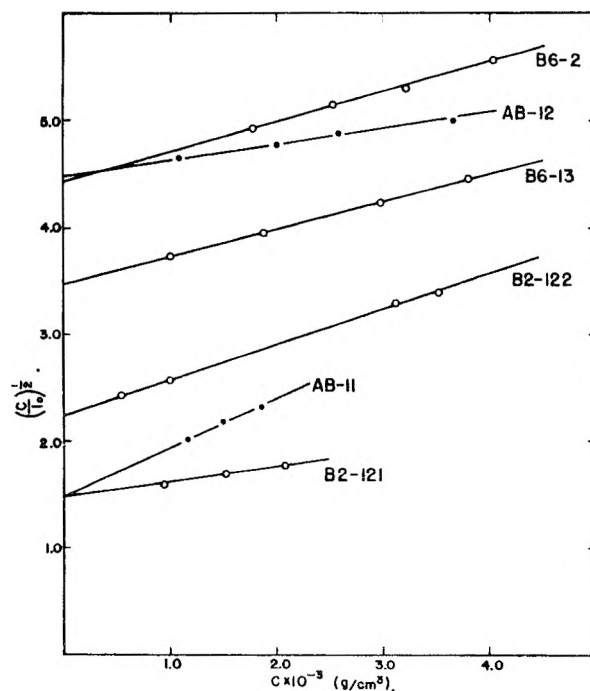


Fig. 3.—Concentration dependence of the zero angle intercepts for poly-(1-butene) in *n*-nonane. Atactic fractions at 35° designated by ● and isotactic fractions at 80° by ○.

angular scattering data for isotactic fraction B6-13. The filled circles in this plot represent values of the reciprocal scattering function extrapolated to infinite dilution. Values of the *z*-average mean-square radius of gyration, $\langle s^2 \rangle_z$, were calculated from the (slope/intercept) ratio of this latter line through use of the equation

$$\langle s^2 \rangle_z = \left(\frac{\text{slope}}{\text{intercept}} \right) \frac{3}{16\pi^2} \frac{\lambda^2}{n_0^2} \quad (2)$$

where n_0 is the refractive index of the solvent and λ is the wave length of the incident light, 4.36×10^{-5} cm. The mean-square displacement lengths were calculated on the assumption that $\langle r^2 \rangle_z = 6 \langle s^2 \rangle_z$.

The zero angle intercepts of the lines for finite concentrations shown in Fig. 2 were treated in accordance with the relation

$$(c/I_0)^{1/2} = (c/I_0)_0^{1/2} [1 + \Gamma_2 c] \quad (3)$$

Figure 3 illustrates the data obtained for all fractions plotted in this manner. Molecular weights and values of the second virial coefficient, A_2 , were obtained using the equations

$$\langle M \rangle_w = \frac{C_n/C_n'}{K_V(c/I_0)_0} \quad (4)$$

$$A_2 = \Gamma_2 / \langle M \rangle_w \quad (5)$$

K_V had the values 3.04×10^{-7} and 4.06×10^{-7} mole cm.²/g.² at 35 and 80°, respectively, and the refractive index correction, (C_n/C_n') , which was assumed to be proportional to the square of the refractive index, was 0.862 and 0.835 at the same two temperatures.

The quantities obtained from these solution measurements are collected in Table I. Columns 2 and 3 give values derived from the osmotic measurements for toluene solutions at 45°. Columns 4–6 concern parameters evaluated from the light scattering data obtained using *n*-nonane at 80° (isotactic) and 35° (atactic). The $\langle M \rangle_w$ values enclosed in parentheses in column 4 were calculated from the intrinsic viscosities using relationships given below. Atactic fraction AB-12 degraded between the time of the osmotic pressure and light scattering measurements. A lower limit for this ratio was estimated by setting $\langle M \rangle_w = 185,000$ as calculated from the intrinsic viscosity before degradation. The value of the ratio was undoubtedly closer to 2.0 when the light scattering

measurements were performed. We may therefore expect the entry in column 8 for fraction AB-12 to be somewhat high. This ratio was calculated from the relation

$$\bar{r}^2/M = \langle \bar{r}^2 \rangle_z / \langle M \rangle_w \langle M \rangle_w / \langle M \rangle_z \quad (6)$$

$\langle M \rangle_z$ was estimated by representing the weight fraction distribution by the relation of Zimm^{28,29}

$$f(M) = \frac{y^{h+1}}{h!} M^h e^{-yM} \quad (7)$$

where h , a parameter characterizing the polydispersity, is given by

$$h = (\langle M \rangle_w / \langle M \rangle_n - 1)^{-1}$$

and

$$\frac{\langle M \rangle_z}{h+2} = \frac{\langle M \rangle_w}{h+1} = \frac{\langle M \rangle_n}{h}$$

Phase Equilibrium Measurements.—Liquid-liquid phase diagrams were determined in the vicinity of the critical miscibility temperature for atactic and isotactic poly-(1-butene) in anisole. About 2–3 mg. of Ionol was added to each solution to inhibit degradation. The precipitation temperature of the most concentrated solution was determined first, and subsequent determinations at lower concentrations were made by dilution. The range of temperatures over which phase separation occurred became narrower as the molecular weight of the fractions increased. This temperature range is indicated by the size of the circle shown in Fig. 4, where the precipitation temperature appears plotted against the volume fraction of polymer.

The critical miscibility temperatures, T_c , corresponding to the maximum point of each curve, then were treated in accordance with the relation³⁰

$$\frac{1}{T_c} = \frac{1}{\Theta} \left[1 + \frac{1}{\psi_1} \left(\frac{1}{x^{1/2}} + \frac{1}{2x} \right) \right] \quad (8)$$

Here Θ and ψ_1 are the theta temperature and entropy parameter, respectively, and x is the ratio of the molar volumes of polymer and solvent. Shultz and Flory²⁵ have shown that the precipitation temperature depends upon an average molecular weight between the weight- and z -average. We have calculated x using $\langle M \rangle_w$ values

$$x = \langle M \rangle_w / \bar{v} V_1 \quad (9)$$

where \bar{v} , the partial specific volume, is 1.149 ml./g. for poly-(1-butene) at 30° and the molar volume, V_1 , of anisole is 109.6 ml./mole at 30°. The critical miscibility temperature data appear in Table II. Figure 5 shows these values plotted in accordance with equation 8, and the values of Θ and ψ_1 obtained from these two lines are given in the last two columns of Table II.

Viscosity Measurements.—Data were obtained using as solvents ethylcyclohexane at 70°, n -nonane at 80 and 35° for the isotactic and atactic forms, respectively (conforming to the conditions for the light scattering measurements), and anisole at 89.1 and 86.2° (corresponding to the θ temperatures of the isotactic and atactic polymers, respectively.)

(28) B. H. Zimm, *J. Chem. Phys.*, **16**, 1093 (1948).

(29) B. H. Zimm, *ibid.*, **16**, 1099 (1948).

(30) P. J. Flory, "Principles of Polymer Chemistry," Cornell University Press, Ithaca, N. Y., 1953, p. 545.

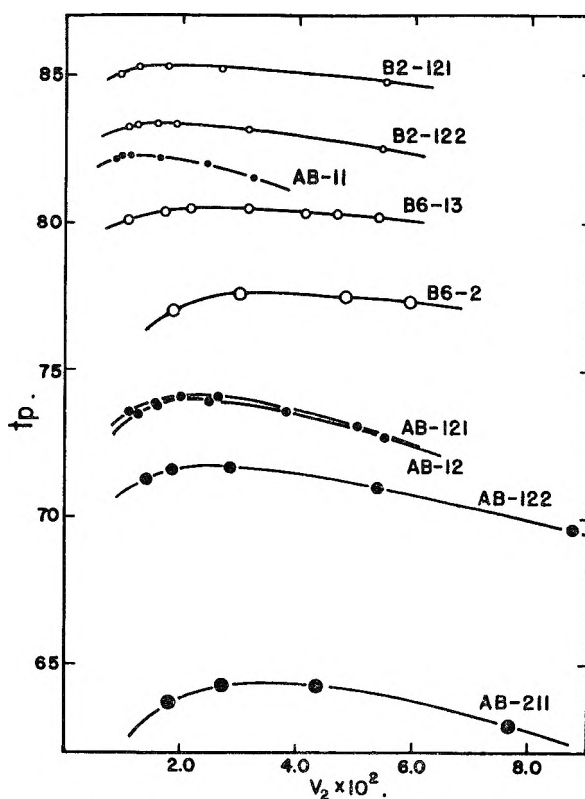


Fig. 4.—Binary phase diagrams for fractions of atactic (●) and isotactic (○) poly-(1-butene) in anisole.

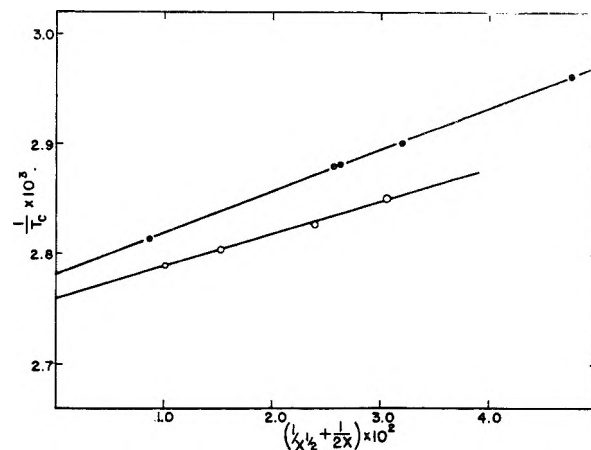


Fig. 5.—Molecular weight dependence of the critical miscibility temperature for atactic (●) and isotactic (○) poly-(1-butene) in anisole.

TABLE II
CRITICAL MISCIBILITY TEMPERATURE DATA FOR
POLY-(1-BUTENE) IN ANISOLE

Fraction	$10^{-3} x$	$t_c, ^\circ\text{C.}$	$10^3/T_c$	Θ ($^\circ\text{K.}$)	ψ_1
AB-11	13.6	82.25 ± 0.05	2.814	359.4	0.740
AB-121	1.56	$74.1 \pm .1$	2.880		
AB-12	1.49	$74.0 \pm .1$	2.881		
AB-122	1.01	$71.7 \pm .1$	2.900		
AB-211	0.46	$64.4 \pm .2$	2.962		
B2-121	9.80	$85.25 \pm .05$	2.790	362.3	0.956
B2-122	4.32	$83.4 \pm .05$	2.804		
B6-13	1.78	$80.5 \pm .1$	2.827		
B6-2	1.10	$77.6 \pm .15$	2.851		
		Difference		2.9	0.216

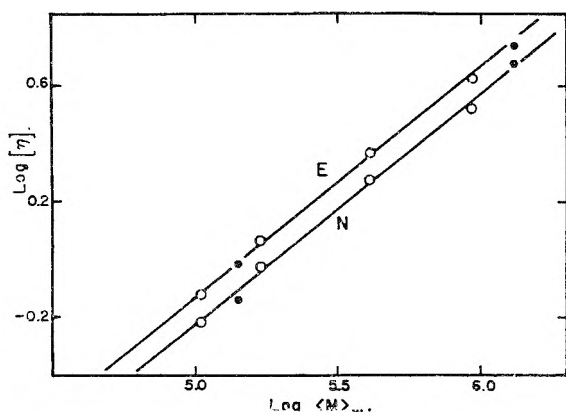


Fig. 6.—Molecular weight dependence of the intrinsic viscosity for atactic (●) and isotactic poly-(1-butene) in ethylcyclohexane (E) and *n*-nonane (N).

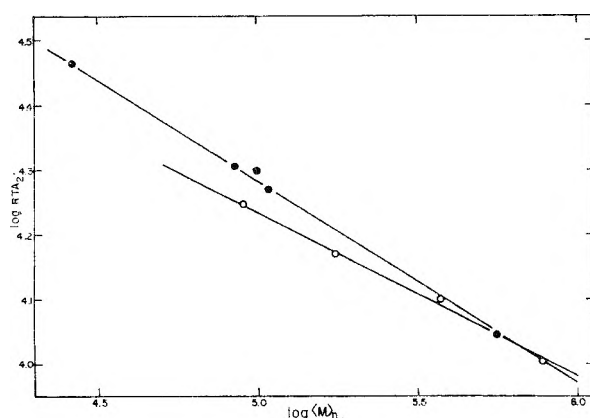


Fig. 7.—Osmotic second virial coefficients for atactic (●) and isotactic (○) poly-(1-butene) in toluene at 45°.

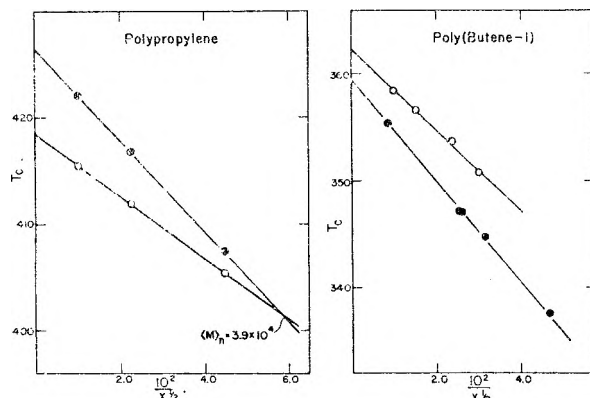


Fig. 8.—Critical miscibility temperatures plotted against $\bar{x}^{-1/2}$ for polypropylene in phenyl ether¹³ (see text) and poly-(1-butene) in anisole. Filled circles represent the atactic form and open circles the isotactic isomer.

The anisole measurements were the last performed. We were unable to recover sufficient polymer from these solutions to check for degradation, as was done in the other cases. The parameter k' in the Huggins relation

$$\eta_{sp}/c = [\eta] + k'[\eta]^2c$$

had the value 0.37 for both modifications in ethylcyclohexane at 70° and for the isotactic polymer in *n*-nonane at 80°. For the atactic polymer in *n*-nonane at 35°, k' was 0.36. The values observed

under theta conditions in anisole for the atactic and isotactic forms were 0.35 and 0.33, respectively. The intrinsic viscosities in dl./g. units are collected in Table III.

TABLE III
INTRINSIC VISCOSITY DATA FOR ATACTIC AND ISOTACTIC
POLY-(1-BUTENE)

Fraction	$10^{-5}(M)_w$	Ethylcyclohexane (70°)	<i>n</i> -Nonane (35 or 80°)	Anisole (θ temp.)
AB-11	13.0	5.52	4.75	1.53
AB-121	(1.49)	1.01
AB-12	1.42	0.965	0.725	0.349
AB-122	(0.966)	.715	...	0.294
AB-211	(0.441)	.379
B2-121	9.35	4.22	3.33	1.29
B2-122	4.12	2.35	1.87	...
B6-13	1.70	1.17	0.946	...
B6-2	1.05	0.758	0.612	0.358

Figure 6 illustrates the customary log-log plot of intrinsic viscosity *vs.* molecular weight for the two good solvents, ethylcyclohexane and *n*-nonane. The relationship obeyed by both atactic and isotactic poly-(1-butene) in ethylcyclohexane at 70° is

$$[\eta] = 7.34 \times 10^{-3} \langle M \rangle_w^{0.80} \quad (10)$$

while for the isotactic form in *n*-nonane at 80° there is obtained

$$[\eta] = 5.85 \times 10^{-3} \langle M \rangle_w^{0.80} \quad (11)$$

It is rather surprising to find that the two points measured at 35° for the atactic fractions in this solvent appear to obey the same relation, despite the 45° temperature difference.

The intrinsic viscosity data measured in anisole under θ conditions are not sufficient to establish a reliable intrinsic viscosity-molecular weight relationship; however, it does appear that the molecular weight exponent must be significantly larger than the value, 0.50, expected for randomly-coiling unperturbed chains. These are 0.59 (isotactic, 89.2°) and 0.64 (atactic, 86.3°).

Discussion

Second Virial Coefficients.—The osmotic second virial coefficient data found in Table I for atactic and isotactic fractions in toluene at 45° appear plotted as $\log RTA_2$ *vs.* $\log \langle M \rangle_n$ in Fig. 7. The atactic isomer exhibits larger values of A_2 up to $\langle M \rangle_n = 7 \times 10^5$. It would be difficult to decide experimentally whether the two lines intersect or converge asymptotically, since the osmotic method becomes insensitive at still higher molecular weights. This behavior is in accord with the osmotic results of Danusso and Moraglio for atactic and isotactic polystyrene in toluene at 30°, and with the light scattering data of Kinsinger and Hughes⁹ for the isomeric polypropylenes in 1-chloronaphthalene at 125°. In the latter case the two lines were reported to cross at $\langle M \rangle_n = 1.2 \times 10^6$; however, the inversion reported at higher molecular weights may have been due to experimental error. The error is somewhat larger for the light scattering method, since an additional extrapolation to zero scattering angle is involved. Our light scattering A_2 values measured in *n*-nonane exhibit consider-

able scatter, in particular the value for fraction B2-121, so that these data are not plotted.

Precipitation Temperatures.—The parameters derived from the phase equilibrium measurements for poly-(1-butene) in anisole are compared in Table IV with those reported by Kinsinger and Wessling¹³ for polypropylene in diphenyl ether.

TABLE IV

COMPARISON OF THERMODYNAMIC PARAMETERS FOR
POLY-(1-BUTENE) AND POLYPROPYLENE

Polymer	θ (°K.)	ψ_1
Isotactic poly-(1-butene)	362.3	0.956
Atactic poly-(1-butene)	359.4	.740
Difference	2.9	.216
Isotactic polypropylene ¹³	419.4	1.414
Atactic polypropylene ¹³	426.5	0.986
Difference	-8.1	0.428

For both polymers the isotactic modification has the larger entropy parameter; however, isotactic poly-(1-butene) also has the higher theta temperature, whereas isotactic polypropylene has the lower theta temperature. The significance of this difference is illustrated in Fig. 8, where the critical miscibility temperatures of these two polymers are plotted against $x^{-1/2}$. The data appearing in Table II were used for poly-(1-butene), while for polypropylene T_c was calculated according to equation 8 for arbitrary x values, making use of θ and ψ_1 as given in Table IV. We observe that for poly-(1-butene) the stereoregular polymer (open circles) has a lower solubility than its random counterpart at all molecular weights. In the case of polypropylene the random atactic polymer is less soluble than the stereoregular polymer for molecular weights above 39,000. This is somewhat unexpected, since the customary separation of the atactic-isotactic mixture is based upon the lower solubility of the stereoregular form, and Danusso and Moraglio⁴ have demonstrated by fractionation experiments that isotactic polystyrene exhibits lower solubility. One must bear in mind, however, that these latter examples may not involve equilibria between two liquid phases. Since there is no evident explanation for the difference in the precipitation temperature behavior shown in Fig. 8, we can only hope that future phase equilibria studies upon other polymers will give further insight concerning this question.

Φ and Molecular Dimensions.—The Flory parameter, Φ , was calculated from the light scattering and intrinsic viscosity data in *n*-nonane at 80° (isotactic) and 35° (atactic) according to the relation³¹

$$\Phi = q_0(M)_w[\eta]/(\langle r^2 \rangle_z)^{3/2} \quad (12)$$

where q_0 corrects the measured averages to number-averages of $(\bar{r}^2)^{3/2}$ and M^{24}

$$q_0 = \frac{(h+2)^{3/2} \Gamma(h+2)}{(h+1)^2 \Gamma(h+1.5)}$$

and h is the parameter appearing in equation 7 representing the molecular weight distribution.

(31) S. Newman, W. R. Krigbaum, C. Laugier and P. J. Flory, *J. Polymer Sci.*, **14**, 451 (1954).

Unperturbed dimensions of poly-(1-butene) and some other polyolefins were estimated from the light scattering data in thermodynamically good solvents through use of equation 6. The molecular expansion factor, $\alpha = (\bar{r}^2/\bar{r}_0^2)^{1/2}$, was calculated using the relation of Orofino and Flory³²

$$A_2 = \frac{2^{3/2}\pi N}{3^3\Phi} \frac{[\eta]}{M} \ln \left[1 + \frac{\pi^{1/2}}{2} (\alpha^2 - 1) \right] \quad (13)$$

In addition to poly-(1-butene) in *n*-nonane, the other polymers for which data are available are: polyethylene at 105° in tetralin³³ and atactic polypropylene at 125° in 1-chloronaphthalene.^{9,34} The results of these calculations appear in Table V.

Examination reveals that these polyolefins exhibit many of the features characteristic of polymer chains of low flexibility, such as the cellulosic derivatives.³⁵⁻³⁷ For example, the Φ values are generally below the asymptotic limit (2.0 to 2.4×10^{21} in good solvents). We may note in passing that the increase in Φ for poly-(1-butene) with molecular weight results in $[\eta]_0$ varying as a power of M greater than $1/2$, as noted above. A wide variety of flexible chain polymers have been shown to have a molecular weight exponent of $1/2$ under θ conditions. Secondly, the α^3 values are low and nearly independent of molecular weight. While the applicability of equation 13 to stiff chain polymers may be questioned, and we regard the α^3 values as approximations only, they do furnish a reliable indication of inflexible chain behavior. Bearing in mind the experimental errors in A_2 , and the uncertainties in the α^3 values, one must conclude from Table V that the estimated (\bar{r}_0^2/M) ratios for these polymers show no definite trend with molecular weight. For this reason we have listed average values for each polymer in the last column. Benoit and Doty³⁹ predicted that this ratio should increase with molecular weight for stiff chain polymers. This has been observed for cellulose trinitrate,³⁵⁻³⁷ but for cellulose tricaproate the ratio decreased with increasing molecular weight.³⁸

It is evident that the polymers in Table V differ in the degree of their "abnormal" behavior. Thus, atactic poly-(1-butene) appears somewhat more "normal" than the isotactic isomer, while the deviations are still less marked for atactic polypropylene. Further evidence for this range of chain flexibilities is found in Table VI, which illustrates chain extension parameters calculated for several polyolefins. These parameters are: the \bar{r}_0^2/lr_{\max} ratio appearing in the semi-flexible chain treatment of Flory,⁴⁰ the persistence length,

(32) T. A. Orofino and P. J. Flory, *J. Chem. Phys.*, **26**, 1067 (1957).

(33) Q. A. Trementozzi, *J. Polymer Sci.*, **36**, 113 (1959).

(34) J. B. Kinsinger, *Dissertation Abstr.*, **19**, 685 (1958).

(35) A. M. Holtzer, H. Benoit and P. Doty, *J. Phys. Chem.*, **58**, 624 (1954).

(36) M. L. Hunt, S. Newman, H. A. Scheraga and P. J. Flory, *ibid.*, **60**, 1278 (1956).

(37) M. M. Huque, D. A. I. Goring and S. G. Mason, *Can. J. Chem.*, **36**, 952 (1958).

(38) W. R. Krigbaum and L. H. Sperling, *J. Phys. Chem.*, **64**, 99 (1960).

(39) H. Benoit and P. Doty, *ibid.*, **57**, 958 (1953).

(40) P. J. Flory, *Proc. Roy. Soc. (London)*, **234A**, 60 (1956).

TABLE V
 Φ AND $\overline{r_0^2}/M$ FOR THREE POLYOLEFINS

Polymer	Fraction	$10^{-4}\langle M \rangle_w$	$\frac{\langle M \rangle_w}{\langle M \rangle_n}$	$10^{-21}\Phi$	$10^{10}\left(\frac{\overline{r^2}}{M}\right)^{1/2}$	$10^4 A_2$	α^2	$10^{10}\left(\frac{\overline{r_0^2}}{M}\right)^{1/2}$	av.
									$10^{10}\left(\frac{\overline{r_0^2}}{M}\right)^{1/2}$
Isotactic poly-(1-butene)	B2-121	9.35	1.21	1.43	136	1.05	1.20	124	113
	B2-122	4.12	1.11	1.24	133	3.56	1.50	117	
	B6-13	1.70	~1	1.14	126	4.31	1.45	111	
	B6-2	1.05	1.17	1.12	120	6.02	1.62	102	
Atactic poly-(1-butene)	AB-11	13.0	2.33	2.32	125	2.4	1.90	101	130
	AB-12	1.42	1.7	1.48	110	2.4	1.35	100	
Polyethylene ³³	1B-1	4.65	1.68	1.40	210	15.9	1.67	177	130
	1B-2	2.69	1.42	0.86	231	18.4	1.40	206	
	3	1.25	1.15	0.86	214	23.1	1.46	188	
Atactic polypropylene ^{9,34}	A-3	3.83	1.24	1.69	124	5.8	2.27	94.1	83.5
	A-4	1.70	1.23	2.10	107	8.3	3.20	72.9	

q_1 of Porod and Kratky,⁴¹ and the ratio $(\overline{r_0^2}/r_{of}^2)^{1/2}$, of the root-mean-square displacement length of the unperturbed chain to that of a chain with fixed valence angles but free rotation. In the first of these quantities r_{max} is the length of the fully extended chain and l is the diameter of a spherical segment of the lattice model chain. The defining relation is⁴⁰

$$\overline{r_0^2}/lr_{max} = (\pi\rho N/4M_0)^{1/2} (\overline{r_0^2}/n)(r_{max}/n)^{-1/2}$$

where n is the number of monomeric units having molecular weight M_0 in the chain, ρ is the polymer density, and N is Avogadro's number. The persistence length, q , was calculated according to the relation given by Benoit and Doty³⁹

$$\overline{r_0^2} = 2qL - q^2(1 - e^{-L/q})$$

where L is the contour length of the chain. Finally $\overline{r_{of}^2}$ appearing in the third ratio was calculated using the Eyring formula⁴²

$$\overline{r_{of}^2} = Nb^2(1 \cos \theta)/(1 + \cos \theta)$$

in which the molecule is represented by N freely-rotating links of length b connected at an angle θ .

 TABLE VI
 MOLECULAR EXTENSION PARAMETERS FOR SEVERAL POLYOLEFINS

Polymer	$10^{10}(\overline{r_0^2}/M)^{1/2}$	$\overline{r_0^2}/lr_{max}$	q (Å.)	$(\overline{r_0^2}/r_{of}^2)^{1/2}$
Polyethylene	190 ³³	8.7	20.2	3.2
Isotactic poly-(1-butene)	113	4.3	14.4	2.7
Atactic poly-(1-butene)	100	3.3	11.2	2.4
Isotactic polystyrene	75 ⁷	2.7	11.5	2.5
Atactic polystyrene	70 ²⁴	2.4	10.1	2.3
Atactic polypropylene	83.5 ⁹	-.92 ³⁴	2.0-2.3	5.9-7.0
Polyisobutylene	76 ⁴³	1.9	7.3	1.8

The entries are listed in decreasing order of the $\overline{r_0^2}/lr_{max}$ ratio given in column 3. One sees immediately that these polyolefins exhibit a considerable range of chain flexibility and that some of

(41) G. Porod, *Monatsh. Chem.*, **80**, 25 (1949); O. Kratky and G. Porod, *Rec. trav. chim.*, **68**, 1106 (1949).

(42) H. Eyring, *Phys. Rev.*, **39**, 746 (1932).

(43) T. G. Fox, Jr., and P. J. Flory, *J. Am. Chem. Soc.*, **75**, 37 (1953); E. D. Kunst, *Rec. trav. chim.*, **69**, 125 (1950).

these are surprisingly highly extended. For comparison, estimated⁴⁴ values of this ratio for several synthetic fibers range from 3.5 to 4.5, although these must be regarded as lower limits, since Φ was assumed to have its asymptotic value for these calculations. For both poly-(1-butene) and polystyrene the stereoregular isotactic form is somewhat more highly extended than the atactic modification. The polyolefins as a class should provide a good test of the semiflexible chain treatment of Flory,⁴⁰ since the intermolecular attractions should be relatively weak. He predicted from entropy considerations alone that a polymer should exhibit crystallinity if the ratio in the third column exceeds 2.2. If one excludes the atactic polymers, since Flory's treatment did not take cognizance of the irregularity introduced by randomly occurring d - or l -configurations along the chain, then it appears that his prediction is confirmed. On the other hand, there is surprisingly little correlation between the molecular extensions and the polymer melting points.

Conclusions

Our observations for the two modifications of poly-(1-butene) in thermodynamically good solvents may be summarized as follows. The isotactic modification exhibited lower values of the second virial coefficient, as measured in toluene at 45°, up to $\langle M \rangle_n = 7 \times 10^5$. Nevertheless, the intrinsic viscosity-molecular weight relationships of the two forms in another good solvent, ethylcyclohexane at 7°, were indistinguishable. Similar results were obtained by Danusso and Moraglio for the polystyrenes,⁴ and by Kinsinger and Hughes for the polypropylenes.⁹ Thus, this type of behavior appears to be general.

Turning to theta solvent systems, our results for poly-(1-butene) in anisole and those of Kinsinger and Wessling¹³ for polypropylene in phenyl ether are in agreement in that differences are observed between the stereoregular and random polymer, and in assigning a higher entropy parameter, ψ_1 , to the isotactic modification. However, for poly-(1-butene) the isotactic form also exhibits the larger θ temperature, whereas the reverse was found for polypropylene. Thus, atactic poly-(1-butene) is more soluble in anisole than its stereore-

(44) W. R. Krigbaum, *J. Polymer Sci.*, **28**, 213 (1958):

regular counterpart for all molecular weights, whereas for polypropylene in phenyl ether the random atactic form should be less soluble for molecular weights above 39,000. This difference is surprising, and merits further investigation.

Finally, the unperturbed dimensions estimated for poly-(1-butene) from light scattering measurements performed in thermodynamically good solvents indicate that the stereoregular form is somewhat more highly extended. This observation is in agreement with the result obtained in a similar manner for polystyrene.⁶ This demonstrates the influence of the sequence of asymmetric carbon atom configurations upon the unperturbed di-

mensions, as well as upon the thermodynamic interactions. It is unfortunate that dn/dc for the theta solvent we examined, anisole, was too small to permit a direct measure of the unperturbed dimensions, since the uncertainties involved in estimating α^3 could thereby have been avoided.

Acknowledgment.—This investigation was supported by the Allegany Ballistics Laboratory, an establishment owned by the United States Navy and operated by Hercules Powder Company under Contract NOrd 10431. J. E. K. wishes to express his gratitude to the Allied Chemical and Dye Corporation for a fellowship during his final year of graduate study.

ON THE POLYELECTROLYTE BEHAVIOR OF HEPARIN. I. BINDING OF SODIUM IONS

BY F. ASCOLI, C. BOTRÉ AND A. M. LIQUORI*

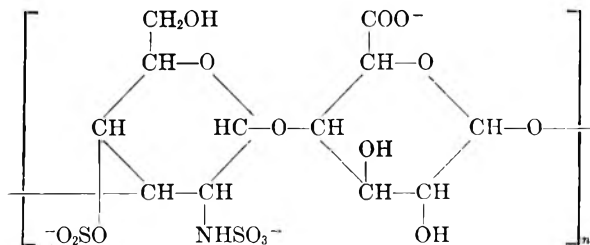
Laboratorio Ricerche sulla Struttura e l'Attività di Composti Chimici, Istituto di Chimica Farmaceutica, Università, Roma, Italia
**Istituto di Chimica fisica, Università, Napoli, Italia*

Received April 24, 1961

The binding capacity toward Na^+ counterions of heparin has been investigated. The results are completely consistent with those previously obtained for other anionic polyelectrolytes. A quantitative correlation between degree of association of the counterions to the macroion and spacing between ionizable groups along the macroion is shown to hold very satisfactorily for a number of polyelectrolytes with a cellulosic skeleton.

Introduction

Previous studies on synthetic polyelectrolytes have shown that a definite relation holds between the average repeat of ionizable groups along the chain and the degree of association of Na^+ counterions¹⁻³ in salt-free solution. In the light of these findings we have carried out a similar investigation on heparin, a well known blood anticoagulant, which is the sodium salt of a natural polymer of the D-glucuronic acid and D-glucosamine, with the well established formula⁴



The polyelectrolyte character to be expected from the above formula suggested to us to investigate the ion binding capacity of this substance. Determinations of Na^+ ion activity in salt-free solutions were carried out at different concentration of heparin by means of membrane electrodes.⁵ The results are completely consistent with those

previously obtained for other polyelectrolytes with a cellulosic skeleton,¹ such as sodium carboxymethylcellulose at different degrees of substitution and sodium cellulose sulfate.

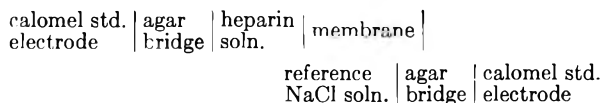
Experimental

Material.—Heparin supplied by B.D.H., London, 95.4 units/mg., was used. After dialysis against distilled water at 5° for two days and freeze-drying, known amounts were weighed and dissolved in water. The concentration was also checked by determining the sodium content. This latter was measured by means of a Flame Photometer "Evans Electro Selenium Ltd., England". Analytical grade sodium chloride was used.

Determination of Na^+ Ion Activity.—The method employed has been discussed extensively in previous papers.^{5,6} It is based on the use of a highly cation selective membrane of about 0.1 mm. thickness, made of polystyrenesulfonic acid supported on a collodion matrix. The acid value of the polystyrene sulfonic acid used was 4.36 meq./g., while 5.43 meq./g. is the theoretical value calculated for a linear polymer, having one sulfonic acid group for each benzene ring. The membrane was equilibrated in sodium chloride solution before use.

The cell used was fully described in previous papers.^{5,6} A PYE precision potentiometer with -0.5 to 1750 mv. circuit with each division of the slide-wire equal to 100 $\mu\text{v.}$, equipped with a standard Weston cell and a Multiflex Lange galvanometer (4.0×10^{-9} amp./mm.) as zero instrument were used. All determinations were carried out at room temperature.

The e.m.f. of the following chain was measured



The NaCl solution was chosen in order to obtain a potential difference equal to zero. Then, the heparin solution (5 ml., $2 \times 10^{-2} M_{\text{Na}^+}$) was diluted or concentrated stepwise,

(1) A. M. Liquori, F. Ascoli, C. Botré, V. Crescenzi and A. Mele, *J. Polymer Sci.*, **40**, 169 (1959).

(2) H. P. Gregor and D. H. Gold, *J. Phys. Chem.*, **61**, 1347 (1957).

(3) M. Nagasawa and I. Kagawa, *J. Polymer Sci.*, **25**, 61 (1957).

(4) M. L. Wolfrom, R. Montgomery, J. V. Karabinos and P. Rathgeb, *J. Am. Chem. Soc.*, **72**, 5796 (1950).

(5) C. Botré, V. Crescenzi and A. Mele, Proc. Intern. Symposium Coordination Compounds, Rome, 1957; *Ricerca Sci.*, **28A**, 369 (1958).

(6) C. Botré, V. Crescenzi and A. Mele, *J. Phys. Chem.*, **63**, 650 (1959).

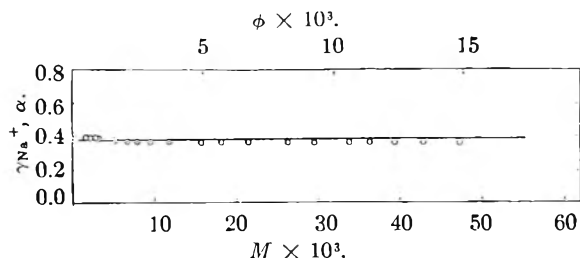


Fig. 1.—The curve represents the degree of dissociation α versus volume fraction ϕ (upper scale) calculated according to equation 1. The points are the experimental values of the activity coefficient γ_{Na^+} versus concentration of heparin expressed as molarity of sodium ions (lower scale).

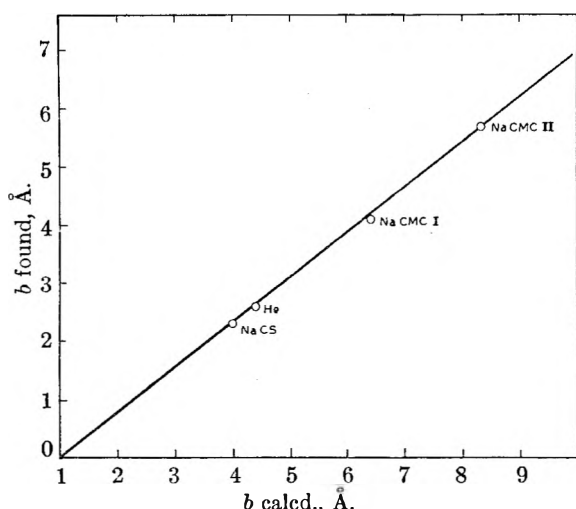


Fig. 2.—Values of spacing b between the ionizable groups, obtained from equations 1 and 2 versus the values of b calculated from the structural model for the following polyelectrolytes having a cellulosic skeleton: NaCS = sodium cellulose sulfate¹; He = heparin; NaCMC = sodium carboxymethylcellulose; I, degree of substitution = 0.94; II, degree of substitution = 0.70.¹

adding water or heparin solution, respectively, and the e.m.f. was recorded at each step.

Neglecting the asymmetry in the liquid junctions, the activity of sodium ions in heparin solution was determined according to the Nernst relation. At each concentration, the activity coefficient γ_{Na^+} was calculated from the ratio between activity and concentration of sodium ions.

Determination of Molecular Weight.—The molecular weight of the sample used, determined by light scattering measurements, was 19.7×10^5 . A Brice Phoenix apparatus was used employing the blue mercury line ($\lambda = 436 \text{ m}\mu$) and a cylindrical cell containing about 15 ml. of solution.

Results and Discussion

In Fig. 1, the points represent the experimental values of the activity coefficient γ_{Na^+} of sodium ions plotted versus the concentration of heparin (lower scale). As may be seen, the values of γ_{Na^+} are low and nearly invariant with the concentration. This characteristic behavior of the activity coefficient is very similar to that already found for highly charged synthetic polyelectrolytes. The

occurrence of closely spaced ionizable groups along the chain of the polyanion is in fact responsible for an intense electrostatic field, which tends to attract the small counterions very strongly, even in a medium of high dielectric constant like water.

The mechanism of counterion association in polyelectrolyte solutions has been described semi-quantitatively by a number of approximate theories, which treat the macroion as a rod or a sphere,⁷⁻¹⁰ with continuous charge density which depends on the distance between the ionizable groups along the chain. This charge density is responsible for the electrostatic interaction between the macroion and the small counterions present in solution and affects their distribution according to the Poisson-Boltzmann equation. The following approximate relation due to Oosawa¹¹ for the cylindrical model has been found particularly useful in treating the experimental data.¹

$$\ln \frac{\alpha}{1-\alpha} = \ln \frac{\phi}{1-\phi} + q\alpha \ln \frac{1}{\phi} \quad (1)$$

α = degree of dissociation

ϕ = volume fraction of the polymer

$q = e_0^2/DkTb$

b = spacing between ionizable groups

D, k, T have the usual meaning

(2)

In order to apply equation 1, the activity coefficient γ_{Na^+} of sodium counterions was identified with the degree of dissociation α . In Fig. 1, the value of α is plotted as a function of ϕ (upper scale) according to equation 1. As said above, the points on the curve represent the experimental values of γ_{Na^+} . A value of 7.0 Å. was taken for the radius of the polyanion in the calculation of the volume fraction ϕ . This value is very uncertain, but fortunately its choice does not affect the result significantly.

The value of q chosen in order to calculate the theoretical curve was 2.8, which corresponds to $b = 2.64 \text{ Å}$. In Fig. 2, the values of b obtained from equations 1 and 2 for several polyelectrolytes with a cellulosic skeleton, as previously reported¹, are plotted against the values derived from the structural models taking into account the different degrees of substitution. The linear relation between the two values of b can be taken as positive evidence of the applicability of Oosawa's theory to this type of polyelectrolyte having a rather rigid skeleton.

Acknowledgment.—This work was sponsored and financially supported by Colgate-Palmolive Company, New York, which is gratefully acknowledged. We wish to acknowledge the collaboration of Dr. F. Servello in the light scattering measurements.

(7) F. E. Harris and S. A. Rice, *J. Phys. Chem.*, **58**, 725 (1954).

(8) S. A. Rice, *J. Am. Chem. Soc.*, **78**, 5247 (1956).

(9) F. T. Wall and J. Berkowitz, *J. Chem. Phys.*, **26**, 114 (1957).

(10) R. M. Fuoss, A. Katchalsky and S. Lifson, *Proc. Natl. Acad. Sci. U. S.*, **37**, 579 (1951).

(11) F. Oosawa, *J. Polymer Sci.*, **23**, 421 (1957).

SPECIES OF COBALT(II) IN ACETIC ACID. PART II. COBALT(II) IN THE PRESENCE OF LITHIUM BROMIDE, LITHIUM CHLORIDE AND AMMONIUM THIOCYANATE

BY P. J. PROLL AND L. H. SUTCLIFFE

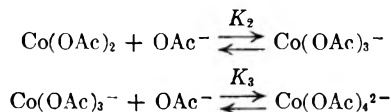
Department of Inorganic and Physical Chemistry, University of Liverpool, Liverpool, England

Received April 28, 1961

The effect of the addition of inorganic bromides, chlorides and thiocyanates to solutions of cobalt(II) in acetic acid has been studied in detail, over the temperature range 25.0 to 64.0°. From ion migration and spectrophotometric experiments the ionic species present are postulated to be $\text{Co}(\text{X})^+$, $\text{Co}(\text{X})_2$, $\text{Co}(\text{X})_3^-$ and $\text{Co}(\text{X})_4^{2-}$, where X represents the bromide, chloride or thiocyanate, the latter two species being favored by the addition of the corresponding inorganic salts. The equilibrium constants K_2 and K_3 for the formation of the $\text{Co}(\text{X})_3^-$ and the $\text{Co}(\text{X})_4^{2-}$ have been evaluated for the bromide and chloride at 25°, and the product of these equilibrium constants for the thiocyanate has been found. An attempt has been made to calculate the oscillator strengths of the $\text{Co}(\text{X})_4^{2-}$ ions; for the chloride ion the agreement with previous workers is reasonable.

Introduction

In a previous paper from this Laboratory¹ it has been shown that the heating of, or the addition of inorganic acetates to, cobaltous acetate in anhydrous acetic acid converts the pink octahedral form $\text{Co}(\text{OAc})_2 \cdot 4\text{HOAc}$ into the blue tetrahedral form $\text{Co}(\text{OAc})_4^{2-}$, the latter species having an absorption maximum at 565 $m\mu$ and an extinction coefficient of about 1700 $M^{-1} \text{ cm}^{-1}$, and the former species a maximum at 526 $m\mu$ with an extinction coefficient of 17.0 $M^{-1} \text{ cm}^{-1}$. Two equilibria were found to be associated with this conversion, namely



It also was possible to estimate the values of the constants K_2 and K_3 from spectrophotometric measurements. The importance of these equilibria in both catalytic and non-catalytic reactions was demonstrated and it was concluded that $\text{Co}(\text{OAc})_4^{2-}$ is probably the most reactive species. Cobaltous bromide or cobaltous acetate with added lithium bromide in anhydrous acetic acid also is used as an autoxidation catalyst,^{2,3} but little attention has been paid to the role of the catalyst, hence it was decided to make a detailed spectrophotometric investigation of this system. At the same time the effects of lithium chloride and of ammonium thiocyanate also were investigated in detail since preliminary experiments showed that similar optical effects are produced by them.

The method used in this series of experiments is identical with that used in the addition of inorganic acetates to cobaltous acetate in anhydrous acetic acid^{1,4}; a set of absorption curves corresponding to increasing concentrations of the complexing agent is obtained. It has been pointed out by Libus, Ugniewska and Minc⁵ that the application of the method of continuous variations even in a modified

form may lead to erroneous conclusions when applied to a system in which two coordination numbers are exhibited by the central metal atom. Much of the work reported in the literature on similar systems has been done using this continuous variation method and is therefore unsatisfactory. Various alcohols have been employed as solvents but since tetrahedral complexes of cobalt(II) are favored by a low dielectric constant, acetic acid is a better solvent for the study of these complexes. Apart from postulating the species present little attention has been given so far to the evaluation of the equilibrium constants involved in these systems. The present paper is concerned with the bromide, chloride and thiocyanate complexes of cobalt(II) in anhydrous acetic acid and the evaluation of the equilibrium constants concerned.

Experimental

The necessity for obtaining completely anhydrous reagents has been shown to be very important in our previous paper.¹ The preparation of anhydrous acetic acid and cobaltous acetate already have been described.¹ The precautions taken in the preparation of the other reagents are as follows.

Cobaltous Bromide.—The British Drug Houses (B.D.H.), product was recrystallized from purified acetic acid and then pumped under a vacuum for about a week at 100° until the bright green anhydrous product was obtained.

Cobaltous Chloride.—The Oakes and Eddon product was recrystallized from purified acetic acid and then pumped under a vacuum for about a week at 100° until the very pale blue anhydrous product was obtained.

Lithium Bromide and Chloride.—The B.D.H. laboratory reagents were dried under a vacuum for two days at 100°.

Ammonium Thiocyanate.—Hopkins and Williams Analytical Reagent (A.R.) quality ammonium thiocyanate was dried under a vacuum for a day at 100°.

Hydrogen Bromide and Chloride.—The Hopkins and Williams A.R. aqueous products were used after adding the correct amount of acetic anhydride to react with all the water present. The acetic anhydride being added very slowly because of the heat produced in the reaction with the consequent loss of the bromide or chloride. The concentration of bromide or chloride present was estimated by first diluting with water and adding nitric acid and excess silver nitrate, then estimating this excess with potassium thiocyanate using ferric alum as an indicator.

Ion Migration Experiments.—The apparatus and method used has been described previously in part I of this series of papers.¹

Spectrophotometry.—All equilibrium measurements were made by means of a Unicam S.P. 500 spectrophotometer fitted with a thermostated cell compartment enabling solutions to be maintained at a given temperature to within $\pm 0.05^\circ$.

(1) P. J. Proll, L. H. Sutcliffe and J. Walkley, *J. Phys. Chem.*, **65**, 455 (1961).

(2) D. A. S. Ravens, *Trans. Faraday Soc.*, **55**, 1768 (1959).

(3) C. E. H. Bawn, R. B. F. Kilgannon and T. K. Wright, to be published.

(4) P. J. Proll and L. H. Sutcliffe, *Trans. Faraday Soc.*, **57**, 1078 (1961).

(5) W. Libus, A. Ugniewska and S. Minc, *Roczniki. Chemii*, **34**, 29 (1960).

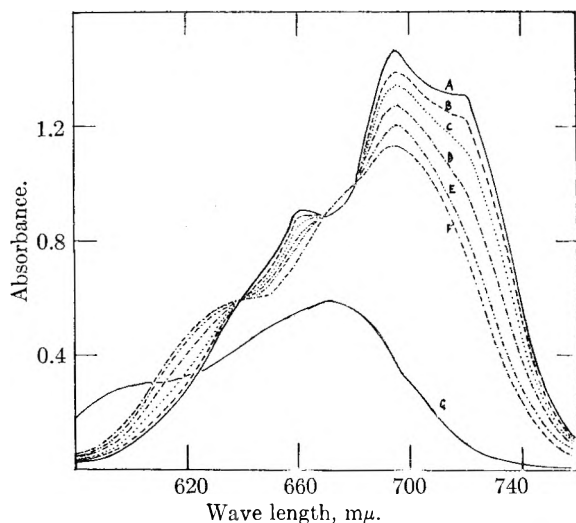


Fig. 1.—The absorption spectra of Co(II) with added lithium bromide in acetic acid solution at 25.0°: A = 0.710 *M*; B = 0.533 *M*; C = 0.355 *M*; D = 0.178 *M*; E = 0.0888 *M*; F = 0.0444 *M* lithium bromide. G is the absorption spectrum of CoBr₂. The cobalt(II) concentration is constant at 1.82 × 10⁻³ *M*.

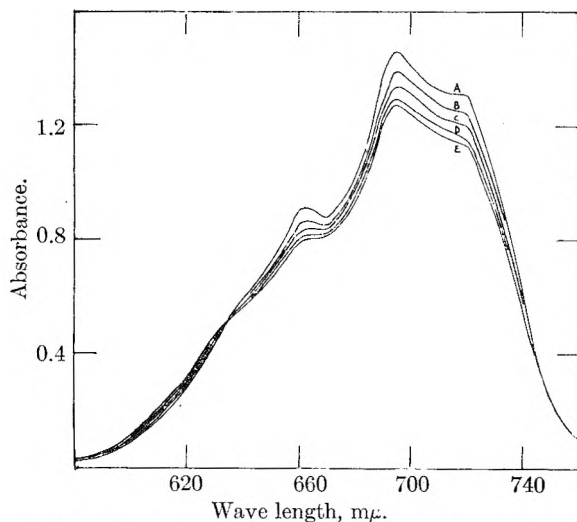


Fig. 2.—The effect of temperature on the absorption spectrum of 1.82 × 10⁻³ *M* Co(II) with a constant lithium bromide concentration of 0.71 *M*: A = 25°; B = 38.0°; C = 47.8°; D = 58.7°; E = 64.0°.

Results and Discussion

Ion Migration.—Ion migration experiments on cobaltous bromide and chloride solutions, and solutions containing excess of the corresponding lithium salt led to the conclusion that there are four likely species of the types CoX⁺, CoX₂, CoX₃⁻, CoX₄²⁻, where X represents the bromide or chloride. The negatively charged species were favored by the addition of the corresponding lithium salt, and the positively charged species were favored by the addition of water.

Spectrophotometry. (a) Addition of Bromide.—Figure 1 shows the absorption curves of Co(II) corresponding to the different concentrations of lithium bromide in anhydrous acetic acid solution. All the curves refer to a constant concentration of Co(II), namely 1.82 × 10⁻³ *M*. It was found from the molar extinction coefficients of cobaltous

bromide in anhydrous acetic acid that the Beer-Lambert law is obeyed in the peak region over the concentration range studied of 1.0 × 10⁻³ to 6.0 × 10⁻³ *M*.

From the ion migration experiments it was found that although cobaltous bromide in anhydrous acetic acid contains some ionic species their actual concentration was very small, that is, the main species is the neutral molecule. Since the solution is blue in color the main complex is probably the tetrahedral CoBr₂·2HOAc. This is in agreement with other workers⁵ who used various alcohols as solvents and assumed that the undissociated complex is of the form CoBr₂·L₂ where L is a solvent molecule. It therefore was concluded that the molar extinction coefficient of CoBr₂·2HOAc is the same as that of cobaltous bromide in anhydrous acetic acid. This is supported by the fact that the Beer-Lambert law is obeyed over the peak region (600 to 730 mμ).

The curves in Figs. 1 and 2 resulted from experiments performed on both cobaltous bromide and cobaltous acetate in anhydrous acetic acid, the cobaltous concentration being the same in both cases. For the same concentration of excess lithium bromide the molar extinction coefficient obtained was the same in both instances. At low concentrations of added lithium bromide, small differences did occur, due to the back reaction of the equilibrium



This effect being more important, of course, in the situation in which lithium bromide was added to cobaltous acetate. Temperature had little or no effect on the peak region of the spectrum of cobaltous bromide alone in anhydrous acetic acid principally because the dissociation constant of acetic acid is very small.

Cobaltous bromide has a maximum in the absorption spectrum at a wave length of 670 mμ; added lithium bromide shifts this maximum slightly to a wave length of 695 mμ and also increases the intensity of this maximum. Figure 3 shows the plot of the observed extinction coefficient against the concentration of lithium bromide at the wave length of 695 mμ. A similar plot for the acetates has been found to give a straight line,^{1,4} but in this case a curve is obtained, which must be due to the fact that CoBr₃⁻ is a tetrahedral complex and therefore has a large extinction coefficient and is present in some quantity.

The results of Libus, Ugniewska and Minc,⁵ who used ethanol and isopropyl alcohol as solvents, have been plotted in a similar manner as shown in Fig. 4. The curves are like those obtained with acetic acid as solvent.

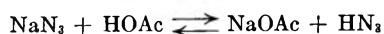
(b) Addition of Chloride.—Figure 5 shows the absorption spectra of Co(II) with various concentrations of lithium chloride in anhydrous acetic acid solution. All the curves correspond to a constant concentration of Co(II), namely 1.82 × 10⁻³ *M*. Cobaltous chloride in acetic acid solution was found to obey Beer-Lambert's law over the peak region as did cobaltous bromide solutions in this solvent. In conjunction with the ion migration experiments and the blue coloration of the cobaltous chloride solutions, it was concluded that the main species is

$\text{CoCl}_2 \cdot 2\text{HOAc}$, and that the molar extinction coefficient of cobaltous chloride in acetic acid is due mainly to this complex. The absorption maximum of cobaltous chloride in acetic acid is at a wave length of $670 \text{ m}\mu$; addition of lithium chloride increases the intensity of absorption and shifts the maximum to $685 \text{ m}\mu$. Figures 5 and 6 are the results of experiments performed on both cobaltous acetate and cobaltous chloride in anhydrous acetic acid. For the same concentration of excess lithium chloride, the same observed molar extinction coefficient of Co(II) was obtained for both cobalt salts. At low concentrations of lithium chloride, small deviations were noticed but as in the previous system, namely with added bromide, this was probably due to the acetate ions produced.

Figure 7 shows the plot of the observed extinction coefficient at $685 \text{ m}\mu$ against the concentration of lithium chloride in acetic acid solution at five temperatures in the range 25 to 64° . Figure 8 shows the results of other workers^{5,6} for different solvents plotted in a similar manner to those obtained for the addition of lithium chloride and hydrogen chloride in acetic acid.

(c) **Addition of Thiocyanate.**—Figure 9 shows the absorption curves of Co(II) corresponding to various concentrations of ammonium thiocyanate in anhydrous acetic acid solution. All the spectra were measured with a constant concentration of Co(II) , namely $1.82 \times 10^{-3} \text{ M}$. Cobaltous thiocyanate in acetic acid solution obeys Beer-Lambert's law over the peak region; the solutions are blue in acetic acid, hence it was concluded that the main species is the neutral tetrahedral molecule, namely, $\text{Co(CNS)}_2 \cdot 2\text{HOAc}$, there being two solvent molecules as in the previously discussed bromide and chloride salts of cobalt(II) in acetic acid solution. The spectrum of cobaltous thiocyanate in acetic acid (see Fig. 9), shows one absorption band in the visible region, the wave length of the maximum being $620 \text{ m}\mu$. The addition of ammonium thiocyanate increases the intensity of the $d \leftarrow d$ transition but there is no shift in the wave length of this maximum. Figure 10 shows the plot of the observed extinction coefficient at the wave length of $620 \text{ m}\mu$ against the concentration of ammonium thiocyanate at a temperature of 25.0° .

The effects of fluoride, cyanide and azide also were tried. The fluoride used was the ammonium salt but this is not very soluble, and did not show any visible effect on the spectrum of cobaltous acetate. Potassium cyanide was found to be very soluble but its addition to cobaltous acetate in anhydrous acetic acid led to some precipitation and hence the system could not be studied by spectrophotometry. Azide was found to affect the spectrum of cobaltous acetate in anhydrous acetic acid in that the peak was shifted to longer wave lengths and there was an increase in the intensity of absorption. It was found, however, that the effect was the same as that of sodium acetate, hence it was concluded that the equilibrium



is present. From this it appears that the dissociation

(6) W. D. Beaver, L. E. Trevorrow, W. E. Estill, P. C. Yates and T. E. Moore, *J. Am. Chem. Soc.*, **75**, 4556 (1953).

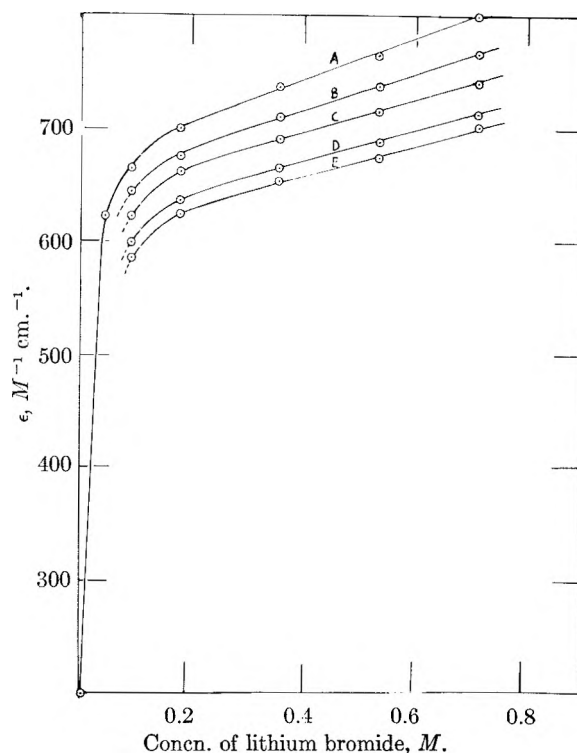


Fig. 3.—The dependence of the molar extinction coefficient ϵ at $695 \text{ m}\mu$ on the concentration of lithium bromide at the temperatures: A = 25.0° ; B = 38.0° ; C = 47.8° ; D = 58.7° ; E = 64.0° .

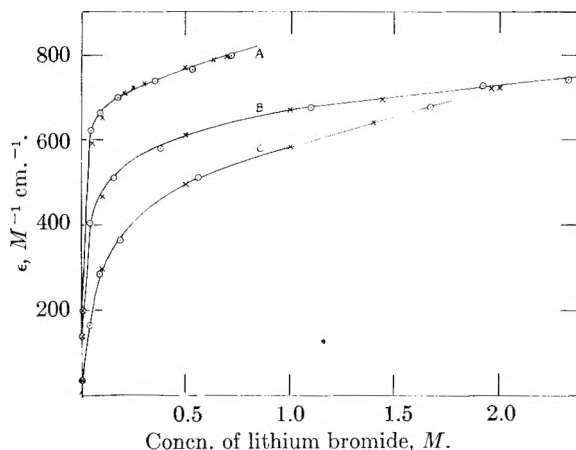


Fig. 4.—Plots of the observed extinction coefficient ϵ at $695 \text{ m}\mu$ against the concentration of lithium bromide. (A) our results using acetic acid as solvent at 25.0° . (B) and (C) the results taken from the work of Libus, Ugniewska and Minc⁵ using (B) isopropyl alcohol and (C) ethanol as solvents at a temperature of $19 \pm 1^\circ$. \circ are the experimental data and \times are the calculated results.

tion constant of HN_3 in acetic acid is very much less than that of acetic acid itself.

Discussion

Calculated curves similar to the experimental curves shown in Figs. 3, 4, 7, 8 and 10 may be generated by considering the effect of the anion X^- on the corresponding cobaltous salt CoX_2 as follows. For simplicity, molecules of solvation are omitted and all the cobalt species are assumed to be of the tetrahedral configuration.

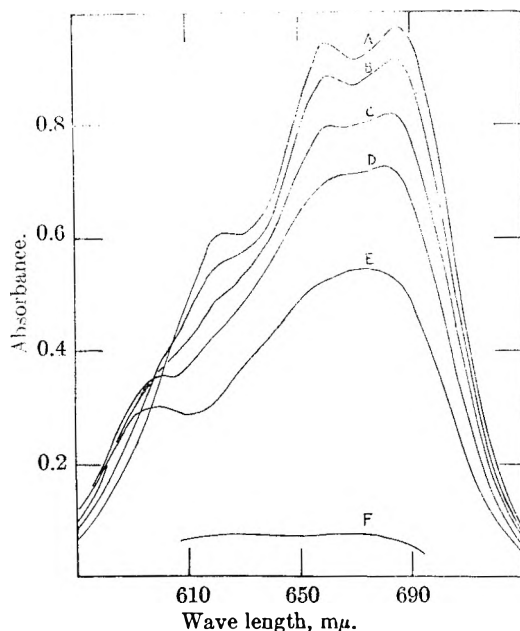


Fig. 5.—The absorption spectra of Co(II) with added lithium chloride in acetic acid solution at 25.0°, the concentration of Co(II) being $1.82 \times 10^{-3} M$. Concentrations of lithium chloride are: A = 0.500 M ; B = 0.250 M ; C = 0.125 M ; D = 0.0625 M ; E = 0.0313 M ; F = $1.82 \times 10^{-3} M$ cobaltous chloride.

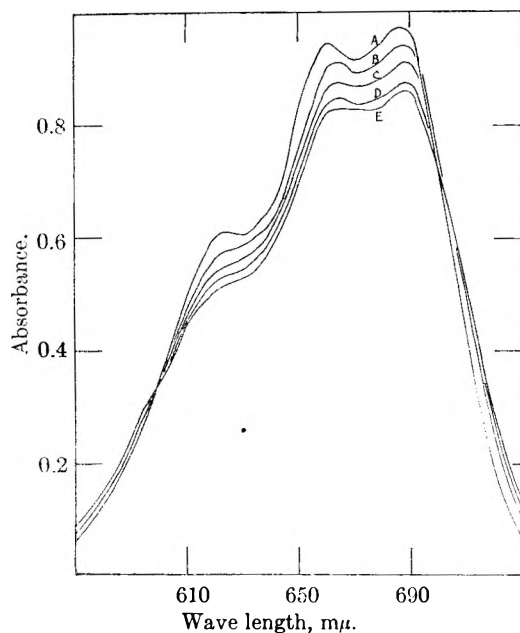
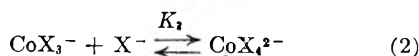
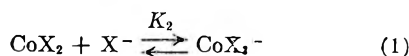


Fig. 6.—The effect of temperature on the absorption spectrum of Co(II) of concentration $1.82 \times 10^{-3} M$, with a constant concentration of lithium chloride of 0.500 M . A = 25.0°; B = 38.0°; C = 47.8°; D = 58.7°; E = 64.0°.



from which it may be shown that the observed extinction coefficient ϵ at a fixed wave length is given by

$$\epsilon = \frac{\epsilon_2 + \epsilon_3 K_2 [\text{X}^-] + \epsilon_4 K_2 K_3 [\text{X}^-]^2}{1 + K_2 [\text{X}^-] + K_2 K_3 [\text{X}^-]^2} \quad (3)$$

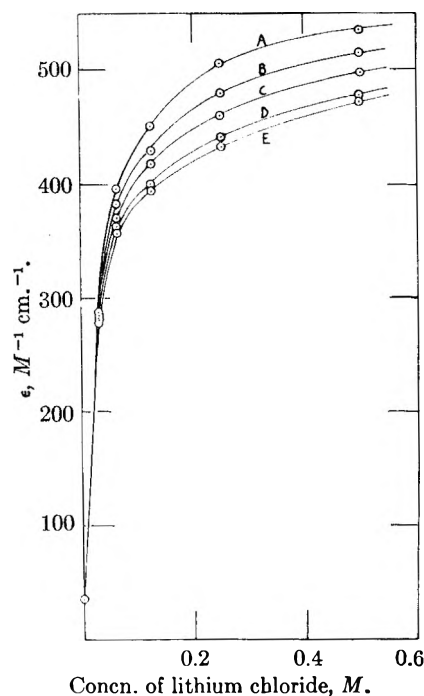


Fig. 7.—The plot of the observed molar extinction coefficient ϵ at 685 $m\mu$ against the concentration of lithium chloride at the temperatures: A = 25.0°; B = 38.0°; C = 47.8°; D = 58.7°; E = 64.0°.

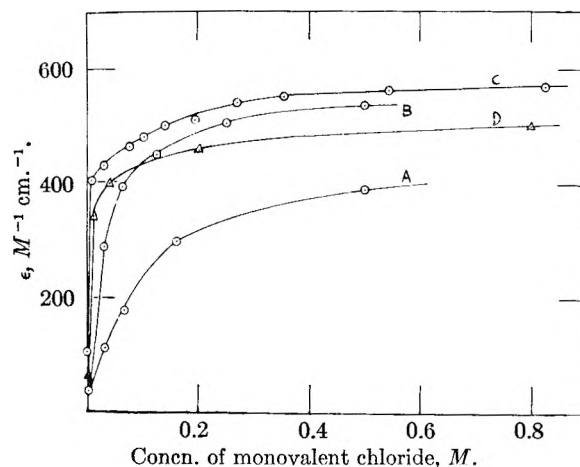


Fig. 8.—The observed molar extinction coefficient ϵ at 685 $m\mu$ vs. the concentration of (A) hydrogen chloride and (B) lithium chloride in anhydrous acetic acid at 25.0°; (C) monobutylammonium chloride in isopropyl alcohol⁵ at $19 \pm 1^\circ$ and (D) lithium chloride in 2-octanol¹ at 30°.

where ϵ_2 , ϵ_3 and ϵ_4 are the molar extinction coefficients of the solvated species CoX_2 , CoX_3^- and CoX_4^{2-} , respectively, at a given wave length.

Since the dissociation constant K_X of salts in anhydrous acetic acid is known to be very small⁷ we may replace $[\text{X}^-]$ by $(K_X [\text{MX}])^{1/2}$, hence equation 3 becomes

$$\epsilon = \frac{\epsilon_2 + \epsilon_3 K_2 K_X^{1/2} [\text{MX}]^{1/2} + \epsilon_4 K_2 K_3 K_X [\text{MX}]}{1 + K_2 K_X^{1/2} [\text{MX}]^{1/2} + K_2 K_3 K_X [\text{MX}]} \quad (4)$$

For all the additions reported in this paper ϵ_2 was identified with the observed extinction coefficient for solutions of CoX_2 with no added halide salts.

(7) S. Bruckenstein and I. M. Kolthoff, *J. Am. Chem. Soc.*, **78**, 2774 (1956).

Considering first the bromide system, an empirical expression, namely

$$\epsilon = \frac{200 + 4600[\text{LiBr}]^{1/2} + 900[\text{LiBr}]}{1.0 + 5.0[\text{LiBr}]^{1/2} + 1.0[\text{LiBr}]} \quad (5)$$

was found to give a curve which shows reasonable agreement with the experimental curve at 25.0° (see Fig. 4A), from which it was deduced that the values of ϵ_3 and ϵ_4 at 695 m μ are 920 and 900 $M^{-1} \text{ cm}^{-1}$, respectively. The dissociation constant of lithium bromide in acetic acid (K_B) has been estimated to be $7.2 \times 10^{-7} M$ at 30°,⁸ but this value is unreliable since it was found from Fuoss-Kraus plots of conductivity data (see Bruckenstein and Kolthoff).⁷ Assuming a positive enthalpy change for K_B , a lower value than the above is required at 25°. A value at 25° of $5 \times 10^{-7} M$ was used for K_B and hence we were able to evaluate K_2 and K_3 to be 7×10^3 and $3 \times 10^2 M^{-1}$, respectively. The reliability of the values will, of course, be subject to some doubt until a more dependable value of K_B is determined. The values for the equilibrium constants K_2 and K_3 are not unreasonable, since in the case of the addition of inorganic acetates to cobaltous acetate in anhydrous acetic acid^{1,4} the product K_2K_3 for the equilibria analogous to (1) and (2) above has a value of $2 \times 10^3 M^{-2}$, being composed of $K_2 = 20 M^{-1}$ and $K_3 = 1 \times 10^4 M^{-1}$. The values of ϵ_3 and ϵ_4 are probably of the right order since at this wave length the extinction coefficients of cobalt(II) with a very large excess of lithium bromide in ethanol or isopropyl alcohol are lower.⁵

Treating the results for alcohol solutions⁵ in a similar manner leads to the conclusion that the value of ϵ_4 is 900 $M^{-1} \text{ cm}^{-1}$ in both of these solvents, as it is in acetic acid at the same wave length of 695 m μ . Since this is the value of the extinction coefficient of CoBr_4^{2-} , it would not be expected to change with solvent as no solvent ligand is involved, as it is tetrahedral. In the case of CoBr_3^- , ϵ_3 was calculated to have values 775 and 770 $M^{-1} \text{ cm}^{-1}$, respectively, for isopropyl alcohol and ethanol compared with 920 $M^{-1} \text{ cm}^{-1}$ for acetic acid. This is not unexpected since it is the extinction coefficient of the CoBr_3^- ion, which must have one solvent ligand attached to it for the tetrahedral configuration. It also was concluded that with ethanol as solvent the value of $K_2K_B^{1/2}$ is 1.3 $M^{-1/2}$ and of $K_2K_3K_B$ is 1.0 M^{-1} ; with isopropyl alcohol as solvent the corresponding values are 3.0 $M^{-1/2}$ and 1.0 M^{-1} , respectively, in the temperature range 18–20°. The agreement between the calculated and observed points is shown in Figs. 4B and 4C. The values of K_B in these solvents are unknown, hence it is not possible to evaluate K_2 or K_3 for either system. The value of the observed molar extinction coefficient of cobaltous bromide in each of the three solvents mentioned previously at 695 m μ is much greater than that of cobaltous acetate at this wave length, which is expected if cobaltous acetate is octahedral and cobaltous bromide is tetrahedral.

The effect of temperature on Co(II)/LiBr solutions is shown in Fig. 3; by finding calculated plots to fit these curves, the variation in the values of

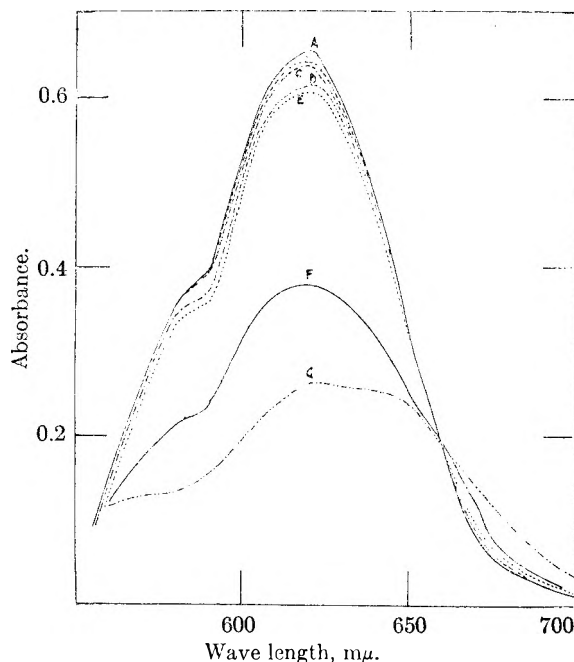


Fig. 9.—The absorption spectrum of Co(II) with added ammonium thiocyanate in acetic acid solution at 25.0°. Concentrations of ammonium thiocyanate are: A = 0.530 M ; B = 0.389 M ; C = 0.265 M ; D = 0.133 M ; E = 0.0663 M ; F = 0.0076 M with the concentration of Co(II) being constant at $1.82 \times 10^{-3} M$; G = $1.82 \times 10^{-3} M$ cobaltous thiocyanate.

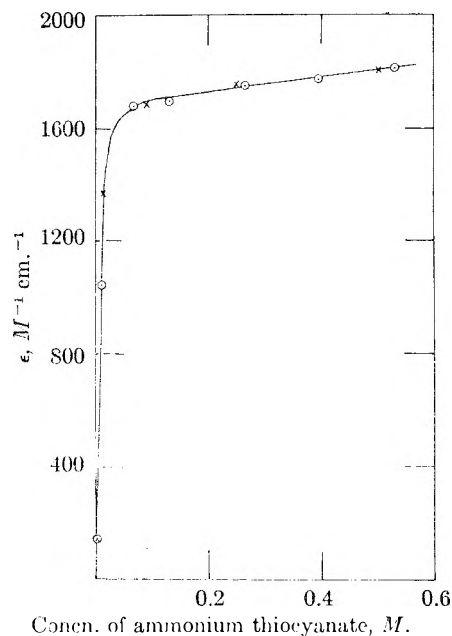


Fig. 10.—The plot of the observed extinction coefficient at 620 m μ against the concentration of ammonium thiocyanate at the temperature 25.0°. O are the observed experimental points and X are the calculated points.

$K_2K_B^{1/2}$ and $K_2K_3K_B$ with temperature was found. This is shown in Table I.

Calculation of the over-all enthalpy changes for the combined processes $K_2/K_B^{1/2}$ and $K_2K_3K_B$ gave values of -2.2 ± 0.5 and -12 ± 4 kcal. mole⁻¹, respectively. As the enthalpy change for the process K_B must be positive, both K_2 and K_3 must correspond to negative changes.

(8) M. M. Jones and E. Griswold, *J. Am. Chem. Soc.*, **76**, 3247 (1954).

TABLE I

Temp., °C.	$K_2K_3^{1/2}(M^{-1/2})$	$K_2K_3K_0(M^{-1})$
25.0	5.0	1.0
38.0	4.0	0.5
47.8	3.7	.2
58.7	3.2	.1
64.0	3.0	.09

TABLE II

Temp., °C.	$K_2K_3^{1/2}(M^{-1/2})$	$K_2K_3K_0(M^{-1})$
25.0	7.0	2.5
38.0	6.0	1.5
47.8	5.5	1.2
58.7	5.0	0.8
64.0	4.8	0.7

Since the expression derived for the observed extinction coefficient of cobalt(II) in the presence of bromide is very dependent on the dissociation constant of the bromide added, it was decided to add other inorganic bromides. Unfortunately, the only other very soluble inorganic bromide is hydrogen bromide, the sodium compound being soluble only to the extent of 0.25 *M*. The addition of hydrogen bromide in acetic acid to cobalt(II) solutions in the same solvent at a temperature of 25.0° resulted in the same effect as described for the addition of lithium bromide. The resulting spectra were identical in shape but the observed molar extinction coefficient was slightly higher for the hydrogen bromide than for the lithium bromide of the same concentration, which indicates that the dissociation constant of hydrogen bromide is slightly higher than that for lithium bromide. The ratio K_B/K_{HB} where K_{HB} is the dissociation constant of HBr in acetic acid is found to be ~ 1.0 . Separate experiments on small concentrations of H, Li, Na and K bromides indicated that the dissociation constants fall in the order $H \geq Li > Na > K$. The only measured value for the dissociation constant of hydrogen bromide in acetic acid is that found by Smith and Elliot⁹ which is known to be inaccurate owing to the use of Fuoss-Kraus plots. The value found was $2 \times 10^{-7} M$ at 25°, which would not fit in a regular order with the results of other workers⁸ for sodium, lithium and potassium, even allowing for the variation of temperature. It might be argued that the forward reaction of the equilibrium



is of importance since the effects of HBr and LiBr are so very similar in magnitude, but it can be shown that the equilibrium constant for this is equal to $K_B K_{Ac} / K_A K_{HB}$ which is of the order of 10^{-8} , where K_A and K_{Ac} are the dissociation constants of lithium acetate and acetic acid, respectively, and the other symbols are as previously designated.

Considering now the chloride system by choosing suitable values for the constants, calculated plots again can be made to fit the experimental curves. By finding the variation with temperature of $K_2 K_C^{1/2}$ and $K_2 K_3 K_C$ (see Table II) it is possible to estimate the over-all enthalpy changes for each of these combined processes. The values found were -2.1 ± 0.5 and -6.2 ± 2 kcal. mole⁻¹.

The value of K_C , the dissociation constant of lithium chloride in acetic acid at 25.0°, has been determined,⁷ hence it is possible to evaluate both K_2 and K_3 at this temperature. The values found were 2.5×10^4 and $1.2 \times 10^3 M^{-1}$, respectively. ϵ_3 and ϵ_4 were found to have values of 600 and 650 $M^{-1} \text{ cm.}^{-1}$, respectively, at 685 μ .

(9) T. L. Smith and J. H. Elliot, *J. Am. Chem. Soc.*, **75**, 3566 (1953).

Because the expression for the observed extinction coefficient with the addition of chloride is very dependent upon the dissociation constant of the chloride concerned it was decided to try the addition of another chloride. As in the case of the bromides, the only other monovalent chloride that is very soluble is hydrogen chloride. The addition of hydrogen chloride in anhydrous acetic acid to cobaltous solutions in the same solvent had the same effect as the addition of lithium chloride in that the shape of the spectra obtained were identical, but the observed molar extinction coefficients for the same concentrations of both chlorides were lower for hydrogen chloride than for lithium chloride. This is shown in Fig. 8, together with the results obtained for alcohol solutions by other workers^{5,6} when replotted. By choosing suitable values for the constants, the plot of the observed extinction coefficient against the concentration of HCl can be fitted and hence the ratio K_C/K_{HC} can be found, where K_{HC} is the dissociation constant of hydrogen chloride in anhydrous acetic acid. The value of this ratio is 12. Kolthoff and Bruckenstein⁷ using potentiometric methods have determined K_C : using K_{HC} determined spectrophotometrically¹⁰ the value of the ratio K_C/K_{HC} is 26. The agreement is reasonable when one considers the difficulties involved in such work. For example, the effect of water in our experiments would lead to an apparent decrease in the value of the dissociation constant concerned, whereas in the potentiometric methods an apparent increase would be observed.

For the system cobaltous chloride plus monobutylammonium chloride in isopropyl alcohol⁵ the following empirical relationship was found

$$\epsilon = \frac{105 + 5600[C_4H_9NH_3Cl]^{1/2} + 6500[C_4H_9NH_3Cl]}{1.0 + 10[C_4H_9NH_3Cl]^{1/2} + 10[C_4H_9NH_3Cl]}$$

This leads to the conclusion that the values of ϵ_3 and ϵ_4 are 560 and 650 $M^{-1} \text{ cm.}^{-1}$, respectively, and the values of $K_2 K_N^{1/2}$ and $K_3 K_2 K_N$ (where K_N is the dissociation constant of $C_4H_9NH_3Cl$ in isopropyl alcohol) both have a value of 10. Since K_N has not been determined only the ratio K_2/K_3 can be obtained; the value of this is 10. In the case of the addition of lithium chloride to cobaltous chloride in 2-octanol⁶ an empirical equation, namely

$$\epsilon = \frac{63 + 4480[LiCl]^{1/2} + 650[LiCl]}{1.0 + 8.0[LiCl]^{1/2} + 1.0[LiCl]}$$

was found to fit the experimental data, from which it was calculated that the values of ϵ_3 and ϵ_4 are 560 and 650 $M^{-1} \text{ cm.}^{-1}$, respectively, and the values of $K_2 K_0^{1/2}$ and $K_3 K_2 K_0$ are 8.0 $M^{-1/2}$ and 1.0 M^{-1} , respectively, where K_0 is the dissociation constant of lithium chloride in 2-octanol.

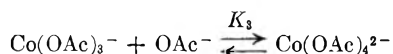
As for the bromide system the value of ϵ_4 does not appear to change from solvent to solvent, but

(10) I. M. Kolthoff and S. Bruckenstein, *J. Am. Chem. Soc.*, **78**, 1 (1956).

once again the value of ϵ_3 does change. In the alcohol solvents a value of $560 M^{-1} \text{ cm.}^{-1}$ is obtained and a value of $600 M^{-1} \text{ cm.}^{-1}$ in acetic acid, which is due to one solvent molecule being included in this species. The order of magnitude of the terms $K_2K_N^{1/2}$ and $K_2K_3K_N$, and $K_2K_0^{1/2}$ and $K_2K_3K_0$ are similar to those obtained with acetic acid as solvent.

For the thiocyanate system a calculated plot fitting the experimental curve was obtained (Fig. 10) with the values of ϵ_3 and ϵ_2 of 900 and $2500 M^{-1} \text{ cm.}^{-1}$, respectively, and $K_2K_T^{1/2}$ and $K_2K_3K_T$ of $23 M^{-1/2}$ and $1.0 M^{-1}$, respectively, at the temperature of 25.0° . The individual values of the constants K_2 and K_3 cannot be determined since the value of K_T , the dissociation constant of ammonium thiocyanate in anhydrous acetic acid, is not known, but the ratio K_2/K_3 was found to be 530. The value of K_T is not expected to be very different from the bromides and chlorides and should be in the range 10^{-6} to $10^{-9} M$ and hence the order of magnitude of the product K_2K_3 will be the same as that found for the bromide and chloride systems, that is, 10^6 to $10^9 M^{-2}$.

In the experiments on the addition of acetates, described in part I, the effect of the addition of water was found to be attributable to a dielectric constant change on the equilibrium



In the present system, the addition of water was found to reduce the molar extinction coefficient of Co(II) in the presence of excess lithium salts, but this is more likely to be due to the increased ionization of the acetic acid, since the blue color is completely destroyed with relatively small amounts of water. The addition of sodium acetate produced the same effect.

The significance of the results in terms of the catalytic activity now can be discussed. The data given in references 2 and 3 shows that reactivity is at a maximum when the ratio of $\text{Br}^-:\text{Co(II)}$ is either 1:1 or 2:1, depending upon the experimental conditions. From the results obtained in this paper, the cobaltous species would be expected to be of tetrahedral structure and can be tentatively given the formulas $(\text{CoBr}\cdot 3\text{HOAc})^+$ and $\text{CoBr}_2\cdot 2\text{HOAc}$. The dissociation of the CoBr_4^{2-} complex on increasing the temperature should favor the production of the latter complex thereby increasing the catalytic activity of the system. The poorer reactivity of the ion CoBr_4^{2-} might be due to the difficulty of producing Co(III), which is not likely to exist as a tetrahedral complex. Tetrahedral complexes with fewer bromine ligands might be more amenable to group transfer of say an acetoxy radical to give octahedral Co(III).

General Conclusions

The addition of acetate, chloride, bromide and thiocyanate, to cobalt(II) in acetic acid solution has been shown to lead to the formation of tetrahedral species of the type CoX_4^{2-} , where X represents the ligands mentioned above. A species of the type CoX_3^- , which is tetrahedral for the chloride, bromide and thiocyanate complexes and prob-

ably tetrahedral for the acetate, also has been shown to be formed. These anionic species of cobalt(II) are both related to the neutral species by equilibria (1) and (2).

The neutral species for the acetate is octahedral, while for the other ligands it is tetrahedral. The spectra observed for all the species are very similar in that they show only one main absorption band in the visible region of the spectrum which is a $d \leftarrow d$ transition. For the neutral species the wave lengths of the absorption maxima fall in the order bromide (672 $m\mu$), chloride (665 $m\mu$), thiocyanate (620 $m\mu$) and acetate (526 $m\mu$). In view of the broad nature of the band and its large extinction coefficient, the transitions must be spin allowed and must be the ${}^4F_1 \leftarrow {}^4F_1$ or the ${}^4A_2 \leftarrow {}^4F_1$ transition in the case of the latter anion since it is of octahedral configuration, and probably the ${}^4F_2 \leftarrow {}^4A_2$ transition in the other cases since they are of the tetrahedral configuration. The addition of excess of acetate, thiocyanate, chloride and bromide shifts the maximum of the absorption spectrum to longer wave lengths in all these systems, the maxima being at 565, 620, 685 and 695 $m\mu$, respectively. To a first approximation this can be assumed to be the order of the decreasing Dq values for Co(II) in a tetrahedral field since the transition is the same for all these ligands. The extinction coefficients obtained for the tetrahedral anionic species of Co(II) at the above maxima are shown in Table III.

TABLE III

Additive	Extinction coefficients ($M^{-1} \text{ cm.}^{-1}$) of		Wave length of max. cm.^{-1}	Half-band width, cm.^{-1}	Estd. oscillator strength of CoX_4^{2-}
	CoX_3^-	CoX_4^{2-}			
Acetate	..	1700	17700	4150	32.5×10^{-3}
Bromide	920	900	14400	1810	7.5×10^{-3}
Chloride	600	650	14600	2270	6.85×10^{-3}
Thiocyanate	1900	2500	16130	1950	22.5×10^{-3}

To a first approximation the Dq values should be in the same order as the oscillator strengths which can be calculated from the extinction coefficient and the half-band width. The oscillator strength F being given by

$$F = 4.32 \times 10^{-9} \int \epsilon \, d\nu \approx 4.6 \times 10^{-9} \epsilon_0 \, d\nu$$

where ϵ_0 is the maximum extinction coefficient and $d\nu$ is the half width in cm.^{-1} (reference 11). Since all the additives cause the formation of both CoX_3^- and CoX_4^{2-} , the resultant spectrum obtained is a mixture of these and that of the neutral molecule, but the absorption spectra do not change appreciably in shape after the addition of a small excess of the additive. Hence to a first approximation the oscillator strengths of the CoX_4^{2-} can be calculated using the half band width as estimated from the spectra obtained at very high concentrations of the additives. The results of these calculations are shown in Table III.

The calculated oscillator strengths fall in the order $\text{Co(OAc)}_4^{2-} > \text{Co(CNS)}_4^{2-} > \text{CoBr}_4^{2-} > \text{CoCl}_4^{2-}$. The order of decreasing Dq values found from the order of the wave lengths of the maxima in the visible region is as above with the bromide and chloride interchanged. The fact that the oscillator

TABLE IV

Additive	Values of $K_2K_X^{1/2}$ and $K_2K_3K_X$ at 25.0°	Over-all enthalpy change, kcal. mole ⁻¹	Over-all free energy change at 25.0°, kcal. mole ⁻¹	Over-all entropy change at 25.0°, cal. mole ⁻¹ deg. ⁻¹
Acetate	$K_2K_A^{1/2} = 0.01 M^{-1/2}$
	$K_2K_3K_A = 0.049 M^{-1}$	1.8 ± 0.1	1.8 ± 0.02	0.0 ± 0.4
Bromide	$K_2K_B^{1/2} = 5.0 M^{-1/2}$	-2.2 ± 0.5	-0.96 ± .04	-4.0 ± 1.7
	$K_2K_3K_B = 1.0 M^{-1}$	-12.0 ± 4.0	0.00 ± .04	-40 ± 14
Chloride	$K_2K_C^{1/2} = 7.0 M^{-1/2}$	-2.1 ± 0.5	-1.16 ± .04	-3.1 ± 1.7
	$K_2K_3K_C = 2.5 M^{-1}$	-6.2 ± 2.0	-0.55 ± .04	-19 ± 7
Thiocyanate	$K_2K_T^{1/2} = 23.0 M^{-1/2}$	-1.86 ± .04
	$K_2K_3K_T = 1.0 M^{-1}$	0.00 ± .04

strength for CoBr_4^{2-} is too large is probably due to the absorption spectrum of cobalt(II) in the presence of excess bromide being much less Gaussian in shape than for the other systems. The value of the oscillator strength of the CoCl_4^{2-} species calculated above of 6.85×10^{-3} agrees reasonably well with the value of 6.0×10^{-3} quoted by Balehausen and Liehr,¹² particularly in view of the approximations involved in these calculations. The oscillator strengths when plotted against the position of the absorption maximum (cm.^{-1}) are reasonably linear, as one would predict.

The good agreement helps to confirm our interpretation of the spectral effects due to the addition of compounds containing the various ligands.

Table IV shows the over-all enthalpy changes, the over-all free energy and over-all entropy changes at 25.0° for the combined processes $K_2K_X^{1/2}$ and $K_2K_3K_X$, where K_X represents the dissociation con-

stant of the inorganic additives, where K_A is the dissociation constant of sodium acetate, K_B and K_C are the dissociation constants of lithium bromide and chloride, respectively, and K_T is the dissociation of ammonium thiocyanate, in all cases acetic acid being the solvent. Since it is reasonably safe to assume that increase in temperature will increase the dissociation of the inorganic additives, the enthalpy change for this process is positive. With this assumption it is possible to estimate the enthalpy change for K_2 for both the bromide and chloride systems to be not greater than -2 kcal. mole⁻¹, and that for K_3 to be not greater than -10 ± 4 and -4 ± 2 kcal. mole⁻¹, respectively. For the bromide and chloride systems it also was found possible to evaluate the difference in the enthalpy changes ($\Delta H_2 - \Delta H_3$) for the processes K_2 and K_3 . This was found to be for the bromide $+7 \pm 3$ kcal. mole⁻¹ and for the chloride $+3 \pm 1$ kcal. mole⁻¹.

The authors are indebted to Dr. J. H. Binks of this Department for much helpful discussion.

(12) C. J. Balehausen and A. D. Liehr, *J. Mol. Spectroscopy*, **2**, 342 (1958).

THE ADSORPTION OF BUTYL, PHENYL AND NAPHTHYL COMPOUNDS AT THE INTERFACE MERCURY-AQUEOUS ACID SOLUTION

By E. BLOMGREN, J. O'M. BOCKRIS AND C. JESCH

John Harrison Laboratory of Chemistry, University of Pennsylvania, Philadelphia 4, Pa.

Received April 27, 1961

The adsorption on mercury from acid solutions of butyl, phenyl and naphthyl compounds having the groups OH, CHO, COOH, CN, SH, S, CO, NH_3^+ and SO_3^- has been examined as a function of concentration and potential. The electrocapillary method was applied. The following quantities have been calculated thermodynamically: the net charge on the solution; the degree of coverage of the surface with organic compound, the net free energy of adsorption of organic adsorbate as a function of coverage and potential; the adsorption of H_3O^+ and Cl^- ions in relation to the adsorption of organic molecules. The effect of diffusion on the rate of attainment of adsorption equilibrium is analyzed. Naphthyl compounds have a 10^3 - 10^4 times higher adsorbability than corresponding butyl compounds, with phenyl compounds intermediate. For substances with the same hydrocarbon radical, the adsorbability varies with the substituent group by a factor of up to 10^4 . Aromatic cations show a special behavior. The orientation of the adsorbed molecules has been determined, and the character of the adsorptive forces is discussed in terms of metal-adsorbate and solution-adsorbate interaction. A method is proposed by which the intrinsic free energy of adsorption of a hydrocarbon radical in an organic substance upon a given metal can be derived. It is about 6 kcal./mole greater for the naphthyl than for the butyl radical. The degree of effectiveness in inhibiting the dissolution of iron and the degree of coverage on mercury show a parallelism for the majority of compounds studied.

Gouy's¹ examination of the surface tension depression of mercury by organic compounds does not permit calculation of surface coverages. Frumkin² determined surface tension depressions for

various concentrations of *l*-amyl alcohol in aqueous solutions and interpreted the results in terms of a semi-empirical adsorption isotherm. Conway, Bockris and Lovrecek³ used the electrocapillary method to examine the adsorption of alkaloids on

(1) G. Gouy, *Ann. chim. phys.*, [7] **29**, 145 (1903); [8] **8**, 291 (1906); [8], **9**, 75 (1906); *Ann. phys.*, [9] **6**, 5 (1916); [9] **7**, 129 (1917).

(2) A. N. Frumkin, *Z. Physik*, **35**, 792 (1926).

(3) B. E. Conway, J. O'M. Bockris and B. Lovrecek, *CITCE Proc.*, **6**, 207 (1955).

mercury. Hansen, *et al.*,⁴ studied the adsorption of *n*-amyl alcohol, *n*-valeric acid, *n*-valeronitrile, *n*-caprylic acid, *n*-diethylketone, acetylacetone and phenol in 0.1 *N* HClO₄ solutions, using capacitance measurements. Blomgren and Bockris⁵ studied adsorption of aromatic aminium ions on mercury by the electrocapillary method. Gerovich and Polyanovskaya⁶ recorded electrocapillary curves for aniline, anilinium ions and tropilium ions in aqueous solutions.

Here the adsorption of butyl, phenyl and naphthyl compounds containing OH, CHO, COOH, CN, SH, S, CO, NH₃⁺ and SO₃⁻ groups is discussed.

In the absence of significant dissociation of the adsorbable organic species, and in the presence of HCl, Gibbs' equation applies⁷ in the form

$$d\gamma = q_s dE_H - \Gamma_{Cl^-} d\mu_{HCl} - \Gamma_A d\mu_A \quad (1)$$

where γ is the surface tension of the mercury, q_s is the total charge per unit area of the interface (solution side), E_H is the potential of the mercury with respect to a hydrogen electrode in the same solution, Γ_{Cl^-} and Γ_A are the surface excesses of Cl⁻ ions and adsorbate molecules, and μ_{HCl} and μ_A are the chemical potentials of HCl and adsorbate in the solution. From (1)

$$q_s = \left(\frac{\partial \gamma}{\partial E_H} \right)_{\mu_{HCl}, \mu_A} \quad (2)$$

$$\Gamma_A = - \left(\frac{\partial \gamma}{\partial \mu_A} \right)_{E_H, \mu_{HCl}} \quad (3)$$

$$\Gamma_{Cl^-} = - \left(\frac{\partial \gamma}{\partial \mu_{HCl}} \right)_{E_H, \mu_A} \quad (4)$$

Furthermore, for an electroneutral adsorbate in a solution of HCl

$$q_s = F(\Gamma_{H_3O^+} - \Gamma_{Cl^-}) \quad (5)$$

The adsorption coefficient k (in cm.³ mole⁻¹) in Langmuir's adsorption isotherm, and the net free energy of adsorption, ΔF_a^0 , *i.e.*, the difference between the standard electrochemical free energies of adsorption of an adsorbate and water (referred to unit mole fraction of water and adsorbate in solution and on the metal surface), is given by⁸

$$\frac{\Gamma_A}{\Gamma_{max} - \Gamma_A} = kC_A = \frac{c_A e^{-\Delta F_a^0/RT}}{0.0555} \quad (6)$$

where c_A is expressed in mole cm.⁻³. Equations for dissociated species have been given.⁵

Experimental

The electrocapillometer has been described.^{5,9} The mercury meniscus was adjusted to a distance of 0.01 cm. from the tip of the capillary. At the beginning of an ex-

periment, pure HCl solution was introduced into the cell and deoxygenated with purified H₂¹⁰; an electrocapillary curve was determined for this solution before the organic material was added. The adsorbate was usually added from a freshly prepared aqueous solution in a buret fused to the capillary compartment. The solution containing the adsorbate also contained HCl in the same concentration as the original solution in the cell ($\pm 1\%$). Corrections were made for the effect on the mercury pressure of the increase in height of the solution surface above the meniscus upon addition of the adsorbate-containing solution. When the solubility of an organic substance in aqueous HCl was so low that the added volume of solution would have exceeded 10% of the original volume in the cell, the adsorbate was added from a solution in redistilled CH₃OH. The maximum concentration of CH₃OH thus introduced was 2.5% by volume. The expected effect upon the interfacial tension of 0.5 dyne cm.⁻¹ was verified.¹¹ The hydrogen electrode was kept in a compartment separated from the capillary compartment by a closed stopcock to eliminate diffusion of organic material to the reference electrode. Liquid junction potentials between these compartments were neglected.

In each experiment, several electrocapillary curves were determined, covering a concentration range selected according to the adsorbability of the substances. The ratio of adsorbate concentrations in solution between two consecutive electrocapillary curve determinations was ≥ 2 .

Purified H₂ was passed through the solutions. For volatile substances the flow of hydrogen was minimized. The effect of volatility was determined by experiments over 18 hours: it had a value of $\Delta\gamma < 0.5$ dyne cm.⁻¹ referred to a level of $\Delta\gamma = 10$ dyne cm.⁻¹.

The HCl and adsorbate solutions were prepared from redistilled HCl and conductivity water. The glassware was cleaned with HNO₃-H₂SO₄ (1:1) mixtures and equilibrium water. The cell was filled with conductance water which was forced out with purified H₂ before the HCl solution was introduced. Pre-electrolysis was applied in test runs. The electrocapillary curve obtained for 0.1 *N* HCl was compared with a "standard curve" for 0.1 *N* HCl solution prepared under rigorous conditions of pre-electrolysis. The maximum deviation accepted between an observed HCl curve and the standard curve was 0.3 dyne cm.⁻¹; when a greater deviation was observed, repeated cleaning of the cell restored the curve to the standard one. Comparison between results obtained for adsorption of organic substances under conditions described above and those obtained with pre-electrolyzed solutions showed differences within evaluation errors¹² (*vide infra*).

Values of q_s were obtained graphically from large scale electrocapillary curves, values of Γ_A and Γ_{Cl^-} from $\Delta\gamma - \log c_A$ and $\Delta\gamma - \log a_{HCl}$ relations, respectively. Activity corrections were employed for HCl¹⁴ but not for organic compounds.

Errors. (a) **Reproducibility.**—This was determined by comparison of results obtained independently by the individual authors.

(1) q_s .—About 2% (referred to a level of 10 μ coul. cm.⁻²) for substances which reached equilibrium within seconds; an average of about 5% for substances which reached equilibrium within minutes (*vide infra*).

(2) Γ_i .—About 10% for substances with negligible time effects; up to 15% for substances with appreciable time effects.

(b) **Inherent Errors.**—These errors arise only with substances which cause a change of $c_{H_3O^+}$ (*e.g.*, amines). Such substances were added in concentrations less than 10% of the HCl concentration. The maximum inherent errors⁹ were

(10) N. Pentland, J. O'M. Bockris and E. Sheldon, *J. Electrochem. Soc.*, **104**, 182 (1957).

(11) R. Parsons and M. A. V. Devanathan, *Trans. Faraday Soc.*, **49**, 673 (1953).

(12) This relative insensitivity of equilibrium adsorption to trace amounts of impurities can be contrasted with the great sensitivity of corresponding kinetic processes (*cf.* Conway, *et al.*).¹³

(13) B. E. Conway, R. G. Barradas and T. Zawadzki, *J. Phys. Chem.*, **62**, 676 (1958).

(14) H. S. Farned and B. E. Owen, "The Physical Chemistry of Electrolytic Solutions," 3rd ed., Reinhold Publ. Corp., New York, N. Y., 1958.

(4) R. S. Hansen, R. E. Minturn and D. A. Hickson, *J. Phys. Chem.*, **60**, 1185 (1956); **61**, 953 (1957).

(5) E. Blomgren and J. O'M. Bockris, *ibid.*, **63**, 1475 (1959).

(6) M. A. Gerovich and N. S. Polyanovskaya, *Nauch. Doklady Vysshei Shkoly, Khim. i Khim. Tekhnol.*, 651 (1958).

(7) *Cf.* R. Parsons, in "Modern Aspects of Electrochemistry," ed. J. O'M. Bockris, Butterworths, London, 1954.

(8) This relation is based on the assumption involved in Langmuir's adsorption isotherm that the total number of sites available for water and for an organic adsorbate are the same. This model becomes increasingly inapplicable as the size of the organic molecules increases. However, the error is tantamount to suppressing a total variation in ΔF^0 due to size of only about 1 kcal. mole⁻¹ for the largest molecules studied in the present work.

(9) (a) S. R. Craxford, Dissertation, Oxford, 1936; L. F. Oldfield, Thesis, London, 1951; M. A. V. Devanathan, Thesis, London, 1951; (b) L. A. Hansen and J. W. Williams, *J. Phys. Chem.*, **39**, 439 (1935).

TABLE I
 TIME EFFECTS AT LOW SURFACE COVERAGES ($\theta < 0.5$)

Substance	$\Gamma_{\max} \times 10^{10}$, mole. cm. ⁻²	E_H , mv.	$k \times 10^{-6}$, cm. ² mole ⁻¹	$K \times 10^4$, cm.	$D \times 10^2$, ^a cm. ² sec. ⁻¹	(τ_{98}) _{Diff} sec.	(τ_{98}) _{exptl}
C ₄ H ₉ ·CHO	7.9	-200	1.5	12	0.70	70	200-400
C ₄ H ₉ ·SH	7.9	-200	0.1	0.8	.70	0.3	60-100
(C ₆ H ₅) ₂ S	3.5	-200	5	18	.60	170	300-600
(C ₆ H ₅) ₂ CO	3.6	50	6	22	.60	220	200-400
C ₆ H ₅ ·CHO	3.6	-200	1	3.6	.72	6	100-230
C ₆ H ₅ ·CHO	3.6	200	0.2	0.7	.72	0.2	ca.30
C ₆ H ₅ ·SH	3.5	-100	6	21	.71	200	100-300
(C ₆ H ₅) ₂ S	2.3	-200	40	92	.60	4400	600-1200
α -C ₁₀ H ₇ ·OH	2.8	-200	50	140	.67	9300	900-1200
α -C ₁₀ H ₇ ·CHO	2.9	300	20	58	.64	1700	600-1200
α -C ₁₀ H ₇ ·COOH	2.2	0	40	88	.61	4000	300 ^c
α -C ₁₀ H ₇ ·NH ₃ ⁺	2.4	300	1	2.4	.66	45	60
β -C ₁₀ H ₇ ·SO ₃ ⁻	2.2	100	6	13	.6	90	30-300 ^d

^a Calculated from Stokes-Einstein's equation. ^b Results of several experiments. ^c Measurements not extended beyond 5 minutes. ^d Measurements only made at $t = 1/2$ min. and 5 min.; constant for $t = 5$ min.

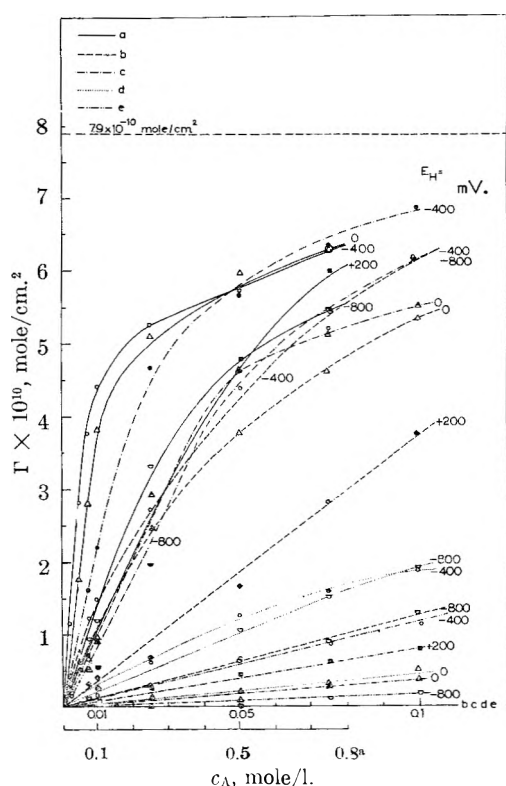


Fig. 1.— Γ_A as a function of c_A at constant potentials: (a) *n*-butyl alcohol; (b) *n*-valeric acid; (c) *n*-valeronitrile; (d) *n*-butylamine; (e) *n*-butylsulfonic acid. For (a)-(c): $c_{\text{HCl}} = 0.1 N$; for (d)-(e): $c_{\text{HCl}} = 1 N$. (Potentials stated on figure.)

$$dq = \pm 0.3 \mu\text{coul. cm.}^{-2}$$

$$d\Gamma_A = \pm 0.06 \times 10^{-10} \text{mole. cm.}^{-2}$$

$$d(F\Gamma_{\text{H}_3\text{O}^+}) = \pm 0.9 \mu\text{coul. cm.}^{-2}$$

$$d(F\Gamma_{\text{Cl}^-}) = \pm 0.6 \mu\text{coul. cm.}^{-2}$$

Results

(a) **Oxidation and Reduction Phenomena.**—Polarographic experiments showed that the only compounds oxidized or reduced under the experimental conditions were *n*-butyl mercaptan, phenyl mercaptan, benzaldehyde and α -naphthaldehyde. Reproducible electrocapillary measurements could be made on butyl mercaptan and phenyl mercaptan in 0.1 *N* HCl only for $E_H < 0.0$ volt. For benzalde-

hyde measurements could not be made for $E_H < -400$ mv. These limitations are consistent with the observed polarographic waves.¹⁵ For α -naphthaldehyde reproducible results were obtained from electrocapillary measurements over the whole potential range although a cathodic wave has been reported¹⁶ at $E_{1/2} = -0.47$ volt.

(b) **Time Effects.**—The surface tension reached constant values in *ca.* 10 sec. for about half of the substances examined. For the others, the time required to reach final values (taken as the time after which $\Delta\gamma$ changed by $<3\%$ in the succeeding 30 minutes) was 2-25 minutes (Table I).

(c) **Surface Coverage as a Function of Solution Concentration of Adsorbate at Constant Potentials.**—Figures 1-3 give typical examples of the adsorption isotherms for the substances examined.

(d) **Maximum Surface Coverage as a Function of Structure.**—Table II shows Γ_{\max} and compares with planar and perpendicular space requirements for a monolayer.

(e) **Surface Coverage as a Function of Potential at Constant Solution Concentrations of Adsorbate.**—Typical examples of Γ as a function of E_H at constant c_A are given in Figs. 4-5. All types of molecules are desorbed at extremes of potential. The neutral molecules have a maximum in Γ near to the e.c.m. on the negative side for aliphatic and on the positive side for aromatic compounds (pure 0.1 *N* HCl: $E_{H,e.c.m.} = -185$ mv.). Aromatic molecules are preferentially adsorbed on the positive branch. C₄H₉NH₃⁺ is preferentially adsorbed on the negative branch and exhibits a decrease of adsorption on the positive branch. The aromatic cations are adsorbed relatively uniformly at all potentials, whereas the aromatic anions are adsorbed preferentially on the positive branch and decreasingly on the negative branch.

(f) **Adsorbability at Electrocapillary Maximum as a Function of Structure.**—The adsorption coefficient, k , (see eq. 6) has values up to 10^3 - 10^4 times higher for naphthyl than for butyl compounds, phenyl compounds having an intermediate degree of adsorbability (Table III). For substances with the same hydrocarbon radical, k in-

(15) R. Pasternak, *Helv. Chim. Acta*, **31**, 753 (1948).

(16) R. W. Schmidt and E. Heilbronner, *ibid.*, **37**, 1453 (1954).

TABLE II
ORIENTATION OF ADSORBED MOLECULES

Substance	Molecular area Å. ²) Fisher-Taylor-Hirschfelder models		Γ _{max} × 10 ¹⁰ (mole cm. ⁻²) Calcd.		Obsd. ^a
	Planar	Perpend.	Planar	Perpend.	
n-Butyl alcohol	36	21	4.6	7.9	>6.5
n-Valeraldehyde	42	21	3.9	7.9	Not attained
n-Valeric acid	43	21	3.8	7.9	>6.5
n-Valeronitrile	40	21	4.1	7.9	>7.0
n-Butylamine	37	21	4.5	7.9	Not attained
n-Butyl mercaptan	39	21	4.3	7.9	Not attained
n-Dibutyl sulfide	64	48 ^b	2.6	3.5 ^b	>3.3
n-Butylsulfonic acid	49	21	3.4	7.9	Not attained
n-Dibutylketone	58	45 ^b	2.8	3.6 ^b	3.7 ± 0.1
Phenol	48	20	3.5	8.2	3.7 ± .2
Benzaldehyde	51	20	3.3	8.2	3.6 ± .1
Benzoic acid	56	20	2.9	8.2	2.6 ± .2
Benzonitrile	51	20	3.3	8.2	3.7 ± .2
Aniline	50	20	3.4	8.2	Not attained
Phenyl mercaptan	49	20	3.4	8.2	3.5 ± 0.1
Diphenyl sulfide	73 ^c	22 ^d	2.3 ^c	7.4 ^d	Not attained
		49 ^e		3.4 ^e	
Phenylsulfonic acid	53	22	3.1	7.4	Not attained
α-Naphthol	66	26	2.5	6.4	2.8 ± 0.2
α-Naphthaldehyde	73	26	2.3	6.4	2.9 ± 0.2
α-Naphthoic acid	75	26	2.2	6.4	Not attained
α-Naphthylamine	68	26	2.4	6.4	2.5 ± 0.1
β-Naphthalene sulfonic acid	77	26	2.2	6.4	2.2 ± 0.1

^a Values marked, e.g., > 6.5, mean that, at the highest measurable concentrations, the adsorption isotherm indicated an approach to the adsorption maximum. "Not attained" means that, at the solubility limit the isotherm was not approaching the saturation value. ^b For symmetrical position of carbon chains with respect to the surface. ^c For symmetrical position of benzene rings with respect to the surface. ^d With one benzene ring attached to the surface and the other projecting into the solution. ^e With both benzene rings in contact with the surface.

creases with the substituent group in the order SO₃⁻ ~ NH₃⁺ < OH < CN < CHO ~ COOH < SH < S < CO; within butyl and phenyl series substituents affect adsorbability by 10³ - 10⁴ times.

TABLE III

ADSORBABILITY OF ORGANIC SUBSTANCES ON MERCURY IN 0.1 N HCl AT E.C.M. AND θ = 0.25

Functional group	k (cm. ³ mole ⁻¹)		
	n-C ₄ H ₉	C ₆ H ₅	C ₁₀ H ₇
SO ₃ ⁻	1 × 10 ³	2 × 10 ⁴	4 × 10 ⁶
NH ₃ ⁺	2 × 10 ³	1 × 10 ⁴	4 × 10 ⁶
OH	1 × 10 ⁴	3 × 10 ⁶	5 × 10 ⁷
CN	3 × 10 ⁴	5 × 10 ⁶
CHO	1 × 10 ⁶	1 × 10 ⁶	7 × 10 ⁷
COOH	4 × 10 ⁶	2 × 10 ⁶	3 × 10 ⁷
SH	7 × 10 ⁴	6 × 10 ⁶
S	6 × 10 ⁶	3 × 10 ⁷
CO	1 × 10 ⁷

(g) **Net Free Energy of Adsorption as a Function of Potential for Constant Surface Coverages.**—Figure 6, which gives examples of the behavior of the examined substances, demonstrates that the free energy of adsorption has a maximum at slightly negative potentials with respect to the e.c.m. for neutral aliphatic compounds. For neutral aromatic compounds, the maximum in |ΔF_a⁰| is found to be at potentials slightly positive to e.c.m. A smaller slope of the ΔF_a⁰-E_H curves on the positive side of e.c.m. for aromatic com-

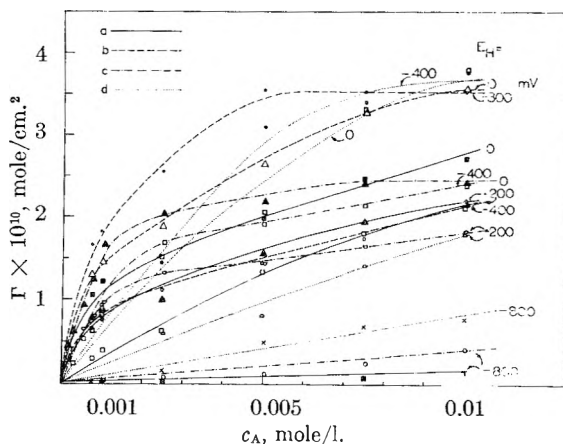


Fig. 2.—Γ_A as a function of c_A at constant potentials and c_{HCl} = 0.1 N: (a) phenol; (b) benzaldehyde; (c) benzoic acid; (d) benzonitrile. (Potentials stated on figure.)

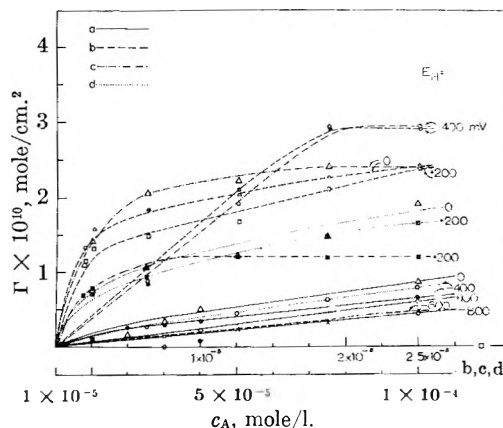


Fig. 3.—Γ_A as a function of c_A at constant potentials and c_{HCl} = 0.1 N: (a) diphenyl sulfide; (b) α-naphthol; (c) α-naphthaldehyde; (d) α-naphthoic acid. (Potentials stated on figure.)

pounds compared with aliphatic compounds was noted.

(h) **Net Free Energy of Adsorption as a Function of Surface Coverage at Constant Potentials.**—All the neutral substances behave as shown in Fig. 7.

(i) **Net Free Energy of Adsorption at Electrocapillary Maximum and at Constant Surface Coverage as a Function of Structure.**—Table IV

TABLE IV

Functional group	ΔF _s ⁰ AND ΔF _a ⁰ AT E.C.M. AND θ = 0.25 (KCAL. MOLE ⁻¹)					
	n-C ₄ H ₉ -ΔF _s ⁰	n-C ₄ H ₉ -ΔF _a ⁰	C ₆ H ₅ -ΔF _s ⁰	C ₆ H ₅ -ΔF _a ⁰	C ₁₀ H ₇ -ΔF _s ⁰	C ₁₀ H ₇ -ΔF _a ⁰
OH	2.5	3.7	2.6	5.6	6.5	8.8
CHO	6.6	6.5	4.5	6.6	6.9	9.0
COOH	2.9	4.5	4.6	6.7	7.7	8.6
CN	3.7	4.5	4.7	6.0
NH ₃ ⁺	1.0-2.4	2.9	1.0-2.4	3.9	1.0-2.4	7.3
SH	5.5	4.9	6.1	7.5
S	7.4	7.4	8.7	8.4
SO ₃ ⁻	1.0-2.4	2.6	1.0-2.4	3.8	1.6	7-7.5
CO	6.1	(8) ^a

^a Estimated from ΔF_a⁰ at high surface coverages.

gives the net free energy of adsorption at e.c.m. and at a (arbitrarily selected) surface coverage of

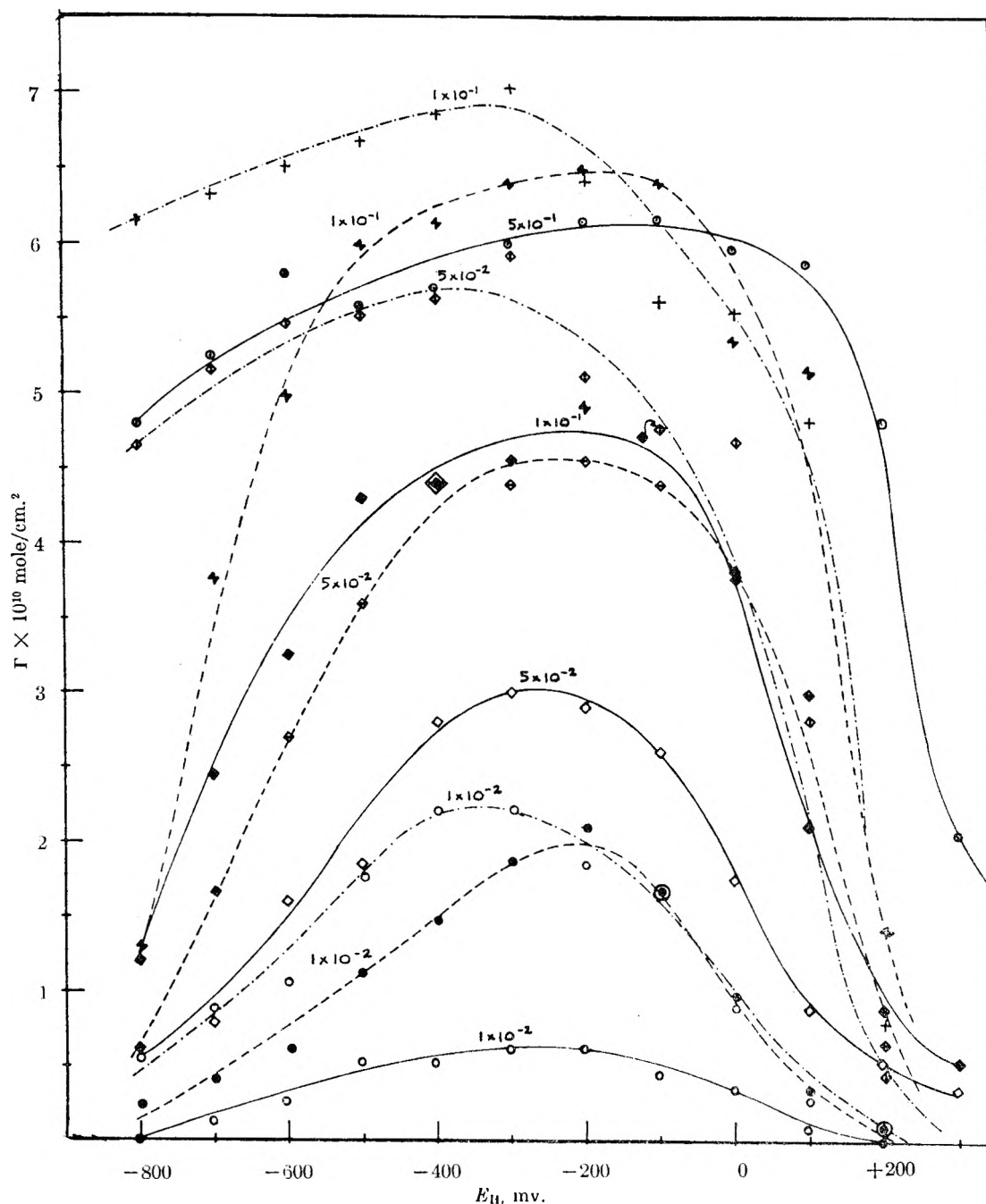


Fig. 4.— Γ_A as a function of E_H for constant adsorbate concentrations and $c_{HCl} = 0.1 N$: (a, —) *n*-butyl alcohol; (b, - - -) *n*-valeric acid; (c, - · - · -) *n*-valeronitrile. (c_A stated on figure.)

25%, and compares with the standard free energy of dissolution (see eq. 14-16). Figure 8 shows the former entity as a function of the latter.

(j) **The Potential of the Electrocapillary Maximum as a Function of Structure of the Adsorbed Organic Molecule at Constant Solution Concentration of Adsorbate.**—As seen from Fig. 9, the e.c.m. is displaced to positive values by aliphatic compounds. It is displaced to negative values by aromatic compounds. Aromatic cations have little effect on the e.c.m.

(k) **The Net Electric Charge on Solution (q_s) as a Function of Surface Coverage at Constant Potentials.**—Adsorption of neutral organic sub-

stances causes q_s to become less positive at negative potentials and less negative at positive potentials (Fig. 9). The q_s - E_H curves for a given substance at various concentrations intersect one another at potentials negative to the e.c.m. for aliphatic substances, and at potentials positive to the e.c.m. for aromatic substances.

Adsorption of aromatic cations causes little change in q_s ; adsorption of aromatic anions causes considerable change in q_s .

(1) **The Surface Excesses of H_3O^+ and Cl^- as a Function of Surface Coverage at Constant Potentials.**— $FT_{H_3O^+}$ in 1 N HCl is reduced by some $5 \mu\text{coulombs cm.}^{-2}$ over the whole potential

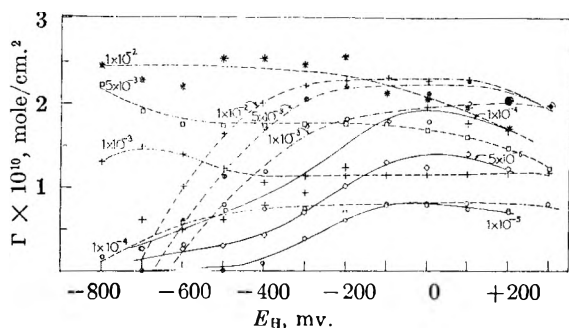


Fig. 5.— Γ_A as a function of E_H for constant adsorbate concentrations and $c_{HCl} = 0.1 N$: (a, —) α -naphthoic acid; (b, - - -) α -naphthylamine; (c, - · - ·) β -naphthalenesulfonic acid. (c_A stated on figure.)

range for $\theta = 0.5 - 0.8$, in the presence of phenol. $F\Gamma_{Cl-}$ decreases considerably on the positive branch in 1 N HCl upon adsorption of phenol. Lesser effects occur at smaller HCl concentrations (Fig. 10).

Discussion

(1) **Comparison with Previous Work.**—The values obtained for $\Delta\bar{F}_a^0$ at the adsorption maximum for valeric acid and valeronitrile are in agreement with those derivable from the results of Hansen, *et al.*,⁴ for the same substances in aqueous perchloric acid.

Values of projected areas for aliphatic substances derived in the present work (Table II) are consistent with values obtained from mono-molecular films of long-chain aliphatic substances at water-air interfaces,¹⁷ but differ from the values of 32–33 Å.² obtained by Hansen, *et al.* For phenol, Hansen, *et al.*'s projected area of 40 Å.² agrees with that reported here.

(2) **Time Effects.**—The slow attainment of equilibrium adsorption may be controlled in rate either by diffusion in solution or by reaction on the surface. The case of diffusion was considered by Sutherland¹⁸ and Delahay and Trachtenberg.¹⁹ A recent treatment was given by Hansen.^{20, 20a}

In the case of diffusion control, ϵ and for $\theta = k_c$ ^{18, 19}

$$\frac{\Gamma_t}{\Gamma_e} = 1 - \exp\left(\frac{Dt}{K^2}\right) \operatorname{erfc}\left(\frac{\sqrt{Dt}}{K}\right) \quad (\text{ref. 18-5})$$

where $K = k\Gamma_{\max}$ and Γ_t , Γ_e , Γ_{\max} denote Gibbs surface excess at time t , at equilibrium, and at maximum adsorption. From (3)

$$d\gamma_t = -RT\Gamma_t \frac{dc(0,t)}{c(0,t)} \quad (7)$$

With $\Gamma_t = k\Gamma_{\max} c(0,t)$ this gives

$$\Delta\gamma_t = RT\Gamma_t \text{ and } \Delta\gamma_e = RT\Gamma_e \quad (8)$$

From ref. 18-5 and (8)

$$\frac{\Delta\gamma_t}{\Delta\gamma_e} = 1 - \exp\left(\frac{Dt}{K^2}\right) \operatorname{erfc}\left(\frac{\sqrt{Dt}}{K}\right) \quad (9)$$

(17) N. K. Adam, "The Physics and Chemistry of Surfaces," Oxford University Press, London, 3rd ed., 1941.

(18) K. L. Sutherland, *Austr. J. Sci. Res.*, **A5**, 683 (1952).

(19) P. Delahay and I. Trachtenberg, *J. Am. Chem. Soc.*, **79**, 2355 (1957).

(20) R. S. Hansen, *J. Phys. Chem.*, **64**, 637 (1960). (20a) The authors are thankful to Dr. R. S. Hansen who drew their attention to the material in (18) and (20). His equation 23 represents the general case of the equation derived hereafter.

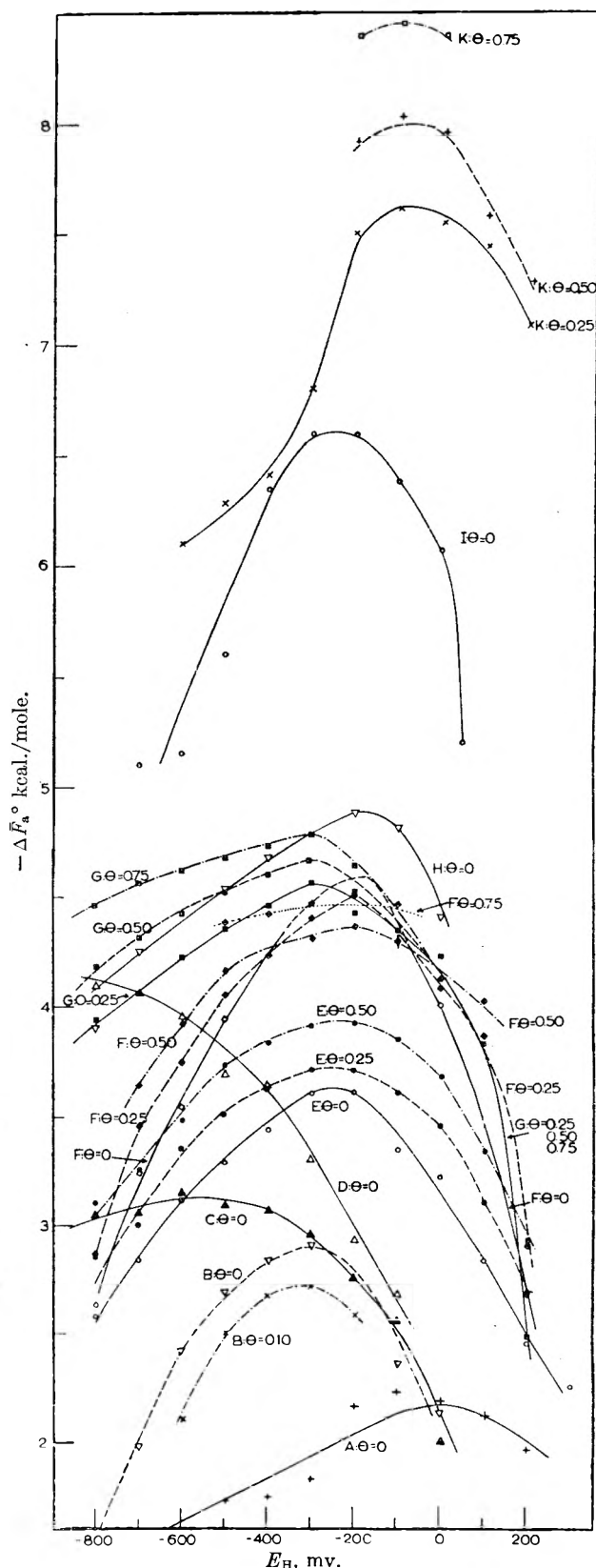


Fig. 6.—Net free energy of adsorption for aliphatic substances as a function of E_H at constant surface coverages: (A) *n*-butylsulfonic acid in 0.1 N HCl; (B) *n*-butylsulfonic acid in 1 N HCl; (C) *n*-butylamine in 1 N HCl; (D) *n*-butylamine in 0.1 N HCl; (E) *n*-butyl alcohol; (F) *n*-valeric acid; (G) *n*-valeronitrile; (H) *n*-butyl mercaptan; (I) *n*-valeraldehyde; (K) *n*-dibutyl sulfide. $c_{HCl} = 0.1 N$ for (E)-(K). (θ stated on figure.)

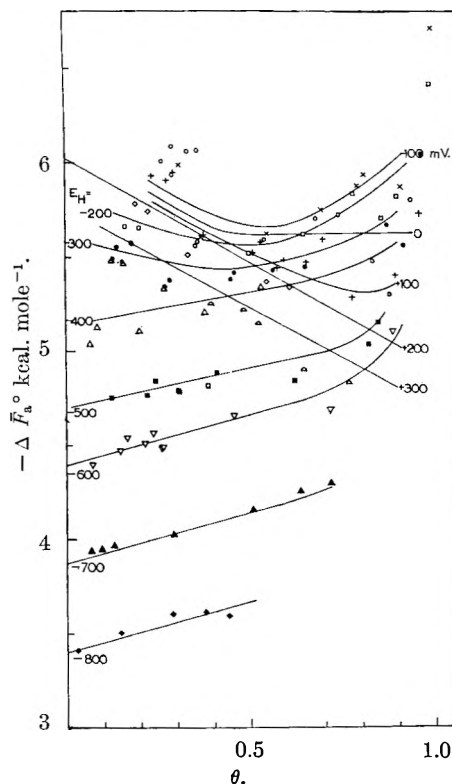


Fig. 7.—Net free energy of adsorption for phenol in 0.1 N HCl as a function of θ for constant potentials. (E_H stated on figure.)

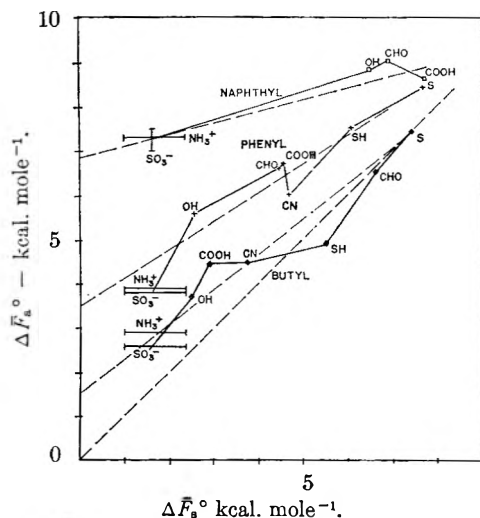


Fig. 8.— $\Delta\bar{F}_a^\circ$ at the electrocapillary maximum and $\theta = 0.25$, as a function of $\Delta\bar{F}_a^\circ$.

where $\Delta\gamma_t$ and $\Delta\gamma_e$ are the value at time t and the final value of the surface tension depression. For $\theta = kc$, the observed surface tensions change with time according to the same rate law as Γ_t .

For high values of t the product of functions in (9) can be expanded in the power series,²¹

$$e^{x^2} \operatorname{erfc}(x) = \frac{1}{\sqrt{\pi}x} \left(1 - \frac{1}{2x^2} + \frac{1.3}{(2x^2)^2} - \frac{1.3.5}{(2x^2)^3} + \dots \right) \quad (10)$$

where $x = \sqrt{Dt}/K$. For $t > 50K^2/D$, the ex-

pansion becomes $1/x\sqrt{\pi}$ to better than 1%, and (9) can be rewritten

$$t = \frac{K^2}{D\pi} \frac{1}{\left(1 - \frac{\Delta\gamma_t}{\Delta\gamma_e}\right)^2} \quad (11)$$

whence $(\tau_{ss})_{\text{Diff}} = 1.1 \times 10^3 K^2/\pi D$. $(\tau_{ss})_{\text{Diff}}$ is the time required theoretically for $\Delta\gamma_t$ to reach a value of $0.97 \Delta\gamma_e$. Thus in the initial part of an adsorption isotherm $(\tau_{ss})_{\text{Diff}}$ is independent of concentration. In Table I, $(\tau_{ss})_{\text{Diff}}$ and $(\tau_{ss})_{\text{exptl}}$ are compared. For certain substances, (e.g., dibutyl ketone), $(\tau_{ss})_{\text{Diff}}$ and $(\tau_{ss})_{\text{exptl}}$ agree. For others (e.g., α -naphthol) the $(\tau_{ss})_{\text{Diff}}$ values are greater than those observed, indicating a convection effect.²²

The consistency of $(\tau_{ss})_{\text{exptl}}$ with $(\tau_{ss})_{\text{Diff}}$ at lower coverages for the majority of the substances suggests that a surface reaction is usually not rate determining. However, a noteworthy exception is with benzaldehyde, where $(\tau_{ss})_{\text{exptl}}$ exceeds $(\tau_{ss})_{\text{Diff}}$. The time constant of the surface reaction thus indicated is about 20 sec.

Conditions for observing an activation-controlled rate process for adsorption become more favorable at higher solute concentrations where $\theta \neq kc$, and $(\tau_{ss})_{\text{Diff}}$ might be expected to decrease with increase of concentration. Under these conditions $(\tau_{ss})_{\text{Diff}}$ can be estimated only by computer calculations.²³ In the absence of these, semiquantitative conclusions drawn from measurements of time effects at high surface coverages²⁴ support the conclusions reported here for lower coverages.

(3) **Orientation of Adsorbed Species.**—Table II demonstrates that the straight chain aliphatic compounds are adsorbed with the hydrocarbon chain perpendicular to the metal. For dibutyl ketone, which has an angular structure, the observed Γ_{max} values agree with an orientation in which the plane of the molecule is perpendicular to the metal and the hydrocarbon chains form equal angles with the metal. At dibutyl sulfide the extrapolated Γ_{max} value (3.5×10^{-10} mole/cm.²) suggests an analogous orientation.

The aromatic substances with planar configurations are adsorbed with the aromatic nucleus parallel to the metal.

No observed Γ_{max} values exceed those for a monolayer.

(4) **Adsorbability as a Function of Molecular Structure.**—The dependence of adsorption upon potential for neutral molecules may be regarded in terms of a competition, controlled by electrostatic forces, between organic molecules and water²⁵ or between organic molecules and ions. The symmetrical character of the Γ -potential relations at constant solution concentration favors the former mechanism.

The shift of the e.c.m. in a positive direction (aliphatics) is consistent with a model of the adsorbed layer in which the aliphatic molecules are

(22) Another effect contributing to smaller values of $(\tau_{ss})_{\text{exptl}}$ than $(\tau_{ss})_{\text{Diff}}$ is that at sufficiently long diffusion times the concentration gradient reaches the end of the capillary so that the condition of "infinite diffusion" is no longer valid.

(23) P. Delahay and C. T. Fike, *J. Am. Chem. Soc.*, **80**, 2628 (1958).

(24) E. Blomgren, J. O'M. Bockris and C. Jesch, unpublished.

(25) J. A. V. Butler, *Proc. Roy. Soc. (London)*, **A122**, 399 (1929);

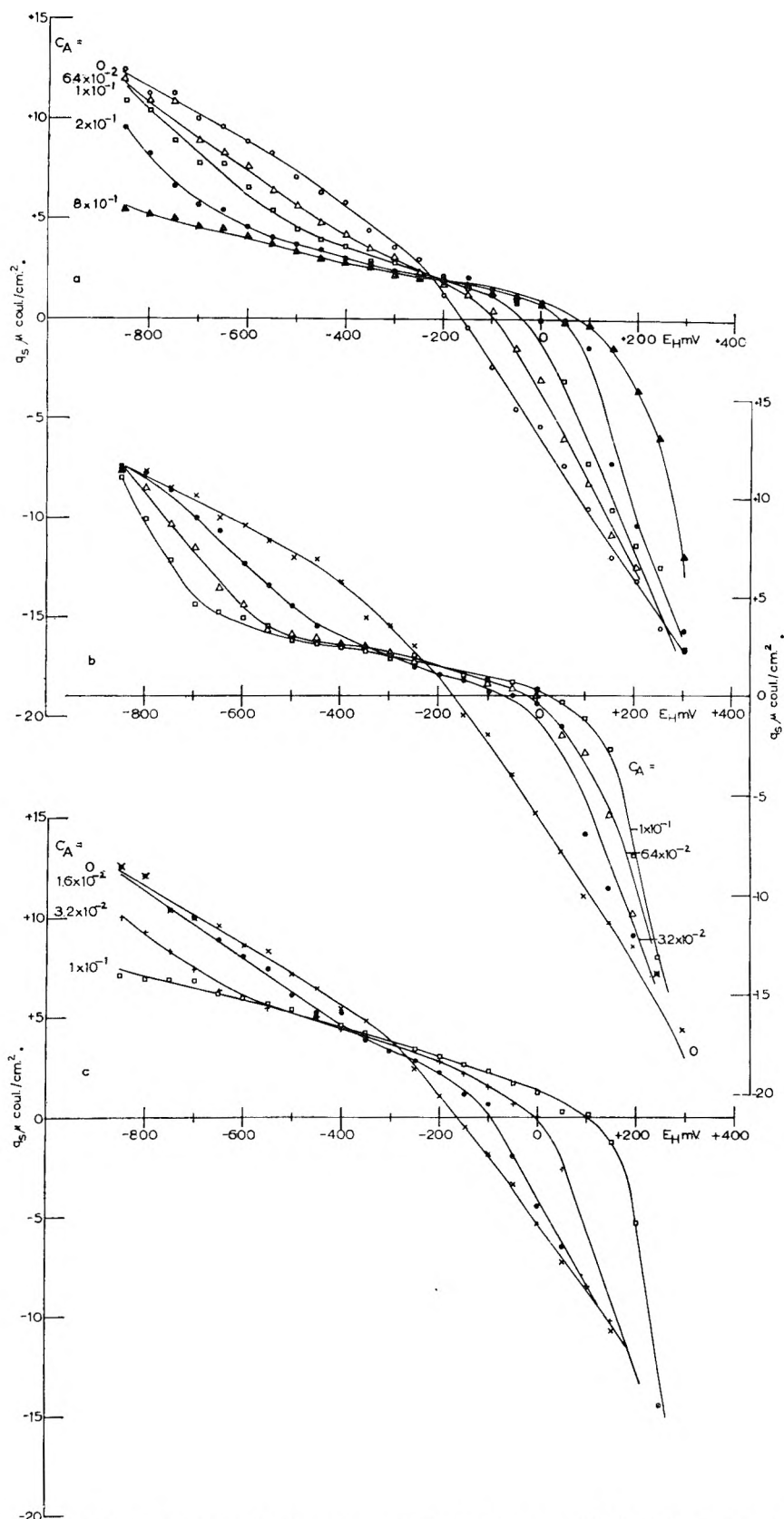


Fig. 9.— q_s as a function of E_H for constant adsorbate concentrations and $c_{\text{HCl}} = 0.1 N$: (a) *n*-butyl alcohol; (n) *n*-valeric acid; (c) *n*-valeronitrile. (C_A stated on figure.)

adsorbed with the substituent groups in the solution (since the dipole moment of the compounds examined has its positive end associated with the hydrocarbon radical, rather than with the substituent group). The shift of the e.c.m. in a negative direction

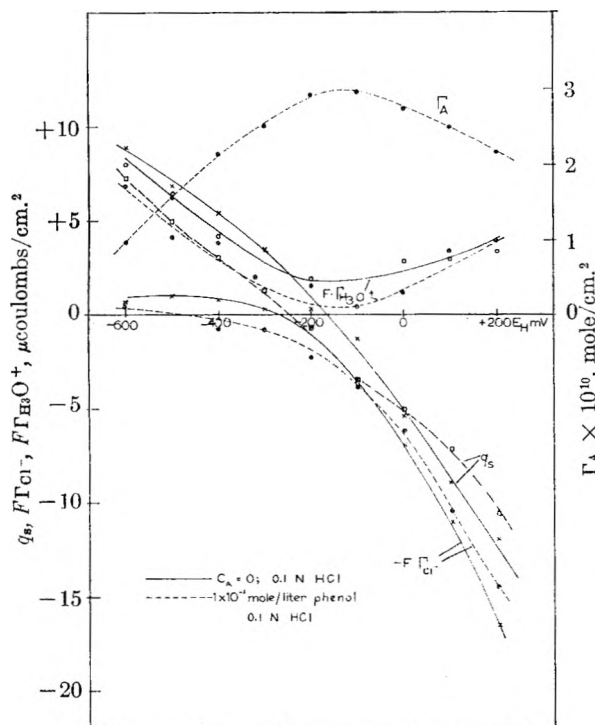


Fig. 10.—Components of charge in the double layer as a function of potential in pure 0.1 *N* HCl, and in 0.1 *N* HCl plus 0.01 *M* phenol.

(aromatics) arises from π -electron interaction with the metal (*cf.* the greater shift for naphthyl compared with phenyl compounds).²⁶

Information on the relative strengths of the adsorbate-metal and adsorbate-solvent interactions may be obtained by consideration of adsorption as a function of structure at the e.c.m. in the solution concerned. The net free energy of adsorption is defined as

$$\Delta \bar{F}_a^0 = (\bar{\mu}_A^{0,a} - \bar{\mu}_A^{0,s}) - (\bar{\mu}_{H_2O}^{0,a} - \bar{\mu}_{H_2O}^{0,s}) \quad (12)$$

where $\bar{\mu}_A^{0,a}$ and $\bar{\mu}_{H_2O}^{0,a}$ are the standard electrochemical potentials of adsorbate and water in the adsorbed state, referred to unit mole fractions on the metal surface, $\bar{\mu}_A^{0,s}$ and $\bar{\mu}_{H_2O}^{0,s}$ are the standard electrochemical potentials of adsorbate and water in solution, referred to unit mole fractions in the solution. The values of $\Delta \bar{F}_a^0$ at the electrocapillary maximum and at constant surface coverage can be taken as a measure of the inherent strength of the net adsorption forces acting on the organic molecules. Conversely, the molar free energy of dissolution, $\Delta \bar{F}_s^0$, defined as

$$\Delta \bar{F}_s^0 = \bar{\mu}_A^{0,s} - \bar{\mu}_A^{0,p} \quad (13)$$

can be taken as a measure of the strength of the forces acting between the adsorbate and the solvent. In (13), $\bar{\mu}_A^{0,p}$ is the standard electrochemical potential of the pure adsorbate in liquid or solid form. For a saturated solution

(26) Dibutyl sulfide has its maximum in $-\Delta \bar{F}_a^0$ markedly on the positive side of the e.c.m. (see Fig. 6(k)). This, together with the displacement of the e.c.m. to negative values, makes one conclude that *n*-butyl sulfide—in contrast to the other aliphatic substances examined—has its functional group to the metal and the hydrocarbon radicals in solution. (*n*-C₄H₉)₂S obeys the linear relation in Fig. 8 (which indicates a strong repelling effect of the S-group from the solution).

$$\bar{\mu}_A^{0,p} = \bar{\mu}_A^{0,s} + RT \ln (a_A^s)_x \quad (14)$$

where $(a_A^s)_x$ is the activity in mole fractions of the organic substance in solution in equilibrium with its pure form in the state stable at the given temperature. From (13) and (14)

$$\Delta \bar{F}_s^0 = -RT \ln (a_A^s)_x = -RT \ln \frac{a_A^s}{55.5} \quad (15)$$

where a_A^s is the molar concentration of the organic substance in a saturated solution.

In Fig. 8, $\Delta \bar{F}_a^0$ at the electrocapillary maximum and $\theta = 0.25$ is plotted as a function of $\Delta \bar{F}_s^0$. The points for substances with the same hydrocarbon radical fall approximately on a straight line with a slope and an intercept for $\Delta \bar{F}_s^0 = 0$ characteristic of the hydrocarbon radical. The significance of the intercepts for $\Delta \bar{F}_s^0 = 0$ is that they give the $\Delta \bar{F}_a^0$ values for hypothetical substances for which the standard chemical potential of the adsorbate in solution is equal to that of the adsorbate in the pure liquid or solid state. Thus, the intercepts give a value of $\Delta \bar{F}_a^0$ for each of the butyl, phenyl and naphthyl series which is free from the effect of differences in molar free energy between solid or liquid lattice and solution for the adsorbate entity.

An approximate value of $\bar{\mu}_{H_2O}^{0,a} - \bar{\mu}_{H_2O}^{0,s}$ involved in the expression for $\Delta \bar{F}_a^0$ may be obtained from the value of the free energy of adsorption of water at low coverages from the gas phase onto a Hg surface, which is²⁷ -6.85 kcal. mole⁻¹. Considering a molecule of water in the bulk as reference state, the standard free energy of transfer of one mole of water from the bulk of solution to the state of adsorption on Hg when no bonding to surrounding liquid water occurs is, therefore, -6.85 kcal. plus the standard free energy per mole of vaporization of liquid water, $+2.05$ kcal., *i.e.*, -4.8 kcal. mole⁻¹. The free energy change for the transfer of one mole of water from the bulk to the surface of Hg in the presence of water is this value increased by the standard free energy per mole of the formation of 2 hydrogen bonds in liquid water, *i.e.*, $-4.8 - (2 \times 0.3)$ ²⁸ = -5.4 kcal. mole⁻¹.

From this figure and the intercepts in Fig. 8, the *intrinsic* standard free energies of adsorption of butyl, phenyl and naphthyl compounds, *i.e.*, the values of $(\bar{\mu}_A^{0,a} - \bar{\mu}_A^{0,s})$ for a hypothetical compound RX of each series such that the standard electrochemical potential of the compound in the solid and liquid lattice and solution are equal, can be calculated

Radical	$(\Delta \bar{F}_a^0)_{\text{intrinsic}}$ (kcal./mole ⁻¹)
Butyl	-6.4
Phenyl	-8.9
Naphthyl	-12.4

These values represent the difference of binding energy of a compound, as defined above, on the surface in the standard state and in the solution in the standard state and are *independent of the free energy changes necessary to displace water from the electrode or the free energy change associated*

(27) C. Kemball, *Proc. Roy. Soc. (London)*, **A187**, 73 (1946).

(28) The values of about 5 kcal. mole⁻¹ represent the heat of formation of an H bond.

with adsorbate-solvent interactions.²⁹ The considerable increase in $-(\Delta\bar{F}_a^0)_{\text{intrinsic}}$ for phenyl and naphthyl radicals, compared with that for butyl, may be noted (π bond attachment).

In $\Delta\bar{F}_s^0$ (eq. 13) it is expected that $\bar{\mu}_A^{0,p}$ (equivalent) to the heat of vaporization of the pure adsorbate) changes little with substituent. This is verified by reference to standard data. Hence the major variation of $\Delta\bar{F}_s^0$ is due to the variation of $\bar{\mu}_A^{0,s}$ with the substituent groups. Furthermore, the linear variation of $\Delta\bar{F}_a^0$ (in which $(\bar{\mu}_{H_2O}^{0,a} - \bar{\mu}_{H_2O}^{0,s})$ is obviously constant) with $\Delta\bar{F}_s^0$ and the slope of the relationship between these two entities, being nearly unity for butyl compounds (Fig. 8), suggest that $\bar{\mu}_A^{0,a}$ (corresponding to the strength of the metal-adsorbate bond) is practically independent of the substituents for butyl compounds. This is consistent with an attachment of the alkyl group to the Hg, the strength of which remains essentially constant as the substituent varies. Hence, it is concluded that for butyl compounds the predominant factor which determines the change of $\Delta\bar{F}_a^0$ with substituent is the strength of the interaction between the solvent and the compound—notably that between the solvent and the functional group. Ideally, this interaction would result in a direct correspondence between solubility and adsorbability and is, as seen from Fig. 8, approximated satisfactorily by butyl compounds, *highly soluble compounds being the least adsorbable* (cf., the concept that strong adsorption is associated with low solubility).³⁰ Since the intrinsic free energies of adsorption defined above are the difference between $\bar{\mu}_A^{0,a}$ and $\bar{\mu}_A^{0,p}$, the latter of which changes little with substituent, the $(\Delta\bar{F}_a^0)_{\text{intrinsic}}$ values given above can be regarded as representing the *intrinsic free energies of adsorptions of the hydrocarbon radicals*.

For phenyl and naphthyl compounds the $\Delta\bar{F}_a^0 - \Delta\bar{F}_s^0$ slope is smaller than for butyl compounds, which indicates that at these compounds the greater part of the adsorption energy is contributed by the constant aromatic nucleus interaction with the metal and only a smaller part by adsorbate-solvent interactions.

(5) **Mechanism of the Effect of Adsorption on the Total Charge of the Interface.**—One has⁶

$$\left(\frac{\partial q_s}{\partial \mu_A}\right)_{E_H} = - \left(\frac{\partial \Gamma_A}{\partial E_H}\right)_{\mu_A} \quad (16)$$

The present results are consistent with (16) as seen from Fig. 9. In particular, the small effect of adsorption of aromatic cations on q_s is consistent with the small variation of Γ_A for these species with potential. Also, the maxima of adsorption coincide with the intersection points between the corresponding $q_s - \mu_A$ curves (the potentials of maximum adsorption can in fact often be determined more accurately from these intersection points than from the $\Gamma_A - E_H$ curves).

(29) These intrinsic free energies of adsorption are analogous to intrinsic acid strengths in which the effect of interaction of the ions with the solvent upon the degree of ionization of the acid molecule has been eliminated.

(30) Valeraldehyde has an abnormally high adsorbability. Also its solubility is abnormally low. As seen from Fig. 8, it lies on the $\Delta\bar{F}_a^0 - \Delta\bar{F}_s^0$ line, which accounts for the change of interaction with the solvent.

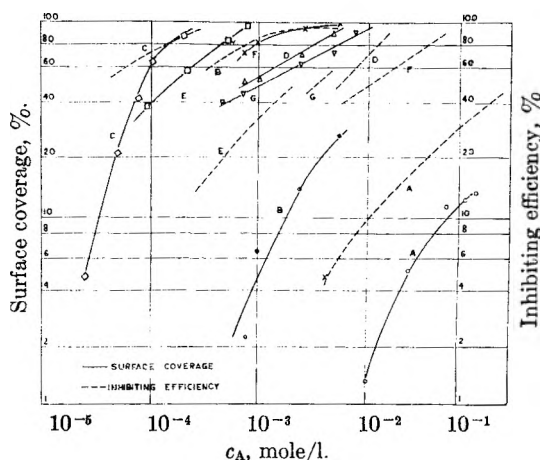


Fig. 11.—Surface coverage on Hg in 0.1 N HCl at e.c.m. and corrosion inhibiting efficiency on mild steel in 1 N H₂SO₄ as functions of concentration: (a) *n*-butylamine; (b) *n*-butyl mercaptan; (c) *n*-dibutyl sulfide; (d) benzaldehyde; (e) phenyl mercaptan; (f) β -naphthalenesulfonic acid; (g) α -naphthylamine.

The fact that q_s changes little upon adsorption of aromatic cations but greatly upon adsorption of molecules is ascribable to a mechanism by which these ions (which are adsorbed practically uniformly over the whole potential range) repel H₃O⁺ ions electrostatically from the surface over the negative branch, and attract Cl⁻ ions electrostatically on the positive branch, to an extent corresponding to the charge of the specifically adsorbed ions. Molecules do not exert similar electrostatic effects to a corresponding extent, the effect of the replacement of water by organic molecules rather depending on the change in mean thickness and dielectric constant of the Helmholtz layer following adsorption of the (larger and less polar) organic molecules. A factor contributing to the decrease in positive charge on the solution which follows aromatic molecule adsorption is that the e.c.m. is displaced towards negative values upon such adsorption. As a consequence, any potential considered on the hydrogen scale is at a more positive value with respect to the e.c.m. after adsorption than before it. The electrostatic attraction of H₃O⁺ ions is hence decreased on the negative branch, and q_s becomes less positive.

(6) **The Dependence of $\Delta\bar{F}_a^0$ upon Surface Coverage.**—The increase of $|\Delta\bar{F}_a^0|$ with θ observed for neutral aliphatic substances on the negative branch at θ up to 0.5 suggests formally that the adsorbed molecules attract one another at low coverage. This effect was allowed for in an empirical correction by Frumkin,² who added a term $2\alpha\theta RT$ (where α is a constant characteristic of the substance) to $\Delta\bar{F}_a^0$. The change in slope of the $\Delta\bar{F}_a^0 - \theta$ relation at $\theta \approx 0.5$ (see Fig. 7) indicates the range of θ within which such a correction term can be validly applied. Possible mechanisms by which an increase of $|\Delta\bar{F}_a^0|$ with θ can be understood are: (i) As adsorption increases, the water layer on the surface breaks up, the adsorption of further molecules thus becoming easier; (ii) It is possible that, at low coverages, the dipoles are not in a perpendicular position and hence

dipole-dipole attraction can occur; (iii) With increasing surface coverage dispersion interaction forces between the adsorbed molecules increase in strength. The rapid increase of $|\Delta\bar{F}_a^0|$ with θ for $\theta > 0.5$ is to be ascribed to the latter phenomenon.

On the positive branch, a decrease, rather than an increase, of $|\Delta\bar{F}_a^0|$ with θ is the regular phenomenon (see Fig. 7). This is interpretable in terms of the energy required to displace the specifically adsorbed Cl^- ions present on this branch from the surface.

The decrease of $|\Delta\bar{F}_a^0|$ with θ over practically the whole potential range with aromatic cations, observed also in the present work, is in accordance with the model already suggested.⁵

(7) **Ionic Composition of the Double Layer.**—The effect of the adsorption of phenol on $\Gamma_{\text{H}_3\text{O}^+}$ for the positive branch at HCl concentrations ≤ 1 mole l^{-1} is interpretable in terms of changes in ϕ_2 , the potential of the Gouy-Helmholtz boundary. It is concluded from results in 1, 0.1 and 0.03 *N* HCl that a surface coverage of phenol of ca. 50% causes a change of ϕ_2 in the positive direction of about 10 mv.

(8) **Mechanism of Corrosion Inhibition.**—Figure 11 compares adsorption on Hg and the corresponding inhibition on steel.^{31, 32}

The range of concentration within which the inhibition occurs coincides with that within which adsorption on mercury occurs (a factor of five in difference is already exceptional). This confirms that adsorbability is the predominant factor in inhibition. Certain deviations from the rule exist, e.g., the order of adsorbability and inhibitory effect is opposite at α -naphthylamine and β -naphthalene sulfonic acid. Hence, either adsorbability on mercury and iron for certain substances (β -naphthalene sulfonic acid) may differ by a factor of up to 10; or a specific effect of adsorbate upon the individual cathodic or anodic reactions is involved, superimposed on the degree of surface coverage effect.

The ionic composition of the double layer in the presence of phenol (*vide supra*) shows that adsorption reduces the H_3O^+ concentration at the outer Helmholtz plane. This factor is expected to decrease the rate of the cathodic partial reaction in

(31) H. H. Uhlig, "Corrosion Handbook," John Wiley and Sons, Inc., New York, N. Y., 1948.

(32) G. G. Eldredge, Thesis, University of Minnesota, 1940.

corrosion, but with neutral organic substances it is concluded to play only a minor role. For organic cations, the effect of adsorption on ϕ_2 is greater.³³

The parallel increase of adsorption on Hg and inhibition of iron corrosion with increasing concentration does not support a mechanism³⁴ in which inhibition is related to attachment of inhibitor molecules to "active centers" on the surface.

Thus (1): Inhibition tends to a maximum upon increase of the degree of conjugate linkage in the compound. (2): For a given degree of conjugate linkage, CN, SH and S substituents tend to give the best inhibitor; OH, NH_3^+ and SO_3^- substituents the least. (3): Inhibiting effects are higher for substances which have smaller free energies of dissolution. (4): The relation between molecular structure and the dependence of adsorption on potential must be taken into account. Certain structures, e.g., primary aliphatic alcohols, are strongly adsorbed at the potential of zero charge on the metal but undergo desorption at 0.1 volts or more away from this.

A molecule with a structure favorable for general purpose inhibition is one which on the negative side of the point of zero charge is attracted by virtue of the positive charge on the substituent; and on the positive side (where charge would normally cause desorption) still is attracted to the metal by π bonding, which increases with positive charge. Such a molecule will inhibit at all potentials except extreme negative or positive potentials. A typical substance exhibiting this lack of potential dependence is a highly conjugated cation, e.g., a phenyl group with a substituent which, in the solution concerned, forms a cation.

Acknowledgments.—The authors are grateful to Dr. W. J. Sweeney of the Esso Research and Engineering Company for sponsorship of this work; and to Dr. H. Northup, and Messrs. R. Maass and R. Merrick of the same company for valuable discussions of corrosion inhibition. They are indebted also to Dr. Halina Wroblowa for discussions and to Mr. K. Müller for confirmatory calculations.

(33) This effect may play a role, e.g., in the reversed order of adsorbability and inhibiting effect at α -naphthylamine and β -naphthalene sulfonic acid.

(34) N. Hackerman and A. C. Makrides, *Ind. Eng. Chem.*, **46**, 523 (1954); N. Hackerman, *Trans. N. Y. Acad. Sci.*, [2] **17**, 7 (1954).

EFFECT OF CRYSTAL ORIENTATION ON OXIDATION RATES OF SILICON IN HIGH PRESSURE STEAM

BY JOSEPH R. LIGENZA

Bell Telephone Laboratories, Inc., Murray Hill, New Jersey

Received May 8, 1961

Silicon crystals oriented in the (110), (311) and (111) planes were oxidized in high pressure steam at temperatures from 773 to 1073°K. and steam pressures from 40 to 150 atm. to determine the role played by the crystal orientation on high pressure steam oxidation rates. For any temperature within the range studied, the oxidation rates are in the order $v_{110} > v_{311} > v_{111}$. The values of the pre-exponential constant k and the apparent activation energy ΔE_a in the observed rate $v = k(P/T)e^{-\Delta E_a/RT}$ were found to depend on the crystal face. In the order (110):(311):(111), the relative k values are 1.00:1.7:1.3 and the apparent activation energies are 28.4 ± 0.5 , 29.9 ± 0.7 and 29.8 ± 0.7 kcal./mole. The oxidation reaction in the total kinetic scheme is postulated to take place at the silica-silicon interface and to be between a silicon bond and a water molecule which had migrated from an interstitial site in the silica film. This model predicts that k will be proportional to N , the number of bonds per cm.² that in any instant of time are available to react with a water molecule. It also enables one to calculate the value of N for any orientation. The relative order of N in the sequence given above is 1.000:1.707:1.227, which is in good agreement with the experimental k order. The model also predicts that the activation energies should be in the order (110) < (311) < (111), which agrees fairly well with the measured activation energies.

Introduction

While the kinetics of oxidation of silicon by high pressure steam¹ and the oxidation mechanism^{2,3} have been described previously, no work had been done to determine the oxidation reaction. It is the purpose of this paper to identify the reacting species involved in the oxidation reaction from a study of the role played by the silicon crystal orientation in oxidation rates. The earlier experiments demonstrated that the oxidation kinetics were linear and that the rate was proportional to the steam pressure.¹ Further, the rate-controlling step in the oxidation process occurred at the interface between the silicon and its oxide² and involved interstitial water molecules in the silica film³ and silicon at the interface. While such an oxidation process is expected to exhibit an orientation dependency and one has been observed accidentally,¹ no deliberate study has been made previously.

Silicon crystals oriented in the (110), (311) and (111) planes were used. The crystals were oxidized in gold-lined metal bombs within the ranges of temperature and pressure where the linear growth law holds. At any temperature within the range studied, the oxidation rates are in the order $v_{110} > v_{311} > v_{111}$, and the largest difference observed was 50%. An examination of the rates showed that the activation energies for the (311) and (111) orientations were identical within the experimental error and larger than that of the (110) orientation. The ratios of the pre-exponential constants in the order (110):(311):(111) are 1.00:1.71:1.3.

The orientation effect can be explained by a reaction between a water molecule from the silica phase with a silicon bond at the silica-silicon interface to form a silicon-oxygen bridge and a hydrogen molecule. Although no correlation can be made between the pre-exponential constants and the silicon bond densities, a very good correlation has been found between the pre-exponential constant and the surface density of silicon bonds at the interface which are available to the water molecules for the different planes studied. This model

also enables one, in a qualitative sense, to explain the relative order of the activation energies, and it is in general agreement with the kinetic laws observed.

Experimental Methods

The bombs, furnace and experimental procedures used in performing the high pressure steam oxidations and the gravimetric techniques used to determine the oxide film thicknesses are the same as those described in the earlier study. Specimens, oriented in the (110), (311) and (111) directions, for oxidation were cut from high purity >50Ω-cm. silicon single crystals in the form of wafers with a geometric area of one cm.². The wafers were mirror polished and before oxidation were lightly etched in a 10:1 HNO₃-HF mixture. Oxide film thicknesses were calculated from weight measurements of the grown film with a precision of ± 50 Å. The oxide film density was assumed to be 2.20 g./cm.³.

Experiments and Results

Since the oxidations were done in a range of pressures and temperatures that are known to yield oxidation rates independent of time and directly proportional to the steam pressure,¹ the oxidation rates in the present experiments were calculated by dividing the measured oxide thickness after an oxidation by the time for oxidation. Three separate experiments were done for every orientation and temperature using a different crystal in each case. Oxidation times were chosen to be sufficiently long to yield film thicknesses of about 1500 Å. at the lowest temperature to 10,000 Å. at the highest. Temperatures were maintained constant to $\pm 1^\circ$ K. in all the experiments. The oxidation rates are expressed in the form $1/P \times dx/dt = K$ and the results of these experiments are given in Table I.

The general result is that the silicon orientation influences the oxidation rate, the relative order in rates being (110) > (311) > (111) for the temperature range investigated. If the average values of K for the orientations and temperatures in Table I are compared against each other as in Table II, a further significant trend in the data is observed. The ratio $\bar{K}_{111}/\bar{K}_{311}$ remains approximately constant with a mean value of 0.80 throughout the temperature range investigated, while the ratios of the average constants \bar{K}_{311} and \bar{K}_{111} to \bar{K}_{110} exhibit a tendency to increase in value with increasing temperatures. This means that the (311) and (111) planes oxidize

(1) J. R. Ligenza, *J. Electrochem. Soc.*, in press.

(2) J. R. Ligenza and W. G. Spitzer, *J. Phys. Chem. Solids*, **14**, 131 (1960).

(3) W. G. Spitzer and J. R. Ligenza, *ibid.*, **17**, 196 (1961).

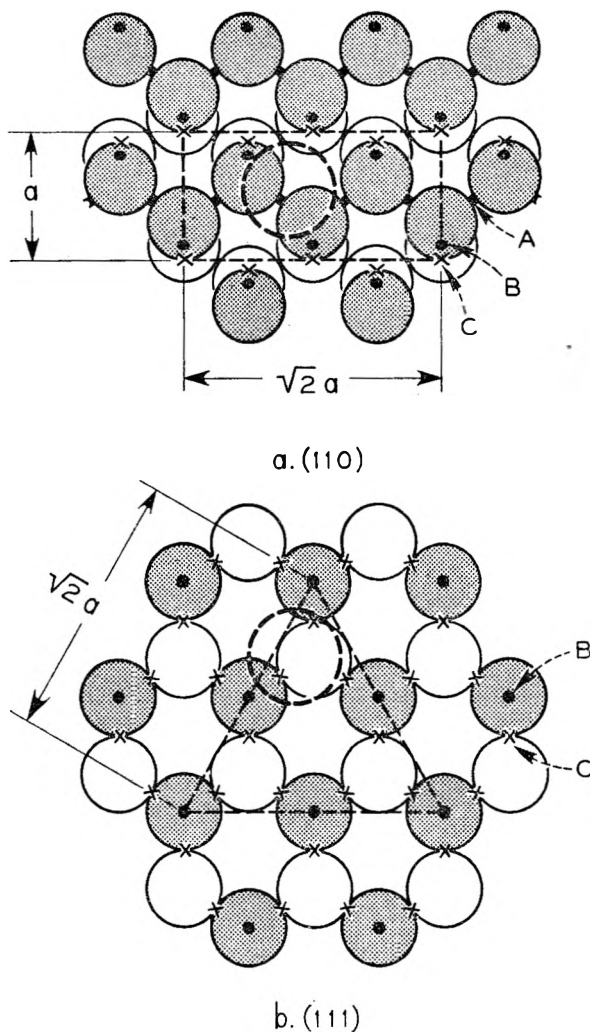


Fig. 1.—(a) A silica-silicon interface in the (110) plane. (b) A silica-silicon interface in the (111) plane. In both (a) and (b) the dimensions of the plane through the unit cell are indicated by straight dashed lines. The lattice parameter a is 5.431×10^{-8} cm.

TABLE I
SILICON OXIDATION RATES IN HIGH PRESSURE STEAM FOR
THE (110), (311) AND (111) PLANES

T , °K.	P , atm.	K_{110}	K_{311} ($\text{\AA} \cdot \text{min.}^{-1} \text{atm.}^{-1}$)	K_{111}
773	150	0.0495	0.0258	0.0217
		.0428	.0267	.0236
		.0381	.0305	.0132
823	120	.1058	.0646	...
		.1073	.0846	...
		.0992	.0934	...
873	100	.379	.228	.231
		.353	.243	.1937
		.375	.257	.2005
923	100	.925	.519	.472
		.738	.500	.448
		.750	.586	.484
973	75	1.781	1.194	0.990
		1.508	1.470	1.123
		1.474	1.481	1.077
1073	40	5.15	5.06	4.41
		5.85	4.44	3.89
		2.94

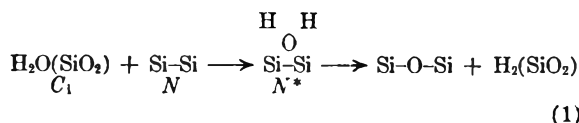
with the same activation energy and the activation energy for the (110) plane is smaller than that of the other two.

TABLE II
RELATIVE VALUES OF THE AVERAGED RATE CONSTANTS \bar{K}

T , °K.	$\bar{K}_{111}/\bar{K}_{110}$	$\bar{K}_{311}/\bar{K}_{110}$	$\bar{K}_{311}/\bar{K}_{111}$
773	0.63	0.45	0.71
823	.78
873	.66	.56	.86
923	.66	.58	.88
973	.87	.67	.77
1073	.86	.68	.78

Discussion

In a previous study of the oxidation mechanism, it was established that the rate-controlling step in the oxidation process occurred at the phase boundary between the silicon and its oxide.² It also was shown that an oxygen bearing species derived from the steam phase entered into the silica film at a rate sufficiently large compared to the oxidation rate to enable it to come to equilibrium with the gas phase. Later studies of the exchange of oxygen between silica and high pressure steam demonstrated that the oxygen bearing species was an interstitial water molecule.³ Perhaps the simplest model one can use for the oxidation reaction is a direct reaction between interstitial water molecules in the silica phase and silicon bonds at the silica-silicon interface. Silicon bonds are expected to be the reaction sites, because the final product, the Si-O-Si bridge, would appear to be formed most easily when the water molecule, prior to reaction, is in a position between the two silicon atoms with which it will eventually bond. The reaction is



where C_i is the concentration of water in the silica film in molecules/cm.³, N is the concentration of reaction sites in sites/cm.² and N^* is the concentration of the activated complex formed by the water molecule and the silicon bond. The hydrogen molecule is assumed to form at a rate equal to the oxidation rate and subsequently to diffuse rapidly away from the interface.

From the nature of the reaction in equation 1, the interface is pictured to be one where all the silicons at the interface are partially bonded to silicons in the silicon phase and to oxide ions in the silica structure. Oxidation occurs when interstitial water molecules in the silica impinge on a silicon bond in the interface layer with the necessary energy. The oxidation rate is

$$v(\text{molecules/cm.}^2\text{-sec.}) = kC_i N e^{-\Delta E/RT} \quad (2)$$

where k is the rate constant for oxidation and ΔE is the activation energy for oxidation. The water concentration in the oxide film is assumed to obey Henry's Law. Then

$$C_i = \frac{PN_0}{RT} e^{\Delta S/R} e^{-\Delta H/RT}$$

and C is directly proportional to the steam pressure, P . Here N_0 is Avogadro's number, ΔS and ΔH are the entropy and enthalpy of solution of water in the oxide film, respectively. The final expression for the oxidation rate is

$$v = \Omega \frac{dx}{dt} = k \frac{N_0 e^{\Delta S/R}}{RT} PN e^{-(\Delta H + \Delta E)/RT} \quad (3)$$

where Ω is a conversion factor of magnitude 3.637×10^{12} to convert dx/dt ($\text{\AA}/\text{min.}$) to ($\text{molecules}/\text{cm}^2\text{-sec.}$). The oxidation rate is then constant at constant temperature and pressure, directly proportional to the steam pressure and proportional to N , the concentration of sites for reaction. Since N will depend on the silicon orientation, the rate will be sensitive to the silicon orientation.

At first sight, N might be expected to be the silicon bond concentration (twice the surface atom concentration) since each bond must eventually react with a water molecule. However, all of the surface silicon bonds are generally not available as reaction sites for water molecules in any given instant of time. The silicon bond is directional and so its availability as a site, in any given instant, will depend on its angle relative to the surface plane, on the positions of adjacent silicon atoms, and on the dimensions of the water molecule. If the water molecule was very small when compared to a silicon atom, all the bonds in the surface plane would be available to it, at any time. It is, however, of such a size that when reacting with some angled bonds, it will screen adjacent bonds from other molecules during the time it takes to react. In other cases it will not be able to reach a surface bond because of the positions of adjacent silicon atoms until enough oxidation has taken place in its vicinity on the more easily reached bonds to expose the bond to reaction. N then will be proportional to the number of bonds per cm^2 that in any given instant of time are available to reaction with a water molecule. This number is difficult to calculate but can be determined from a scale model molecule and crystal set. As an illustration of the method used to determine N , the reader is referred to Fig. 1 where one possible configuration each of the (110) and (111) interface planes is shown. The shaded circles are atoms in the interface bonded to oxygens in the silica structure above by bonds B and to silicon atoms, the unshaded circles, in the silicon lattice by bonds C. The bond A is a silicon bond parallel to the surface plane between two interface atoms. The dashed circle in Fig. 1a represents a water molecule in position over a bond A in the (110) plane. One can place only four water molecules within the (110) plane of a unit cell of area $\sqrt{2} a^2 \text{ cm}^2$, each molecule being in position over a bond A. Because of the position of interfacial atoms in the adjacent row, an angled bond C cannot be reached by a water molecule until the A bonds in its immediate vicinity have reacted. In Fig. 1b, the water molecule is in a position on a (111) interface plane to react with a C bond. The two adjacent C bonds are screened by it from other water molecules. Thus at any instant of time one can place three water molecules over three bonds in the (111) plane of the unit cell of an area $1/2 \sqrt{3}$

$a^2 \text{ cm}^2$. Values of N for the three orientations studied and other calculations pertinent to the discussion are summarized in Table III.

TABLE III

PROPERTIES OF FOUR SILICON CRYSTAL PLANES
The lattice parameter is $a = 5.431 \times 10^{-8} \text{ cm.}$

Orientation	Plane area of unit cell (cm^2)	Si atoms in area	Si bonds in area	Bonds available to water in area
(110)	$\sqrt{2} a^2$	4	8	4
(311)	$1/8 \sqrt{11} a^2$	1.5	3.0	2
(111)	$1/2 \sqrt{3} a^2$	2	4	3
(100)	a^2	2	4	2

	Bonds/ cm^2	Bond density relative to (110)	Available bonds/ cm^2 , N	N relative to (110)
(110)	19.18×10^{14}	1.000	9.59×10^{14}	1.000
(311)	24.54×10^{14}	1.280	16.36×10^{14}	1.707
(111)	15.68×10^{14}	0.817	11.76×10^{14}	1.227
(100)	13.55×10^{14}	0.707	6.77×10^{14}	0.707

The activation energy also is expected to depend on the silicon orientation. Bonds parallel to the surface are expected to react most readily and those at an angle to the surface plane will react less easily because of a steric hindrance presented by the positions of the silicon atoms in the neighborhood of the bond. That is to say, the ease of formation of the activated complex between the water molecule and a silicon bond depends on the relative positioning between the two. The parallel bonds have the most favorable position for the formation of the activated complex and require the least energy to form, *i.e.*, the smallest activation energy. An examination of the surface models for the four planes listed in Table III reveals that four of the eight bonds in the (110) plane and one of the three bonds in the (311) plane are parallel bonds and that none are parallel in the (111) and (100) planes. Furthermore, the bonds in the (100) plane are at a larger angle to the surface plane than those of the (111) plane. On this basis alone, we might expect the activation energies to follow the order $\Delta E_{100} > \Delta E_{111} > \Delta E_{3,1} > \Delta E_{110}$.

To check the predictions, the oxidation rates in Table I are analyzed by the method of least squares in the manner suggested by equation 3 to obtain the pre-exponential constant $kN_0 e^{\Delta S/R}$ and the apparent activation energy $\Delta E_a = \Delta H + \Delta E$.

The results of the least square analysis are given in Table IV.

TABLE IV

PRE-EXPONENTIAL CONSTANTS AND APPARENT ACTIVATION ENERGIES FOR THE OXIDATION OF THE (110), (311) AND (111) SILICON CRYSTAL PLANES IN HIGH PRESSURE STEAM

Orientation	$\Delta H + \Delta E$ (kcal./mole)	$\frac{kN_0 e^{\Delta S/R}}{R}$ (molecule $^\circ\text{K. cm}^{-2}$ sec. $^{-1}$ atm. $^{-1}$)	Relative pre-exponential constant order
(110)	28.4 ± 0.5	$1.2 \pm 0.4 \times 10^{22}$	1.00
(311)	$29.9 \pm .7$	$2.1 \pm 0.8 \times 10^{22}$	1.7
(111)	$29.8 \pm .7$	$1.6 \pm 0.7 \times 10^{22}$	1.3

The data in Table IV bear out the findings of the simpler analysis presented in Table II, where the

activation energies for the (311) and (111) planes were found to be identical and larger than that of the (110) plane.

The assumption that the oxidation rate is the rate of reaction between water molecules and silicon bonds at the silica-silicon interface is substantiated by the data in Table IV. The calculated order for the pre-exponential constants in the series (110):(311):(111) is 1.000:1.707:1.227 (Table III) and the experimental order is 1.00:1.7:1.3 (Table IV). Although the argument for the activation energies is greatly oversimplified, the predicted order (111) > (311) > (110) is close to the experimental order (111) = (311) > (110).

The calculation in Table III shows that N for the (100) plane is the smallest of the four planes listed and would thereby have the smallest pre-exponential constant. The analysis for the activation energy given above predicts that this plane would also have the largest activation energy. It is expected therefore that the oxidation rate of the (100) plane would be smaller than those of the (111), (311) and (110) planes.

Acknowledgments.—The author wishes to express his appreciation to Miss R. E. Cox for carrying out the oxidations, to L. E. Howarth for providing the oriented wafers, and to W. G. Spitzer for his interest and helpful discussions.

THE HEAT OF FORMATION OF THE HYPOBROMITE ION¹

BY J. E. McDONALD² AND J. W. COBBLE

Department of Chemistry, Purdue University, Lafayette, Indiana

Received May 8, 1961

The heat of formation of the hypobromite ion has been determined by measurement of the heat of hydrolysis of bromine in alkaline solutions at 25°. The value so obtained was $\Delta H_f^\circ = -23.05 \pm 0.2$ kcal./mole. With a free energy of $\Delta F_f^\circ = -8.2$ kcal./mole, the partial molal entropy has been determined to be 8.5 ± 0.7 gbs./mole at 25°.

Introduction

As a continuation of the work on the hypohalite ions as chemical calorimetric oxidants, the heat of formation of aqueous hypobromite has been redetermined. All previously listed values^{3,4} have been based upon the older work of Thomsen⁵ and Berthelot.⁶ As a result of certain inconsistencies noted between these thermochemical data and more recent work,⁷ it was of interest to fix the thermodynamic functions of hypobromite more precisely.

Experimental

The calorimeter and associated equipment have been described in detail elsewhere.⁸ All heats of reaction were carried out at $25.0 \pm 0.05^\circ$.

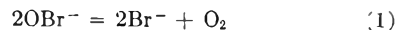
Chemicals.—The bromine was obtained from the Great Lakes Oil Company and certified to be 99.9%. Analysis for water showed less than 50 p.p.m.

Sodium hydroxide solutions were prepared by dilution of a saturated stock solution containing J. T. Bakers Analyzed Reagent with distilled water.

Procedure.—The experimental procedure was essentially the same as that described previously⁸ and involved releasing known amounts of bromine sealed in small glass bulbs into various concentrations of sodium hydroxide solu-

tion. The hypobromite formed was determined immediately on removal from the calorimeter by addition of excess solid KI and titration of the I_3^- so formed with standard thiosulfate.

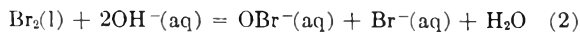
Bromate formed by the disproportionation of the hypobromite does not react with the iodide under the conditions of this titration; therefore a correction must be made for this loss of hypobromite. The rate of disproportionation of hypobromite under the conditions of the calorimetric experiments has been reported to be slow.⁹ This fact was verified by a set of separate experiments which established the rate of this reaction under the experimental conditions existing in this research. The magnitude of this correction varied between 1 and 3% of the number of milliequivalents of OBr^- formed. No other decomposition reaction was considered since the disproportionation has been found to be the predominate mode of hypobromite decomposition. The alternate reaction



has been reported to account for less than 2% of the total decomposition under the conditions of the present experiments.⁹

Results

The stoichiometry of the reaction



was checked by comparison of the amount of bromine used to the quantity of hypobromite formed. The results of the hydrolysis experiments are summarized in Table I.

Using the extrapolated heat of reaction, $\Delta H = -10.35 \pm 0.20$ kcal./mole, and auxiliary thermodynamic data,^{10,11} the heat of formation of $OBr^-(aq)$ is calculated to be $\Delta H_f^\circ = -23.05 \pm 0.20$ kcal./mole. This result compares favorably to that obtained by King and Cobble⁷ in the oxidation of bromide ion by aqueous hypochlorite.

(9) V. P. Kulkarni and G. M. Nabar, *J. Sci. Ind. Research (India)*, **15B**, 708 (1956).

(10) "Selected Values of Chemical Thermodynamic Properties," Circular 500, U. S. Bureau of Standards, Washington, D. C., 1952.

(11) W. M. Latimer, "Oxidation-Reduction Potentials," 2nd Ed., Prentice-Hall, Inc., New York, N. Y., 1952.

(1) This research was supported by the United States Air Force through the Air Force Office of Scientific Research of the Air Research and Development Command under Contract AF 18(600)-1525. Reproduction in whole or part is permitted for any purpose of the United States Government.

(2) From the Ph.D. thesis of J. E. McDonald, Purdue University, 1961; Dow Chemical Fellow, 1959-1960.

(3) "International Critical Tables," Vol. 5, McGraw-Hill Book Co., New York, N. Y., 1933, p. 169.

(4) F. R. Bichowsky and F. D. Rossini, "Thermochemistry of the Chemical Substances," Reinhold Publ. Corp., New York, N. Y., 1936, p. 188.

(5) J. Thomsen, "Thermochemische Untersuchungen," Barth, Leipzig, 1882-1886.

(6) M. Berthelot, *Ann. chim. phys.*, **7**, 413 (1886).

(7) J. P. King and J. W. Cobble, *J. Am. Chem. Soc.*, **82**, 2111 (1960).

(8) J. E. McDonald, J. P. King and J. W. Cobble, *J. Phys. Chem.*, **64**, 1345 (1960).

TABLE I

THE HEAT OF HYDROLYSIS OF BROMINE IN SODIUM HYDROXIDE SOLUTIONS AT 25°

Run no.	NaOH (N)	OBr ⁻ formed (meq.)	Heat evolved (cal.)	-ΔH (kcal./mole)
II	0.10	3.7500	19.9650	10.648
VI	.10	1.8052	9.9340	11.006
VII	.10	1.8862	10.2500	10.868
XV	.10	1.8400	10.1130	10.992
		Av. value		10.879 ± 0.084 ^a
III	0.052	1.8666	9.9485	10.660
IV	.052	1.9009	10.0140	10.536
V	.052	1.8662	9.9528	10.666
XVIII	.052	1.9394	9.9550	10.266
		Av. value		10.532 ± 0.094 ^a
XVI	0.032	1.9147	10.3370	10.798
XVII	0.032	1.9586	10.3610	10.392
		Av. value		10.595 ± 0.203 ^a
IX	0.025	1.8765	9.5470	10.176
XIII	.025	1.8810	9.3090	9.898
XIV	.025	1.8558	10.2180	11.012
		Av. value		10.362 ± 0.335 ^a

Extrapolated value at infinite dilution 10.35 ± 0.20^b^a Standard deviation. ^b Probable error.

One also can compare the value obtained in the present work to that calculated from the data of Thomsen.⁵ The ΔH_f^0 of NaOBr(aq) is given as -79.1 kcal./mole. Subtracting the ΔH_f^0 for Na⁺(aq) one obtains $\Delta H_f^0 = -21.8$ kcal./mole for the

hypobromite. No limits of error are available for this value.

The observed value enables the calculation of several thermochemical quantities which have not been available previously. These are listed in Table II along with the corresponding ones for hypochlorite, which are included for comparison.

TABLE II

THERMOCHEMICAL FUNCTIONS OF THE HYPOHALITES AT 25°

	ΔH_f^0 (kcal./mole)	ΔF_f^0 (kcal./mole)	S^0 (gbs./mole)
OCl ⁻	-26.2	-8.86	8.3
HOCl	-29.65	-19.04	30.9
OBr ⁻	-23.05	-8.2	8.5
HOBr	-29.85	-19.9	25.1

The values for hypobromous acid were obtained by combination of the present data with that of Kelly and Tartar¹² on the heat and free energy of ionization of HOBr, and that of Liebhafsky¹³ on the free energy of hydrolysis of bromine in water.

The listed heat of formation of HOBr is not in agreement with that given in Bichowsky and Rosini,⁴ ($\Delta H_f^0 = -25.2$ kcal./mole), which was in turn based on the older data of Thomsen and on the assumption that the heat of ionization of HOBr was equal to that of HOCl.

The hypochlorite values were calculated from the data of Connick and Chia¹⁴ and that of the authors.⁸

(12) C. M. Kelly and H. V. Tartar, *J. Am. Chem. Soc.*, **78**, 5752 (1956).

(13) H. A. Liebhafsky, *ibid.*, **56**, 1500 (1934).

(14) R. E. Connick and Yuan-tsan Chia, *ibid.*, **81**, 1280 (1959).

A THEORETICAL TREATMENT OF THE SOLUBILITY OF POLYVALENT AMPHOLYTES BINDING OTHER MOLECULES¹

BY FRED M. SNELL AND ESTHER B. NIELSEN

Department of Biophysics, University of Buffalo, Buffalo 14, N. Y.

Received May 3, 1961

The theory of Linderström-Lang describing the solubility of polyvalent ampholytes as a function of pH (proton association) is extended to include interactions of association with one or more other molecular species. Assuming a solution phase saturated with respect to a crystalline phase composed of a single electrically neutral species type of polyvalent ampholyte, the two phase system is univariant at constant temperature, pressure and hydrogen ion activity with respect to variations in the activity of another associating species. The occurrence of discrete phase changes reflecting a change in crystal type is in general expected. The system is invariant at these points and a break in the solubility curves with discontinuity in slope is predicted. Since the average number of molecules of an associating species bound per molecule of polyvalent ampholyte is shown to be related to the slope of the solubility curve, the theory suggests a new method for the study of such interactions.

Introduction

Linderström-Lang² has developed a general theory describing the solubility of a polyvalent ampholyte as a function of pH about its isoelectric point. He introduced in his theory the interaction of the ampholyte with a small ion at one site in an

attempt to rationalize a discrepancy between theory and experiment when the theory was applied in an estimation of the molecular weight of β -lactoglobulin, utilizing the solubility data of Grönwall.³ The possibility of extending this theory to a more general case suggested itself, and is herein developed. The results suggest a new method for the study of interactions between polyvalent ampholytes and other molecules. Such interactions have received considerable attention by Bjerrum,⁴

(1) This investigation was supported by a Public Health Service research grant #RG-6730 and a training grant #2G-718 from the Division of General Medical Sciences, Public Health Service.

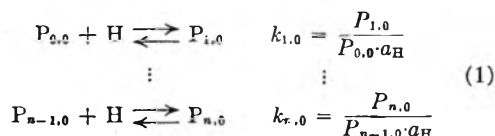
(2) (a) K. Linderström-Lang, *Arch. Biochem.*, **11**, 191 (1946).
(b) K. Linderström-Lang and S. O. Nielsen, "Acid-Base Equilibria of Proteins," in "Electrophoresis," (Milan Bier, ed.) Academic Press, New York, N. Y., 1959, Chap. 2.

(3) A. Grönwall, *Compt. rend. trav. lab. Carlsberg, Ser. chim.*, **24**, 185 (1942).

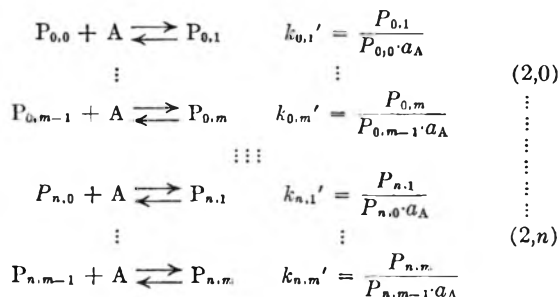
Scatchard,⁵ Klotz⁶ and Gurd.⁷

Theory

Consider a solution of a polyvalent electrolyte which aside from other possible interactions is conceived to associate in particular with protons and one other molecular species. For definiteness this other species may be thought of as some small molecule or ion such as a metal. It will be evident that the treatment to follow may be extended to multi-species associations, but for notational simplicity the theory will be developed for the more limited system described. The independent equations describing the multiple equilibria may be written as



These n equations describe the association of protons with those species of polyampholyte not binding species A.



These $m(n+1)$ equations describe the association of species A with the various species binding i protons. P_{ij} denotes the activity of that species of polyvalent ampholyte, (i), associated with i protons, H, and j other molecules or ions, A. a_H and a_A denote the hydrogen ion activity and the activity of A, respectively. The k_{ij} 's are the thermodynamic association constants. n and m are the total number of binding sites for H and A, respectively, and the individual sites may or may not coincide. In these equations no distinction is made regarding the distribution of either protons or other molecules in their binding to one or more of the several possible sites whose energies of interaction are identical. Equations (1), (2,0) . . . (2, n) together with

$$P_t' = \sum_i^n \sum_j^m P_{ij}' \quad (3)$$

comprise a deterministic set of $(n+1)(m+1)$ equations in the $(n+1)(m+1)$ variables P_{ij} , if $P_{ij}' = P_{ij}$, where the prime denotes a concentration rather than an activity. P_t' denotes the total polyvalent ampholyte concentration. It will be

(4) J. Bjerrum, "Metal Ammine Formation in Aqueous Solution," P. Haase and Son, Copenhagen, 1941.

(5) G. Scatchard, W. L. Hughes, F. R. N. Gurd and P. E. Wilcox, in "Chemical Specificity in Biological Interactions," (F. R. N. Gurd, ed.), Academic Press, New York, N. Y., 1954, Chap. IX.

(6) I. M. Klotz, in "The Proteins" (H. Neurath and K. Bailey, eds.), Academic Press, New York, N. Y., 1953, Vol. I, Part B, p. 727 ff.

(7) F. R. N. Gurd and P. E. Wilcox, "Advances in Protein Chemistry," Vol. XI, Academic Press, New York, N. Y., 1956, p. 311 ff.

assumed that the usual considerations regarding the activity coefficients⁸ may be applied and may for purposes of convenience be incorporated in the thermodynamic constants to give apparent constants without change in notation. Thus the prime notation in equation 3 may be dropped. The equations may be solved for the P_{ij} 's in terms of the k_{ij} 's, a_H , a_A and P_t .

$$P_{ij} = \frac{P_t K_{i0} a_H^i K_{ij}' a_A^j}{\sum_i^n \sum_j^m K_{i0} a_H^i K_{ij}' a_A^j} \quad (4)$$

where

$$K_{i0} \equiv \prod_{r=0}^i k_{r,0} \quad (i = 0, 1, \dots, n) \quad (5)$$

$$K_{00} \equiv 1$$

and where

$$K_{ij}' \equiv \prod_{s=0}^j k_{i,s}' \quad \left\{ \begin{array}{l} i = 0, 1, \dots, n \\ j = 0, 1, \dots, m \end{array} \right\} \quad (6)$$

$$K_{i0}' \equiv 1 \quad (i = 0, 1, \dots, n)$$

Consider now that the solution of polyvalent ampholyte is in saturation equilibrium with one of its particular crystalline entities. It is assumed that the crystal is composed of only one electrically neutral species type, that is, no solid solution phase is allowed. A particular species bearing zero net charge may be designated $(q-zr_s, r_s)$, where r_s refers to the number of molecules or ions, A, of valence z (z includes sign) bound per molecule of P in the crystalline phase and q to the number of protons bound to yield a net charge of zero when $r_s = 0$. As long as the dissolved ampholyte remains in equilibrium with a crystal of type $(q-zr_s, r_s)$ the chemical potential of the ampholyte is fixed. Such a system is composed of four components and two phases, and thus at constant temperature and pressure is bivalent, and

$$P_t = P_t(a_H, a_A) \quad (T, p = \text{constant}) \quad (7)$$

and

$$d \ln P_t = \left(\frac{\partial \ln P_t}{\partial \ln a_H} \right)_{T,p,a_A} \Delta \ln a_H + \left(\frac{\partial \ln P_t}{\partial \ln a_A} \right)_{T,p,a_A} \Delta \ln a_A \quad (8)$$

The coefficients of (8) may be obtained from (4) remembering that the left-hand member, written for the crystalline species, $(q-zr_s, r_s)$, is a constant. It follows that

$$d \ln P_t = [\bar{i} - (q - zr_s)] d \ln a_H + (j - r_s) d \ln a_A \quad (9)$$

with the usual definitions

$$\bar{i} \equiv \frac{\sum_i^n \sum_j^m i K_{i0} a_H^i K_{ij}' a_A^j}{\sum_i^n \sum_j^m K_{i0} a_H^i K_{ij}' a_A^j} \quad (10)$$

and

$$j \equiv \frac{\sum_i^n \sum_j^m j K_{i0} a_H^i K_{ij}' a_A^j}{\sum_i^n \sum_j^m K_{i0} a_H^i K_{ij}' a_A^j} \quad (11)$$

The system under consideration is univariant if either of the variables, a_H or a_A , is held constant. If then at constant a_H , a_A is varied, the coexistence of two distinct crystalline phases, *e.g.*, $(q-zr_s, r_s)$ and $[q-z(r_s + 1), r_{s+1}]$, respectively, comprises an invariant system and no change in either P_t or a_A is possible until one crystal form is entirely converted to the other. In general, such a phase change results in a discrete break in the function $P_t(a_H, a_A)$ at constant T, p, a_H , for the coefficient $(\bar{j} - r_s)$ appearing in equation 9 is discontinuous. On either side of this break, r_s and r_{s+1} must differ by a rational number.

Similar considerations are valid if a_H is varied at constant T, p, a_A . Depending upon the lattice energies of the various crystals, which are related to the various standard chemical potentials, μ_s^0 , where s represents one of the crystal types, $(q-zr_s, r_s)$, different curves relating $\ln P_t$ to $\ln a_A$ are to be expected. Some examples are illustrated in Fig. 1.

From the foregoing analysis and the illustrative curves of Fig. 1 several conclusions of significance are evident: (1) the slope of the curve relating $\ln P_t$ to $\ln a_A$ at constant p, T and a_H is given by $(\bar{j} - r_s)$; (2) at the points of discontinuity in slope which denote a change in crystalline phase in an invariant system, the change in r_s is related to the two slopes by

$$\Delta r_s = r_{s+1} - r_s = (\bar{j} - r_s) - (\bar{j} - r_{s+1}) \quad (12)$$

(3) From the above two conclusions it follows that \bar{j} may be determined at any point along the curve relating $\ln P_t$ to $\ln a_A$, assuming an initial value of r, r_0 , is known. Thus

$$\bar{j} = \text{slope} + r_0 + \sum_{s=1} \Delta r_s \quad (13)$$

(4) The numerical magnitudes of the slopes and the r_s 's are independent of the units in which P_t (and a_A) is expressed. Therefore, knowledge of \bar{j} (or r_s) together with an independent chemical analysis of the solution (or crystal where $r_s \neq 0$) for the number of moles of A bound per gram of P_t in solution (or crystal) suffice to allow an estimation of the molecular weight of P ; (5) Equations 7-9 may be extended easily to include additional molecular associations. For example, if

$$P_t = P_t(a_H, a_{A1}, a_{A2}, \dots) \quad (14)$$

then it follows that

$$d \ln P_t = \left[\bar{i} - \left(q - \sum_k z_k r_{sk} \right) \right] d \ln a_H + \sum_k (\bar{j}_k - r_{sk}) d \ln a_{Ak} \quad (15)$$

where the coefficients are the usual partials

$$\left(\frac{\partial \ln P_t}{\partial \ln a_{Ak}} \right)_{T, p, a_H, a_{Aj}}$$

in which a_{Aj} indicates that all a_A are to be held constant, other than the k th in computing the partial.

Discussion

In the foregoing a general thermodynamic theory has been developed pertaining to the associative interactions of polyvalent electrolytes with other molecules. The theory in essence pertains to the properties of a univariant two phase system at

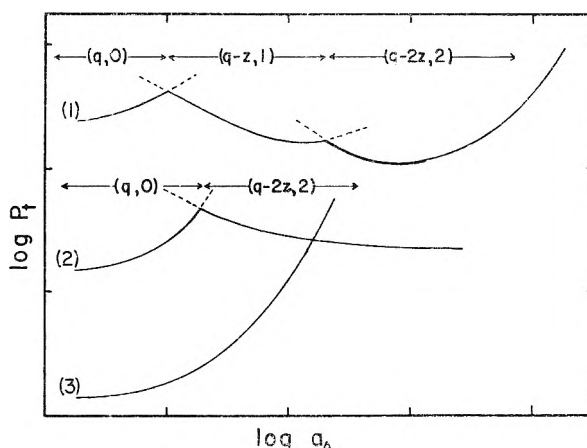


Fig. 1.—Curve 1 illustrates an example of two phase changes of crystalline types $(q,0) \rightarrow (q-z,1) \rightarrow (q-2z,2)$ with their associated characteristic slope changes. The curve at larger values of $\log a_A$ is that to be expected with the occurrence of higher complexes which, however, are more soluble than $(q-2z,2)$. Curve 2 illustrates a single phase change of crystalline types $(q,0) \rightarrow (q-2z,2)$ with the latter more soluble than the former. At large values of $\log a_A$ it is evident that $\bar{j}(\max) = 2$. Curve 3 illustrates an example in which the complex concentrations do not exceed their solubilities, and therefore no discontinuities occur. The limiting slope at large $\log a_A$ gives $\bar{j}(\max)$.

saturation equilibrium, which becomes invariant with discrete crystalline phase changes.

Of the several assumptions made the one involving the use of activities, which involves primarily electrostatic corrections, presents no more than the usual difficulties and has been thoroughly discussed elsewhere, (*e.g.*, ref. 6, p. 766). By far the most stringent assumption from an experimental point of view is that which demands that any crystalline phase present in the system be composed of a single species type of polyvalent ampholyte. In other words, for functions of the type illustrated in Fig. 1 to be obtained experimentally it is necessary that each of the two possible crystalline phases possess a distinct standard chemical potential independent of variations in solution composition, thereby excluding solid solutions. However from phase rule considerations the mere presence of components of the system other than the polyampholyte in the solid phase is not excluded; thus the crystal may contain solvent or any of the components A_k , provided there is equality of the chemical potentials of each component in each phase and μ_s^0 is unaffected.

It is well known that protein crystals are generally loosely structured and penetrable to a degree by small molecules of the "mother liquor".⁷⁻⁹ Little is known regarding the forces involved in crystal formation in such systems in comparison to that of simple molecules. Nevertheless it is reasonable to suppose that the association of one or several small molecules to a polyampholyte is not likely to alter greatly the over-all crystal lattice energies or unit cell dimensions making solid solutions somewhat probable. However, it is

(8) J. T. Edsall and J. Wyman, "Biophysical Chemistry" Vol. I, Academic Press, New York, N. Y., 1958, p. 320 ff.

(9) B. H. Zimm, in "Biophysical Science—A Study Program," (J. L. Oncley, ed.), John Wiley and Sons, Inc., New York, N. Y., 1959, p. 123.

conceivable that specific regions occupying only a fraction of the molecular surface may be primarily involved in lattice stability, in which case the theoretical considerations might be applied to such regions. Amorphous precipitates are common and are even more loosely structured and cannot in general be expected to conform to the assumption if one considers the entire surface of the molecule. Here again, however, only specific regions on the surface may be involved in precipitate stability and the remainder of the surface may have only a minor influence on solubility. In dealing with the interaction of proteins with large molecules such as peptides or other proteins, association is more likely to significantly alter lattice parameters and thus in cases of reasonable crystalline behavior more likely to conform to the assumption. Such also would be the case in dealing with the smaller proteins as well as polypeptides or even peptides themselves interacting with small molecules, and it would be in these situations that an examination of the validity and value of the theory should be made. Finally, surface forces of solid phases may well contribute significantly to affect solubility, especially in the case of microcrystals and presumably amorphous precipitates where the surface area to volume ratio may be large. These forces are difficult to evaluate and have been specifically neglected in the theoretical development presented herein.

There appears to be no published data with which the theory may be tested adequately. However, it is possible that the experiments which would conform to the condition of saturation demanded in the theory have not been done because it was not realized heretofore that the results would have any significance. The results of Edelman and Bryan¹⁰ on the solubility of antigen-antibody complexes are suggestive of the type of discrete phase changes predicted by the theory (see their Figs. 3 and 4).

The chief importance of the present theory is that it indicates a new method to add to the existing methods for the study of the interactions of poly-ampholytes. This method may have particular advantages in certain circumstances, *e.g.*, in the study of ion-ampholyte interactions at those large values of ion activities which present difficulties in other methods. Furthermore, it is not inconceivable that, assuming knowledge of the associative interactions considered in this theory, a study of the solubility of an ampholyte system and its deviations from theoretical behavior may be exploited to advantage in understanding the properties of certain solid solutions, pseudo crystals and mixed crystals, as well as amorphous precipitates and gels.

Acknowledgment.—We are very grateful to Dr. Sidney Katz for a number of helpful discussions.

(10) I. S. Edelman and W. P. Bryan, *J. Am. Chem. Soc.*, **82**, 1491 (1960).

DIELECTRIC POLARIZATION AND HYDROGEN BONDING OF ADSORBATE: METHANOL AND ISOBUTANE ON POROUS VYCOR GLASS

BY D. FIAT, M. FOLMAN AND U. GARBATSKI

Department of Chemistry, Israel Institute of Technology, Haifa, Israel

Received May 4, 1961

Dielectric properties of methanol and isobutane adsorbed on porous Vycor glass were investigated at low surface coverages. Changes in capacity were measured with an accuracy of $2 \times 10^{-4} \mu\text{mf.}$ by means of a high precision capacitance meter. The structure and the shape of the adsorbent allow the adsorbate-adsorbent system to be treated as a solution. Molar polarizations P_m and molar differential polarizations $P_{\text{diff.}}$ of the adsorbate as a function of V (the amount adsorbed) were calculated using Onsager's equation. For methanol the curve $P_{\text{diff.}}$ against V shows an initial rise, passes through a maximum and decreases at higher coverages. For methylated adsorbent the shape of the curve is markedly changed. Isobutane shows a completely different picture. $P_{\text{diff.}}$ has no maximum, it decreases steeply at low surface coverages and approaches slowly a constant value which is close to that of the liquid. The molar differential polarization for methanol shows a non-normal dependence on temperature at low coverages. The results obtained are explained by interaction (in the case of methanol, hydrogen bonding) between the adsorbate and the OH groups of the adsorbent.

Introduction

The work presented here is a continuation of the research on dielectric properties of adsorbed molecules described previously.¹ Dielectric properties of adsorbed vapors and gases on high surface area solids have been studied by a few workers,²⁻⁸ but no

satisfactory conclusions could be drawn from the experimental results, this being mainly due to the lack of knowledge of the electric field at the adsorption site. This knowledge is essential for calculation of the dielectric properties (as dielectric constant or dielectric polarization) of the adsorbate from the compound quantities obtained from measurements for the combined system composed of the adsorbate, adsorbent and the gas phase in equilibrium.

The difficulties encountered in this type of calculation together with results obtained until now are reviewed by Channen and McIntosh⁹ and discussed in our previous publication.¹

The main purpose of this work was to investigate the dielectric properties of adsorbate-adsorbent

(1) D. Fiat, M. Folman and U. Garbatski, *Proc. Roy. Soc. (London)*, **A260**, 409 (1961).

(2) R. McIntosh, E. K. Rideal and J. A. Snelgrove, *ibid.*, **A208**, 292 (1951).

(3) L. N. Kurbatov, *J. Phys. Chem. U.S.S.R.*, **24**, 899 (1950); **28**, 287 (1954).

(4) S. Kurosaki, *J. Phys. Chem.*, **58**, 320 (1954).

(5) J. A. Snelgrove, H. Greenspan and R. McIntosh, *Can. J. Chem.*, **31**, 72 (1953).

(6) M. H. Waldman, J. A. Snelgrove and R. McIntosh, *ibid.*, **31**, 998 (1953).

(7) S. E. Petrie and R. McIntosh, *ibid.*, **35**, 183 (1957).

(8) J. M. Thorp, *Trans. Faraday Soc.*, **E5**, 442 (1959).

(9) E. W. Channen and R. McIntosh, *Can. J. Chem.*, **33**, 172 (1955).

systems at low surface coverages and on a system which enables one to make certain assumptions which seem valid and justify the use of a solution-like model. The adsorbent chosen was one plate of high surface area porous Vycor glass.

Experimental

In order to work at low surface coverages and to find out whether the heterogeneity of the adsorbent's surface influences the measured properties it is necessary to use a very precise capacitance meter. The one used was of a resonance type¹⁰ described previously in detail.¹ It consisted of an oscillator and a wave meter. The measuring cell was in the oscillator circuit in parallel with a precision condenser of coaxial type. At a frequency of 1 Mc. it was possible to measure changes in capacity up to an accuracy of 2×10^{-4} $\mu\mu\text{f}$.

The condenser suspended inside the cell was of two silver plates 33×33 mm. and connected to two Kovar glass seals. The solid adsorbent of porous Vycor glass 1 mm. in thickness was placed between them. In order to fix the distance between the silver plates, glass spacers were placed between them, 0.02 to 0.03 mm. thicker than the adsorbent plate. The lower part of the cell, which contained the condenser, could be heated up to 500° (for desorption) and could be maintained at any other temperature by the use of thermostats.

Materials.—The porous Vycor glass adsorbent was the same as already used and described. Its surface area measured by B.E.T. method using argon at -196° was $190 \text{ m.}^2/\text{g}$. Before each run the glass was cleaned by heating at 450° in an oxygen atmosphere and subsequent evacuation for several hours. Helium was of pure grade at least 99.99%, argon 99.9%. Methyl alcohol was refluxed over metallic Mg for 12 hours, distilled, into a twin bulb and freed from air by bulb-to-bulb distillation. Isobutane and butane, 99% pure as provided by J. H. Matheson and Co., were cleaned by bulb-to-bulb distillation, the middle fraction being used in measurements.

The methylation of the surface of the glass adsorbent was performed using methanol vapors as described previously.¹ It is known that this procedure exchanges about 80% of the surface OH groups.

Procedure.—The amounts adsorbed were measured with a conventional volumetric type apparatus. After each admission of gas the changes in capacitance as well as pressures were measured at the same time until equilibrium was reached. Desorptions were carried out by opening the cell to an evacuated volume.

Method of Calculation

The method of calculation of the dielectric properties such as dielectric constant and dielectric polarization has been described previously in detail.¹

Here it is important to stress that the system considered is a continuous geometrically defined plate and the only inhomogeneity arises from microporosity of the Vycor glass lying in the range of $15\text{--}20 \text{ \AA}$. As these inhomogeneities are on a molecular scale, the adsorbent-adsorbate system was treated as a solution and its dielectric properties evaluated correspondingly relying on Onsager's equation and assuming additivity of specific polarizations of the constituent phases of the system.

The final equations obtained are

$$P_a \varphi_a = \frac{(\epsilon - 1)(2\epsilon + 1)}{9\epsilon} - \frac{(\epsilon_g - 1)(2\epsilon_g + 1)}{9\epsilon_g} \varphi_g - \frac{(\epsilon_v - 1)(2\epsilon_v + 1)}{9\epsilon_v} \varphi_v \quad (1)$$

where P_a is the specific polarization of the adsorbate, ϵ is the dielectric constant and φ the volume fraction. The subscripts g, a, v, designate the solid silicate, the adsorbate and the vapor in equilibrium, respectively.

In the case of methyl alcohol, where the equilibrium pressures are low, ϵ_v is practically 1 and the last term in equation 1 may be neglected.

From $P_a \varphi_a$ the molar polarization of the adsorbate is found

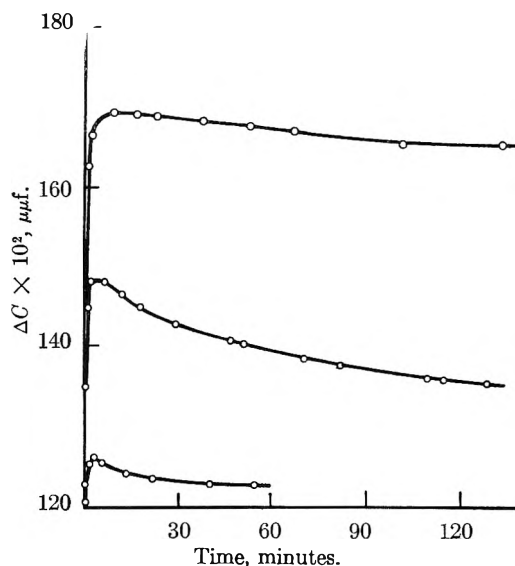


Fig. 1.—The changes in capacitance of the test condenser with time after admission of CH_3OH at different surface coverages.

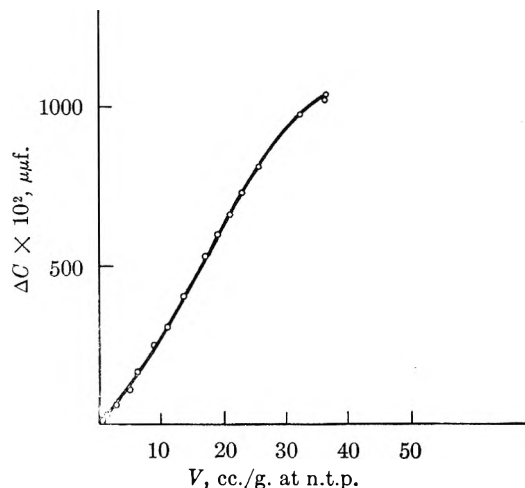


Fig. 2.—The change in capacitance of the test condenser (ΔC) as a function of the amount of CH_3OH adsorbed (V) at 23° .

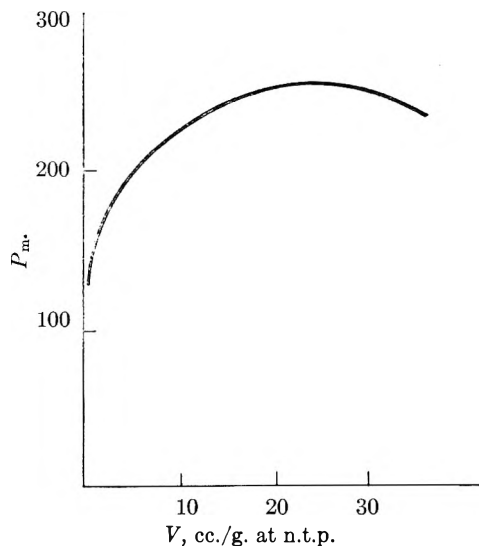


Fig. 3.—The molar polarization P_m of the adsorbate as a function of the amount of CH_3OH adsorbed.

(10) R. J. W. Le Fevre, J. G. Ross and B. M. Smythe, *J. Chem. Soc.*, 76 (1950).

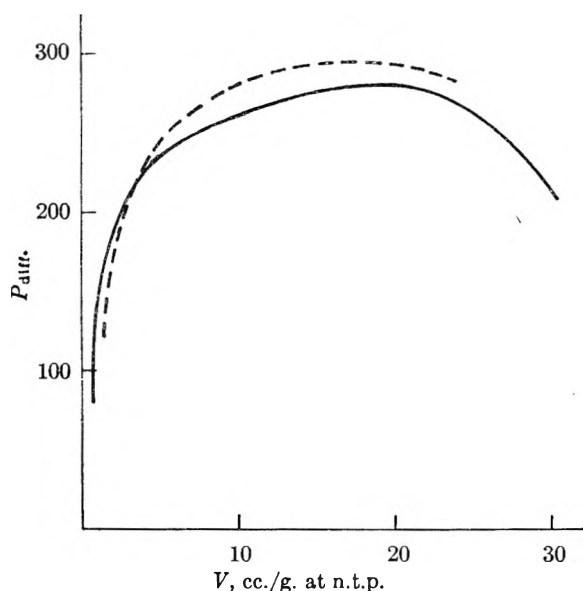


Fig. 4.—The molar differential polarizations P_{diff} of the adsorbate as a function of amount of CH_3OH adsorbed at 0° (—) and 23° (---).

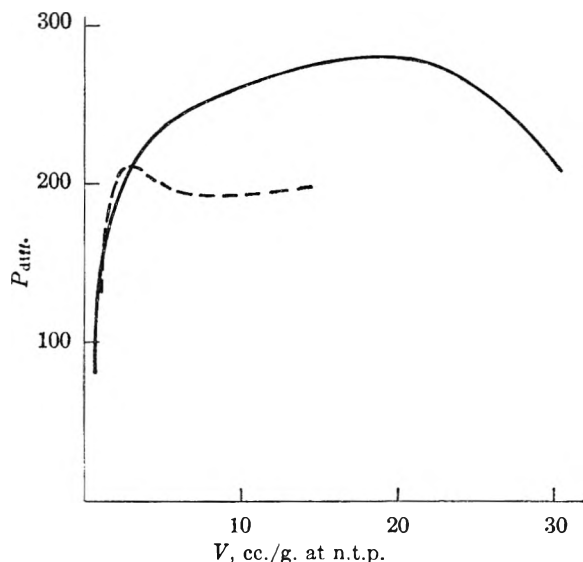


Fig. 5.—The molar differential polarization P_{diff} of the CH_3OH adsorbate as a function of the amount adsorbed at 23° , after methylation of the surface of the adsorbent. —, before methylation; —, after methylation.

$$P_m = P_a \varphi_a \times V \times \frac{M_a}{W_a} \quad (2)$$

where V is the total volume of the plate adsorbent, M_a and W_a are the molecular weight and the weight of the adsorbate, respectively.

Changes in the dielectric properties due to adsorption are ascribed to the adsorbate only.

It seemed very convenient to define and use a new function P_{diff} , which as distinct from P_m gives the molar differential polarization of the adsorbate accordingly

$$P_{diff} = P_m + V \left(\frac{\partial P_m}{\partial V} \right)_T \quad (3)$$

Results

As already mentioned changes in the capacity of the test condenser were measured, together with the amount adsorbed. After admission of each dose of vapor ΔC was recorded every 30 seconds. It was found that especially at low coverages on admission

of methyl alcohol vapor ΔC increases sharply (Fig. 1), passes through a maximum and approaches slowly an equilibrium value. This behavior is parallel to that of ammonia and will be explained in a similar fashion.

The dependence of capacitance on amount adsorbed (Fig. 2) is not linear, nor does it show any sudden change in slope or may it be looked at as composed of linear sections.

The values of P_m vs. V at 23° (Fig. 3) show an initial rise up to 250 cc. at a coverage of about 25 cc./g. and decrease afterwards. This behavior is still more pronounced in P_{diff} (Fig. 4). The function rises from 90 cc. at a coverage of 1.0 cc./g. up to 285 at 23 cc./g. and goes down to nearly 190 cc. at 31 cc./g. adsorbed (the maximum coverage measured). It should be noted that the graph for 0° (dotted curve) intersects that for 23° at low coverage (3.0 cc./g.). A similar effect has been shown in the adsorption of ammonia.¹

When methanol is adsorbed on methylated glass, where most OH groups have been exchanged by methoxy groups, the maximum in P_{diff} (Fig. 5) is sharper and occurs at a much lower coverage (3.5 cc./g.). After that point it decreases and changes rather slowly with further adsorption. Whereas methanol as adsorbate shows very similar behavior to that of ammonia,¹ with butane and isobutane a quite different picture was obtained.

On admission of new doses of vapor equilibrium values of ΔC are reached quickly without any maximum and ΔC reaches its final values monotonously. The curve ΔC vs. V (Fig. 6) is not linear but as distinct from ammonia and methanol the curve is everywhere concave toward the V -axis and no point of inflection is found. Accordingly P_m shows no maximum (Fig. 7) but decreases steeply at low coverages from a value of about 85 cc. at 0.5 cc./g. and then reaches slowly a value of approx. 35 cc. P_{diff} behaves similarly, it decreases to about 28 cc. at a coverage of 15 cc./g. The curves for adsorption on methylated glass are given by dotted lines; they show decrease of the polarization at lower coverages than on unmethylated glass.

Discussion

The various phenomena and results given above fall into a coherent picture when one relates them to the known characteristics of the adsorbent's surface.

It has been shown already that in addition to the usual heterogeneity of the surface of the porous glass there exist at least two types of adsorption sites, one being the OH groups, the other oxygen or silicon atoms. The concentration of the OH groups is very high and is not much decreased even by heating and prolonged evacuation at 450 – 500° . These OH groups give rise to a number of interesting phenomena when polar molecules are adsorbed on them through hydrogen bonding.¹¹

The energies of adsorption for polar adsorbates are usually different for the two types of sites. It also has been shown that the two types of sites differ in their adsorption kinetics; such molecules as NH_3 and CH_3OH are adsorbed more rapidly on

(11) M. Folman and D. J. C. Yates, *Proc. Roy. Soc. (London)*, **A246**, 32 (1958).

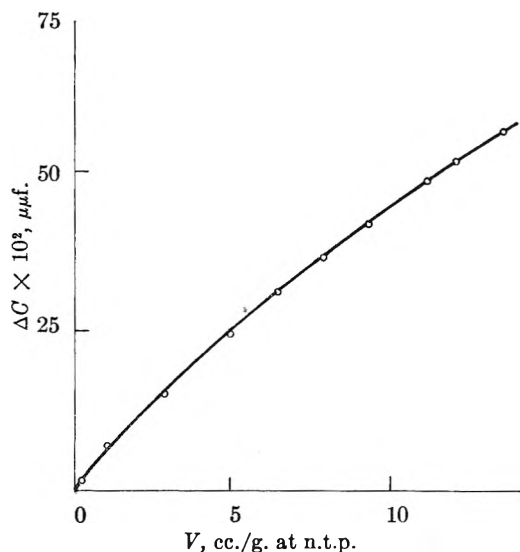


Fig. 6.—The change in capacitance of the test condenser (ΔC) as a function of the amount of isobutane adsorbed (V) at 22° .

the OH groups. This has been shown by means of infrared spectra.¹² A confirmation of this fact in our measurements is the occurrence of a maximum in the ΔC vs. time curves; it will be shown (this will be proved later) that those molecules of CH_3OH that are adsorbed on the OH groups giving hydrogen bonds give higher values of polarization than the molecules adsorbed on the other type of sites; when the CH_3OH vapor is admitted to the cell the adsorption takes place at the beginning mainly on the OH sites (this being the faster reaction) and afterwards as the pressure drops due to adsorption a redistribution of the adsorbate takes place leading to an equilibrium distribution. A similar phenomenon was found in the case of NH_3 .¹ No similar time effects were observed in the case of adsorption of isobutane. This may be due also to the fact that the adsorption of isobutane is very fast and equilibria were obtained usually two or three minutes after admission of a dose of gas.

The explanation of the time effects fits very well the whole picture and finds its confirmation in infrared spectra taken at different time intervals.¹² Nevertheless there may exist an additional reason for the observed effect. The diffusion of adsorbate molecules to the inner regions of the glass adsorbent is certainly a process requiring activation energy for surface migration, thus it is not an instantaneous process. If the polarization of molecules situated at the very narrow capillaries and cracks is lower as compared to more accessible sites, and time is needed to reach these places again a similar effect should be observed.

The most significant result is in the fact that none of the ΔC vs. V curves shows linearity. This is true much beyond the limits of experimental error, corresponds to former results obtained with NH_3 and contrasts with other findings published until now. The ΔC vs. V curve for methyl alcohol is an S-shaped curve with an inflection point at about 18–20 cc./g.

(12) M. Folman and D. J. C. Yates, *Trans. Faraday Soc.*, **54**, 1684 (1958).

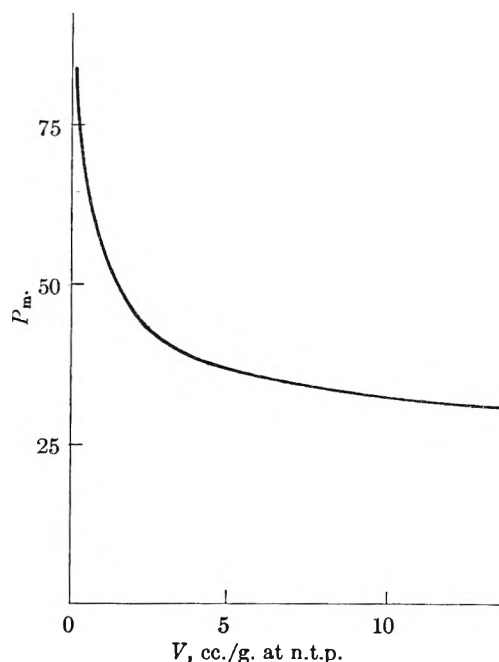


Fig. 7.—The molar polarization P_m of the adsorbate as a function of the amount of isobutane adsorbed (V).

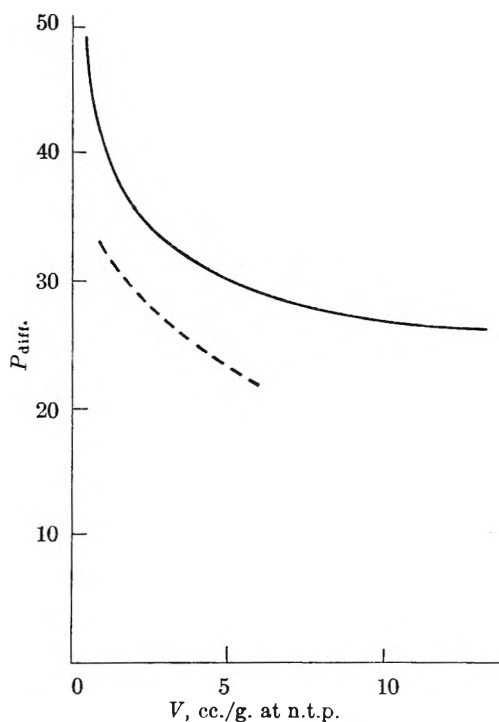


Fig. 8.—The molar differential polarization P_{diff} of the isobutane adsorbate as a function of the amount adsorbed (V) at 22° after methylation of the surface of the adsorbent. —, before methylation; ---, after methylation.

Such a result has to be expected if one considers the possibility of an influence of the adsorbent on the dielectric properties of the adsorbate and takes into account the heterogeneity inherent in the adsorbent's surface. This influence is much more pronounced in the $P_m - V$ plots. Here we find a very marked change in P_m ; from approx. 120 cc. at very low coverage through a maximum of 250 cc. (for 23°) to decreasing values for higher coverages.

The existing heterogeneity of the surface is still more directly expressed in P_{diff} which gives the molar polarization of the adsorbate added at different surface coverages.

The values found here go from 150 cc. at the lowest amount adsorbed through a maximum at 285 cc./g. The molar polarization of gaseous CH_3OH at 23° is 71 cc./mole; liquid methyl alcohol has a molar polarization of 293 at the same temperature. This large difference is explained by the existence of hydrogen bonding in the liquid state which is a phenomenon usually found with this type of compound.

It is known from previous work that CH_3OH is adsorbed on the porous glass, giving hydrogen bonds with the surface OH groups as well as on the other type of sites. Moreover the energy of these hydrogen bonds is very close to that in the liquid methanol.¹² This is inferred from the infrared spectrum, where the shift in the OH stretching frequency of the hydrogen bonded surface OH groups equals the shift of frequency obtained when intermolecular hydrogen bonding occurs in liquid methanol. As adsorption takes place simultaneously on both types of sites, the figure 285 for the maximum should be considered as a lower limit for the polarization of methanol molecules adsorbed on the OH groups. An even higher value of polarization would have been obtained if CH_3OH were adsorbed on the OH groups only. At low coverages adsorption takes place preferentially on high energy sites, where freedom of rotation is most probably restricted, resulting in lower values of polarization. After most of the OH groups have been occupied again a decrease in P_{diff} occurs. This is in accordance with the view that non-hydrogen bonded adsorbate molecules have a lower molar polarization.

In order to check this supposition the adsorption of methanol on methylated glass was investigated. Here the maximum in P_{diff} is much lower; (203 instead of 285 cc./mole) and occurs at 4 cc./g. adsorbed instead of 25 cc./g. It is clear that the removal of approximately 80% of the OH groups shifts the maximum to lower coverages. At the same time the relative amount adsorbed on OH groups decreases, lowering the value of the maximum.

Temperature Dependence.—The temperature dependence of P_{diff} is a normal one at higher surface coverages, *i.e.*, with increasing temperature the polarization decreases. At low surface coverage (less than 0.5–0.6 cc./g.) the dependence on temperature is not normal. The molar polarization increases with increasing temperature, similar to NH_3 as found previously. The explanation of this is based on the belief that due to the high energy of adsorption for the first amounts adsorbed the adsorbate molecules are tightly bound to the surface being located on the most active spots (most probably very narrow capillaries and cracks). Freedom of rotation movement is hindered and the contribution from the orientation polarization is small. With increasing temperature the freedom of rotation is enhanced and a higher value of P_{diff} obtained. (In addition to that the energy of adsorption in such a system is lowered with temperature.) On

increasing the coverage the freedom of rotation of additional amounts of adsorbate is increased so much that the term $\mu^2/3kT$ determines the overall dependence of the polarization on temperature.

Isobutane.—The ΔC vs. V curve of isobutane has no inflection point and it is concave towards the abscissa. Accordingly P_m and P_{diff} show no maximum but a steep decrease at low coverages. P_{diff} at the lowest coverage measured is 49 cc./mole and at the highest adsorption measured, 26 cc./mole. This value is quite near the molar polarizations of gaseous and liquid isobutane (22 cc./g.).

The P_{diff} for methylated glass decreases from 32 to 22 cc./mole lying in the whole range lower than the curve for unmethylated glass. The first conclusion which may be drawn is that in this case also the molar polarization is higher for isobutane molecules adsorbed on the OH groups. Secondly these OH groups are the more energetic sites for adsorption of isobutane and are preferentially populated at low coverages. The third conclusion arises from the fact that in isobutane contrary to NH_3 and CH_3OH there is no initial rise in P_{diff} at small amounts adsorbed. This may be explained by the assumption that the most energetic adsorption regions, which are smallest cracks and capillaries, are not accessible for larger molecules. To check this assumption B.E.T. surface area measurements were made with butane. It was found that in this case the area of the accessible surface is smaller by $1/3$ than with argon. Although isobutane is generally considered as a non-polar molecule, recent measurements by means of microwaves¹³ confirmed that it possesses a dipole moment of 0.13 D. In view of this the interaction with the OH groups may be understood. It leads to higher energy and preferential adsorption on these sites. It also explains the higher values of polarization (as compared to the liquid) by enhancement of the dipole moment.

Preliminary experiments with butane show the existence of the same phenomena as with isobutane.

Conclusions

It now seems in place to sum up the results obtained with the three adsorbates of different polarity, and to compare their behavior. In the three cases investigated a strong dependence of molar polarization on amount adsorbed was found at low surface coverages (between $\theta = 0$ and approx. $\theta = 0.5$).

Assuming that the measured changes of molar polarization are due to the adsorbate only we find that NH_3 , CH_3OH and isobutane show increase of molar polarizations due to adsorption on the OH groups as compared to gas phase values. This increase may be related to the strength of interaction in adsorption. As was shown previously, NH_3 gives very strong hydrogen bonds with the surface OH groups (much higher than in the liquid state), thus the molar polarization of the adsorbate is much higher than that of the liquid.

Methanol gives hydrogen bonds with the surface

(13) D. R. Lide, Jr., and D. E. Mann, *J. Chem. Phys.*, **29**, 914 (1958).

OH group of energy near to that which exists in the liquid, (as obtained from shifts in OH stretching frequency in infrared); therefore the molar polarization of adsorbed methyl alcohol is near to that of the liquid. Isobutane with its low dipole moment interacts much more strongly with the polar sur-

face OH groups than in the liquid state, and, consequently the adsorbate on these OH groups shows a higher polarization than the liquid.

Acknowledgment.—The authors are indebted to Dr. M. E. Nordberg of the Corning Glass Works, Corning, N. Y., for the gift of the porous Vycor glass.

MEASUREMENTS OF INTRAMOLECULAR HYDROGEN BONDING BY NUCLEAR MAGNETIC RESONANCE AND INFRARED SPECTROSCOPY

By JOHN R. MERRILL

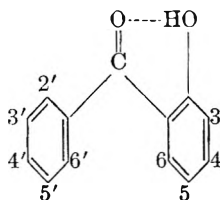
Radiation Physics Laboratory, Engineering Department, E. I. du Pont de Nemours & Company, Wilmington, Delaware

Received May 6, 1961

The hydroxyl proton chemical shifts of a series of substituted 2-hydroxybenzophenones dissolved in carbon tetrachloride vary by 2.35 p.p.m. at room temperature. The individual shifts change only about 0.3 p.p.m. from -25 to $+80^\circ$, and are similarly insensitive to concentration. The infrared O-H stretching bands have half-intensity widths of ~ 400 cm^{-1} , and peaks at 2940 to 3200 cm^{-1} . A correlation is found between the hydroxyl shifts and the O-H frequencies. Both hydroxyl groups of 2,2'-dihydroxybenzophenones appear to be chelated, although less strongly than those of the 2-hydroxybenzophenones.

Introduction

Intramolecular hydrogen bonds between the carbonyl and hydroxyl groups of 2-hydroxybenzophenones form six-atom chelate rings



The proton magnetic resonance and infrared spectroscopy studies reported here concern the strengths of chelation in a series of these compounds. Competition between intramolecular and intermolecular hydrogen bonding is examined in a non-hydrogen-bonding solvent. Chelation strengths are compared for derivatives with one and two hydroxyl groups *ortho* to the carbonyl group and with other substituents on the aromatic rings. The hydroxyl proton chemical shifts and their dependence on temperature and concentration^{1,2} and the displacement of the O-H fundamental stretching frequency² are used to establish the nature and relative strengths of the hydrogen bonds.

Experimental Procedures

Proton magnetic resonance spectra were obtained with a Varian Associates V-4300B spectrometer at a fixed frequency of 40 Mc. A thermostat, similar in design and operation to that described by Brownstein,³ was constructed to fit the Varian NMR probe for measurements at controlled temperatures. Samples were spun in 5-mm. o.d. glass tubes. The temperature near the sample was measured with a thermocouple located within the thermostat. A graph of differences between this temperature and that of a liquid sample was constructed for correcting the thermostat readings taken during calibration of spectra. Temperatures were

measured with a precision of $\pm 0.5^\circ$ and an accuracy of $\pm 1^\circ$.

All spectra were recorded from carbon tetrachloride solutions of the hydroxybenzophenones at concentrations of 0.3–1.0 *M*. To avoid interactions with an added reference compound, hydroxyl shifts were calibrated with respect to other resonance peaks of each hydroxybenzophenone. All major peaks were calibrated at each temperature to establish that only the hydroxyl shifts changed. The reference peaks were assigned their room-temperature shifts in c.p.s. at 40 Mc. from external tetramethylsilane. The hydroxyl shifts from internal tetramethylsilane at 23° also were determined, and found to be about 12 c.p.s. to higher field than those referred externally.

Spectra were calibrated with audiofrequency modulation techniques. Three to six calibrations were made at each temperature and the results averaged. Tests of the calibration procedures and the internal consistency of the shift data indicate that the measurements are accurate to a few tenths of a c.p.s. Resolution, expressed as the half-peak width of a tetramethylsilane resonance, was about 1 c.p.s.

Infrared absorption spectra were recorded on a Perkin-Elmer model 221 grating spectrophotometer with a nominal resolution of 2 cm^{-1} . When possible, 0.3 *M* solutions in carbon tetrachloride were used in cells of 0.1-mm. path length. For the less soluble derivatives, and for dilution studies, 1–10-mm. cells were used. Spectra also were taken after deuterium had been substituted for the hydroxyl hydrogen atoms. Exchange with deuterium was accomplished by shaking a carbon tetrachloride solution of each hydroxybenzophenone with a 200-fold molar excess of heavy water for a few minutes. The hydroxybenzophenones are relatively insoluble in water, as is carbon tetrachloride. After the two liquid phases were allowed to separate, the carbon tetrachloride solution of deuterioxybenzophenone was pipetted off. The contribution of the C-H stretching absorptions which overlay the hydrogen-bonded O-H band can be seen by comparing, or instrumentally subtracting, spectra of the normal and deuterated compounds (Fig. 1). Replacement of the hydroxyl protons with deuterium was verified by n.m.r. spectroscopy.

Results

The room-temperature hydroxyl proton shifts (Table I) range from 409 to 503 c.p.s. toward low field from internal tetramethylsilane, or from -0.23 to -2.58 p.p.m. on Tiers' scale.⁴ All the 2-hydroxyl peaks were narrow, with half-peak widths of 2 c.p.s. except that of 2,2'-dihydroxybenzophenone, which was 5 c.p.s. in width. The hy-

(1) J. A. Pople, W. G. Schneider and H. J. Bernstein, "High-resolution Nuclear Magnetic Resonance," McGraw-Hill Book Co., Inc., New York, N. Y., 1959, p. 400.

(2) G. C. Pimentel and A. L. McClellan, "The Hydrogen Bond," W. H. Freeman and Co., San Francisco, California, 1960.

(3) S. Brownstein, *Can. J. Chem.*, **37**, 1119 (1959).

(4) G. V. D. Tiers, *J. Phys. Chem.*, **62**, 1151 (1958)

TABLE I
INFRARED O-H AND O-D STRETCHING FREQUENCIES AND HYDROXYL PROTON RESONANCE SHIFTS
OF HYDROXYBENZOPHENONES DISSOLVED IN CARBON TETRACHLORIDE

Compound	-benzophenone	2-OH, ^a cm. ⁻¹	2-OH/2-OD (ratio)	4-OH, ^b cm. ⁻¹	4-OH/4-OD (ratio)	2-OH, ^c c.p.s.
16	2,2',4,4'-tetrahydroxy-5,5'-di- <i>t</i> -butyl-	3200	1.33	3595	1.36	^d
17	2,2'-dihydroxy-	3200	1.33	415
11	2,2',4-trihydroxy-	3190	1.34	3595	1.36	^d
7A, B	2,2'-dihydroxy-4-methoxy-	3190	1.35	459, 409
14	2,2'-dihydroxy-4,4'-dimethoxy-	3150	1.34	^d
5	2-hydroxy-5-chloro-	3100	1.34	471
13	2,2'-dihydroxy-4,4'-didodecyloxy-	3100	1.32	449
10	2,4-dihydroxy-5-hexyl-	3010	1.34	3595 ^e	1.36	501
4	2-hydroxy-4-methoxy-	2960	1.33	502
8	2-hydroxy-4-decyloxy-	2940	1.32	503

^a Best value for center of broad infrared absorption band (half-intensity widths ca. 400 cm.⁻¹). ^b Non-hydrogen-bonded 4-hydroxyl groups. ^c Down-field n.m.r. shift from internal tetramethylsilane at 40 Mc. and 23°. ^d Too insoluble in CCl₄ for measurement. ^e At high concentrations, intermolecularly hydrogen-bonded 4-hydroxyl groups produce a peak centered at 3325 cm.⁻¹.

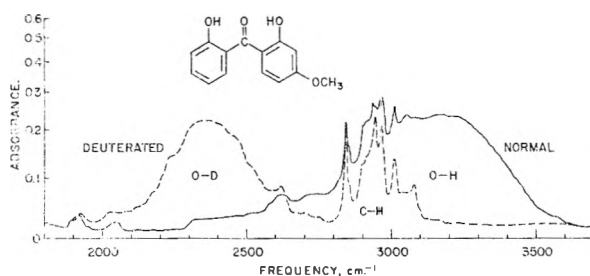


Fig. 1.—Infrared spectra of normal (—) and deuterated (---) 2,2'-dihydroxy-4-methoxybenzophenone in CCl₄. Concentration, 0.3 M; cell path, 0.1 mm.

droxyl proton chemical shifts are plotted against temperature in Fig. 2. For all compounds, a decrease in temperature causes the hydroxyl shifts to move to lower field, the direction associated with stronger or more complete hydrogen bonding. The changes are small, approximately 10 c.p.s. over the available temperature range of -25 to +80°.

The hydroxyl shifts are also relatively insensitive to concentration. For example, the shift of 2-hydroxy-4-decyloxybenzophenone undergoes an 8-c.p.s. decrease upon eighteen-fold dilution. Both hydroxyl peaks of 2,2'-dihydroxy-4-methoxybenzophenone, which is less soluble, behave similarly (Table II). The direction of the changes indicates less hydrogen bonding at lower concentrations.

No free hydroxyl peaks were observed in the in-

TABLE II

INFLUENCE OF CONCENTRATION ON HYDROXYL SHIFT ^a				
2-Hydroxy-4-decyloxybenzophenone		2,2'-Dihydroxy-4-methoxybenzophenone		
Concn., M	Hydroxyl shift, ^b c.p.s.	Concn., M	Hydroxyl shift, ^c c.p.s.	
3.5	518	1.5	474	424
2.3	516	1.0	471	421
1.2	514	0.5	470	420
0.6	512	0.3	470	420
0.2	510			

^a Measured in carbon tetrachloride at 21°. ^b Down-field shift from external tetramethylsilane (calibrated from major -C₁₀H₂₁ peak, assigned a constant shift of 68 c.p.s.). ^c Down-field shift from external tetramethylsilane (calibrated from -OCH₃ peak, assigned a constant shift of 168 c.p.s.).

frared spectra of 2-hydroxybenzophenones, even at low concentrations. The chelated hydroxyl groups have O-H stretching bands displaced to lower frequencies, with half-peak widths of about 400 cm.⁻¹. The corresponding O-D bands are about 300 cm.⁻¹ in width. The broadness of the bands, the imperfect subtraction of interfering C-H peaks, and the partial overlap of O-H and O-D absorptions combine to limit the accuracy with which the bands can be located. The best estimates of band-center frequencies for the derivatives studied range from 2940 to 3200 cm.⁻¹ (Table I). The index numbers in Table I were assigned to the derivatives arbitrarily, to identify points on the graphs.

The maximum uncertainty in locating the center of each O-H band is indicated by the horizontal lines in Fig. 3. In most cases the centers probably have been located more closely. The O-H/O-D frequency ratio is normally reported within the range of 1.29-1.38.⁵ This ratio was calculated for each hydroxybenzophenone after both the O-H and O-D peak locations had been determined. It varies from 1.32 to 1.35 for 2-hydroxyl groups, and is near 1.36 for 4-hydroxyl groups (Table I). The relative constancy of this ratio suggests that the peaks have been located accurately. At an O-H frequency of 3000 cm.⁻¹, a ratio change from 1.32 to 1.35 corresponds to a frequency change of 70 cm.⁻¹.

To investigate the possible confusion of 2-hydroxyl bands with hydrogen-bonded 4-hydroxyl bands in some of the derivatives, spectra were taken from concentrated and dilute solutions of 2,4-dihydroxy-5-hexylbenzophenone. At 0.5 M, a band attributable to intermolecular hydrogen bonding is prominent at 3325 cm.⁻¹. At 0.01 M, this band has virtually disappeared, and most of the 4-hydroxyl groups contribute to a narrow free peak at 3595 cm.⁻¹. The other 4-hydroxyl compounds examined have maximum solubilities near 0.01 M. Interference from a bonded 4-hydroxyl band does not appear to be a major problem at these low concentrations.

No fine structure could be definitely ascribed to the O-H or O-D absorptions, which are single,

(5) Reference 2, p. 112.

fairly symmetrical bands. Spectra of normal and deuterated 2,2'-dihydroxy-4-methoxybenzophenone are shown in Fig. 1.

The carbonyl group C=O stretching absorption of benzophenone is near 1670 cm^{-1} . Broader, structured C=O bands from the hydroxybenzophenones occur at 1620-1640 cm^{-1} . The direction of this frequency shift is that expected for hydrogen bonding.² The carbonyl peaks are not sufficiently consistent in shape to be located with the precision required for comparison with the hydroxyl-group infrared or n.m.r. shifts. These frequencies are similar to those reported for crystalline anthraquinone and its hydroxy derivatives.⁶ Broad O-H stretching bands of some chelated hydroxyquinones have been assigned near 2900 cm^{-1} .⁷

Discussion

The chemical shift of the hydroxyl proton of a 2-hydroxybenzophenone can be expected to arise in a complex manner. Diamagnetic currents induced in the adjacent aromatic ring,^{8,9} and the angle, strength and extent of formation of hydrogen bonds are factors that should influence the observed shifts. If the subsidiary contributions are similar for all the derivatives, it is possible that the hydroxyl shifts are related monotonically to the hydrogen-bond strengths.

As shown in Fig. 2, the individual 2-hydroxyl shifts are all relatively insensitive to temperature, changing only some 10 c.p.s. over a range of about 100°. This behavior contrasts with that of an intermolecularly hydrogen-bonded 4-hydroxyl group, whose shift changes about 1 c.p.s. per degree at the concentrations employed here. Similarly, the 2-hydroxyl shifts are relatively independent of concentration, as shown in Table II. Although the 2-hydroxyl shifts include a small intermolecular contribution at high concentrations, they primarily reflect the strength of chelation.

The infrared spectra also support virtually complete chelation of the 2-hydroxyl groups. Their O-H stretching absorptions are displaced some 400 to 660 cm^{-1} from the free O-H frequency near 3600 cm^{-1} , and are broadened some twenty-fold. Even at concentrations of 0.01 *M*, no free O-H peak is detected for the 2-hydroxy compounds.

In the unsymmetrically substituted compound 7 (2,2'-dihydroxy-4-methoxybenzophenone) residence times for the two hydroxyl proton sites are sufficiently long to give two narrow resonance peaks separated by 50 c.p.s. Despite this difference in shift, the behavior of both peaks meets the criteria for chelation. Furthermore, the infrared O-H and O-D bands each appear single and no broader than those of other derivatives (Fig. 1). No changes are found in infrared spectra taken at concentrations from 1.5 to 0.01 *M* that would suggest intermolecular hydrogen bonding of one of the hydroxyl groups. Although the separation of the n.m.r. peaks may indicate different chelation

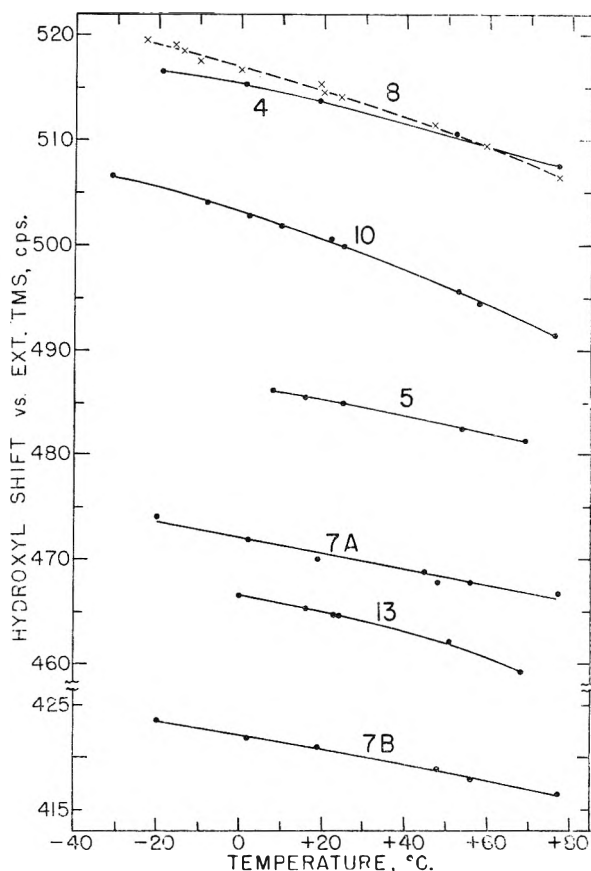


Fig. 2.—Hydroxyl proton chemical shifts of 2-hydroxybenzophenones vs. temperature. The derivatives are identified by number in Table I.

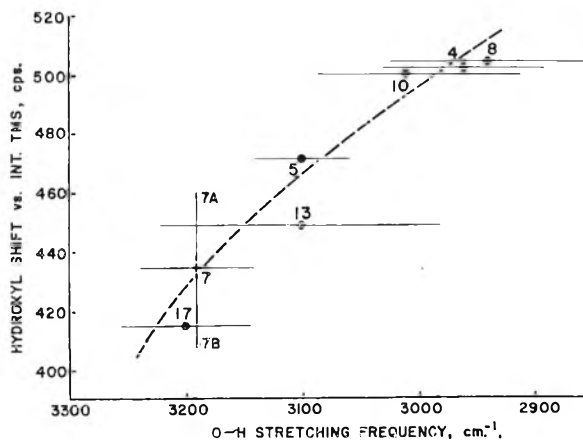


Fig. 3.—Correlation of hydroxyl proton chemical shift with infrared O-H stretching frequency. Compounds are identified in Table I.

strengths for the two *ortho*-hydroxyl groups, other magnetic shielding effects also may contribute.

The O-H infrared absorption bands cannot be located with the same accuracy as the n.m.r. resonances. However, the symmetry of the O-H bands, and the previously mentioned isotopic shift between their frequencies and those of the narrower, more readily located O-D bands are helpful in establishing band-center frequencies. The lines in Fig. 3 indicate the maximum uncertainty in locating the centers through inspection of each

(6) M. St. C. Flett, *J. Chem. Soc.*, 1441 (1948).

(7) D. Hadzi and N. Sheppard, *Trans. Faraday Soc.*, **50**, 911 (1954).

(8) Reference 1, p. 181.

(9) L. W. Reeves, *Can. J. Chem.*, **38**, 748 (1960).

O-H band itself. (C-H interference varies with the different compounds). The actual centers are more likely to occur near the middle of each range.

Figure 3 shows that the larger chemical shifts correspond to lower O-H frequencies. Each of these respective trends is associated with stronger hydrogen bonding. A similar correlation has been found by Reeves, Allan and Strømme for intramolecular bonds in phenols and naphthols.¹⁰

Figure 3 and the additional infrared data in Table I indicate that the 2-hydroxybenzophenones have the strongest hydrogen bonds. Double chelation of the carbonyl group in 2,2'-dihydroxybenzophenones appears to reduce the strength of each bond, although not markedly. Again, the relative independence of the n.m.r. and infrared parameters to temperature and concentration indicates that both hydroxyl groups in these compounds are chelated.

According to Stuart-Briegleb atom models, coplanarity of the two aromatic rings with the carbonyl group of benzophenone is prevented by steric hindrance between the 6- and 6'-hydrogen atoms. The minimum angle between rings appears to be about 30°. The hydroxyl group and its phenyl ring, and the carbonyl group of 2-hydroxy-

benzophenone can be coplanar. In a 2,2'-dihydroxybenzophenone, simultaneous planarity of both rings and their hydroxyl groups with the carbonyl group is impossible without distortion of bond angles. To line up with the carbonyl oxygen atom, each hydroxyl group must turn out of the plane of its phenyl ring. A 15°-offset of each ring from the carbonyl group would seem to be the required compromise, at least for those derivatives in which both rings are identically substituted. It was noted that the separate hydroxyl proton resonances from compound 7 may arise because of unequal hydrogen-bond strengths. In this and other unsymmetrically substituted 2,2'-dihydroxybenzophenones, the phenyl ring whose hydroxyl group is more strongly chelated may be held more nearly coplanar with the carbonyl group than the other ring. A steric hindrance to planarity could partly account for the weaker chelation of each hydroxyl group in the 2,2'-dihydroxybenzophenones.

Acknowledgments.—Helpful discussions were held with W. D. Phillips of our Central Research Department, and with H. Kobsa of the Pioneering Research Laboratory, Textile Fibers Department and R. Dessauer of Jackson Laboratory, Organic Chemicals Department, who also supplied the compounds for this study.

(10) L. W. Reeves, E. A. Allan and K. O. Strømme, *Can. J. Chem.*, **38**, 1249 (1960).

SOLUBILITY OF CALCIUM CARBIDE IN FUSED SALT SYSTEMS

BY WILLIAM A. BARBER AND CAROL L. SLOAN

Central Research Division, American Cyanamid Co., Stamford, Connecticut

Received May 12, 1961

Calcium carbide, CaC₂, has been found to be soluble in a number of pure alkali and alkaline earth salts and salt mixtures at temperatures up to 1000°. The highest solubilities were observed with lithium salts. The variation of solubility with temperature has been determined in several of these solvents. Measured solubilities are compared with those predicted theoretically for the ideal case.

Introduction

Information on the solubility of CaC₂ is exceedingly scarce. No material which is liquid at or near room temperature is known to dissolve CaC₂. It has been mentioned¹ incidental to some work on Li₂C₂ that CaC₂ is soluble in some hydride-containing melts, but no quantitative information has been presented. It is known that CaC₂ forms eutectics with CaO² and with CaCN₂,³ but, because these mixtures melt above 1000°, they have limited utility. We now wish to report the results of a study concerning the solubility of calcium carbide in fused alkali and alkaline earth salts and their mixtures below 1000°.

Experimental

Apparatus.—For preparing solutions a vertical, electrically heated furnace (Hevi-Duty Electric Co.) was used which accommodates a cylindrical tube of 1.25 inches o.d. Since Pyrex or Vycor glass containers were found to be attacked by some melts, especially those containing Li⁺, the experiments were performed using stainless steel tubes. Although stainless steel is not completely inert to the melt,

no significant amounts of corrosion products appeared in the filtered mixtures (determined by ultraviolet emission spectroscopic analysis: Fe < 1 p.p.m.; Cr, Ni, Mn not detectable).

The apparatus used is a modification of that described by Solomons, *et al.*,⁴ and is pictured in Fig. 1. The melt was supported either on a coarse porosity Micrometallic stainless steel filter or a solid stainless steel disc perforated with 1/32" holes. Since the remainder of the apparatus was of Pyrex glass, the joints of the furnace tube were wrapped with water-cooled copper coils to protect the glass connections from thermally caused stress. Temperatures were measured with a Chromel-Alumel thermocouple inserted in a stainless steel thermocouple well and read on a Leeds & Northrup Type K potentiometer.

Materials.—Argon gas (Linde High Purity grade) was further dried by passing it through activated alumina (pre-dried at 400° for several hours).

The calcium carbide used was ordinary commercial grade material (about 85% pure). The major impurity, CaO, was found to be insoluble in most of the melts studied. The carbide was broken into approximately 1/8 to 1/4 inch lumps at the time of use, and finer material was discarded.

Reagent grade salts were used without further purification. LiCl and CaCl₂ were placed in graphite crucibles and pre-melted in a Lindberg crucible furnace under a flow of argon gas. This procedure served to remove any water picked up in handling and provided blocks of salt which were easier to keep dry. Any additional water present in the salts was

(1) A. Guntz and F. Benoit, *Compt. rend.*, **176**, 970 (1923).

(2) G. Flusin and C. Aall, *ibid.*, **201**, 451 (1935).

(3) H. Franck and H. Heimann, *Z. Elektrochem.*, **33**, 469 (1927).

(4) C. Solomons, *et al.*, *J. Phys. Chem.*, **62**, 248 (1958).

removed during the experiment either by vaporization or by reaction with excess CaC_2 . Such reaction produced CaO which was insoluble in the melt and acetylene which was pyrolyzed or swept away. The more satisfactory procedure for dehydrating molten chlorides in an atmosphere of HCl^5 could not be used in our stainless steel apparatus.

Procedure.—In a typical experiment, the thermocouple well was inserted, and lumps of solid calcium carbide were added to the tube. (Powdered carbide could not be used since surface tension caused it to float and contact was poor.) The solid solvent salt was added next. If the molten salt was expected to have a density greater than the carbide, a tightly fitting stainless steel screen was placed above the carbide and below the salt layer to keep the carbide submerged when the salt was molten.

After the glass equipment was assembled, the system was flushed thoroughly with a stream of dry argon passing upward through the tube. When the temperature was raised to the desired value, the gas flow, besides providing an inert atmosphere, served to keep the melt above the disc, to agitate the carbide particles in the melt, and to reduce by its stirring action any temperature gradients caused by uneven furnace heating. The temperature could be held for extended periods at the desired value $\pm 3^\circ$.

After holding the melt in contact with the solid calcium carbide for the desired period of time (usually three hours), the argon flow was reduced or shut off entirely, and the melt was allowed to filter through the disc under gravity, if possible, or under argon pressure if necessary. As the filtrate was collected it solidified immediately. This quenching action produced a visibly homogeneous mixture (usually gray) of carbide and salt which, after cooling under argon, was removed and analyzed for carbide content.

Analytical Methods.—The method employed for the determination of carbide was developed particularly for this problem and is useful in the presence of halide, base or free active metal. Based upon a procedure for the determination of gaseous acetylene,⁶ the method involves precipitation of the carbide as cuprous acetylide. The precipitate is washed free of excess copper and redissolved, and the copper concentration is determined colorimetrically. Reproducible results have been obtained on samples containing from 0.01 to $\sim 85\%$ carbide.

The approximate sample size for analysis was estimated by a preliminary test. An accurately weighed sample was dropped into 15 ml. of precipitating solution (2 g. of $\text{Cu}(\text{NO}_3)_2 \cdot 3\text{H}_2\text{O}$; 8 g. of $\text{NH}_2\text{OH} \cdot \text{HCl}$; 8 ml. of NH_3 , aq. (28%); diluted to 100 ml.). The resulting dark red precipitate was filtered, rinsed thoroughly with wash solution (10 g. of $\text{NH}_2\text{OH} \cdot \text{HCl}$ per liter made weakly alkaline with NH_3), and decomposed in 12 ml. of dissolving solution (82 ml. of H_2SO_4 (98%) and 8 ml. of H_2O_2 (30%) diluted to 500 ml.). The resulting cupric solution was transferred to a 100-ml. volumetric flask, and concentrated ammonia was added until the blue color of the $\text{Cu}(\text{NH}_3)_4^{++}$ ion was just visible. An additional 20 ml. of ammonia was added, and the blue solution was diluted to volume with water. The blank was prepared from 12 ml. of dissolving solution and 26 ml. of concentrated ammonia diluted to 100 ml. Using the transmittance measured at 800 μ (constant slit) on a Beckman DU Spectrophotometer, the copper concentration was obtained from a previously prepared calibration curve. From this information, the initial carbide concentration was calculated. When necessary, the quenched filtrate also was titrated with standard HCl to give the total base formed.

Results

All lithium salts tried, with the exception of LiNO_3 , were found to be good solvents for CaC_2 . All other alkali salts tried were found to be non-solvents. Some of the salts which dissolve CaC_2 are given in Table I. Members of the LiCl-LiF-LiH system, which were found to be exceptionally good solvents, were studied in greater detail and are treated separately.

The LiCl-LiF-LiH System.—Data obtained for the pure salts LiCl and LiF are shown in Fig. 2. Results with LiH , in which solution seems to be

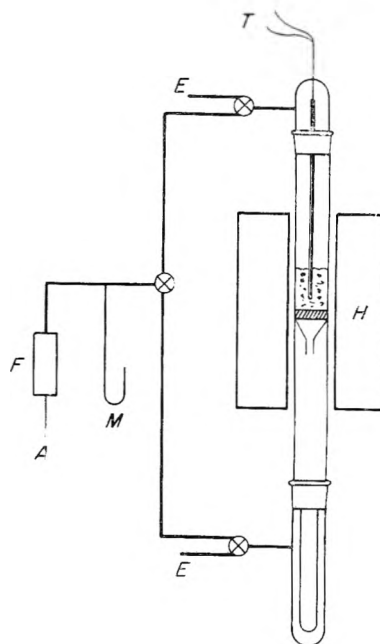


Fig. 1.—Apparatus: A, argon inlet; E, gas exit line; F, flowmeter; H, furnace; M, mercury manometer; T, thermocouple.

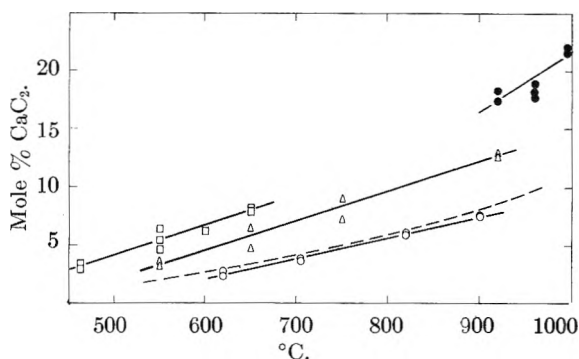


Fig. 2.—Solubility of CaC_2 in fused salts: O, LiCl ; ●, LiF ; Δ, LiCl-LiF eutectic; □, LiCl-LiF-LiH eutectic; —, ideal.

TABLE I
SOLVENTS FOR CALCIUM CARBIDE

Pure salts	M.p., °C.	T, °C.	Wt. % CaC_2	Mole % CaC_2	Ideal mole %
LiBr	547	820	6.0	8.0	13.0
CaCl_2	772	820	6.2	10.4	13.0
BaCl_2	962	1000	4.3	13.2	21.6
Salt mixtures—composition mole %					
80 CaCl_2 20 CaF_2	650E ^a	820	6.8	10.8	13.0
59 LiCl 41 KCl	352E	820	3.6	3.2	13.0
80 LiCl 20 KCl	510	820	7.1	5.5	13.0
72 LiCl 28 NaCl	552E	820	8.6	6.5	13.0
70 LiBr 30 NaBr	537E	820	2.5	3.6	13.0
63 LiCl 37 CaCl_2	496E	820	7.3	7.7	13.0

^a E indicates eutectic.

accompanied by a chemical reaction, were erratic and are not presented.

Among the three binary systems, only the eutectics were considered for study, because interest was directed primarily toward low-melting solvents. The data shown in Fig. 2 for the LiCl-LiF system

(5) H. A. Laitinen, et al., *J. Electrochem. Soc.*, **104**, 516 (1957).

(6) G. Almasy and I. Pallai, *Magyar Kém. Folyóirat*, **59**, 200 (1953).

were determined using the composition reported for the eutectic by Haendler, *et al.*⁷ No solubility measurements were made in the LiF–LiH system since a eutectic was not observed. This has recently been confirmed by Messer and Mellor.⁸ It was necessary to determine the approximate composition of the LiCl–LiH eutectic. This was found to be 63 mole % LiCl (m.p. 486°). Unfortunately, solubility studies in this system have been complicated by the same difficulties as with pure LiH and, therefore, results have not been included.

It was necessary also to establish the approximate composition of the ternary eutectic. We found

	Mole %	Wt. %
LiCl	56	76
LiF	23	19
LiH	21	5

m.p. 454°

Solubility results obtained in this mixture are shown also in Fig. 2.

Character of the Dissolved Carbide.—Several of the quenched filtrates were examined by X-ray diffraction. The powder patterns obtained were in all cases those of CaC₂, showing that metathesis had not occurred. Also, these CaC₂ lines were sharper than those obtained from the starting material, indicating that recrystallization of CaC₂ had taken place. Moreover, a rather large freezing point depression (11.5°) was observed for a 10% solution of CaC₂ in LiCl. This is additional evidence that the CaC₂ is actually dissolved in the molten salt.

Generalizations.—Of the alkali halides, only lithium salts are suitable solvents for CaC₂. Sodium, potassium and cesium chlorides all react to some extent to give a small amount of free alkali metal with no trace of dissolved carbide in the filtrate.

Magnesium chloride undoubtedly dissolves CaC₂ but it also reacts with it to give MgC₂ and/or Mg₂C₃. The system is further complicated by the thermal instability of Mg₂C₃ which decomposes to magnesium metal and carbon. Calcium and barium chlorides dissolve small amounts of CaC₂. Low melting eutectics containing AlCl₃, such as LiCl–AlCl₃ and NaCl–AlCl₃, do not dissolve any detectable CaC₂ at 200–300°.

(7) H. M. Haendler, *et al.*, *J. Electrochem. Soc.*, **106**, 264 (1959).

(8) C. E. Messer and J. Mellor, *J. Phys. Chem.*, **64**, 503 (1960).

ZnCl₂, PbCl₂ and CdCl₂ also were investigated as solvents for CaC₂. These post-transition metal salts were reduced by the carbide nearly quantitatively to free metal.

Discussion

The solubilities reported are believed to be close to equilibrium values. When equilibrium was approached from both higher and lower temperatures, the solubilities found were in good agreement.

Ideality.—The solubility of CaC₂ in any solvent in which it behaves ideally can be calculated from the relation⁹

$$\ln x = -\frac{\Delta H_f}{R} \left(\frac{1}{T} - \frac{1}{T_0} \right)$$

where

- x = mole fraction of solute
- ΔH_f = heat of fusion of solute
- R = gas constant
- T_0 = melting point of solute
- T = the desired temperature

The values $\Delta H_f = 7680$ cal./mole¹⁰ and $T_0 = 2573^\circ\text{K}$.¹¹ have been used to determine the ideal solubility curve in Fig. 2. It can be seen that the solubility of CaC₂ in LiCl is below, but closely approaches, the ideal case. In systems containing LiF and LiH, however, the observed solubilities are much greater than would be expected if these solutions were ideal.

Of all the alkali and alkaline earth salts tried, lithium salts (with the smallest cation) are the best solvents for CaC₂. Of the lithium salts, those with small anions (LiF, LiH) are best. Cation size, then, appears to be of primary importance and anion size of secondary importance in determining the solvating power of these salts for CaC₂.

With regard to other solutes, it may be mentioned that Li₂C₂ has been found to be soluble in LiCl and to a lesser extent in NaCl, and that Ca₃N₂ is slightly soluble in CaCl₂.

Acknowledgment.—The authors are grateful to Mr. Stephen Arcano for his assistance with much of the experimental work.

(9) See for example E. A. Guggenheim, "Thermodynamics," North-Holland Publishing Co., Amsterdam, 1949, p. 237.

(10) E. Schlumberger, *Z. angew. Chem.*, **40**, 141 (1927).

(11) C. Aall, "Contribution à l'étude du Carbure de Calcium Industriel," Imprimerie Allier, Grenoble, 1938.

EFFECTS OF HIGH ENERGY RADIATION ON SOME INCLUSION
COMPOUNDS OF UREA, THIOUREA AND HYDROQUINONEBY WILLIAM SEAMAN¹*Department of Chemistry, King's College, University of Durham, Newcastle-upon-Tyne 1, England*

Received May 12, 1961

The following inclusion compounds were irradiated with cobalt-60 γ -rays: urea with 1,4-dichlorobutane (I), 1-chlorododecane (II), 1,5-dibromopentane (III), 1-bromodecane (IV), *n*-octadecane (V), sebacic acid (VI), cetyl alcohol (VII) and stearic acid (VIII); thiourea with 2-bromo-*n*-octane (IX), dicyclohexylamine (X), cyclohexanol (XI), cyclohexene (XII), cyclohexanone (XIII), 2,3-dimethylnaphthalene (XIV), 2-methylnaphthalene (XV) and camphene (XVI); and hydroquinone with sulfur dioxide (XVII) and hydrogen sulfide (XVIII). Comparisons were made with the corresponding irradiated physical mixtures in cases where the guest compounds were solid. From infrared absorption spectral evidence, explanations are suggested, based on spatial and chemical factors, for the occurrence or absence of interactions between host and guest and between components of the physical mixtures.

Organic inclusion compounds are characterized by a definite spatial relationship between the host and guest molecules.^{2,3} It would be expected that if such compounds were irradiated, the occurrence or absence of interactions between host and guest, the nature of such interactions if they occur, and the differences in these respects between an inclusion compound of two substances and a random physical mixture of the same substances might depend upon the contiguity or lack of contiguity of certain groups and atoms as well as upon their chemical characteristics. The aim of the work reported here was to survey several classes of inclusion compounds in order to see what the nature of such effects was. It was thought that such a study should make a contribution to the field of solid state irradiation reactions and serve as a guide for a more detailed study of individual inclusion compounds.

The polymerization by irradiation of a number of substances bound as channel compounds with thiourea and urea has been reported.⁴ That work was not concerned, however, with interaction between host and guest but only with stereospecific effects on the polymerization of the included monomers. A study also has been reported on the radiolysis of pentane adsorbed on synthetic zeolites.⁵

In this work the inclusion compounds listed in the Abstract were irradiated with cobalt-60 γ -rays in a nitrogen atmosphere to dosages of from 8.5 to 76 megareps. Corresponding to the compounds containing solid guest constituents (V, VI, VII, VIII, XIV, XV and XVI), physical mixtures of the guest and host compounds also were made and irradiated. Some of the compounds and mixtures, before and after irradiation, were separated into their components by treatment with water and solvent extraction. Infrared absorption spectra were obtained in order to determine whether interactions had occurred between host and guest and between the components of the physical mixtures and, where possible, to interpret the nature of the interaction.

Results

In Tables I, II and III are listed those infrared absorption bands of the irradiated and unirradiated samples and, where applicable, of the physical mixtures, for which irradiation caused a change in intensity, or a change in frequency of no less than 5 cm.^{-1} , or caused the appearance or disappearance of a band, except that the appearance or disappearance of weak shoulders was not listed. For XVII (see text) and XVIII the absorption band changes are given for the solids recovered by evaporating an aqueous solution of the clathrates before and after irradiation, as well as for the irradiated and unirradiated clathrates. For V, VIII and IX absorption band changes also are given for the water-soluble and ether-soluble or carbon tetrachloride-soluble fractions obtained from the irradiated and unirradiated compounds and mixtures after heating with water. (The fact that for V, VIII, IX, XVII and XVIII infrared absorption differences ascribable to irradiation are present even after solution and separation by solvents precludes the possibility of explaining the results that follow as being due to polymorphic modifications brought about by irradiation.)

The symbols s, m, and w in the tables refer, respectively, to strong absorption bands (peak height from baseline equal to 50 to 100% of the strongest band in the spectrum); medium (20 to 50%); and weak (less than 20%). The symbol sh refers to "shoulder." Absorption band frequencies are in cm.^{-1} .

Urea Channel Compounds.—The oxygenated compounds VI, VII and VIII show few changes (Table I), possibly because the presence of oxygen in the guest molecules minimizes the tendency for transfer of electrons from (oxygen-containing) urea. On the other hand, the corresponding physical mixtures are much more reactive, which emphasizes the significance of spatial factors. The data for the ether-soluble and water-soluble fractions of the water-treated irradiated and unirradiated mixtures and compounds V and VIII indicate that some irradiation effects persist even after separation of the compound and mixture into their components, and that these effects are not identical for the compound and the mixture.

The compounds II, III and IV (Table I) show varying degrees of change. It might be expected

(1) On leave from Research Laboratories, Organic Chemicals Division, American Cyanamid Company, Bound Brook, New Jersey (present address).

(2) W. Schlenk, *Ann.*, **565**, 204 (1949).

(3) H. M. Powell and J. H. Rayner, *Nature*, **163**, 566 (1949).

(4) J. F. Brown, Jr., and D. W. White, *J. Am. Chem. Soc.*, **82**, 5671 (1960); D. M. White, *ibid.*, **82**, 5678 (1960).

(5) J. W. Sutherland and A. O. Allen, *ibid.*, **83**, 1040 (1961).

TABLE I
INFRARED ABSORPTION BANDS OF UREA COMPOUNDS AND MIXTURES (CM.⁻¹)

1,4-Dichlorobutane compound (I) (15.0 mrep.) ^a (See text)		1,5-Dibromopentane compound (III) Before irradiation After irradiation (68 mrep.)		1-Bromodecane compound (IV) Before irradiation After irradiation (76 mrep.)	
		3262 w	3262 w, sh		
		3225 w	3226 s		
		2817 w	2790 w		
1-Chlorododecane compound (II) Before irradiation After irradiation (18.4 mrep.)		1675 w	1675 w, sh		
		1667 w	1661 s		
3400 s	3413 s	1626 w	1616 w	3226 s	3221 s
3218 s	3226 s	1486 w, sh	1486 w	1250 w	1250 w, sh
2981 w	2994 w	1464 s	1464 w, sh	1070 w	1064 w
1634 w, sh	1629 w, sh	1453 w, sh	1453 s		
1618 w, sh	1613 w, sh	1290 w	1290 w, sh		
1468 w, sh	1460 w, sh	1269 w	1274 w		
1379 w, sh	1379 w	785 m	787 s		
n-Octadecane (V)					
Mixture ^b		Ether-sol., after irradiation and hydrolysis of		Water-sol., after irradiation and hydrolysis of	
Before irradiation	After irradiation (26.8 mrep.)	Mixture	Compound	Mixture	Compound
3414 s	3401 s	3428 m	3410 w	2930 w	2912 w
3221 m	3215 m	1661 w	1656 w	1669 m	1678 m
1070 w	1058 w	1626 w	1618 w	1613 m	1618 m
	Compound	719 m	717 s	1543 w, sh	1538 w, sh
3390 s	3410 s			1527 w, sh	1520 w, sh
3218 m	3226 m				
1471 w, sh	1466 w, sh				
Sebacic acid (VI)					
Mixture ^d		Compound		Cetyl alcohol (VII)	
Before irradiation	After irradiation (21.8 mrep.) ^a	Before irradiation	After irradiation (21.8 mrep.) ^a	Before irradiation	After irradiation (15.3 mrep.) ^a
3413 s	3401 s	3367 w	3367 w, sh	3410 s	3425 s
3333 m	3356 s	1466 w, sh	1471 w, sh	3342 w, sh	3342 m
3218 m	3211 m	1453 w, sh	1460 w, sh	3262 w, sh	3262 w
2928 s	2928 m	943 w	952 w	3226 m	3229 w, sh
	1709 w			2915 s	2921 s
1484 w	1486 s			1630 w	1613 w
1462 s				1488 m	1486 w
1410 w	1408 w, sh			1462 m	1460 s
1321 w	1321 w, sh				1339 w
1302 s	1300 m			1163 m	1157 s
1253 w	1250 w, sh			1117 w	1117 w, sh
1238 s	1238 w			1099 w	1087 w
1186 m	1186 w, sh			1060 m	1062 w
1163 w, sh	1163 s			1039 w	1044 w
1156 s				955 w	1000 w
1011 w	1013 m			729 w	
1004 w					Compound
930 m	942 w			1681 w, sh	1681 w
753 w					
721 w	721 w, sh				
656 w					
Stearic acid (VIII)					
Mixture ^c		Ether-soluble after hydrolysis of		Water-soluble after hydrolysis of	
Before irradiation	After irradiation (8.5 mrep.) ^a	Unirradiated	Irradiated	Unirradiated	Irradiated
3419 s	3410 m	1645 w	1645 w, sh	3431 m	3448 m
3248 w, sh	3255 w, sh	1464 w	1464 m	3339 m	3344 w
1661 s	1661 w				2912 w
1464 s	1466 m	2916 s	2912 m	2845 w, sh	2845 w
1323 w	1330 w		803 w	2795 w	2804 w
1161 s	1156 s	725 w, sh	727 w	1592 w, sh	1592 s
1053 w	1064 w			1466 s	1458 s
1000 w, sh	1000 w			1156 s	1149 m
789 w, sh	788 s			1042 w	1047 w
784 s	784 w, sh				Compound
715 m	718 w			3346 w	3333 w
				2795 w	2793 m

Mixture ^c		Stearic acid (VIII)		Water-soluble after hydrolysis of Mixture	
Before irradiation	After irradiation (8.5 mrep.) ^a	Unirradiated	Irradiated	Unirradiated	Irradiated
Compound		1667 m	1675 m		
1290 w	1282 w			1460 s	1466 s
		787 m	786 s		
		715 w	715 m		

^a Sample also irradiated with 3-Mev. electrons to dose of 75 mrep. gave substantially the same spectrum. ^b Two grams of octadecane and 6.6 grams of urea. ^c Four grams of stearic acid and 11.8 grams of urea. ^d Three grams of sebacic acid and 9.69 grams of urea. ^e Three grams of hexadecanol-1 and 9.15 grams of urea.

TABLE II

INFRARED ABSORPTION BANDS OF THIOUREA COMPOUNDS AND MIXTURES (CM.⁻¹)

—2-Bromo- <i>n</i> -octane compound (IX)—		—Cyclohexanol compound (XI)—		—Cyclohexanone compound (XIII)—	
Before irradiation	After irradiation (14.4 mrep.)	Before irradiation	After irradiation (20.9 mrep.)	Before irradiation	After irradiation (18.4 mrep.)
1610 s	1610 w, sh	1701 w	1695 w	3276 w	3276 m
1590 w	1590 s	1647 w, sh	1653 w, sh	1812 w	1802 w
	1433 m	1468 s	1466 m	1715 m	1709 m
1412 m	1414 w		1195 w	1684 w, sh	1697 w, sh
1389 w, sh	1389 w	1024 w, sh	1024 w	1653 w, sh	1681 w, sh
730 s	730 w, sh	729 s	729 w, sh	1587 w, sh	1587 w
718 w	717 s	717 w, sh	717 s	1563 w, sh	1558 w, sh
CCl ₄ -sol. after hydrolysis of compound				1488 m	1484 w, sh
2954 m	2956 w	—Cyclohexene compound (XII)—		1475 w	1466 m
2928 m	2926 w	Before irradiation	After irradiation (68 mrep.)	1408 m	1403 m
2857 m	2851 w	3383 m	3383 w, sh	1389 w, sh	1379 w, sh
1463 m	1461 w	3282 w	3279 m	1307 w	1299 w
1451 w, sh	1451 w	3177 m	3165 m	1217 w	1209 w
977 w	978 m	2937 w, sh	2924 w, sh	1111 w	1105 w
		2915 w, sh	2915 w	1086 m	1081 m
H ₂ O-sol. after hydrolysis of compound			2849 w	1047 w	1047 w, sh
3175 m	3169 m	2833 w, sh	2833 w	906 w	898 w
1195 w	1200 w	1493 w, sh	1493 s	861 w	855 w
		1473 m	1477 w		
Dicyclohexylamine compound (X)		1408 s	1412 m		
	(19.6 mrep.) ^a	1134 w, sh	1134 w		
	(See text)	730 s	730 w, sh		
		717 w, sh	717 s		
—2,3-Dimethylnaphthalene (XIV)—		—2-Methylnaphthalene (XV)—		—Camphene (XVI)—	
Mixture ^c		Mixture ^e		Mixture ^g	
Before irradiation	After irradiation ^b (16.0 mrep.)	Before irradiation	After irradiation ^b (11.4 mrep.)	Before irradiation	After irradiation ^b (10.3 mrep.)
1764 w, sh	1764 w	1613 s	1618 s	3012 w, sh	3003 w, sh
875 m	875 s		1242 w †	1590 w, sh	1592 w
		1082 m	1082 s	1468 m	1468 s
		1053 w	1053 w, sh	1406 m	1408 s
		882 w	895 w	1235 w	1245 w
		848 w	854 w		1130 w ^h
		812 m	812 m †		877 w ^h
		† Absent at 75 mrep.			
Compound		Compound		Compound	
Before irradiation	After irradiation ^{b,d} (16.0 mrep.)	Before irradiation	After irradiation ^{b,d} (11.4 mrep.)	Before irradiation	After irradiation ^{b,d} (10.3 mrep.)
3061 w, sh	3050 w, sh		1712 w		
2725 w	2717 w, sh	1563 w, sh	1558 w, sh	1590 w, sh	1590 w
2679 w	2668 w	813 s	813 m	1487 w	1487 m
1808 w	1803 w	764 w	764 w, sh	1471 m	1466 m
	1739 w*	720 s	720 s †	1408 m	1389 w
		† At 75 mrep. and no exposure to air—720 w, sh		1049 w, sh	1052 w
1464 w	1466 w, sh				796 w
	890 w			729 w	729 w, sh §
	* (75 mrep.)			§ At 75 mrep.—741 w	

^a Sample irradiated with 3-Mev. electrons to dose of 75 mrep. gave substantially the same spectrum. ^b Possible exposure of tube contents to air by breakage during irradiation. ^c 7.33 grams of thiourea and 3 grams of 2,3-dimethylnaphthalene. ^d Substantial agreement with spectrum from sample irradiated with 3-Mev. electrons to dose of 75 mrep. and avoidance of tube breakage and exposure to air. ^e 8.19 grams of thiourea and 3 grams of 2-methylnaphthalene. ^f After irradiation of a sample to a dose of 75 mrep. with 3-Mev. electrons, spectrum taken in a Perkin-Elmer Model 321 Spectrophotometer was substantially identical except for the absence of 1242 w and 812 m. ^g 7.6 grams of thiourea and 4 grams of camphene. ^h After dose of 75 mrep. of 3-Mev. electrons.

TABLE III
INFRARED ABSORPTION BANDS OF HYDROQUINONE-HYDROGEN SULFIDE CLATHRATE (XVIII) (FOR SULFUR DIOXIDE CLATHRATE (XVII) SEE TEXT)

Unirradiated	Irradiated (11.2 mrep.)	Residue after hydrolysis of—	
		Unirradiated	Irradiated
	2493 w	4861 w	
1639 w	1645 w	3668 w	3660 w
1600 w	1605 w	3262 w	
1120 w, sh	1120 w	1923 w, sh	1923 w 1730 w

that I, also a halogen derivative, would undergo reaction. Yet it did not. The explanation for this apparent anomaly probably lies in the fact that the crystal lattice of I is different⁶ from that which is common to all the others, so that in spite of the presence of chlorine, transfer of electrons is impeded by lack of juxtaposition of suitable groups. V showed a similar reactivity for mixture and compound, but the bands affected for each are not the same, which is also true for the ether-soluble and water-soluble fractions (Table I). With such a non-polar compound the spatial factors might determine which bands are affected.

The impossibility of irradiating mixtures of the solid components of I, II, III and IV without resorting to special freezing techniques prevented a direct comparison between mixture and channel compound such as was obtained with V, VI, VII and VIII. The question could be asked whether some of the effects ascribed to irradiation of the channel compound for II, III and IV could not have been due to independent effects for each of the components. Lack of reaction in I would, however, seem to indicate that any effects on the individual components in II, III and IV would have had to result from the presence of both components, and must, therefore, have been mediated by the spatial arrangements in the channel compound.

Thiourea Channel Compounds.—Of the thiourea compounds (Table II) only X showed no change. Yet XI, XII and XIII, also cyclohexane derivatives, reacted strongly. For X it is a question whether lack of reaction was caused by failure of the NH group of the guest molecule to act as a more powerful electron acceptor from the CS group in thiourea than the NH₂ groups in thiourea did, or whether the NH group of the guest molecule is spatially inaccessible to reaction with thiourea.

Of the seven thiourea compounds affected by radiation, five showed some change in the band at or near 730, which has been assigned^{7,8} to a composite CS and NCN stretch, NH₂ bending and CN stretch, or in the associated band at about 714–720, or in both. In some there was a weakening of the 730 band and a strengthening of the band at about 718, or a shift of both bands to lower wave numbers, whereas uncomplexed thiourea (Table IV) after irradiation to 75 mrep., had its absorption strengthened around 730 and showed no band at about 718. The changes for the inclusion compounds in these regions could be caused either by hydrogen bonding of the NH₂ or CS group of thio-

urea by the guest molecule for some compounds, or by a loosening of hydrogen bonds already formed in the inclusion compound for others. The band around 1470, which has been assigned,⁸ together with 730, to a CN stretching mode, was affected along with the 730 and 720 bands for some of the compounds.

TABLE IV
INFRARED ABSORPTION SPECTRUM OF THIOUREA BEFORE AND AFTER IRRADIATION

Before irradiation ^a	After irradiation ^b (75 mrep. ^c)
3366 s	
3270 w	3250 m
3150 m	
3100 w, sh	3080 w, sh
2920 w	
2680 w	
1730 w	
1613 s	1600 s
1590 w, sh	1560 w, sh
1498 w, sh	1543 w, sh
1475 s	1455 m
1415 s	1400 m
	1228 w
	769 w
	728 s
730 m	

^a Grubb Parsons double-beam GS2 spectrophotometer.

^b Perkin-Elmer Model 321 infrared spectrophotometer.

^c 3-Mev. electrons.

Band changes for the water-soluble and carbon tetrachloride-soluble fractions of compound IX (Table II) indicate that some of the irradiation effects persisted even after resolution of the compound into its components.

Hydroquinone Clathrates.—Irradiation of the hydroquinone-sulfur dioxide clathrate XVII to a dose of 11.4 mrep. resulted in no spectral change except for the formation of a weak band at 803. The residue left after sulfur dioxide was driven off by heating with water showed, upon irradiation, a shift from 3257 s to 3283 s and from 2331 w to 2326 w. These bands were absent in the clathrate. These changes point to an irradiation reaction for which the infrared evidence seems to have been hidden by clathration. Another possible explanation would be that irradiation had sensitized the hydroquinone so that a reaction occurred upon heating with water and drying. It also was found that sulfur was present in the liberated fractions to varying extents, but this could not be definitely identified as being due to an irradiation effect.

With the hydroquinone-hydrogen sulfide clathrate XVIII (Table III) there are several differences between the irradiated and unirradiated samples. A weak band appeared at 2493, which is absent after heating with water and is therefore not due to hydroquinone. It may be an SH band, indicating thiol formation by irradiation. With the hydroquinone-hydrogen sulfide clathrate, as with the sulfur dioxide clathrate, binding of sulfur occurred to varying degrees in the products obtained after heating with water. This too could not be definitely identified as being due to an irradiation effect. As with the hydroquinone-sulfur dioxide clathrate, the

(6) W. Schlenk, *Ann.*, **565**, 233 (1949).

(7) E. Spinner, *Spectrochim. Acta*, **12**, 99 (1959).

(8) J. E. Stewart, *J. Chem. Phys.*, **26**, 252 (1957).

residue after heating with water showed some differences between the irradiated and unirradiated.

In addition to differences between the products obtained by heating the irradiated and unirradiated clathrates with water, there are differences in absorption between the products of water-treatment of the unirradiated sulfur dioxide and hydrogen sulfide clathrates. This, together with retention of sulfur, already noted, would indicate that reversion of the clathrate to hydroquinone by release of hydrogen sulfide and sulfur dioxide, respectively, is not an uncomplicated process, at least in the presence of water and air, but may be accompanied by the formation of by-products.

Experimental

Preparation of Inclusion Compounds.—Compounds XVII and XVIII were prepared by passing SO_2 and H_2S , respectively, into aqueous solutions of hydroquinone. The thiourea and urea channel compounds were prepared by crystallization from a solution of the components, as directed by Schlenk,^{2,9} or by closely analogous procedures. Intermediates used were of the best commercially available grades. The inclusion compounds were freed of solvent by pressing between absorbent paper and drying in a desiccator over a suitable reagent at room temperature.

Irradiations.—Eight-cm. lengths of 1-cm. diameter borosilicate glass tubing were drawn out at both ends. About a 1-g. sample was spread evenly over the length of the tube, and nitrogen, purified by passage over heated copper, was passed over the sample to displace the air. The tube was sealed at both ends during the passage of the nitrogen stream.

The sample tubes were exposed to a cobalt-60 γ -ray flux at a dose rate of 0.17 or 0.05 mrep. per hour, depending on the position in the irradiator.

The infrared absorption curves of some of the compounds

(9) W. Schlenk, *Ann.*, **573**, 159 (1951).

and mixtures were confirmed, as indicated in the Results on separate samples irradiated beforehand with an electron flux under a beam of 3-Mev. electrons from a Van de Graaff accelerator while the tubes were immersed in ice-water to prevent heating above 20–25°.

Infrared Absorption Curves.—The infrared absorption curves, from which the bands reported in the Results were taken, were obtained on samples incorporated into potassium bromide discs and run on a Grubb Parsons double-beam GS2 spectrophotometer. Confirmatory curves run on the samples irradiated with 3-Mev. electrons were obtained with samples in potassium bromide discs run on a Perkin-Elmer Model 321 Infrared Spectrophotometer, which has a coarser resolution than the Grubb Parsons spectrophotometer.

Acknowledgment.—I am grateful to Prof. J. J. Weiss for the use of his laboratory and for helpful consultations; to Dr. R. E. Dodd for assistance in the interpretation of infrared curves; to Mrs. B. S. Crawford, for infrared curves on the Grubb Parsons spectrophotometer; to Dr. R. F. Stamm and Mr. G. Butler of the Stamford, Connecticut, Laboratories of American Cyanamid Company for carrying out irradiations with 3-Mev. electrons and to Dr. R. F. Stamm for his criticism of the manuscript; to Dr. J. L. Gove and Mr. T. C. Mowatt of the Bound Brook, New Jersey, Research Laboratories of American Cyanamid Company for infrared curves on the Perkin-Elmer Spectrophotometer; to Mr. D. Stewart, at the same location, for help in collating the infrared data; and to Prof. S. W. Fenton, Department of Chemistry, University of Minnesota, for his criticism of the manuscript.

I also thank the American Cyanamid Company for a research and travel leave and grant which made this work possible.

DETERMINATION OF MOLECULAR WEIGHTS OF CHARGED POLYMERS FROM EQUILIBRIUM ULTRACENTRIFUGATIONS

By STIG R. ERLANDER

Northern Regional Research Laboratory,¹ Peoria, Illinois

Received May 15, 1961

Equations for determining the weight and Z-average molecular weights of charged polymers are derived. The results indicate that the concentration dependence of charged or uncharged polymers is a function of the concentration coefficient term B , the weight-average molecular weight, and the concentration of the polymer where all are obtained at both the meniscus and bottom of the centrifuge cell. The concentration dependent term in determining the Z-average molecular weight from $1/\bar{M}_z^{\text{app}} = 1/\bar{M}_z + B'C$ appears to be $2(\bar{M}_w/\bar{M}_z)$ times as large as that obtained in determining the weight-average molecular weight. The equations have been applied to the schlieren and interference optical systems.

Johnson, Kraus and Scatchard² derived certain equations for determining the degree of polymerization of a charged solute. They redefined their polymeric component as $\{\text{PX}_z - (Z/2)\text{BX}\}$ instead of PX_z where P is the polymer having a net charge of Z , X is the associated anion (or cation) and BX is the buffer or salt present in the three component system. By subtracting $(Z/2)\text{B}^+$ ions plus $(Z/2)\text{X}^-$ ions (or a total of Z ions) from the sum of $(Z + 1)$ ions (the dissociation of PX_z into

$\text{P}^{+Z} + \text{ZX}^-$), the result is that one ion (P^{+Z}) remains. Johnson, *et al.*,² concluded that this definition of the polymeric component reduces the errors in determining the degree of polymerization from refraction index data. They have applied this definition to both the schlieren² and interference optical systems.³ The resulting equation $N = [S/A_2'/1 - (Z'\eta S/A_2')]$ derived in their first paper² (their equation 29) has been examined briefly by Williams, *et al.*,⁴ in their review. In this equation N is the degree of polymerization, A_2

(1) A laboratory of the Northern Utilization Research and Development Division, Agricultural Research Service, U. S. Department of Agriculture. Article not copyrighted.

(2) J. S. Johnson, K. A. Kraus and G. Scatchard, *J. Phys. Chem.*, **58**, 1034 (1954).

(3) J. S. Johnson, G. Scatchard and K. A. Kraus, *ibid.*, **63**, 787 (1959).

(4) J. W. Williams, K. E. Van Holde, R. L. Baldwin and H. Fujita, *Chem. Revs.*, **58**, 733 (1958).

$= M_2(1 - \bar{V}_2 \rho)\omega_2/2RT$, \bar{V}_2 = the partial specific volume, ρ = the density of the solution,⁵ ω = the angular velocity, R = the gas constant, T = absolute temperature, $A_2 = A_p x_2 - (Z/2)$, $A_{BX} = A_p - (Z/2) A_B$, $n = Zm_2/2m_3$, $m_2 = m_p$ = molality of component -2 or the polymeric component, $m_3 = (m_B) + (Z/2)m_2$, m_B = molality of the buffer, $S = d \ln m_2/d(r^2) = d \ln (dm_2/r dr)/d(r^2) = d \ln (dn^*/r dr)/d(r^2)$, r is the distance from the center of the rotor to a specific position in the centrifuge cell and dn^*/dr is the refractive index of the solution minus the refraction index of the solvent in a double sector cell. The prime designates those values for the monomer unit. The assumption² that $d \ln (dm_2/r dr) = d \ln m_2$ can be shown to be essentially equivalent to the assumption that the Z -average and weight average degrees of polymerization are equal: $(\bar{M}_z)_2 = (\bar{M}_w)_2$. This equality was implied in a later paper by Johnson, Kraus and Holmberg.⁶

Johnson, *et al.*,^{2,3,6} were interested primarily in obtaining the degree of polymerization (N , N_w or N_z). In this paper equations are derived for the molecular weight of a polyelectrolyte, and not for its degree of polymerization, by defining the components in the same manner as Johnson, *et al.*^{2,3,6} In addition, the concentration coefficient for the weight and Z -average molecular weights for a specific radius and for the entire sample are derived for a heterogeneous polymer. The resulting equations are applied to the schlieren and interference optical systems.

Homogeneous Solute in a Three-component System.—From the equations of Johnson, *et al.*,^{2,6} using the definitions given

$$d \ln a_2 = d \ln m_2 m_x^{Z/2} m_B^{-Z/2} G_2 = A_2 d(r^2) \quad (1)$$

where a_2 is the activity of component -2; m_2 , m_x and m_B are the molalities of components 2, X and B; and G_2 is the activity coefficient product³ of component -2. Now $m_3 = m_B + (Z/2)m_2 = m_x - (Z/2)m_2$. Substitution of this m_x into equation 1 yields

$$d \ln a_2 = d \ln \left[m_2 \left(\frac{m_B + Zm_2}{m_B} \right)^{Z/2} G_2 \right] = A_2 d(r^2) \quad (2)$$

Separation and differentiation of the logarithm terms in equation 2 gives

$$2A_2 = \left(\frac{1}{m_2} \right) \left(\frac{dm_2}{r dr} \right) \left\{ 1 + \frac{m_2 d}{dm_2} \left[\left(\frac{Z}{2} \right) \ln \left(\frac{m_B + Zm_2}{m_B} \right) + m_2 \left(\frac{d \ln G_2}{dm_2} \right) \right] \right\} \quad (3)$$

Since

$$\frac{m_2 d}{dm_2} \left\{ \left(\frac{Z}{2} \right) \ln \left[\frac{(m_B + Zm_2)/m_B}{m_B} \right] \right\} = \frac{m_2}{dm_2} \left\{ \left(\frac{Z}{2} \right) \left[\frac{d(Zm_2/m_B)}{(m_B + Zm_2)/m_B} \right] + \ln \left[1 + \left(\frac{Zm_2}{m_B} \right) \right]^{1/2} \right\}$$

equation 3 then can be put into the form

(5) R. J. Goldberg, *J. Phys. Chem.*, **57**, 194 (1953).

(6) J. S. Johnson, K. A. Kraus and R. W. Holmberg, *J. Am. Chem. Soc.*, **78**, 26 (1956).

$$2A_2 = \left(\frac{1}{m_2} \right) \left(\frac{dm_2}{r dr} \right) \left\{ 1 + \left(\frac{d \ln G_2}{dm_2} \right) m_2 + \frac{\left(\frac{Z^2}{2} \right) \left[1 - \left(\frac{m_2}{m_B} \right) \left(\frac{dm_B}{dm_2} \right) \right] m_2}{(m_B + Zm_2)} + \left[\ln \left[1 + \left(\frac{Zm_2}{m_B} \right) \right]^{1/2} + \frac{1}{2 \left[1 + \left(\frac{m_B}{Zm_2} \right) \right]} \right] \left(\frac{dZ}{dm_2} \right) m_2 \right\} \quad (4)$$

If we assume that the solution is dilute enough so that molarities and molalities are essentially equivalent, then substitution of $m_2 = C_2/M_2$ and of $m_B = C_B/M_B$ (where C is in weight per volume units and M is the molecular weight of the respective component) into equation 4 gives

$$2A_2 = \left(\frac{1}{C_2} \right) \left(\frac{dC_2}{r dr} \right) \left\{ 1 + \left(\frac{d \ln G_2}{dC_2} \right) C_2 + \frac{\left(\frac{Z^2}{2M_2} \right) \left[1 - \left(\frac{d \ln C_B}{d \ln C_2} \right) \right] C_2}{\left[\left(\frac{C_B}{M_B} \right) + \left(\frac{Z}{M_2} \right) C_2 \right]} + \left(\ln \left[1 + \left(\frac{Z}{M_2} \right) \left(\frac{M_B C_2}{C_B} \right) \right] \right)^{1/2} + \frac{1}{2 \left[1 + \left(\frac{M_2}{Z} \right) \left(\frac{C_B}{M_B C_2} \right) \right]} \right\} \left(\frac{dZ}{dC_2} \right) C_2 \quad (5)$$

If we assume that $(ZC_2/M_2) \ll C_B/M_B$, that $d \ln C_B/d \ln C_2 \ll 1$, and that $dZ/dC_2 = 0$, then equation 5 becomes

$$2A_2 = \frac{M_2(1 - \bar{V}_2 \rho)\omega^2}{RT} = \frac{1}{C_2} \left(\frac{dC_2}{r dr} \right) \left\{ 1 + \left[\frac{d \ln G_2}{dC_2} + \frac{Z^2 M_B}{2M_2 C_B} \right] C_2 \right\} \quad (6)$$

where $A_2 = A_p - (Z/2) A_B$.

The equation by Williams, *et al.*,⁴ using equation 29 of Johnson *et al.*,⁶ for N is

$$M_2 \frac{(1 - \bar{V}_2 \rho)\omega^2}{RT} = \frac{1}{C_2} \left(\frac{dC_2}{r dr} \right) \left[1 + \left(\frac{Z^2 M_B}{2M_2 C_B} \right) C_2 \right] \quad (7)$$

Consequently, the assumptions for equation 6 are essentially equivalent to the assumptions⁶ that $1 - \eta^2 = 1$ and $d \ln m_3/d(r^2) = 0$ where $\eta = ZM_2/2M_3$ and $m_3 = m_B + (Z/2)m_2$.

Heterogeneous Solute in a Three-component System. Determination of $\bar{M}_{w,r}$ and $\bar{M}_{z,r}$.—For multicomponent⁷ charged polymers equation 5 can be put into the following form for the i th component of the polymer (PX-(Z/2)BX) at a specific radius r

$$2A_i = \frac{M_i(1 - V_i \rho)\omega^2}{RT} = \left(\frac{1}{C_i} \right) \left(\frac{dC_i}{r dr} \right) \left[1 + K_i C_i \right] \quad (8)$$

where

$$K_i = \frac{d \ln G_i}{dC_i} + \frac{\left(\frac{Z_i}{M_i} \right)^2 \left[1 - \left(\frac{d \ln C_B}{d \ln C_i} \right) \right] M_i}{2 \left[\frac{C_B}{M_B} + \frac{Z_i C_i}{M_i} \right]} + \left\{ \ln \left[1 + \left(\frac{Z_i}{M_i} \right) \left(\frac{M_B C_i}{C_B} \right) \right] \right\}^{1/2} + \frac{1}{2 \left[1 + \left(\frac{M_i}{Z_i} \right) \left(\frac{C_B}{M_B C_i} \right) \right]} \left\{ \left[\frac{d(Z/M_i)}{dC_i} \right] M_i \right\}$$

(7) S. R. Erlander and J. F. Foster, *J. Polymer Sci.*, **37**, 103 (1959).

and where

$$A_i = A_{pi} - \left(\frac{Z_i}{2}\right) A_B$$

and assuming interactions between different species are negligible. For the heterogeneous polymer the subscript "2" has been dropped. In terms of molecular weights the definition of A_i becomes⁸

$$M_i = (M_p)_i \left[1 - \left(\frac{Z_i}{2}\right) \left(\frac{M_B}{(M_p)_i}\right) \frac{(1 - \bar{V}_B \rho)}{(1 - (\bar{V}_p)_i \rho)} \right] \frac{(1 - (\bar{V}_p)_i \rho)}{(1 - \bar{V}_i \rho)} \quad (9)$$

It can be assumed in equation 9 that $\bar{V}_i = (\bar{V}_p)_i$. Equation 8 can be put into the form

$$2A_i = \frac{1}{C_i} \left(\frac{dC_i}{r dr}\right) [1 + B_i M_i C_i] \quad (10)$$

where

$$B_i = K_i/M_i$$

If all the values of B_i are the same ($B_i = B$) and in addition $[d(Z'/M')/dC]_i = 0$, then B can be expressed as

$$B = \frac{d \ln G'}{M' dC} + \frac{1}{2} \left(\frac{Z'}{M'}\right)^2 \left[\frac{1 - \left(\frac{d \ln C_B}{d \ln C}\right)}{\left(\frac{C_B}{\bar{M}_B}\right) + \left(\frac{Z'C}{\bar{M}'}\right)} \right] \quad (11)$$

The primed values represent the values for the monomer unit. Any molecular average such as the weight of Z -average also could be substituted for these primed values as long as the ratio (Z'/M') is the same for all monomer units. In addition, $C' = C$ since the concentration is based on weight per unit volume and not moles per unit volume.

The quantity B_i would appear to be more constant than K_i for different polymer species since B_i is proportional to $(Z_i/M_i)^2$ instead of (Z_i^2/M_i) as in K_i . Also $(d \ln G_i/dC_i)/M_i$ may be more constant than $(d \ln G_i/dC_i)$ because the quantity $(d \ln G_i/dC_i)$ most likely increases with molecular weight.

Assuming that all B_i are the same, summing over all n terms, and putting all terms under a common denominator gives

$$\frac{2 \sum_{i=1}^n A_i C_i \prod_{\substack{j=1 \\ j \neq i}}^n [1 + B M_j C_j]}{\prod_{i=1}^n [1 + B M_i C_i]} = \frac{d \sum_{i=1}^n C_i}{r dr} \quad (12)$$

If all of the B and higher terms (*i.e.*, all C^2 and higher terms) in the numerator and all of the B^2 and higher terms (*i.e.*, all C^2 and higher terms) in the denominator of equation 12 are eliminated, then equation 12 can be written as

$$\frac{2 \sum_{i=1}^n A_i C_i}{1 + B \sum_{i=1}^n M_i C_i} = \frac{d \sum_{i=1}^n C_i}{r dr} \quad (13)$$

Now the definition⁹ of a weight-average value

(8) It should be pointed out that for ultracentrifugation studies the relationship $M_2 = M_p - (Z/2)M_B$ is not true. That is, the activities of the polymer and the buffer are related to (S/D) values and not to molecular weight values as in the case of osmotic pressure. Hence, the relationship $(S/D)_2 = (S/D)_p - (Z/2)(S/D)_B$ or its equivalent $A_2 = A_p - (Z/2)A_B$ must be used instead of $M_2 = M_p - (Z/2)M_B$.

is $\bar{M}_w = \sum M_i C_i / \sum C_i$. Thus $\sum M_i C_i = \bar{M}_w C$ or $\sum A_i C_i = \bar{A}_w C$ where $C = \sum C_i$ when the summation is carried out over all terms. It must be assumed⁷ that all partial specific volumes are the same ($V_i = V$) in order that $\sum M_i C_i = \bar{M}_w C$ or $\sum M_i N_i = \sum C_i = C$. Substitution of these values into equation 13 gives

$$\frac{2\bar{A}_w C}{1 + B\bar{M}_w C} = \frac{dC}{r dr} \quad (14)$$

or upon rearrangement

$$2\bar{A}_{w,r} = \left(\frac{1}{C_r}\right) \left(\frac{dC}{r dr}\right)_r [1 + B_r \bar{M}_{w,r} C_r] \quad (15)$$

where the subscript "r" has been added to emphasize that this equation is true only at a specific point r . Again, if we assume that all partial specific volumes of the n species are the same ($\bar{V}_i = \bar{V}$), then equation 15 becomes

$$\frac{1}{\bar{M}_{w,r}^{app.}} = \frac{1}{\bar{M}_{w,r}} [1 + B_r \bar{M}_{w,r} C_r] \quad (16)$$

where

$$\bar{M}_{w,r}^{app.} = \left[\frac{RT}{(1 - \bar{V}_p)\omega^2} \right] \left(\frac{1}{C_r} \right) \left(\frac{dC}{r dr} \right)_r$$

$$B_r = \frac{K_r}{\bar{M}_{w,r}} = \left\{ \frac{[d \ln \bar{G}_2 dC]_w}{\bar{M}_w} + \left(\frac{1}{2} \right) \left(\frac{Z_w}{\bar{M}_w} \right)^2 \left[\frac{1 - \left(\frac{d \ln C_B}{d \ln C} \right)}{\left[\frac{C_B}{\bar{M}_B} + \frac{Z_w C}{\bar{M}_w} \right]} \right] \right\}_r$$

assuming, as in equation 11, that $B_i = B$ and that $(dZ/dC)_i = 0$.

To determine the Z -average molecular weight, equation 8 may be multiplied by A_i and summed as in equation 13, again assuming that all B and higher terms of B in the numerator and all B^2 and higher terms of B in the denominator are zero. Thus

$$\frac{2 \sum_{i=1}^n A_i^2 C_i}{1 + B \sum_{i=1}^n M_i C_i} = \frac{d \sum_{i=1}^n A_i C_i}{r dr} \quad (17)$$

If the definitions^{7,9} of Z - and weight-average values are used, then $\sum A_i^2 C_i = \bar{A}_z \bar{A}_w C$ and $\sum A_i C_i = \bar{A}_w C$. By substituting these values into equation 17 and using equation 15 for the definition of $\bar{A}_{w,r}$, equation 17 yields at the point r

$$\frac{2\bar{A}_z \bar{A}_w C}{(1 + B\bar{M}_w C)} = \frac{d(\bar{A}_w C)}{r dr} \quad (18)$$

or

$$2\bar{A}_z = d \left[\frac{\left(\frac{dC}{r dr}\right) (1 + B\bar{M}_w C)}{dC} \right] \quad (19)$$

Thus in a plot of $[(dC/r dr) (1 + B\bar{M}_w C)]$ versus C the tangent to the curve at the point C_1 (or r_1) equals $2\bar{A}_{z,r_1}$. At a variable point C_2 on the curve, the C coordinate will change from C_1 to C_2 or a difference of $\Delta C = C_2 - C_1$. The corre-

(9) W. C. Lansing and E. O. Kraemer, *J. Am. Chem. Soc.*, **57**, 1369 (1935).

sponding change in the other coördinate is $\Delta[(dC/dr)(1 + B\bar{M}_wC)] = (dC/dr)_2(1 + B\bar{M}_wC)_2 - (dC/dr)_1(1 + B\bar{M}_wC)_1$. The slope of the chord between these two points will approach the tangent to the curve at C_1 as point 2 approaches point 1. Consequently, the differential equation 19 can alternatively be defined as

$$2\bar{A}_{z,r} = \lim_{\substack{\Delta C \rightarrow 0 \\ \text{or } \Delta r \rightarrow 0}} \left[\frac{\Delta \left[\frac{dC}{r dr} (1 + B\bar{M}_wC) \right]}{\Delta C} \right] = \lim_{\Delta r \rightarrow 0} \quad (20)$$

$$\left[\frac{\left(\frac{dC}{r dr} \right)_2 (1 + B\bar{M}_wC)_2 - \left(\frac{dC}{r dr} \right)_1 (1 + B\bar{M}_wC)_1}{C_2 - C_1} \right]$$

where $\Delta r = r_2 - r_1$. Multiplying numerator and denominator by $(1 + B_1\bar{M}_{w1}C_1)(1 + B_2\bar{M}_{w2}C_2)$, equation 20 then becomes

$$2\bar{A}_{z,r} = \lim_{\Delta r \rightarrow 0} \left[\frac{(1 + B_1\bar{M}_{w1}C_1)(1 + B_2\bar{M}_{w2}C_2) \left(\frac{dC}{r dr} \right)_2 - (1 + B_1\bar{M}_{w1}C_1)(1 + B_2\bar{M}_{w2}C_2) \left(\frac{dC}{r dr} \right)_1}{(C_2 - C_1)(1 + B_1\bar{M}_{w1}C_1)(1 + B_2\bar{M}_{w2}C_2)} \right] \quad (21)$$

which is true where molarities can be substituted for molalities. Assuming that $(1 + B_1\bar{M}_{w1}C_1)(1 + B_2\bar{M}_{w2}C_2) = 1 + B_1\bar{M}_{w1}C_1 + B_2\bar{M}_{w2}C_2$ and that $(C_2 - C_1)(1 + B_1\bar{M}_{w1}C_1) = (C_2 - C_1)(1 + B_2\bar{M}_{w2}C_2) = C_2 - C_1$, i.e., all C_1C_2 , C_1^2 or C_2^2 terms are negligible or all B^2 terms in the numerator and B and B^2 terms in the denominator are negligible, we have

$$2\bar{A}_{z,r} = \lim_{\Delta r \rightarrow 0} \left[\frac{(1 + B_1\bar{M}_{w1}C_1 + B_2\bar{M}_{w2}C_2) \Delta \left(\frac{dC}{r dr} \right)}{\Delta C} \right] \quad (22)$$

Letting Δr approach zero gives

$$2\bar{A}_{z,r} = \frac{(1 + 2B_r\bar{M}_{w,r}C_r) d \left(\frac{dC}{r dr} \right)}{dC} \quad (23)$$

As in equations 15 and 16 where $\bar{V}_i = \bar{V}$, equation 23 can be put into the form

$$\frac{1}{\bar{M}_{z,r}^{app.}} = \frac{1}{\bar{M}_{z,r}} [1 + 2B_r\bar{M}_{w,r}C_r] \quad (24)$$

where B_r is defined as in equations 16 or 11 and

$$\bar{M}_{z,r}^{app.} = \left[\frac{RT}{(1 - \bar{V}_p)\omega^2} \right] \left[\frac{d \left(\frac{dC}{r dr} \right)}{dC} \right]$$

Equations 16 and 24 can be simplified by assuming that $Z_wC/\bar{M}_w \ll C_B/M_B$, that $(d \ln C_B/d \ln C) \ll 1$, and that $(dZ/dC) = 0$. These assumptions would be equivalent to those made by Johnson, *et al.*,² as illustrated in deriving equation 6.

The definition as given above in equation 9 for M_i is $M_i = M_{pi} - (Z_i/2)M_BQ$ where $Q = (1 - \bar{V}_{Bp})/(1 - \bar{V}_{pp})$ assuming that $V_{pi} = V_p$ for all i th species and that $\bar{V}_{pi} = \bar{V}_i$. Using this definition and in addition assuming as pointed out by Johnson, *et al.*,³ that $C_p = C_2$ as in their equation 3 and that $(Z_i/M_{pi}) = (Z'/M_p') = \text{constant}$, then the definition of \bar{M}_w or $\bar{M}_{w,r}$ as given in the above equations is

$$\bar{M}_w = \frac{\Sigma M_i C_i}{\Sigma C_i} = \frac{\Sigma M_{pi} C_{pi}}{\Sigma C_{pi}} - \frac{Q(M_B/2)\Sigma Z_i C_{pi}}{\Sigma C_{pi}}$$

or

$$\bar{M}_w = (\bar{M}_w)_p - Q \left(\frac{M_B}{2} \right) Z_w = (\bar{M}_w)_p \left[1 - \left(\frac{M_B}{2} \right) \left(\frac{Z'}{M_p'} \right) \left(\frac{1 - \bar{V}_{Bp}}{1 - \bar{V}_{pp}} \right) \right] \quad (25)$$

since $\Sigma Z_i C_{pi} = \Sigma (Z_i/M_{pi}) M_{pi} C_{pi} = (Z'/M_p') \Sigma M_{pi} C_{pi}$ assuming Z_i/M_i is constant for all i th species. Correspondingly, the definition of \bar{M}_z is

$$\bar{M}_z = \frac{\Sigma M_z^2 C_i}{\Sigma M_i C_i} = \frac{\Sigma M_{pi}^2 C_{pi} - Q M_B \Sigma Z_i M_{pi} C_{pi} + \left(\frac{Q M_B}{2} \right)^2 \Sigma Z_i^2 C_{pi}}{\Sigma M_{pi} C_{pi} - Q \left(\frac{M_B}{2} \right) \Sigma Z_i C_{pi}} \quad (26)$$

Assuming as in equation 25 that $Z_i/M_i = Z'/M_p' = \text{a constant}$ and dividing numerator and denominator by $\Sigma M_{pi} C_{pi}$, then

$$\bar{M}_z = (\bar{M}_z)_p - Q M_B \left(\frac{Z'}{M_p'} \right) (\bar{M}_z)_p + \left(\frac{Q M_B}{2} \right)^2 \left(\frac{Z'}{M_p'} \right)^2 (\bar{M}_z)_p \left[1 - Q \left(\frac{M_B}{2} \right) \left(\frac{Z'}{M_p'} \right) \right]$$

or

$$\bar{M}_z = (\bar{M}_z)_p \left[1 - \left(\frac{M_B}{2} \right) \left(\frac{Z'}{M_p'} \right) \left(\frac{1 - \bar{V}_{Bp}}{1 - \bar{V}_{pp}} \right) \right] \quad (27)$$

If it is assumed that $(m_p)_i = m_i$ as given in the Introduction and in the paper by Johnson, *et al.*,² then C_i is unequal to $(C_p)_i$. Assuming that molarities are equal to molalities as in equation 5, then $(C_i/M_i) = (C_p/M_p)_i$ or $C_i = C_{pi}(M_i/M_{pi}) = C_{pi}[1 - (QM_B/2)(Z'/M_p')]$. Thus assuming that Z_i/M_{pi} is the same for all i th species, then C_i equals C_{pi} times a constant. For equations 25, 26 and 27 this constant, i.e., $[1 - Q(M_B/2)(Z'/M_p')]$ cancels. Since equations 25, 26 and 27 convert the *extrapolated* molecular weight to the molecular weight of the polymer at infinite dilution, then the assumption that molarities are equal to molalities is true. Consequently, the same result is obtained assuming either $(m_p)_i = m_i$ or $(C_p)_i = C_i$. From equations 25 and 27 and the definition of M_i , the same quantity must be divided into M_i , \bar{M}_w or \bar{M}_z in order to obtain the corresponding molecular weight of the polymer, i.e., the quantity $[1 - (M_B Z'/2M_p')((1 - \bar{V}_{Bp})/(1 - \bar{V}_{pp}))]$.

Equations 16 and 24 show that the concentration dependence for determining $\bar{M}_{z,r}$ is $2(\bar{M}_{w,r}/\bar{M}_{z,r})$ times as large as that for determining $\bar{M}_{w,r}$ from an equation of the form $1/M(\text{app.}) = (1/M) + BC$. This ratio equals exactly two if the equation is in the form $1/M(\text{app.}) = (1/M)(1 + KC)$. This result is expected since Van Holde and Baldwin¹⁰ have shown that the concentration dependence for calculating the molecular weight of a single species using an \bar{M}_z equation is twice the concentration dependence using an \bar{M}_w equation. However, for heterogeneous systems the two "B" coefficients will be equal if $\bar{M}_{z,r} = 2\bar{M}_{w,r}$. Thus, the constants for the concentration dependence of $\bar{M}_{w,r}$ and $\bar{M}_{z,r}$ may be another test for heterogeneity.

(10) K. E. Van Holde and R. L. Baldwin, *J. Phys. Chem.*, **62**, 734 (1958).

Similar equations to equations 16 and 24 can be developed assuming that all K_i are equal instead of assuming that all B_i are equal. In this case $K_i = K$ would be substituted for BA_i in equation 12 with the result that K_r is substituted for $B_r\bar{M}_{w,r}$ in equations 16 and 24 giving

$$1/\bar{M}_{w,r}^{\text{app}} - 1/\bar{M}_{w,r} + (K_r/\bar{M}_{w,r})C_r \quad (28)$$

and

$$1/M_{z,r}^{\text{app}} = 1/M_{z,r} + 2(K_r/\bar{M}_{z,r})C_r \quad (29)$$

The concentration dependence for determining $\bar{M}_{z,r}$ is $2(\bar{M}_{w,r}/\bar{M}_{z,r})$ times as large as that for determining $\bar{M}_{w,r}$. This ratio is therefore the same for either constant B_i or constant K_i .

Determination of \bar{M}_w and \bar{M}_z .—Values for \bar{M}_w and \bar{M}_z for a total polymer may be obtained by integrating from the meniscus (a) to the bottom (b) of the ultracentrifuge cell by the method of Van Holde and Baldwin.¹⁰ Hence, for the conservation of mass in an ultracentrifuge cell whose cross-sectional area is proportional to the radius, we have

$$\int_a^b rC_i dr = \frac{C_i^0(b^2 - a^2)}{2} \quad (30)$$

where the value of $(rC_i)dr$ as obtained from equation 10 is

$$(rC_i)dr = \frac{dC_i}{2A_i} + \frac{BM_iC_i dC_i}{2A_i}$$

The quantity B is defined as in equations 11 or 16.

The integrated form of $\int_a^b BM_iC_i dC_i$ can be assumed to be equal to $(M_i/2) [(BC_i^2)_b - (BC_i^2)_a]$ although this assumption may in some cases diverge significantly from the true value.¹¹ In addition, if it is assumed that $(B_a - B_b)$ is zero, then the quantity $(BC_i^2)_b - (BC_i^2)_a$ equals $(C_b - C_a)_i(B_aC_{ia} + B_bC_{ib})$. Integration of equation 30 then yields

$$(C_b - C_a)_i = \frac{A_iC_i(b^2 - a^2)}{[1 + (1/2)(B_aM_iC_{ia} + B_bM_iC_{ib})]} \quad (31)$$

Summing equation 31 over all species, placing all terms over a common denominator and neglecting all B and higher terms in the numerator, plus all B , and higher terms in the denominator (using the same assumptions as in equations 12 and 13) gives

$$C_b - C_a = \frac{\Sigma A_iC_i^0(b^2 - a^2)}{1 + (1/2)(B_a\Sigma M_iC_{ia} + B_b\Sigma M_iC_{ib})} \quad (32)$$

or

$$\frac{1}{\bar{M}_w^{\text{app}}} = \frac{1}{\bar{M}_w} + \frac{[(B\bar{M}_wC)_a + (B\bar{M}_wC)_b]}{2\bar{M}_w} \quad (33)$$

where

(11) If it is considered that $(d \ln G'/M'dC)$, (Z'/M') , $(d \ln C_B/d \ln C_i)$, and (C_B/M_B) are constant from a to b and that $dZ/dC = 0$ then integration of equation 30 yields

$$C_i^0(b^2 - a^2)A_i = \left[1 + \frac{d \ln G'}{(M'dC)} \left(\frac{C_a + C_b}{2} \right) \right] \Delta C_i + \left[1 - \left(\frac{d \ln C_B}{d \ln C} \right) \right] \left\{ \frac{Z'\Delta C_i}{M'} - \Delta \left[\left(\frac{C_B}{M_B} \right) \ln \left(\frac{C_B}{M_B} + \frac{Z'C_i}{M'} \right) \right] \right\}$$

Even with these assumptions the concentration dependent term appears unwieldy.

$$\bar{M}_w^{\text{app}} = \left(\frac{C_b - C_a}{C_i^0(b^2 - a^2)} \right) \left(\frac{2RT}{(1 - \bar{V}_\rho)\omega^2} \right)$$

and

$$[(B\bar{M}_wC)_a + (B\bar{M}_wC)_b] = \{(B\bar{M}_w^{\text{app}}C)_a[1 + B\bar{M}_wC_a] + (B\bar{M}_w^{\text{app}}C)_b[1 + B\bar{M}_wC_b]\}$$

The quantities \bar{M}_w^{app} , $\bar{M}_{wb}^{\text{app}}$, B_a and B_b are defined as in equation 16. The value of \bar{M}_w is related to $(\bar{M}_w)_p$ and M_B as given in equation 25.

If \bar{M}_{wa} and B_a are numerically close to \bar{M}_{wb} and B_b , respectively, then equation 33 can be written

$$\frac{1}{\bar{M}_w^{\text{app}}} = \frac{1}{\bar{M}_w} + B \left(\frac{C_a + C_b}{2} \right) \quad (34)$$

where the terms in equation 34 are defined as in equations 16, 25 and 33.

Lansing and Kraemer⁹ have shown that \bar{M}_z can be obtained from

$$\bar{M}_z = \frac{\bar{M}_{wb}C_b - M_{wa}C_a}{C_b - C_a} \quad (35)$$

Substitution of (\bar{M}_wC) at a or b as obtained from equation 16 into equation 35 gives

$$\bar{M}_z = \left[\frac{\left(\frac{dC}{r dr} \right)_b (1 + B\bar{M}_wC)_b - \left(\frac{dC}{r dr} \right)_a (1 + B\bar{M}_wC)_a}{C_b - C_a} \right] \left[\frac{RT}{(1 - \bar{V}_\rho)\omega^2} \right] \quad (36)$$

Multiplying numerator and denominator by $(1 + B\bar{M}_wC)_a (1 + B\bar{M}_wC)_b$ and eliminating all C_aC_b , C_a^2 or C_b^2 terms as in deriving equation 22 gives

$$\bar{M}_z = \left[\frac{RT}{(1 - \bar{V}_\rho)\omega^2} \right] \left[\frac{\Delta \left(\frac{dC}{r dr} \right)}{\Delta C} \right] [1 + (B\bar{M}_wC)_a + (B\bar{M}_wC)_b] \quad (37)$$

or

$$\frac{1}{\bar{M}_z^{\text{app}}} = \frac{1}{\bar{M}_z} + \left[\frac{(B\bar{M}_wC)_a + (B\bar{M}_wC)_b}{\bar{M}_z} \right] \quad (38)$$

where

$$\bar{M}_z^{\text{app}} = \left[\frac{RT}{(1 - \bar{V}_\rho)\omega^2} \right] \left[\frac{\Delta \left(\frac{dC}{r dr} \right)}{\Delta C} \right]_{(a \text{ to } b)}$$

and $(B\bar{M}_w)_r$ is defined as in equation 16. If \bar{M}_{wb} is numerically close to \bar{M}_{wa} and B is independent of r , then

$$\frac{1}{\bar{M}_z^{\text{app}}} = \left(\frac{1}{\bar{M}_z} \right) + 2B \left(\frac{\bar{M}_w}{\bar{M}_z} \right) \left(\frac{C_a + C_b}{2} \right) \quad (39)$$

The quantity \bar{M}_z is related to $(\bar{M}_z)_p$ and M_B as given in equation 27.

A comparison of equation 33 with equation 38 or a comparison of equation 34 with equation 39 indicates that the concentration dependence obtained from a $1/\bar{M}_z$ vs. $f(C)$ plot will be essentially $2(\bar{M}_w/\bar{M}_z)$ times as large as that from a $(1/\bar{M}_w)$ vs. $f(C)$ plot. This comparison agrees with that for $\bar{M}_{w,r}$ and $\bar{M}_{z,r}$.

Interference Optics.—Equations 16 and 24 were derived primarily for schlieren optics. By changing (dC_r/C_r) to $(d \ln C_r)$, equation 16 can be converted to the interference optical system; that is

$$M_{w,r}^{\text{app}} = \left[\frac{2RT}{(1 - \bar{V}_\rho)\omega^2} \right] \left(\frac{d \ln C_r}{d(r^2)} \right) \quad (40)$$

for equation 16. The equation for $\bar{M}_{z,r}$ (equation

24) can be converted from terms involving (dC/dr) to terms involving the concentration by changing $\bar{M}_{z,r}^{\text{app}}$.

$$\bar{M}_{z,r}^{\text{app}} = \left[\frac{2RT}{(1 - \bar{V}_p)\omega^2} \right] \left\{ \frac{d}{d(r^2)} \left[\frac{C d \ln C}{d(r^2)} \right]_r \right\} / \left[\frac{C d \ln C}{d(r^2)} \right]_r \quad (41)$$

or

$$\bar{M}_{z,r}^{\text{app}} = \left[\frac{2RT}{(1 - \bar{V}_p)\omega^2} \right] \frac{d \ln}{d(r^2)} \left[\frac{C d \ln C}{d(r^2)} \right]_r \quad (41')$$

To determine $\bar{M}_{z,r}$ one must first plot $(\ln C_r)$ vs. (r^2) . In addition, the logarithm of the resulting slopes of this curve times C_r must be plotted against (r^2) . It would appear therefore that the interference optical system would involve a cumbersome method for determining $\bar{M}_{z,r}$. The equations for \bar{M}_w and \bar{M}_z have been evaluated by Lansing and Kraemer⁹ using values of C and have been discussed by Richards and Schachman.¹² Thus, equation 33 for \bar{M}_w can be used directly from data obtained from the interference optical system. In addition, since $(dC/r dr)_r = 2C_r [d \ln C_r/d(r^2)]$ then equation 38 can be written in terms of C_r by using equation 41' for a to b or

$$\bar{M}_z^{\text{app}} = \left[\frac{2RT}{(1 - V_p)\omega^2} \right] \left[\frac{\Delta \left[C \left(\frac{d \ln C}{d(r^2)} \right) \right]}{\Delta C} \right]_{(a \text{ to } b)} \quad (42)$$

and equation 16 for values of B_a and B_b .

Refractive Increment.—According to Johnson, *et al.*,⁶ the refractive difference n^* between solution and solvent (background) is given by

$$n^* = k_2 C_2 + k_3 (C_3 - C_{bg}) \quad (43)$$

where $k_2 = \partial n^*/\partial C_2 = (\partial n^*/\partial C_p) - (Z/2)(\partial n^*/\partial C_B)$, $k_3 = \partial n^*/\partial C_B$ and $C_3 = C_B + (Z/2)C_2$ and where $C = C_2$ is the concentration of $\text{PX}_z - (Z/2)\text{BX}$. As noted above the concentration of the polymer C_p is equal to a constant times C_3 , *i.e.*, $C = C_p \cdot \{1 - (M_B/2)(Z'/M_p') [(1 - \bar{V}_{Bp})/(1 - \bar{V}_{p\rho})]\}$, if Z'/M_p' and \bar{V}_p are the same for all species. It is assumed here that extraneous gradients due to pressure and to distortion of cell windows^{2,6} are essentially eliminated by using the double sector cell. The value of C_2 may be calculated according to the method given by Johnson, *et al.*⁶ Differentiation of equation 43 yields

$$\frac{dn^*}{dC_2} = k_2 + k_3 \left[\frac{d(C_3 - C_{bg})}{dC_2} \right]$$

It can be generally assumed that dn^*/dC_2 is proportional to a constant² if the concentration of the polymer is low and if the change in the difference in concentration of the buffer in the two cell compartments at any radius r is small, *i.e.*, $d(C_3 - C_{bg})/dC_2 = (Z/2) + (C_2/2)(dZ/dC_2) + (d[C_B - C_{bg}]/dC_2) = (Z/2)$. Thus this assumes that the charge Z is constant and that $C_B - C_{bg} = 0$ or is constant from the meniscus to the bottom of the cell. However, dn^*/dC_2 also will be proportional to a constant if the change in Z or the change in $(C_B - C_{bg})$ or both is proportional to the polymer concentration. Because this is most likely true

(12) E. G. Richards and H. K. Schachman, *J. Phys. Chem.*, **63**, 1578 (1959).

concerning $(C_B - C_{bg})$, the schlieren optical system would appear to be more desirable than the interference optical system for charged polymers. Except for the value of C in the concentration dependency term BC , the refractive increment constant k_2 will cancel in the equations for $\bar{M}_{w,r}$, \bar{M}_w and \bar{M}_z . The initial concentration C^0 may be obtained by trapezoidal summation from a synthetic boundary cell or from a sedimentation pattern in a double sector cell.^{7,13} Thus

$$C^0 = \sum_{r=a}^{r=p} \left(\frac{r}{a} \right)^2 \left(\frac{dC}{dr} \right) \Delta r \quad (44)$$

where a = the distance to the meniscus in a sedimentation pattern or the initial line between solvent and solution in a synthetic boundary cell and where p = the plateau region. The concentration at the meniscus C_a then can be obtained from¹³

$$C_a = C^0 + \left(\frac{1}{b^2 - a^2} \right) \left[\sum_{r=a}^{r=b} r^2 \left(\frac{dC}{dr} \right) \Delta r - b^2 \sum_{r=a}^{r=b} \left(\frac{dC}{dr} \right) \Delta r \right] \quad (45)$$

The concentration at any point r in the ultracentrifuge cell then is obtained from

$$C_r = C_a + \sum_{r=a}^{r=b} \left(\frac{dC}{dr} \right) \Delta r \quad (46)$$

where $\Delta r = (r_2 - r_1)$ is an arbitrary distance for trapezoidal integration. Assuming that dn^*/dC is a constant, then (dC/dr) may be replaced by $k_2(dn^*/dr)$ in equations 44, 45 and 46. Hence, $\bar{M}_{w,r}$, $\bar{M}_{z,r}$, \bar{M}_w and \bar{M}_z can be obtained directly from values of dn^*/dr in schlieren patterns by extrapolating to $C = 0$ or $n^* = 0$.

Discussion and Summary

Equations are derived for the molecular weight of homogeneous and heterogeneous polymers by using the definition of Johnson, *et al.*,² for the polymer component: $A_i = (A_p)_i - (Z/2)A_B$. In deriving equation 5 and all later equations, it has been assumed that molarities are equal to molalities and that interactions between different species are negligible. The first assumption should be true as long as both solutes are dilute and the solution is incompressible.⁴ The assumptions that $(Z_2/M_2) = (d \ln C_B/d \ln C_2) = 0$ and that $\{ \ln [1 + (Z/M_2) \cdot (M_B C_2/C_B)]^{1/2} + 1/[1 + (M_2/Z)(M_B C_2)] \} [d(Z/M)/dC_2] M_2 = 0$ for the equation derived for a homogeneous polymer (equation 6) are essentially equivalent to the assumptions made by Johnson, *et al.*,² in deriving their equation (equation 29 of reference 2); *i.e.*, $(1 - \eta^2) = 1 - [(Z/2)(C_2 M_3) \cdot (M_3/M_2)]^2 = 0$ and $d \ln (C_3/M_3)/d(r^2) = 0$. It was further assumed by them² and in equation 6 that the activity coefficient of the polymer is the same at all radii. In applying these assumptions to equations 11, 16, 34 and 39, the B coefficient becomes equal to $B = (Z'/M')^2/(2C_B/M_B)$. Solving for Z' gives: $Z' = [2B(C_B/M_B)]^{1/2} (M')$ or $Z_w = [2B(C_B/M_B)]^{1/2} (\bar{M}_w)$ assuming that (Z'/M') is constant for all species. Hence, the

(13) H. K. Schachman, "Ultracentrifugation, Diffusion, and Viscometry," Academic Press, New York, N. Y., 1957, p. 51.

charge Z of the polymer can be obtained from the concentration coefficient B and the extrapolated molecular weight. This is a modification of the method given by Johnson, *et al.*³

A comparison of equations 16 and 24 or equations 33 and 38 suggests that the assumption $d \ln C/d(r^2) = d \ln [dC/r dr]/d(r^2)$ made by Johnson, *et al.*,² is equivalent to the assumption: $\bar{M}_w = \bar{M}_z$.

Equations for charged heterogeneous polymers (equations 16, 24, 33, 34, 38 and 39) were derived by assuming that certain values of B and B^2 and higher terms can be considered negligible and that all partial specific volumes are equal. The equations are readily applicable to data obtained from the interference or schlieren optical system.

It should be emphasized that equation 33 for \bar{M}_w of all species from the meniscus to the bottom of the cell was not derived rigorously with regard to the concentration dependent term B . On the other hand, equation 38 was derived using no assumptions with regard to the integration of the B

term. Thus, the concentration dependent term for \bar{M}_z can be considered to be more reliable. A comparison of the concentration dependent term for $\bar{M}_{w,r}$ and $\bar{M}_{z,r}$ (equations 16 and 24) or for \bar{M}_w or \bar{M}_z (equations 33 and 38) indicates that this coefficient for $\bar{M}_{z,r}$ or \bar{M}_z is $2(\bar{M}_w/\bar{M}_z)$ times as large as that for the corresponding $\bar{M}_{w,r}$ or \bar{M}_w . This statement is in agreement with the results of Van Holde and Baldwin¹⁰ for a single species.

From equations 25 and 27 it is seen that the extrapolated values of \bar{M}_w and \bar{M}_z are functions of (Z'/M_p') , the charge of a monomer unit divided by its molecular weight. The quantity $(d \ln G/dC)_i$ in the coefficient B is most likely a constant only if the temperature and pressure are not varied and thus may be considered as a partial derivative. It also might be added that all of the above equations appear to be valid for the Archibald approach-to-equilibrium method since the meniscus and bottom of a cell can be considered as being at equilibrium at all times (ref. 4, p. 780).

ACTIVITY COEFFICIENTS OF LiNO_3 , HNO_3 AND NH_4NO_3 IN DOWEX-1 ANION-EXCHANGE RESIN

By J. DANON

Centro Brasileiro de Pesquisas Físicas, Av. Wenceslau Braz 71, Rio de Janeiro, Brazil

Received May 23, 1961

Activity coefficients of LiNO_3 , HNO_3 and NH_4NO_3 in the resin phase were measured with Dowex-1, 8% DVB. The results obtained with the nitrates suggest that the internal medium of the exchanger behaves like a concentrated aqueous solution without notable interaction between the various ionic species inside the resin phase. The large uptake of HNO_3 by the resin is attributed to an interaction of this acid with the exchanger.

When an ion exchange resin is immersed in an electrolytic solution, a given amount of electrolyte penetrates the resin phase. The difference in ionic composition between the two phases depends on the type of resin, its degree of cross-linking and on the activity of the ions of the aqueous solution. These systems can be treated by thermodynamic methods by considering a two-phase equilibrium and it is thus possible to calculate the activity coefficients of the electrolyte in the resin phase.

With anion-exchange resins such measurements were made mostly with chloride systems.¹⁻³ In the present work we have extended these studies to the nitrate systems. Anion-exchange resins have been used for the investigation of nitrate complexes and the quantitative treatment of these results depends on the knowledge of the activities of the electrolytes in the resin phase.^{4,5}

We assume with Nelson and Kraus² that J is an electrolyte of the $M_{\gamma^+}X_{\nu^-}$ where γ^+ and ν^- are the number of positive ions (M) and negative ions (X). The equilibrium distribution of J is described by the equality of the thermodynamic activities in the two phases

$$a_J = a_{J(r)} \quad (1)$$

where the subscript (r) denotes the resin phase. Equality 1 implies that the same standard states are selected for J in the two phases.

Relation 1 can be written as a function of data on electrolyte invasion

$$a_J = m_M \nu^+ \cdot m_X \nu^- \cdot \gamma_{\pm}^{\nu} = m_{M(r)} \nu^+ \cdot m_{X(r)} \nu^- \cdot \gamma_{\pm}^{\nu(r)} \quad (2)$$

where m represent the molal concentration of the ions and γ_{\pm} the mean activity coefficients.

Experimental

The amount of electrolyte in the resin was measured by the volumetric method.¹ Dowex-1 resin, 8% DVB, 50-100 mesh was washed with 4 M HCl in order to remove impurities and converted to the nitrate form with dilute HNO_3 . After being washed with water the resin was dried over Anhydron at 60° to constant weight.

About 1 g. of resin was placed in a small sintered glass funnel. Nitrate solutions of known composition were passed through the funnel until partition equilibrium was attained. The funnel next was centrifuged to constant weight and the resin was washed with water in order to remove the imbibed electrolyte.

HNO_3 was titrated with standard NaOH. LiNO_3 was determined by flame photometry in an ElectroSelenium photometer which was previously calibrated with solutions of known concentrations of LiNO_3 prepared from standard Li_2CO_3 . NH_4NO_3 was determined by displacing NH_4OH with concentrated NaOH in a distillation apparatus and the products were collected over H_2SO_4 of known molarity. All determinations were made at least twice. Analytical reagents were used throughout.

The determination of the interstitial volume of the resin bed was made with spherical glass beads of the same mesh.

(1) K. A. Kraus and G. E. Moore, *J. Am. Chem. Soc.*, **75**, 1439 (1953).

(2) F. Nelson and K. A. Kraus, *ibid.*, **80**, 4154 (1958).

(3) D. H. Freeman, *J. Phys. Chem.*, **64**, 1048 (1960).

(4) Y. Marcus and C. D. Coryell, *Bull. Research Council Israel*, **8A**, 1, 17 (1959).

(5) J. Danon, *J. Inorg. & Nuclear Chem.*, **13**, 112 (1960).

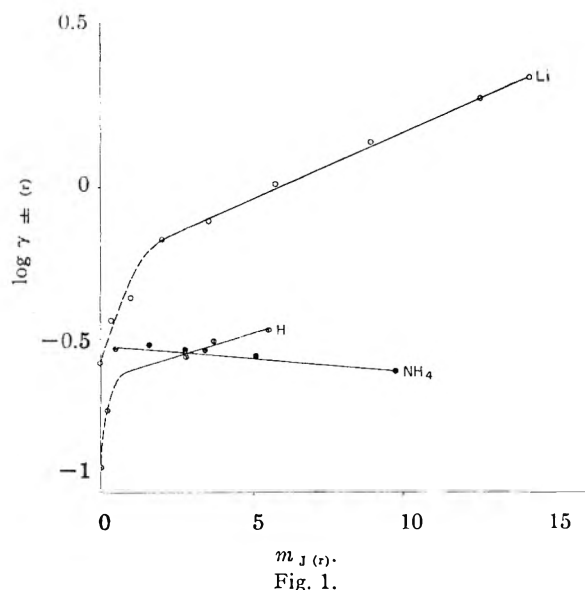


Fig. 1.

The value obtained, 0.0345 l. per l. of bed, is slightly higher than that found for 200-230 mesh Dowex-1 (0.033 l./l.). This difference is probably a consequence of the difference in mesh of the two batches.

The water content of the resin was determined by the difference in weight of the dry resin and the resin equilibrated with water after centrifugation and corrected for the interstitial water. The value obtained, 1.465 ± 0.005 kg. of wet resin per kg. of dry resin, gives a water content of the wet resin of 31.85%.

The volume of the resin bed in the several media investigated was determined by measuring with a cathetometer the height of the bed after centrifugation in a calibrated sintered funnel. The value found averaged 2.12 ± 0.08 l. per kg. of dry resin. The changes of this observed value with the various electrolytes are within the experimental error in the measurement of the volumes.

The capacity of the resin for nitrate ions was measured by two different procedures. The resin was converted to the chloride form with NaCl solution and the chloride ion was next eluted with NaClO₄ and titrated with AgNO₃ solution of known molarity. Other measurements were made by eluting the nitrate ion with NaClO₄. The nitrate was next reduced with Devarda's alloy and NaOH and the NH₄OH formed were distilled over E₂SO₄ of known molarity. The average value obtained in ten determinations was 2.952 ± 0.005 moles per kg. of dry resin. This yields a molality of the nitrate functional group of the resin of 6.325 equivalents per kg. of resin water.

All determinations were made at room temperature ($25 \pm 3^\circ$).

Results and Discussion

The results obtained are summarized in Table I.

The results obtained for the nitrate systems show a close similarity with other systems.

For LiNO₃ the relation Γ between the activity coefficients in the resin and the aqueous solution remains essentially constant and close to 0.7 as m_J changes from 3 to 13. The value of Γ is notably close to that found for LiCl² (~ 0.8).

The values of $\gamma_{\pm(r)}$ for NH₄NO₃ are also constant in the molality range 1 to 23. Although the value of Γ increases it remains close to unity until very high molalities of the aqueous phase.

The constancy of Γ at values not far from unity confirms the conclusions of previous studies^{1,2} that the internal media of the exchanger behaves like a concentrated aqueous solution without a notable interaction between the imbibed electrolyte and the "resin-electrolyte."

TABLE I^a

m_J	$m_{J(r)}$	$m_{X(r)}$	Γ	$\gamma_{\pm(r)}$
LiNO ₃				
0.077	0.010	6.434	0.298	0.261
0.736	.333	6.712	.492	.359
1.506	.993	7.513	.551	.432
2.922	2.006	8.720	.697	.668
4.14	3.54	10.55	.68	.78
5.97	5.79	13.25	.68	1.02
8.50	9.00	17.07	.69	1.42
11.38	12.61	21.38	.70	1.94
12.84	14.15	23.21	.70	2.24
NH ₄ NO ₃				
1.05	0.45	6.92	0.59	0.30
2.85	1.52	8.32	.80	.30
4.99	2.70	9.86	.96	.29
6.65	3.43	10.82	1.09	.29
10.09	5.11	12.95	1.23	.27
22.80	9.21	18.43	1.74	.25
HNO ₃				
0.068	0.034	6.360	0.147	0.121
0.317	0.235	6.615	.254	.186
1.816	2.743	9.582	.354	.275
2.684	4.664	11.880	.360	.313
3.043	5.491	12.850	.362	.330
5.504	11.62	20.23	.36	...
10.28	29.00	41.77	.29	...
15.06	63.35	85.36	.20	...

^a Values of mean activity coefficients in aqueous solutions were taken from Robinson and Stokes "Electrolytic Solutions," Butterworths Publications, London, 1955.

TABLE II^a

Electrolyte	m_{NO_3}	$\log \gamma_{\pm(r)}$	$m_{Li(r)}$ range
LiNO ₃	$6.3 + 1.20 m_{Li(r)}$	$-0.26 + 0.043 m_{Li(r)}$	3-13
HNO ₃	$6.3 + 1.22 m_{H(r)}$	$-.03 + .03 m_{H(r)}$	$\sim 1-3$
NH ₄ NO ₃	$6.3 + 1.31 m_{NH_4(r)}$	$-.52 - .009 m_{NH_4(r)}$	1-22

^a The small number of determinations of $\gamma_{\pm(r)}$ at low m_J values did not permit the calculation of the corrections according to the methods of Freeman.³ It has been possible, however, to verify that the fractional retention for LiNO₃ is less than 0.1.

With HNO₃ as well as for HCl and H₂SO₄,² a strong interaction between the electrolyte and the resin is demonstrated by the excess uptake of acid even at moderate concentrations of the external electrolyte. This is reflected on the values of Γ which are quite below unity for the all range of m_J values. A comparison between the values of Γ obtained for the three acids shows that for a given molality of the aqueous phase we have

$$\Gamma_{HNO_3} < \Gamma_{H_2SO_4} < \Gamma_{HCl}$$

This decrease of the value of Γ follows the increase in reactivity of these acids with the aromatic groups of the resin, suggesting that the large uptake of acids from the aqueous solution is probably due to this type of acid-base reaction.

It has been shown recently³ that the theory of specific interactions for concentrated solutions leads to the following relation between activity coefficients $\gamma_{\pm(r)}$ and internal concentration of electrolytes in the resin phase

$$\log \gamma_{\pm(r)} = \beta_1 m_{J(r)} + \beta_2 m_{X(r)} \quad (3)$$

where β_1 and β_2 represent the sums of coefficients

which are independent of the concentrations. If $m_{X(r)}$ is linearly dependent on $m_{J(r)}$, relation (3) becomes

$$\log \gamma_{\pm(r)} = a + bm_{J(r)} \quad (4)$$

The chloride systems were found to vary according to relation (4) at external electrolyte concentrations above about one molal.³ Below this concentration negative deviations of linearity occur. The devia-

tions are due to the relatively low values of $\gamma_{\pm(r)}$ at low external electrolyte concentrations which has been attributed to consistent experimental errors and the influence of impurities of the resin phase.³

A similar behavior was observed with the nitrate systems as is illustrated in Fig. 1.

The results of applying relations 3 and 4 are given in Table II.

AN ULTRASENSITIVE THERMISTOR MICROCALORIMETER AND HEATS OF SOLUTION OF NEPTUNIUM, URANIUM AND URANIUM TETRACHLORIDE¹

BY G. R. ARGUE,² E. E. MERCER² AND J. W. COBBLE

Department of Chemistry, Purdue University, Lafayette, Indiana

Received May 24, 1961

A sensitive solution microcalorimeter using a thermistor-amplifier bridge and automatic recording has been constructed and evaluated. The sensitivity of the instrument is 1×10^{-6} ; with magnesium, heats of solution in 1 M HCl have been measured to $\pm 0.2\%$ with samples as small as 19.51 μg . The device has been designed primarily for use in determining the thermodynamic functions of actinide elements and their compounds. The heats of formation of U(IV) in 1 M HCl, $\text{U}^{+4}(\text{aq.})$ and $\text{UCl}_4(\text{c})$ have been redetermined and new values are reported for Np(IV), Np(III) in 1 M HCl and $\text{Np}^{+4}(\text{aq.})$, $\text{Np}^{+3}(\text{aq.})$.

Introduction

Microcalorimeters suitable for carrying out heats of solution and reaction of actinide and other scarce elements have been reported and described by Westrum and Eyring,³ Gunn and Cunningham,⁴ and White and Salman.⁵ In general, these instruments have sensitivities such that precise heat data for some reactions can be obtained with samples of a few milligrams. However, still more sensitive calorimeters will be required to extend heat measurements on the actinides and their compounds beyond the transcurium elements. There are a number of ways in which the sensitivity of small microcalorimeters can be improved, but the most feasible method appears to be the substitution of thermistors as the temperature sensing element. Such applications are not new,^{6,7} but the current availability of extremely stable thermistors with high temperature coefficients makes their application to microcalorimetry extremely desirable; in addition, such use further lends itself to automatic recording devices. This latter feature in itself increases the accuracy of microcalorimetry, and this communication reports the details of an automatic recording thermistor microcalorimeter approximately four times more sensitive than any yet described. Further, experience with this device has led to recommendations for future microcalorimeters of even higher

sensitivity; such instruments probably qualify to be called ultramicrocalorimeters.

The calorimeter has been used in redetermining the heats of formation of U(IV) and Np(IV) in acid solutions, and the heat of formation of $\text{UCl}_4(\text{c})$. New measurements on the heats of solution of $\text{UCl}_4(\text{c})$ in perchloric acid solutions, and neptunium in HCl solutions, allows accurate estimations of the heats of formation of $\text{U}^{+4}(\text{aq.})$ and $\text{Np}^{+4}(\text{aq.})$ at infinite dilution. Finally, a new method has been used to directly determine the heat of formation of $\text{Np}^{+3}(\text{aq.})$.

Experimental

Calorimeter.—The microcalorimeter body was a modification of the design of Westrum and Eyring.³ It was constructed from a small tantalum beaker having a volume of approximately 7 cc., being about 4 cm. in length. The top was fitted with a tantalum lid which could be fastened to make a vacuum tight seal and was suspended by a Kel-F plastic⁸ hanger from the top of a "submarine jacket" (Fig. 1). A 40 mil diameter Pyrex stirring rod running down the center of this hanger and a glass thermistor probe piercing the lid through a vacuum tight seal provided the essential parts of the device. An aluminum radiation shield supported on lucite legs was used. This submarine type of calorimeter also has been used by others^{3,4}; the principal advantages of this arrangement have been studied and summarized recently elsewhere.⁹

A synchronous 288 r.p.m. motor was mounted directly above the stirring rod on a guided spring suspension. A slight vertical movement of the suspension broke the sample bulb fastened to the end of the stirring rod.¹⁰ The whole stirring apparatus could be covered by a plastic bag to maintain an inert or reducing atmosphere on the inside of the calorimeter, which otherwise is open to the air through the stirring shaft.

The heater consisted of approximately 120 inches of No. 39 single silk coated manganin wire having a resistance of 100

- (1) Supported by the U. S. Atomic Energy Commission.
- (2) From the Ph.D. theses of G. R. Argue and E. E. Mercer, Purdue University, 1960.
- (3) E. F. Westrum and LeRoy Eyring, *J. Am. Chem. Soc.*, **74**, 2045 (1952).
- (4) S. R. Gunn and B. B. Cunningham, *ibid.*, **79**, 1563 (1957).
- (5) B. C. L. Salman and A. G. White, *J. Chem. Soc.*, 3197 (1957).
- (6) While this research was in progress, White (ref. 5) has independently reported the use of thermistors in a microcalorimeter of much less sensitivity than the device described in this communication.
- (7) H. A. Skinner and H. O. Pritchard, *J. Chem. Soc.*, 272 (1950).

(8) Manufactured by the Industrial Plastic and Equipment Co. Orange, New Jersey.

(9) S. Sunner and I. Wadsö, *Acta Chem. Scand.*, **13**, 97 (1959).

(10) Unless care is taken to line up the centers of the rod, bulb and anvil (Fig. 1), the stirring rod also may break.

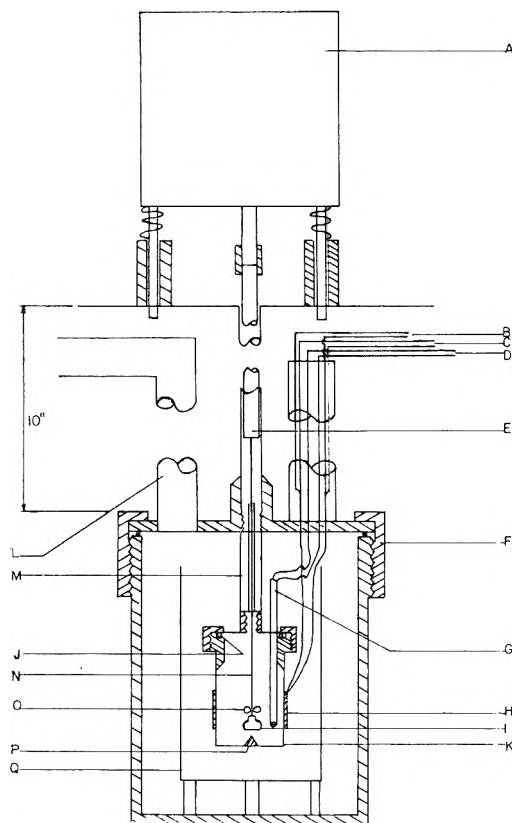


Fig. 1.—The submarine and microcalorimeter assembly: A, stirring motor (spring mounted); B, leads to heater; C, leads from heater to potentiometer; D, thermistor leads to bridge; E, glass stirring rod; F, submarine; G, thermistor; H, heater; I, sample bulb; J, "O" ring; K, tantalum calorimeter body; L, vacuum line; M, Kel-F hanger; N, 40 mil glass stirring rod; O, platinum propeller; P, anvil; Q, radiation shield.

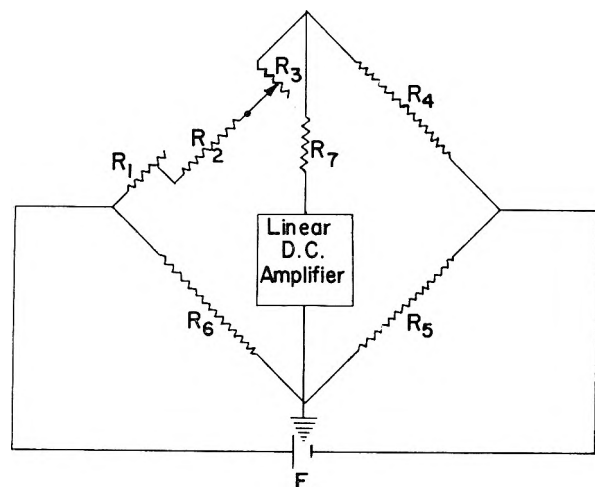


Fig. 2.—Thermistor bridge: R_1 , 10 turn 50 k Ω Heliopot; R_2 , 70 k Ω ; R_3 , 40 Ω (ten); R_4 , R_5 , 100 k Ω ; R_6 , Thermistor; R_7 , 25 k Ω ; E , 1.019 volts.

ohms and wound non-inductively in a single layer on the outside of the tantalum calorimeter body. A coating of Armstrong C-7 cement¹¹ was painted onto the windings to firmly fix the heater in place, and the ends were attached to a plastic ring attached in turn to the calorimeter body just above the heater. At this point, the manganin leads were connected to No. 30 copper wire leads which then con-

(11) Armstrong Products Company, Warsaw, Indiana.

nected to insulated lugs on the lid of the submarine. The potential measuring leads also were located at these lugs. The justification for locating the leads two inches away from the end of the manganin heater was, (1) the resistance involved is only 0.03% of the total heater resistance, and, (2) the heat generated in these leads is all delivered to the end at the lower temperature when the calorimeter is more than 0.004° from equilibrium.¹²

A "dummy" heater similar to the calorimeter heater was suspended in oil and thermostated to $\pm 0.1^\circ$, and was used in the circuit on a "standby" position. This heater allowed preliminary setting of the current flow in the heater circuit; fluctuations in the circuit voltages and currents thus were minimized in the usual manner. The current source was an electronic constant potential source¹³ capable of supplying 500 ma. at an extremely stable voltage essentially independent of the current loads. This power source was found to be a considerable improvement over the use of storage cells.¹⁴ Heater currents were measured by determination of the potential across a standard 100 ohm resistance which could be placed in series either with the calorimeter or dummy heater. A Leeds and Northrup Model K-3 rack mounted "guarded" potentiometer was used for this purpose.

Time measurements were obtained from a 60 cycle synchronous clock which was powered by a constant 110 v., 60,000 cycle power supply¹⁵ regulated by a tuning fork. The clock was provided with an electric clutch arrangement so that there was an insignificant delay (≤ 0.001 min.) involved in stopping and starting the timer. A single switch operated both the clock and the heater through a suitable relay arrangement.

The temperature sensing device finally adopted was a Fenwall¹⁶ type GA51P68 thermistor having a resistance of $\sim 100,000$ ohms and a 4% temperature coefficient at 25°. The thermistor was placed in one arm (R_6) of a Wheatstone bridge (Fig. 2). The other resistors of the bridge (R_{1-5}) were kept in oil and thermostated at 25°. A 1.0193 standard cell was used as a current source, which was about 5×10^{-6} ampere during a measurement. The signal from the bridge was amplified by a d.c. current amplifier,¹⁷ the output of which was used to drive a 0-10 mv. Brown recorder. The scale of the recorder was extended ten-fold by inserting a set of ten carefully adjusted and thermostated resistors of the proper impedance in another arm of the Wheatstone bridge (R_3); the range thus could be continually extended during a run by proper switching.¹⁸

The linearity of the thermistor itself was demonstrated to be satisfactory ($\leq 0.1\%$) over a 0.1° range by comparison to a calibrated platinum resistance thermometer. In actual practice the total temperature range of any run was about 0.01-0.04°. The system had a temperature sensitivity of at least $1 \times 10^{-5}^\circ$, with a reasonable noise level, and the effective heat capacity was from 7-10 cal./deg. (depending upon the volume of solution used). The sensitivity has been increased recently by another factor of two to $5 \times 10^{-6}^\circ$, which corresponds to a thermal sensitivity of 5×10^{-5} cal.¹⁹ The effective sensitivity limit is essentially imposed by three considerations. The first is the low current requirements of such a continually recording system, since too high a current in the thermistor introduces too much self-heating. The second is the electronic noise level of the first vacuum tube in the amplifier; the present device operates near this noise limit. The third consideration is the

(12) For the details of the calculations leading to this conclusion the reader is referred to the Ph.D. thesis by one of the authors (E. E. M.).

(13) Kay-Lab Corp., San Diego, Calif.

(14) Although they were not available during the initial phases of this research, constant current power supplies now can be obtained commercially, and the use of one such type manufactured by John Fluke, Inc., Seattle, Washington, has essentially eliminated the need for current measurements.

(15) Riverbank Laboratories, Geneva, Illinois.

(16) Fenwall Electronics, Inc., Framingham, Mass.

(17) Leeds and Northrup Model 9836-B, Philadelphia, Pa.

(18) In recent modifications this set of fixed resistors has been replaced by a precision, calibrated slide wire of a helipot design; this modification in effect provides for infinite expansion of the recorder scales within the linearity limits of the bridge.

(19) This was accomplished by the simple modification of replacing R_7 and the current amplifier (Fig. 2) with a Leeds and Northrup Voltage amplifier, Model 9835B.

thermal leak modulus, which was as high as 8×10^{-3} deg. min.⁻¹ deg.⁻¹ in the present device. Thus the full sensitivity of the thermistor was not utilized in the present apparatus. However, the future models of this instrument will involve a twin differential calorimeter which will allow the use of larger currents (hence a smaller noise level) and will increase the sensitivity significantly. It is not at all out of the realm of possibility that such devices can have stable operating characteristics with sensitivities of the order of 1×10^{-7} .

The assembled calorimeter and submarine jacket was immersed to a depth of 10 inches in a large 60 gallon water thermostat controlled to $\pm 0.0004^\circ$ for extended periods of time. This control was achieved largely through efficient and rapid stirring and the use of proportional infrared heaters which also were thermistor controlled. A vacuum of $\leq 0.01 \mu$ was maintained around the calorimeter by a suitable mercury diffusion and mechanical fore-pump. The whole apparatus was kept in an air-conditioned room controlled to $\pm 2^\circ\text{F}$.

Chemicals.—Metallic uranium was obtained in the form of thin foils from the M. and C. Nuclear Corporation and was reported to be $\geq 99.9\%$ pure. The oxide film was removed by first washing the sample in 10 M nitric acid followed by rinsing with water, acetone and ether, and finally air dried. Neptunium metal was prepared on a few milligrams scale by the fluoride reduction method previously reported by others.²⁰ Reagent grade barium was used as the reducing agent. Anhydrous NpF₄ was obtained by first precipitating the hydrous fluoride with HF from a Np(IV) nitrate solution. The precipitate was washed repeatedly with absolute alcohol and finally centrifuged at ~ 3500 r.p.m. into a small solid pellet.²¹ The pellet was dried under an infrared heat lamp, and transferred to a previously degassed and heated thoria crucible. The thoria crucible was placed on a small tantalum platform inside a larger outer tantalum crucible. Clean, freshly cut barium was placed under the platform and the crucible covered with a tantalum lid containing a small hole (to prevent excessive pressure differentials from moving the lid). This whole assembly was hung inside a wire wound (tantalum) resistance coil and evacuated. After a pressure of $\leq 10^{-5}$ mm. was obtained, the temperature of the assembly was slowly raised to 300° to remove any possible trace of volatile impurities. The reduction itself then was carried out by rapidly increasing the temperature to 1300° . A spectrographic analysis of a typical run is given in Table I. X-Ray analysis of two separate pieces indicated that the metal was α -neptunium, probably coated with NpO. The amount of this coating appeared to vary with the time of exposure to air, was believed to be thin, and largely removed by mechanical and chemical cleaning before use. The analysis indicates that the material was effectively 99.9% heavy elements.

TABLE I
SPECTROGRAPHIC ANALYSIS OF A NEPTUNIUM METAL SAMPLE^a

Element	$\mu\text{g.}/70 \mu\text{g.}$ of sample	Blank, $\mu\text{g.}$	Net, $\mu\text{g.}$
Al	0.01	0.01	0.0
Ba	.01	.01	.0
Ca	.03	.01	.02
Mg	.02	.02	.0
Th	< .1	< .1	0
U	< .5	< .5	0.0
Pu	< 1.0	< 1.0	0

^a Determined by courtesy of George Shalimoff at the Lawrence Radiation Laboratory, Berkeley, California.

Alpha pulse analysis showed that no other transuranic elements were present except plutonium, which was $\sim 0.1\%$. Since this would presumably be present as metallic plutonium no detectable errors would result from this source.

(20) S. Fried and N. Davidson, *J. Am. Chem. Soc.*, **70**, 3539 (1948).

(21) The authors are extremely grateful to Drs. B. B. Cunningham and J. C. Wallman of the Lawrence Radiation Laboratory for kindly pointing out this pelletizing procedure which has considerably improved the quality and yield of metal that can be obtained.

Any traces of thorium would have originated from the thoria crucible. While these may have been present in the analytical sample, any such surface contaminate was removed from the calorimetric samples by a chemical nitric acid treatment. Alternatively, if the thorium were present as the metal the same argument as used for trace plutonium metal also would apply.

Uranium tetrachloride was prepared by the reaction of "active" uranium dioxide with carbon tetrachloride at 500° , and was purified by sublimation in a carrier stream of nitrogen.²² "Active" uranium dioxide was prepared by the reduction of uranium trioxide with methane at 450° and was analyzed by ignition in air to U₃O₈ at 800° . Uranium trioxide was obtained from uranyl nitrate by precipitating ammonium diuranate from a uranyl solution followed by heating of this material in air at 350° . The Pyrex tubing and furnaces in which uranium dioxide and carbon tetrachloride reacted was arranged in such a way so that sublimation of the UCl₄ could be carried out in the same system. The purified UCl₄ so obtained was sealed off in the Pyrex reactor, and transferred to an inert atmosphere box where samples of the desired size (~ 1 mg.) were removed, weighed and sealed in glass sample bulbs for use. UCl₄ was analyzed by hydrolysis in 0.5 M NaOH solutions. The resulting uranium(IV) precipitate was separated by centrifugation and the supernatant analyzed for chloride by the Mohr volumetric method. Uranium analyses were made by first oxidizing a solution of the uranium chloride with excess permanganate in 2 M sulfuric acid. The resulting mixture was passed through a Jones reductor; the resulting solution was air oxidized to remove small traces of U(III) and then titrated with standard permanganate. The preliminary permanganate oxidation was necessary to prevent subsequent chloride interference. A typical result obtained was:

Anal. Calcd. U, 62.66; Cl, 37.34. *Found:* U, 62.77; Cl, 37.29.

Magnesium used for chemical calibrations was obtained by cutting singly distilled metallic crystals.

Potassium chloride was Mallinckrodt A. R. Grade, dried at 250° for 24 hours and stored over P₂O₅.

J. T. Baker A. R. grade concentrated hydrochloric acid was diluted with conductivity water before use.

Perchloric acid solutions were made up from G. F. Smith doubly distilled concentrated acid diluted with conductivity water. All acid solutions were standardized with standard sodium hydroxide and phenolphthalein.

Weighings.—These were carried out either on a calibrated quartz fiber torsion micro-balance²³ (sens., 0.06 $\mu\text{g.}$) or on an automatic semi-micro Mettler balance (sens., 5 $\mu\text{g.}$).

Procedure.—One or more electrical calibrations were made before and after each chemical determination and the average energy equivalent was used for the calculation of the chemical heats. Drift lines were usually taken for 20–30 minutes and the rate and amount of electrical heating were both varied so as to simulate the chemical calorimetric run as closely as possible. This is one extremely important advantage of automatic recording. The six-tenths rise time^{24a} was used to obtain the total resistance and heat change. The calorie is taken as 4.1840 abs. joules, and errors are reported as standard deviations as recommended by Rossini.^{24b}

Calibration.—Although there was no reason to doubt the performance of the calorimeter, several chemical calibrations also were performed. The first of these was the heat of solution of magnesium metal in 1.00 M HCl at 25° . This type of reaction was similar to, although somewhat faster than, to that expected for the dissolving of heavy element metals in acids. The results of seven runs are summarized in Table II. The value obtained, $\Delta H_2 = -111.21 \pm 0.21$ kcal./mole compares favorably with the results reported previously for this heat of -111.322 ± 0.041 kcal./mole.²⁵

(22) H. R. Hoekstra and J. J. Katz, Chapter 6, "The Actinide Elements," Vol. 14A, edited by G. T. Seaborg and J. J. Katz, McGraw-Hill Book Co., New York, N. Y., 1954, p. 151.

(23) Micro-chemical Specialties Co., Berkeley, California.

(24)(a) H. C. Dickinson, *U. S. Bur. Standards Bull.*, **11**, 189 (1914);

(b) F. D. Rossini and W. E. Deming, *J. Wash. Acad. Sci.*, **29**, 419 (1939).

(25) C. H. Shomate and E. H. Huffman, *J. Am. Chem. Soc.*, **65**, 1625 (1943).

TABLE II

THE HEAT OF SOLUTION OF MAGNESIUM IN 1.00 M HCl AT 25°

Wt. of Mg. μg.	H, cal.	-ΔH ₂ , ^a kcal./mole
48.85	0.22355	111.63
49.15	.22229	110.32
45.64	.20968	112.06
41.30	.18805	111.06
43.74	.19879	110.86
41.78	.19053	111.24
19.51	.08899	111.27

Av. 111.21 ± 0.21

^a Includes a correction of 0.33 kcal./mole for vaporization of the solvent by escaping hydrogen.

Another calibration was carried out by dissolving anhydrous potassium chloride in water to give a solution which was $5 \times 10^{-3} M$. These data are listed in Table III. The heat so obtained, $\Delta H_3 = 4.147 \pm 0.006$ kcal./mole agrees well with the literature value of 4.143.²⁶ This latter measurement required a longer time and a larger sample, and the two calibrations probably represent two extremes of variables in chemical reactions for which this calorimeter was designed. Several empty bulbs were broken in the calorimeter and no heat effect was observed in these cases. The over-all performance as indicated by these preliminary tests was considered satisfactory.

TABLE III

THE HEAT OF SOLUTION OF POTASSIUM CHLORIDE IN WATER AT 25°

Sample wt., mg.	H, cal.	ΔH ₃ , kcal./mole
3.588 ^a	0.19915	4.138
3.130	.17359	4.135
3.600	.20026	4.147
3.588	.20055	4.167

Av. 4.147 ± 0.006

^a These amounts are such as to give a final solution approximately $5 \times 10^{-3} M$ in KCl.

Experimental Results

The Heat of Solution of Uranium.—When actinide metals are dissolved in acids under conditions to give the (IV) oxidation state, a black insoluble residue usually is formed. While this precipitate has been reported as a hydrous oxide²⁷ for uranium, it also has been referred to as a dihydride²⁸ or a mixture of ThO, HCl and H₂O²⁹ in the case of thorium. Since there is, therefore, some doubt as to the exact nature and reproducibility of the material, best calorimetric procedure requires other dissolving conditions so as to eliminate its formation. This can be done by adding fluosilicate ion to the dissolving solution.³⁰ Such a procedure probably results in the formation of fluoride complexes of the actinide(IV) ion, but this heat has been experimentally fixed for thorium(IV) under concentration conditions similar to those used in this research as -0.3 kcal./mole. Presumably this same value is valid for U(IV).

The second problem in the heat of solution of uranium metal is the exact nature of the chemical

(26) As estimated from the data recorded in "Selected Values of Chemical Thermodynamic Properties," Circular 500, Bureau of Standards, 1949; however, these values are apparently subject to some disagreement as discussed in reference 9.

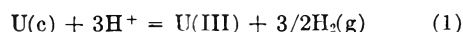
(27) R. C. Young, *J. Inorg. & Nuclear Chem.*, **7**, 418 (1959).

(28) W. J. James and M. E. Straumanis, *Acta Cryst.*, **9**, 376 (1956).

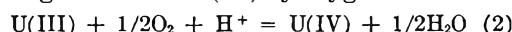
(29) L. I. Katzin, *J. Am. Chem. Soc.*, **80**, 3908 (1958).

(30) L. Eyring and E. F. Westrum, *ibid.*, **72**, 5555 (1950).

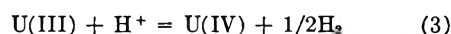
reaction taking place in the calorimeter. The first step of the reaction in concentrated acid can be assumed to be



which is consistent with the other actinide and lanthanide elements which have stable +3 aqueous oxidation states. However, +3 solutions immediately change color and are oxidized to +4 either by H⁺ or traces of oxygen in the uranium system. When the calorimeter was operated in a normal air atmosphere, erratic values for the heat of solution were obtained, some of which were 15 kcal./mole higher than those to be reported in this section. Under these conditions and from a knowledge of the heats involved, it would appear that about half of the U(III) from reaction 1 was being oxidized to U(IV) by oxygen



When the calorimeter solution was initially purged with hydrogen and also kept under an atmosphere of hydrogen, the data became more precise and the heats were lower. Under these conditions it will be assumed that all of the U(III) was oxidized by H⁺



The results of the heat of solution of uranium in 6 M HCl solution which was 0.005 M in SiF₆⁼ are reported in Table IV. It was found that HCl concentrations $\geq 6 M$ were necessary to obtain moderately rapid and complete calorimetric reactions.

TABLE IV

THE HEAT OF SOLUTION OF URANIUM IN 6.03 M HCl (0.005 M Na₂SiF₆) AT 25°

Sample wt., μg.	H, cal.	ΔH ₄ , ^a kcal./mole
217.58	0.13525	148.64
259.03	.15949	147.23
316.61	.19326	145.97
280.09	.17242	147.20
259.63	.16113	148.40
310.84	.19135	147.20
264.68	.16837	146.70
337.96	.20748	146.81
235.93	.14395	145.92
320.32	.19531	145.81
260.18	.15861	145.78

Av. -146.88 ± 0.33^b^a Includes -0.65 kcal./mole for the heat of evaporation of water by escaping hydrogen. ^b Standard deviation.

The Heat of Solution of UCl₄(c).—The heat of solution of anhydrous uranium tetrachloride was carried out in various acidic solvents in order to be able to complete certain thermochemical cycles. The first series of measurements (Table V) were in 6.03 M HCl which was also 0.005 M in Na₂SiF₆ to give a final solution essentially identical with that resulting from the dissolution of uranium metal (Table IV).

It should be noted that the heat obtained was several kilocalories higher than that found by Killner.³¹

The heat of solution of UCl₄(c) in perchloric

(31) Referred to by Brewer, *et al.*, p. 22 of ref. 36.

TABLE V

THE HEAT OF SOLUTION OF $UCl_4(c)$ IN 6.03 M HCl (0.005 M

Sample wt., mg.	H , cal.	$-\Delta H_s$, kcal./mole
0.430	0.04874	43.06
0.506	.05771	43.33
1.145	.12965	43.01
1.297	.14679	43.00

Av. 43.10 \pm 0.08^a^a Standard deviation.

acid of various concentrations was required to estimate the heat of formation of U^{+4} at infinite dilution. These data are summarized in Table VI. When the concentration of the perchloric acid was $\leq 0.01 M$, there was calorimetric evidence of a slow secondary reaction taking place after the initial rapid solution reaction. It is assumed that this secondary heat was due to the polymerization of $U(IV)$ ³² at these low acidities. In order to obtain useful data from this lower acid concentration an estimation was made from previous runs of the shape of the calorimetric heating curve; in this manner the secondary heat could be subtracted from the total heat evolved. The values recorded for 0.01 M $HClO_4$ given in Table VI were obtained by this method. However,

TABLE VI

THE HEATS OF SOLUTION OF $UCl_4(c)$ IN $HClO_4$
(HCl SOLUTIONS) AT 25°

Acid concn.	Sample wt., mg.	H , cal.	$-\Delta H_s$, kcal./mole
0.01 M $HClO_4$ ^a	1.106	0.159	54.5
	1.131	0.163	54.7
			Av. 54.6 \pm 0.5
0.050 M $HClO_4$	0.711	0.10649	56.9
	0.735	.11169	57.7
	1.142	.17247	57.4
		Av. 57.3 \pm 0.3	
0.135 M $HClO_4$	0.463	0.06803	55.8
	.670	.09762	55.4
	.950	.13869	55.6
		Av. 55.6 \pm 0.15	
0.200 M $HClO_4$	1.390	0.21370	58.4
	0.777	0.12213	59.7
		Av. 59.1 \pm 0.6	
1.00 M $HClO_4$	1.904	0.30554	61.0
1.00 M HCl	0.697	0.10462	57.0

^a Data at this concentration corrected for polymerization of $U(IV)$.

the estimated accuracy of such a procedure is only ± 0.5 kcal./mole and would be even poorer at lower acid concentrations. Consequently, there appears to be little point in extending heats of dilution data for $U(IV)$ below 0.01 M E^+ even at these low uranium concentrations ($\sim 10^{-4}$ M $U(IV)$).

A value for the heat of solution of $UCl_4(c)$ in 1 M HCl was desired and this heat also is listed in Table VI.

The Heat of Solution of Neptunium.—In the reaction between neptunium metal and 1 M HCl

to give $Np(IV)$, a black precipitate is formed, similar to the behavior of uranium under these conditions. Therefore, the dissolving solution also contained 0.005 M Na_2SiF_6 . The data for four separate determinations are listed in Table VII.

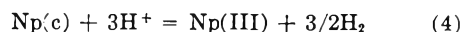
TABLE VII

THE HEAT OF SOLUTION OF NEPTUNIUM IN 1.00 M HCl
(0.005 M Na_2SiF_6) AT 25°

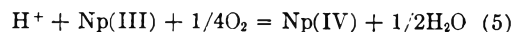
Sample wt., $\mu g.$	H , cal.	$-\Delta H_s$, ^a kcal./mole
186.47	0.14068	165.2
577.61	.40129	165.1
207.88	.14727	165.9
108.97	.07590	165.5

Av. 165.4 \pm 0.4^b^a Includes -0.4 kcal./mole for evaporation of water by escaping hydrogen. ^b Standard deviation.

In the case of neptunium the stoichiometry of the reaction is assumed to be



followed by



The evidence for this assumption rests largely on the fact that $Np(III)$ appears to be stable for extended times in strong acid solutions in the absolute absence of oxygen.³³ This latter observation suggests the possibility of measuring directly the heat of solution to give $Np(III)$. Therefore a second series of experiments was performed by placing the calorimeter assembly under an atmosphere of hydrogen and carefully purging the dissolving solution.

The results of these experiments scattered between -133 to -160 kcal./mole, indicating at least partial oxidation to $Np(IV)$. The use of a coil of platinum coated with platinum black wound around the thermistor was only partially successful. It thus appeared that the absolute elimination of the traces of oxygen required to partially oxidize such a small amount of neptunium was not to be readily achieved.

In this respect the observation of Gelman and Mefodieva³⁴ that closed acid solutions of $Np(III)$ in the presence of an excess of sodium formaldehyde sulfoxylate appear to be stable over extended periods of time without rigorously removing traces of oxygen suggested a new method of stabilizing $Np(III)$. This observation suggests that sulfoxylic acid is capable of removing the last traces of oxygen from an enclosed system. Further tests showed that the rate of oxidation of H^+ by the sodium formaldehyde sulfoxylate reagent under the conditions in the calorimeter was sufficiently slow and constant so that its presence was easily corrected for as a constant, but small, heat source. Part of this reaction may have been due to traces of oxygen which either slowly desorbed from, or leaked into, the calorimeter system. In any event, breaking a sample bulb of air in the calorimeter gives an immediate thermal response. Further,

(33) J. C. Hindman, L. B. Magnusson and T. J. LeChapelle, *ibid.*, **71**, 687 (1949).(34) A. D. Gelman and A. P. Mefodieva, *Doklady Akad. Nauk, S. S. S. R.*, **117**, 225P (1957).(32) K. A. Kraus and F. Nelson, *J. Am. Chem. Soc.*, **72**, 3901 (1950).

there is little reason to expect that formaldehyde, or sulfoxylate, thiosulfate or sulfate ions (the last two of which are possible products of the oxidation of sulfoxylate) complex Np(III) at these low concentrations or in competition with 1 *M* Cl⁻. This situation suggests that it should be possible to use sodium formaldehyde sulfoxylate as a chemical "protective" reagent during the calorimetric dissolution of neptunium to Np(III).

The data are summarized in Table VIII for the heat of solution of neptunium in 1.00 *M* HCl which is 0.005 *M* in sodium formaldehyde sulfoxylate. This same type of experiment should be applicable to Pu(III).

TABLE VIII

THE HEAT OF SOLUTION OF Np(c) IN 1.00 *M* HCl (0.005 *M* NaHSO₂·CH₂O·2H₂O) AT 25°

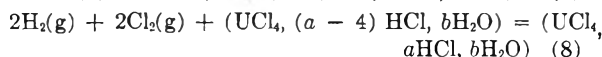
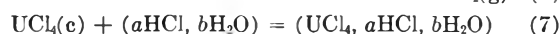
Sample wt., μg.	<i>H</i> , cal.	-Δ <i>H</i> _s ^a kcal./mole
61.26	0.03227	125.2
155.17	.08195	125.4
474.14	.25132	126.0
57.22	.03026	125.6

Av. 125.6 ± 0.3^b

^a Includes -0.4 kcal./mole for evaporation of water by escaping hydrogen. ^b Standard deviation.

Thermodynamic Calculations and Discussion

The Heat of Formation of UCl₄(c).—From the two sets of data given in Tables IV and V, the heat of formation of UCl₄(c) from its elements can be calculated. These experiments were designed so that the resulting solutions were almost identical after the reactions had taken place. Further, the effect of any fluoride complexing should also cancel out. In detail, the calculation is made as



Typical values are: *a* = 4200, *b/a* = 8.13. The proper addition of reactions 6 through 8 gives



The sum of reactions 6 and 7 is given by the difference in the heats involved in Tables IV and V: Δ*H*₅ - Δ*H*₄. To this must be added the heat for reaction 8, which is the apparent heat of formation of the hydrochloric acid solution. This quantity has been determined to be -36.85 kcal./mole from auxiliary thermodynamic data.³⁵ Such a calculation, Δ*H*₅ - Δ*H*₄ + 4(-36.85) gives -251.2 ± 0.4 kcal./mole for the standard heat of formation of UCl₄(c) at 25°. This value is in good agreement with the two other previous values reported: -251.3³⁶ and -250.9³⁷ kcal./mole. This is some-

(35) Auxiliary thermochemical data for this and other calculations are taken from "Selected Values of Thermodynamic Properties," National Bureau of Standards Circular 500 (1952).

(36) W. Biltz and C. Fendius, *Z. anorg. u. allgem. Chem.*, 176 (1928); recalculated and corrected by L. Brewer, L. A. Bromley, P. W. Gilles and N. L. Longren, U. S. Atomic Energy Commission Report BC-82 (1947); paper 33, vol. 1, page 219, "The Chemistry of Uranium," edited by J. J. Katz and E. Rabinowitch, U. S. A. E. C. Tech. Info. Service Extension, Oak Ridge, Tenn. (1958).

(37) C. H. Barkeley, U. S. Atomic Energy Commission Report RL 4.6.906 (1945); the value given was based upon a new heat of ox-

idation of ferrous to ferric ion used by Barkeley to oxidize U(III) to U(IV).

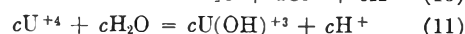
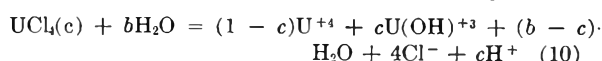
what surprising in the case of the first of these values, since there is some doubt as to the completeness of the calorimetric reaction and/or the purity of the uranium. Nevertheless, it is gratifying that Δ*H*_f⁰ for UCl₄(c) is fixed so well, since it is a key intermediate in evaluating many of the thermodynamic functions of the aqueous ions of uranium.

The Heat of Formation of U(IV) and U⁺⁴(aq.).—In principle, the heats of formation of U(IV) under various conditions and at infinite dilution can be obtained from measurements of the heats of solution of UCl₄(c) in various acid media. In practice the situation is complicated because of the difficulty in extrapolating data on a highly charged ion to infinite dilution. Further, even at the low uranium concentrations used in this research, the U⁺⁴ ion is appreciably hydrolyzed at 0.1 *M* H⁺. Lastly the polymerization reaction below 0.01 *M* H⁺ prevents one from obtaining information in either U⁺⁴ or U(OH)⁺³ at very low ionic strengths.

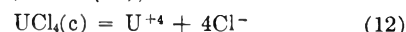
Nevertheless, good estimations can be made on the heat of formation of U⁺⁴(aq.) from the heats of dilution of UCl₄ in non-complexing media. To this end, the data obtained in Table VI will be used to estimate some new thermochemical properties.

The heats of formation of U⁺⁴ in 1 *M* HCl and 1 *M* HClO₄ can be calculated with the usual assumptions. From the heat of solution of UCl₄ in 1 *M* HCl and 1 *M* HClO₄, and taking the heats of formation of Cl⁻ in HCl and HClO₄ as the same value, -39.6 kcal./mole, the partial heats of formation of U(IV) become: Δ*H* = -149.8 ± 0.4 kcal./mole in 1 *M* HCl; Δ*H* = -153.8 ± 0.4 kcal./mole in 1 *M* HClO₄. These formal heats are of use in comparing with other actinide species which have only been determined in high acid concentrations.

The heat of formation of U⁺⁴(aq.) at infinite dilution may be obtained from the data on the heats of solution of UCl₄(c) in various concentrations of HClO₄ (Table VI). At most of these concentrations hydrolysis of the U⁺⁴ is significant and must be subtracted out by use of the cycle



Subtracting (11) from (10), one obtains



The heat of reaction 10 is recorded as a function of acid concentration in Table VI. A value of *c* for these equations may be calculated from the hydrolysis constants for reaction 11 as recorded by Kraus and Nelson.³⁸ The heat of reaction 11, Δ*H*_{hyd}, also has been determined by these authors. The calculated heat of reaction 12 as a function of total acid concentration or ionic strength is listed in Table IX.

The value for Δ*H*₉ at 0.200 *M* HClO₄ appears to be somewhat out of order, but this probably follows

dation of ferrous to ferric ion used by Barkeley to oxidize U(III) to U(IV).

(38) K. A. Kraus and F. Nelson, *J. Am. Chem. Soc.*, 72, 3901 (1950); 77, 3721 (1955).

TABLE IX

THE HEAT OF SOLUTION OF $UCl_4(c)$ IN $HClO_4$ AT 25° CORRECTED FOR HYDROLYSIS

$HClO_4$ concn., M	K_H	c (fraction hydrolyzed)	$-\Delta H_s$, kcal./mole
0.010	0.135	0.918	65.4
.050	.082	.619	64.5
.135	.057	.297	59.1
.200	.049	.197	61.3
0 (extrapolated)			66.0 ± 1.0

from the fact that K_{hyd} is not well defined at this ionic strength. Small changes in K_{hyd} can change the value of ΔH_s by 0.5 to 1.0 kcal. The extrapolated value of ΔH_s^0 becomes -66.0 ± 1.0 kcal./mole. Combined with heats of formation of $HCl(aq.)$ and $UCl_4(c)$, the heat of formation of $U^{+4}(aq.)$ at infinite dilution at 25° becomes -157.1 ± 1.0 kcal./mole. It also follows that the heat of formation of $U(OH)^{+3}$ becomes -213.7 ± 1.0 kcal./mole using the value of 11.7 kcal./mole for ΔH_{hyd}^0 .³⁸

The heats of formation for $U^{+4}(aq.)$ and $U(OH)^{+3}$ given here are 10.4 and 9.6 kcal./mole, respectively, more negative than the currently listed values.³⁶ This is not very surprising considering the manner in which the older literature values were obtained, *i.e.*, assuming that the heat effect on transferring U^{+4} from 0.5 M $HClO_4$ to water at infinite dilution is zero, and ignoring any hydrolysis.

The Heat of Formation of $Np^{+3}(aq.)$.—From the data on the heat of solution of Np metal in 1 M HCl under reducing conditions (Table VIII), the heat of formation of $Np(III)$ in 1 M HCl becomes -125.6 ± 0.3 kcal./mole. This may be compared to the presently accepted value of -127.4 estimated from the potentials in 1 M HCl .³ There are two sources of data which allow estimations of the heat of dilution of $NpCl_3$ in 1 M HCl to infinite dilution. The heat of dilution of a solution of $CeCl_3$ at unit ionic strength to infinite dilution³⁹ is -1.9 kcal./mole. This probably provides a good estimation of the heat of dilution since the crystal radius of cerous is almost identical to that of Np^{+3} . The heat of solution of $LaCl_3$ in HCl solutions of various concentrations had been reported by Klemm.⁴⁰ Although these heat data at higher concentrations appear somewhat low, indicating that the $LaCl_3$ may not have been completely anhydrous, the heat of dilution from 1 M HCl solutions to infinite dilution can be estimated to be -1.6 kcal./mole. This latter value probably represents a lower limit, although the chemical environment is closer to the case under consideration than the pure $CeCl_3$ solutions. As a good approximation, a value of -1.8 ± 0.2 kcal./mole will be adopted. The heat of formation of $Np^{+3}(aq.)$ at infinite dilution now can be reliably set at -127.4 ± 0.4 kcal./mole.

The Heat of Formation of $Np^{+4}(aq.)$.—The heat of formation of $Np(IV)$ in 1 M HCl can be obtained from the data in Table VII, and an estimate can be made also for the heat of formation at infinite

(39) F. H. Spedding and G. Atkinson as reported in "The Structure of Electrolytic Solutions," edited by W. J. Hamer, John Wiley and Sons, New York, N. Y., 1959, p. 319.

(40) W. Klemm, *Z. anorg. u. allgem. Chem.*, **249**, 23 (1942).

dilution. This will be done by assuming that the differences between the heats of formation of $U(IV)$ in 1 M HCl and infinite dilution will be closely similar to the corresponding values for neptunium.⁴¹

From the data of Table VII, and making a small correction of 0.3 kcal./mole for the presence of fluosilicate,³⁰ the heat of the sum of reactions 4 and 5 is -165.1 ± 0.3 kcal./mole. Subtraction of the heat of formation of $1/2$ mole of water (-34.2 kcal./mole) results in a heat of formation of $Np(IV)$ in 1 M HCl of -130.9 ± 0.3 kcal./mole. Although this is within experimental error of the corrected value³ of -131.5 ± 0.3 kcal./mole reported previously in 1.5 M HCl , it is believed that the present value is to be preferred in 1 M HCl .

The difference between the heats of formation of $U(IV)$ in 1 M HCl and infinite dilution as previously given is 7.3 kcal./mole. Therefore, the estimated heat of formation of $Np^{+4}(aq.)$ becomes -138.2 ± 1 kcal./mole. Similarly, the heat of formation of $Np(IV)$ in 1 M $HClO_4$ becomes -134.9 ± 0.3 kcal./mole.

Table X contains a summary of the new thermodynamic functions reported in this communication. Free energies have been calculated by estimation of the entropies from various sources as indicated in the table.

TABLE X

SUMMARY OF THERMODYNAMIC PROPERTIES FOR URANIUM AND NEPTUNIUM SPECIES AT 25°

Species	ΔH_f^0 , kcal./mole	ΔF_f^0 , kcal./mole	S^0 , cal./ mole/ deg.
$U^{+4}(aq.)$	-157.1 ± 1.0	-148.2 ± 1.0	$(-80)^a$
$U(OH)^{+3}(aq.)$	-213.7 ± 1.0	-203.9 ± 1.0	$(-27)^b$
$U(IV)$ in 1 M HCl	-149.8 ± 0.4		
$U(IV)$ in 1 M $HClO_4$	$-153.8 \pm .4$		
$UCl_4(c)$	$-251.2 \pm .4$	-230.0 ± 0.4	47.4 ^c
$Np^{+4}(aq.)$	-138.2 ± 1.0	-128.1 ± 1.0	$(-84)^a$
$Np(IV)$ in 1 M HCl	-130.9 ± 0.3		
$Np(IV)$ in 1 M $HClO_4$	$-134.9 \pm .3$		
$Np(III)$ in 1 M HCl	$-125.6 \pm .3$		
$Np^{+3}(aq.)$	$-127.4 \pm .4$	-126.8 ± 0.4	$(-37)^a$
$NpCl_4(c)$	$-232.3 \pm .4^d$	-211.1 ± 0.6	(48)

^a Estimated by the method of R. E. Powell and W. M. Latimer, *J. Chem. Phys.*, **19**, 1139 (1951). ^b From $\Delta S_{hyd} = 36$ as reported by K. A. Kraus and F. Nelson (ref. 38) and an entropy of $U^{+4}(aq.)$ as given. ^c J. J. Katz and G. T. Seaborg, "The Chemistry of the Actinide Elements," John Wiley & Sons, New York, N. Y., 1957, p. 162. ^d Assuming the heat of solution of $NpCl_4(c)$ to be the same as $UCl_4(c)$; see reference 41.

The potential for the Np^{+3} - Np^{+4} couple at infinite dilution can be calculated with fair accuracy from the free energies in Table VIII as 0.056 volt, which may be compared to the "formal" potential in 1 M HCl of -0.137 volt.³³

(41) In this respect, the heat of solution of solid $ThCl_4$ reported in reference 42 in 1 M HCl is given as -57.4 kcal./mole, which may be compared to the corresponding uranium data in Table VI of -57.0 kcal./mole. However, the ionic crystal radii of Th^{+4} , U^{+4} and Np^{+4} are 0.95, 0.89 and 0.88 Å., respectively, so that the difference between the uranium and neptunium heats might reasonably be expected to be much smaller. It is on the basis of this reasoning that the heats of dilution of $NpCl_4$ solutions will be assumed to be the same as those for UCl_4 solutions.

(42) E. F. Westrum, Jr., and H. P. Robinson, Atomic Energy Commission Declassified Report AEC-D-2554, 1949.

Acknowledgments.—The authors are indebted to Dr. Jonathan Amy for his assistance in the preliminary design of the calorimeter bridge, and to Mr. Roy Hayes for his aid in electronic circuitry.

Dr. J. C. Wallman and D. B. McWhan of the Lawrence Radiation Laboratory were most generous in their aid and suggestions in the neptunium metal preparation.

POLYMORPHISM OF THE RARE EARTH SESQUIOXIDES¹

BY I. WARSHAW AND RUSTUM ROY

Contribution No. 60-92, College of Mineral Industries, The Pennsylvania State University, University Park, Pa.

Received May 25, 1961

Under equilibrium conditions the polymorphic forms of the rare earth sesquioxides transform reversibly from one form to the other. The sesquioxides of the largest ions, La, Ce and Pr, exhibit the A-type structure, Nd_2O_3 exists both as A- and C-type, while Sm_2O_3 , Eu_2O_3 , Gd_2O_3 , Tb_2O_3 and Dy_2O_3 exist both as B- and C-type oxides. The remaining rare earth sesquioxides occur only in the C-type structure. The C to B transition temperature increases linearly with decreasing ionic radius of the rare earth cation.

Introduction

The proper understanding of the polymorphic relationships among the rare earth sesquioxides is fundamental to any study involving these compounds and is of special importance when one considers the use or reaction of the rare earth oxides at elevated temperatures. A number of investigators, starting with Goldschmidt, *et al.*,² in 1925, have tried to outline the polymorphic relationships among the rare earth sesquioxides, but there is wide disagreement among all the studies.

The reasons for the widely differing results are readily apparent. Sufficiently pure rare earth oxides were not available to the earlier investigators, and thus it is to be expected that their work should contain many incorrect results. Purified rare earth sesquioxides were used for the more recent studies, but, with only minor exceptions, the experiments were not carried out with a view to studying equilibrium assemblages. Obviously, unless equilibrium is attained, it is impossible to compare the results obtained in one laboratory with those obtained in another. Due to the fact that they are reconstructive transformations, the inversions are particularly sluggish and in some instances it is difficult to attain equilibrium. This, however, does not detract from the fact that with time the compounds may invert even at low temperatures, and thus it is necessary to know what will happen under equilibrium conditions. In view of the fact that the authors were undertaking a program on the crystal chemistry of rare earth compounds and phase equilibrium studies involving the rare earth oxides, the re-examination of the polymorphism of the rare earth sesquioxides under equilibrium conditions was of particular importance.

The first studies of the polymorphism of the rare earth sesquioxides were carried out by Goldschmidt, Ulrich and Barth² in 1925, and followed by Goldschmidt, Barth and Lunde³ in 1925. They found that the rare earth sesquioxides could exist in three polymorphic forms, which they denoted as A,

B and C, and classified the structures as being hexagonal, probably monoclinic and cubic, respectively. They also noted slight differences within the B-type structures and classified them either as B₁ or B₂. In their earlier work they studied the reversibility of the transformations and concluded that the A to B transformations were reversible, while the B to C transitions were more complex, being monotropic for Sm_2O_3 but enantiotropic for Dy_2O_3 . While a single tentative stability diagram was presented in the first paper by Goldschmidt, *et al.*, eight generalized possible diagrams are given in the second paper. This larger number of diagrams is due to the inconclusive nature of the results and to the possibility that some of the polymorphs may be metastable.

Lohberg⁴ prepared C-type La_2O_3 and Nd_2O_3 by gentle heating of the respective nitrate compounds. While Bommer⁵ was able to confirm the existence of C-type Nd_2O_3 , he was not able to form C-type Ce_2O_3 or Pr_2O_3 .

Iandelli⁶ heated a number of the rare earth sesquioxides at various temperatures to obtain the approximate transformation temperature. From his study he postulated that the transformation temperature varied almost linearly with the atomic number. He obtained C-type La_2O_3 and Pr_2O_3 , but below 600° the former compound always consisted of a mixture of the C- and A-type structures.

Shafer and Roy⁷ studied the transformation temperatures for Nd_2O_3 , Sm_2O_3 and Gd_2O_3 by hydrothermal techniques and as a result they chose what they considered the most probable of the eight diagrams proposed by Goldschmidt, *et al.*,³ indicating the relationships among the various polymorphic forms of the rare earth sesquioxides. Moreover, they confirmed the existence of B-type Nd_2O_3 , which was found previously only by Goldschmidt, *et al.*

The polymorphism of the trivalent rare earth oxides was reinvestigated more recently by Roth and Schneider.⁸ They concluded that each oxide

(4) K. Lohberg, *Z. physik. Chem.*, [B], **23**, 402 (1935).

(5) H. Bommer, *Z. anorg. u. allgem. Chem.*, **241**, 273 (1939).

(6) A. Iandelli, *Gazz. chim. ital.*, **77**, 312 (1947).

(7) M. W. Shafer and R. Roy, *J. Am. Ceram. Soc.*, **42**, 563 (1959).

(8) R. S. Roth and S. J. Schneider, *J. Research Natl. Bur. Standards—A. Phys. and Chem.*, **64A**, 309 (1960).

(1) Dissertation of I. Warsaw in the Department of Geophysics and Geochemistry at The Pennsylvania State University.

(2) V. M. Goldschmidt, F. Ulrich and T. Barth, *Skrifter Norske Videnskaps-Akad. Oslo. I Mat. Naturv. Kl.*, No. 5 (1925).

(3) V. M. Goldschmidt, T. Barth and G. Lunde, *ibid.* No. 7 (1925).

	RARE EARTH SESQUIOXIDES														
	La	Ce	Pr	Nd	Sm	Eu	Gd	Tb	Dy	Ho	Er	Tm	Yb		Lu
Goldschmidt <i>et al.</i> (1925)	A	A	A (810) A ₁	A (1000) E ₁	A (1850) B ₁ (735) C	B ₁ (800) C	B _{1,2} (875) C	b (1150) C	b ₂ (1600) C	C	C	C	C	C	Temp. indicated were determined from diagram. All A to B and some B to C transformations were found to be reversible.
Shafer and Roy (1959)	a	a	a	A (1030) B 9.5 C	B 840 C	b	B 1025 C	b	b	b	c	c	c	c	Most temp. shown were determined from data and are ±20°. All transformations were considered reversible.
Iandelli (1947)	A		A	A	B 1150	B 1350									Temp. shown were determined from data and are ±50°. Max. temp. attained was 1500°.
Roth and Schneider (1960)	A	a	A	A	B 950	B 1075	1250								Temp. shown are given by authors. Limits of error were not given. All transformations are considered to be irreversible; all low-temp. forms believed to be metastable.
Warsaw and Roy	A	a	A	A	B 875	B 1100	B 1200	B 1875	B 2150						All transformations are reversible. All the polymorphs shown are stable within their respective temp. ranges.

Note: The existence of the polymorphic forms shown in small letters is indicated in the diagram or text of the paper; however, no experimental evidence is given in the paper.

a While the C-type polymorph is indicated in the diagram, the authors express doubt that it exists.

Fig. 1.—Comparison of the data given by several investigators on the existence of the high (A), medium (B), and low (C) temperature forms of the rare earth oxides and their transformation temperatures.

exists stably in only one form, the A-type for La_2O_3 to Nd_2O_3 , the B-type for Sm_2O_3 to Gd_2O_3 , and the C-type for all the remaining trivalent oxides. While they found that Nd_2O_3 , Sm_2O_3 , Eu_2O_3 and Gd_2O_3 could exist as C-type at lower temperatures, they concluded that these polymorphs were metastable and that all low-temperature forms inverted irreversibly to the stable form at higher temperatures.

All of the above work is summarized in Fig. 1. While most of the inversion temperatures shown in the figure are those specifically stated by the respective authors or taken from their tables of data, the temperatures given in parentheses were estimated by us from diagrams given in the respective papers.

Experimental

Equipment and Techniques.—For the most part the furnaces and equipment used throughout this study have been described previously. This includes platinum-wound quenching furnaces,⁹ the strip-furnace¹⁰ and hydrothermal equipment.¹¹

Because of the temperatures involved, the strip-furnace was used extensively. During the course of this study the maximum temperature attainable with this furnace was extended from 1850°, the melting point of 60 platinum-40 rhodium, to 2400° by the use of iridium strips. Since it is preferable to heat iridium in an oxygen-free atmosphere, a plastic box utilizing an O-ring seal was constructed to maintain a purified nitrogen atmosphere around the sample. By attaching the optical pyrometer to the base of the furnace, it was possible to be only a few inches from the sample. As a result the sample could be observed more closely and the sample temperature could be determined with greater accuracy.

At temperatures below 1000°, hydrothermal techniques were frequently used to aid diffusion of the ions and to establish equilibrium more rapidly. A variation in this

technique, known as "leak quenching,"¹² was employed so that the oxide being studied was in contact with water only at the highest temperature of the experiment. In this method, the water is added after the material is up to temperature and removed (leak-quenched) before the temperature quench. After the water vapor is released, the sample is dried at the temperature of the run for one-half to three hours before being quenched to room temperature. The longer drying times are required for low temperature runs. Leak-quenching was necessary to prevent the hydration of the rare earth oxides during cooling. With the oxides of all of the rare earths smaller than neodymium, the water vapor could act only as a catalyst because the temperatures of the experiments to determine oxide phase transitions were well above those at which hydrates could form.

Temperature Measurement.—The temperatures which are reported throughout this study were obtained by the use of Chromel-Alumel thermocouples if the temperature was below 1000°, of calibrated platinum-platinum-10 rhodium thermocouples when temperatures were in the range of 1000 to 1500° and of a calibrated optical pyrometer when the temperature exceeded 1500°. The melting points of the elements or compounds used as calibration standards were

Diopside	$\text{CaMgSi}_2\text{O}_6$	1391.5°
Pseudowollastonite	CaSiO_3	1544°
Platinum, C.P.	Pt	1773°
Corundum	Al_2O_3	2050°

Reagents and Preparation of Mixtures.—The purity of the rare earth sesquioxides is of special interest. For this study the rare earth compounds were at least 99.8% pure, with most of the compounds being 99.9% pure. While no quantitative analyses of the starting materials were carried out, semi-quantitative X-ray fluorescence analysis of most of the compounds used indicated only traces of contaminating rare earth ions in any particular compound, generally within the manufacturer's stated limits.

The nature of the starting materials used in this study varied with the particular experiment. Poorly crystallized, reactive hydroxides were used to avoid the metastable persistence of certain oxide starting materials. The former were prepared by dissolving the oxides in nitric acid followed by precipitation with ammonium hydroxide. The precipitates were separated and washed by centrifugation and then were dried at 105°. In order to test reversibility, it was essential to start with the various polymorphic forms of the oxides. The determination of the equilibrium temperature was made by heating both polymorphs of a certain oxide side by side at various temperatures followed by examination of both to detect changes in either one. In this manner it was

(9) E. S. Shepard, G. A. Rankin and F. E. Wright, *Amer. J. Sci.*, **178**, 293 (1909).

(10) M. L. Keith and R. Roy, *Am. Mineralogist*, **39**, 1 (1954).

(11) R. Roy and O. F. Tuttle, "Physics and Chemistry of the Earth," Vol. I, edited by L. H. Ahrens, Kalervo Rankama, Frank Press and S. K. Runcorn, Pergamon Press, London and New York, (Ch. VI 1956).

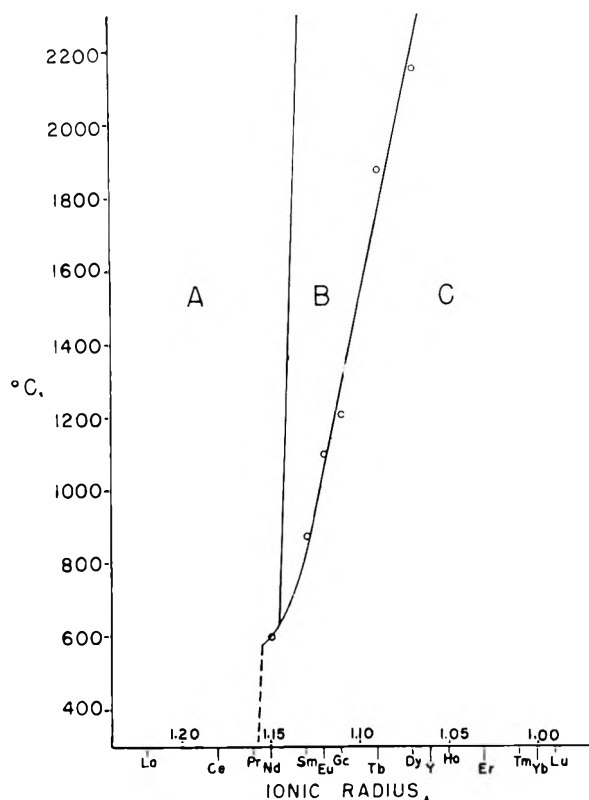


Fig. 2.—Temperature stability relationships of the rare earth sesquioxide polymorphs.

readily possible to determine which polymorph was the stable form at any given temperature.

Identification of Phases.—The phases formed under given conditions were identified in every case by powder X-ray diffractometry using Norelco and GE instruments. In this study the distinctions are simple and unequivocal.

Results

The results of the critical experiments are listed in Table I and are plotted in Fig. 2.

In Fig. 2, one can readily observe the relationships of the various polymorphs to each other and the dependence of the C to B inversion temperature on the radii of the rare earth ions. The linear relationship between the ionic radius and the transformation temperature for those compounds which involve both C- and B-type polymorphs is very striking. The second feature of the diagram is the fact that the boundary between the A- and B-type polymorphs is almost vertical so that Nd_2O_3 does not exhibit any B-type structure and Sm_2O_3 does not exhibit the A-type structure even near its melting point. While the boundary is drawn in such a manner that it appears that promethium sesquioxide would exhibit all three polymorphs there is no experimental evidence for this. The problem of what forms Pm_2O_3 would exhibit is strictly hypothetical and is not likely to be solved readily since promethium-147 has a very short half-life.

Discussion

The diagram shown in Fig. 2 most nearly corresponds to that previously determined by Shafer and Roy.⁷ However, there are considerable differences between this work and all previous studies regarding the inversion temperatures, the various

TABLE I
THERMAL DATA FOR ONE-COMPONENT RARE EARTH SES-
QUOXIDE SYSTEMS

Temp. (°C.)	Time	Pressure (p.s.i.)	Reactants	Products
The system Nd_2O_3				
560	22 da.	..	A	A + tr. C
600	66 hr.	5000	A	C (+ hydrate)
600	66 hr.	5000	Hydroxide gel	C (+ hydrate)
600	1 hr.	..	C + hydroxide	C + tr. A
600	2 hr.	..	Hydroxide gel	C
600	2 da.	..	Hydroxide gel	C + A
696	24 hr.	8000	C + A	A
715	20 hr.	4000	C	A (+ hydrate)
715	20 hr.	4000	Hydroxide gel	A (+ hydrate)
The system Sm_2O_3				
860	5 hr.	5000	Hydroxide gel	C
872	48 hr.	5000	B	C
880	20 hr.	5000	C	B
890	4 hr.	5000	Hydroxide gel	B
2350	30 min.	..	C	B
The system Eu_2O_3				
974	22 hr.	3000	B	C
1096	24 hr.	..	C	C
1105	30 hr.	..	C	C + small amt. B
1145	18 hr.	..	C	B
The system Gd_2O_3				
980	24 hr.	3000	Hydroxide gel	C
1182	35 hr.	..	B	B + small amt. C
1190	24 hr.	..	Hydroxide gel	C
1215	30 hr.	..	Hydroxide gel	B
1235	20 hr.	..	C	C + small amt. B
1309	18 hr.	..	Hydroxide gel	B
The system Tb_2O_3				
1800	30 min.	..	C	C
1860	30 min.	..	B	B + small amt. C
1870	30 min.	..	B	B + tr. C
1880	30 min.	..	C	C + small amt. B
1945	30 min.	..	C	B + C
2200	15 min.	..	C	B
The system Dy_2O_3				
2050	15 min.	..	C	C
2080	30 min.	..	B	C + B
2190	15 min.	..	C	B + C
2300	10 min.	..	C	B + small amt. C

forms in which the various oxides can exist and their stability relationships.

The results found in this investigation are almost a composite of certain statements by all the previous workers who have studied this subject. To begin with, all the transformations, especially the C to B, are reversible. While Goldschmidt, *et al.*,^{2,3} and Shafer and Roy⁷ found this to be true for some of the sesquioxides, Roth and Schneider⁸ claim that all the transformations are monotropic and that the low temperature forms are always metastable.

The linear relationship between the transformation temperature and the ionic radius of those oxides which exhibited both B- and C-type structures was mentioned in a general sense by Iandelli.⁶ However, his ideas were based on his inaccurate data and, moreover, he included the C to A as well

as the C to B transformations in his statement.

The almost vertical boundary between the A- and B-type polymorphs also was postulated by Roth and Schneider,⁸ while both Goldschmidt, *et al.*,² and Shafer and Roy⁷ show the boundary to have a moderate slope. These moderate slopes are due to the fact that Goldschmidt, *et al.*, obtained A-type Sm_2O_3 and B-type Nd_2O_3 while Shafer and Roy also found B-type Nd_2O_3 . It is believed that the availability of purer samples accounts for some of the differences between the present and previous studies. It is especially likely that the sesquioxides which Goldschmidt, *et al.*, used were impure since Bommer,⁵ who claimed that he used the purest rare earth oxides which were available in 1939, points out that his samarium oxide contained 0.8% europium and 0.3% gadolinium.

The differences between this work and that of Roth and Schneider⁸ are mostly due to their not using hydrothermal techniques to attain equilibrium at the lower temperatures and to the fact that, with only three exceptions, their study was limited to a maximum temperature of 1500°. In one instance they used an arc image furnace to melt Dy_2O_3 , but they were not able to quench the sample rapidly and did not observe the B-type polymorph.

The sesquioxides of the largest ions (La, Ce, Pr and Nd) most commonly exhibit the A-type structure. Lanthana has been reported⁴ to exist in the C form, but it has not been possible to repeat this preparation of C-type La_2O_3 . This polymorph has been prepared hydrothermally from the appropriate A- or B-type oxides of Nd, Sm and Eu. It should be emphasized here that, in the method used, the oxides were in contact with water only at the highest temperature of the run. It is not possible to obtain C-type oxides for the still larger rare earths hydrothermally since the A-type polymorph is stable down to the upper temperature limit for the oxyhydroxides. The inversion of A to C by dry heating has not been effected except in the instance

of neodymia, which indicates either that C is not a stable form of La_2O_3 , Ce_2O_3 or Pr_2O_3 or that the inversion temperature is too low for it to occur in a reasonable length of time.

The A \rightleftharpoons C transition of Nd_2O_3 is about 600° whereas Roth and Schneider⁸ stated that a temperature of 650° was required to change C to A.

While Shafer and Roy⁷ found that Nd_2O_3 could exist as the B-type polymorph as well as in the A and C forms, it was not possible to reproduce their results even though the same conditions and hydrothermal equipment were used in this study. This is probably due to a sample of higher purity being used in the present study.

The intermediate rare earth oxides exist in both the B- and C-type polymorphs and these transformations are reversible, as shown in Table I. These include Sm_2O_3 , Eu_2O_3 , Gd_2O_3 , Tb_2O_3 and Dy_2O_3 . While B-type Dy_2O_3 was reported previously by Goldschmidt, *et al.*,^{2,3} neither they nor any other previous investigators mentioned B-type Tb_2O_3 even though this oxide transforms at a lower temperature than Dy_2O_3 . As for Dy_2O_3 , it should be noted that it has not been possible to obtain pure B-type. As stated previously, the transformations are very sluggish and thus a considerable length of time is required to transform completely a particular sample. With our equipment it was not possible to maintain approximately 2400° for more than 15 to 30 minutes and thus the samples of Dy_2O_3 consist of both the B- and C-type polymorphs. The interpretation of such data is based on the fact that one polymorph will not grow at the expense of a second unless the first is the stable form under the conditions of the experiment.

The sesquioxides of the smallest ions, Y, Ho, Er, Tm, Yb and Lu, exist only as the C-type polymorph. All previous studies agree on this point.

Acknowledgment.—This work forms part of a research program in crystal chemistry supported by the Chemical Physics Branch of the U. S. Army Signal Corps.

THE DIPOLE MOMENTS OF SOME PHOSPHITE ESTERS AND THEIR DERIVATIVES

BY THEODORE L. BROWN, J. G. VERKADE AND T. S. PIPER

Noyes Chemical Laboratory, University of Illinois, Urbana, Ill.

Received June 5, 1961

The dipole moments of the constrained phosphite esters 1-methyl-4-phospha-3,5,8-trioxabicyclo[2.2.2]octane (I) and 1-phospha-2,8,9-trioxa-adamantine (VI) have been determined in dioxane solution. In addition the moments of the phosphate and thiophosphate of I have been determined. The constraints imposed by the bonding in I preclude free rotation about the P-O-R bonds, thus permitting a better estimate of the apparent P=O and P=S group moments. These are 2.95 and 2.62 D, respectively.

Introduction

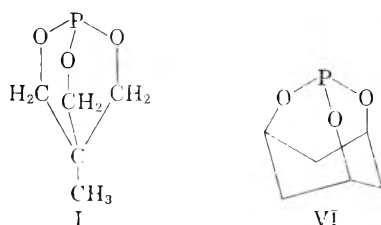
This paper reports the measurements of the dipole moments of the constrained phosphite esters, 1-methyl-4-phospha-3,5,8-trioxabicyclo[2.2.2]octane (I) and 1-phospha-2,8,9-trioxa-adamantine (VI). In addition the moments of a number of re-

lated compounds have been determined. Rotation of the alkoxy groups about the P-O bond is not possible in either I or VI. The interpretation of the dipole moments of these compounds, and more particularly of the difference in moment between phosphite and phosphate or thiophosphate, is more straightforward than in ordinary phosphite compounds.

TABLE I
DIPOLE MOMENT DATA FOR COMPOUNDS IN DIOXANE AT 25.0°
Values in parentheses refer to cyclohexane solution at 25.0°

Compound	Mol. wt.	α	β	P_2 (cm. ³)	MR (cm. ³)	μ (Debyes)
I CH ₃ C(CH ₂ O) ₃ P	148.10	14.60 (8.89)	-0.179 (- .45)	388 (348)	33.6 ^a	4.15 (3.91)
II CH ₃ C(CH ₂ O) ₃ PO	164.10	38.6	- .311	1068	33 ^b	7.10
III CH ₃ C(CH ₂ O) ₃ PS	180.17	32.0	- .237	984	41 ^c	6.77
IV (C ₂ H ₅ O) ₃ P	156.16	2.22 (1.44)	+ .062 (- .22)	110 (102)	42 ^d	1.82 (1.71)
V CH ₃ C(CH ₂ O) ₃ As	192.03	3.72	- .340	152	37 ^e	2.36
VI C ₆ H ₅ O ₃ P	130.11	17.2	- .290	485	36 ^a	4.7

^a From the value for triethyl phosphite using accepted values of C-C and C-H bond refractivities: A. I. Vogel, W. T. Cresswell, G. H. Jeffrey and J. Leicester, *J. Chem. Soc.*, 514 (1952). ^b From I, and comparison of triethyl phosphite (41.3 cm.³) with triethyl phosphite, (42.3 cm.³). ^c From I, and comparison of MR values of POCl₃ (25.1 cm.³) and PSCl₃ (32.8 cm.³). ^d From n_D^{20} 1.4079 and d_4^{25} 0.9687. ^e From I, by adding 3 cm.³; based on comparison of triphenylarsine with triphenylphosphine (E. Bergmann and W. Shütz, *Z. physik. Chem.*, B19, 401 (1932)), and of arsenic trichloride with phosphorus trichloride (J. W. Smith, *Proc. Roy. Soc. (London)*, 136, 256 (1932)).



Experimental

Dipole Moment Measurements.—The apparatus and procedure and purification of solvents have been described previously.¹ For some of the measurements a new heterodyne beat apparatus of conventional design was employed.² Weight fractions were in the range 0.002 to 0.015.

Preparation of Compounds.—The derivatives of pentaglycerol CH₃C(CH₂OH)₃ were prepared by a method previously described.³ Triethyl phosphite (Eastman-yellow label) was fractionally distilled. The fraction boiling at 48° (12.5 mm.)⁴ was taken. The synthesis previously reported⁵ for PO₃C₆H₅ (VI) affords a relatively low yield (20%). A method⁶ for the preparation of phosphites similar to compound I was extended. Phloroglucinol (1,3,5-trihydroxybenzene) was hydrogenated to *cis*-1,3,5-trihydroxycyclohexane by a previously described method⁵ with the modification that high pressure (10 atm.) was used. Hydrogen absorption essentially ceased after 6 hr. A mixture of *cis*-1,3,5-trihydroxycyclohexane and a 5 mole excess of trimethylphosphite was allowed to stand (with occasional shaking) under nitrogen for 10 days at 50°. At the end of this time the reaction mixture was a clear colorless solution. When the methanol formed in the reaction and the excess trimethylphosphite had been removed *in vacuo*, a white crystalline residue remained. The white solid was sublimed at 100° (0.05 mm.), the sublimate recrystallized from a minimum of pentane at -80° and the product re-sublimed at 100° (0.05 mm.), yield, 70%, m.p. (uncor.), 208–209°.

Anal. Calcd.: C, 45.00; H, 5.67. Found: C, 45.05; H, 5.77.

Results

The method of Halverstad⁷ and Kumler,⁷ with slight modification,¹ was employed in calculations of the dipole moments. The data and results are shown in Table I. Values for molar refractions were

- (1) T. L. Brown, *J. Am. Chem. Soc.*, **81**, 3232 (1959).
- (2) A. W. Cordes, Ph.D. Thesis, University of Illinois, 1960.
- (3) J. G. Verkade and L. T. Reynolds, *J. Org. Chem.*, **25**, 663, (1960).
- (4) A. Ford-Moore and J. Williams, *J. Chem. Soc.*, 1465 (1947).
- (5) H. Stetter and K. Steinacker, *Ber.*, **85**, 451 (1952).
- (6) W. S. Wadsworth and W. D. Emmons, Abstracts, 138th Meeting A.C.S., New York, p. 97P; M. S. Newman, private communication.
- (7) I. F. Halverstadt and W. D. Kumler, *J. Am. Chem. Soc.*, **64**, 2988 (1942).

estimated as indicated by the footnotes to Table I. Since all of the dipole moments are quite large, an uncertainty of one or two cm.³ in MR results in a very small uncertainty in the calculated dipole moment. No allowance was made in the calculations for atom polarization. The estimated uncertainty in the values of dipole moments is 0.05 D or less for all compounds except VI. This compound appeared to be more susceptible to oxidation than any of the others, and the quality of the data indicate an uncertainty in the moment of perhaps 0.2 Debye.

Discussion

The dipole moment values listed in Table I afford a number of interesting comparisons with the values for other phosphorus-containing compounds, Table II.

TABLE II

A COMPARISON OF SOME PHOSPHITE, PHOSPHATE AND THIO-
PHOSPHATE COMPOUNDS

	μ (D)	$\Delta\mu$ (D)
(C ₂ H ₅ O) ₃ (IV)	1.82	1.3
(C ₂ H ₅ O) ₃ PO ^a	3.07	
CH ₃ C(CH ₂ O) ₃ P(I)	4.15	2.95
CH ₃ C(CH ₂ O) ₃ PO(II)	7.10	
CH ₃ C(CH ₂ O) ₃ P(I)	4.15	2.62
CH ₃ C(CH ₂ O) ₃ PS(III)	6.77	
(C ₆ H ₅) ₃ P ^b	1.45	2.86
(C ₆ H ₅) ₃ PO ^b	4.31	
(C ₆ H ₅) ₃ P	1.45	3.29
(C ₆ H ₅) ₃ PS ^b	4.74	
(C ₆ H ₅ O) ₃ P ^c	2.03	0.78
(C ₆ H ₅ O) ₃ PO ^c	2.81	
(C ₆ H ₅ O) ₃ P	2.03	0.55
(C ₆ H ₅ O) ₃ PS ^c	2.58	

^a W. J. Svirbely and J. J. Lander, *J. Am. Chem. Soc.*, **70**, 4121 (1948). Value for benzene solution. ^b K. A. Jensen, *Z. anorg. u. allgem. Chem.*, **250**, 268 (1943). Values for benzene solution. ^c G. L. Lewis and C. P. Smyth, *J. Am. Chem. Soc.*, **62**, 1529 (1940). Values for benzene solution.

The moment of I is considerably greater than that of IV; this may be due in part to a greater lone pair moment in the former as a result of the tying back of the alkyl groups, but the major part of the increase probably arises from the presence of rotation about the P-O bonds in IV. Spectral evi-

dence⁸ indicates rotational isomerism in triethylphosphate, and it is very likely also present in the phosphite IV.⁹ Presuming that rotational isomerism exists in both triethyl phosphate and triethyl phosphite, the difference in moments between these two does not afford a good measure of the P=O group moment, because the conformations of the isomers, and the distributions between them, may be different in the two compounds. This objection is absent from the comparison of I with II, or of I with III in the case of the P=S group.

The difference in moments between triphenyl phosphine and triphenyl phosphine oxide (Table II), is close to the difference between I and II. It is interesting in the light of this that the difference between triphenyl phosphine and triphenyl phosphine sulfide is significantly larger than that between I and III. A similar situation is encountered in the series triphenyl phosphite, phosphate and thiophosphate, but here the variation in moment may include contributions from rotational

isomerism. The present results, therefore, appear to be the first which show unambiguously that the P=S group moment in thiophosphates is lower than the P=O group moment in the analogous phosphates, as distinct from the phosphine analogs in which the opposite is true.

It is widely recognized that the relatively low values for the P=O and P=S group moments are the result of π -bonding between oxygen or sulfur and phosphorus.^{10,11} Undoubtedly π -bonding also occurs in phosphites, and the difference in the moments of I and II or I and III includes changes in the bonding between phosphorus and the alkoxy oxygens in going from the phosphite to the phosphate or thiophosphate. It is clear that the group moments obtained by the comparisons made above are only *apparent* values, and include a number of contributions which cannot, on the basis of the dipole moment data alone, be separately evaluated.

Acknowledgments.—We thank the National Science Foundation for a grant and a fellowship (J.G.V.).

(10) J. W. Smith, "Electric Dipole Moments." Butterworths, London, 1955, p. 230.

(11) G. M. Phillips, J. S. Hunter and L. E. Sutton, *J. Chem. Soc.*, 146 (1945).

(8) F. S. Mortimer, *Spectrochim. Acta*, **9**, 270 (1957).

(9) Measurement of the dipole moments of both I and IV at 35.0° in dioxane gave values of 4.17 and 1.60 D, respectively. The moment of I is therefore essentially constant, whereas the moment of IV decreases by about 0.2 D. The existence of a temperature-dependent distribution of rotational forms in IV is indicated.

A COMPLETE IONIZATION SCHEME FOR CITRIC ACID

BY R. BRUCE MARTIN

Cobb Chemical Laboratory, University of Virginia, Charlottesville, Va.

Received May 29, 1961

Titration analysis of citric acid and selected methyl esters indicates that about 60% of the monoionized and 45% of the diionized species are symmetrical.

Recently two independent determinations were made of the relative ionizing tendency of the two kinds of carboxylic acid groups in citric acid. A nuclear magnetic resonance (n.m.r.) study indicated that ionization from the terminal carboxylic acid groups is predominant.¹ By measuring the relative chemical shifts of the methylene doublet as citric acid underwent progressive ionization and comparing these values with a scale for the chemical shift established by similar measurements on selected methyl esters, the mole fractions of the several ionic species could be estimated. In a second study, analysis of X-ray diffraction data demonstrates that the central carboxylic acid group is ionized in solid sodium dihydrogen citrate.² These two studies are not necessarily contradictory because the ionization favored in the solid state may not be favored in solution.

For many purposes it is the equilibria in solution that are of interest. A more direct method than n.m.r. exists for estimating the favored ionizations in citric acid with the aid of selected methyl esters.

Titration of the esters and comparison with the accurately known acid ionization constants of citric acid³ permits quantitative determination of the favored ionizations. This paper presents a titration analysis of the same esters used in the n.m.r. study and arrives at the opposite conclusion; the ionization from the central carboxylic acid group is predominant.

Experimental

Citric acid trimethyl ester⁴ had m.p. 75–76°, lit. 76°⁴ and 73–73.5°.¹ Citric acid symmetrical dimethyl ester⁵ had m.p. 116–118°, lit 125–126°⁶ and 115–117°.¹ *Anal.* Calcd. for monohydrate: C, 40.3; H, 5.9; eq. wt., 238. Found: C, 40.9; H, 6.0; eq. wt., 257. Titrations were performed at 25° on a Beckman Model G pH meter by addition of standard base from an ultramicroburet. No salt was added to keep the ionic strength low so the thermodynamic ionization constants of citric acid³ could be used. Because of the problem of ester purity and the selectivity of the hydrolyses described later, the results are rounded to 0.05 log units, but should be considered reliable to only ± 0.1 log units.

Results

The complete ionization scheme for citric acid is

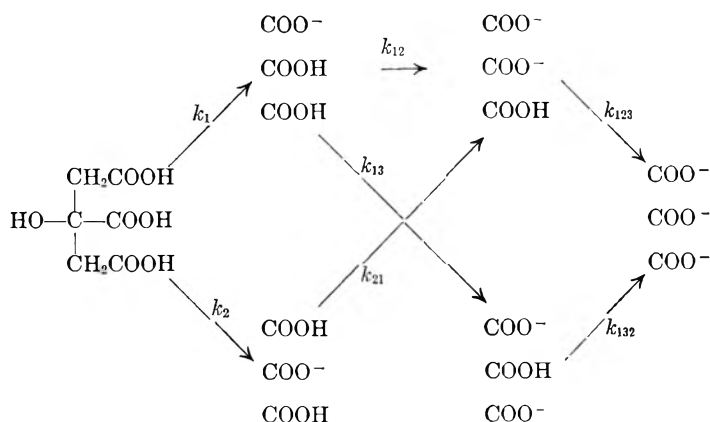
(3) R. G. Bates and G. D. Pinching, *ibid.*, **71**, 1274 (1949).

(4) W. E. Donaldson, R. F. McCleary and E. F. Degering, *ibid.*, **56**, 459 (1934).

(5) G. Schroeter, *Ber.*, **38**, 3190 (1905).

(1) A. Loewenstein and J. D. Roberts, *J. Am. Chem. Soc.*, **82**, 2705 (1960).

(2) J. P. Glusker, D. van der Helm, W. E. Love, M. L. Dornberg and A. L. Patterson, *ibid.*, **82**, 2964 (1960).



where the k 's are microscopic acid ionization constants, and the last subscript refers to the number of the carboxylic acid group ionizing in the indicated equilibrium. This scheme is simpler than that of the general case of a tribasic acid⁶ because the equivalence of the terminal carboxylic acid groups introduces an element of degeneracy. From the definitions of the micro and macroconstants, it may be shown that the macroconstants determined by titration are related to the microconstants by

$$K_1 = 2k_1 + k_2 \quad (1)$$

$$K_1K_2 = k_1k_{13} + 2k_2k_{21} = 2k_1k_{12} + k_1k_{13} \quad (2)$$

$$K_1K_2K_3 = k_1k_{12}k_{123} = k_1k_{13}k_{132} = k_2k_{21}k_{123} \quad (3)$$

$$K_3^{-1} = 2k_{123}^{-1} + k_{132}^{-1} \quad (4)$$

The accurately known macroconstants at zero ionic strength and 25° are³: $pK_1 = 3.13$, $pK_2 = 4.76$ and $pK_3 = 6.40$.

Two of the seven microconstants must be independently determined if the complete ionization scheme is to be delineated. Preparation of appropriate esters to block selected ionizations permits the microscopic ionization constants of unblocked groups to be estimated. The equivalence of an ester and an un-ionized carboxylic acid group finds support in the identical chemical shifts in the n.m.r. spectra of citric acid and its methyl esters.¹ Hydrogen bonding effects are probably minimal in the case of citric acid.⁷

The complete ionization scheme may be worked out from titration with standard acid after selective hydrolysis of one or two terminal ester groups of the trimethyl ester. Addition of one equivalent of base to trimethyl citrate and titration with acid after 10 minutes yield $pk_1 = 3.85$ over a range of acid to base ratios from 0.4 to 2.5. From equation 1, $pk_2 = 3.35$. Addition of two equivalents of base and titration with acid after 10 minutes yield two overlapping ionizations which may be analyzed by a pM vs. α plot.⁸ The results are $pk_1 = 3.85$, which checks well with the above value, and $pk_{13} = 4.40$. From equation 2, $pk_{12} = 4.60$, $pk_{21} = 5.10$ and from equation 3, $pk_{123} = 5.85$, $pk_{132} = 6.05$. The last two results are in agreement with equation 4.

(6) R. B. Martin, J. T. Edsall, D. B. Wetlaufer and B. R. Hollingworth, *J. Biol. Chem.*, **233**, 1429 (1958).

(7) F. H. Westheimer and O. T. Benfy, *J. Am. Chem. Soc.*, **78**, 5309 (1956).

(8) J. T. Edsall, R. B. Martin and B. R. Hollingworth, *Proc. Natl. Acad. Sci.*, **44**, 505 (1958).

Though the complete scheme has been worked out as described in the previous paragraph, some checks in addition to the one for pk_1 are desirable. Titration of citric acid symmetrical dimethyl ester over a range of acid to base ratios from 0.4 to 2.5 yields $pk_2 = 3.40$, in satisfactory agreement with the above value of 3.35. Addition of two moles of base to the same ester, titration with acid, and analysis by a pM vs. α plot⁸ yield a macroconstant K_E at the high pH end of the curve which is given by $pK_E = 5.25$. From the ionization scheme, this constant is related to the macroconstants by $K_E^{-1} = k_{12}^{-1} + k_{21}^{-1}$. From the microconstant values already estimated, the calculated $pK_E = 5.20$, in satisfactory agreement with the experimental value. Thus two more checks lend confidence to the estimated microconstant values.

Discussion

Relationships between the microconstants could be estimated by electrostatic theory, but the results would probably not be too reliable. Comparison with model compounds is perhaps more profitable. The k_1k_{13} ionization sequence occurs in glutaric acid where the difference in the logarithms of the micro ionization constants is 0.47.⁹ In this work $pk_{13} - pk_1 \approx 0.55$, in fair agreement with the model compound result.

The ratio of monoionized citric acid molecules with the terminal carboxylic acid groups ionized to those with the central group ionized is given by $2k_1/k_2$. From this work this ratio is about 0.6 so that the inverse ratio of central group ionized to terminal groups ionized is 1.6. At any pH in a solution of citric acid, 40% of the monoionized species have terminal carboxylic acid groups ionized. Thus the symmetrical monoionized citric acid species is predominant.

The only groups of citric acid not insulated from each other by at least two tetrahedral carbon atoms are the hydroxy group and the central carboxylic acid group. It might be expected that the central carboxylic acid group would be the most influenced by other groups on the molecule. Comparison of pK_a values of glycolic (hydroxyacetic) acid, $pK_a = 3.8$ with acetic acid, $pK_a = 4.7$, demonstrates the acid strengthening effect of a hydroxy group on a neighboring carboxylic acid group. On these grounds the central carboxylic acid group of citric acid should be more acidic than the two terminal

(9) R. H. Jones and D. I. Stock, *J. Chem. Soc.*, 102 (1960).

carboxylic acid groups. A more quantitative, but still approximate, comparison may be made by considering the $pK_a = 4.5$ for β -hydroxypropionic acid. The difference of 0.7 log unit for the effect of a hydroxy group in the α - and β -positions is slightly larger than the difference $pk_1 - pk_2 \simeq 0.5$ of this work.

The results from the n.m.r. analysis indicated 80% of the monoionized species are in the unsymmetrical form.¹ Assuming results of this paper correct, why are the n.m.r. results in error? The n.m.r. analysis for determining the relative importance of the k_1 and k_2 ionizations depends upon a comparison of chemical shifts of 9.7 and 7.3 c./sec. relative to un-ionized citric acid, for the unsymmetrical and symmetrical monoionized species, respectively. The observed shift, on the same scale, for free monoionized citric acid of 9.2 c./sec. indicates only 20% of the symmetrical monoionized species. Uncertainties of about 0.5 c./sec. allow for a considerable margin of error when the difference of the numbers being compared is only 2.4 c./sec. Assuming, however, the correctness of the standard chemical shifts obtained on the esters, the n.m.r. analysis may be brought into agreement with the results of this paper if the 9.2 c./sec. value were 8.2 c./sec. Apart from the n.m.r. measurements, the only assumption in deriving the 9.2 c./sec. value is a value for $pK_1^\circ = 3.13$. An analysis shows, however, that if a value of $pK_1 = 3.08$ had been used, a value of 8.2 c./sec. would have been obtained. This value of pK_1 , lower by only 0.05 log units, is a more reasonable value for the first ionization constant of citric acid when the minimum ionic strength is $0.2 M^3$ as in the n.m.r. study. According to the view presented here, the n.m.r. study gave an incorrect result not because of the n.m.r. data itself, but due to an inappropriate choice of pK_1 to which the interpretation is sensitive. By selecting a value of pK_1

more applicable to the conditions of the experiment, the n.m.r. results are consistent with the results of this study.

Considering the diionized species, it may be shown that the ratio of the unsymmetrical to symmetrical microforms is given by $2k_{132}/k_{123}$. This ratio is 1.3 from the constants given above. Thus about 55% of the diionized species are unsymmetrical. The statistically expected ratio and percentage are 2.0 and 67%, respectively. To the extent that the symmetrical diionized species permits greater separation of charges it would be favored. That this effect is not more pronounced is explained by examination of molecular models which indicate that the three carboxylic acid groups may distribute themselves nearly equidistant from one another. Several factors are operative in this situation, however.

The results just quoted for the diionized species are in sharp disagreement with the n.m.r. results which were interpreted to indicate that 100% of the diionized species are symmetrical.¹ Once again the discrepancy may be eliminated by lowering the impossibly high (in comparison with the ester standards) 20.2 c./sec. chemical shift to 16.9 c./sec. This change is in the direction expected for the effect of ionic strength on the assumed ionization constants. A decrease in pK_2 of only 0.08 log unit can bring agreement between all results. To a first approximation, ionic strength does not change the ratio of the microforms of species of the same charge, but ionic strength does change the ratio of forms with differing charges.

Acknowledgment.—This research was supported by grants from the National Science Foundation and the National Institutes of Health. The author thanks Charles W. Hill and Alice Parcell for performing the measurements.

HIGH TEMPERATURE PHASE RELATIONS IN THE FERRITE REGION OF THE Ni-Fe-O SYSTEM

BY M. W. SHAFER

International Business Machines Corporation, Yorktown Heights, New York

Received May 29, 1961

Thermogravimetric analysis and quenching experiments have been used to determine phase equilibria in the ferrite region of the Ni-Fe-O system. The area where single phase nickel ferrite spinels exists has been determined for oxygen pressures of 10^0 , $10^{-0.7}$ and 10^{-2} atmosphere at 1400, 1500 and 1600°. Liquidus temperatures and compositions also have been determined and are presented in terms of the ternary system Ni-Fe-O.

Introduction

This paper describes the results of a research program designed to improve the compositional control of ferromagnetic oxides with the spinel structure. Since the majority of these oxides can be thought of as solid solutions of transition metals in magnetite (Fe_3O_4), the problem of composition control is essentially one of determining the extent of the solid solution, *i.e.*, the spinel field boundary. Once this is done as a function of temperature, the task of preparing single phase polycrystalline

ceramics or even single crystals of any composition within the spinel field is relatively easy. The region of our primary interest in this work is the nickel ferrite spinel region, which will be discussed in terms of the phase equilibrium relations in the Ni-Fe-oxygen system.

Various people such as Blum and Zneimer,¹ Van Uitert² and Okazaki³ have studied some

(1) S. Blum and J. Zneimer, *J. Am. Ceram. Soc.*, **40** [6], 208 (1957).

(2) L. Van Uitert, *J. Chem. Phys.*, **23** [10], 1883 (1955).

(3) C. Okazaki, *J. Phys. Soc. Japan*, **15**, 2013 (1960).

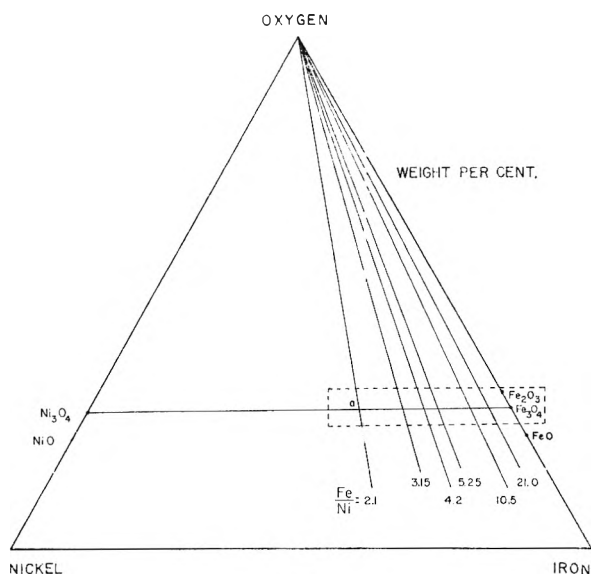


Fig. 1.

property of the nickel ferrite system as a function of composition, from which we can partially characterize the extent of spinel field. However, the most thorough work on the subject was by Paladino,⁴ whose use of vacuum techniques in determining the phase equilibrium enabled him to give an excellent description of the phase relations up to 1300°.

Experimental Method

Materials and General Procedure.—All starting materials used in the determination of the phase relations were prepared by coprecipitating the hydroxides of iron and nickel with NaOH. After very thorough washing, the precipitates were dried at 110°, fired at 800–900° for 24 hours, and then finely ground in a mortar. The iron–nickel ratio then was determined very precisely by chemical analysis for each of these starting mixtures.

The two general methods used in determining the phase equilibrium were quenching and thermogravimetric analysis. In the quenching experiments mixtures with known iron–nickel ratios were held in platinum or rhodium vials at constant temperature until equilibrium was reached among the gas, liquid and crystalline phases. This time varied from several hours at the lower temperatures to a matter of minutes above 1600°. The mixtures then were quenched and the phases present and their compositions were determined by microscopic examination and chemical analysis.

In some cases a more precise determination of the solidus temperature was obtained by vertically suspending an extruded rod of starting material in a tube furnace and recording the temperature at which a “rounding” was observed due to liquid formation. This procedure is described in more detail in a paper by Moruzzi and Shafer⁵ on liquidus determinations in the La₂O₃–Fe₂O₃ system.

In the thermogravimetric analysis 8–10 g. samples were suspended in Pt–Rh crucibles and slowly heated in various atmospheres, and the weight gain or loss was observed on an automatic recording balance. An excellent check on the equilibrium rates could be obtained by observing the weight change–time plot of the thermobalance. When no further weight changes were observed, it was assumed the system had reached equilibrium.

The oxygen pressures used in this investigation ranged from 10⁻² to 10⁰ atmosphere. Runs at P_{O₂} = 10⁰ atm. were made by passing purified tank oxygen directly through the furnace and runs at P_{O₂} = 10^{-0.7} atm. (air) were made by passing through dry air. Lower oxygen pressures were obtained by mixing oxygen and nitrogen. The rate of flow of each gas was measured by a calibrated flow meter. The

flow rate through the furnace was approximately 100 cc./min.

Apparatus and Analysis.—Vertical platinum-wound quenching furnaces, controlled by duration-adjusting-type temperature controllers, were used for temperatures below 1600°. A vertical furnace with uniquely designed molybdenum rods as the heating element was used in conjunction with a current-adjusting-type saturable-core reactor and a Leeds & Northrup AZAR recording controller for experiments above 1600°. Tungsten–rhenium thermocouples were used above 1600° for both the read and control couples. The control couple was suspended adjacent to the molybdenum element and both were contained in a forming gas atmosphere (10% H₂–90% N₂). Since tungsten–rhenium thermocouples cannot be used in an oxidizing atmosphere, the furnace chamber was flushed with forming gas after the sample had been removed and the reading couple then inserted in the same position as the sample. All temperatures were automatically recorded and any changes could easily be detected. It is believed that for the length of time the samples were being equilibrated, *i.e.*, up to several hours, the furnace temperature did not fluctuate any more than ±1/2° in the 1700° region. However, the accuracy of the temperatures reported is of the order of ±2° where Pt–10% Rh couples were used (below 1600°) and considerably poorer at higher temperatures where the tungsten–rhenium couples were used.

Phase identification was accomplished by microscopic examination of polished quenched samples using the usual metallographic techniques. Positive phase identification of selected samples was obtained by X-ray diffraction with a Norelco diffractometer.

The total iron, ferrous iron and nickel content of the quenched samples were determined by chemical analysis. The samples were put into sulfuric acid solution under deoxygenated nitrogen or in sealed tubes from which the air was removed. Ferrous and total iron were determined on separate aliquots; ferrous by directly titrating with dichromate and total by first reducing with stannous chloride and then titrating. The nickel was determined as nickel dimethylglyoxime on those samples where it was present in sufficient quantities, otherwise it was titrated with cyanide.

It should be pointed out, however, that in an investigation such as this where we are dealing with small compositional changes in the spinel phase, the limiting factor in accurately describing the phase relationship is the composition determination of the equilibrated phases. If we look at the binary diagram for the iron–oxygen system (Fig. 6) we can see that the single phase spinel area (Fe₃O₄ solid solution) covers a composition range from 27.63 wt. % oxygen for stoichiometric magnetite to 28.3% oxygen for magnetite in equilibrium with oxygen gas at 1460°. Now since this probably represents the maximum difference in oxygen content we will encounter, it is a formidable task indeed, by using wet chemical analyses methods on quenched samples, to determine compositions within a range where the differences in oxygen content are considerably smaller. For example, the average deviation of the most careful oxygen determinations was about 0.30% absolute which corresponds to an oxygen variation of about 0.03 wt. %. Such variations are more tolerable at the higher iron nickel ratios where it will be seen that the field is wider and the isobars are more separated than at lower iron nickel ratios where the field has very little width and there are very little compositional differences between the three isobars.

Also, this deviation did not allow a determination of the compositions where the isobars leave the spinel field with a degree of precision which was desired. As was pointed out earlier, one of the primary objects of this work was to determine with a fair degree of certainty just at what point for a given oxygen pressure the spinel phase would lose oxygen and the (NiFe)O phase would begin to form. Since this could not be done satisfactorily by using conventional wet chemical methods to analyze quenched samples, several other techniques were used. The most successful and the one which gave the greatest precision was thermogravimetric analysis. It was carried out on a slightly modified Stanton thermobalance which enabled us to uniformly heat 10-g. samples up to a temperature of 1620°. Weight changes down to 1 mg. could be detected and automatically recorded. By using samples of a total weight of about 10 g., the precision over wet chemical methods was improved by a factor of 40. Consequently, the resulting diagrams have been con-

(4) A. Paladino, *J. Am. Ceram. Soc.*, **42** [4], 168 (1959).

(5) V. Moruzzi and M. W. Shafer, *ibid.*, **43** [7], 367 (1960).

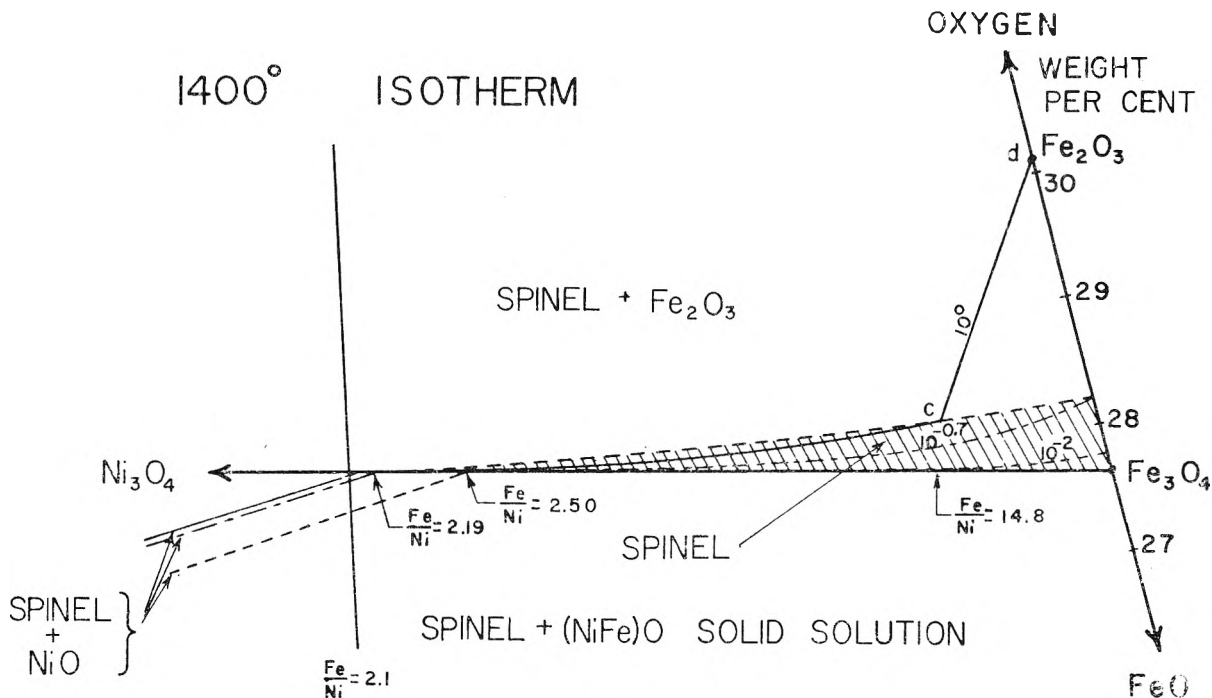


Fig. 2.

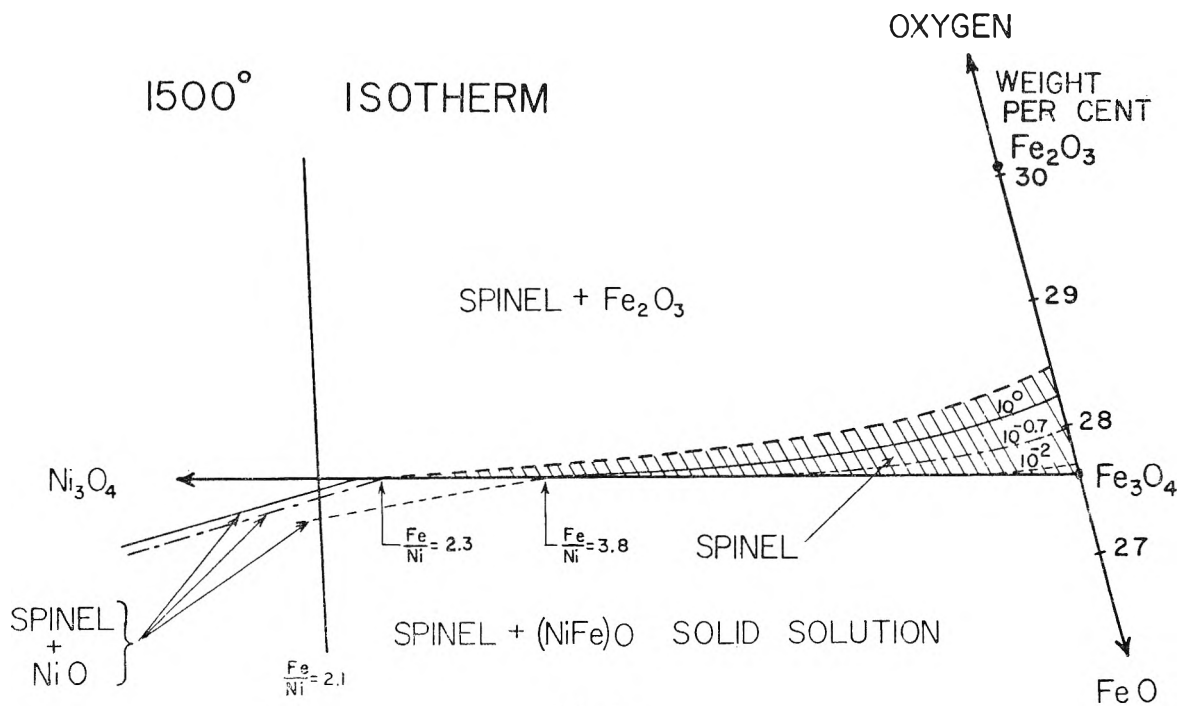


Fig. 3.

structured mainly from these data. It should be pointed out that to determine exact ternary compositions from thermobalance curves showing only weight changes, it is necessary that a known composition be used as a reference point. In this case the points used for reference were the compositions on the Ni_3O_4 - Fe_3O_4 join where we have an exact metal to oxygen ratio of 3:4. The justification for selecting these is based on the fact that Paladino's work firmly established the conditions up to 1300° under which stoichiometric nickel ferrite spinels can exist.

The compositions, under a different set of conditions, then could be found by measuring the weight gain or loss of the sample in terms of deviations from the Ni_3O_4 - Fe_3O_4 join. Of course, the success of this method is contingent on the as-

sumption that any weight changes were due only to a gain or loss of oxygen.⁶ It should be pointed out that although the total composition of the solid can be obtained by this method, it will not tell us anything about the phases present. The metallographic microscope proved to be a very successful tool in this determination. By examining polished quenched ceramic discs, as little as 0.1% Fe_2O_3 could be detected in the spinel phase. It was somewhat more difficult to detect

(6) This was not entirely the case for at the higher temperatures there was a measurable vaporization of the platinum container, in addition to a slight loss of oxide itself into the vapor phase. However, this was corrected easily by the addition of the appropriate calibration factor.

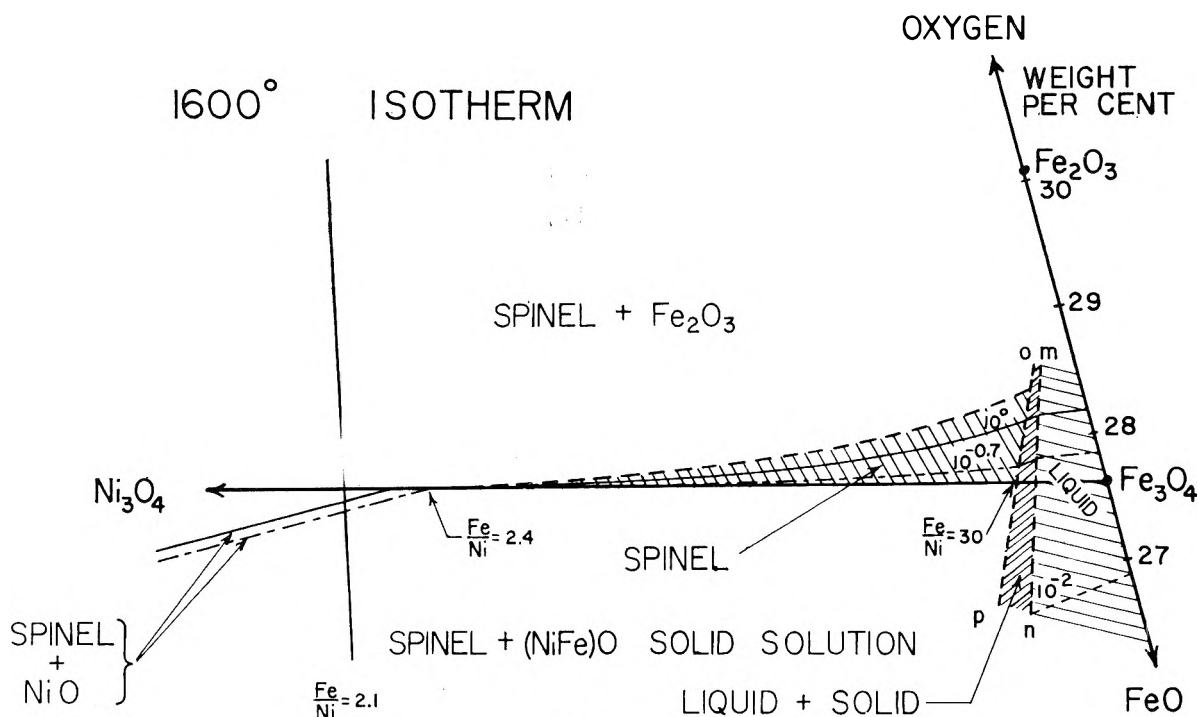


Fig. 4.

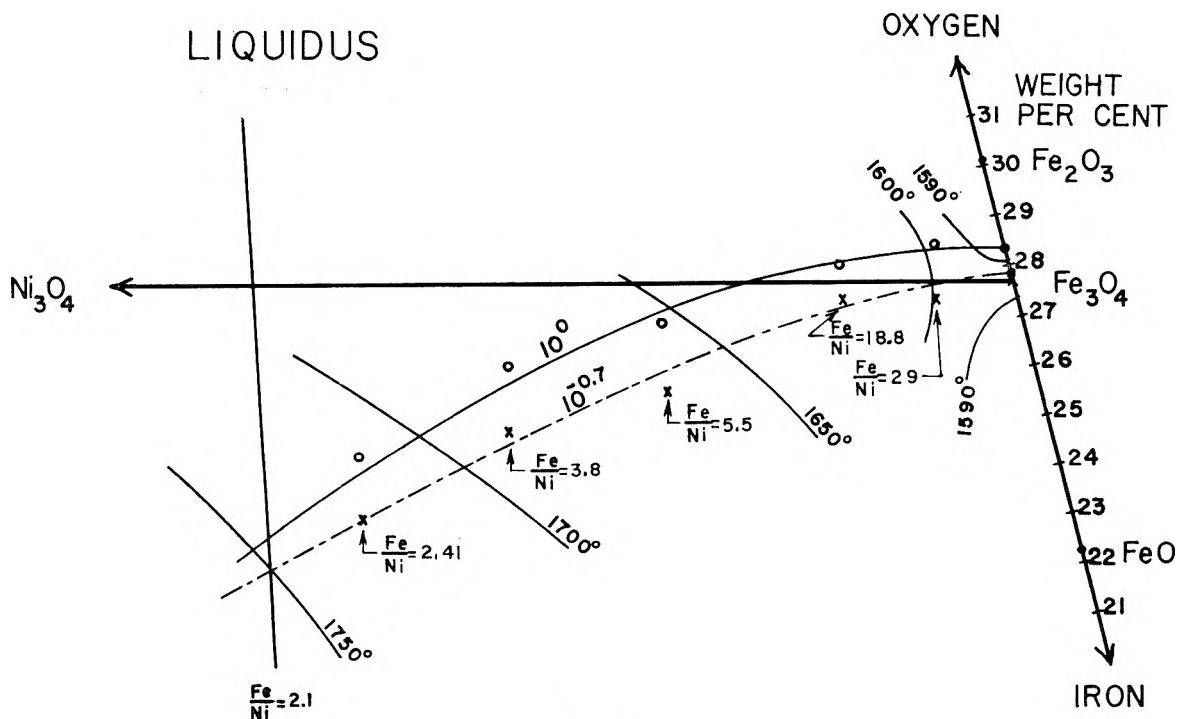


Fig. 5.

the (NiFe)O phase in the spinel matrix because its first appearance was in the grain boundaries. There was very good agreement however, between the points where the isobars cross the Ni_3O_4 - Fe_3O_4 join, *i.e.*, where spinel starts to decompose to a (NiFe)O phase, as determined by microscopic examination, and where they cross as determined from weight loss measurements on the thermobalance. These points were checked further by cell dimension measurements⁷ and good agreement was obtained.

Results

The results of the quenching and thermogravimetric analysis experiments can be shown best in terms of the ternary system Ni-Fe-oxygen. This is illustrated in Fig. 1 which is a compositional plot on a weight per cent. basis and shows the composition of the compounds existing in the binary systems Ni-O and Fe-O. The nickel ferrite

(7) J. E. Weidenborner and M. W. Shafer, to be published.

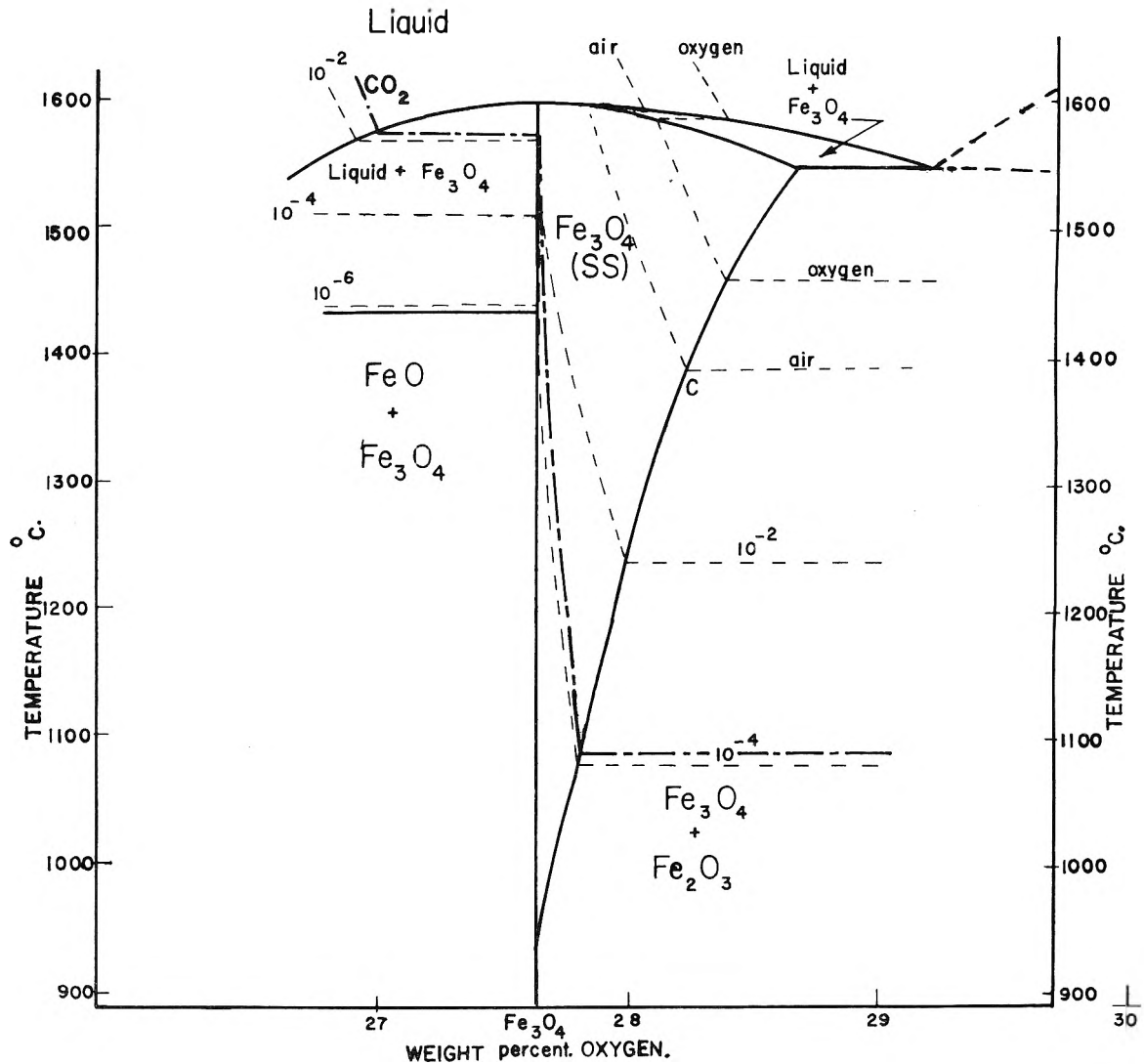


Fig. 6.

spinel region, the area of our interest, is outlined by the dashed lines along the join between Fe_3O_4 and Ni_3O_4 . It is on this line where we have a metal to oxygen ratio of exactly three to four, in other words, the proper ratio for the formation of phases with the spinel structure. Since we are only defining compositions in Fig. 1, it is irrelevant whether Ni_3O_4 actually exists as a crystalline phase.

The straight lines (light solid lines) emanating from the oxygen corner of the triangle and crossing the Ni_3O_4 - Fe_3O_4 join are lines of constant Fe/Ni ratio (iso-Fe-Ni lines). Each such line specifies a composition with a predetermined Fe/Ni ratio. For purposes of orientating the reader, the actual ratio values for some representative lines are shown in Fig. 1. For example, the point where the Fe/Ni = 2.1 line intersects the Ni_3O_4 - Fe_3O_4 join (point a in Fig. 1) would denote a composition of NiFe_2O_4 , i.e., nickel ferrite.

The phase diagrams in Figs. 2, 3, 4 and 5 have been constructed from data obtained from the quenching and thermobalance experiments. Although the phase relations are presented in terms of the Ni-Fe-O system, the area shown in these

diagrams only includes that portion of the ternary which is outlined by the dashed lines in Fig. 1. Figures 2, 3 and 4 are isothermal sections for temperatures of 1400, 1500 and 1600°, respectively and Fig. 5 is a projection of the liquidus surface. The data for the binary system iron-oxygen has been taken from the published works of Darken and Gurry⁸ and Smiltens.⁹ The medium, solid and dashed lines in these diagrams are the isobars for the oxygen pressures (P_{O_2}) used in this investigation, 10^0 , $10^{-0.7}$ and 10^{-2} atm. These will be straight lines in regions where two condensed phases are in equilibrium and their extremities will denote the composition of the two phases in equilibrium. For example, in Fig. 2 the two solid phases in equilibrium with $P_{\text{O}_2} = 10^0$ are spinel and Fe_2O_3 , and their compositions are given by points c and d, respectively. In the single solid phase regions such as the spinel field it is no longer a requirement that the isobars be straight lines, and indeed this is the case. Here the composition of the one solid phase in equilibrium with

(8) L. S. Darken and R. W. Gurry, *J. Am. Chem. Soc.*, **68**, 798 (1946).

(9) J. Smiltens, *ibid.*, **79**, 4877 (1957).

TABLE I
OXYGEN PERCENTAGES FOR Fe/Ni RATIOS AT EACH TEMPERATURE AND OXYGEN PRESSURE

Fe/Ni	1400°			1500°			1600°		Liquidus	
	10 ⁰	10 ^{-0.7}	10 ⁻²	10 ⁰	10 ^{-0.7}	10 ⁻²	10 ⁰	10 ^{-0.7}	10 ⁰	10 ^{-0.7}
∞	30.01	28.20	27.73	28.24	28.18	27.73			28.30	27.91
29.5	29.41	28.13	27.67	28.07	27.83	27.60 ^a	28.04	27.67	28.35	27.60
15.5	28.73	28.15	27.62	28.15	27.72	27.58 ^a	27.90	27.64	28.1	27.30
13.8	28.50	28.15	27.63	27.97	27.67	27.57 ^a				
9.0	27.94	27.92	27.54 ^a	27.84	27.55 ^a	27.55 ^a	27.72	27.55		
5.67	27.69	27.76	27.57 ^a	27.65	27.50 ^a	27.51 ^a	27.55	27.51 ^a	27.11	26.01
4.25	27.68	27.64	27.48 ^a	27.51	27.48 ^a	27.49 ^a				
3.80	27.62	27.57	27.46 ^a	27.46	27.46 ^a	27.44	27.46 ^a	27.46 ^a	25.84	24.80
2.43	27.40 ^a	27.40 ^a	27.39 ^a	27.40 ^a	27.41 ^a	27.35	27.39 ^a	27.40 ^a	24.5	23.6
2.26	27.39 ^a	27.39 ^a	27.35	27.39 ^a	27.38 ^a	27.36	27.39 ^a	27.37		
2.19	27.39 ^a	27.37 ^a	27.28	27.39 ^a	27.35	27.30	27.38 ^a	27.33		
2.13	27.39 ^a	27.35	27.27	27.35	27.31				23.5	23.0
22.01	27.35	27.35	27.27	27.35	27.32		27.32	27.30		
1.86	27.32	27.31		27.31						

^a Indicates a metal to oxygen ratio of 3:4.

the gas phase is given at the point of intersection of the isobar and the iso-Fe-Ni line.

In Fig. 5, where we have only liquid in equilibrium with the gas phase, the liquid composition is given at the point where the isobar intersects the iso-Fe-Ni line. Temperatures are indicated in Fig. 5 by the light solid lines.

The shaded portion of Figs. 2, 3 and 4 shows the approximate compositional limits where nickel ferrite spinel can exist as a single phase. The two two-phase regions adjacent to it are the spinel and Fe₂O₃ region on the oxygen-rich side and the spinel and (NiFe)O region on the metal-rich side.

Table I also summarizes the results of the experimental work and gives the composition of the spinel phase for P_{O₂} of 10⁰, 10^{-0.7} and 10⁻² atm. at temperatures of 1400, 1500, 1600°, and the liquidus.

Discussion

It should be noted from Figs. 2, 3 and 4 and from Table I that the nickel ferrite spinel field has considerable width on the oxygen side of the Fe₃O₄-Ni₃O₄ join. In other words, the spinel phase has the ability to take a fraction of a per cent. of oxygen into solid solution. This is not an uncommon phenomenon and has been observed in most iron-rich spinels. Structurally such spinels have a complete oxygen lattice with some cation sites unoccupied (probably on B sites) and are often referred to as spinels with "cation vacancies." Since a vacancy is essentially created by the oxidation of 3 ferrous ions to 2 ferric ions, the actual number can be controlled by controlling the oxygen pressure above the condensed phase. This is clearly illustrated in the portion of the iron-oxygen system, shown in Fig. 6, where the oxygen content, *i.e.*, the Fe⁺⁺⁺/Fe⁺⁺ ratio of the Fe₃O₄ phase, is strongly dependent on the oxygen partial pressure of the gas phase with which it is in equilibrium. This area of oxygen solid solutions with spinel or cation vacancies would be expected to be a maximum in the binary iron-oxygen system where there are a maximum number of ferrous ions present in the spinel structure, *i.e.*, 1/3. Now as we substitute nickel(II) for iron(II) on the B sites of the spinel structure, we are essentially

reducing the number of ferrous ions which can participate in vacancy formation. Consequently, the extent of the solid solution should be reduced unless vacancies can be introduced by the oxidation of nickel(II) to nickel(III). This latter possibility is unlikely considering the fact that the third ionization potential of nickel¹⁰ is about 6 e.v. larger than that of iron. Likewise, there is no strong evidence from magnetic moment measurements that suggests the presence of nickel(III) in the spinel lattice at these temperatures. So assuming only vacancies caused by ferrous iron oxidation, one would expect a linear decrease in the extent of the solid solution from a maximum value at Fe₃O₄ to zero at Ni₁Fe₂O₄, where the ferrous iron concentration is zero. This is essentially what was determined and is shown in Figs. 2, 3 and 4. It is seen in Fig. 2, the 1400° isotherm, that the spinel field has maximum width along the iron-oxygen binary (Fe/Ni = ∞) which corresponds to point c in Fig. 6, and decreases almost linearly with nickel additions until Fe/Ni = 2.3 concentration. Beyond this point the field has no width, even at P_{O₂} = 10⁰. However, as was inferred earlier, it is probable that at only moderately higher oxygen pressure the field would continue to have width until a Fe/Ni = 2.1 concentration, the point where all the iron(II) is replaced by nickel(II). Still at much higher oxygen pressures, it is also probable that the field can have width all across the Fe₃O₄-Ni₃O₄ join to Ni₃O₄ (Fe/Ni = 0).

In Fig. 2, the 1400° isothermal section, the composition of the condensed phases in equilibrium with the various oxygen pressures used in this investigation should be noted. Both the 10^{-0.7} and 10⁻² atm. isobars lie wholly within the spinel field in the iron-oxygen binary and remain there until the nickel concentration reaches a Fe/Ni = 2.50 for P_{O₂} = 10⁻² and 2.19 for P_{O₂} = 10^{-0.7}. In other words, the spinel composition is given along the isobars as they pass through the single phase spinel field and the iron-rich spinels in P_{O₂} = 10^{-0.7} and to a lesser extent in P_{O₂} =

(10) R. Parsons, "Handbook of Electrochemical Constants," Academic Press, Inc., London, 1959.

10^{-2} atm. have excess oxygen in solid solution. At $\text{Fe/Ni} = 2.50$ for $P_{\text{O}_2} = 10^{-2}$ atm. and 2.19 for $P_{\text{O}_2} = 10^{-0.7}$ the isobars cross the Ni_3O_4 - Fe_3O_4 join and leave the spinel field. At this point, as the nickel concentration increases, they become tie lines showing two phases in equilibrium. In this case the two phases are a spinel, whose composition is given by the point where the isobar crosses the join, and a $(\text{NiFe})\text{O}$ solid solution. Since we were concerned mainly with the spinel phase in this investigation no effort was made to determine the composition of the $(\text{NiFe})\text{O}$ solid solution. However, its existence has been shown by several investigators.^{11,12} In a like manner the oxygen isobar leaves the field but at a point very close to $\text{Fe/Ni} = 2.1$ ($\text{Ni}'\text{Fe}_2\text{O}_4$). The analysis results were such that it was difficult to precisely define this point.

The 1500° isothermal section in Fig. 3 shows essentially the same behavior as observed at 1400° . In this case, however, the 10^0 atm. oxygen isobar falls wholly within the spinel field meaning one would have to go to oxygen pressures greater than 1 atm. to have spinel in equilibrium with Fe_2O_3 at 1500° . Again all three isobars leave the spinel field at higher nickel concentrations and become tie lines showing the spinel- $(\text{Ni-Fe})\text{O}$ equilibria.

In Fig. 4, the 1600° isotherm, the width of the spinel field is somewhat decreased and the isobars become tie lines at higher iron concentrations than at lower temperatures. It is seen that 1600° is above the liquidus temperature for the iron-rich portion of the system. It can be seen readily from the iron-oxygen binary in Fig. 6 that at 1600° only liquid oxide is in equilibrium with the gas phase. The highest temperature at which a crystalline phase is present is 1597° , the melting point of stoichiometric magnetite. As the nickel concentration is increased there is a corresponding increase in the liquidus temperature and at 1600° the liquidus composition is shown by the line mn. There is a rather narrow compositional range of liquid plus solid coexisting as the phases in equilibrium. The composition of the solidus is given along line op and has the $\text{Fe/Ni} = 30$ at the $P_{\text{O}_2} = 10^{-0.7}$ isobar intersection. Further nickel additions yields only single phase spinel in air and oxygen until a $\text{Fe/Ni} = 2.41$, at which point the $(\text{NiFe})\text{O}$ phase begins to form. Because of certain experimental difficulties the condensed phase compositions in the $P_{\text{O}_2} = 10^{-2}$ atm. isobar were not determined.

The liquid oxide compositions at liquidus temperatures are shown in Fig. 5 for the $10^{-0.7}$ and 10^0 isobars. Since this is not an isothermal section, the temperatures are indicated by the light solid lines crossing the isobars. It is evident that there is a rather linear increase in the liquidus temperature from about 1590° to about 1740° as the nickel concentration increases from $\text{Fe/Ni} = \infty$ to $\text{Fe/Ni} = 2.1$. Note that within the experimental error of the determination,¹³ the isobars

are smooth curves with no major discontinuity. This is an indication that the liquid structure is essentially the same across the system. In other words, the arrangement of ions in the iron oxide liquid is unaffected by nickel additions. Since the isobars cross to the metal side of the Ni_3O_4 - Fe_3O_4 join at rather low nickel concentrations, *i.e.*, in $P_{\text{O}_2} = 10^{-0.7}$ $\text{Fe/Ni} = 29$, and $P_{\text{O}_2} = 10^0$ $\text{Fe/Ni} = 8$, the liquids for the most part contain considerably less oxygen than the 3:4 spinel ratio. Of course this does not mean that if an oxygen deficient liquid is frozen under equilibrium conditions the resulting crystalline phase would have the same composition as the initial liquid. The actual situation is one in which the crystalline phase in equilibrium with the oxygen deficient liquid has a composition which corresponds to a metal to oxygen ratio of 3:4. Consequently, the spinel phase with compositions on the Ni_3O_4 - Fe_3O_4 join¹⁴ is the crystalline phase in equilibrium with many of the oxygen deficient liquid compositions. The exceptions are those liquid compositions with an Fe/Ni of less than 2.95. For these liquid compositions the spinel phase in equilibrium with the liquid remains at the point where the $\text{Fe/Ni} = 2.95$ line intersects the Ni_3O_4 - Fe_3O_4 join. In other words, by freezing a liquid in a $P_{\text{O}_2} = 10^0$ the maximum amount of nickel contained in the resulting spinel, regardless of the nickel concentration of the liquid, is where the $\text{Fe/Ni} = 2.95$. This corresponds to a composition of $\text{Ni}_{0.76}\text{Fe}_{2.24}\text{O}_4$ since it falls on the Ni_3O_4 - Fe_3O_4 join where the metal to oxygen ratio is 3 to 4. Further nickel additions will just result in a spinel of this composition and a nickel oxide precipitate. Of course, the corresponding spinel composition formed from liquids cooled in $P_{\text{O}_2} = 10^{-0.7}$ would have a somewhat higher iron-nickel ratio. On the other hand, it would be necessary to go to oxygen pressures greater than one atmosphere to increase the nickel concentration in the spinel phase which can be formed by freezing a liquid. It should be pointed out that no definite effort was made to determine the crystalline compositions in equilibrium with the liquid, and that the evidence for establishing the $\text{Fe/Ni} = 2.95$ composition as the limiting spinel compositions is based only on the results of crystal growth experiments. Under these conditions a known iron-nickel ratio is slowly cooled from above the liquidus temperature to a point where it is completely frozen. It is from the results of the chemical analysis of these crystals that the $\text{Fe/Ni} = 2.95$ and several other points were determined. This method would essentially give the compositions of the crystals in equilibrium with the last liquids to crystallize rather than that of the crystals at the liquidus temperature. However, all evidence indicates that the tempera-

ture at these temperatures the contamination from the container, *i.e.*, rhodium crucibles, was quite severe. It appeared that a quantity of rhodium metal would dissolve in the molten oxide and precipitate out on cooling. Since reaction rates at these temperatures are very rapid, it is also possible that we were not preventing oxidation state changes during quenching.

(14) Since there was no evidence from this or any previous work of nickel ferrite spinels with metal ions in solid solution, *i.e.*, anion vacancies, this statement is justified.

(11) V. Arkharov, A. Varskaya, M. Zhvavleva and G. Chufarov, *Doklady Akad. Nauk S.S.S.R.*, **87**, 49 (1952).

(12) J. Benard, *Ann. Chim.*, **12**, 5 (1959).

(13) As is evident from the experimental points shown in Fig. 5, the scatter is quite bad. This probably can be explained by the fact

ture range where liquid and crystal coexist in equilibrium is rather small. This tends to make any compositional changes, which occur as we cool through this region, likewise rather small.

The equilibrium relationships are essentially the same as those where we are only dealing with solid-solid equilibria—that is, as the nickel con-

centration increases it is necessary to have a corresponding increase in oxygen pressure to prevent the decomposition of the spinel phase.

Acknowledgments.—The author gratefully acknowledges the assistance of H. G. Schaefer in the preparation of the starting materials and G. L. Evans and J. Kuptsis in the chemical analysis.

CALCIUM-CALCIUM HYDRIDE PHASE SYSTEM¹

BY D. T. PETERSON AND V. G. FATTORE

Institute for Atomic Research, Iowa State University, Ames, Iowa
Sicedison S.p.A., Centro Studi e Ricerche Bollate, Milan, Italy

Received May 31, 1961

The CaH₂ phase diagram was studied by thermal analysis and chemical analysis of equilibrated phases. The maximum solubility of CaH₂ in calcium metal is 24 mole % at the peritectic temperature of 890°. Calcium metal undergoes an allotropic transition at 448 ± 2° and melts at 839 ± 2°. An intermediate phase, stable between 320 to 600°, is produced by hydrogen. Calcium hydride shows an allotropic transformation at 780°.

Introduction

The calcium-calcium hydride system has been studied by several authors by determining pressure-composition isotherms. By this method it was possible to investigate only the portion of the system above 550°, because below this temperature the pressure is too small to be measured with reasonable accuracy. Hurd and Walker² have summarized the work up to 1931. Since that time the structure of CaH₂ has been determined by Zintl and Harder.³ Johnson, *et al.*,⁴ and Treadwell and Stecher⁵ have studied the system by pressure composition isotherms and obtained concordant results. In the temperature range of these measurements, hydrogen dissolves in the calcium phase up to about 20 mole % CaH₂. From this composition to about 90 mole % CaH₂, the calcium and CaH₂ phases coexist and, at constant temperature, the pressure is fixed. The CaH₂ phase varies in composition with the hydrogen pressure and approaches very near CaH_{2.0} as an upper limit.

Pure calcium was reported by Smith, *et al.*,⁶ to be f.c.c. up to 464° and b.c.c. above this temperature, but contamination caused the appearance of other allotropic forms. Hydrogen was shown to play an important role in the allotropic behavior of calcium. Other investigators have reported different allotropic forms and transformation temperatures for calcium. These results have been summarized and discussed by Schottmiller, *et al.*⁷ The study of this system was expected to give some explanation of the observed phenomena. Dif-

ferential thermal analysis, equilibration experiments and X-ray examination were the experimental methods employed in this work.

Experimental Methods

Materials.—The calcium metal used in this investigation was purified by distillation at 950° under a pressure not exceeding 1 × 10⁻⁵ mm. Chemical and spectrographic analysis of this calcium showed that its purity was about 99.94%, if the hydrogen and oxygen contents were not considered. The main impurities are: Mg, 300 p.p.m.; C, 100 p.p.m.; Si, 100 p.p.m.; N, 50 p.p.m.; Fe, 20 p.p.m. Oxygen was not determined. The hydrogen content varied from 120–220 p.p.m., corresponding to 0.24–0.44 mole % of CaH₂. To avoid contamination, the calcium always was kept out of air and handled in a glove box previously evacuated to 5–10 μ and filled with argon whose purity was over 99.9%. Very pure hydrogen for charging the specimens was obtained by heating uranium hydride above 300°.

Thermal Analysis.—The calcium (7–8 g. of distilled crystals) was placed into the thermal analysis capsule in the glove box. The capsule was of type 304 stainless steel and was 6.5 cm. long, 1.9 cm. inside diameter and 1.5 mm. wall thickness. The suitability of type 304 stainless steel as an inert crucible for molten calcium was verified by analyzing the calcium after heating to 900° in the thermal analysis capsule. The total increase in metallic impurities was only 0.03 atomic %. In addition, the melting point was determined in a tantalum thermal analysis capsule and the same melting temperature was found as in stainless steel capsules. There was a thermocouple well 1.3 cm. deep and 3 mm. in diameter in the bottom of the capsule. The top end was only partially closed by welding on a cover in order to allow rapid access of hydrogen to the calcium during charging. The capsule was placed in a 45 cm. long quartz tube which was closed at one end and at the other end a stopper with a stopcock was sealed with Apiezon W wax. After this operation the tube was taken from the glove box and joined to the charging apparatus. This consisted of a resistance furnace for heating the specimen, a calibrated volume and a manometer for measuring the hydrogen, a uranium hydride hydrogen generator and a mechanical vacuum pump. The apparatus was evacuated and filled with a known amount of pure hydrogen which was allowed to react with the specimen at about 510–530°. After charging to the desired concentration of CaH₂, the quartz tube was transferred again to the glove box. The capsule was taken out and the cover completely sealed by welding. The capsule then could be handled out of the glove box without danger of contamination and it was ready for the thermal analysis.

The loss of hydrogen from the capsule by diffusion through the walls of the capsule during the thermal analysis was reduced by placing the capsule in a close-fitting quartz tube which was evacuated and closed. The amount of hydrogen

(1) Contribution No. 1024. Work was performed in the Ames Laboratory of the U. S. Atomic Energy Commission.

(2) C. B. Hurd and K. E. Walker, *J. Am. Chem. Soc.*, **53**, 1681 (1931).

(3) E. Zintl and H. Harder, *Z. Elektrochem.*, **41**, 33 (1935).

(4) W. C. Johnson, M. F. Stubbs, A. E. Sidwell and A. Pechukas, *J. Am. Chem. Soc.*, **61**, 318 (1939).

(5) W. D. Treadwell and J. Stecher, *Helv. Chim. Acta*, **36**, 1820 (1953).

(6) J. F. Smith, O. N. Carlson and R. W. Vest, *J. Electrochem. Soc.*, **103**, 409 (1956).

(7) J. C. Schottmiller, A. J. King and F. A. Kanda, *J. Phys. Chem.*, **62**, 1446 (1958).

which escaped was determined by measuring the pressure with a manometer. In all cases, the change in composition due to the evolution of hydrogen was negligible. A differential thermal analysis was used to give greater sensitivity in detecting small heat effects. The sample thermocouple (Chromel-Alumel) was calibrated at the melting point of a N.B.S. standard aluminum sample and a sample of electrolytic silver. The differential thermocouple was placed in an empty capsule similar to the sample capsule but shorter and located just below the quartz tube. The thermal analyses were repeated several times for each sample at various rates of heating and cooling. Except for the transformation of 320–360°, the heating and cooling arrests came at identical temperatures and were not significantly changed by changes in the heating or cooling rate.

Equilibration Experiments.—The calcium rods used for these experiments were 1.9 cm. long and 1.3 cm. in diameter. These rods were obtained by melting distilled calcium crystals in a pure iron crucible in the glove box filled with argon, and casting into a steel mold. After casting, the calcium rods were machined in a lathe in the glove box to a smooth surface and the desired size. The calcium cylinder was placed in an open stainless steel capsule and loaded into the Vycor charging tube in the glove box. The charging was done at the temperature chosen for the equilibration. Hydrogen was added to the sample to transform 25–30% of the calcium to CaH_2 . After adding the hydrogen, the temperature of the sample was maintained for 5 hours to be sure that equilibrium was reached. The charged specimen consisted of a very brittle outside layer of the hydride phase and a soft core of the metal phase. In the glove box, the two layers were separated and samples were taken to be analyzed for hydrogen. These analyses were done by a hot vacuum extraction method, to be published. The accuracy of the method was $\pm 2\%$ of the amount of hydrogen present.

X-Ray Examination.—A number of samples of various hydrogen contents were examined at room temperature by powder X-ray diffraction. The powder obtained by filing the metal phase or by crushing the CaH_2 phase was passed through a 250 mesh screen and placed in a 0.3 mm. diameter glass capillary. This operation was performed in the glove box and the open end of the capillary was sealed with Apiezon W wax before bringing the capillary into the air. Some specimens were heated to 300–500° in the capillary to remove the distortion caused by filing or crushing. The diffraction patterns were obtained with copper $K\alpha$ radiation.

Results

The calcium-calcium hydride system is quite similar to the barium-barium hydride system⁸ except for the additional complexity arising from the allotropy of calcium. The phase diagram is shown in Fig. 1. The melting point of calcium was found to be $839 \pm 2^\circ$. The thermal arrest for the liquidus and solidus rose smoothly with increasing hydrogen content to a peritectic at 890° and 24 mole % CaH_2 . The solid solubility limit of CaH_2 in calcium was observed by both thermal analysis and equilibration experiments. The solid solubility limit increased with temperature, and, in the range 780–890°, it was in good agreement with the values obtained by Johnson, *et al.*,⁴ and by Treadwell and Stecher⁵ through pressure-composition isotherm studies. Thermal analysis showed a phase transition in pure calcium metal at $448 \pm 2^\circ$ on heating and $442 \pm 2^\circ$ on cooling which must be the f.c.c. \rightarrow b.c.c. transformation found by Smith, *et al.*⁶ A new phase, gamma, appears in this temperature range with increasing hydrogen contents. This gamma phase seems to not be an allotropic modification of calcium metal which is stabilized by hydrogen but a calcium-hydrogen intermediate phase that can exist only in the temperature range 320–600°. Postulated detail

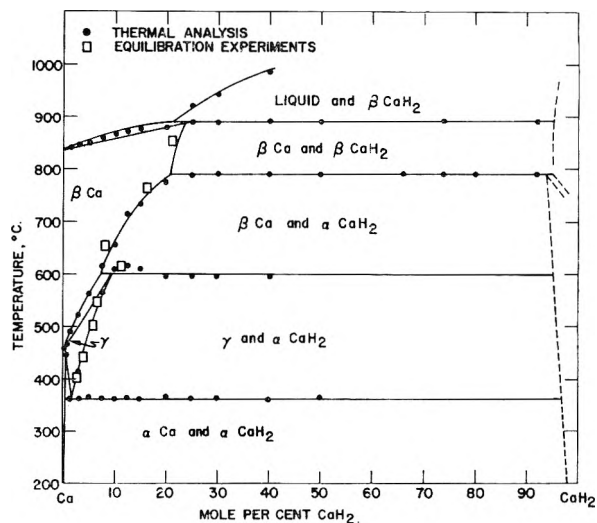


Fig. 1.—The calcium-calcium hydride phase diagram.

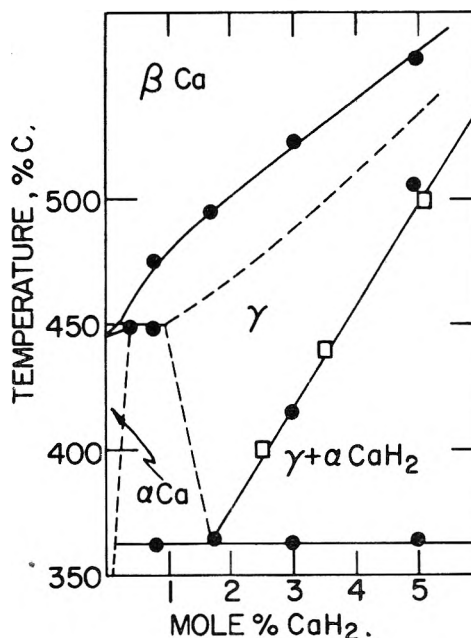


Fig. 2.—Postulated extent of the γ -phase in the calcium-calcium hydride system.

of the calcium-calcium hydride system in this range is shown in Fig. 2. A peritectoid decomposition of α -calcium solid solution into β -calcium and the α -phase is postulated at about 449° . A specimen of the calcium which contained 220 p.p.m. hydrogen and gave an arrest at 448° on heating and 438° on cooling was placed in a sealed tantalum thermal analysis capsule and degassed by heating for 2 days at 900° under a high vacuum. The melting point was unchanged from 839° and the transformation temperature was unchanged on heating, but on cooling was raised to 442° . The thermal arrest, which was rather indistinct originally, was sharp, and occurred at an invariant temperature after degassing. Analysis of the calcium after degassing showed 110 p.p.m. of hydrogen. These observations supported the conclusion that pure calcium has only two allotropic forms, but the origin of the γ -phase could not

(8) D. T. Peterson and M. Indig, *J. Am. Chem. Soc.*, **82**, 5645 (1960).

be firmly established. The γ -phase at $600 \pm 5^\circ$ and 11 mole % CaH_2 undergoes a peritectoid transformation to β -calcium and CaH_2 . At 320 – 360° and near 1.5 mole % CaH_2 , an eutectoid decomposition of γ into α -calcium and calcium hydride takes place. This thermal arrest was the only one which was not found at essentially the same temperature during heating as during cooling. The arrest was always found at 360° on heating and at 320° on cooling. Decreasing the rate of heating or cooling did not significantly change the temperature at which this arrest was observed. X-Ray diffraction at room temperature showed the presence of f.c.c. calcium with a lattice constant of $5.592 \pm 0.002 \text{ \AA}$. in equilibrium with CaH_2 . The constant lattice of the pure calcium (110 p.p.m. H_2) was $5.59 \pm 0.002 \text{ \AA}$.

The composition of the CaH_2 phase in equilibrium with the metal phase could not be determined by analyzing the CaH_2 layer on the outside of equilibration specimens. The hydrogen contents of samples of the CaH_2 layer were erratic and generally below the lower composition limit for CaH_2 obtained by thermal analysis and pressure – composition isotherms. The analytical method had been shown to give satisfactory results on homogeneous samples of CaH_2 so the low results must have been due to occlusions of calcium metal during the growth of the CaH_2 layer. The thermal arrest at 780° was found to originate in the CaH_2 phase and was interpreted as a phase transition in CaH_2 similar to that found in BaH_2 . This could not be checked by high temperature X-ray diffraction because of the reactivity and high dissociation pressure of CaH_2 in this temperature range. The X-ray diffraction pattern of CaH_2 at room temperature was found to be identical with that reported by Zintl and Harder³ except that a few of the very weak lines were not observed.

Discussion

The melting point of calcium metal has been reported at temperatures between 839 and 851° by several investigators. Variation in the hydrogen content could be responsible for these different results. On the basis of the effect of hydrogen on the melting temperature and of the purity of the calcium used in this investigation, it seems reasonable to give $839 \pm 2^\circ$ as the melting point for pure calcium metal.

The allotropy of calcium has been studied by a number of investigators using methods such as

differential thermal analysis, electrical resistivity, dilatometry, thermal expansion, X-ray analysis and thermoelectric power. There was considerable disagreement in the results which can be divided into two groups: those showing only one transition and those showing more than one transition. Rinck,⁹ Graf,¹⁰ Ebert, *et al.*,¹¹ Schulze, *et al.*,¹² and Smith, *et al.*,⁶ found only one transformation which was observed at 450 – 460° . Bastien,¹³ Graf¹⁴ Schulze,¹⁵ Sheldon,¹⁶ Melsert, *et al.*,¹⁷ and Schottmiller, *et al.*,⁷ found two transformations: the first in the range 270 – 350° and the second in the range 460 – 610° . Calcium was reported to be f.c.c. up to the first transition, h.c.p. from the first to the second and b.c.c. above the second transition. In addition, some of these authors found a low symmetry or "complex" phase between 270 – 460° which was introduced by contaminants. None of the investigators reported the hydrogen content of their specimens although the calcium which was used might have contained significant quantities of hydrogen. Smith and Bernstein¹⁸ studied the influence of specific contaminants on the calcium transformations. They reported that the presence of the h.c.p. phase was associated with hydrogen contamination of the calcium.

This investigation shows the importance of hydrogen in the allotropy of calcium and supports the conclusion that pure calcium undergoes only one allotropic transformation which is the transition from f.c.c. to b.c.c. at 448° . However, a small amount of hydrogen induces the appearance of a γ -phase, the presence of which in the specimens of some previous investigators can explain the differing results reported. The identity of the temperature range over which gamma is stable, and the temperature range reported by Sheldon and by Schottmiller, *et al.*, for the h.c.p. phase leave little doubt that α is the h.c.p. phase.

(9) E. Rinck, *Compt. rend.*, **192**, 421 (1931).

(10) L. Graf, *Metallwirtschaft*, **12**, 649 (1933).

(11) F. Ebert, H. Hartmann and H. Peisker, *Z. anorg. u. allgem. Chem.*, **213**, 126 (1933).

(12) A. Schulze and H. Schulte-Overberg, *Metallwirtschaft*, **12**, 633 (1933).

(13) P. Bastien, *Compt. rend.*, **193**, 831 (1934).

(14) L. Graf, *Physik. Z.*, **35**, 551 (1934).

(15) A. Schulze, *ibid.*, **36**, 595 (1935).

(16) E. A. Sheldon, Thesis, Syracuse University, 1949.

(17) H. Melsert, T. J. Tiedema and N. G. Burgers, *Acta Cryst.*, **9**, 525 (1956).

(18) J. F. Smith and B. T. Bernstein, *J. Electrochem. Soc.*, **106**, 448 (1959).

THE DIELECTRIC CONSTANT OF WATER AS A FUNCTION OF TEMPERATURE AND PRESSURE^{1,2}

BY BENTON B. OWEN, ROBERT C. MILLER,³ CLIFFORD E. MILNER AND HAROLD L. COGAN

Contribution No. 1654 from the Sterling Chemistry Laboratory, Yale University, New Haven, Connecticut

Received June 5, 1961

Using the resonant frequency of a coaxial cavity excited in TEM modes at frequencies between 50 and 480 mc./sec., the dielectric constant of water was determined at 5° intervals between 0 and 70°, and at 100 bar intervals between 1 and 1000 bars. The results are expressed as a set of isothermal and isobaric equations whose parameters were evaluated by the method of least squares. The dielectric constant of water and its temperature and pressure derivatives at 1 atmosphere are tabulated at 5° intervals from 0 to 70°.

Introduction

The temperature and pressure derivatives of the dielectric constant of water are of great importance in the theory of electrolytic solutions, and in the proper treatment of the experimental data leading to certain partial molal quantities.⁴ There have been numerous determinations of the temperature coefficient, and at the time that this project was begun the results of Wyman and Ingalls⁵ were accepted so generally that our interest was thought to lie only in the pressure derivatives, which were very imperfectly known.

Dr. Robert Miller³ assembled, or designed and constructed as necessary, the electronic equipment capable of determining the resonant frequency of a coaxial cavity filled with water at various temperatures and pressures. The dielectric constant, D , and the observed fundamental resonant frequency, f_{obsd} , of the cavity at any temperature and pressure, are simply related to their values, D_0 and f_0 , at the standard temperature (25°) and the standard pressure (1/bar), by the equation

$$D = D_0(L_0/L)^2(f_0/f_{\text{obsd}})^2 \quad (1)$$

The factor, L_0/L , is the ratio of the electrical length of the resonant cavity under the standard and the arbitrarily variable conditions, respectively. Neglecting for the moment the difference between the electrical length and the directly measurable axial dimension of the cavity, this length is readily calculable at any temperature and pressure from the linear coefficients of compressibility and expansibility of copper, and to a close approximation

$$(L/L_0) = 1 - 0.25 \times 10^{-6}(P - 1) + 16 \times 10^{-6}(t - 25) \quad (2)$$

If we designate by f the observed resonant frequency at any temperature and pressure corrected for the change in the length of the cavity from the standard conditions, then

$$f = (L/L_0)f_{\text{obsd}} \quad (3)$$

(1) Financial support under the National Science Foundation Grants Nos. 63, 489 and 3054 is gratefully acknowledged.

(2) This communication is based upon the Dissertations submitted to the Graduate School of Yale University of Clifford E. Milner (1955) and Harold L. Cogan (1958) in partial fulfillment of the requirements for the degree of Doctor of Philosophy.

(3) Post-doctoral research assistant 1953-1954.

(4) H. S. Harned and B. B. Owen, "The Physical Chemistry of Electrolytic Solutions," Third Edition, Reinhold Publ. Corp., New York, N. Y., 1958, chapters 5 and 8.

(5) J. Wyman, Jr., and E. N. Ingalls, *J. Am. Chem. Soc.*, **60**, 1182 (1938).

and we obtain the inverse proportionality

$$D = D_0(f_0/f)^2 \quad (4)$$

between D and f^2 .

Ideally, the absolute value of the dielectric constant could be evaluated by equation 4 if f_0 is determined for the completely evacuated cavity, for in this case D_0 would be unity. Unfortunately, the accuracy of this absolute evaluation is limited by the difficulty in estimating the small variation in electrical length resulting from the gross dissimilarity in the electrical properties of the contents of the cavity as we pass from vacuum to water. This difficulty will be discussed later in connection with the quality factor, Q , for the cell. At this point it need only be remarked that the electrical properties of the cell contents (water) change relatively little as the temperature and pressure are varied over the experimental range. Consequently, the measurements which lead to evaluation of the temperature and pressure coefficients are made under conditions of essentially constant electrical length.

Apparatus and Experimental Procedure

Figure 1 shows the pressure bomb partially cut away so as to make visible one half of a longitudinal cross-section of the coaxial cavity cell, the electrical connectors, terminating resistors and loops. The cell⁶ was made of pure copper, carefully broached or turned to uniform dimensions, polished and gold-plated on all inside surfaces before it was assembled. It consists of a right cylinder, 1.74" o.d. and 1.560" (± 0.002) i.d., coaxial with a solid rod, 0.4382" (± 0.0002) diam., and closed by plane, parallel end-plugs 12.287" (± 0.001) apart. The bottom end-plug is fitted with a flexible monel bellows which, under increasing pressures, supplies water to the cell through the slanting silver tube shown just above the bellows. The bottom end-plug and bellows were silver-soldered in place following experience acquired by soldering a series of dummy cells and sawing them longitudinally for examination of the joints. Careful inspection showed no spalling of the gold plate after soldering the bottom end-plug.

Since a check on spalling would be impossible with both end-plugs in place, the top end-plug was soft-soldered to avoid the risk of over-heating the gold plate. During this soldering operation the endplug was bolted into position so that its gold-plated plane surface was pressed firmly against the gold-plated lips of the central rod and surrounding cylinder. By this procedure it was hoped that the soft solder would maintain the top end-plug in place without forming a significant part of the circuit in the cell. This hope seems to have been realized, because the observed Q of the cell, filled

(6) The cell A, herewith described, was used for measurements at all temperatures except 35°. A Cell B, similar to Cell A in design and dimensions, was constructed by electroforming, in an effort to improve electrical quality of the cavity by elimination of certain soldered joints. This effort was not successful, for the Q of Cell B was slightly less than that of Cell A, and dropped rapidly after several series of measurements had been made at the higher temperatures. The drop in Q was not remedied by careful cleaning and refilling, so Cell B was retired from further use.

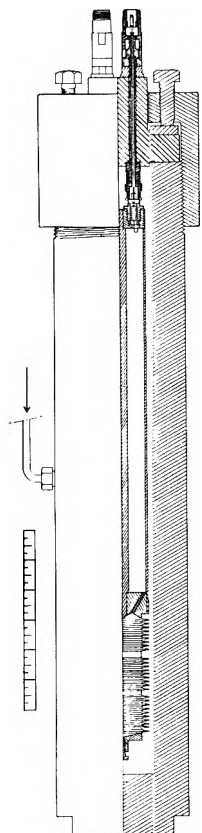


Fig. 1.—Cell and bomb assembly.

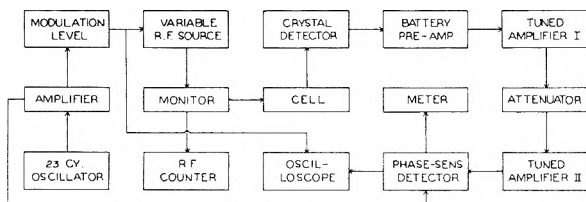


Fig. 2.—Block diagram of the measuring circuits.

with dry nitrogen at 1 atmosphere, was about 65% of the theoretical value,⁷ calculated from the resistivity of pure copper and the assumption of ideal coaxial geometry for the cell.

The coupling loops were formed from the "pig-tails" of the terminating 52 ohm resistors, one of which is shown in Fig. 1 embedded in Shell Epon Resin within a UG-291/U connector whose base has been altered for this purpose. Each such connector is attached to the end-pug by four screws, so as to exert pressure upon the 0.015" pure gold gaskets located near their lower extremities. These gaskets effect good electrical contact and a water-tight seal. The UG-291/U connectors on the cell fit into properly spaced UG88/U connectors attached to the RF leads through the bomb head, and are hung thereby in the oil-filled bomb.

The kovar and glass leads which conduct the RF current through the bomb head are an important feature of the apparatus, since the insulation in these leads withstands the working pressures by glass-to-meta. seals rather than by the usual retaining glands whose shoulders would make the proper resonance determination difficult by reflection of the RF current. Each lead was constructed from a 1/2" kovar rod 4.5" long, drilled axially with a 0.1" hole and turned down to 1/4" for 3.5" of its length. Into this hole was inserted a closely fitting glass capillary 4.5" long, and this was threaded upon a 0.02" kovar wire, centered and held taught by a special jig. Following a few trials, the conditions of heating were found which produced reliable glass-to-kovar seals that could

withstand pressures of 1000 bars over long periods without leakage. After slowly cooling a lead to room temperature, it was returned to the lathe to be threaded, and to eliminate the effects of warping by means of a shallow cut. The top end of each lead was screwed into the modified base of a UG/23B/U connector. These connectors are shown, in the round and in cross-section, surmounting the bomb head in Fig. 1. The use of these special leads and UF connectors permitted the withdrawal of a very "clean" output signal from the cell for the precise determination of the resonance frequency.

Before the cell was used for dielectric constant measurements, its operating characteristics were investigated. The coupling coefficient, β , between the two loops was found to be less than 0.01, the standing wave ratio, r , was 1.05, and the quality factor, Q , was about 120 with water in the cell. These figures indicate that the ratio of the measured resonance frequency to the true resonance frequency (ideally determined without coupling) is

$$1 \pm \beta(r^2 - 1)/4Qr = 1 \pm 0.000002$$

which is unity within the limits of sensitivity of our measuring equipment. This conclusion was directly verified by doubling the area of the output loop without noticeably affecting the measured resonance frequency.

The electronic equipment used in the determination of the resonance frequency of the water-filled cell was arranged according to the block diagram shown in Fig. 2. The variable RF source is a Hewlett-Packard 608A signal generator, slightly modified to allow modulation from an external 23 cy. source. This modulation frequency was chosen to simplify the problem of eliminating hum (60 cy. and its multiples and submultiples) from the power supplies and pick-up from power lines in the laboratory. This choice was not necessarily a happy one, because during long periods of the day the power mains feeding our equipment through a Sorensen 10 kw. voltage regulator carried some irregular voltage fluctuations of such low frequencies that their pick-up by our multistage amplifiers, and other very sensitive apparatus, could not be eliminated from the 23 cycle circuits by choke and condenser filters of practical sizes. These fluctuations often introduced irksome delays into measurement schedules. Our 23 cycle oscillator produces this frequency with high stability as the difference between the frequencies of two similar crystal oscillators, one operating at 80.86 kc. and the other pulled off this frequency to yield the 23 cycle difference. The outputs of those oscillators are fed into a mixer circuit,⁸ and the difference frequency is filtered and amplified and delivered through a modulation level control to the variable RF source.

The output of the Hewlett-Packard 608A signal generator is controlled by an attenuator, and a built-in monitoring circuit indicates the output level in volts and the % modulation of the signal. The modulated RF signal is led through Type N connectors and short lengths of RG-58A/U coaxial cable to the input connector on the cell, and to the frequency-measuring device, which was either a TS-174/U Signal Corps frequency meter, or a Hewlett-Packard 524B electronic counter equipped with a 525B frequency converter. Some measurements on the cell filled with nitrogen involved frequencies of the order 480 mc., and consequently required the use of a Hewlett-Packard 540A transfer oscillator in conjunction with the electronic counter.

The output connector of the cell is attached directly to a Type N fitting containing a 1N28B, or 1N32 crystal which detects and delivers the 23 cycle modulating frequency to a battery-operated, low-noise preamplifier situated near the bomb. This preamplifier employs two subminiature triodes, a 6247 and a 5703WA. The 6247 operates as a class A amplifier (of gain 10) with a high impedance output, and the 5703WA acts as a cathode follower which serves to drop the output impedance low enough to drive a stepup interstage transformer used to isolate the ground of the preamplifier from that of following tuned amplifiers and the phase-sensitive detector.

The tuned amplifiers I and II are of the type designed by Sturtevant.⁹ They include sufficient frequency-independent feed-back to ensure stability and a linear gain characteristic.

(8) B. Chance, "Waveforms," Vol. 19, M.I.T. Radiation Laboratory Series, McGraw-Hill Book Co., New York, N. Y., 1949, pp. 124-125.

(9) J. M. Sturtevant, *Rev. Sci. Instr.*, **18**, 124 (1947).

(7) T. Moreno, "Microwave Transmission Design Data," McGraw-Hill Book Co., New York, N. Y., 1948, p. 226.

but are made highly selective by the use of frequency-dependent feed-back (23 cycles) supplied by a twin-T network. Two separate feed-back loops, each including a cathode follower, connect the plate of the second amplifier tube to the cathode of the input tube, and direct coupling is used throughout each loop to avoid phase shift and adapt the circuits to use with low frequencies. Three amplifier stages of this type are used; two are used in Tuned Amplifier I, and one in Tuned Amplifier II. Between these amplifiers is an Attenuator driven by a 12A Y7 cathode follower.

The output from Tuned Amplifier II is coupled to the grids of a twin-triode 6SN7 cathode follower, one half of which is used to supply 23 cycles to the vertical plates of the oscilloscope, and one-half to supply the 23 cycle signal to the phase-sensitive detector.¹⁰ The output of this detector passes through a variable time-constant RC filter, and then to one grid of a 6SN7 difference amplifier, the other grid of which is maintained at a constant reference voltage. The difference voltage is amplified and directly connected to the grids of a pair of 6V6 tubes in a differential cathode-follower whose d.c. output is registered on the meter as a quantitative measure of the power transmitted through the cavity.

Resonance also is indicated by a Lissajous figure on the oscilloscope screen, as the result of the combination of two 23 cycle signals, one applied to the horizontal plates from the 23 cycle oscillator, and the other applied to the vertical plates from the output of the tuned amplifier. The frequency of the 23 cycle oscillator is adjusted so that the phase-shift in the tuned amplifier is zero.

The pressure bomb containing the cell, and shown in Fig. 1, is an Aminco super-pressure bomb rated at 15,000 p.s.i. The inside diameter of this bomb is 2-1/16", and its inside length is 20-5/8". Pressure is applied to the cell by forcing oil into the bomb through the inlet shown in Fig. 1 on the left-hand side of the bomb. Pressures are measured with the aid of a 16" bourdon type gage made by the Heise Bourdon Tube Company of Newtown, Connecticut. This gage was calibrated by the manufacturer, and checked from time to time by comparison with an Aminco dead-weight gage. It is believed that the uncertainties in pressure measurements range from about 1/2 bar at the lower pressures to 1.5 bars at the highest pressure.

The temperature of the oil-bath surrounding the bomb can be maintained constant to $\pm 0.003^\circ$ during a run, and is measured by means of a platinum resistance thermometer. The oil-bath is surrounded by a large thermostat containing water and ethylene glycol which can be maintained within 0.1° of the nominal working temperatures between 0 and 70°. Both the oil-bath and its surrounding thermostat are very efficiently stirred, and thoroughly insulated.

The distilled water used in the measurements was further purified by redistillation from dilute alkaline permanganate in a Barnstead still, or deionization by passage through a column containing Amberlite MB-1 resin. No water samples were used which had a specific conductivity greater than 1.5×10^{-6} mho.

During the filling operation the carefully cleaned cell, with bellows screw-plug and connector assemblies removed, was inverted into a large glass test-tube attached to a vacuum line and to a flask containing the water sample. The water was degassed by boiling under vacuum, and when cooled to room temperature it was siphoned into the test-tube containing the cell. Throughout this siphoning, both the water vessel and the test-tube must be maintained under vacuum so as to make it possible to eliminate air bubbles from the bellows. This procedure brings the water sample in contact with the outside surfaces of the cell, which must be scrupulously clean. To facilitate this cleaning, all metallic surfaces of the cell, which are not stainless steel or monel, were gold-plated.

After the test-tube and cell are completely filled with the water sample, the vacuum is broken, the test-tube opened and the bellows screwplug inserted under water. Taking precautions not to allow air to be drawn into the cell through the connector openings when the test-tube is inverted, the cell now can be removed from the test-tube. The connectors and their gold gaskets are fixed in place while maintaining a slight outward flow of water by compression of the bellows.

Because of the large heat capacity of the bomb, a minimum

of three hours was always allowed for equilibrium in the cell whenever a major adjustment (0.2° or more) of the temperature of the oil thermostat was made. Adequate time was allowed also for dissipation of the heat of compression after any adjustments in pressure; two hours were allowed after the usual increment of 100 bars in pressure. In principle, the operating procedure involves bringing the cell to temperature equilibrium at 1 atmosphere and measuring the resonant frequency, then at succeeding pressure intervals of 100 bars measuring the resonant frequencies until 1000 bars are attained. In practice, the vagaries of our a.c. power source and occasional malfunctioning of thermostatic and electronic equipment caused the time schedule for such a series to vary from two days to as much as a week or more before the temperature of the oil-bath could be raised 5° and another series of pressures investigated. Because such a schedule required that the cell be subjected to high pressures for long periods of time, and the bellows permitted the pressure within the cell to be less than that in the bomb by almost 1 bar at 1000 bars, there was always the possibility that oil might leak into the cell through some imperfection in a gasket or soldered joint, or what seems more likely, oil might leak along the epoxy resin-to-metal seal in the base of the connectors at the top of the cell. Evidence of such leakage was assiduously looked for, but never directly demonstrated. On the other hand, the *Q* of the cell cavity would be expected to be sensitive to the presence of very small traces of oil on an inner surface of the cell, particularly in the neighborhood of the lcops, so we believe leakage to be responsible for the observed drop in *Q* from 120 for the freshly filled cell to about 95 for a cell used over a complete series of pressure intervals at five or six different temperatures. In any case, thoroughly cleaning the cell with acetone, followed by methanol and water, and refilling it with a freshly purified water sample, as previously described, would result in bringing the *Q* back to 120, or more. Altogether, four separate fillings are involved in obtaining the results reported in this paper.

Resonance in the cell was detected by graphical determination of the frequency at which the reading of the meter connected to the phase-sensitive detector is a maximum for a given constant power input to the cell. This meter reading is proportional to the power transferred through the cell because the crystal detector at the output of the cell acts as a square law detector. Originally, a duplicate unit, consisting of a micromatch unit (ahead of the cell) connected to a crystal detector, preamplifier, tuned amplifier, phase-sensitive detector and meter, was used to monitor the RF power input to the cell, but this was disconnected when it was found to offer no practical advantage over the monitoring system built into the RF source itself. Accordingly, as the RF frequency was continuously varied, the input voltage to the cell was held constant, usually at 1 volt, and the % modulation was held constant. The power transferred through the cell was plotted against frequency, and the maximum determined by extending a plot of median frequencies (averages for equal power outputs) to its intersection with the power-frequency curve. The results were discarded if the plot of median frequencies was not a straight line for power levels greater than 0.7 of the maximum.

The *Q* of the loaded cell was determined from the ratio

$$Q = f_0 / (f_2 - f_1) \quad (5)$$

where f_0 is the resonance frequency, and f_2 and f_1 are the frequencies at half power above and below resonance. Under our experimental conditions, the fundamental resonance frequency was of the order of 50 to 60 megacycles per second, but the output from the crystal detector was improved by working at higher harmonics with consequent improvement in the signal to noise ratio in the output from the tuned amplifiers. On the other hand, the frequency range between the 0.7 power readings on each side of the maximum was proportional to the harmonic number, and as a consequence a greater time was required to make a series of measurements at the higher harmonics. As a result of these and other experimental considerations, the third harmonic was used for measurements at 0 to 30°, and the second harmonic was used from 25 to 70°. The frequencies at the lower temperatures were determined with a TS-174/U Signal Corps Frequency Meter and a 1N28B in the crystal detector; at the higher temperatures the measurements were speeded up by the acquisition of the Hewlett-Packard 524B

(10) Reference 7, pp. 309-10. Cf. also E. C. Pollard and J. M. Sturtevant, "Microwaves and Radar Electronics," John Wiley and Sons, Inc., New York, N. Y., 1948, Fig. 10.16, p. 310.

electronic counter and the use of a 1N32 in the crystal detector.

Experimental Results

At each constant temperature the fundamental resonant frequencies, corrected to constant cell length by equations 2 and 3, were represented originally by quadratic functions of P by the method of least squares. The parameters of these equations, particularly the coefficient of P^2 , are sensitive to experimental error, because f changes less than 2.4% for an increment of 1000 bars, and the number of pressure increments (ten) at each temperature is small for statistical purposes. Consequently the values of the desired derivative

$$\left(\frac{\partial \ln D}{\partial P}\right)_T = -2 \left(\frac{\partial \ln f}{\partial P}\right)_T \quad (6)$$

obtained from the parameters of these quadratic equations did not vary smoothly with the temperature. The simple isothermal curve-fitting was therefore abandoned in favor of a regression analysis computer program¹¹ which increased the validity of the least squares procedure by treating all of our data simultaneously as a matrix of 165 frequencies at 15 temperatures and 11 pressures. The coefficients of fit resulting from this treatment are so satisfactory that the extensive data need not be tabulated here. The dependent variable, $\log f$, differs from its values calculated from the parameters resulting from the regression analysis (without regard to sign) by only 3.6×10^{-6} on the average, and for only seven points does the difference exceed the calculated 95% confidence limit of 10.5×10^{-6} . The standard estimate of error¹² is 5.2×10^{-6} , and a least-squares fitting of the experimental against calculated values of $\log f$ results in a straight line of slope 1.0000087 and intercept 0.167×10^{-6} .

Although the data subjected to this statistical treatment were not obtained under identical experimental conditions,¹³ the same coaxial cavity, Cell A, was used in all of the measurements except those at 35°. Measurements were made at both 25 and 35° with Cell B while its Q was satisfactorily high, so we used the ratio

$$f^A(1,25)/f^B(1,25) = 54.213/54.263 = 0.99907$$

as a multiplier of the frequencies $f^B(P, 35)$, measured with Cell B at 35° to refer them to the electrical length of Cell A. The two values, 54.213 and 54.263, were obtained by fitting the data at eleven pressures for each cell at 25° to a quadratic in P by the method of least squares.

The function selected for the regression analysis represents the logarithm of the frequency as a

(11) We are very grateful to Mr. Norman Hyatt of the Olin Mathieson Chemical Company, for making this program available to us, and to Mr. Nicolas Antonoff, Jr. for undertaking the calculations and statistical analysis under the part-time support of NSF Grant 15046.

(12) The standard deviation, σ_r . Cf. K. A. Brownlee, "Industrial Experimentation," Chemical Publishing Co., New York, N. Y., 1952, p. 65.

(13) The third harmonic was measured at 0 through 25° with a TS-174/U Signal Corps frequency meter, and the second harmonic was measured at 25 through 70° with a Hewlett-Packard electronic counter, but comparisons of the fundamental resonant frequencies in a number of runs showed that these measuring procedures gave the same results within the curve-fitting error.

quadratic in the Centigrade temperature, t , and the gage pressure, $p = P - 1$, in bars. Thus

$$10^6 \ln f = 10^6 \ln f(0,0) = a_1 p + a_2 p t + a_3 p t^2 + a_4 p^2 + a_5 p^2 t + a_6 p^2 t^2 + a_7 t + a_8 t^2 \quad (7)$$

and, by combination with equation 6, the dielectric constant and its derivatives are given by

$$-10^6 \ln D = -10^6 \ln D(0,0) + 2a_1 p + 2a_2 p t + 2a_3 p t^2 + 2a_4 p^2 + 2a_5 p^2 t + 2a_6 p^2 t^2 + 2a_7 t + 2a_8 t^2 \quad (8)$$

$$-10^6 \left(\frac{\partial \ln D}{\partial P}\right)_T = 2a_1 + 2a_2 t + 2a_3 t^2 + 4a_4 p + 4a_5 p t + 4a_6 p t^2 \quad (9)$$

$$-10^6 \left(\frac{\partial \ln D}{\partial T}\right)_P = 2a_2 p + 4a_3 p t + 2a_4 p^2 + 4a_5 p^2 t + 2a_7 + 4a_8 t \quad (10)$$

$$-10^6 \left(\frac{\partial^2 \ln D}{\partial P^2}\right)_T = 4a_4 + 4a_5 t + 4a_6 t^2 \quad (11)$$

$$-10^6 \left(\frac{\partial^2 \ln D}{\partial T^2}\right)_P = 4a_8 + 4a_3 p + 4a_6 p^2 \quad (12)$$

$$-10^6 \left(\frac{\partial^2 \ln D}{\partial P \partial T}\right) = 2a_2 + 4a_3 t + 4a_5 p + 8a_6 p t \quad (13)$$

The values of the parameters resulting from the least squares treatment of our matrix of data are given in Table I. The constant $D(0,0)$, whose logarithm is included in the table, is the dielectric constant of water at $t = 0$ and $p = P - 1 = 0$.

TABLE I

PARAMETERS OF EQUATIONS 7 TO 13

$\ln f(0,0) =$	3.935390	$a_5 \times 10^6 =$	2.7395
$a_1 =$	-22.5713	$a_6 \times 10^6 =$	-0.1476
$a_2 \times 10^2 =$	-3.2066	$a_7 \times 10^{-3} =$	2.30064
$a_3 \times 10^4 =$	-2.8568	$a_8 =$	-0.13476
$a_4 \times 10^3 =$	1.1832	$\ln D(0,0) =$	4.476150

This quantity was calculated from $f(0,0)$ and the measured resonant frequency of the cavity filled with nitrogen. Equation 6 requires that the product Df^2 is a constant for a cell of constant electrical length, so we can equate $D(0,0)f^2(0,0)$ for water to $D_0 f_0^2$ for nitrogen if the condition of constancy of electrical length is fulfilled. All of our observed resonant frequencies are corrected by equation 2 for changes in length due to temperature and pressure, but when the cell is used to compare fluids of such widely different electrical properties as water and nitrogen, a frequency-dependent correction must be applied. In making this correction, observed resonant frequencies are multiplied by a term containing the quality factor, Q^W , for the wall of the cavity. Thus

$$f = (1 + (2Q^W)^{-1})f_{\text{obs}} \quad (14)$$

The Q determined by equation 5 differs somewhat from Q^W because of imperfections in the geometry of the cavity and losses in the dielectric. When the cell is filled with nitrogen the measured Q is so high (1,600) and the losses in the dielectric are so low that it is a permissible approximation to equate Q with Q^W , so that the correction term, $1 + 1/(2Q^W)$, becomes 1.000313 for f_0 in the presence of nitrogen. With water in the cell this approximation is not permissible, because the measured Q is low (90 to 120) and the losses in the dielectric are relatively high. We therefore propose as a working

hypothesis that the ratio $Q^W/f^{1/2}$ is independent of the contents of the cell and obtained¹⁴ an estimated value of 850 for Q^W in the presence of water, so that the correction term, $1 + 1/(2Q^W)$, becomes 1.000588 in this case. With the cell filled with pure dry nitrogen at 25° and under a pressure of 769 mm. the resonant frequency was found to be 479.847 megacycles per second, and the dielectric constant of nitrogen under these conditions is 1.000544.¹⁵

The introduction of these figures into equations 2 and 14 leads to 230,251.6 for the product $D(0,0)f^2(0,0)$, and to 87.896 for $D(0,0)$. This value for $D(0,0)$ is 0.18% higher than the result (87.740) recently obtained at the National Bureau of Standards¹⁶ at 0° and 1 atmosphere. Although this difference in the *absolute* value of the dielectric constant possibly does not exceed the error introduced into our calculations by the assumptions regarding Q^W for the cell containing water, these assumptions should have a much smaller effect upon the temperature and pressure derivatives of D . Table II gives the values of D and the various derivatives calculated from equations 8 through

TABLE II
RESULTS DERIVED FROM EQUATIONS 8 THROUGH 13 AT
 $P = 1 \text{ BAR}^a$

t	D	$\left(\frac{\partial \ln D}{\partial P}\right)_T$	$\left(\frac{\partial \ln D}{\partial T}\right)_P$	$\left(\frac{\partial^2 \ln D}{\partial P^2}\right)_T$	$\frac{\partial^2 \ln D}{\partial T \partial P}$
0	87.896	45.14	-46.01	-47.34	64.1
5	85.897	45.48	-45.99	-52.76	69.8
10	83.945	45.84	-45.96	-57.90	75.5
15	82.039	46.23	-45.93	-62.74	81.3
20	80.176	46.65	-45.91	-67.28	87.0
25	78.358	47.10	-45.88	-71.53	92.7
30	76.581	47.58	-45.85	-75.49	98.4
35	74.846	48.09	-45.82	-79.15	104.1
40	73.151	48.62	-45.80	-82.52	109.8
45	71.496	49.19	-45.77	-85.58	115.6
50	69.878	49.78	-45.74	-88.36	121.3
55	68.299	50.40	-45.72	-90.84	127.0
60	66.756	51.05	-45.69	-93.02	132.7
65	65.249	51.73	-45.66	-96.91	138.4
70	63.776	52.43	-45.64	-98.51	144.1

^a The coefficient $(\partial^2 \ln D / \partial T^2)_P = 54 \times 10^{-8}$ at one bar at all temperatures.

13 at 1 atmosphere over the temperature range 0 to 70°. In order to compare our results with those of others, Fig. 3 shows our results, and those of Wyman and Ingalls⁵ and of Lees¹⁷ plotted relative to the values reported by the Bureau of Standards.¹⁶ It is clear that our results agree with those of Lees, both in absolute magnitude and in temperature dependence. We call particular attention to this unpublished work of Lees because it was carefully

(14) $Q^W/137^{1/2} = 1600/480^{1/2}$, where the right-hand member refers to nitrogen and the left-hand member to water. The value 137 is an average of the frequencies at which measurements were made with water in the cell (third harmonic below 25°, and second harmonic above), and 480 is the frequency with nitrogen in the cell.

(15) G. Birnbaum, J. S. Kryder and H. Lyons, *J. Appl. Phys.*, **22**, 95 (1951).

(16) C. G. Malmberg and A. A. Maryott, *J. Research Natl. Bur. Standards*, **56**, 1 (1956).

(17) W. L. Lees, Dissertation, June (1949), Department of Physics, Harvard University.

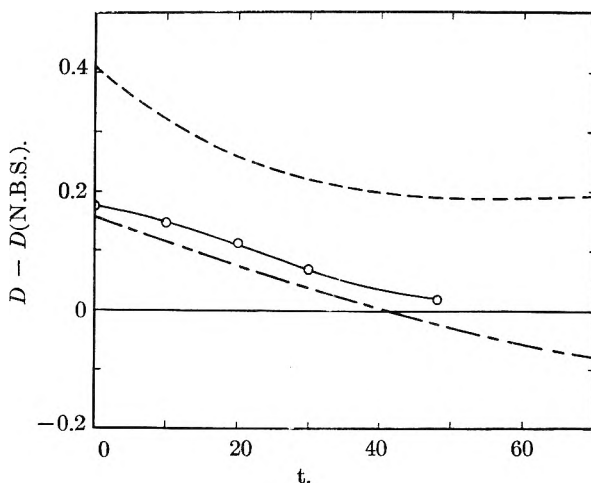


Fig. 3.—Plots of dielectric constants relative to values reported by the National Bureau of Standards. ——— N.B.S. (Malmberg and Maryott, Ref. 16); - - - This Research; —○—, Lees, Ref. 17; - - - - , Wyman and Ingalls, Ref. 5.

done and permits comparison with our results at two higher pressures, 196.1 and 980.7 bars. Thirty years ago Lattey, Gatty and Davies¹⁸ studied the temperature dependence of the dielectric constant of water, and compared their results with those of seven previous investigators. A similar comparison of more recent results was made by Malmberg and Maryott.¹⁶ The reader is referred to both of these comparisons which clearly show the marked disagreement between results obtained by different experimental methods, as well as by different investigators using rather similar methods. Our values of $\partial \ln D / \partial T$ are very nearly the means of those of Lattey, Gatty and Davies¹⁸ and of Malmberg and Maryott.¹⁶

TABLE III
THE RATIO $D(t,P)/D(t,1)$

t	P	This paper	W. L. Lees ^a
0	196.1	1.00875	1.00913
0	980.7	1.0±284	1.04394
10	196.1	1.00886	1.00914
10	980.7	1.0±303	1.04373
20	196.1	1.00900	1.00924
20	657.1	1.02959	1.0296 ^b
20	980.7	1.04339	1.04392
30	196.1	1.00919	1.00927
30	980.7	1.04393	1.04422
50	196.1	1.00959	1.00970
50	980.7	1.04553	1.04586

^a Reference 17—The values given in this column differ slightly from those in ref. 17. They were kindly supplied to us as the result of a recalculation by Dr. Lees. ^b Reference 22.

Comparisons of the pressure coefficient, $\partial \ln D / \partial P$, are even more unsatisfactory, because the number of previous measurements is small and the data very limited. Harris, Haycock and Alder¹⁹ report coefficients differing from ours by factors varying from 1.1 at 14.5° to 0.1 at 60.7°. Two

(18) R. T. Lattey, O. Gatty and W. D. Davies, *Phil. Mag.*, **12**, 1019 (1931).

(19) F. E. Harris, E. W. Haycock and B. J. Alder, *J. Phys. Chem.*, **57**, 978 (1953).

series of measurements at a single temperature lead to 44.0×10^{-6} at 16.3° (Falkenberg²⁰) and 66.7×10^{-6} at 20° (Kyropoulos²¹). Lees¹⁷ made measurements at 0, 10, 20, 30 and 50° , and at pressures up to 12,000 kg./cm.², but since the pressure intervals he employed are too great to permit accurate evaluation of $\partial \ln D / \partial P$ at 1 bar, we have compared

(20) G. Falkenberg, *Ann. Physik*, **61**, 145 (1920).

(21) S. Kyropoulos, *Z. Physik*, **40**, 50* (1926).

our results with his in terms of the ratio $D(t, P) / D(t, 1)$ at those temperatures and pressures at which our measurements overlap. This comparison is shown in Table III, where it can be seen that our ratios are about 0.02% lower than Lees at 196 bars, and about 0.06% lower at 981 bars. The very close agreement with the ratio of Schaife²² at 20° is not significant because his data were rounded off to the nearest 0.1 unit of the dielectric constant.

(22) B. K. Schaife, *Proc. Phys. Soc.*, **68B**, 790 (1955).

THE LOW TEMPERATURE MAGNETIC PROPERTIES AND MAGNETIC ENERGY LEVELS OF SOME RARE EARTH CHELATES OF ACETYLACETONE AND ETHYLENEDIAMINETETRAACETIC ACID^{1,2}

By J. J. FRITZ, P. E. FIELD AND INGMAR GRENTHE³

College of Chemistry and Physics, Pennsylvania State Univ., University Park, Pa.

Received June 12, 1961

The magnetic susceptibilities of powdered specimens of nine acetylacetonates and three ethylenediaminetetraacetate complexes of the rare earths have been measured from 1.3 to 20°K . Measurements were made with an AC bridge using frequencies from 100 to 2000 cycles. In the case of dysprosium acetylacetonate (only) relaxation effects were observed, corresponding to a spin-lattice relaxation time of about a millisecond. The temperature dependence of the susceptibilities has been analyzed for crystalline fields of cubic and of trigonal symmetry. The results are better represented by the cubic field, but show distinct deviations corresponding to lower symmetry.

Introduction

The magnetic properties of compounds of the rare earth elements have been a subject of lively interest for many years. Measurements made on the hydrated sulfates, mainly at ordinary temperatures, aided in verification of some of the earliest theoretical work on the paramagnetism of ionic solids.⁴ These along with spectroscopic investigations of the solid compounds,⁵ led to positive identification of J -values of the lowest multiplet states as consistent with those observed for the gaseous ions spectroscopically. Unfortunately the low temperature measurements necessary for description of the "splitting" of the ground state under various possible crystal environments have been rather sparse.

Except for a few scattered measurements on oxides and halides, the only compounds for which extensive low temperature measurements have been made are the hydrated sulfates and the ethyl sulfates. Magnetic properties on a number of the sulfates have been measured down to 14°K ., mainly at Leiden, and $\text{Gd}_2(\text{SO}_4)_3 \cdot 8\text{H}_2\text{O}$ has been subjected to extensive measurements down to 0.1°K . at Leiden and Berkeley. Becquerel, van den Handel, and others⁶ measured the optical

rotations down to 1.5°K . of single crystals of five of the ethyl sulfates and made direct magnetic susceptibility measurements of some of these. More recently, experimental and theoretical groups at Oxford University have carried out an extensive program of magnetic resonance experiments on the ethyl sulfates and have presented theoretical analyses of some of these.⁷ These measurements were made primarily on "diluted" specimens containing a fraction of an atomic per cent. of the ion being investigated in a crystal compound primarily of the isomorphous, but diamagnetic lanthanum ethyl sulfate. In a few cases observations were made on the "concentrated" (*i.e.*, undiluted) paramagnetic salt itself.

In a way it is fortunate that the low temperature magnetic properties of rare earth compounds were not investigated more thoroughly in the past, since the susceptibilities of the rare earths vary tremendously, and it has been possible only recently to obtain substantial amounts of rare earth salts sufficiently pure that the effect of contamination by other rare earth elements could be neglected.

In connection with work on the formation constants of rare earth chelates⁸ we were able to obtain pure specimens of the acetylacetonates of all the stable rare earths and of the ethylenediaminetetraacetates of four of them.⁹ We have summarized the results of the low temperature magnetic measurements on nine of the acetylacetonates

(1) Presented in part at the 139th National Meeting of the American Chemical Society at St. Louis, Mo., March, 1961.

(2) The authors wish to thank the Office of Naval Research for financial aid under Contract No. Nonr 65624, and the National Science Foundation for support under Grant No. 9928.

(3) On leave from University of Lund (Sweden).

(4) See, for example, J. H. Van Vleck, "The Theory of Electric and Magnetic Susceptibilities," Oxford Univ. Press, New York, N. Y., 1932, Chap. IX.

(5) See, for example, F. H. Spedding and H. F. Hamlin, *J. Chem. Phys.*, **5**, 429 (1937).

(6) J. Becquerel, W. J. De Haas and J. van den Handel, *Physica*, **5**, 857 (1938), which gives reference to previous work; also *Comm. Phys. Lab. Univ. Leiden*, No. 242d, 244b, 2, d, 262a (1936-1940).

(7) R. J. Elliott and K. W. H. Stevens, *Proc. Roy. Soc. (London)*, **A219**, 275 (1953). This paper summarizes much of the theoretical work and gives many references to earlier publications, both experimental and theoretical.

(8) I. Grenthe and W. C. Fernelius, *J. Am. Chem. Soc.*, **82**, 6258 (1960).

(9) The tetraacetates were loaned to us by Prof. T. Moeller of the University of Illinois. We wish to express our particular gratitude to him for his kindness in making these specimens available.

(acac) and three of the EDTA complexes in a previous publication.¹⁰ The purpose of this communication is to present these results in detail along with theoretical analysis of their significance. The acetylacetonates have the formula $M(\text{CH}_3\text{COCH}_2\text{COCH}_3)_3 \cdot \text{H}_2\text{O}$, with each diketone ligand doubly coordinated to the metal through its oxygens. The structures of the crystals have not yet been determined, nor the location of the water of hydration. In the EDTA complexes the ethylenediaminetetraacetic acid ($\text{HOOCCH}_2\text{N}-\text{CH}_2-\text{CH}_2-\text{N}(\text{CH}_2\text{COOH})_2$) is presumably hexacoordinate, with points of attachment to the metal ion at the two nitrogens and the four carbonyl oxygens; these complexes have the general formula $\text{Na}[M(\text{EDTA})] \cdot 8\text{H}_2\text{O}$. Again, the crystal structure is as yet unknown. Our original hope was that the chelate compounds (especially the acetylacetonates) would have octahedral coordination leading to a crystal field of nearly cubic symmetry about the paramagnetic ions; in this case the powder susceptibilities would have provided enough information for analysis of the energy level structure. There is now evidence, to be discussed herein, that this should not be so and that the crystal field should be of distinctly lower symmetry, in which case powder susceptibilities are insufficient for complete analysis, but do serve to restrict the alternatives and in some cases give definitive answers.

Experimental

Susceptibility measurements were carried out by essentially the methods previously described,¹¹ in which the inductance of a 4700-turn coil ($L_0 \approx 0.047$ henry), was observed successively with and without a cylindrical specimen of the material inserted in the core of the coil. Whereas previously measurements were made only at 400 cycles, in this investigation the behavior of all specimens was examined at 400 and 1000 cycles in order to detect any relaxation effects present. In all cases but one the susceptibilities obtained at 400 and 1000 cycles were identical from 1.5 to 20°K., and no further observations of the effect of frequency were made. In one case (dysprosium acetylacetonate), strong dependence of susceptibility on frequency was observed at and below 4.2°K.; the (dynamic) susceptibility of this specimen was observed at five frequencies from 100 to 2000 cycles. In earlier measurements all specimens used were 10.0 cm. long and 0.5 cm. in diameter. Because of limited amounts of material available, some of the rare earth specimens had to be formed into specimens of smaller diameter, and there were minor variations in their lengths. Separate calibration specimens were prepared for each diameter used; auxiliary experiments showed that, above 8 cm., the length of the specimen did not affect the results, provided that the calibration constant was adjusted proportionately to account for the actual length of the specimen.

Measurements were made at four temperatures between 1.2 and 4.2°K. and at three or four temperatures between 9 and 20°K. The acetylacetonates were prepared according to the methods of Stites, *et al.*¹² The EDTA salts were used as obtained from Moeller (see footnote 9). All were in the form of fine powders, which were packed tightly in cylindrical Pyrex sample tubes of appropriate size and then sealed under a mixture of helium (for thermal conductivity) and dry air. The amounts of specimen varied from 0.52 to 2.3 g.; the exact weight of each specimen is

TABLE I MAGNETIC SUSCEPTIBILITY OF CHELATES					
Temp., °K.	χ_m	$\chi_m T$	Temp., °K.	χ_m	$\chi_m T$
Pr(acac) ₃ ·H ₂ O; wt. 1.3666 g.			Tb(acac) ₃ ·H ₂ O; wt. 0.8549 g.		
20.24	0.039	0.78	20.24	0.455	9.2
16.99	.045	.77	17.01	.530	9.0
15.12	.048	.72	15.17	.605	9.2
4.20	.084	.351	9.90	.914	9.1
3.11	.088	.272	4.19	2.01	8.43
1.98	.090	.179	3.07	2.63	8.08
1.31	.095	.125	1.96	3.84	7.51
			1.24	5.30	6.58
Nd(acac) ₃ ·H ₂ O; wt. 0.5695g.			Ho(acac) ₃ ·H ₂ O; wt. 0.5824 g.		
20.24	0.054	1.09	20.24	0.506	10.2
16.97	.057	0.97	16.91	.509	10.0
15.09	.057	.86	15.08	.651	9.8
4.20	.192	.81	9.45	.944	8.9
3.10	.235	.73	4.17	1.848	7.71
1.98	.353	.70	3.09	2.306	7.12
1.34	.491	.67	1.96	2.940	5.76
			1.31	3.197	4.18
Gd(acac) ₃ ·H ₂ O; wt. 0.5222 g.			Er(acac) ₃ ·H ₂ O; wt. 1.0402 g.		
20.27	0.378	7.7	20.27	0.376	7.6
16.94	.448	7.6	17.00	.426	7.2
15.05	.500	7.5	15.07	.472	7.1
4.19	1.705	7.15	9.29	.702	6.5
3.11	2.238	6.95	4.19	1.396	5.86
1.98	3.158	6.26	3.11	1.864	5.80
1.406	3.439	4.48	1.97	2.993	5.89
			1.33	4.489	5.96
			1.27	4.875	6.19
Tm(acac) ₃ ·H ₂ O; wt. 0.8246 g.			Na[Nd(EDTA)]·8H ₂ O; wt. 1.0474 g.		
20.24	0.336	6.8	20.21	0.037	0.75
16.96	.401	6.8	17.05	.041	.70
15.04	.447	6.7	15.17	.049	.74
9.64	.694	6.7	4.19	.163	.684
4.19	1.440	6.04	3.10	.206	.639
3.127	1.821	5.69	1.98	.320	.634
1.944	2.324	4.52	1.30	.473	.617
1.324	2.628	3.48			
Yb(acac) ₃ ·H ₂ O; wt. 0.8937 g.			Na[Gd(EDTA)]·8H ₂ O; wt. 0.6089 g.		
20.25	0.071	1.44	20.22	0.414	8.4
17.02	.073	1.24	17.01	.481	8.2
15.09	.082	1.24	15.04	.552	8.3
4.19	.301	1.25	4.19	1.959	8.2
3.08	.393	1.21	3.10	2.653	8.22
1.96	.630	1.23	1.98	4.131	8.16
			1.24	6.251	7.77
Na[Pr(EDTA)]·8H ₂ O; wt. 2.2630 g.					
20.23	0.029	0.59			
17.04	.032	.54			
15.12	.032	.48			
4.20	.034	.142			
3.10	.034	.105			
1.98	.038	.075			
1.30	.040	.062			

(10) J. J. Fritz, I. Grenthe, P. E. Field and W. C. Fernelius, *J. Am. Chem. Soc.*, **82**, 6199 (1960).

(11) J. J. Fritz, R. V. G. Rao and S. Seki, *J. Phys. Chem.*, **62**, 703 (1958).

(12) J. G. Stites, C. N. McCarthy and L. L. Quill, *J. Am. Chem. Soc.*, **70**, 3142 (1948).

listed with the results of the susceptibility measurements. The purities were 99.9% or better, with the exception of the neodymium, and the carbon-hydrogen analysis gave excellent agreement with calculated values (see ref. 10).

The over-all accuracy of the measurements, based on previous comparisons of materials of known susceptibility, is estimated as 2-3%. The precision was determined by an uncertainty of about 0.3 microhenry in observation of the inductance, corresponding to from 0.001 to 0.003 in the molar susceptibility, depending on the size of the specimen. The precision was never poorer than 3% in the liquid helium range, and in most cases the internal consistency was better than 1%. Corrections for diamagnetism, as estimated from atomic susceptibilities, were equal to or less than the precision of measurement and therefore were not applied.

Results

The molar susceptibilities (χ_m) and the $\chi_m T$ products for all of the compounds except dysprosium acetylacetonate are given in Table I. The constants of Curie-Weiss expressions for the susceptibility have been given previously.¹⁰ Certain generalizations are immediately apparent from the table. Both chelates of praseodymium show a relatively small change of susceptibility from 20 to 1.3°K., although there is more variation than has been observed previously for the sulfate and ethyl sulfate. This behavior indicates that the ground state of the ion is almost certainly a singlet in all of these compounds. The EDTA complexes of neodymium and gadolinium and the acetylacetonate complex of ytterbium have nearly constant χT products over the entire range investigated, indicating a ground multiplet separated widely from higher multiplets (if any). The remaining substances show various deviations from constancy in their χT products, indicating a relatively narrow spacing of multiplets.

The magnetic susceptibility of dysprosium acetylacetonate is given in Table II as a function of both temperature and frequency. The values given for the (static) susceptibility at zero frequency were obtained by plotting the reciprocal of the susceptibility against the square of the frequency for the low frequency points; they are somewhat more uncertain than the measured values.

Cubic Field Model.—Ideally, a theoretical analysis of the magnetic susceptibility should start from knowledge of the structural arrangement of the groups around the paramagnetic ion, from which the symmetry of the crystalline environment can be deduced. As has frequently been the case in other investigations, the structure of these chelates is not known. In fact, Hoard¹³ has suggested that the acetylacetonates and EDTA complexes of the rare earths are likely to be seven-coordinate, with at most a twofold axis of symmetry. This structure could give rise to a crystal field of very low symmetry.

Although the actual crystal symmetry is almost certainly much lower than cubic, some general inferences can be drawn by comparison of the results with the relatively simple theory obtained for a cubic crystalline field. Detailed theoretical

TABLE II
MAGNETIC SUSCEPTIBILITY OF DYSPROSIUM
ACETYLACETONATE

Temp., °K.	Frequency	(weight 0.5673g.)	
		χ_m	$\chi_m T$
20.24	400	0.718	14.5
	1000	.728	14.7
17.01	400	.836	14.2
	1000	.836	14.2
15.12	400	.925	14.0
	1000	.931	14.1
4.185	0	(2.86)	(12.1)
	100	2.88	12.07
	200	2.74	11.49
	400	2.54	10.64
	1000	1.98	8.29
	2000	1.32	5.53
3.091	0	(3.50)	(10.8)
	100	3.4	10.69
	200	3.21	9.94
	400	2.69	8.33
	1000	1.75	5.42
	2000	1.17	3.61
1.971	0	(4.59)	(9.1)
	100	4.49	8.84
	200	4.13	8.12
	400	3.21	6.34
	1000	2.08	4.11
	2000	1.47	2.91
1.324	0	(5.44)	7.2
	100	5.45	7.22
	200	4.63	6.12
	400	3.55	4.69
	1000	2.26	2.99
	2000	1.65	2.19

treatments are available for praseodymium,¹⁴ neodymium,¹⁴ erbium¹⁵ and ytterbium.¹⁶

The ground state of the praseodymium ion is 3H_4 , which is split by a cubic electric field into a singlet (lowest), a triplet, a doublet and a second triplet. The singlet derives from linear combinations of levels with J_z of 0 and ± 4 , and is heavily weighted with respect to $J_z = 0$. The spacing between the several levels is determined by a simple parameter a , reflecting the strength of the crystal field.¹⁴ At very low temperatures the susceptibility approaches a constant value. The magnitude of the approximately constant susceptibility of praseodymium acetylacetonate below 4°K. indicates that the singlet level of this compound is about 25 cm.^{-1} below the next multiplet. The susceptibility above 15°K. is distinctly lower than that predicted for a cubic crystal field, indicating that a field of lower symmetry produces a sizable splitting of the otherwise triplet level. The lower susceptibility of the EDTA complex indicates a separation of nearer 60 cm.^{-1} between singlet and multiplet; similar departures from the predictions of cubic field theory above 15°K. are observed for this salt also.

(13) "On the Stereochemistry of Ethylenediaminetetraacetate Complexes of the Iron Group and Related Cations," by J. L. Hoard, G. S. Smith and M. Lind. We thank Dr. Hoard for communication in advance of this paper prepared for presentation at the Sixth International Conference on Coordination Chemistry.

(14) W. G. Penney and R. Schlapp, *Phys. Rev.*, **41**, 194 (1932).

(15) F. H. Spedding, *J. Chem. Phys.*, **5**, 316 (1937).

(16) W. G. Penney, *Phys. Rev.*, **43**, 485 (1933).

A cubic field splits the $^4I_{9/2}$ ground state of neodymium into a doublet (lowest) and two quartet states. The cubic field model¹⁴ gives a limiting value of 0.67 for χT at very low temperatures, which is slightly higher than the limiting value observed for both the acetylacetonate and the EDTA complex. The data for the former compound can be fit, to a poor approximation, by an energy level pattern in which the next multiplet is about 50 cm^{-1} above the ground doublet. For the EDTA complex it is possible to observe only that the separation between the two multiplets is again considerably greater than for the acetylacetonate.

The inadequacy of the cubic field approximation is illustrated more clearly by erbium acetylacetonate. The $^4I_{15/2}$ state of the erbium ion is split by a cubic field into three quartets and two doublets, with two quartets lowest. The lowest value of χT for the ground quartet¹⁵ is 10.6; by contrast χT observed for erbium acetylacetonate is about 6 in the helium range and only 7.6 at 20.3°K. This indicates clearly that the ground level is only a doublet, with the next multiplet at least some tens of wave numbers higher.

In the case of ytterbium, the $^2F_{7/2}$ ground state is split by a cubic field into two doublets (lowest) and a quartet. The value of χT due to the ground doublet¹⁶ is 1.07. The observed value for ytterbium acetylacetonate is nearly constant below 20°K. at about 1.24. Apparently the ground state is indeed a doublet of slightly different character from that predicted by cubic field theory, with the next multiplet quite far (at least 100 cm^{-1}) above it.

Previous attempts to fit the properties of gadolinium salts by means of cubic field theory have had only very moderate success. In both the acetylacetonate and the EDTA complexes the χT product above 10°K. is near (in the latter case, slightly above) the value (7.9) required for full occupancy of the 8S state. The Weiss constants for the two substances are 0.47 and 0.08°K., respectively, indicating that whatever the detailed character of the pattern, the over-all splitting must be less than 1 cm^{-1} in both cases and substantially less for the EDTA complex.

In view of the rather indifferent success of the cubic field model in predicting the observed susceptibilities, we did not extend the treatment to the remaining substances for which data were available. For those examined above, it is evident that the states observed are either singlets or doublets separated substantially from the next higher multiplets, and that any low-lying triplet or quartet states predicted by cubic field theory are further split under the influence of the existing interactions.

Crystal Fields of Lower Symmetry.—Elliott and Stevens^{7,17} have examined the resonance behavior, and in some cases the susceptibility, of the rare earth ethyl sulfates using a model in which the electric field has C_{3h} symmetry. While there are good reasons to believe that the symmetry in the chelate compounds is lower than this,¹³ their

model contains strong weighting of axial terms and should aid in the identification of states. Their formalism provides simple identification of the terms arising from purely axial symmetry in terms of potentials V_2^0 , V_4^0 and V_6^0 which may be taken as parameters, and tabulated matrix elements for these potentials for states of particular J and J_z . In addition they tabulate the matrix elements for the non-axial V_6^0 potential which mixes states differing by ± 6 in J_z , and provide a general formulation for the matrix elements of other non-axial terms. Moreover, they were able to show that, to first order, the field parameters for the various ethyl sulfates were similar and were related in a simple manner one to the other, leading to the hope that a similar situation should prevail with other series of related compounds.

The clearest situation obtains in the case of praseodymium, where for both chelates the ground state is a singlet. For a purely axial field, the singlet ($J_z = 0$) is lowest only if the parameters V_4^0 and V_6^0 are positive, *not* negative as in the case of the ethyl sulfates. (As a check, the "zero'th order" axial levels used as a starting point by Penney and Schlapp¹⁴ are reproduced, except for choice of zero, by using on y $V_4^0 = -443a$, with a as before a *negative* number; the choices of a required for the approximate fit of the previous section give V_4^0 of the order of 40 to 80 cm^{-1} .) A field similar to that used by Elliott and Stevens,⁷ with negative potentials, puts the $J_z = 0$ singlet highest. Additional singlets arise, to first order, only from the $J_z = \pm 3$ doublet. A large value of V_6^0 could produce a low-lying singlet from this, but it seems unlikely that any reasonable potential would bring this singlet lower than doublets arising from $J_z = \pm 2, \pm 4$, and further calculations have not been made. It appears, however, that the properties of the praseodymium chelates can be interpreted more readily in terms of a field nearer cubic in symmetry than by one approximately C_{3h} .

Ytterbium acetylacetonate has a nearly constant χT product, indicating that a doublet state is lowest. A large positive value of V_4^0 would put, to zero'th order, the $J_z = \pm 1/2$ level lowest, with approximately the observed susceptibility. A mixture of this state with another of $^2F_{7/2}$ multiplet could explain the observed results. The C_{3h} potential puts the $J_z = \pm 3/2$ level lowest, with χT about four times too small. The C_{3h} potential can be made to fit the data only by using a V_6^0 term large enough to bring the doublets arising from $J_z = \pm 5/2, \pm 7/2$ lowest. Again this does not seem particularly promising, and detailed calculations were not made. In any case the next doublet must be many wave numbers above the ground state. A zero'th order calculation using a V_4^0 potential of approximately 50 cm^{-1} would bring the $J_z = \pm 7/2$ level only about 20 cm^{-1} higher, but admixture of states in a nearly cubic field could increase the separation of the resultant states substantially.

In the case of the neodymium chelates, no clear distinctions can be drawn. It should certainly be possible to explain the properties of the ground doublet by altering the admixture of the $J_z =$

$\pm 1/2, 7/2, 9/2$ states in a nearly cubic field, but the observed susceptibility also could be produced by the $J_z = \pm 5/2, 7/2$ combination used in the Elliott and Stevens⁷ treatment. Clearly more information is required before further explanations can be made. The situation with dysprosium is particularly ambiguous, since χT is still dropping rapidly below 1.5°K . The best that can be said here is that the results are not inconsistent with either a nearly cubic field or one of approximately C_{3h} symmetry.

For erbium ($^4I_{15/2}$), the zero'th order results of a positive V_4^0 is to put the $J_z = \pm 11/2$ doublet lowest. This doublet produces about the observed χT product (ignoring the apparent upturn at low temperatures as perhaps due to cooperative interactions). However, in a nearly cubic field the admixtures of various states are so complicated as to make almost any type of ground state possible. The $\pm 7/2, \pm 5/2$ doublet lowest in a field of C_{3h} symmetry would give a χT product only slightly too low, and is also a possibility.

Finally, in the cases of terbium, holmium and thulium, neither χ nor χT is at all constant. Since the number of values of J_z involved is large in each case (13, 17, 13, respectively) no attempt has been made to obtain any correlations.

In general it can be said that the effective fields due to the crystalline environment appear to have symmetry nearer cubic than either axial or C_{3h} , but with stronger interactions than would be found for a purely cubic crystal field and considerable "mixing" of states with different J_z . In all cases additional measurements are needed for unambiguous choice of the ground state and the splitting pattern. In particular, knowledge of the principal susceptibilities, either by direct measurement or by resonance experiments to get g_{\parallel} and g_{\perp} , would clarify the interpretation considerably with regard to the low-lying levels. Finally, spectroscopic observations would aid immensely in elucidation of the over-all energy level pattern.

Spin-lattice Relaxation in Dysprosium Acetylacetonate.—We already have observed¹⁰ that a Debye plot of the susceptibility of $\text{Dy}(\text{acac})_3 \cdot \text{H}_2\text{O}$ gives values for the spin-lattice relaxation time, τ , of about a millisecond. The actual values obtained were 0.9, 1.4, 1.6 and 1.8×10^{-3} second at

4.2, 3.1, 2.0 and 1.3°K , respectively. Although the times observed are of the same order of magnitude as those of Cooke,¹⁸ *et al.*, the temperature variation is much smaller, particularly below 3°K . The simple Debye plot fit the data within experimental error up to 400 cycles, but at higher frequencies the susceptibility fell less rapidly than required for this treatment.

The modified Debye treatment used by Gorter,¹⁹ with an additional parameter, F , gave a better representation of the data, but still deviated badly at the higher frequencies. The best value of F was 1.0 below 400 cycles and 0.75 at frequencies of 1000 and 2000 cycles. It appears that there are probably two distinct relaxation mechanisms involved.

Conclusions

The widely varied susceptibilities of the acetylacetonate complexes of the rare earth elements are consistent with an internal crystalline field producing interactions similar to, but more complex than, those due to a cubic field. In all cases the lowest energy levels are doublets (or in the case of praseodymium, a singlet) rather than higher multiplets; the next lowest levels range from approximately 20 to 100 or more cm^{-1} above the ground state. In the cases of praseodymium and neodymium, the EDTA chelate showed stronger interactions than did the acetylacetonate; in the case of gadolinium the EDTA produced distinctly less effect on the separation of states. Evidently the lowest levels in all cases correspond to mixtures of states of two or more values of J_z . Possible ground state configurations have been suggested, but additional experimental evidence is required to eliminate ambiguities of choice.

Acknowledgments.—We wish to thank Dr. W. C. Fernelius for assistance in preparation or procurement of the specimens used in these investigations, and for helpful suggestions throughout. We wish to thank Mr. L. F. Shultz for preparation of refrigerants, and Prof. J. G. Aston and Prof. J. A. Sauer for encouragement and helpful discussions.

(18) A. H. Cooke, D. T. Edmonds, F. R. McKim and W. R. Wolf, *Proc. Roy. Soc. (London)*, **A252**, 246 (1959).

(19) C. J. Gorter, "Paramagnetic Relaxation," Elsevier Publishing Co., New York, N. Y., 1947, p. 22.

RATE OF ELIMINATION OF WATER MOLECULES FROM THE FIRST COÖRDINATION SPHERE OF PARAMAGNETIC CATIONS AS DETECTED BY NUCLEAR MAGNETIC RESONANCE MEASUREMENTS OF O¹⁷

BY ROBERT E. CONNICK AND E. DIANE STOVER

Department of Chemistry and the Radiation Laboratory, University of California, Berkeley, Calif.

Received June 19, 1961

Earlier nuclear magnetic resonance measurements on the rates of exchange of water molecules between bulk water and the first coordination sphere of cations have been amplified and refined using water enriched in O¹⁷. Limits for the rates of these processes were calculated from the transverse relaxation time. A sideband technique was used in making the measurements. The following lower limits for the first-order rate constants for the exchange of a particular water molecule in the first coordination sphere were found: Mn²⁺, 2.2×10^7 sec.⁻¹; Cu²⁺, 3.3×10^6 sec.⁻¹; Co²⁺, 3.1×10^6 sec.⁻¹; Ni²⁺, 3.2×10^4 sec.⁻¹ and Fe³⁺, 2.4×10^4 sec.⁻¹.

In a previous paper² preliminary results were reported on the effect of paramagnetic ions on the width of the nuclear magnetic resonance signal of O¹⁷ in water. The corresponding T_2 values were interpreted in terms of an exchange between bulk water molecules and the water in the first coordination sphere of the metal ions, and from the data a lower limit for the rate of this exchange could be calculated. In the present work the measurements have been repeated with greater precision by using water enriched in O¹⁷, and the linear dependence of the line width on the concentration of the paramagnetic ion has been established.

During the course of the work the longitudinal relaxation time, T_1 , was measured for O¹⁷ existing in the form of water. Also, the acidity dependence of the transverse relaxation was determined.

Experimental

A sideband technique³⁻⁵ was used with a Varian Associates model V-4200 wide-line nuclear magnetic resonance (variable frequency) spectrometer. The frequency was 5.77 Mc., corresponding to a ca. 10 kgauss field, for all but the final cobalt experiments where it was 5.44 Mc. The sweep frequency was 400 c.p.s. and the sweep amplitude ca. 0.9 gauss. The T_2 measurements were all taken at the same rf power setting of ca. 0.06 gauss, where no saturation was occurring. For the T_1 measurements the radio-frequency was increased from the non-saturating value of ca. 0.05 to 0.25 gauss. The phasing of the audio-amplified voltage delivered to the synchroverter phase detector was tuned so that the zeroth harmonic was eliminated; the first sideband was detected as an absorption signal. The time constant of the integrating filter was 0.64 sec., and the polarizing magnetic field was scanned at a sweep speed of 1.3 gauss per min.

Samples of 4-ml. volume were contained in 15×125 mm. Pyrex tubes fitted with ground glass jointed caps.

The enriched water, obtained from the Weizmann Institute of Science, had 0.7 atom % O¹⁷ and ca. 10 atom % deuterium.⁶ The solutions of paramagnetic ions contained 0.10 M HClO₄ in addition to the salt, except for the chromic perchlorate solutions. The water was recovered by distillation. Perchlorate salts were employed in an attempt to minimize complex formation.

In early measurements the samples were degassed on a vacuum line and the sample tube refilled with nitrogen in

order to prevent dissolved O₂ in the water from broadening the resonance. It was found that this effect was not measurable, and the degassing technique was dropped for later samples.

The spectra were taken at a temperature of ca. 26°.

Results and Discussion

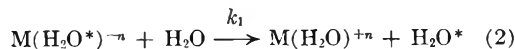
The line widths (*i.e.*, half widths at half height) and transverse relaxation times, T_2 , for the various solutions are given in Table I. The dependence of line-width on concentration of paramagnetic ion is shown in Fig. 1. The absorption curves of some of the more concentrated solutions were broadened considerably, making accurate measurement of line width difficult. This accounts at least in part for the scatter.

If it is assumed that the spin of an O¹⁷ nucleus can undergo transverse relaxation by two independent, first-order processes, *i.e.*, relaxation in the bulk water and relaxation caused by paramagnetic ions, one can write

$$\frac{1}{T_2} = \frac{1}{(T_2)_D} + \frac{1}{(T_2)_P} \quad (1)$$

where $(T_2)_D$ refers to the relaxation time in the diamagnetic bulk water and $(T_2)_P$ refers to the relaxation time arising from the presence of the paramagnetic ions. According to this equation the line width, which is inversely proportional to T_2 at a given frequency, should be linearly dependent on the concentration of paramagnetic ion. This was found to be the case in Fig. 1.

As shown earlier² $(T_2)_P$ can be related to a lower limit for the rate of exchange of water molecules between the first coordination sphere of the metal ion and the bulk water.⁷ The values of the first-order rate constant for the loss of a particular water molecule from the first coordination sphere



are given in Table II, as calculated from the data of Table I. It was assumed that every metal ion had a coordination number of 6.

In the last column of Table II are reported for comparison the values obtained earlier. When allowance is made for the large experimental uncertainty in the previous measurements, the results for Mn⁺⁺, Ni⁺⁺ and Co⁺⁺ compare favor-

(7) From the chromic ion results, where such an exchange is known to be very slow (J. P. Hunt and H. Taube, *J. Chem. Phys.*, **19**, 602 (1951)) it is inferred that the much more rapid relaxation observed with the other ions must be occurring in the first coordination sphere.

(1) Presented at the September 1960 meeting of the American Chemical Society, New York.

(2) R. E. Connick and R. E. Poulson, *J. Chem. Phys.*, **30**, 759 (1959).

(3) K. V. Vladimirovskii, *Doklady Akad. Nauk, S.S.S.R.*, **58**, 1625 (1947).

(4) H. Primas, *Helv. Phys. Acta*, **31**, 17 (1958).

(5) J. V. Acrivos, Lawrence Radiation Laboratory Report UCRL 9649, 1961, University of California, Berkeley, California.

(6) The deuterium was measured by comparing the n.m.r. signal of deuterium with that of a diluted D₂O solution.

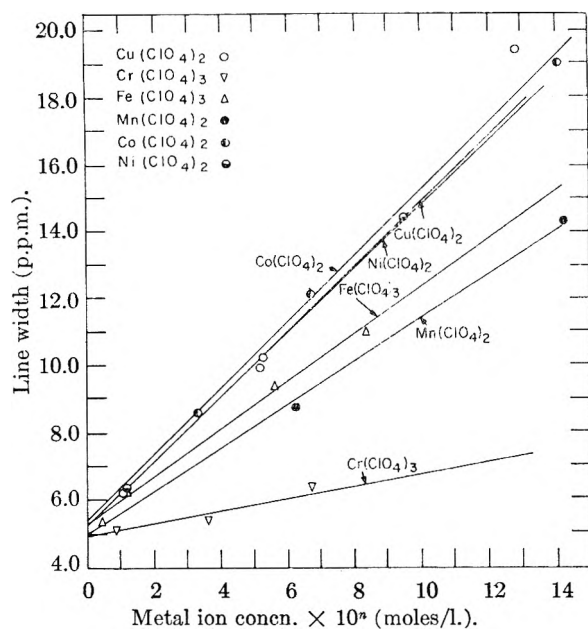


Fig. 1.—Variation of line width with concentration. Concentrations of metal perchlorate solutions are multiplied by 10^4 where n is: 4 for Cu^{2+} , 3 for Cr^{3+} , 2 for Fe^{3+} , 5 for Mn^{2+} , 2 for Ni^{2+} , and 3 for Co^{2+} .

TABLE I

LINE WIDTHS AND TRANSVERSE RELAXATION TIMES OF O^{17} IN SOLUTIONS OF PARAMAGNETIC IONS AT ROOM TEMPERATURE

0.10 M HClO_4 present except in $\text{Cr}(\text{ClO}_4)_3$ experiments.			
Solution	Molar concn.	Line width, p.p.m. ^a	$T_2 \times 10^3$, sec.
$\text{Cu}(\text{ClO}_4)_2$	1.10×10^{-4}	6.2	4.5
	5.25×10^{-4}	10.2	2.7
	1.28×10^{-3}	19.4	1.4
$\text{Cr}(\text{ClO}_4)_3$	0.088	5.1	5.5
	.36	5.34	5.2
	.67	6.4	4.3
$\text{Fe}(\text{ClO}_4)_3$	4.44×10^{-3}	5.29	5.2
	1.14×10^{-2}	6.30	4.4
	5.57×10^{-2}	9.33	3.0
	8.32×10^{-2}	11.0	2.5
$\text{Mn}(\text{ClO}_4)_2$	6.24×10^{-6}	8.74	3.2
	1.43×10^{-4}	14.3	1.9
$\text{Ni}(\text{ClO}_4)_2$	1.19×10^{-2}	6.34	4.3
	5.17×10^{-2}	9.89	2.8
	9.44×10^{-2}	14.4	2.1
$\text{Co}(\text{ClO}_4)_2$ ^b	3.28×10^{-3}	8.58	3.4
	6.70×10^{-3}	12.1	2.2
	1.41×10^{-2}	19.0	1.5
H_2O^{17}	5.20 ± 0.37	5.3 ± 0.3^c

^a Field inhomogeneity was less than 0.5 p.p.m. ^b Measured at 5.44×10^6 c.p.s. All others measured at 5.77×10^6 c.p.s. ^c Average of 8 different spectra.

ably. There is an appreciable discrepancy in the case of Cu^{2+} and a large discrepancy between the Fe^{3+} results. The source of these discrepancies is unknown. In the latter case, at least, instrumental distortion of the absorption² could scarcely account for the difference. Likewise the replacement of 2.0 and 4.0×10^{-3} M $\text{Fe}(\text{NO}_3)_3$ by $\text{Fe}(\text{ClO}_4)_3$ seems unimportant. It should be emphasized that the present results for what is partially a D_2O solvent would be expected to differ somewhat from those for H_2O , but not greatly.

TABLE II

CALCULATED LOWER LIMITS FOR FIRST-ORDER RATE CONSTANTS FOR WATER EXCHANGE (EQUATION 2)

Solution ^a	Lower limit for k_1 , sec. ⁻¹	Lower limit for k_1 , sec. ⁻¹ from Connick and Poulson ²
$\text{Cu}(\text{ClO}_4)_2$	3.3×10^8	6×10^5
$\text{Fe}(\text{ClO}_4)_3$	2.4×10^4	1.1×10^6
$\text{Mn}(\text{ClO}_4)_2$	2.2×10^7	1×10^7
$\text{Ni}(\text{ClO}_4)_2$	3.2×10^4	4×10^4
$\text{Co}(\text{ClO}_4)_2$	3.1×10^6	2×10^6

^a Since the relaxation is not occurring in the first coordination sphere for Cr^{3+} , no value for k_1 can be calculated.

Eigen⁸ has compared the rates of formation of inner sulfate complexes of metal ions with the lower limit for the rates of exchange of water molecules measured previously.² It is of interest to repeat the comparison with the newer data. In Table III is given in the second column the first-order rate constant for the conversion of an outer sphere sulfate complex to an inner sphere complex.⁸ In the 3rd column are listed the lower limits for the water exchange found here. Except for Cu^{2+} , the relative orders and absolute values are remarkably similar, as might be expected if the primary impediment to the formation of the activated complexes is the partial removal of a water molecule from the first coordination sphere.^{8,9} Although the water exchange data are only lower limits, this rather striking comparison supports the idea that the rate of exchange is actually being measured.

TABLE III

COMPARISON OF RATES OF FORMATION OF SULFATE COMPLEXES WITH LOWER LIMITS FOR RATES OF EXCHANGE OF WATER MOLECULES

Ion	First-order rate constant for formation of sulfate complex, sec. ⁻¹	Lower limit for k_1 , sec. ⁻¹
Mn^{2+}	4×10^6	2.2×10^7
Cu^{2+}	$\sim 10^4$ (?)	3.3×10^8
Co^{2+}	2×10^6	3.1×10^6
Ni^{2+}	1×10^4	3.2×10^4

The new value for the exchange of waters bound to Fe^{3+} can be compared with the rates of formation of FeCl^{2+} and FeSCN^{2+} complexes. In each case a water molecule in the first coordination sphere is being replaced. At 25° in 0.1 M HClO_4 and an ionic strength of 1.0 and 0.40 M, respectively, the apparent bimolecular rate constants for the formation of the complexes are 1.9×10^{210} and $3.3 \times 10^2 \text{ M}^{-1} \text{ sec.}^{-1}$,¹¹ respectively, for FeCl^{2+} and FeSCN^{2+} . The lower limit for the bimolecular rate constant for water exchange, where any of the six waters may be replaced, is from the present work $2.6 \times 10^3 \text{ M}^{-1} \text{ sec.}^{-1}$. The values are much more nearly the same than was thought previously² and lend support to the idea that the rate in each case is primarily controlled by the elimination of the water molecule.^{8,9}

(8) M. Eigen, *Z. Elektrochem.*, **64**, 115 (1960).

(9) F. Basolo and R. G. Pearson, "Mechanisms of Inorganic Reactions," John Wiley and Sons, Inc., New York, N. Y., 1958, p. 163.

(10) R. E. Connick and C. P. Coppel, *J. Am. Chem. Soc.*, **81**, 6389 (1959).

(11) J. F. Below, Jr., R. E. Connick and C. P. Coppel, *ibid.*, **80**, 2961 (1958).

The value of $2.2 \times 10^7 \text{ sec.}^{-1}$ for the lower limit of k_1 of Mn^{++} can be compared with that of $4 \times 10^7 \text{ sec.}^{-1}$ found by Bernheim, *et al.*,¹² for the rate of replacement of protons in the first coordination sphere of Mn^{++} from measurements of the proton relaxation time in aqueous manganous solutions at 27° .¹³ It has been pointed out by Pearson, *et al.*,¹³ that the similarity in these two rates indicates the protons are entering and leaving the first coordination sphere by exchange of an entire water molecule. The difference could arise from: (a) the experimental accuracy of the two measurements, (b) the effect on the rate of the replacement of H_2O by D_2O , (c) a rate of relaxation of an O^{17} in the first coordination sphere which is comparable to the rate of displacement of the oxygen, or (d) a proton replacement mechanism which is independent of water exchange and having about the same rate as the latter.

Acidity Dependence of T_2 of O^{17} in Water.—In order to ascertain whether the acidity was at all critical, T_2 was determined in solutions of varying pH which contained the enriched water and amounts of perchloric acid or sodium hydroxide necessary to give the observed pH. The data are shown in Table IV. Since this work was completed Meiboom¹⁴ has published data on T_2 and T_1 of O^{17} of water as a function of pH from pH 3.3 to 12.1. He found T_2 to be $4.4 \times 10^{-3} \text{ sec.}$ over most of this pH range as compared to an average value of $5.3 \times 10^{-3} \text{ sec.}$ in Table IV. The slightly smaller value obtained by Meiboom might have arisen from instrument broadening in the derivative method, as found in the work reported earlier.¹

The pronounced effect of pH on T_2 observed by Meiboom near the neutral region is absent from Table II because no measurements were made near pH 7. The only run where a significant derivation from constancy would be expected is that at pH 8.0 where Meiboom's theoretical curve predicts a value of $3.2 \times 10^{-3} \text{ sec.}$ The absence of such an effect in Table IV should not be construed as a

(12) R. A. Bernheim, T. H. Brown, H. S. Gutowsky and D. E. Woessner, *J. Chem. Phys.*, **30**, 950 (1959).

(13) The comparison made earlier (R. G. Pearson, J. Palmer, M. M. Anderson and A. L. Allred, *Z. Elektrochem.*, **64**, 110 (1960)) mistakenly quoted a sevenfold too high value from ref. 2.

(14) S. Meiboom, *J. Chem. Phys.*, **34**, 375 (1961).

disagreement because of the uncertainty in both the T_2 measurement and the pH determination.

TABLE IV

VARIATION OF T_2 OF O^{17} IN WATER WITH pH		
pH	Line-width, p.p.m.	$T_2 \times 10^3, \text{sec.}$
0.87	4.80	5.75
1.00	5.20 ± 0.37	5.3 ± 0.3^a
3.0	5.23	5.25
5.5	5.37	5.14
8.0	5.34	5.17
10.5	5.53	4.98

^a From Table I.

T_1 of O^{17} in Water.—The saturation technique was used to measure T_1 in water enriched in O^{17} and containing $0.1 M \text{ HClO}_4$. In the side band method the absorption is of the form⁵

$$\text{constant} \times \frac{\gamma H_1 J_1^2(\beta) T_2 \beta^{-1}}{1 + T_2^2 (\Delta_{\pm 1} \omega)^2 + \gamma^2 H_1^2 J_1^2(\beta) T_1 T_2} \quad (3)$$

where $J_1(\beta)$ is the first Bessel function, $B = |\gamma| H_m / \omega_m$, (the subscript m refers to modulation), $\Delta_{\pm 1} \omega = \Delta \omega \pm \omega_m$, and the other symbols have their usual significance. The effective field, H_1 , was found at high power from the relation

$$\delta = 2(\omega_m^2 - \gamma^2 H_1^2)^{1/2} \quad (4)$$

where δ is the sideband separation; lower power values were read from the dial settings in terms of the high power value.

Four separate saturation runs gave an average value of 0.178 gauss for H_1 at maximum peak amplitude and correspondingly $4.1 \times 10^{-3} \text{ sec.}$ for T_1 . This value may agree with T_2 within the experimental accuracy, as might be expected for a quadrupole relaxation mechanism. Divergent values have been reported by Shulman and Wyluda¹⁵ and Meiboom.¹⁴ Our value agrees well with that of $4.4 \times 10^{-3} \text{ sec.}$ reported by the latter investigator.

We wish to acknowledge our great indebtedness to Dr. J. V. Acrivos for making available to us the sideband method of detection on the wide line apparatus, and to thank Professor R. J. Myers for his helpful counsel. The research was supported by the United States Atomic Energy Commission.

(15) R. G. Shulman and B. J. Wyluda, *J. Chem. Phys.*, **30**, 335 (1959).

THE RATE OF DISSOCIATION OF PERCHLORATE ION IN FUSED SODIUM HYDROXIDE^{1,2}

BY RALPH P. SEWARD AND HARRY W. OTTO

*Dept. of Chemistry, The Pennsylvania State University, University Park, Penna.**Received June 19, 1961*

Sodium perchlorate in fused sodium hydroxide at temperatures from 360 to 420° is found to decompose to chlorite in two consecutive first-order reactions. Rate constants for conversion of perchlorate to chlorate and from chlorate to chlorite have been evaluated, the first step being the faster. Respective activation energies of 47.3 and 53.2 kcal. mole⁻¹ have been calculated. Decomposition rates are much greater in fused sodium hydroxide than in fused sodium nitrate. It is suggested that the decomposition is promoted by hydroxyl ion through the formation of a peroxide intermediate.

When the present investigation was initiated no study of the rate of a homogeneous liquid phase reaction in a non-reacting fused salt solvent had appeared in the literature. It was thought that the decomposition of an oxygen containing anion in fused sodium hydroxide might be such a reaction and that its investigation would be worthwhile. Sodium hydroxide was chosen as the solvent because of its low melting point and an earlier interest in the nature of this material, although its use precluded the use of glass containers and thus introduced some experimental problems. A preliminary trial showed that perchlorate decomposed at a satisfactory rate at 350–400° while bromate decomposed too rapidly for measurement and iodate disproportionated rapidly to periodate and iodide without loss of oxygen. Furthermore, the decomposition of the alkali metal perchlorates as pure salts in both solid and liquid state already had been investigated.³

The over-all progress of the reaction was followed by the determination of the concentration of chloride ion in samples taken at suitable intervals. Determination of chloride rather than oxygen was chosen because it is known⁴ that fused sodium hydroxide reacts with oxygen gas, forming up to 3 wt. % sodium peroxide. After it was apparent that a considerable amount of chlorate accumulated during the reaction, experiments were carried out in which both chlorate and chloride were determined in the samples. As the disappearance of chlorate based on these analyses followed a smooth first-order relation, it was concluded that no significant concentrations of chlorite or hypochlorite were present during the reaction. Hypochlorite could not be detected by qualitative tests. Thus the concentration of undecomposed perchlorate could be calculated by subtracting the sum of chlorate and chloride concentrations from the total chlorine concentration. A trace of chlorine was found in the gaseous product but this was too small for quantitative determination.

It was found that the rate of decomposition of perchlorate in fused sodium hydroxide was some 10⁴ times the rate calculated by extrapolation of the rates observed for decomposition in pure liquid

potassium perchlorate at somewhat higher temperatures.³ The difference in the rates of decomposition of potassium perchlorate and of sodium perchlorate in fused sodium hydroxide being relatively insignificant, it is apparent that the hydroxyl ion is an important factor in determining the rate of decomposition of perchlorate ion. For this reason rates of decomposition of perchlorate were measured in various sodium nitrate–sodium hydroxide mixtures.

Investigation of other factors which it was thought might influence the reaction rate included the addition of insoluble aluminum, barium oxide and magnesium oxide, soluble sodium peroxide, barium peroxide and water. The effect of substitution of lithium, and in part potassium, for sodium also was investigated.

Aluminum containers were used for the sodium hydroxide fusions in this work. When aluminum is immersed in fused sodium hydroxide, gas evolution from the surface of the metal occurs but this lasts only a few seconds. It is proposed that the protective coating consists of a layer of an insoluble sodium aluminate since if the metal is removed, washed and then returned to the melt, the brief attack occurs again. While nickel is satisfactory in resistance to corrosion by fused sodium hydroxide at moderate temperatures, the unfortunate tendency of the liquid to creep up the walls of the container, to solidify when it reaches a cooler spot, is much more noticeable in nickel than in aluminum. Corrosion of the aluminum containers did occur but slowly enough so that they could be used for many hours with only a few milligrams loss in weight.

Experimental

Apparatus.—Reactions were carried out in aluminum cups 1 inch in diameter and 2.75 inches tall with 1/8 inch wall thickness. Constancy of temperature was achieved by fitting the reaction cups into holes in an aluminum cylinder, 4 inches in diameter and 7 inches in height. The cylinder had also a thermocouple well and a well for a Fenwall Thermoswitch bimetallic temperature controller. In use, the aluminum cylinder fitted into a four-inch iron pipe which was surrounded on the sides and bottom by about 3 inches of insulation. A Transite cover reduced heat loss at the top. A main heater of electrical wiring kept the cylinder nearly up to the desired temperature and a smaller intermittent heater operating through the Thermoswitch kept the temperature constant to about ±1°. During runs the temperature control was improved to ±0.5° by manual adjustment of the heating current. Temperatures were measured with a Chromel–Alumel thermocouple which had been calibrated with N.B.S. samples of tin, lead and zinc. The thermocouple e.m.f. was measured to ±1 microvolt with a Leeds and Northrup Type K2 potentiometer. On immersion of the thermocouple in the reacting mixtures, temperatures were found of the order of 1° lower than that

(1) This work was supported by the U. S. Atomic Energy Comm. under Contract AT(30-1)-1881.

(2) From the Ph.D. thesis of Harry Otto, The Pennsylvania State University, June 1961.

(3) A. E. Harvey, M. T. Edmison, E. D. Jones, R. A. Seybert and K. A. Catto, *J. Am. Chem. Soc.*, **76**, 3270 (1954).

(4) H. Lux, R. Kuhn and T. Niedermaier, *Z. anorg. allgem. Chem.*, **298**, 285 (1959).

of the aluminum cylinder and the recorded temperatures corrected for this difference. This effect is attributed to heat loss through the aluminum sampling pipets which protruded through holes in the cover, this heat loss more than compensating for the slightly exothermic nature of the reaction.

In carrying out a reaction, the reaction cup was first preheated to $470 \pm 10^\circ$ in a separate furnace, about 15 g. of sodium hydroxide pellets added, and the molten hydroxide kept at this temperature for an hour to remove water. The cup then was transferred to the aluminum cylinder and, after giving it time to come to the cylinder temperature, preheated samples of the perchlorate or chlorate were added, and the mixture briefly stirred manually to ensure homogeneity. During reaction the solution was adequately stirred by the evolution of oxygen gas.

Approximately one-g. samples of the melt were removed at various intervals by means of aluminum pipets, dropped on a cool metal plate, weighed after solidifying and cooling, and dissolved in water. Chloride then was determined gravimetrically as silver chloride. Since the densities of the reacting solutions were not known, all concentrations were calculated as moles per kg. of solution. When chlorate also was to be determined, a separate aliquot of the dissolved sample was acidified with sulfuric acid, sodium bisulfate added to reduce the chlorate, and chlorate and chloride combined determined as silver chloride. In samples containing nitrate, reduction of chlorate in alkaline solution by zinc was found more satisfactory.

The chemicals used were Reagent Grade commercial products except lithium perchlorate which was prepared from lithium carbonate and perchloric acid. The perchlorates were recrystallized and dried by heating to 150° or higher at less than 5 mm. pressure. No chloride or chlorate could be detected in them. Sodium hydroxide pellets were dried as described above and contained up to 0.5% sodium carbonate. Other chemicals were untreated before use except for thorough drying.

Results and Discussion

Homogeneity of the Reaction.—Although visual observation showed sodium perchlorate to be readily dissolved in fused sodium hydroxide, a portion of the binary phase diagram was investigated to show what the limits of homogeneity were. By recording cooling curves, it was found that a eutectic exists at 243° and 15 mole % sodium perchlorate. At the temperatures at which the rate experiments were done, the solubility of sodium perchlorate is much greater than 15 mole %. From the freezing points in the dilute perchlorate region, the heat of fusion of sodium hydroxide was calculated as 1530 cal./mole, in good agreement with the calorimetric value of 1520 cal. obtained by Douglas and Dever,⁵ thus indicating that the solutions are essentially ideal.

The solubility of sodium perchlorate in sodium nitrate (m.p. 309°) also was investigated. In this system a eutectic was found at 228° and 38 mole % sodium perchlorate. At 309° the liquid phase is 50 mole % sodium perchlorate. Retortillo and Moles⁶ have shown that the sodium hydroxide-sodium nitrate system is completely liquid at all compositions when above 320° .

Several decomposition rate experiments were carried out with aluminum turnings added to the reaction cups, thus increasing the area of aluminum surface by as much as a factor of four. No detectable change in the reaction rate was found, indicating that the reaction occurs in the liquid phase with no significant contribution from the metal surface.

(5) T. B. Douglas and J. L. Dever, *J. Research Natl. Bur. Standards*, **53**, 81 (1954).

(6) N. M. Retortillo and E. Moles, *Anales soc. espan. fis. quim.*, **31**, 830 (1933).

Decomposition rates in the presence of added magnesium oxide and barium oxide were measured. Both oxides are insoluble in sodium hydroxide although any moisture present would form some soluble barium hydroxide in the case of the barium oxide addition. A small decrease in rate was found with magnesium oxide and a small increase with barium oxide. No reason can be advanced for these effects which, in any case, are too small to have any great significance.

The Over-all Decomposition Rate.—The rate of production of chloride ion from sodium perchlorate in fused sodium hydroxide was measured at various constant temperatures from 358 to 416° . In all cases plots of the logarithm of total chlorine concentration less the chloride concentrations, as a measure of the concentration of unreacted material, *versus* time showed initial curved portions of increasing slope followed by straight lines. The reaction thus appeared, after an initial induction period, to be first order. Specific rates, calculated from the linear portions of the plots, were independent of the initial perchlorate concentration as shown in Table I.

A plot of the logarithms of the rate constants *versus* reciprocal temperature for twenty individual experiments over a 60° range of temperature was linear within the expected precision. It is estimated that uncertainties in individual reaction rate constants may be as much as $\pm 15\%$, the largest uncertainty being due to the large temperature coefficient. A least squares treatment of the data gave

$$\log k \text{ (min.}^{-1}\text{)} = -11.44 (10^3)/T + 15.18 \quad (1)$$

for relating rate constants to temperature.

The Rate of Decomposition of Chlorate.—The concentration *versus* time curves for perchlorate decomposition in sodium hydroxide, as described in the previous section, suggested that the decomposition occurred in two steps, the specific rate of the second step being somewhat smaller than that of the first. As a likely intermediate was chlorate, measurements of the decomposition rate starting with sodium chlorate were made. In these runs both chlorate and chloride concentrations in the samples were determined. On subtracting the combined chlorate and chloride from total chlorine, it was found that at no time was there as much as 0.5% of the total in the form of perchlorate. Plots of the logarithm of chlorate concentration *versus* time were linear with no suggestion of the induction period observed when starting with perchlorate. First-order rate constants were evaluated from such plots at four different temperatures and found to be related to temperature by

$$\log k_{\text{ClO}_3^-} \text{ (min.}^{-1}\text{)} = -11.62(10^3)/T + 15.53 \quad (2)$$

Rate constants calculated from equation 2 at 630 to 690°K. are 17 to 23% higher than those calculated from equation 1. While this discrepancy is slightly higher than the supposed uncertainty of 15%, it was concluded that both equations relate to the same reaction, namely the decomposition of the chlorate ion.

The Rate of Decomposition of Perchlorate.—Reaction rates again were determined with sodium perchlorate as the starting material, but with analy-

TABLE I
 RATE CONSTANTS FOR SODIUM PERCHLORATE DECOMPOSITION

Temp., °C.	387	387	386	386	386	387	406	406
Initial mole ratio NaClO ₄ /NaOH	0.0103	0.0142	0.0167	0.0198	0.0209	0.0246	0.0150	0.0214
10 ³ k, min. ⁻¹	7.03	6.62	5.84	5.93	6.22	6.41	21.0	21.8

ses for both chloride and chlorate. Perchlorate concentrations were obtained by subtracting the sum of chlorate and chloride concentrations from total chlorine. Perchlorate concentration was found to decrease rapidly while chlorate concentration rose to a maximum and then decreased. Plots of the logarithm of perchlorate concentration *versus* time were linear and first-order rate constants were evaluated. Equation 3 was obtained from the constants at three different temperatures.

$$\log k_{\text{ClO}_4} (\text{min.}^{-1}) = -10.35(10^{-3})/T + 14.78 \quad (3)$$

Comparison of equations 3 and 2 shows that, in the temperature range of interest, the specific rate for perchlorate decomposition is 12 to 18 times that for chlorate decomposition. Kinetic quantities as calculated from equations 2 and 3 are given in Table II.

 TABLE II
 KINETIC QUANTITIES FOR THE DECOMPOSITION OF CHLORATE AND PERCHLORATE IN FUSED SODIUM HYDROXIDE

Decomposing ion	Activation energy, kcal. mole ⁻¹	Arrhenius frequency factor, sec. ⁻¹	Activation entropy, cal. mole ⁻¹ deg. ⁻¹
Chlorate	53.2 ± 2.7	5.53 × 10 ¹³	2.73
Perchlorate	47.3 ± 2.4	5.95 × 10 ¹²	-0.70

Relation of Rate of Dissociation to Hydroxyl Ion Concentration.—As the rate of dissociation of perchlorate ion in sodium hydroxide turned out to be so much larger than the rate predicted from measurements on pure liquid perchlorates, it was of interest to investigate the effect of a variation in hydroxyl ion concentration. For this purpose rate experiments were run in various mixtures of sodium nitrate and sodium hydroxide. The results of experiments done at 400 ± 1° are shown in Table III.

 TABLE III
 THE DECOMPOSITION OF SODIUM PERCHLORATE IN SODIUM NITRATE-HYDROXIDE MIXTURES

Mole % NaOH	16	24	48	66	78	100
10 ³ k (min. ⁻¹)	1.94	2.18	2.53	3.05	5.67	15.2

In pure sodium nitrate at 400° the decomposition of sodium perchlorate is too small to measure. As shown by gas evolution, sodium chlorate does decompose in pure sodium nitrate. Thus the hydroxyl has a large effect on the decomposition of perchlorate and a significant but lesser effect on the decomposition of chlorate. The constants of Table III were calculated as described in the section on the over-all decomposition and should be essentially those for chlorate decomposition. The constants of Table III do not show any simple dependence on the hydroxyl concentration. Retortillo and Moles⁶ found maxima in the temperature-composition diagram for the sodium hydroxide-sodium nitrate system corresponding to the compounds NaOH·NaNO₃ and (NaOH)₂·NaNO₃. They assumed these compounds to be evidence for the existence of

ortho nitrate ions in the melt. If such ions are formed, the sodium hydroxide mole fraction would not be a true measure of hydroxyl ion concentration in the mixture.

The Addition of Water, Chloride and Peroxide.—The rate of decomposition of perchlorate in sodium hydroxide was measured with the perchlorate added as hydrated sodium perchlorate and also with sodium hydroxide which had been subjected to less rigorous drying. As no significant change in rates was observed, it was concluded that the rate is not sensitive to small amounts of water.

As the rate of decomposition of potassium perchlorate in sodium hydroxide had been found to be unaffected by addition of potassium chloride, no further experiments were done involving chloride addition.

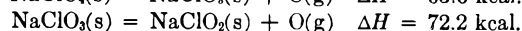
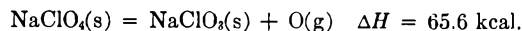
Rate experiments were done in the presence of added peroxide since qualitative tests showed that small amounts of peroxide always were formed when perchlorate or chlorate decomposed in sodium hydroxide, accumulating to a maximum concentration and then gradually disappearing. The results of these tests were inconclusive. At 360 and 384° the rate of decomposition of sodium perchlorate was not altered by the addition of sodium peroxide, which is readily soluble in sodium hydroxide. At 402°, however, peroxide additions caused a significant increase in the rate. Barium peroxide, in contrast, reduced the decomposition rate.

Decomposition rates for potassium perchlorate in sodium hydroxide were measured while the effect of peroxide was being considered, since more peroxide is formed by reaction of potassium hydroxide with oxygen than is formed in the sodium system.⁴ Here, too, there was a significant increase at 402°, 60% greater rate than for sodium perchlorate, but at 380 and 386° no difference between sodium and potassium perchlorates.

The Rate of Decomposition of Lithium Perchlorate in Lithium Hydroxide-Lithium Nitrate Solution.—Experiments with a system having only lithium cations were done to avoid the presence of peroxide which is reported not to be formed from oxygen and lithium hydroxide. As the melting point of lithium hydroxide is higher than the temperature at which the work on the sodium cation system had been done, its melting point was lowered by adding lithium nitrate. These experiments yielded concentration time curves quite like those obtained with the sodium cation system. The decomposition rate constants at 400° are greater, however, in the lithium system than in the sodium system, 5.3 × 10⁻³ compared with 3.3 × 10⁻³ min.⁻¹ for a solvent 38 mole% hydroxide, and 35 × 10⁻³ compared with 5.6 × 10⁻³ min.⁻¹ in a solvent 73 mole % hydroxide. These observations suggest that a change in cation may be more important than the presence or absence of peroxide.

Mechanism of Perchlorate and Chlorate De-

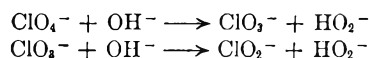
composition.—Harvey, Edmison, Jones, Seybert and Catto³ found the activation energy for the decomposition of pure potassium perchlorate to be 70 kcal., which coincides with the energy needed to break a chlorine-oxygen bond with formation of potassium chlorate and a gaseous oxygen atom. For the sodium salts at 298°K., the corresponding energies are⁷



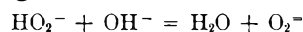
The experimental activation energies for perchlorate and chlorate decomposition in sodium hydroxide are 47.3 and 53.2 kcal., less by 18.3 and 19.0 kcal, respectively. This suggests that the influence of the fused salt medium is essentially the same for perchlorate

(7) W. M. Latimer, "Oxidation Potentials," Prentice-Hall Book Co., New York, N. Y., 1952.

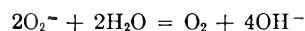
and for chlorate decomposition. That the hydroxyl ion is the important factor is indicated by the reduction in rate attendant on diluting the hydroxyl with nitrate. A mechanism which would be consistent with the observations is



followed by a rapid conversion of ClO_2^- to Cl^- . It not likely that any significant concentration of HO_2^- could accumulate as equilibrium should lie toward the right in



and the presumably rapid reaction



would cause the eventual disappearance of peroxide.

THERMODYNAMIC CONSIDERATIONS IN THE ALUMINUM-PRODUCING ELECTROLYTE

BY W. B. FRANK

Aluminum Company of America, Alcoa Research Laboratories, Physical Chemistry Division, New Kensington, Pennsylvania

Received June 19, 1961

The thermodynamic values for Na_3AlF_6 , NaF and AlF_3 appearing in the literature are corrected for an apparent error in temperature measurement. The free energy change for the postulated dissociation mechanism $\text{Na}_3\text{AlF}_6 \rightleftharpoons 3\text{NaF} + \text{AlF}_3$ is calculated at 1300°K. Dissociation according to this scheme is absent or very slight. Thermochemical properties are developed for undissociated liquid cryolite and molten sodium tetrafluoroaluminate. The use of these functions substantiates the dissociation mechanism of molten cryolite as $\text{Na}_3\text{AlF}_6 \rightleftharpoons 2\text{NaF} + \text{NaAlF}_4$. The possibility of the formation of sodium aluminate by dissolution of aluminum oxide in fused cryolite is considered. To a nominal alumina content of about 4 weight % this reaction is thermodynamically possible at 1300°K.: $2\text{Na}_3\text{AlF}_6 + 2\text{Al}_2\text{O}_3 = 3\text{NaAlO}_2 + 3\text{NaAlF}_4$.

Introduction

In the industrial production of aluminum, an electrolyte consisting primarily of aluminum oxide dissolved in molten cryolite is used. Despite the intensive experimental and theoretical interest in this system, there is disagreement in the literature concerning the ionic constitution of the solvent and the interaction of the solvent with the solute. It has been established that cryolite dissociates appreciably at high temperatures. However, the nature and degree of dissociation remain controversial. While most investigators accept chemical interaction between alumina and molten cryolite, in contrast to physical solution, numerous aluminates and oxyfluoroaluminates have been proposed as reaction products. Fairly complete and reliable thermochemical data are now available for the pertinent constituents of the electrolyte to undertake a thermodynamic study of the dissociation mechanism and a treatment of one of the proposed schemes of solution.

The high temperature heat content measurements on cryolite by O'Brien and Kelley¹ do not agree with the measurements of Albright.² The discrepancy in the two data sets results in a significant difference in derived thermochemical functions at high temperatures. For example, the use of the data of O'Brien and Kelley results in a value

for $(F_{1300} - H_{298})$ of -130.04 kcal., while that of Albright gives a value of -132.76 kcal. Comparison of the heat content curve of O'Brien and Kelley with that of Albright shows good agreement for the heats of transition and fusion (2.16 vs. 2.38 kcal. and 27.64 vs. 27.91 kcal., respectively). However, the transition temperatures and melting points of the two studies differ appreciably (Fig. 1). The investigation of O'Brien and Kelley included heat content measurements for sodium fluoride and aluminum trifluoride. The melting point reported for sodium fluoride was also considerably higher than that observed by other investigators. Listed in Table I are the transformation temperatures reported by O'Brien and Kelley with other recent determinations of these temperatures in the literature. The mean values and standard deviations for the transition temperature of cryolite and melting points of cryolite and sodium fluoride from the six other investigations are $558 \pm 6^\circ$, $1008 \pm 3^\circ$, and $995 \pm 2^\circ$. It is seen that each temperature reported by O'Brien and Kelley is consistently higher than the mean values of other investigations and well beyond the standard deviation in all cases. The temperature measurements of O'Brien and Kelley appear to be about 20° high at 1000° with a smaller error at lower temperatures.

Because of the importance of accurate thermodynamic data for Na_3AlF_6 , NaF and AlF_3 to the understanding of the aluminum-producing electrolyte, and because the measurements for NaF

(1) C. J. O'Brien and K. K. Kelley, *J. Am. Chem. Soc.*, **79**, 5616 (1957).

(2) D. M. Albright, Thesis, Carnegie Institute of Technology, 1956.

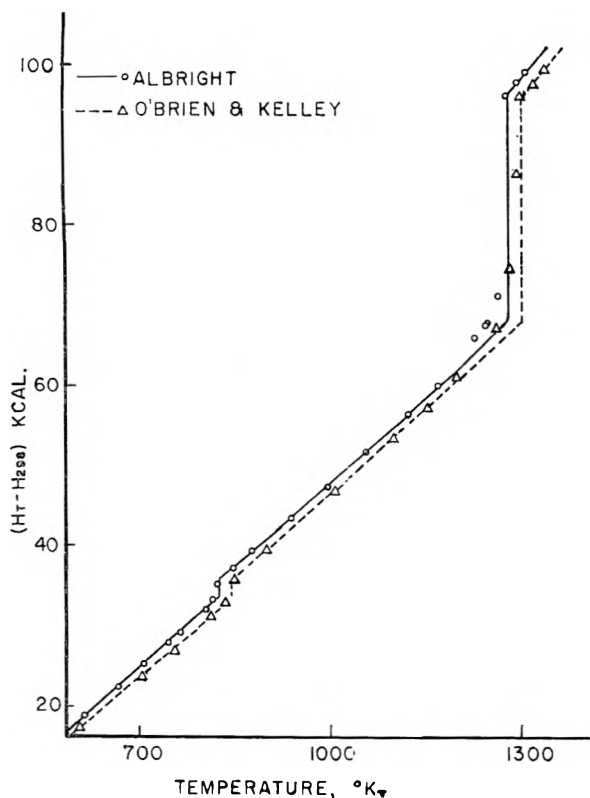


Fig. 1.—Comparison of heat content measurement for cryolite by two investigations.

TABLE I

	Transition temp., Na ₃ AlF ₆ , α → β	—M.p., °C.—	
		Na ₃ AlF ₆	NaF
O'Brien and Kelley ¹	572°	1027°	1012°
Albright ²	550	1006	..
Landon and Ubbelohde ³	565	1013	997
Grijotheim, <i>et al.</i> ^{4,5}	560	1008	994
Phillips, <i>et al.</i> ⁶	..	1009	994
Rolin ⁷	..	1009	997
Foster ⁸	..	1004	992

and AlF₃ are the only reliable high temperature data available for these compounds, a correction for the apparent error in temperature measurement has been carried out.

Method of Temperature Correction.—To obtain better agreement with the transition temperatures of cryolite and sodium fluoride of the other investigations and to facilitate comparison of the corrected values with the measurements of Albright, the error in temperature at the melting point of cryolite is set at 21°. Because of the quantity measured, ($H_T - H_{298}$), there is no error at 25°. The deviation in temperature measurement is

(3) G. J. Landon and A. R. Ubbelohde, *Proc. Roy. Soc. (London)*, **240A**, 160 (1957).

(4) K. Grijotheim, "Contribution to the Theory of Aluminum Electrolysis," *Kgl. Norske Videnskab. Selskabs Skrifter*, No. 5, (1956).

(5) J. Brynestad, K. Grijotheim and S. Urnes, *Metallurgia ital.*, **52**, No. 8, 495 (1960).

(6) N. W. F. Phillips, R. H. Singleton and E. A. Hollingshead, *J. Electrochem. Soc.*, **102**, 690 (1955).

(7) M. Rolin, *Bull. soc. chim. France*, 671 (1960).

(8) P. A. Foster, Jr., Melting Points Employed at Alcoa Research Laboratories.

assumed to be linear over the reported temperature range from 298 to 1450°K. Each temperature reported by O'Brien and Kelley is corrected by use of the equation

$$T = 298.1 + \frac{980.9}{1001.9} (T_0 - 298.1) \quad (1)$$

where

T = corrected temp. in °K.

T_0 = reported temp. in °K.

The melting points for cryolite and sodium fluoride resulting from this equation are 1006 and 991°. The transition temperature for cryolite becomes 560°. These temperatures are in good agreement with the average values of the other determinations, 1008, 995 and 558°.

Corrected Thermodynamic Functions.—The temperature associated with each heat content determination of O'Brien and Kelley was corrected by equation 1. Expressions relating the observed heat content with the corrected temperature were developed by regression analysis with an I.B.M. 650 computer. Expressions for C_p , ($S_T - S_{298}$) and ($F_T - H_{298}$) were calculated from the corrected equations for heat content and values for S_{298}^0 . Listed below are the resulting expressions for the thermochemical properties of sodium fluoride, aluminum trifluoride and cryolite. The units for ($H_T - H_{298}$) and ($F_T - H_{298}$) are cal. mole⁻¹. The units for C_p and ($S_T - S_{298}$) are cal. deg.⁻¹ mole⁻¹.

Sodium Fluoride.—

NaF(s) (298.1–1264.3°K.)

$$H_T - H_{298} = 8.412T + 3.115 \times 10^{-3}T^2 - 1.965 \times 10^5 T^{-1} - 2144$$

$$C_p = 8.412 + 6.23 \times 10^{-3}T + 1.963 \times 10^5 T^{-2}$$

$$S_T - S_{298} = 19.373 \log T - 9.815 \times 10^4 T^{-2} + 6.23 \times 10^{-2}T - 48.69$$

$$F_T - H_{298} = 44.842T - 3.115 \times 10^{-3}T^2 - 9.815 \times 10^4 T^{-1} - 19.373T \log T - 2144$$

Fusion—1264.3°K.

$$\Delta H_m = 7.92 \text{ kcal.}$$

$$\Delta S_m = 6.26 \text{ cal. deg.}^{-1} \text{ mole}^{-1}$$

NaF(l) (1264.3–1400°K.)

$$H_T - H_{298} = 16.866T - 89$$

$$C_p = 16.866$$

$$S_T - S_{298} = 38.842 \log T - 95.00$$

$$F_T - H_{298} = 99.601T - 38.842T \log T - 89$$

Aluminum Trifluoride.—

AlF₃(s,α) (298.1–718°K.)

$$H_T - H_{298} = 17.152T + 5.945 \times 10^{-3}T^2 + 1.553 \times 10^5 T^{-1} - 6299$$

$$C_p = 17.152 + 1.189 \times 10^{-2}T - 1.953 \times 10^5 T^{-2}$$

$$S_T - S_{298} = 39.501 \log T + 1.189 \times 10^{-2}T + 9.765 \times 10^4 T^{-2} - 102.386$$

$$F_T - H_{298} = 103.648T - 5.945 \times 10^{-3}T^2 + 9.765 \times 10^4 T^{-1} - 39.501T \log T - 6299$$

Phase Transition, α→β—718°K.

$$\Delta H_{tr} = 0.16 \text{ kcal.}$$

$$\Delta S_{tr} = 0.23 \text{ cal. deg.}^{-1} \text{ mole}^{-1}$$

(9) E. G. King, *J. Am. Chem. Soc.*, **79**, 2056 (1957).

AlF₃(s,β) (718–1400°K.)

$$\begin{aligned}
 H_T - H_{298} &= 21.222T + 1.63 \times 10^{-3}T^2 - 6562 \\
 C_p &= 21.222 + 3.26 \times 10^{-3}T \\
 S_T - S_{298} &= 48.874 \log T + 3.26 \times 10^{-3}T - 122.541 \\
 F_T - F_{298} &= 127.883T - 1.63 \times 10^{-3}T^2 - 48.874T \log T - 6562
 \end{aligned}$$

Sodium Hexafluoroaluminate, Cryolite.—**Na₃AlF₆(s,α)** (298.1–833.5°K.)

$$\begin{aligned}
 H_T - H_{298} &= 45.51T + 1.603 \times 10^{-2}T^2 + 1.755 \times 10^5T^{-1} - 15580 \\
 C_p &= 45.51 + 3.206 \times 10^{-2}T - 1.755 \times 10^5T^{-2} \\
 S_T - S_{298} &= 104.81 \log T + 3.206 \times 10^{-2}T + 8.775 \times 10^4T^{-2} - 269.891 \\
 F_T - H_{298} &= 258.491T - 1.603 \times 10^{-2}T^2 + 8.775 \times 10^4T^{-1} - 104.81T \log T - 15580
 \end{aligned}$$

Phase Transition, α→β—833.5°K.

$$\begin{aligned}
 \Delta H_{tr} &= 2.22 \text{ kcal.} \\
 \Delta S_{tr} &= 2.66 \text{ cal. deg.}^{-1} \text{ mole}^{-1}
 \end{aligned}$$

Na₃AlF₆(s,β) (833.5–1279°K.)

$$\begin{aligned}
 H_T - H_{298} &= 36.40T + 0.01714T^2 - 6331 \\
 C_p &= 36.4 + 0.03428T \\
 S_T - S_{298} &= 83.829 \log T + 0.03428T - 207.673 \\
 F_T - H_{298} &= 187.073T - 0.01714T^2 - 83.829T \log T - 6331
 \end{aligned}$$

Phase Transformation—1279°K. This transition does not represent true melting of solid to pure liquid cryolite, but, as will be shown, a transformation from β-cryolite to a liquid solution of cryolite and its dissociation products.

$$\begin{aligned}
 \Delta H_{\beta \rightarrow \text{soln.}} &= 26.71 \text{ kcal.} \\
 \Delta S_{\beta \rightarrow \text{soln.}} &= 20.88 \text{ cal. deg.}^{-1} \text{ mole}^{-1}
 \end{aligned}$$

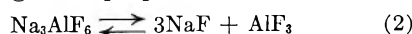
Solution Resulting from Liquefaction of One Mole of Solid Cryolite (1279–1350°K.).—The following expressions do not represent liquid cryolite at unit activity, but rather a solution of varying concentrations of cryolite and its dissociation products.

$$\begin{aligned}
 H_T - H_{298} &= 96.814T - 28855 \\
 C_p &= 96.814 \\
 S_T - S_{298} &= 222.963 \log T - 575.217 \\
 F_T - H_{298} &= 615.031T - 222.693T \log T - 28855
 \end{aligned}$$

Substituting $T = 1300$ into the last expression gives a value of -131.90 kcal., which is in fair agreement with the value of this function at 1300°K. from Albright's data, -132.76 kcal.

Results and Discussion

A. Dissociation Mechanism of Cryolite. Dissociation to Sodium Fluoride and Aluminum Trifluoride.—Pearson and Waddington¹⁰ presented evidence for partial dissociation of cryolite in the molten state to sodium fluoride and aluminum trifluoride (or their ions). The variation of density of sodium fluoride–aluminum fluoride fusions indicated dissociation of 20% at 1000° and 30% at 1100° according to the proposed reaction



Pearson and Waddington state that thermodynamic considerations led to the conclusion that "cryolite is about 15% dissociated at 1000° , the dissociation increasing with temperature." It was suggested that the order of dissociation de-

rived from the density study thus was confirmed. However, because of errors in the thermodynamic treatment and revised thermochemical data, this conclusion is not justified.

Pearson, in a more recent examination¹¹ of the dissociation mechanism, developed values for the dissociation constant for reaction 2 of 1.7×10^{-5} and 4.6×10^{-5} at 1000 and 1100° from the thermodynamic data available at that time. These revised values for the dissociation constants were not high enough to explain the position and shape of the density maxima of the fused sodium fluoride–aluminum fluoride system. Pearson suggested that this discrepancy between the appreciable degree of dissociation derived from density data and the limited degree of dissociation calculated from thermodynamic considerations "could well be accounted for by complex formation, which, in effect, would enhance the dissociation of cryolite." Nevertheless the dissociation mechanism proposed in the original work of Pearson and Waddington is cited in current publications and recent textbooks as a representation of the dissociation occurring in NaF–AlF₃ fusions.

The values of the free energy change for reaction 2 at 1006 and 1100° were recalculated using the functions developed earlier in this study. The free energies of formation of sodium fluoride, aluminum trifluoride and cryolite were calculated at 1006 and 1100° from the relation

$$\Delta F_{f,T}^0 = (F_T - H_{298})_{\text{compound}} - \Sigma(F_T - H_{298})_{\text{elements}} + \Delta H_{f,298}^0 \quad (3)$$

The values of $(F_T - H_{298})$ for the compounds are from the expressions developed for NaF(l), AlF₃(β), and the solution of the stoichiometric composition, 3NaF·AlF₃. The values of $(F_T - H_{298})$ for the elements are calculated from JANAF Thermochemical Tables.¹² The values used for the heats of formation of sodium fluoride and aluminum fluoride were -136.30^{12} and -356.3 kcal.¹² The value used for the heat of formation of cryolite was -784.88 kcal. [average of values -784.8^{13} and -784.95 kcal.¹⁴].

From the free energies of formation of the products and reactant, the free energy changes at 1006 and 1100° for reaction 2 are 27 and 28 kcal. These values correspond to equilibrium constants of 3×10^{-5} and 4×10^{-5} (from $\Delta F^0 = -RT \ln K$). The equilibrium constant for the reaction can be expressed in terms of the degree of dissociation, α , as

$$K = \frac{27\alpha^4}{(1 + 3\alpha)^2(1 - \alpha)} \quad (4)$$

Substitution of the value of the equilibrium constant into equation 4 and solving for the degree of dissociation

$$\begin{aligned}
 \alpha_{1006^\circ} &= 0.033 \\
 \alpha_{1100^\circ} &= 0.036
 \end{aligned}$$

(11) T. G. Pearson, "The Chemical Background of the Aluminum Industry," Royal Institute of Chemistry, No. 3 (1955).

(12) JANAF Interim Thermochemical Tables, Thermal Laboratory, Dow Chemical Company, Midland, Michigan, Dec. 31, 1960.

(13) J. P. Coughlin, *J. Am. Chem. Soc.*, **80**, 1802 (1958).

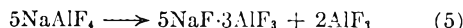
(14) P. Gross, C. Hayman and D. L. Levi, "Physical Chemistry of Process Metallurgy," Part 2, Interscience Publishers, New York, N. Y., 1961, p. 903.

(10) T. G. Pearson and J. Waddington, *Discussions Faraday Soc.*, **1**, 307 (1947).

A cryoscopic study⁵ of the sodium fluoride-aluminum fluoride system examined reaction 2 as a possible dissociation scheme for molten cryolite. In this study, the fluorides of sodium and aluminum were considered to be completely ionized. The expression relating the degree of dissociation and the equilibrium constant is therefore somewhat different from equation 4. The best agreement with the experimentally determined phase diagram was obtained with constant values of $K = 3.0 \times 10^{-5}$ and $\alpha = 0.07$ in the temperature range 940–1008°.

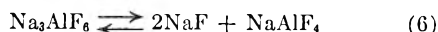
The degree of dissociation to sodium fluoride and aluminum trifluoride necessary to explain lowering of liquidus temperatures ($\alpha = 0.07$) and density data ($\alpha = 0.2-0.3$) in the NaF- AlF_3 system is not consistent with thermodynamic considerations. Thermodynamic calculations show that dissociation according to this scheme would be less than 4%. The cryoscopic studies of the NaF- AlF_3 system by Brynestad, *et al.*,⁵ and Rolin⁷ eliminated reaction 2 as a dissociation mechanism for cryolite on the basis of other considerations. The extensive dissociation indicated by physico-chemical observations must be predominantly by a reaction with products other than sodium fluoride and aluminum fluoride.

Evidence for the Existence of NaAlF_4 in NaF- AlF_3 Fusions.—A maximum occurs in the equilibrium diagram of the NaF- AlF_3 system at a composition corresponding to the compound Na- AlF_4 .⁴ This compound was first identified by Howard¹⁵ by chemical and X-ray powder diffraction methods in quenched vapors over fusions near the composition NaF· AlF_3 . The compound also was found in rapidly cooled fusions having 1:1 mole ratio of NaF/ AlF_3 . However, at temperatures below 500°, the compound undergoes a solid state transformation



Because of this disproportionation reaction, the preservation of the compound at low temperatures is difficult.

A significant activity of NaAlF_4 in melts near the cryolite composition is suggested by vapor composition^{16,17} and vapor pressure^{17,18} studies. Landon¹⁹ concluded that the ion AlF_4^- is abundantly present in fused cryolite from considerations of electronic structure and electrical conductivity. Cryoscopic treatments of the NaF- AlF_3 system^{4,5,7} and the Na_2SO_4 - Na_2AlF_6 system²⁰ considered several possible mechanisms and selected the following as the most probable dissociation scheme for molten cryolite



The above reaction also was chosen from the three dissociation mechanisms tested, as the best repre-

(15) E. H. Howard, *J. Am. Chem. Soc.*, **76**, 2041 (1954).

(16) H. Ginsberg and A. Bohm, *Z. Elektrochem.*, **61**, 2, 315 (1957).

(17) A. Vajna and R. Bacchiega, *Met. ital.*, **52**, 481 (1960).

(18) M. M. Vetyukov, M. L. Bluiustein and V. P. Poddymov, *Zar. Tsvet. Met.*, **2**, 126 (1959).

(19) G. J. Landon, "The Melting Mechanism of Cryolite, Na_3AlF_6 ," *Cong. Intern. Chim. Pure et Appl.* 16, Paris (1957).

(20) K. Grjotheim, T. Halvorsen and S. Urnes, *Can. J. Chem.*, **37**, 1170 (1959).

sentation for the variation in density in the fused NaF- AlF_3 system.²¹ In this investigation, the degree of dissociation was determined as a function of temperature and the heat of reaction 6 was calculated in the temperature range 1000–1090°.

B. Thermochemical Properties of Undissociated Cryolite.—Because of the partial dissociation of cryolite at high temperatures, the experimentally determined heat content data above 1006° does not represent liquid cryolite at unit activity. The observed heat content is really that of a solution of cryolite and its dissociation products. However, from the knowledge of the dissociation mechanism and the degree of dissociation as a function of temperature, the thermodynamic functions for the hypothetical undissociated cryolite can be derived. The following data are available on the constitution²¹ and heat content of one mole of solid cryolite and the solution resulting from its fusion. The values for heat content are from the expressions developed earlier.

Temp., °K.	Phase	Degree of dissociation	Composition (moles)			$H_T - H_{298}$, kcal.
			Na_3AlF_6	NaF	NaAlF_4	
1279	s, β	...	1.000	58.26
1279	l, soln.	0.353	0.647	0.706	0.353	94.97
1329	l, soln.	.399	.601	.798	.399	99.81
1379	l, soln.	.445	.555	.890	.445	104.65

The heat content of the solution is related to the heat content of undissociated cryolite and the heat of dissociation as

$$(H_T - H_{298})_{\text{soln.}} = (H_T - H_{298})_{\text{u.l.}} + \alpha \Delta H_r \quad (7)$$

where

$$(H_T - H_{298})_{\text{soln.}} = \text{heat content of the soln. of cryolite and its dissociation products}$$

$$(H_T - H_{298})_{\text{u.l.}} = \text{heat content of hypothetical undissociated liquid cryolite}$$

$$\alpha = \text{degree of dissociation}$$

$$\Delta H_r = 22.5 \text{ kcal.},^{21} \text{ heat of reaction 6}$$

Substituting the proper values and solving equation 7 for the heat content of undissociated liquid cryolite at three different temperatures

$$(H_{1279} - H_{298})_{\text{u.l.}} = 87.03 \text{ kcal.}$$

$$(H_{1329} - H_{298})_{\text{u.l.}} = 90.83 \text{ kcal.}$$

$$(H_{1379} - H_{298})_{\text{u.l.}} = 94.64 \text{ kcal.}$$

From the above values an expression for the heat content of undissociated liquid cryolite is developed (units: cal. mole⁻¹)

$$(H_T - H_{298})_{\text{u.l.}} = 76.12T - 10330 \quad (8)$$

Differentiating equation 8 with respect to temperature, the heat capacity of liquid cryolite at unit activity is

$$C_p = 76.12 \text{ cal. deg.}^{-1} \text{ mole}^{-1} \quad (9)$$

From the heat content of solid β -cryolite at the "melting point" and the heat content of undissociated liquid cryolite at the same temperature, the true heat of melting can be obtained.

$$\Delta H_m = (H_{1279} - H_{298})_{\text{u.l.}} - (H_{1279} - H_{298})_{\text{s},\beta} = 18.76 \text{ kcal.} \quad (10)$$

The entropy of undissociated liquid cryolite can be obtained from the equation

(21) W. B. Frank and L. M. Foster, *J. Phys. Chem.*, **64**, 95 (1960).

$$(S_T - S_{298})_{u.1.} = (S_{1279} - S_{298})_{\alpha,\beta} + \Delta S_m + (S_T - S_{1279})_{u.1.} \quad (11)$$

where

$$(S_{1279} - S_{298})_{\alpha,\beta} = 96.62 \quad (12)$$

$$\Delta S_m = 14.67 \quad (13)$$

$$(S_T - S_{1279})_{u.1.} = \int_{1279}^T 76.12 dT/T = 175.304 \log T - 544.647 \quad (14)$$

Substituting the values of equations 12, 13 and 14 into equation 11

$$(S_T - S_{298})_{u.1.} = 175.304 \log T - 433.358 \quad (15)$$

From equations 8 and 15 and the value for $S_{298}^0 = 57.0 \text{ cal. deg.}^{-1} \text{ mole}^{-1}$,⁹ the following expression for the function, $F_T - H_{298}$, for undissociated liquid cryolite is derived.

$$(F_T - H_{298})_{u.1.} = 452.478T - 175.304T \log T - 10330 \quad (16)$$

These functions represent the hypothetical supercooled liquid cryolite at unit activity. If it were not for the partial dissociation of solid cryolite at high temperatures (the substantial heat effect due to dissociation of β -cryolite²² above 880° is obvious in the heat content measurements) fusion would occur at a considerably higher temperature. This hypothetical melting point of undissociated cryolite can be calculated from the Schroder-van Laar equation

$$-\ln a_1 = \frac{\Delta H_m}{R} \left(\frac{1}{T} - \frac{1}{T_0} \right) \quad (17)$$

where

a_1 = 0.379, activity of undissociated cryolite in the melt at the liquidus temp.

ΔH_m = 18764 cal., true heat of fusion

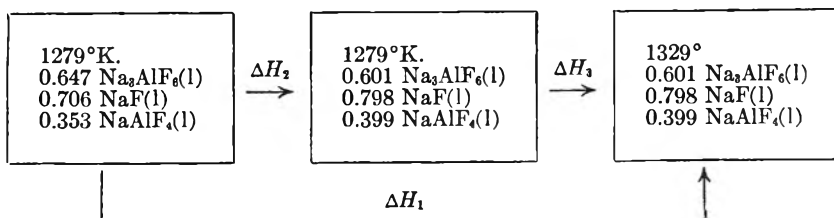
T = 1279°K., liquidus temp.

T_0 = hypothetical melting point

Solving equation 17 for the melting point of undissociated cryolite

$$T_0 = 1472^\circ\text{K.} \quad (18)$$

C. Thermochemical Properties of Sodium Tetrafluoroaluminate.—Some of the thermodynamic functions for molten sodium tetrafluoroaluminate now can be developed. Knowing the heat content of the solution resulting from liquefaction of one mole of solid cryolite, its composition as a function of temperature, and the heat capacities of two of its components (undissociated liquid cryolite and molten sodium fluoride), the heat capacity of the third component (NaAlF_4) can be calculated. The total heat absorbed in changing the composition of the solution and raising the temperature from 1279 to 1329°K. can be represented as the sum of two steps



(22) Measurements of heat content from 880–1006° were not used in developing the expression for the heat content of β -cryolite.

$$\Delta H_1 = \Delta H_2 + \Delta H_3 \quad (19)$$

$$\Delta H_1 = (H_{1329} - H_{298})_{\text{soln.}} - (H_{1279} - H_{298})_{\text{soln.}} \quad (20)$$

$$\Delta H_2 = \Delta n_{\text{Na}_2\text{AlF}_6} \Delta H_D \quad (21)$$

where

$$\Delta n_{\text{Na}_2\text{AlF}_6} = 0.046, \text{ mole } \text{Na}_2\text{AlF}_6 \text{ dissociating}$$

$$\Delta H_D = 22.5 \text{ kcal.},^{21} \text{ heat of dissociation}$$

$$\Delta H_3 = [n_{\text{Na}_2\text{AlF}_6} C_p(\text{Na}_2\text{AlF}_6) + n_{\text{NaF}} C_p(\text{NaF}) + n_{\text{NaAlF}_4} C_p(\text{NaAlF}_4)] \Delta T \quad (22)$$

where

$n_{\text{Na}_2\text{AlF}_6}$, n_{NaF} and n_{NaAlF_4} = number of moles of each component

$C_p(\text{Na}_2\text{AlF}_6)$, $C_p(\text{NaF})$ and $C_p(\text{NaAlF}_4)$ = heat capacity of each component

$\Delta T = 50^\circ$, temperature increment

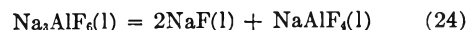
By solving equation 22 for the heat capacity of sodium tetrafluoroaluminate and substitution of the appropriate values

$$C_p(\text{NaAlF}_4) = 42.4 \text{ cal. deg.}^{-1} \text{ mole}^{-1} \quad (23)$$

Similar calculations for the temperature interval from 1329 to 1379°K. give the same value for the heat capacity of molten sodium tetrafluoroaluminate.

This derived value for heat capacity is in good agreement with the values estimated for NaAlF_4 by two methods suggested by Kubaschewski and Evans.²³ The first method for estimation of heat capacities of inorganic liquids at high temperatures assigns 7.25 cal. deg.⁻¹ g.-atom⁻¹, giving a value of 43.5 cal. deg.⁻¹ mole⁻¹. The second method assumes that the heat capacity of a compound is the sum of the heat capacities of the components at the same temperature. The sum of the heat capacities of sodium fluoride(I) and aluminum trifluoride(β) at 1329°K. is 42.4 cal. deg.⁻¹ mole⁻¹.

Since the heat of formation²⁴ from the elements at room temperature and low temperature heat content data²⁴ are not available for NaAlF_4 , its thermodynamic properties cannot be expressed in the conventional form. However, the free energy of formation from the elements can be developed. The equilibrium constant for the dissociation reaction is known as a function of temperature.²¹



The free energy change for the reaction can be expressed in terms of the free energies of formation of the reactants and products as

$$\Delta F^0_r = -RT \ln K_D = 2\Delta F^0_{\text{NaF}} + \Delta F^0_{\text{NaAlF}_4} - \Delta F^0_{\text{Na}_2\text{AlF}_6} \quad (25)$$

where

ΔF^0_r = free energy change for reaction 24

K_D = equilibrium constant for reaction 24

ΔF^0_{NaF} , $\Delta F^0_{\text{NaAlF}_4}$ and $\Delta F^0_{\text{Na}_2\text{AlF}_6}$ = standard free energies of formation of sodium fluoride, sodium tetrafluoroaluminate and undissociated cryolite

(23) O. Kubaschewski and E. Evans, "Metallurgical Thermochemistry," Pergamon Press, New York, N. Y., 3rd Edition, 1958, pp. 184–186.

(24) These quantities would be difficult, if not impossible, to measure experimentally because of the instability of the compound at low temperature.

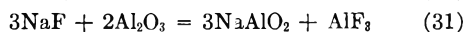
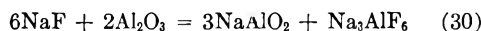
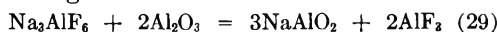
The values of the free energies of formation of sodium fluoride and undissociated cryolite are obtained from equation 3. The value of $(F_T - H_{298})$ for undissociated cryolite is calculated from equation 16. The values of $(F_T - H_{298})$ for the elements are calculated from JANAF Thermochemical Tables.¹² By substitution of the numerical values of ΔF^0_r , $\Delta F^0_{\text{Na}_2\text{AlF}_6}$ and ΔF^0_{NaF} into equation 25, the following values were calculated for the free energy of formation of sodium tetrafluoroaluminate at three temperatures

$$\Delta F^0_{1273} = -401.18 \text{ kcal.} \quad (26)$$

$$\Delta F^0_{1223} = -397.21 \text{ kcal.} \quad (27)$$

$$\Delta F^0_{1373} = -393.31 \text{ kcal.} \quad (28)$$

D. The Formation of Sodium Aluminate in Cryolite-Alumina Fusions.—A recent Russian publication²⁵ states that "the formation of sodium aluminate during the solution of aluminum oxide in molten cryolite is thermodynamically inconceivable. With the addition of surplus sodium fluoride, the possibility of the formation of NaAlO_2 increases but still remains only slightly probable thermodynamically." These conclusions were based on large positive values derived for the free energy changes at 1300°K. for the reactions



The values obtained by Ivanova for the free energy changes at 1300°K. were 126,527, 30,167 and 78,347 cal. for reactions 29, 30 and 31.

New pertinent thermochemical data are available since the investigation of Ivanova. The values for the heats of formation of some of the compounds involved have been drastically revised. The values used in the original study are compared with the presently accepted values in Table II.

TABLE II
HEAT OF FORMATION AT 25°, $\Delta H^0_{f, 298}$ (KCAL.)

Compound	Value used by Ivanova	Presently accepted value
Na_2AlF_6	-759.60	-784.8 ¹³ -798.95 ¹⁴
Al_2O_3	-399.09	-400.4 ¹²
NaAlO_2	-270.84	-270.84 ²⁶
AlF_3	-311.00	-356.3 ¹²
NaF	-136.30	-136.3 ¹²

No measurements of the heat capacity of sodium aluminate above room temperature were available at the time of the investigation of Ivanova. The values for the high temperature heat capacity were estimated and thermodynamic functions were calculated based on these estimates. Christensen, *et al.*,²⁷ have since reported the heat capacity of sodium aluminate to a temperature of 1700°K.

The free energies of formation for products and reactants of reactions 29, 30 and 31 were calculated at 1300°K. using the best thermochemical values presently available. The resulting free energies of formation and the sources of the thermodynamic values used in their calculations are

(25) L. Ivanova, *Izvest. Vysshikh Ucheb. Zavedenii Tsvet. Met.*, **2**, 67 (1959).

(26) J. P. Coughlin, *J. Am. Chem. Soc.*, **80**, 1802 (1958).

(27) A. V. Christensen, K. C. Conway and K. K. Kelley, Bureau of Mines Report of Investigations 5585 (1960).

Na_2AlF_6	$\Delta F^0_{f, 1300}$ -610.16	$(F_{1300} - H_{298})_{\text{compound}}$ from expression for soln. of stoichiometric composition $3\text{NaF} \cdot \text{AlF}_3$; $(F_{1300} - H_{298})$ for the elements ¹² ; $\Delta H^0_{f, 298}$ ^{13,14}
Al_2O_3	-301.67	$\Delta F^0_{f, 1300}$ ¹²
NaAlO_2	-199.64	$\Delta H^0_{f, 298}$ ²⁶ ; S^0_{298} ²⁶ ; $(H_{1300} - H_{298})$ and $(S_{1300} - S_{298})$ ²⁷
AlF_3	-275.80	$(F_{1300} - H_{298})_{\text{compound}}$ from expression for $\text{AlF}_3(\beta)$; $(F_{1300} - H_{298})$ for the elements ¹² ; $\Delta H^0_{f, 298}$ ¹²
NaF	-102.41	$(F_{1300} - H_{198})_{\text{compound}}$ from expression for $\text{NaF}(1)$; $(F_{1300} - H_{298})$ for the elements ¹² ; $\Delta H^0_{f, 298}$ ¹²

The resulting free energy changes at 1300°K. for reactions 29, 30 and 31 are 63, 9 and 36 kcal., respectively. The equilibrium constants for reactions 29, 30 and 31 are 3×10^{-11} , 3×10^{-2} and 9×10^{-7} (from $\Delta F^0_r = -RT \ln K$). The free energy change for each of the reactions is significantly lower than the value obtained in the original study. Thus the probability of sodium aluminate formation by these reactions is considerably greater than Ivanova concluded.

In the study of Ivanova, the criteria of Dodge²⁹ for whether or not a reaction takes place were adopted: (1) If $\Delta F < 0$, the reaction is possible; (2) If ΔF has a value of 0-10 kcal., the reaction is improbable but may occur; (3) If $\Delta F > 10$ kcal., the reaction is highly improbable and occurs only under "unusual" circumstances.

Dodge, in presenting these criteria for the feasibility of a given reaction for an industrial process, emphasized that they are only guides useful in exploratory work. He points out that commercial processes often are based on reactions having positive values for the free energy change. There is no definite value for the free energy change which can be specified as indicating that a reaction will or will not take place. The statement that a reaction "is thermodynamically inconceivable" has no meaning without qualification. Starting with reactants uncontaminated by products, any reaction will have a tendency to proceed to some extent even though the degree may be infinitesimal. The value for the free energy change and the resultant equilibrium constant ($\Delta F^0 = -RT \ln K$) merely specify a limiting relationship for activities of the products and reactants. While a large positive value for ΔF , (*i.e.*, a small value for the equilibrium constant) generally suggests that at equilibrium the activities of the products are small compared to the activities of the reactants, the expression for the equilibrium constant must be examined carefully before drawing conclusions as to the possible extent of the reaction.

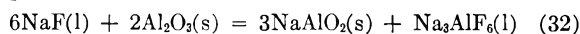
Reaction 30 has in fact been demonstrated to proceed quantitatively at about 1300°K. Albert and Breit,³⁰ by rapidly cooling mixtures containing sodium fluoride and aluminum oxide held at 1050°, observed the stoichiometric yield of sodium aluminate by titration of the aqueous extract of the

(28) E. G. King, *J. Am. Chem. Soc.*, **77**, 3180 (1955).

(29) B. F. Dodge, "Chemical Engineering Thermodynamics," McGraw-Hill Book Co., New York, N. Y., 1944.

(30) O. Albert and H. Breit, *Aluminum Ranshoffen*, No. 3, 3 (1955).

quenched specimen. Cryolite was identified by an X-ray powder diffraction pattern as the second product of the reaction. It has been established that the sodium aluminate formed is almost completely insoluble^{31,32} in the resulting liquid phase at temperatures of about 1000°. Specifying the phases for reaction 30 at 1300°K.

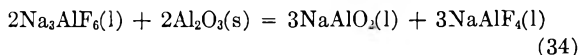


Because the reactant alumina and the product sodium aluminate are solid phases at unity activity, the equilibrium constant for reaction 32 can be written

$$K = \frac{a_{\text{Na}_3\text{AlF}_6}}{a_{\text{NaF}}^6} \quad (33)$$

The value for this function is calculated for various nominal alumina contents assuming quantitative formation and complete insolubility of sodium aluminate and no dissociation of the cryolite formed. The value of this function increases with increased initial alumina content and reaches the value 3×10^{-2} [value calculated for K from free energy change for reaction 32] at a weighed-in alumina content of about 10%. Thus the quantitative formation of sodium aluminate by reaction 32 at 1300°K. is not surprising with a large excess of sodium fluoride.

In light of the present knowledge of the constitution of molten cryolite, a more realistic mechanism for the formation of sodium aluminate in cryolite-alumina melts is



The free energies of formation for the products and reactants of this reaction are calculated at 1300°K. The free energies of formation at 1300°K. for NaAlO_2 and Al_2O_3 are -199.64 ³³ and -301.67 kcal., the same values cited previously. A value of -399.51 kcal. is obtained for the free energy of formation of NaAlF_4 at 1300°K. by interpolation of equations 26 and 27. A value of -610.03 kcal. is obtained for the free energy of formation of undissociated cryolite from the expression for $(F_T - H_{298})_{u.l.}$ From the free energies of formation of the products and reactants, the free energy change for reaction 34 becomes 25.9 kcal. This corresponds to an equilibrium constant of 4.5×10^{-5} .

Since the solubility of alumina at 1300°K. is

(31) E. Bonnier, *Ann. Phys.*, **8**, (12), 258 (1953).

(32) A. Seyyedi and G. Petit, *J. phys. radium*, **20**, 832 (1959).

(33) The free energy of formation of supercooled liquid sodium aluminate should be used in calculating the free energy change for reaction 34. Since no data are available for molten sodium aluminate the free energy of formation of the solid is used as an approximation.

about 14%,³⁴ the sodium aluminate, if present, must be a constituent of the melt at low alumina contents. The equilibrium constant for reaction 34 can be written

$$K = \frac{a_{\text{NaAlO}_2}^3 a_{\text{NaAlF}_4}^3}{a_{\text{Na}_3\text{AlF}_6}^2} \quad (35)$$

To test the possibility of reaction 34 proceeding quantitatively for reasonable alumina contents, the activities of all species were calculated assuming stoichiometric formation of sodium aluminate, ideality of the melt, and equilibrium between Na_3AlF_6 , NaF and NaAlF_4 as specified by the equilibrium constant at 1300°K.²¹

$$K_D = \frac{a_{\text{NaF}}^2 a_{\text{NaAlF}_4}}{a_{\text{Na}_3\text{AlF}_6}} = 0.108 \quad (36)$$

The resulting activities and the value of the expression representing the equilibrium constant are given in Table III.

TABLE III

Nominal wt. % Al_2O_3	$a_{\text{Na}_3\text{AlF}_6}$	a_{NaF}	a_{NaAlF_4}	a_{NaAlO_2}	$\frac{a_{\text{NaAlO}_2}^3 a_{\text{NaAlF}_4}^3}{a_{\text{Na}_3\text{AlF}_6}^2}$
0	0.360	0.427	0.213	0	0
2.7	.329	.385	.239	.047	1.3×10^{-5}
5.4	.294	.346	.266	.093	1.8×10^{-4}
8.1	.260	.310	.293	.138	1.0×10^{-3}

It is seen that the function representing the equilibrium constant reaches the value 4.5×10^{-5} at an alumina content of about 4%. This means that it is possible for alumina to react quantitatively with cryolite to form sodium aluminate up to this composition. The activities shown for the two highest alumina contents are meaningless since quantitative reaction is thermodynamically impossible. If alumina reacts according to reaction 34 in the dilute range it must dissolve by a second mechanism at higher alumina contents.

It is interesting to note that an independent study, freezing point lowering in the cryolite-alumina system,³⁵ suggested reaction 34 as the mechanism for the solution of alumina in cryolite to an alumina content of about 5%. Above this composition, a rather sharp deviation from this reaction mechanism was observed. Thus both the cryoscopic study and thermodynamic considerations suggest that alumina can react stoichiometrically with cryolite to form sodium aluminate and sodium tetrafluoroaluminate to a nominal alumina content of 4–5%. Additional aluminum oxide apparently dissolves by a second mechanism.

(34) P. A. Foster, Jr., *J. Am. Ceram. Soc.*, **2**, 66 (1960).

(35) P. A. Foster, Jr., and W. B. Frank, *J. Electrochem. Soc.*, **107**, No. 12, 997 (1960).

THE ASSOCIATION OF PHENOL IN WATER SATURATED CARBON TETRACHLORIDE SOLUTIONS

BY RICHARD M. BADGER AND RALPH C. GREENOUGH

Contribution No. 2721 from Gates and Crellin Laboratories of Chemistry, California Institute of Technology, Pasadena, California

Received June 26, 1961

The association of phenol in CCl_4 solution has been shown to be greatly promoted by the presence of water, and several kinds of evidence indicate that the predominant polymer species is a "hemihydrate dimer." Spectroscopic evidence shows that the hydrogen atoms of the water are not involved in hydrogen bonding and it is presumed that the polymer owes its stability to bonds formed through the agency of the hydrogen atoms of the phenol hydroxyls.

Introduction

The association through hydrogen bonding of several alcohols and of phenol in anhydrous non-polar solvents has repeatedly been investigated by several methods, but so far without completely definitive results. Not only have the details of the continued association process been elusive, but no really conclusive evidence exists regarding the structures of the polymeric species.¹ The most common method of attack has been the spectrophotometric measurement of monomer concentration as a function of total concentration. But although this and the n.m.r. method may adequately measure the over-all association they are not very powerful in elucidating the intermediate steps in the process. Different authors have accounted reasonably well for the over-all association on the assumptions, (a) that the association constants, K_n , for the processes: $M_{n-1} + M \rightarrow M_n$, are all the same²; (b) that they increase in systematic fashion³ with n ; and (c) that all constants are the same except for the dimerization constant, which is taken to be considerably smaller.⁴ Recent workers appear to agree that the tendency for dimerization is comparatively weak and attempts have been made to account for recent n.m.r. observations on the assumption that the trimer is the predominant species.⁵

There is, however, direct evidence for the existence of a dimer species in not inconsiderable amount. In the case of phenol, for example, the comparatively narrow and only slightly shifted association bands which first put in their appearance at very moderate concentrations would be difficult of other interpretation.⁶ Van Thiel, Becker and Pimentel in their studies of methanol in solid nitrogen matrices were able to distinguish several polymeric species,⁷ the first of which to appear at low concentrations is almost certainly a dimer.

The structures of the phenol and alcohol polymers, particularly that of the dimer, present some

interesting problems which are difficult to solve conclusively. The question as to whether one or two hydrogen bonds are involved in the dimer has not been answered definitively. The latter alternative is interesting since it seems to find no analog in the known bonding situations in crystals.

An early attempt was made by Philbrick⁸ to study the association of phenol in CCl_4 by measurement of the partition between aqueous and CCl_4 solutions, but was unsuccessful for reasons which are not obvious. His measurements on benzene solutions by the same methods appeared to succeed and he obtained a dimerization constant apparently confirmed by the careful isopiestic measurements of Lassetre and Dickinson⁹ on anhydrous solutions. In the light of the observations which will be presented below it is possible that this apparent agreement should be reconsidered.

Some years ago one of us reinvestigated the partition of phenol between CCl_4 and water, extending the measurements to higher concentrations. The results were simple and reproducible but indicated that the association process in CCl_4 was greatly affected by the presence of water. This, together with other evidence suggested that a "hemihydrate dimer" is the predominant polymeric species under these conditions. Confirmatory spectroscopic evidence has been obtained recently which has thrown further light on the nature of this entity.

Experimental Observations

The results of the measurement of the partition of phenol between CCl_4 and water at 28° are shown in Fig. 1.

The data are represented by the following equation which relates the partition ratio to the concentration in the aqueous phase

$$P = C_{\text{CCl}_4}/C_{\text{H}_2\text{O}} = 0.350 + 1.88C_{\text{H}_2\text{O}} \quad (1)$$

where the concentration units are formula weights of phenol per liter of solution at 28°.

From the steep slope of the plot one may conclude that phenol is rather strongly associated in water saturated CCl_4 , and from its linearity that the associated species is practically exclusively dimer up to concentrations about 0.3 F in the CCl_4 phase. On the assumption that association is negligible in the aqueous phase one may calculate an association constant. This "dimer" constant, $K_p = 1.88/2(0.35)^2 = 7.7 \text{ l. mole}^{-1}$, is several times as large as that which has been estimated for anhydrous solutions. (Wulf and Jones³ and Coggeshall and Saier⁴ estimated K_2 to be 1.8 and 1.38 l. mole^{-1} , respectively, at about 25°.)

As will be seen later, this constant does not have a very simple significance. Furthermore it is highly probable that higher association has contributed slightly to the slope of Fig. 1 without introducing a detectable curvature.

(1) For a useful review of this subject and a comprehensive bibliography see: G. D. Pimentel and A. L. McClellan, "The Hydrogen Bond," W. H. Freeman and Co., San Francisco, Calif., 1960.

(2) H. Kempster and R. Mecke, *Z. physik. Chem.*, **46**, 229 (1941).

(3) O. R. Wulf and E. J. Jones, *J. Chem. Phys.*, **8**, 745 (1940).

(4) H. O. Coggeshall and E. L. Saier, *J. Am. Chem. Soc.*, **73**, 5414 (1951).

(5) (a) M. Saunders and J. B. Hyne, *J. Chem. Phys.*, **29**, 1319 (1958); (b) E. B. Becker, *ibid.*, **31**, 269 (1959).

(6) J. J. Fox and A. E. Martin, *Proc. Roy. Soc. (London)*, **A162**, 419 (1937).

(7) M. Van Thiel, E. D. Becker and G. C. Pimentel, *J. Chem. Phys.*, **27**, 95 (1957).

(8) F. A. Philbrick, *J. Am. Chem. Soc.*, **56**, 2581 (1934).

(9) E. N. Lassetre and R. G. Dickinson, *ibid.*, **61**, 54 (1939).

Since it was evident that water plays some part in the association demonstrated by the partition measurements it seemed that these measurements could be related to the solubilization of water in CCl_4 by phenol. The water solubility was first estimated by titrating fairly concentrated aqueous solutions of phenol into CCl_4 -phenol solutions to the appearance of turbidity. Since the water solubility is small in the range studied it was not very practicable to titrate with pure water, but by using aqueous phenol solutions the volumes to be measured were made significant, and a reasonably reproducible end-point was obtained nevertheless. The experimental results are represented by the open circles in Fig. 2.

It is evident that there was a significant overshoot of the end-point in the titrations since the curve does not extrapolate to the known solubility of water in CCl_4 (about 0.012 formal at 28°), on which there is reasonable agreement.¹⁰ However, the trend of solubility with phenol concentration is well shown. This trend is confirmed by our later spectrophotometric measurements represented by the black circles.

A very qualitative comparison of the partition and solubility measurements suggests that the water solubilized by phenol resides predominantly in a hemihydrate phenol dimer and that the stability of this complex is responsible for the increased association of phenol in the presence of water. One can show by a very simple experiment that the water is indeed carried predominantly by a phenol polymer species. If a water saturated solution of phenol in CCl_4 is diluted with anhydrous CCl_4 , turbidity immediately appears with subsequent separation of an aqueous phase.

To account quantitatively for the water solubilization, however, it seems necessary to assume that a small fraction of the water is carried by a phenol monomer. This would be difficult to measure directly, but can probably be estimated with sufficient accuracy. In CCl_4 solutions phenol forms 1/1 complexes with ether, acetone, etc., which are presumably analogous to the complex with water. Since the association constants for all of these lie in the range 8-10 l. mole⁻¹¹¹ we shall probably not be greatly in error in assuming that in the water saturated CCl_4 solution (free water concentration about 0.012 formal) the ratio of hydrated to unhydrated phenol monomer is about 0.1. To predict quantitatively the water solubilization we shall assume that in the water saturated solutions the association of phenol to the hemihydrate dimer and the various anhydrous polymers occur independently and that for the latter we may adopt the values of Coggeshall and Saier,⁴ reduced by about 8% to account for the difference in temperature, ($25-28^\circ$).¹² The constant, K_p , obtained from the partition data we interpret as shown in the following collection of the data employed, in which Ph_2W and Ph_2 represent the concentrations of hydrated and anhydrous dimer, and PhW and Ph , those of the corresponding monomers.

$$K_p = \frac{(\text{Ph}_2\text{W} + \text{Ph}_2)}{(\text{PhW} + \text{Ph})^2} = 7.7 \text{ l. mole}^{-1};$$

$$K_2 = \frac{\text{Ph}_n}{(\text{Ph})^2} = 1.29 \text{ l. mole}^{-1}$$

$$\frac{\text{PhW}}{\text{Ph}} = 0.1 \text{ (in water satd. soln);}$$

$$K_n = \frac{\text{Ph}_n}{(\text{Ph})(\text{Ph}_{n-1})} = 2.72 \text{ l. mole}^{-1} (n \geq 3)$$

The solubilization of water in CCl_4 by phenol predicted on the basis of these assumptions is shown by the solid curve of Fig. 2. An alternative calculation in which the monomer is assumed to be unhydrated is represented by the dashed line. It seems very probable that our assumptions are essentially correct though they may err in some details. In particular it is probable that K_p has been overestimated, probably by about 10%, for the reasons given above. If so it may be necessary to admit a slightly greater hydration of the monomer, or some hydration of higher polymers, in order to account for the water solubilization.

(10) (a) C. W. Clifford, *Ind. Eng. Chem.*, **13**, 631 (1921); (b) C. K. Rosenbaum and J. H. Walton, *J. Am. Chem. Soc.*, **52**, 3568 (1930); (c) A. J. Stasermann, *Rec. trav. chim.*, **60**, 836 (1941)

(11) See ref. 1, p. 378 for collected data.

(12) R. Mecke estimates the mean heat of association to be about 4.35 kcal. See R. Mecke, *Discussions Faraday Soc.*, **9**, 161 (1950).

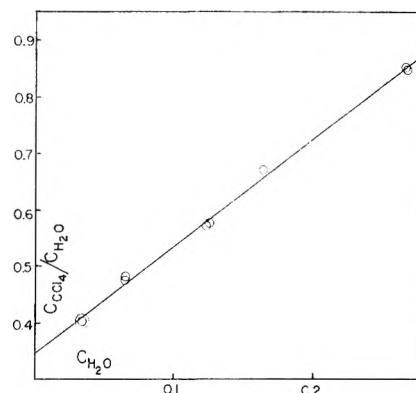


Fig. 1.—The partition of phenol between CCl_4 and water at 28° . Concentration units are formula weights per liter at 28° .

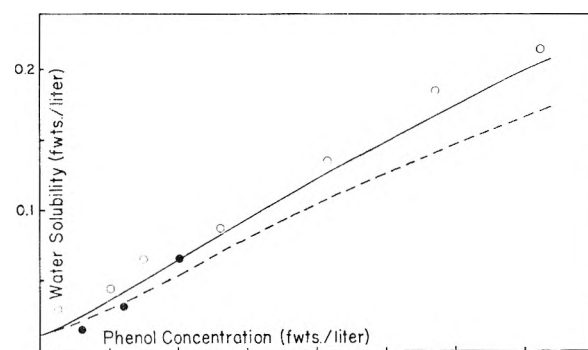


Fig. 2.—The solubility of water in phenol- CCl_4 solutions: (a) open circles, titration data; (b) closed circles, spectrophotometric data; (c) continuous curve calculated as described in text; (d) broken curve, calculated assuming no monomer hydration.

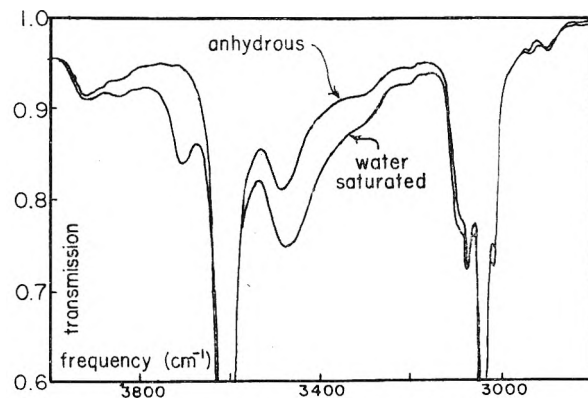


Fig. 3.—Spectra of 0.06 F phenol solution in CCl_4 near 3μ : (a) anhydrous; (b) water saturated (2 mm. paths, slit width 3 cm.^{-1}).

Spectrophotometric Measurements.—Supporting evidence for the above considerations has been provided recently by the spectrophotometric measurements presented in Figs. 3 and 4, which permit one to draw some conclusions regarding the structure of the associated species.

In anhydrous solutions in CCl_4 the spectrum of phenol gives evidence for more than one associated species. At low concentrations an association band is observed which is comparatively sharply peaked at 3500 cm.^{-1} . The increase of intensity with concentration is appreciably greater on the low frequency side but the over-all increase is much less than should occur if it were due entirely to trimers or higher polymers. At about $0.2 F$ the maximum has shifted to about 3460 cm.^{-1} and is less sharply peaked. At low concentrations the band shows some evidence of structure but

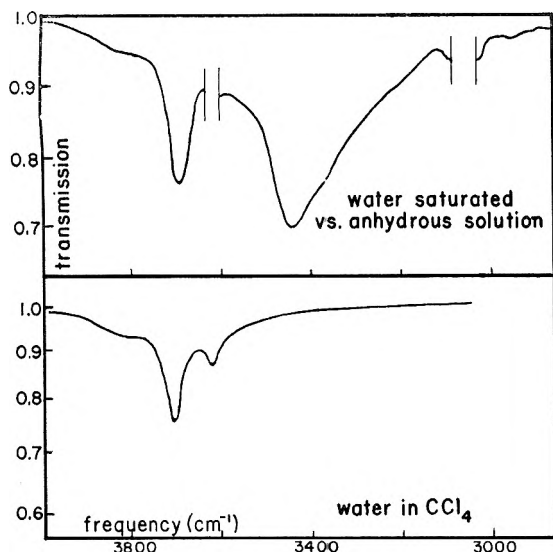


Fig. 4.—Difference spectrum of water saturated versus anhydrous phenol in CCl_4 . Concentration 0.125 F (2 mm. paths). Spectrum of water saturated CCl_4 given for comparison (7.9 mm. path, slit width 3 cm.^{-1}).

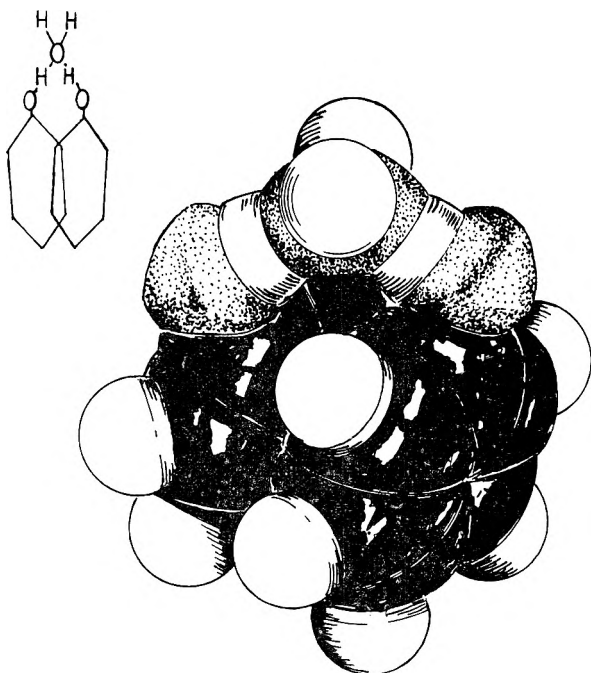


Fig. 5.—Possible configuration of a hemihydrate dimer of phenol.

from the behavior of these features with increase in concentration it seems reasonably certain that they are due to very weak overtone or combination bands not affected by hydrogen bonding.

If a given solution is saturated with water the association band shows a very significant increase in intensity, very roughly doubling although it is very difficult to make an objective estimate because of the overlapping of several bands. The maximum shifts to lower frequencies (about

3440 cm.^{-1}), but the high frequency tail increases in extent. Furthermore new features appear on the high frequency side of the monomer peak.

The change in appearance on water saturation is shown in Fig. 3 but is most strikingly evident in Fig. 4 which presents the difference spectrum of an anhydrous versus a water saturated solution of the same phenol concentration. The spectrum of water saturated CCl_4 in a path 3.9 times as long is shown also for comparison. The water peaks at 3710 and 3620 cm.^{-1} presumably represent ν_3 and ν_1 , respectively, but the high frequency shoulder has not been satisfactorily explained so far as we are aware. The attribution to a hindered rotation seems very dubious in view of the observations presented here.

In the region not obscured by the intense phenol monomer OH peak, the high frequency features of the hydrous phenol spectrum appear identical with the water spectrum, including the high frequency shoulder. The absence of any significant modification is somewhat surprising but seems conclusive evidence that in the water molecule associated with phenol, neither hydrogen is engaged in a hydrogen bond. One is forced to the conclusion that the association results rather from bonding through the hydroxyl hydrogen of phenol to the oxygen of the water molecule.

The high frequency features of the hydrous phenol spectrum are considerably overlapped by the monomer band as well as the tail of the association band at lower frequency so that no really objective apportionment of intensities can be made. Nevertheless we have estimated the concentration of solubilized water in three solutions on the assumption that the extinction coefficient for the solubilized water is the same as that for "free" water in CCl_4 , as found in the careful measurements of Fox and Martin.¹³ The points shown as closed circles in Fig. 2 support this assumption and confirm the belief that the water is remarkably little perturbed by the association.

The relatively high stability of the hydrous dimer presumably results in large part from the two strong hydrogen bonds which can be formed, in place of the one strong, or two weak bonds, in the anhydrous species. It seems quite possible that additional stability is gained, at the expense of some loss in entropy, from the van der Waals attraction between phenyl groups. A conceivable configuration of the hydrous dimer is shown in Fig. 5, which was drawn from a Pauling-Corey model.

In this connection it is of interest that phenol forms a crystalline hemihydrate¹⁴ of which a preliminary X-ray structure determination has been made recently.¹⁵ This appears to show the presence of chains which could be regarded as built up by unfolding and connecting, with hydrogen bonds, a succession of the basic units proposed in this article. Methuen and v. Stackelberg make a point of the fact that the hemihydrate is difficult to obtain directly from the supersaturated solution and suggest that the associated species in solution differ in some way from those in the crystal. The model of Fig. 5 suggests such a possible difference.

It should be added that phenol forms 2/1 intermolecular compounds with several organic compounds, for example acetone¹⁶ and acetamide¹⁷ and that vapor pressure measurements suggest the presence of 2/1 complexes in the binary liquid systems with methanol, ethanol and acetone¹⁸ as the second component.

(13) J. J. Fox and A. E. Martin, *Proc. Roy. Soc. (London)*, **A174**, 234 (1940).

(14) F. H. Rhodes and A. L. Markely, *J. Phys. Chem.*, **25**, 527 (1921).

(15) B. Methuen and M. v. Stackelberg, *Z. Elektrochem.*, **64**, 387 (1960).

(16) J. Schmidlin and R. Lang, *Ber.*, **43**, 2512 (1910).

(17) R. Kreegan, *Monatsh.*, **38**, 479 (1918).

(18) G. Weissenberger, *Z. anorg. Chem.*, **152**, 333 (1926).

THE TRANSMISSION AND ADDITIVITY OF POLAR EFFECTS

BY C. D. RITCHIE

*Department of Chemistry, The William M. Rice University, Houston, Texas**Received June 30, 1961*

Several recent developments in the field of structure-reactivity relationships made it appear advisable to re-examine the basis of the linear-polar-energy equation which has been proposed by Taft. A test for the self-consistency of the σ^* parameters is derived from simple symmetry considerations similar to those used by Hine for the Hammett equation. It is found that σ^* values for alkyl groups are not consistent with those for other groups. The implications of the inconsistency are examined, and new σ^* values are proposed. The discussion then is extended to the additivity of substituent effects. It is shown that a "saturation effect" is observable even in cases where linear-free-energy equations are obeyed. Some conclusions regarding the transmission properties of groups are also possible from these arguments.

Introduction

Taft¹ has recently suggested a relationship, $I = \sigma^* \rho^*$, for the purpose of separating polar effects from others in chemical rates and equilibria. Examples of the use of this relationship for the evaluation of steric,² resonance,³ hyperconjugative,⁴ and solvation⁵ effects have been offered.

Although the existence of linear-free-energy equations may be justified on fairly sound theoretical bases,^{6,7} the evaluation of the σ^* parameters is an empirical process. Ideally, the evaluation should be carried out using reaction series in which one can be certain that only polar effects are operative.⁸ In practice, it becomes difficult to find series with enough substituents in which this ideal may be approached.

Working on a suggestion by Ingold,⁹ Taft¹⁰ used the difference in the rates of acid- and base-catalyzed ester hydrolyses as the standard series for the evaluation of σ^* . Although the assumption that only polar effects influence these differences seemed reasonable, it could be checked only by comparing σ^* values obtained with other independent observations. Taft¹¹ has presented several lines of evidence which appear to verify individual constants, however, all of the values have not been verified.

Hine's recent work with the symmetry properties of the Hammett equation¹² suggested that the analogous arguments applied to the Taft equation would provide a test for the self-consistency of the σ^* values.

It also appeared that Miller's¹³ recent work on multiple variations in structure-reactivity correlations might provide a method of gaining information concerning the additivity of substituent effects.

(1) R. W. Taft, Jr. in "Steric Effects in Organic Chemistry," edited by M. S. Newman, John Wiley and Sons, Inc., New York, N. Y., 1956, pp. 622 ff.

(2) Ref. 1, pp. 633-636, 642-645.

(3) Ref. 1, pp. 636-642; R. W. Taft, Jr., and I. C. Lewis, *J. Am. Chem. Soc.*, **81**, 5343 (1959).

(4) M. M. Kreevoy and R. W. Taft, Jr., *ibid.*, **77**, 5590 (1955).

(5) H. K. Hall, Jr., *ibid.*, **79**, 5439 (1957).

(6) J. Hine, *ibid.*, **82**, 4877 (1960).

(7) W. F. Sager and C. D. Ritchie, *ibid.*, **83**, 3498 (1961).

(8) For efforts toward this ideal, see: J. D. Roberts and W. T. Moreland, *ibid.*, **75**, 2167 (1953); S. Siegel and J. M. Komorny, *ibid.*, **82**, 2547 (1960).

(9) C. K. Ingold, *J. Chem. Soc.*, 1032 (1930).

(10) R. W. Taft, Jr., *J. Am. Chem. Soc.*, **74**, 3120 (1952).

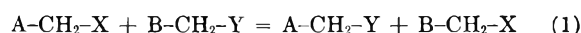
(11) *Cf. ref. 1*, pp. 613-618.

(12) J. Hine, *J. Am. Chem. Soc.*, **81**, 1126 (1959).

(13) S. I. Miller, *ibid.*, **81**, 101 (1959).

Development of Equations

Consider the reaction



where the equilibrium constant¹⁴ for the reaction is correlated by

$$\log K = (\sigma^*_A - \sigma^*_B)\rho^*_{XY} \quad (2)$$

For the Taft equation to have general applicability, also

$$\log K = (\sigma^*_X - \sigma^*_Y)\rho^*_{AB} \quad (3)$$

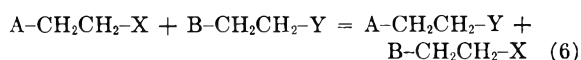
Combining equations 2 and 3, and rearranging gives

$$\frac{\rho^*_{XY}}{(\sigma^*_X - \sigma^*_Y)} = \frac{\rho^*_{AB}}{(\sigma^*_A - \sigma^*_B)} \quad (4)$$

Since ρ^*_{XY} must be independent of σ^*_A and σ^*_B , and ρ^*_{AB} independent of σ^*_X and σ^*_Y , these ratios must both equal a constant which we denote by $\tau(CH_2)$. Thus, we find

$$\rho^*_{XY} = \tau(CH_2)(\sigma^*_X - \sigma^*_Y) \quad (5)$$

Now consider the reaction



Again for the Taft equation to apply

$$\log K (\sigma^*_{ACH_2} - \sigma^*_{BCH_2})\rho^*_{XY} = (\sigma^*_{XCH_2} - \sigma^*_{YCH_2})\rho^*_{AB} \quad (7)$$

Substituting in (7) the expression for ρ^* from (5), and rearranging

$$\frac{\sigma^*_A - \sigma^*_B}{\sigma^*_{ACH_2} - \sigma^*_{BCH_2}} = \frac{\sigma^*_X - \sigma^*_Y}{\sigma^*_{XCH_2} - \sigma^*_{YCH_2}} \quad (8)$$

Since the σ^* values of the A's, B's, X's, and Y's are independent of one another, these ratios must be equal to a constant which we denote $\tau(CH_2)/\tau(CH_2CH_2)$.¹⁵ The relationship 8 then requires that

$$\sigma^*_A = \frac{\tau(CH_2)}{\tau(CH_2CH_2)} \sigma^*_{ACH_2} + \text{constant} \quad (9)$$

By considering reactions in which methylene groups are successively interposed between the substituent and the reaction site, equation 9 may be generalized to the statement that there is a constant fall-off factor for each methylene group between a substituent and reaction site.

The derivation of equation 9, and its generalization, requires no other assumptions than the gener-

(14) The "inductive energy" (*cf. ref. 2*), I , may be substituted in place of $\log K$ in any of the equations presented without affecting the arguments.

(15) As can be seen from inspection, $\tau(CH_2CH_2)$ is the constant in the expression for ρ^* of equation 6 if we were to use σ^* of A, B, X and Y. That is $\rho^*_{XCH_2, YCH_2} = \tau(CH_2CH_2)(\sigma^*_X - \sigma^*_Y)$ for equation (6).

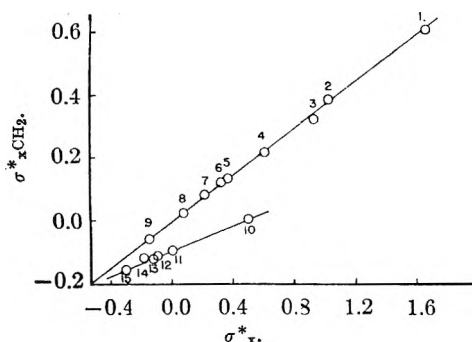


Fig. 1.—Plot of data for equation 9: 1, CH_3CO ; 2, ClCH_2 ; 3, CF_3CH_2 ; 4, C_6H_5 ; 5, $\text{CH}_2\text{CH}=\text{CH}$; 6, $\text{CF}_3\text{-CH}_2\text{CH}_2$; 7, $\text{C}_6\text{H}_5\text{CH}_2$; 8, $\text{C}_6\text{H}_5\text{C}\equiv\text{CH}_2$; 9, $\text{cyclo-C}_6\text{H}_{11}$; 10, H; 11, CH_3 ; 12, C_2H_5 ; 13, $n\text{-C}_3\text{H}_7$; 14, $i\text{-C}_3\text{H}_7$; 15, $t\text{-C}_4\text{H}_9$. (Values taken from ref. 1, p. 619).

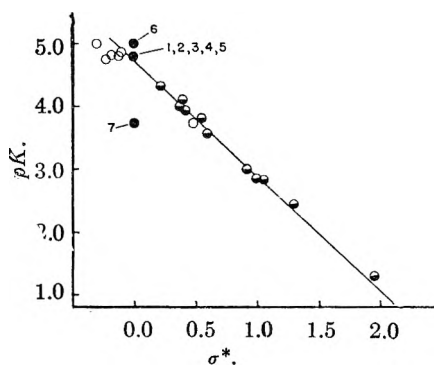
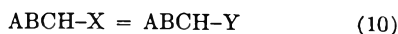


Fig. 2.—Taft plot of ionization of aliphatic acids: \circ , values for alkyl groups from ref. 1; \bullet , values for alkyl groups from this paper; \ominus , groups other than alkyl; 1, CH_3 ; 2, C_2H_5 ; 3, $n\text{-C}_3\text{H}_7$; 4, $i\text{-C}_3\text{H}_7$; 5, $\text{sec-C}_4\text{H}_9$; 6, $t\text{-C}_4\text{H}_9$; 7, H. (Primary references for the data are given in ref. 1.)

ality of the linear-polar-energy equation, and the possibility of assigning σ^* values to groups A and ACH_2 in the same reaction series. In short, equation 9 is a necessary condition for the existence of the linear-polar-energy equation.

Another informative manipulation of the Taft equation results from the consideration of multiple variations in structure.¹³

Consider the reaction



Application of the Taft equation gives

$$\log K_{\text{AB}} = \sigma^*_{\text{A}}\rho^{\text{B}}_{\text{XY}} + \log K_{\text{BH}} = \sigma^*_{\text{B}}\rho^{\text{A}}_{\text{XY}} + \log K_{\text{AH}} \quad (11)$$

Also by the Taft equation

$$\log K_{\text{BH}} = \sigma^*_{\text{B}}\rho^{\text{H}}_{\text{XY}} + \log K_{\text{HH}}, \text{ and, } \log K_{\text{AH}} = \sigma^*_{\text{A}}\rho^{\text{H}}_{\text{XY}} + \log K_{\text{HH}} \quad (12)$$

Combination of (11) and (12) gives

$$\sigma^*_{\text{A}}\rho^{\text{B}}_{\text{XY}} + \sigma^*_{\text{B}}\rho^{\text{H}}_{\text{XY}} = \sigma^*_{\text{B}}\rho^{\text{A}}_{\text{XY}} + \sigma^*_{\text{A}}\rho^{\text{H}}_{\text{XY}} \quad (13)$$

Calling upon the necessary independence of the various σ^* and ρ^* , and rearranging, gives

$$\frac{\rho^{\text{B}}_{\text{XY}} - \rho^{\text{H}}_{\text{XY}}}{\sigma^*_{\text{B}}} = \frac{\rho^{\text{A}}_{\text{XY}} - \rho^{\text{H}}_{\text{XY}}}{\sigma^*_{\text{A}}} = \text{constant} = q^{16} \quad (14)$$

By the same arguments used earlier

$$\rho^{\text{A}}_{\text{XY}} = \tau(\text{CHA})(\sigma^*_{\text{X}} - \sigma^*_{\text{Y}}), \text{ and } \rho^{\text{B}}_{\text{XY}} = \tau(\text{CHB})(\sigma^*_{\text{X}} - \sigma^*_{\text{Y}}) \quad (15)$$

Now, combining equations 5, 14 and 15

$$q = \frac{[\tau(\text{CHA}) - \tau(\text{CH}_2)](\sigma^*_{\text{X}} - \sigma^*_{\text{Y}})}{\sigma^*_{\text{A}}} \quad (16)$$

But q must be independent of A and B, therefore

$$\frac{q}{\sigma^*_{\text{X}} - \sigma^*_{\text{Y}}} = \frac{\tau(\text{CHA}) - \tau(\text{CH}_2)}{\sigma^*_{\text{A}}} = \text{constant} \quad (17)$$

Thus, we find the interesting result that the transmission constant is a function of the groups attached to the transmitting atom. This effect is the same as that which has been called a "saturation effect."¹⁷

As Miller has pointed out,¹³ the general equation for symmetric dual substitution is

$$\log K_{\text{AB}} = (\sigma^*_{\text{A}} + \sigma^*_{\text{B}})\rho^{\text{H}}_{\text{XY}} + \sigma^*_{\text{A}}\sigma^*_{\text{B}}q + \log K_{\text{HH}} \quad (18)$$

For triple substitution on a single carbon, a rather lengthy algebraic process gives¹⁸

$$\log K_{\text{ABC}} = (\sigma^*_{\text{A}} + \sigma^*_{\text{B}} + \sigma^*_{\text{C}})\rho^{\text{H}}_{\text{XY}} + (\sigma^*_{\text{A}}\sigma^*_{\text{B}} + \sigma^*_{\text{A}}\sigma^*_{\text{C}} + \sigma^*_{\text{B}}\sigma^*_{\text{C}})q + \log K_{\text{HHH}} \quad (19)$$

Discussion

A plot of the σ^* values to which equation 9 should be applicable is shown in Fig. 1. It is seen that alkyl groups fall on a separate line from that defined by other substituents.

Since most of the arguments which have been presented by Taft¹¹ tend to substantiate the σ^* values for groups other than alkyl, our conclusion must be that the σ^* values for alkyl groups are not consistent with the generality of the Taft equation. If we assume that the σ^* value of zero for the methyl group is correct, equation 9 requires that σ^* values for all n -alkyl groups are zero. Branched alkyl groups cannot strictly be considered in the simple equation 3, since these involve multiple substitution. Equations 18 and 19, however, give $\log K_{\text{alkyl}} = \log K_{\text{methyl}}$, since σ^* values for the n -alkyl groups are zero. Thus, branched alkyl groups may be considered to have σ^* equal to zero.

Several plots of the Taft equation, using these required values, are shown in Figs. 2-4. It is seen that the data are correlated as well with these new values as with those previously assigned. In some cases, notably with the basicity of primary and secondary amines, the new values give better fits than do the old ones.

It should be noted that the points for the hydrogen substituted compounds deviate seriously from the plots for the acidity of aliphatic acids and for the hydrolysis of acetals and ketals. No single substituent constant for hydrogen will improve the correlations shown.

Thus, if the linear-polar-energy equation exists, the assumptions made in the original evaluation of σ^* constants must be in error. This is not hard to understand in terms of Miller's arguments. If other effects are operative in ester hydrolyses, it would be expected that they interact with the polar effect. Assuming that the other effect could be expressed analytically, this interaction would lead to a cross term in the equation for $\log K$. From the above arguments concerning q , this cross

(17) Ref. 1, pp. 623-625.

(16) An analogous equation has been derived by: C. D. Ritchie, J. D. Saltiel and E. S. Lewis, *J. Am. Chem. Soc.*, **83**, 4601 (1961).

(18) The straightforward process analogous to that above gives three q 's. It is easy to show, using the symmetry of the substitution, that these three q 's are equal.

term should be a function of ρ^* . Since ρ^* for the acid- and base-catalyzed ester hydrolyses are not the same, it would not be expected that this cross term would cancel in the difference of the log K values for the two reactions.

The possible misinterpretations which have resulted from the use of σ^* values for alkyl groups in the past are obvious and need not be dwelled upon.

Equations 14 through 19, of course, become trivial if q is zero. Past data have dealt with such narrow ranges of structures,¹³ or with cases in which substituents were so far separated,¹⁶ that it has been difficult to assess the significance of the q terms in equations such as (18).

From the derivation of equation 18, it is seen that if the linear-free-energy equations are to be applicable at all to multiple substitution, the evaluation of σ^* for multiply substituted methyl groups will give q . That is, if σ^* for an X_2CH group is twice σ^* for the XCH_2 group, q is zero; if not, then q is not zero.

Taft¹⁹ recently has pointed out that σ^* for an X_2CH group is generally 1.7 σ^* for the XCH_2 group, and that σ^* for an X_3C group is 2.2 σ^* for the XCH_2 group. Since the data used deals necessarily with halogen substitution, for which σ^* of XCH_2 is nearly the same in each case, with σ^* equal 1.0, equations 18 and 19 require that q is equal to $-0.30 \rho^*_{XY}$. Equation 17 then requires that electron withdrawing substituents decrease the transmission properties of the carbon to which they are bonded

$$\frac{\tau(\text{CHA}) - \tau(\text{CH}_2)}{\tau(\text{CH}_2)} = -0.30 \sigma^*_{\text{A}} \quad (20)$$

Conclusions

The results presented above point out the difficulties in the disentanglement of various effects on reactivity. It would appear that the only safe way of proceeding in the separation of polar effects from others is to study series in which all other effects are carefully controlled.

Acknowledgments.—Grateful acknowledgment is made to the Robert A. Welch Foundation for the

(19) (a) R. W. Taft, Jr., Paper presented before the Hydrocarbon Symposium, Houston, Texas, January 1961; (b) R. W. Taft, Jr., personal communication, April 1961.

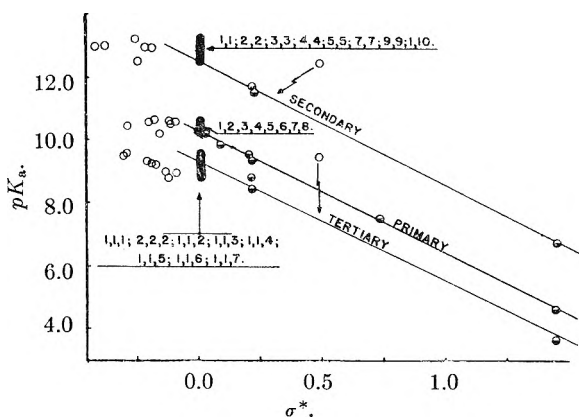


Fig. 3.—Taft plot of the ionization of aliphatic amines: O, values for alkyl groups from ref. 1; ●, values for alkyl groups from this paper; ○, groups other than alkyl. pK_a for primary amines used to establish line for all amines. $pK_a + 2.00$ is shown for secondary amines; $pK_a - 1.00$ shown for tertiary amines. 1, CH_3 ; 2, C_2H_5 ; 3, $n\text{-C}_3\text{H}_7$; 4, $n\text{-C}_4\text{H}_9$; 5, $i\text{-C}_3\text{H}_7$; 6, $t\text{-C}_4\text{H}_9$; 7, $sec\text{-C}_4\text{H}_9$; 8, $neo\text{-C}_6\text{H}_{11}$; 9, $i\text{-C}_4\text{H}_9$; 10, H. (Data taken from ref. 5.)

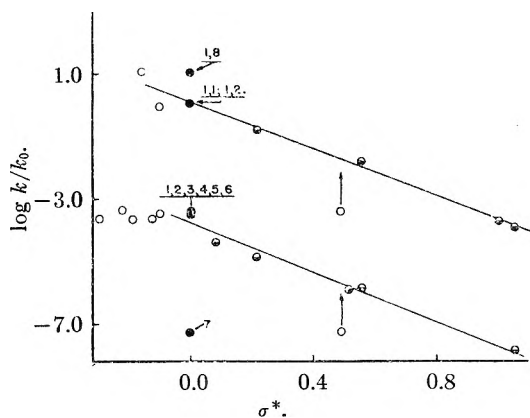


Fig. 4.—Taft plot for the hydrolysis of acetals and ketals: O, values for alkyl groups from ref. 1; ●, values for alkyl groups from this paper; ○, groups other than alkyl; 1, CH_3 ; 2, C_2H_5 ; 3, $i\text{-C}_3\text{H}_7$; 4, $t\text{-C}_4\text{H}_9$; 5, $i\text{-C}_4\text{H}_9$; 6, $(\text{C}_2\text{H}_5)_2\text{CH}$; 7, H; 8, $neo\text{-C}_6\text{H}_{11}$. (Data taken from ref. 4.)

support of this work, and to Prof. E. S. Lewis for many helpful discussions and suggestions.

A SPECTROPHOTOMETRIC STUDY OF THE REACTION BETWEEN FERRIC ION AND HYDRAZOIC ACID¹

BY R. M. WALLACE AND E. K. DUKES

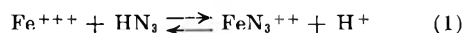
Savannah River Laboratory, E. I. du Pont de Nemours & Co., Aiken, South Carolina

Received July 10, 1961

A spectrophotometric study of the reaction between Fe^{+++} and HN_3 demonstrated that the complex FeN_3^{++} was formed. The molar extinction coefficient of FeN_3^{++} was 3.68×10^3 at the absorption peak of 460 $m\mu$. Equilibrium constants for the reaction $\text{Fe}^{+++} + \text{HN}_3 \rightleftharpoons \text{FeN}_3^{++} + \text{H}^+$ were measured under a variety of conditions. The equilibrium constant at 25°, extrapolated to infinite dilution, was 1.71; the ΔH of the reaction was 2010 ± 100 cal. Anomalous results for the equilibrium constant at very low acid concentrations were attributed to the hydrolysis of Fe^{+++} to FeOH^{++} .

Introduction

The reaction between aqueous hydrazoic acid and ferric ion to produce an intensely red-colored solution has been known for many years.² Early investigators assumed that the color was due to the compound $\text{Fe}(\text{N}_3)_3$; however, Ricca³ has presented evidence to indicate that the reaction involved is



Ricca's conclusion was based on the observations that the color faded upon acidification and aeration, that the color migrated toward the cathode in an electrolysis cell, and that the differences between the observed and calculated conductivities of solutions prepared by adding hydrazoic acid to ferric chloride could best be explained by the release of one hydrogen ion for every ferric ion undergoing reaction.

Although the reaction has been used as the basis for a spectrophotometric analysis for hydrazoic acid,⁴ no systematic investigation of the reaction has been made. The purpose of the present investigation was to verify reaction 1 spectrophotometrically and to determine the equilibrium constant for the reaction.

Experimental

Materials.—Solutions of ferric nitrate, sodium azide, nitric acid, sodium nitrate, perchloric acid and sodium perchlorate were prepared from reagent-grade chemicals.

Solutions of sodium azide were standardized by adding ceric ion to an aliquot of the solution and titrating the excess ceric ion with ferrous ion.

Solutions of ferric nitrate were standardized by reducing the ferric ion to ferrous ion and measuring the absorbance of the ferrous *o*-phenanthroline complex.

Apparatus.—Absorbance measurements were made with either a Beckman DU spectrophotometer and matched 1.0-cm. Corex cells or with a Cary recording spectrophotometer and matched 2.5-cm. Corex cells. The desired temperatures were maintained by using jacketed cells in conjunction with a thermostatically controlled water-bath.

A Beckman Model H2 pH meter was used for pH measurements.

Procedure.—Aliquots of standard solutions of sodium azide and ferric nitrate were added to a 10-ml. volumetric flask that already contained the other reagents such as nitric acid. After the solution was diluted to 10 ml. with water, an aliquot was withdrawn for acid determination and the remainder of the solution was used for absorbance measurements. For measurements at 0.01 *M* H^+ , all reagents were added to a small beaker and diluted to about 9 ml. The solution was adjusted to pH 2 with dilute NaOH

or HNO_3 and then was transferred to a 10-ml. volumetric flask for final dilution. Absorbance measurements were made against a reference of the same composition as the sample but containing no hydrazoic acid.

When it was necessary to have large concentrations of HN_3 present at low acidities, as was the case in the determination of the extinction coefficient of FeN_3^{++} , the following procedure was used. An aqueous solution of HN_3 (about 0.5 *M*) was prepared by passing a solution of NaN_3 through a column filled with "Dowex" 50 cation exchange resin in the acid form. The solution was analyzed for hydrazoic acid by a method described previously.⁵ Aliquots of the pure HN_3 solution, HNO_3 , $\text{Fe}(\text{NO}_3)_3$, and water then were mixed to obtain the desired final concentrations.

Calculations

The equilibrium constant for reaction 1 can be expressed as follows, if activities are replaced by concentrations.

$$K_c = \frac{(\text{FeN}_3^{++})(\text{H}^+)}{(\text{Fe}^{+++})(\text{HN}_3)} \quad (2)$$

where the quantities in parentheses are the equilibrium concentrations of the respective components.

Since the ferriazide complex, FeN_3^{++} , is the only absorbing species in the region of the spectrum studied, and since the equilibrium concentrations of the ferric ion and the hydrazoic acid will be the concentrations of these components added less the amounts consumed in forming the complex, equation 2 becomes

$$K_c = \frac{A(\text{H}^+)}{\epsilon \left[(\text{Fe})_a - \frac{A}{\epsilon} \right] \left[(\text{HN}_3)_a - \frac{A}{\epsilon} \right]} \quad (3)$$

where A is the absorbance for a 1-cm. light path, ϵ is the molar extinction coefficient of the ferriazide complex, and $(\text{Fe})_a$ and $(\text{HN}_3)_a$ are the respective concentrations of the ferric ion and hydrazoic acid added to the solution.

If the hydrazoic acid is present in large excess so that its concentration remains essentially unchanged by the formation of the complex, but an appreciable fraction of the ferric ion is consumed in forming the complex, equation 3 can be rearranged to give

$$\frac{(\text{Fe})_a}{A} = \frac{1}{\epsilon} + \frac{(\text{H}^+)}{\epsilon K_c} \times \frac{1}{(\text{HN}_3)_a} \quad (4)$$

A plot of $(\text{Fe})_a/A$ vs. $1/(\text{HN}_3)_a$ at constant acidity should therefore give a straight line with intercept $1/\epsilon$, permitting the determination of the extinction coefficient.

(1) The information contained in this article was developed during the course of work under contract AT(07-2)-1 with the U. S. Atomic Energy Commission.

(2) Curtius and Rissom, *J. prakt. Chem.*, **58**, Series 2, 261 (1898).

(3) B. Ricca, *Gazz. chim. ital.*, **75**, 71 (1945).

(4) C. E. Roberson and C. M. Austin, *Anal. Chem.*, **29**, 854 (1957).

(5) E. K. Dukes and R. M. Wallace, *Anal. Chem.*, **33**, 242 (1961).

Results

Application of the method of continuous variations⁶ to the system ferric nitrate-hydrazoic acid in nitric acid demonstrated that one mole of ferric ion and one mole of hydrazoic acid are involved in the formation of the colored complex. Figure 1 shows plots of absorbance vs. the mole fraction of HN_3 for solutions in which the sum of the concentrations of Fe^{+++} and HN_3 as constant. The results at 7 M HNO_3 were obtained with a total concentration of 0.16 M (Fe^{+++} plus HN_3) and those at 0.01 M HNO_3 at a total concentration of 4.0×10^{-3} M (Fe^{+++} plus HN_3). In each case the maximum occurred at mole fraction 0.5, indicating the formation of 1:1 complex.

Further evidence for the existence of a 1:1 complex was the constancy of the quantity $A/(\text{Fe})_a - (\text{HN}_3)_a$ at constant acidity and at various concentrations of added Fe^{+++} and HN_3 . The constancy of this quantity also shows that no significant amounts of Fe^{+++} or HN_3 were consumed in forming the complex in these measurements. The values of this quantity in 1 M HNO_3 for various concentrations of added Fe^{+++} and HN_3 are shown in Table I. The values are seen to be constant within experimental error, as would be expected for the proposed reaction. Similar measurements made in 5, 6 and 7 M HNO_3 also gave constant values for $A/(\text{Fe})_a(\text{HN}_3)_a$.

TABLE I
VALUES OF $A/(\text{Fe})_a(\text{HN}_3)_a$ IN 1 M HNO_3

$(\text{HN}_3)_a, M$	$(\text{Fe})_a, M$	Absorbance	$\frac{A}{(\text{Fe})_a(\text{HN}_3)_a}$
0.0096	0.0250	0.468	1950
.0147	.0125	.357	1942
.0147	.0150	.432	1959
.0196	.0125	.477	1947
.0245	.0100	.481	1963

Determination of the Molar Extinction Coefficient of FeN_3^{++} .—The molar extinction coefficient of FeN_3^{++} was determined in 0.05 and 0.10 M HNO_3 by a method based on equation 4. In each determination, solutions were prepared containing the desired acid concentration, a small amount of ferric ion, and varying concentrations of hydrazoic acid. The absorbance of each of these solutions was determined at 460 $m\mu$, and the ratio $(\text{Fe})_a/A$ was plotted vs. the reciprocal of the hydrazoic acid concentration as shown in Fig. 2. The resulting straight lines were extrapolated to $1/(\text{HN}_3)_a$ equal zero, and the extinction coefficients were calculated from the intercepts. A least squares fit of the data gave extinction coefficients of 3.69×10^3 and 3.66×10^3 for the 0.05 and 0.10 M HNO_3 , respectively. The average value of 3.68×10^3 was used in subsequent calculations.

It was not possible to obtain reliable estimates of the extinction coefficients at acid concentrations much greater than 0.1 M; the higher acidities reduced the fraction of the iron present as the complex, and required a much greater extrapolation. However, since the extinction coefficient did not

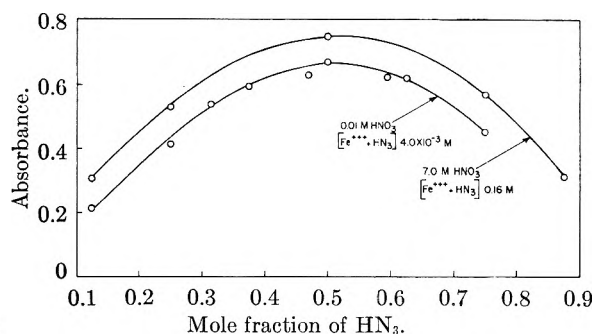


Fig. 1.—Stoichiometry of the reaction between Fe^{+++} and HN_3 .

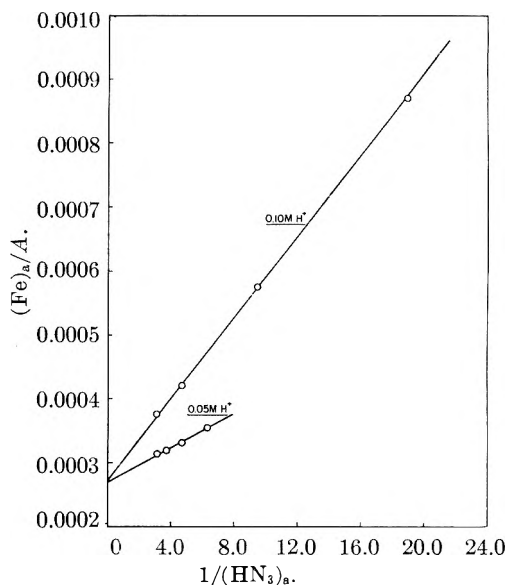


Fig. 2.—Determination of molar extinction coefficient of FeN_3^{++} at 460 $m\mu$.

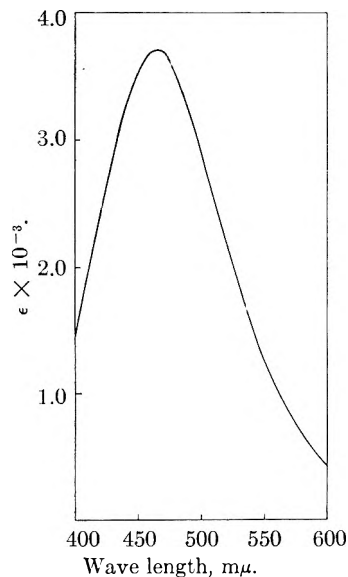
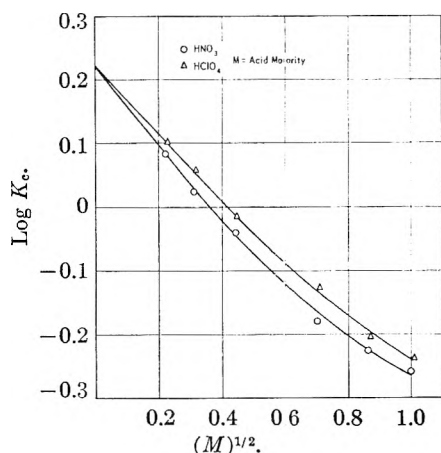
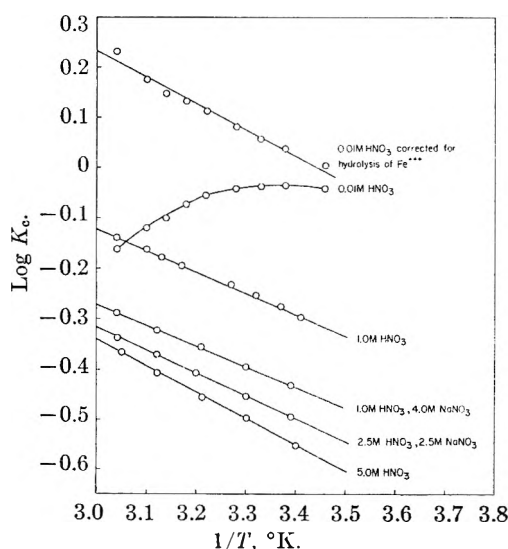


Fig. 3.—Absorption spectrum of FeN_3^{++} .

change when the acidity was doubled, it was assumed to be constant in all experiments.

The determination of the extinction coefficient at one wave length together with absorbance measurements at other wave lengths permitted the deter-

(6) W. C. Vosburgh and G. R. Cooper, *J. Am. Chem. Soc.*, **63**, 437 (1941).

Fig. 4.—Log K_c vs. $(M)^{1/2}$ at 23°.Fig. 5.—Effect of temperature on K_c .

mination of the absorption spectrum of FeN_3^{++} shown in Fig. 3. The maximum in the curve occurs at 465 rather than 460 $m\mu$, but the difference in the extinction coefficients at these two wave lengths is so small that 460 $m\mu$ was used in all these studies.

Effect of Acid Concentrate on Equilibrium Constant.—If equation 1 were valid, the equilibrium constants calculated from equation 3 should be independent of the hydrogen ion concentration, providing the ionic strength was held constant. Equilibrium constants therefore were determined in solutions containing mixtures of HClO_4 and NaClO_4 in which the ionic strength was maintained constant at 0.50 and 1.00 M and the acid concentration was varied from 0.01 to 0.50 M . The results shown in Table II demonstrate that the equilibrium constant is independent of acidity over the range studied. The only significant discrepancies occurred in those measurements at 0.01 M acid; these points have been disregarded in taking the average, for reasons that will be discussed later.

Although the acid concentration did not affect the equilibrium constant significantly, the ionic strength did affect it markedly. The average value of the equilibrium constant decreased from 0.735

TABLE II
EQUILIBRIUM CONSTANTS AT 23° IN MIXTURES OF HClO_4
AND NaClO_4

H^+ , M	K_c	
	0.50 M	1.00 M
0.01	0.679	0.545
.05	.765	.626
.10	.718	.616
.50	.723	.594
Av.	.735	.612

to 0.612 when the ionic strength was increased from 0.50 to 1.00 M .

Equilibrium constants also were determined in nitric acid solutions at concentrations between 0.05 and 8.23 M and in perchloric acid solutions at concentrations between 0.05 and 1 M in the absence of any added salts, so that the ionic strength was equal to the acid concentration. The results of these measurements are shown in Table III. A comparison of the results obtained in nitric and perchloric acids at the same ionic strength shows the equilibrium constants in the perchlorate system to be slightly higher than comparable ones in the nitrate system. The difference is not large but is greater than the experimental error and may be due to some specific interaction between the nitrate and ferric ions. Such an interaction would lower the actual ferric ion concentration without our having taken the decrease into account in our calculation of K_c by equation 3 and would result in values of K_c that are too small.

TABLE III
EQUILIBRIUM CONSTANTS AT 23° IN HNO_3 AND HClO_4

HNO_3 , M	K_c	HClO_4 , M	K_c
0.0496	1.210	0.0509	1.264
.0992	1.059	.102	1.146
.198	0.913	.204	0.969
.496	.661	.509	.747
.744	.596	.764	.623
.992	.550	1.02	.576
2.05	.411		
3.07	.340		
4.05	.304		
5.13	.277		
6.15	.272		
7.13	.259		
8.23	.256		

When $\log K_c$ was plotted against the square root of the acid concentrations as shown in Fig. 4 for the data in Table III, a reasonably good straight line was obtained for acid concentrations below 0.5 M in the perchlorate system. Extrapolation of this line to zero ionic strength gave a value of 1.67 for the equilibrium constant at infinite dilution at 23°. A similar plot of the data obtained in nitric acid can be extrapolated linearly to a value only slightly lower than that obtained in perchloric acid. A smooth curve drawn through the points in the nitrate system, however, can be made to pass through the same point at zero ionic strength as that found in the perchlorate system. The probable interaction between ferric and nitrate ions suggests that the linear extrapolation in the perchlorate system will yield the most reliable value for K_c at infinite dilution.

Although K_c was independent of acidity at lower ionic strengths, it varied slightly with acidity when the ionic strength was 5 *M*. Equilibrium constants of 0.370, 0.320 and 0.281 were obtained for solutions that were 1, 2.5 and 5.0 *M*, respectively, in HNO_3 to which sufficient NaNO_3 was added to maintain a constant ionic strength of 5.0 *M*. These variations are greater than the experimental errors.

Effect of Temperature on Equilibrium Constant.

Equilibrium constants were determined at various temperatures in the range 20 to 58° in solutions which were 0.01, 1.0 and 5.0 *M* in HNO_3 as well as solutions which were 1.0 and 2.5 *M* in HNO_3 and contained sufficient NaNO_3 to maintain a constant ionic strength of 5.0 *M*. The results of these measurements are shown in Fig. 5 in which $\log K_c$ is plotted against $1/T$. The straight lines that are obtained for all except the lowest acid concentration have negative slopes, which demonstrate that the reaction is endothermic. Enthalpies of reaction in the various media are shown in Table IV. The value obtained in 5.0 *M* HNO_3 is significantly higher than the others, which indicates that the medium has an appreciable effect on ΔH at higher acidities. An average of the first three values in Table IV, 2.01 ± 0.10 kcal./mole, is probably the most reliable estimate of ΔH because of the above-mentioned effect of acidity.

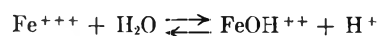
TABLE IV

ENTHALPY OF REACTION IN VARIOUS MEDIA

Medium	ΔH , kcal./mole
1.0 <i>M</i> HNO_3	+2.03
1.0 <i>M</i> HNO_3 , 4.0 <i>M</i> NaNO_3	+1.89
2.5 <i>M</i> HNO_3 , 2.5 <i>M</i> NaNO_3	+2.10
5.0 <i>M</i> HNO_3	+2.42

Anomalous Behavior at 0.01 *M* HNO_3 .—The variation of K_c with temperature in 0.01 *M* HNO_3 appears to be inconsistent with that found in the other solutions. The plot of $\log K_c$ vs. $1/T$ is not only curved but it actually has a positive slope over most of the range of temperatures studied. The values of K_c , however, were calculated with equation 3, which ignores the hydrolysis of ferric ion at low acidities.

The hydrolysis of ferric ion according to the reaction



$$K_h = \frac{(\text{FeOH}^{++})(\text{H}^+)}{(\text{Fe}^{+++})}$$

has been studied previously. Lamb and Jacques⁷ report a value of 2.5×10^{-3} for the equilibrium constant, K_h , at 25°, while Arden⁸ found it to be 1.25×10^{-3} . Rabinowitch and Stockmayer⁹ reported the enthalpy of reaction to be $+12.3 \pm 1$ kcal./mole.

Using a value of 2.0×10^{-3} for K_h at 25° and 12.3 kcal./mole for ΔH , we have calculated K_h at various temperatures and corrected the apparent values of K_c obtained in 0.01 *M* HNO_3 by multiplying them by $[1 + K_h/(\text{H}^+)]^{-1}$. The corrected values are shown in Fig. 5. The line drawn through the corrected points now has a negative constant slope from which the enthalpy of the ferriazide reaction was found to be $+2.38$ kcal./mole. Although this result is not in perfect agreement with those obtained in solutions of higher acidity, it is sufficiently close to demonstrate that the apparent anomaly was due to the hydrolysis of the Fe^{+++} ion. It was because of this hydrolysis and the uncertainty involved in correcting for it that the results obtained previously in 0.01 *M* HClO_4 were disregarded when averages were determined for K_c .

The following thermodynamic quantities for reaction 1 were estimated at 25° and infinite dilution from the value of K_c at infinite dilution at 23° and the enthalpy of the reaction.

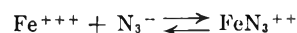
$$K_c = 1.71$$

$$\Delta F_{25^\circ} = -318 \text{ cal.}$$

$$\Delta H_{25^\circ} = 2010 \pm 100 \text{ cal.}$$

$$\Delta S_{25^\circ} = 7.8 \pm 0.3 \text{ e.u.}$$

From the value for K_c given above and the dissociation constant for hydrazoic acid, 2.8×10^{-6} , reported by Quintin,¹⁰ the equilibrium constant for the following reaction was determined.



$$\frac{(\text{FeN}_3^{++})}{(\text{Fe}^{+++})(\text{N}_3^-)} = 6.1 \times 10^4$$

(7) A. B. Lamb and A. G. Jacques, *J. Am. Chem. Soc.*, **60**, 1215 (1938).

(8) T. V. Arden, *J. Chem. Soc.*, 350 (1951).

(9) E. Rabinowitch and W. H. Stockmayer, *J. Am. Chem. Soc.*, **64**, 335 (1942).

(10) M. Quintin, *Compt. rend.*, **210**, 625 (1940).

THE KINETICS OF THE HYDROLYSIS OF THE BICHROMATE ION

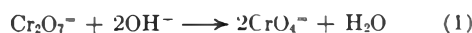
BY ASSA LIFSHITZ AND B. PERLMUTTER-HAYMAN

*Department of Physical Chemistry, Hebrew University, Jerusalem, Israel**Received July 10, 1961*

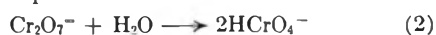
The hydrolysis of the bichromate ion to chromate ion is investigated, using the continuous flow method. A re-investigation of the reaction in the presence of sodium hydroxide shows that the reaction is second order (and not first order as reported previously) with $k_{OH^-}^{II} = (4.3 \pm 0.35) \times 10^2 \text{ mole}^{-1} \text{ l. sec.}^{-1}$. Similarly, in the presence of ammonia, it is second order, with $k_{NH_3}^{II} = (7.4 \pm 0.3) \times 10^2 \text{ mole}^{-1} \text{ l. sec.}^{-1}$. In the presence of the ions phenolate and carbonate the second-order rate constants are much lower, but have been estimated only approximately. A possible mechanism is suggested.

Introduction

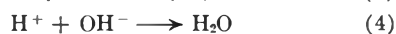
The hydrolysis of the bichromate ion in alkaline solution proceeds according to the stoichiometric equation



The reaction was found by La Mer and Read¹ to be first order with respect to bichromate, and zero order with respect to OH^- . The rate-determining step therefore was assumed to be



followed by fast neutralization according to²



The reaction was found to proceed at a rate which can be measured conveniently by the continuous flow method. (In fact it is quoted as a classical example of the use of the thermal method.³) Employing thermocouples as temperature indicators, the authors found an initial "instantaneous" temperature rise, ΔT_0 , which they ascribed to the fast neutralization of that part of HCrO_4^- which is present in the solution at $t = 0$, owing to equilibrium 2 which is set up in the original bichromate solution. The instantaneous temperature rise was followed by a more gradual one which was ascribed to reaction 1. In 8 experiments, in which the initial stoichiometric concentration of $\text{Cr}_2\text{O}_7^{2-}$ was varied between 0.01 to 0.03 *M*, and that of OH^- between 0.02 to 0.08 *M*, the authors found a first-order rate constant of $8.83 \pm 0.41 \text{ sec.}^{-1}$ at 25°. In order to check our apparatus,⁴ we had previously duplicated one of these experiments (without, however, paying too much attention to the exact value of $[\text{OH}^-]$) and, fitting the data to a first-order rate law, had found a slightly higher value, namely 9.4 sec.^{-1} . At the time, the agreement was considered satisfactory.

Now, the fact that reaction 2 represents the rate-determining step in the hydrolysis in the presence of sodium hydroxide does not prove that a different reaction path might not be available in the pres-

ence of other substances which are capable of converting bichromate into chromate by shifting equilibrium 2 to the right: a direct reaction between $\text{Cr}_2\text{O}_7^{2-}$ and OH^- is unfavorable from an electrostatic point of view; a direct reaction between $\text{Cr}_2\text{O}_7^{2-}$ and an uncharged base might be more probable. It seemed interesting to get some information about this point. We therefore decided to investigate the influence of ammonia on the rate of hydrolysis.

Preliminary experiments, where excess sodium hydroxide had been added in order to keep the ammonia concentration constant during each experiment, showed that the hydroxyl ion concentration had a considerable influence on the rate of hydrolysis. We therefore decided to reinvestigate the reaction in the presence of OH^- . Furthermore, in order to elucidate the influence of charge type, we carried out a few experiments where equilibrium 2 was shifted to the right by $\text{C}_6\text{H}_5\text{O}^-$ and by CO_3^{2-} .

In the general case, the stoichiometric equation takes the form



whereas instead of 4 we write



where B is NH_3 , $\text{C}_6\text{H}_5\text{O}^-$ or CO_3^{2-} , and A the corresponding conjugate acid.

Methods

Experimental.—We also employed a continuous flow apparatus, using the thermal method. Temperature differences were measured by the use of thermistors (Stantel, type F2311/300). A 5-decade Rubicon "High Precision" Wheatstone bridge together with a mirror galvanometer (Kipp and Zonen, double coil, Model A 53) allowed temperature differences to be estimated with an accuracy of $\pm 0.002^\circ$.

The reagents were contained in 10-liter Pyrex flasks with ground glass connections, surrounded by wire netting, and immersed in a thermostat. The thermostat was heated by a single 500 w. immersion heater in series with two resistances. One of them was regulated by hand, according to room temperature, to keep the temperature very slightly below that desired; the other could be short-circuited by a Sunvic hot-wire electronic relay (type EA3(M)), controlled by a mercury thermoregulator, having a capillary of 0.4 mm. diameter. Temperature fluctuations were approximately $\pm 0.002^\circ$ inside the thermostat when measured with a Beckmann thermometer, and presumably less in the vessels containing the reactants. The temperature was 25°.

A pressure of up to 750 mm. was applied over the solutions in order to drive them through the mixing chamber. This was an ordinary 3-way capillary T stopcock, the stem acting as observation tube. The inner diameter was about 2 mm. Within the limit of experimental error, mixing was complete at the first thermistor. The volume between the mixing chamber and each thermistor was determined by weighing the amount of mercury which filled it

(1) V. K. La Mer and C. L. Read, *J. Am. Chem. Soc.*, **52**, 3098 (1930).

(2) Recent views on the subject (see, e.g., M. Eigen, *Z. Elektrochem.*, **64**, 121 (1960); A. Weller, *ibid.*, **34**, 395 (1960)) make it seem more likely that the neutralization should proceed directly according to



However, this does not affect the kinetic results.

(3) F. J. W. Roughton in A. Weissberger, "Technique of Organic Chemistry," Vol. VIII, Interscience Publishers, Inc., New York, N. Y., 1953, p. 669.

(4) E. Giladi, A. Lifshitz and B. Perlmutter-Hayman, *Bull. Research Council Israel*, **A8**, 75 (1959).

exactly. The time during which reaction took place was obtained by dividing this volume by the flow velocity (between 5 and 8 cm.³ sec.⁻¹). Seven thermistors, placed in the observation tube at a distance of about 1.5 cm. from each other, thus enabled us to measure reaction times between 7 and 52 msec. Three additional thermistors were placed after comparatively large volumes (1.4, 2.4, and 4.4 cm.³), and were intended to show ΔT_∞ , the temperature change at the end of the reaction.

The whole apparatus,⁴ and the principle of the thermal method^{1,3} are described elsewhere in greater detail.

The stoichiometric concentration of $\text{Cr}_2\text{O}_7^{2-}$ was measured by titration with FeSO_4 (using diphenylamine as an indicator), both of the original solution and of the reaction mixtures. The ratio of the two concentrations gives the dilution factor which was around 0.5 but varied considerably from one experiment to the other. The concentration of the base was measured only *before* dilution, and its concentration in the reaction mixture was calculated by multiplying by the dilution factor.

Methods of Calculation.—Let us define the first-order rate constant, k^I , by the equation

$$dx/dt = k^I (a - x_t) \quad (\text{I})$$

and the second-order rate constant, k^{II} , by the equation

$$dx/dt = k^{II} (a - x_t)(b - 2x_t) \quad (\text{II})$$

where a is the initial stoichiometric concentration of $\text{Cr}_2\text{O}_7^{2-}$ in the reaction mixture, b that of the base, and x_t the amount of bichromate hydrolyzed at time t (*i.e.*, $[\text{CrO}_4^{2-}] = 2x_t$).

The back reaction need not be taken into account, since even in the presence of ammonia—the weakest base employed—the reaction goes $\geq 99\%$ to completion. This means that $x_\infty = a$ when $b/2 \geq a$; otherwise we have $x_\infty = b/2$.

The values of x_t were calculated from the measured temperature changes, ΔT_t , using the relation

$$x_t = x_0 + (\Delta T_t - \Delta T_0)/(-\Delta H_1) \quad (\text{III})$$

where ΔH_1 is the enthalpy change in reaction 1 or 1a, as the case may be, and the specific heat of the reaction mixture is taken as unity.

Substituting (III) into (I) and integrating we get for k^I

$$k^I t = \ln (\Delta T_\infty - \Delta T_t) + \text{const.} \quad (\text{IV})$$

(provided⁵ $b \geq 2a$). Similarly, substituting III into II we get for k^{II}

$$k^{II} t = -\Delta H_1/2 (\Delta T_\infty - \Delta T_t) + \text{const.}' \quad (\text{V})$$

when $b \approx 2a$. When $b > 2a$, we get

$$k^{II} t = \frac{1}{b - 2a} \ln \frac{-\Delta H_1 (b/2 - x_0) - (\Delta T_t - \Delta T_0)}{\Delta T_\infty - \Delta T_t} + \text{const.}'' \quad (\text{Va})$$

when $b < 2a$, a and $b/2$ exchange places in equation Va. When $b \gg a$, we again use equation IV, replacing k^I by $k^{II}(b - x)$.

The quantities x_0 , ΔT_0 , ΔT_∞ and ΔH_1 , appearing in equations I to V, were obtained in the following way:

(a) From the known concentration of the bichromate solution before mixing, and a knowledge of the dilution factor, we can calculate x_0 , provided we know the equilibrium constant of reaction 2. This is given in the literature⁶ as $K_2 = 3.03 \times 10^{-2}$, which can be corrected to our ionic strength ($\mu = 0.1$ to 0.2) by using the Davies equation⁷; we get $K_2^0 = (1.64$ to $1.85) \times 10^{-2}$. The values of x_0 usually were about $1/5$ to $1/4$ those of a .

(b) The values of ΔT_0 can in principle be obtained from an extrapolation of the ΔT vs. time plot to $t = 0$. However, in most cases this proves to be a fairly long, and therefore inaccurate extrapolation (see fig. 1 for a typical plot).

(5) Otherwise, we have to write

$$k^I t = \ln \left[\frac{\Delta T_\infty - \Delta T_t}{-\Delta H_1} + a - b/2 \right] + \text{const.}''' \quad (\text{IVa})$$

(6) W. G. Davis and J. E. Prue, *Trans. Faraday Soc.*, **51**, 1045 (1955).

(7) R. A. Robinson and R. H. Stokes, "Electrolyte Solutions," Butterworth Scientific Publ., London, 1955, p. 230.

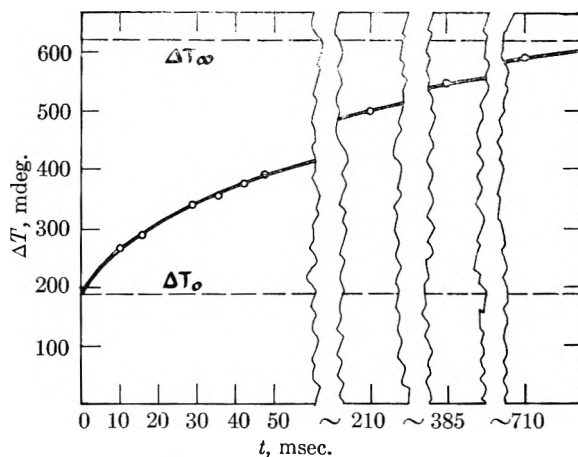


Fig. 1.—The change of temperature with time, for a typical experiment (run 7). The extrapolation to zero time is carried out with the aid of equation VI.

Only in the case of carbonate could ΔT_0 be determined accurately (see Results). We therefore made use of the relation

$$\Delta T_0 = -2x_0(\Delta H_3 + \Delta H_4) \text{ or } 2x_0(\Delta H_3 + \Delta H_{4a}) \quad (\text{VI})$$

as the case may be. Now, the value of ΔH_4 has been measured exactly, and the values of ΔH_{4a} for NH_3 and CO_3^{2-} can be calculated from the temperature dependence of the appropriate equilibrium constants. However, ΔH_3 is not reliably known.¹ We calculated its value from the experiments in the presence of carbonate, using relation VI; from this, we calculated ΔT_0 for all the other experiments, again using relation VI.

(c) The values of ΔT_∞ are equal to the readings of the thermistors farthest away from the mixing chamber, provided at least the two last thermistors record identical values. Otherwise we cannot be sure whether the reaction has indeed gone to completion at the last point measured. This condition was fulfilled only in 8 out of 17 runs.

Now, since x_∞ is known, ($x_\infty = a$, or $b/2$, whichever is less), we could calculate ΔT_∞ from equation III (substituting ∞ for t in the indices) if ΔH_1 were known. No sufficiently reliable measurements are available, however. We therefore calculated ΔH_1 from the 8 experiments where we have reason to believe ΔT_∞ to be reached, and used the result in order to calculate ΔT_∞ from equation I in all other cases.

Results

Experiments in the Presence of Sodium Hydroxide.—Figure 1 shows the dependence of the temperature change on time for a typical experiment (run 7). Details of 7 experiments are given in Table I. Columns 2 and 3 show the initial stoichiometric concentrations of bichromate and hydroxide, respectively. In column 4 we report the initial rapid temperature rise, calculated from equation VI. Columns 5 and 6 show that only in those experiments where hydroxide was in considerable excess did the reaction go to completion during the approximately 0.8 second of observation. From these experiments we calculated ΔH_1 (see column 7)

$$\Delta H_1 = -21.8 \pm 0.6 \text{ kcal. mole}^{-1}$$

In order to calculate the specific rate with respect to bichromate, we plotted the right-hand side of eq. IV (or IVa) against time. Concave curves were obtained in every case, *i.e.*, the specific rate decreases as the reaction proceeds. An example is shown in Fig. 2 (again, run 7). The initial slopes are reported in the table under the heading

TABLE I
 DETAILS OF EXPERIMENTS CARRIED OUT IN THE PRESENCE OF OH⁻

1	2	3	4	5	6	7	8	9	10
Run no.	a × 10 ³	b × 10 ³ Molar	ΔT ₀ × 10 ^{3a}	ΔT × 10 ³ Read from the two last thermistors	ΔT × 10 ³	-ΔH ₁ ^b	ΔT _∞ × 10 ³	k ^I , sec. ⁻¹	k ^{II} , mole ⁻¹ l. sec. ⁻¹
1	18.0	103.0	130	434	434	22.2	434	45	480 ^c
2	16.9	106.5	122	395	397	21.5	397	43	475 ^c
3	20.6	254	151	479	479	21.8	479
4	17.8	275	129	410	410	21.0	410	~130	~430 ^c
5	28.8	49.3	208	520	551		590 ^b	17	505 ^c
6	27.7	51.5	200	543	576		611 ^b	15	455 ^d
7	26.3	54.1	189	548	589		619 ^b	14	465 ^d

^a From equation VI. ^b From equation III. ^c From equation Va. ^d From equation V.

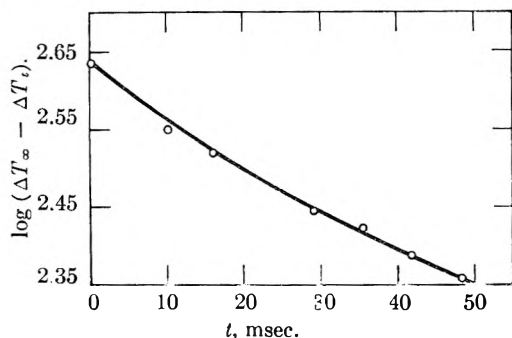


Fig. 2.—The dependence of $\log(\Delta T_{\infty} - \Delta T_t)$ on time, for run 7. For a 1st-order reaction, a straight line would be obtained.

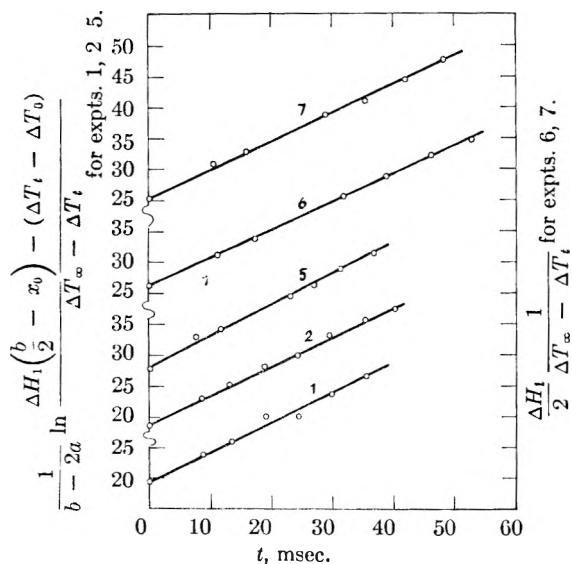


Fig. 3.—Plots of the right-hand side of equation V (expts. 6 and 7) and of equation Va (expts. 1, 2, 5) against time for experiments carried out in the presence of NaOH. Straight, parallel lines correspond to 2nd-order kinetics.

k^I . It is immediately seen that *these do not represent true rate constants*, but increase in a way roughly proportional to b . (Run 3 was so fast that the rate constant could not be evaluated. The results of run 4 are only approximate, since they pertain only to a fairly advanced stage of the reaction.)

We therefore tried whether the results would fit a second-order rate equation. In Fig. 3 we plotted the right-hand side of equation V and Va, respectively, against time. Straight and practically parallel lines are seen to be obtained, *i.e.*, the slopes, which are equal to k^{II} , exhibit no trend with

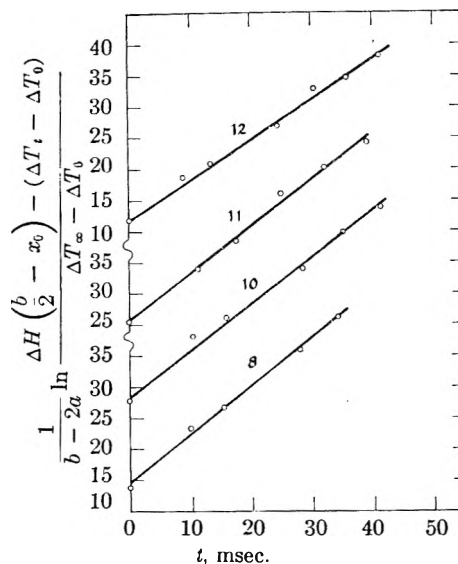


Fig. 4.—Plots of the right-hand side of equation V against time, for experiments carried out in the presence of NH₃. Straight, parallel lines correspond to 2nd-order kinetics.

the concentration of reactants. The values are given in the last column of Table I. We get

$$k^{II}_{OH^-} = (4.6 \pm 0.35) \times 10^2 \text{ mole}^{-1} \text{ l. sec.}^{-1}$$

Experiments in the Presence of Ammonia.—The results of 5 experiments are shown in Table II. Again, ΔH_{1a} can be calculated from those experiments which indeed went to completion. As a mean of 3 experiments we get

$$\Delta H_{1a(NH_3)} = -20.7 \pm 1.0 \text{ kcal. mole}^{-1}$$

The kinetic results are similar to those obtained in the previous section. The values of k^I decrease during each run; the initial values, given in the table, clearly depend on the concentration of the base. On the other hand, k^{II} is constant during each run and exhibits no trend with initial concentrations. This can be seen from Fig. 4, where we again plotted the right-hand side of equation Va against time. From the slopes (see last column of Table II) we get

$$k^{II}_{NH_3} = (7.4 \pm 0.3) \times 10^2 \text{ mole}^{-1} \text{ l. sec.}^{-1}$$

Experiments in the Presence of Sodium Phenolate.—These experiments are only qualitative, especially because we had some difficulties in titrating chromate in the presence of phenol. In one of the two experiments carried out, ΔT_{∞} was reached, and the result was used for the calculation of ΔT_{∞} .

TABLE II
 DETAILS OF EXPERIMENTS CARRIED OUT IN THE PRESENCE OF NH₃

1	2	3	4	5	6	7	8	9	10
Run no.	$a \times 10^3$ Molar	$b \times 10^3$	$\Delta T_0 \times 10^{3a}$	$\Delta T \times 10^3$ Read from the two last thermistors	$\Delta T \times 10^3$	$-\Delta H_{1a}^b$	$\Delta T_\infty \times 10^3$	$k_I, \text{sec.}^{-1}$	$k^{II}, \text{mole}^{-1} \text{l. sec.}^{-1}$
8	20.2	150	119	464	465	21.8	464	70	785
9	22.9	144	135	490	488	19.8	489	72	750
10	22.7	53.8	187	478	502	..	516	18	750
11	17.6	80.0	146	412	409	21.5	410	42	755
12	47.0	114	273	971	1015	..	1053	35	660

^a From equation VI. ^b From equation III. ^c From equation Va.

in the other experiment. Although the phenolate was present in large excess ($b = (178 \text{ and } 400) \times 10^{-3} M$), k^I was low. However, it remained constant during each run. We obtained $k^I = 5$ and 9 sec.^{-1} , respectively, and $k^{II} = 30$ and $23 \text{ mole}^{-1} \text{ l. sec.}^{-1}$, respectively. The latter two values were considered identical within the limits of accuracy in the presence of phenol. Therefore

$$k^{II}_{\text{C}_6\text{H}_5\text{O}^-} \approx 26.5 \pm 3.5 \text{ mole}^{-1} \text{ l. sec.}^{-1}$$

Experiments in the Presence of Sodium Carbonate.—The reaction in the presence of sodium carbonate was found unsuitable for kinetic measurements in our apparatus. However, these experiments form the basis of our calculations of ΔT_0 , and are therefore reported here.

In 4 experiments, the reaction mixture contained 0.035 to 0.036 M $\text{K}_2\text{Cr}_2\text{O}_7$ and 0.045 to 0.098 M Na_2CO_3 . The first seven thermistors registered a small and constant temperature rise of 0.073 to 0.079° . Only at the three last points was a further gradual rise in temperature observed.

This behavior is due to two reasons: (a) The reaction is slow, as verified qualitatively by an improvised "stopped flow" method and an improvised calorimetric flow method, based on visual comparison. (b) The total heat of reaction is low, because⁸

$$\Delta H_{4a}(\text{CO}_3^{2-}) = -3.6 \text{ kcal. mole}^{-1}$$

which is much lower than in the case of OH^- or NH_3 (where $\Delta H_4 = -13.6 \text{ kcal. mole}^{-1}$ and⁹ $\Delta H_{4a}(\text{NH}_3) = -12.4 \text{ kcal. mole}^{-1}$). This gives a total heat of reaction of approximately $-2.5 \text{ kcal. mole}^{-1}$, and approximate values of ΔT_∞ between 0.100 and 0.150° at our concentrations, values which were not reached in our experiments.

A rough estimate of $k^{II}_{\text{CO}_3^{2-}}$ from these values of ΔT_∞ , and the last three values of ΔT_i (for which the values of t are uncertain, since the flow through the larger volumes is not sufficiently well-defined) gave: $k^{II}_{\text{CO}_3^{2-}} \approx 10 \text{ mole}^{-1} \text{ l. sec.}^{-1} \pm 100\%$.

With such a value of the rate constant it can be calculated that ΔT_i in the observation tube proper should change by no more than about 0.002° ; *i.e.*, it is constant within the limit of experimental accuracy.

We therefore may consider the mean value given by the first 7 thermistors to be equal to ΔT_0 . On this assumption, we calculate from equation VI

$$\Delta H_3 = -1.3 \pm 0.13 \text{ kcal. mole}^{-1}$$

which in turn enables us to calculate ΔT_0 in the other 3 series of experiments.

This also enables us to calculate ΔH_2 , which is not reported in the literature. We get

$$\Delta H_2 = 8.0 \pm 0.6 \text{ kcal. mole}^{-1}$$

and

$$\Delta H_2 = 6.7 \pm 1.0 \text{ kcal. mole}^{-1}$$

depending on whether we use ΔH_1 or $\Delta H_{1a}(\text{NH}_3)$. The discrepancy is seen to lie within the limit of experimental error, and may be ascribed to the fact that ΔH_2 is obtained as the difference between comparatively large quantities.

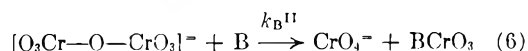
Discussion

Our experimental results lead us to the conclusion that reaction 2 does not represent the rate-determining step in the hydrolysis of bichromate in alkaline solution. The values of k^I corresponding to such a mechanism decrease during any given run (unless the base is in large excess, as was the case for phenolate). More important, they change from one run to the other, increasing with increasing concentration of the base. Finally, they depend on the nature of the base, being much higher in the presence of OH^- and NH_3 than in the presence of CO_3^{2-} and $\text{C}_6\text{H}_5\text{O}^-$.

Although we have considered the problem from several angles, we have no explanation to offer for the discrepancy between this result and the first-order constants reported by La Mer and Read¹ for the reaction in the presence of sodium hydroxide. It should be added that there also exists some disagreement between our value of ΔH_1 , and that reported by these authors ($\Delta H_1 = -15.3 \text{ kcal. mole}^{-1}$).

The constancy of the second-order rate constant in each series of experiments on the one hand, and its dependence on the bases employed, on the other, indicate that these bases bring about the reaction not simply by neutralizing the HCrO_4^- formed in the hydrolysis, and thus shifting the equilibrium to the right; instead, they seem to react directly with the bichromate ion in a rate-determining bimolecular step. Several instances of such behavior have been reported in recent years.¹⁰

The mechanism of our reaction can be pictured as consisting of a rupture of a Cr-O bond in the rate-determining step, according to

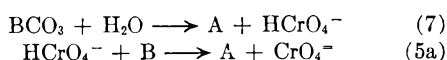


(8) See ref. 7, p. 496.

(9) R. P. Bell, "The Proton in Chemistry," Cornell University Press, Ithaca, N. Y., 1958, p. 65.

(10) See, for instance, quotations in footnote 2; see also: A. Lifshitz and B. Perlmutter-Hayman, *Bull. Research Council Israel*, **8A**, 160 (1959); *J. Phys. Chem.*, **65**, 753 (1961).

followed by a rapid sequence



When the reactant is OH^- step 7 is of course redundant.

Since the choice of bases which can bring about the hydrolysis of bichromate is rather limited, no definite pronouncement can be made at present about the connection between k^{II}_{B} and the nature of the reagent employed.

However, a comparison between $k^{\text{II}}_{\text{OH}^-}$ and

$k^{\text{II}}_{\text{C}_6\text{H}_5\text{O}^-}$ seems to show a certain correlation between the basicity of the reactant and the rate constant. Such a correlation is to be expected in view of the existence of general free energy relationships.¹¹ On the other hand, it is not surprising that any such correlation should be counteracted by the influence of the charge type. This influence can be inferred from the similarity between $k^{\text{II}}_{\text{OH}^-}$ and $k^{\text{II}}_{\text{NH}_3}$, and from the extremely low value for $k^{\text{II}}_{\text{CO}_3^{2-}}$.

(11) A. A. Frost and R. G. Pearson, "Kinetics and Mechanism," John Wiley and Sons, Inc., New York, N. Y., 1953, p. 214 ff.

NOTES

MOLECULAR ORBITAL CALCULATIONS FOR CYCLOOCTATETRAENE¹

BY GUENTER AHLERS AND JAMES F. HORNIG

Department of Chemistry, University of California, Riverside, California

Received December 2, 1960

Calculations for the molecule cyclooctatetraene indicate that a simple extension of Hückel type molecular orbital theory² may be used in this case to estimate the relative stability of geometric configurations of a molecule with a non-planar π -electron system. It is necessary only to modify the resonance integral β to take into account the relative twist of neighboring p orbitals. The effect on β of varying bond lengths is somewhat larger here than in planar ring systems, so we have taken it into account by means of an approximation due to Mulliken.³ The effect of bond length is smaller than that due to twist, so that the qualitative results do not depend critically on the approximation.

Hückel recognized that cyclooctatetraene probably would be puckered, so his calculations for a planar model would not be appropriate. Lippincott and Lord⁴ demonstrated by analysis of Raman spectra that the molecule was indeed puckered. The detailed geometric configuration of the molecule became the subject of numerous investigations, and the boat, crown and chair configurations (Fig. 1) all were proposed. The most recent investigation is the electron diffraction study by Bastiansen, *et al.*,⁵ which establishes the boat configuration. The present calculations support this result.

Modified Resonance Integral.—Experimental bond angles of cyclooctatetraene indicate that the σ bonds may deviate substantially from sp^2 hybridiza-

tion. For the degree of approximation intended here, we assume that the π electron orbitals still can be described adequately by linear combinations of hydrogen-like 2p orbitals. For neighboring hydrogen-like 2p orbitals twisted through an angle ϕ , the resonance integral is proportional to $\cos \phi$

$$\beta_\phi = \beta^0 \cos \phi$$

The effect of variations in the bond length, ρ , on the resonance integral has been estimated by Mulliken.³ We incorporate his results in a factor $k(\rho)$

$$\beta_\rho = k(\rho)\beta_{1.39}$$

As Mulliken points out, this estimate already includes a contribution from the compression energy of the σ bonds. More refined estimates of $k(\rho)$ would yield slightly different results, but since the contribution is smaller than that from twist, this approximation is satisfactory.

If the effects of stretching and twisting are independent, the resonance integral may be written

$$\beta_{\rho\phi} = k(\rho) \cos \beta^0_{1.39}$$

Here $\beta^0_{1.39}$ is the value appropriate to an untwisted bond of length 1.39 Å. The π electron energy of any particular configuration may be calculated by evaluating the secular equation containing the values of $\beta_{\rho\phi}$ appropriate to the assumed geometry.

Boat Configuration (D_{2d}).—In this configuration the molecule has four untwisted bonds (type a, Fig. 1A) and four bonds (type b) with a relative twist, ϕ , given by

$$\cos \phi = \cot^2 \theta$$

where θ is the C-C-C bond angle. The a and b bond types will have different lengths, so the secular equation will contain two different resonance integrals

$$\begin{aligned} \beta_a^0 &= k(a) \beta^0_{1.39} \\ \beta_b^0 &= k(b) \cot^2 \theta \beta^0_{1.39} \end{aligned}$$

The secular equation may be solved analytically, giving a ground state energy for the eight π electrons of

$$E_{\pi^{\text{boat}}} = 8\alpha + 4\{k(a) + [k(a)^2 + k(b)^2 \cot^2 \theta]^{1/2}\} \beta^0_{1.39}$$

Here α is the coulomb integral.

(1) Based on a thesis submitted by Guenter Ahlers in partial fulfillment of the requirements for the degree of Bachelor of Arts, University of California, Riverside, California.

(2) E. Hückel, *Z. Physik*, **70**, 204 (1931).

(3) R. S. Mulliken, C. A. Rieke and W. G. Brown, *J. Am. Chem. Soc.*, **63**, 41 (1941).

(4) E. R. Lippincott and R. C. Lord, *ibid.*, **73**, 3889 (1951).

(5) O. Bastiansen, L. Hedberg and K. Hedberg, *J. Chem. Phys.*, **27**, 1311 (1957).

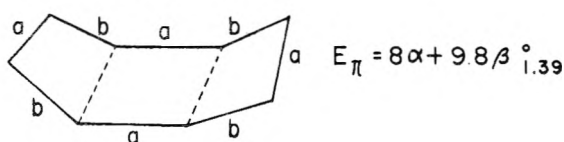
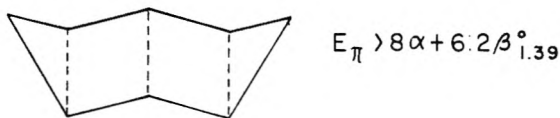
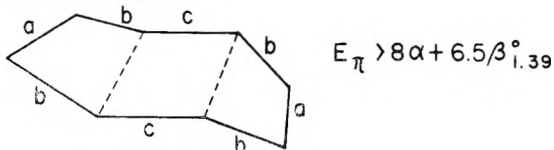
A. BOAT (D_{2d})B. CROWN (D_{4d})C. CHAIR (C_{2h})

Fig. 1.—Ground state pi electron energies calculated for three configurations of cyclooctatetraene.

Using Bastiansen's molecular parameters, $\theta = 126.5^\circ$, $a = 1.33 \text{ \AA}$., $b = 1.46 \text{ \AA}$., and Mulliken's data for $k(\rho)$, one obtains

$$E_{\pi}^{\text{boat}} = 8\alpha + 9.8\beta^0_{1.39}$$

Crown Configuration (D_{4d}).—All eight bonds are equivalent in this configuration (Fig. 1B), with a relative twist, ϕ , given by

$$\cos \phi = \frac{|\cos \theta + 2 \cos \pi/4 - 1|}{1 + \cos \theta}$$

Solution of the secular equation gives a ground state energy of

$$E_{\pi}^{\text{crown}} = 8\alpha + 9.66\beta_{\rho}\phi$$

For $\rho = 1.42 \text{ \AA}$., $\theta = 125^\circ$, this gives

$$E_{\pi}^{\text{crown}} = 8\alpha + 3.3\beta^0_{1.39}$$

Since $\beta^0_{1.39}$ is negative, this configuration is unstable with reference to the boat configuration by $5.5 |\beta^0_{1.39}|$. Assuming even the most favorable bond length, that appropriate to benzene, $\tau = 1.39 \text{ \AA}$., and a relatively flattened molecule, $\theta = 130^\circ$, gives

$$E_{\pi}^{\text{crown}} = 8\alpha + 6.2\beta^0_{1.39}$$

which is still $3.6 |\beta^0_{1.39}|$ less stable than the boat form.

Chair Configuration (C_{2h}).—The chair configuration has three kinds of bonds (Fig. 1). The four type **b** bonds are twisted by an angle ϕ_b given by

$$\cos \phi_b = \cot^2 \theta$$

just as in the boat configuration. The two type **a** bonds are untwisted, but the remaining two type **c** bonds are twisted by an angle ϕ_c given by

$$\cos \phi_c = |2 \cot^2 \theta - 1|$$

The twist in the **c** bond is considerable, so that neighboring p orbitals are eclipsed completely in the vicinity of $\theta = 125^\circ$.

A numerical solution of the secular equation involving three different resonance integrals showed that the chair configuration is considerably less

stable than the boat, though comparable to the crown form. For the calculation we chose parameters relatively favorable for stability: $\theta = 130^\circ$, $a = 1.33 \text{ \AA}$., $b = 1.46 \text{ \AA}$., and $c = 1.50 \text{ \AA}$.. The energy in this configuration was found to be

$$E_{\pi}^{\text{chair}} = 8\alpha + 6.5\beta^0_{1.39}$$

Conclusions

The boat configuration is favored energetically over the crown and chair configurations by about $3.5 \beta^0_{1.39}$ in these calculations, thus agreeing with Bastiansen's experimental results favoring the boat configuration. It is interesting to note that although the calculation is intended primarily to give relative results for several possible configurations, the predicted stabilization energy of the boat configuration is comparable to the experimental resonance energy. The energy of four isolated double bonds would be $8k(1.33)\beta^0_{1.39}$ or $9.5\beta^0_{1.39}$, so our calculations predict a stabilization energy of $0.3|\beta^0_{1.39}|$, or about 11 kcal./mole, using -37 kcal./mole as a reasonable estimate of $\beta^0_{1.39}$.^{6,7} The experimental resonance energy is 4 kcal./mole.

It may be possible to estimate the relative stability of various configurations of other non-planar π electron systems in this way. Reliable quantitative calculations, or comparisons of configurations differing widely in C-C-C bond angles would require a more careful treatment which included change in hybridization and an explicit evaluation of the energy of the σ system.

(6) G. Glockler, *J. Chem. Phys.*, **21**, 1242 (1953); R. S. Mulliken and R. G. Parr, *ibid.*, **19**, 1271 (1951).

(7) H. D. Springall, T. R. White and R. C. Cass, *Trans. Faraday Soc.*, **50**, 815 (1954).

A NEW METHOD FOR STUDYING PORE SIZES BY THE USE OF DYE LUMINESCENCE¹

BY JEROME L. ROSENBERG AND DONALD J. SHOMBERT

Contribution No. 1032 from the Department of Chemistry, University of Pittsburgh, Pittsburgh 13, Pennsylvania

Received January 10, 1961

In connection with some recent work on the mechanism of the reaction of oxygen with photoexcited adsorbed dyes,² we found that the penetration of oxygen through the pores of the adsorbent was rate-limiting in some cases. It occurred to us that photochemical observations under these conditions might be used to study the pore characteristics of the adsorbent. This note summarizes the experimental basis and outlines the possibilities of application for such a porosimeter.

Procedure.—The method of study has been described in detail previously.² Briefly, a suitable phosphorescent dye was adsorbed on the porous substance. The principal criteria in the selection of the dye were high adsorbability

(1) Presented before the 138th National Meeting of the American Chemical Society, New York, September 13, 1960. This work was supported by the National Science Foundation under Grant NSF-G6271. The material presented here is abstracted from a dissertation presented to the University of Pittsburgh by Donald J. Shombert in partial fulfillment of the requirements for the Ph.D. degree in January, 1959.

(2) J. L. Rosenberg and D. J. Shombert, *J. Am. Chem. Soc.*, **82**, 3257 (1960).

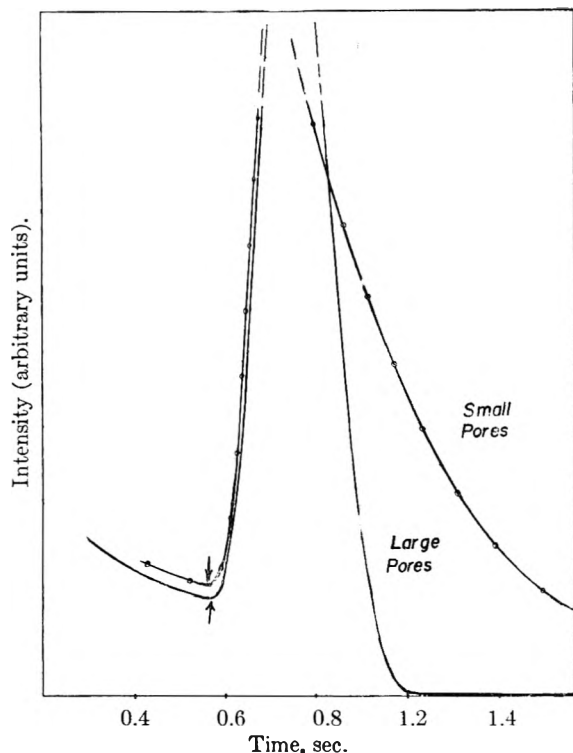


Fig. 1.—Effect of pore size on rate of chemi-luminescence. Concentration, $2.5 \mu\text{mole acriflavine/g. silica}$; observation wave length, $500 \text{ m}\mu$; temperature, -100° ; oxygen pressure at infinite time, 0.04 mm . Arrows denote admission of oxygen. Large- and small-pore gels as described in text.

(minimum of 10^{-8} mole of dye per gram of adsorbent) and a phosphorescence, of convenient mean life (about one second), quenched readily by oxygen. Typical systems are acriflavine-silica gel and fluorescein-alumina. The adsorbate sample was placed on a vacuum line, where it was baked out. Its phosphorescence, excited with a flash lamp, was intercepted by a photomultiplier tube, and the intensity-time curve was displayed on an oscilloscope. While the phosphorescence still was decaying oxygen was admitted to the sample through a solenoid-operated mercury valve. By a proper choice of optical filters between the sample and the photomultiplier, it was possible to observe either the direct triplet to ground delayed emission of β -phosphorescence or the chemi-luminescence accompanying the oxygen-dye reaction (Fig. 1 in ref. 2). The former process could be observed readily at any temperature from -160° to room temperature; the latter was most conveniently studied at -100° .

Results

The rate of either type of luminescence decay following admission of oxygen was found to depend on the rate of penetration of oxygen through the pores of the adsorbent. This fact was proved by two types of observation on adsorbates of acriflavine on silica gel.

(a) Although the phosphorescence at -100° persisted for about a second if oxygen at a pressure of 10^{-3} mm . was admitted to the sample within 0.1 second after a flash, the luminescence was completely quenched in less than 10 milliseconds if the same pressure of oxygen was equilibrated with the sample before the flash. The rate-limiting factor in the former case must be the flow of oxygen to the site of dye adsorption. Greater discrepancies existed at higher pressures. Two regions of hindered gas flow can be distinguished in these gels, flow

between the gel granules and flow within the pores of a single granule. Adsorption can be excluded as the rate-limiting process on the grounds (a) that the amount of oxygen adsorbed on the gel at these temperatures is insufficient to account for the quenching observed,³ and (b) that the kinetic evidence, from both steady state and transient experiments, indicates that oxygen quenching is a diffusion-limited process,² about one in ten collisions being effective in quenching.

Flow between the granules is quite fast and limitations due to this region can be eliminated by using samples with a small number of granules. We found that if the oxygen was added after the flash, the time of rise of chemiluminescence intensity depended on the time for passage of gas between the granules and the rise time could be shortened to less than 0.1 second by reducing the number of granules in the sample. The time for decay after the maximum, however, was independent of the number of granules in the sample. Therefore the decay time in oxygen is related to the time of flow of oxygen through the pores of a single granule.

(b) Experiments of this kind were performed under identical conditions for two samples that differed only in the average pore size of the gel. In both cases the gel contained 2.5 micromoles of acriflavine per gram, the temperature was -100° , the chemi-luminescence was observed through a $500 \text{ m}\mu$ interference filter, and the oxygen pressure after admission was 0.04 mm . The two gels had the same granule size and equal amounts were used for the two experiments. One gel, a standard Davison preparation, had fairly small internal pores, 30 to 50 \AA . The other gel, made by sintering of pure silica beads, is known to have fairly large internal pores, about 300 \AA , and to be free of small pores.⁴ The final decay of luminescence was much faster in the large pore gel, presumably because oxygen can reach the dye sites more rapidly (Fig. 1). Similar differences in the slopes of decay of the β -phosphorescence were observed for samples that differed in internal pore size.

Discussion

We propose that these differences in luminescence decay rate might be used to determine the internal pore sizes of adsorbent substances. The method is applicable to any substance which can adsorb a suitable phosphorescent dye, so long as the adsorbent transmits the dye's excitation and luminescent bands. Complications due to dye-gel interaction⁵ have ruled out a complete kinetic analysis of the system. Nevertheless, a single experimental parameter, such as the rate constant for the apparently exponential decay portion of the chemi-luminescence curves in Fig. 1, should be relatable to an

(3) Oxygen adsorption was not measured under these experimental conditions, but estimates were made by extrapolating data from higher pressures as determined for similar samples by W. D. Urry, *J. Phys. Chem.*, **36**, 1831 (1932). These extrapolations indicate that the mole ratio of adsorbed oxygen to dye was less than 0.01.

(4) We are indebted to Dr. W. Keith Hall, of Mellon Institute, for furnishing this silica sample, described as X-88 aerogel in Fig. 5 of W. K. Hall, D. S. MacIver and H. P. Weber, *Ind. Eng. Chem.*, **52**, 421 (1960). Curve C in this same reference describes a material similar in porosity to the Davison gel used by us.

(5) J. L. Rosenberg and D. J. Shombert, *J. Am. Chem. Soc.*, **82**, 3252 (1960).

average pore size. The relationship could be determined by calibration against a primary pore-size measurement. The range of 10 to 1000 Å. in pore diameter would be involved. If the method were to be used, adsorbent granules should be of the same over-all dimensions to avoid differences in the rate of flow between granules. At least one granule dimension should be greater than 1 millimeter so that the inter-granular flow does not become rate-limiting.

AN OXIDE OF TERVALENT NICKEL

BY P. S. AGGARWAL AND A. GOSWAMI

National Chemical Laboratory, Poona-8, India

Received April 11, 1961

While iron and cobalt exist in di- and trivalent states in the oxides of compositions MO , M_2O_3 , and M_3O_4 , the existence of anhydrous Ni_2O_3 has been doubted by many workers. Attempts to prepare this by heating the hydroxide, basic carbonate or nitrate of nickel in air or oxygen resulted in the formation of NiO only.¹ Cairns and Ott² prepared from solutions a compound of the composition $Ni_2O_3 \cdot 2H_2O$, which decomposed to $Ni_2O_3 \cdot H_2O$ and finally to NiO , as revealed by X-ray studies. No line characteristic of N_2O_3 was at all detected. Rooksby³ showed, by X-rays, that different oxides of nickel, black or otherwise, obtained from various sources consisted only of NiO . During electron diffraction studies of evaporated films of nickel, on hot rocksalt substrates *in vacuo*, we observed many rings in diffraction patterns, which could not be explained by the presence of Ni and NiO alone, but required the existence of an oxide having a hexagonal structure.

Nickel was evaporated from a nickel filament (spec. pure, supplied by M/s. Johnson and Matthey & Co., London) at a pressure of about 10^{-1} to 10^{-2} mm. (obtained by a rotary oil pump) on the cleavage face of rocksalt crystals kept at about 400° . After removal of the films from the substrate in the usual way, these were examined in the E.D. camera by transmission methods.

TABLE I^a

Ni_2O_3			Co_2O_3 ⁴		
	$a_0 = 4.61$ $c_0 = 5.81$ $c_0/a_0 = 1.22$			$a_0 = 4.64$ $c_0 = 5.75$ $c_0/a_0 = 1.24$	
d	Intensity	hkl	d	Intensity (X-rays)	
3.23	vf	101	3.21	90	
2.80	s	002	2.87	100	
2.30	ms	110	2.33	100	
2.02	s	200	
1.77	s	112	1.78	100	
1.62	s	202	1.63	90	
..	..	210	1.57	50	
1.40	f	004	1.39	90	
1.11	f	

^a v, very; f, faint; s, strong; and m, medium.

Patterns thus obtained, consisting of rings and spots, mostly were due to nickel, though sometimes extra rings of NiO and the unknown oxide were

noticed. The epitaxially grown nickel films mostly developed parallel orientations. They were occasionally mixed with a small amount of crystals which were aximuthally rotated by 45° , *i.e.*, they thus had $\langle 110 \rangle$ axis parallel to $\langle 110 \rangle$ axis of $NaCl$. $\{111\}$ twinned structures of the oxide were observed also. In some cases the patterns due to unknown oxide were predominant. Using 220 rings of either NiO or Ni , the d_{hkl} values were evaluated and rings indexed. Table I shows these values which agree well with a hexagonal structure having $a_0 = 4.61$ Å., $c_0 = 5.61$ Å. and $c_0/a_0 = 1.22$.

It is, however, interesting to note that cobaltic oxide (Co_2O_3) has a similar hexagonal structure ($a_0 = 4.64$ Å., $c_0 = 5.75$ Å., $c_0/a_0 = 1.24$) with its d values and intensities of rings⁴ very close to those of the oxide of nickel mentioned above (Table I). From the consideration of similarities in the properties of cobalt and nickel compounds and their isomorphous nature and also of the fact that similar chemical compounds have similar structures, it may be concluded that the observed hexagonal structure is very likely due to the formation of the oxide of trivalent nickel (Ni_2O_3), as in the case of cobaltic oxide (Co_2O_3). It may, however, be pointed out here that in the absence of accurate intensity data of Co_2O_3 , the comparison cannot be carried out too far.

(4) A.S.T.M. Card No. 2-0770.

PRIMARY STEPS IN THE PHOTOLYSIS OF METHYL CARBONATE¹

BY M. H. J. WIJNEN

Radiation Research Laboratories, Mellon Institute, Pittsburgh, Pa.

Received May 1, 1961

Investigations of the photolysis of methyl acetate^{2,3} have shown that the main primary process produces methoxy radicals according to



A similar step in the photolysis of methyl carbonate would lead to CH_3OCO and CH_3O radicals and possibly to $2CH_3O$ and CO if the CH_3OCO radicals would decompose into carbon monoxide and methoxy radicals. This investigation has been undertaken to investigate the feasibility of using the photolysis of methyl carbonate as a source for methoxy radicals.

Experimental

Since it has been observed⁴ that methyl carbonate decomposes thermally on quartz, the photolysis was studied at 6 and at 80° only. The usual photochemical technique has been applied. A Hanovia Type 73A10 (S-500) medium pressure arc was used to obtain the data at 80° . Constant temperature at 80° was maintained by an aluminum block furnace. Temperature control at 6° was obtained by placing the cell in a water-bath and transmitting the light through a 5 mm. layer of water into the cell. A Hanovia medium pressure arc (Type 16A13) was used as the light source for the experiments at 6° . Analysis of the reaction products

(1) This investigation was supported, in part, by the U. S. Atomic Energy Commission.

(2) (a) W. L. Roth and G. K. Rollefson, *J. Am. Chem. Soc.*, **64**, 490 (1942); (b) P. Ausloos, *Can. J. Chem.*, **36**, 383 (1958).

(3) (a) M. H. J. Wijnen, *J. Chem. Phys.*, **27**, 710 (1957); (b) **28**, 271 (1958); (c) **28**, 939 (1958).

(4) M. H. J. Wijnen, *ibid.*, **34**, 1465 (1961).

(1) R. W. Cairns and E. Ott, *J. Am. Chem. Soc.*, **55**, 527 (1933).

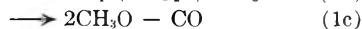
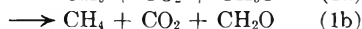
(2) R. W. Cairns and E. Ott, *ibid.*, **55**, 534 (1933).

(3) H. P. Rooksby, *Nature*, **152**, 304 (1943).

was carried out by gas chromatography. The following reaction products were observed: CO, CO₂, CH₄, C₂H₆, CH₃OH, CH₃OCH₃ and CH₂O. No quantitative analysis was carried out for formaldehyde. The amounts of methyl ether produced were too small to be measured accurately. Table I gives the observed product distribution under various conditions of light intensities and initial pressures. The conversion was on the order of 0.5% of the starting material.

Discussion.

Within experimental error CO and CO₂ are directly proportional to incident light intensity and to initial pressure. Accepting, therefore, that they are produced in the primary process, the steps to be considered are



It is obvious that as an intermediate the CH₃OCO radical may have been formed. Attempts to identify methyl oxalate and methyl acetate as reaction products failed. This indicates that under our experimental conditions the CH₃OCO radical must decompose readily if formed. Surprising is the relatively large amount of methane formed. In addition to primary step 1b, methane could conceivably be produced by the reactions

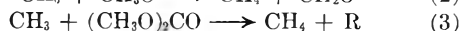


TABLE I

PHOTOLYSIS OF METHYL CARBONATE						
(CH ₃ O) ₂ -CO, molec./cc. × 10 ⁻¹¹	Intensity relative %	R _{CO}	R _{CO₂}	R _{CH₄}	R _{C₂H₆}	R _{CH₃OH}
Temp., 6°						
4.84	100	29.0	162.1	70.1	28.0	85.0
1.80	100	12.2	66.7	36.0	5.4	32.9
4.80	9	2.0	11.4	7.9	1.5	6.8
4.12	9	1.9	12.1	6.4	1.2	4.2
5.28	25	5.9	41.3	21.6	4.2	21.0
1.81	60	8.3	49.5	20.3	4.5	27.1
4.43	30	6.1	41.8	15.1	6.7	20.5
Temp., 80°						
12.60	100	15.9	208.6	51.4	45.9	122.8
6.58	100	9.5	93.4	24.0	21.6	47.0
3.65	100	5.9	61.1	18.7	8.2	28.8
11.78	100	11.9	157.5	34.3	33.1	61.2
11.95	25	2.5	31.5	7.0	6.5	17.7
11.81	9	1.4	17.5	3.6	3.2	6.4
11.90	50	6.6	72.4	15.5	13.1	50.7

Previous results^{3b} indicate that $k_2/k_4 \approx 1.4$ (where k_4 is the rate constant of reaction 4).

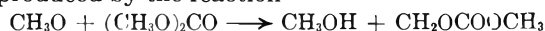


Since only trace amounts of methyl ether have been detected, reaction 2 may be excluded as contributing in any appreciable extent to the amount of methane produced. Reaction 3 undoubtedly requires an activation energy of not less than 8 kcal. in analogy to other activation energies for the abstraction of a primary hydrogen by methyl radicals. This reaction thus is not likely to occur to any large extent at the relatively low temperatures of our investigation. It therefore seems reasonable to suggest primary step 1b as the main source of methane production. It may be mentioned that molecular rearrangements have been observed also in the photolysis of other esters.^{2b}

The recombination of methyl radicals, produced by step 1a, is suggested as the sole mode of ethane formation. Step 1a also produces methoxy radicals which may form methanol *via* disproportionation and/or hydrogen abstraction. The amount of methanol produced by step 1c, if occurring, could not exceed twice the amount of CO produced. Our results at 80° indicate that $R_{\text{CH}_3\text{OH}} \gg 2R_{\text{CO}}$ thus confirming step 1a also through the production of methanol.

The large yield of CO₂ indicates clearly that primary steps 1a and 1b constitute a major part of the total primary process. Steps 1c and/or 1d are suggested to explain the formation of carbon monoxide. Since methoxy radicals produced by step 1c may form methanol and formaldehyde it is difficult to choose between these two steps. We are inclined to give a slight preference to step 1d based on the following observation. We may calculate the importance of the CO and CH₄ producing primary steps if we accept $R_{\text{CO}} + R_{\text{CO}_2}$ as a measure of the total primary process. Such calculations indicate that the fractions of the primary process leading to CO and CH₄ are roughly 0.14 and 0.4 at 6° and 0.08 and 0.23, respectively, at 80°. This is not necessarily a temperature effect since different light sources and thus possibly different wave lengths were used. The contribution of the CO and CH₄ producing steps to the total primary process thus varies considerably with the experimental conditions of our investigation. Nevertheless, the ratio $R_{\text{CO}}/R_{\text{CH}_4}$ remains approximately constant. This indicates that CO and CH₄ may originate from the same electronic excitation level. This would be the case if CO is produced by molecular rearrangement step 1d which is similar to the production of methane by step 1b. This consideration does not exclude the possibility that step 1c also may occur to some extent. Our data do not suggest the occurrence of primary steps other than steps 1a to 1d.

It is clear from primary steps 1a and 1b that $(R_{\text{CH}_4} + 2R_{\text{C}_2\text{H}_6})/R_{\text{CO}_2}$ should be equal to unity. The actual observed value indicates $(R_{\text{CH}_4} + 2R_{\text{C}_2\text{H}_6})/R_{\text{CO}_2} \approx 0.7$. This deficiency in methyl radicals may be explained by the addition of methyl radicals to the CH₂OCOOCH₃ radical which is produced by the reaction



That methoxy radicals are able to abstract primary hydrogens at the relatively low temperatures of our investigation has been shown previously.³ Since we have not analyzed for formaldehyde, it is not possible to carry out material balance calculations for the methoxy radical.

Acknowledgment.—The author wishes to express his sincere thanks to Mr. J. A. Guercione for his aid in this investigation.

VAPOR PRESSURES OF PLATINUM METALS. II. RHODIUM

BY LLOYD H. DREGER AND JOHN L. MARGRAVE

Department of Chemistry, University of Wisconsin, Madison, Wisconsin

Received May 27, 1961

New vapor pressure data are reported here for

metallic rhodium which previously has not been studied quantitatively. The recent survey of Honig¹ cites only an estimated vapor pressure and heat of sublimation.

Experimental Apparatus and Techniques

The apparatus used was a microbalance inside a vacuum system and has been described previously along with the calculation methods.² The high purity wire (99.99 + %) was suspended from a single crystal MgO hook and no reaction was observed.

Discussion of Results

The results of the sublimation studies on Rh are summarized in Table I. Monatomic Rh(g) was assumed to be the only important gaseous species. Combination of the vapor pressures with free energy functions from Stull and Sinke³ allows computation of a third law heat of vaporization at 298°K. A plot of P vs. $1/T$ yields the heat of sublimation at the high temperature from the slope and correction to 298°K. can be accomplished by using heat content data from Stull and Sinke.³

From Table I, the heat of sublimation of Rh at 298°K. is 134.2 ± 0.8 kcal./mole and the extrapolated normal boiling point is $3900 \pm 100^\circ\text{K}$. The second law treatment of $\log P$ vs. $1/T$ data yields $\Delta H_{298}^0 = 135 \pm 2$ kcal./mole, in good agreement.

TABLE I

VAPOR PRESSURE DATA FOR RHODIUM METAL

The $\log P$ vs. $1/T$ plot gives $\Delta H = 137.7$ at $T_{\text{avg}} = 1925$ which when corrected to 298°K. using Stull and Sinke's data gives $\Delta H_{298}^0 = 135 \pm 2.0$ kcal./mole.

Run no.	$T, ^\circ\text{K}$.	P_{mm}	ΔH_{298}^0 (kcal./mole)
12	1942	1.17×10^{-6}	138.5 ^a
13	1942	3.50×10^{-6}	134.2
14	1942	2.72×10^{-6}	135.2
15	1975	4.16×10^{-6}	135.8
16	2068	5.32×10^{-4}	131.6
17	2068	3.09×10^{-4}	133.8
18	2068	3.60×10^{-4}	133.2
19	2068	3.33×10^{-4}	133.5
20	2068	3.01×10^{-4}	133.9
21	1962	1.33×10^{-4}	130.4 ^a
22	1975	7.19×10^{-6}	133.6
23	2006	1.19×10^{-4}	133.7
25	1744	4.73×10^{-7}	135.7
26	1857	7.29×10^{-6}	134.2
27	1857	5.80×10^{-6}	135.1
28	1803	2.22×10^{-6}	134.7
29	1803	2.00×10^{-6}	135.1

$$\Delta H_{298}^0 = 134.2 \pm 0.8 \text{ kcal./mole}$$

^a Large deviation. Given 0 weight in average.

NOTE ADDED IN PROOF.—Two recent reports verify the results reported here. Hampson and Walker⁴ have reported

(1) R. C. Honig, "Vapor Pressure Data for the More Common Elements," R. C. A. Laboratories, David Sarnoff Research Center, Princeton, N. J., 1957.

(2) L. H. Dreger and J. L. Margrave, *J. Phys. Chem.*, **64**, 1323 (1960).

(3) D. R. Stull and G. C. Sinke, "Thermodynamic Properties of the Elements," *Advances in Chemistry Series*, No. 18, Amer. Chem. Soc. (1956).

(4) (a) R. F. Hampson and R. F. Walker, *J. Research Natl. Bur. Standards*, **66A**, 289 (1961); Abstracts, XVII Intern. Congr. Pure and Appl. Chem., Montreal, August, 1961 p. 101.

data for rhodium which indicate $\Delta H_{298} = 132.5 \pm 2.0$ kcal./mole, while Panish and Reif⁵ have reported $\Delta H_{298} = 132.8 \pm 0.3$ kcal./mole.

Acknowledgment.—The authors are pleased to acknowledge the financial support of this research by the Wisconsin Alumni Research Foundation and the Atomic Energy Commission. Samples of high purity Rh wire were generously provided by the International Nickel Company through the courtesy of E. M. Wise.

(5) M. B. Panish and L. Reif, *J. Chem. Phys.*, **34**, 1915 (1961).

THERMODYNAMICS OF IONIZATION OF AQUEOUS *meta*-CHLOROPHENOL

BY W. F. O'HARA AND L. G. HEPLER

Department of Chemistry, University of Virginia, Charlottesville, Va.

Received June 1, 1961

It has been found¹ that the differences in free energies of ionization of the three mono nitrophenols in aqueous solution are due to entropy rather than enthalpy effects. The entropies of ionization are different because the anions of *o*-nitrophenol and *p*-nitrophenol distribute their negative charge to the nitro group more than do anions of *m*-nitrophenol, in accord with conventional ideas about the small tendency of *meta* substituents, as compared to *ortho* and *para* substituents, to take part in resonance with the phenolic function. The differences in charge distribution cause differences in solute-solvent interactions, which show up most clearly in the entropies of ionization.

Enthalpies and entropies of ionization of *o*-chlorophenol and *p*-chlorophenol also were investigated.¹ The heat of ionization of aqueous *m*-chlorophenol has been investigated in a continuation of earlier work and the results are presented and discussed here.

Experimental

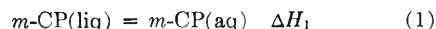
The solution calorimeter we used has been described.^{2,3} All heats of solution and heats of reaction with NaOH(aq) were measured in a volume of 950 ml. at $25.0 \pm 0.1^\circ$.

Eastman white label *m*-chlorophenol was doubly distilled in an all-glass apparatus with Vigreux column at atmospheric pressure. Only the fraction having n_{40}^D 1.5560 and melting between 32.0 and 33.1° was used. The *m*-chlorophenol was used in the supercooled state in the calorimetric runs because it was conveniently handled in the liquid state and was found not to solidify in the sample bulbs during an experiment.

Sodium hydroxide solutions were prepared and standardized by common procedures.

Results and Discussion

Heats of solution of liquid *m*-chlorophenol in 950 ml. of water were determined. The calorimetric reaction equation is



Results of these experiments, listed in Table I, were extrapolated to zero concentration to give $\Delta H_1^0 = 674 \pm 15$ cal./mole.

Heats of neutralization of *m*-chlorophenol by

(1) L. P. Fernandez and L. G. Hepler, *J. Am. Chem. Soc.*, **81**, 1783 (1959).

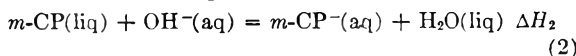
(2) C. N. Muldrow and L. G. Hepler, *ibid.*, **79**, 4045 (1957).

(3) R. L. Graham and L. G. Hepler, *ibid.*, **78**, 4846 (1956).

TABLE I

HEATS OF SOLUTION OF <i>m</i> -CP(LIQ)	
Moles <i>m</i> -CP/950 ml. H ₂ O	ΔH_1 (cal./mole)
0.01080	663
.01887	678
.02825	664
.03737	658

aqueous NaOH also were determined. The calorimetric reaction equation is

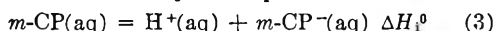


Results of these experiments, listed in Table II, were extrapolated to zero concentration to give $\Delta H_2^0 = -7.54 \pm 0.07$ kcal./mole.

TABLE II

HEATS OF NEUTRALIZATION OF <i>m</i> -CP(LIQ) BY NaOH(AQ)		
Moles <i>m</i> -CP/950 ml.	<i>M</i> of NaOH	ΔH_2 (kcal./mole)
0.00139	0.0593	-7.52
.00250	.0593	-7.52
.00437	.0988	-7.47
.00841	.0988	-7.44
.00922	.0988	-7.42
.01448	.0988	-7.44
.02244	.1236	-7.48

Combination of ΔH_1^0 with $\Delta H^0 = 13,500$ cal./mole for ionization of water⁴ gives $\Delta H_i^0 = 5286$ cal./mole for the ionization of aqueous *m*-chlorophenol as indicated by the equation



Bordwell and Cooper⁵ have determined the thermodynamic ionization constant of *m*-chlorophenol (aq) at 25° to be 8.32×10^{-10} . We calculate the standard free energy of ionization of *m*-chlorophenol (aq) to be $\Delta F_i^0 = 12390$ cal./mole and combine this value with our ΔH_i^0 to obtain $\Delta S_i^0 = -23.8$ cal./mole deg.

Thermodynamic data for the ionization of all three monochlorophenols in aqueous solution are listed in Table III.

TABLE III

THERMODYNAMICS OF IONIZATION OF AQUEOUS CHLOROPHENOLS			
Compound	$K \times 10^{10}$	$\frac{\Delta H_i^0}{\text{(cal./mole)}}$	$\frac{\Delta S_i^0}{\text{(cal./mole deg.)}}$
<i>o</i> -CP	33.4	4636	-23.5
<i>m</i> -CP	8.32	5286	-23.8
<i>p</i> -CP	4.18	5800	-23.5

Previous investigations of other phenols^{1,6} have shown that interpretation of acidity of these compounds must be based on consideration of what we call *internal* and *external* contributions to the thermodynamic functions. By *external* contribution we mean solute-solvent interactions and by *internal* contribution we mean differences in enthalpy and entropy within the acid molecule and its anion. We therefore write

$$\Delta S_i^0 = \Delta S_{\text{int}} + \Delta S_{\text{ext}} \quad (4)$$

(4) H. M. Papee, W. J. Canaday and K. J. Laidler, *Can. J. Chem.*, **34**, 1677 (1956).

(5) F. G. Bordwell and G. D. Cooper, *J. Am. Chem. Soc.*, **74**, 1058 (1952).

(6) L. G. Hepler and W. F. O'Hara, *J. Phys. Chem.*, **65**, 811 (1961).

and

$$\Delta H_i^0 = \Delta H_{\text{int}} + \Delta H_{\text{ext}} \quad (5)$$

Pitzer⁷ has shown that all ΔS_{int} values for a series of similar acids are substantially the same so we write

$$\Delta S_{\text{int}}(\textit{o}\text{-CP}) = \Delta S_{\text{int}}(\textit{m}\text{-CP}) = \Delta S_{\text{int}}(\textit{p}\text{-CP}) \quad (6)$$

Because the entropies of ionization of the three monochlorophenols are very nearly the same we also write

$$\Delta S_{\text{ext}}(\textit{o}\text{-CP}) = \Delta S_{\text{ext}}(\textit{m}\text{-CP}) = \Delta S_{\text{ext}}(\textit{p}\text{-CP}) \quad (7)$$

It can be shown that several different models for solute-solvent interactions lead to ΔH_{ext} proportional to ΔS_{ext} .⁶ We therefore also conclude that

$$\Delta H_{\text{ext}}(\textit{o}\text{-CP}) = \Delta H_{\text{ext}}(\textit{m}\text{-CP}) = \Delta H_{\text{ext}}(\textit{p}\text{-CP}) \quad (8)$$

and that

$$\Delta H_{\text{int}}(\textit{o}\text{-CP}) < \Delta H_{\text{int}}(\textit{m}\text{-CP}) < \Delta H_{\text{int}}(\textit{p}\text{-CP}) \quad (9)$$

Thus observed acid strength differences for these compounds are due to differences in ΔH_{int} .

ΔH_{int} is the energy required to break one mole of O-H bonds. The O-H bond strengths in similar molecules are roughly proportional to the squares of the O-H stretching frequencies.⁶ It has been found by Ingold⁸ and others that the O-H stretching frequency is greater for *p*-chlorophenol than for *m*-chlorophenol, in accord with the order of ΔH_{int} values we have found. Interpretation of the spectrum of *o*-chlorophenol is complicated because of intramolecular hydrogen bonding but the maximum is at a still lower frequency than that for *m*-chlorophenol as expected from the order of ΔH_{int} values. There is no indication that intramolecular hydrogen bonding is of much importance to the thermodynamics of dissociation of aqueous *o*-chlorophenol, at least as compared to O-H bond breaking and solute-solvent interactions.

Most of the many more or less successful attempts to correlate or explain acid strengths in terms of molecular structure have involved application of theories of resonance, inductive effects, etc., to predict relative values of what we have called ΔH_{int} . It generally has been implicitly assumed that ΔH_{ext} , ΔS_{ext} and ΔS_{int} contribute only insignificantly to differences in acid strength. Pitzer⁷ has shown that it is ordinarily proper to ignore ΔS_{int} but our work on nitrophenols¹ and methyl substituted phenols⁶ has shown that it is sometimes entirely incorrect and misleading to ignore ΔH_{ext} and ΔS_{ext} . It therefore is interesting to note that the monochlorophenols are the only class of phenols so far studied for which consideration of ΔH_{int} values alone is sufficient to predict relative ionization constants correctly and by the right reasoning.

In the case of the monochlorophenols it is inductive and field effects which cause the observed variation in bond strengths and hence in ΔH_{int} , ΔH_i^0 and K .

Acknowledgment.—We are grateful to the National Science Foundation and the Alfred P. Sloan Foundation for support of this and related research.

(7) K. S. Pitzer, *J. Am. Chem. Soc.*, **59**, 2365 (1937).

(8) K. U. Ingold, *Can. J. Chem.*, **38**, 1092 (1960).

H₂ AND C₁-C₇ YIELDS FROM THE RADIOLYSIS OF 2,2,4- TRIMETHYLPENTANE

By J. A. KNIGHT, R. L. MCDANIEL, R. C. PALMER AND
FRED SICILIO

Radioisotopes Laboratory, Engineering Experiment Station, Georgia
Institute of Technology, Atlanta, Georgia

Received June 16, 1961

Work current in this Laboratory is concerned with a detailed study of the radiolysis chemistry of branched hydrocarbons. Radiolysis products, hydrogen and hydrocarbons through C₇, from the X-irradiation (50 kvp.) of 2,2,4-trimethylpentane, have been identified and quantitative yields established by gas chromatography. Products with $G \geq 0.1$, in order of decreasing yield, are hydrogen, isobutane, isobutylene, methane, 4,4-dimethyl-*cis*-pentene-2, propylene, neopentane, 2,2- and/or 2,4-dimethylpentane, and propane.

Experimental

Materials.—The 2,2,4-trimethylpentane, Eastman, used in this work was percolated through activated alumina before use. The infrared spectra of the "treated" 2,2,4-trimethylpentane and of a sample of Phillips research grade material were identical. Authentic hydrocarbon samples for identification of radiolysis products were obtained from Matheson, Phillips, or National Bureau of Standards.

X-Ray Apparatus.—A Machlett OEG-60 end-window (beryllium) tube, housed in a lead-lined box, was used with a GE XRD-5 X-ray diffraction unit power supply with voltage stabilizer. All irradiations were performed at 50 kvp. and 50 ma., at a dose rate of 8.2×10^{17} e.v./g./min. for the volumes of samples studied.

Irradiation Cell.—Irradiations were performed in an open-window stainless-steel cell with an inside diameter of 67 mm. and inside depth of 37 mm. The cell, supported by a magnetic stirrer on a laboratory jack, is sealed to the end of the X-ray tube with an "O" ring above the liquid level. Inlet and outlet tubes allow inert gas to be bubbled through the cell. The outlet tube is connected to a condenser so that condensable vapors are returned to the cell. The cell is jacketed, and coolant water was used during these irradiations to maintain the cell at approximately 20°.

Irradiation and Sampling Technique for Volatile Radiolysis Products.—During the irradiation of 2,2,4-trimethylpentane, the sample was stirred and helium gas at a known flow rate in the range of 5 to 10 ml. per min. was bubbled continuously through the hydrocarbon. This served to constantly remove volatile radiolysis products—hydrogen, neopentane and the C₁ through C₄ hydrocarbons. The exit helium gas, along with the volatile radiolysis products, passed through 1/4-inch o.d. copper tubing to a sampling loop of a solenoid-operated gas sampler¹ connected to a gas chromatographic unit. Thus, it was possible periodically to subject the helium sweep gas to chromatographic analysis.

In the analysis for hydrogen and methane, the sweep gas, after leaving the irradiation cell, was passed through a cold trap containing 3 ml. of 2,2,4-trimethylpentane, at a temperature of -78°. After steady state conditions were attained, hydrogen and methane passed through the trap. The sweep gas then was passed through the gas-sampling loop. In the analysis for volatile radiolysis products other than hydrogen and methane, the cold trap was omitted.

Hydrocarbon Radiolysis Products in the C₅-C₇ Range.—Samples of the irradiated 2,2,4-trimethylpentane were fractionally distilled with a 1.2 by 33-cm. column packed with Podbielniak Heli-Pak 3013 stainless steel packing. The distillations were performed very slowly in order to concentrate the radiolysis products of carbon content less than C₈ in the initial fractions. Fractions of 1 ml. or less were taken, and chromatograms obtained on each fraction. The chromatograms showed that all of the radiolysis products of carbon content less than C₈ were contained in the first three fractions.

(1) R. C. Palmer, D. K. Davis and W. V. Willis, *Anal. Chem.*, **32**, 894 (1960).

Analytical Work.—Hydrogen and methane were identified and determined quantitatively with a 50-ft. column of Linde 13X Molecular Sieve, 20 to 40-mesh. Other hydrocarbon radiolysis products were identified with two columns, one a 50-ft. column of 20% (by weight) tri-*m*-cresyl phosphate on 30 to 60-mesh Chromosorb and the other a 50-ft. column of 20% dimethylsulfolane on 30 to 60-mesh Chromosorb. The gas chromatographic unit was calibrated for thermal response to hydrogen and to each of the hydrocarbon radiolysis products. Microliter syringes with fixed needles were utilized for injecting samples of known amounts for calibration, and sample sizes were used which corresponded to the ranges of the amounts of the radiolysis products. Peak areas were measured with a planimeter. Thermal response was linear in the range of sample volumes employed.

Dosimetry.—The energy absorbed by 2,2,4-trimethylpentane was determined by polyethylene-ferrous ion dosimetry measurements,² in which the dose received by a hydrocarbon is compared to the dose received by a corresponding quantity of polyethylene, in g./cm.². The dose determined in this manner compares to within 5% of the dose received by an equivalent volume, as determined by electron density ratio, of Fricke dosimeter solution [$G(\text{Fe}^{+++}) = 15.5$].

Results and Discussion

The radiolysis products, hydrogen and those hydrocarbons in the range C₁-C₇, found in this investigation are listed in Table I. The data represent the results of some 30 individual irradiations.

TABLE I
RADIOLYSIS PRODUCTS FROM 2,2,4-TRIMETHYLPENTANE
(HYDROGEN AND C₁-C₇ CARBON CONTENT)

Product ^a	G ^b
Hydrogen	2.2
Methane	1.1
Ethane	0.05
Ethylene	.02
Propane	.1
Propylene	.3
Isobutane	1.6
Isobutylene	1.4
Neopentane	0.2
Isopentane	.05
Neohexane	.02
2,2- and/or 2,4-dimethylpentane	.2
4,4-Dimethylpentene-1	.04
4,4-Dimethyl- <i>trans</i> -pentene-2	.06
4,4-Dimethyl- <i>cis</i> -pentene-2	.45

^a Three additional products with low yields have been identified tentatively as: 2-methylpentane, $G = 0.02$; 4-methylpentene-1, $G = 0.003$; 4-methyl-*trans*-pentene-2, $G = 0.005$. ^b Yield in molecules per 100 e.v., as determined by extrapolation to zero dose.

Hydrogen and Methane.—Dewhurst,³ in his work on branched chain alkanes, reported G -values for hydrogen and methane of 3.0 and 0.7, respectively, but did not report any other radiolysis products for 2,2,4-trimethylpentane. Our values of 2.2 and 1.1 for $G(\text{H}_2)$ and $G(\text{CH}_4)$, respectively, differ from the values reported by Dewhurst. However, he employed 800 kvp. electrons and a sealed system whereas we used 50 kvp. X-rays with a dynamic system. Tolbert and Lemmon⁴ calculated $G(\text{H}_2)$ and $G(\text{CH}_4)$ as being 1.9 and 0.82,

(2) R. C. Palmer, R. W. Carter and D. C. Bardwell, *Intern. J. Appl. Radiation and Isotopes*, **9**, 60 (1960).

(3) H. A. Dewhurst, *J. Am. Chem. Soc.*, **80**, 5607 (1958).

(4) B. M. Tolbert and R. M. Lemmon, *Radiation Research*, **3**, 52 (1955).

respectively, from the data reported by Schoepfle and Fellows⁵ for the irradiation of 2,2,4-trimethylpentane with 0.17 mev. electrons.

C₁-C₇ Radiolysis Products.—The radiolytic hydrocarbon products in the C₁-C₇ range can be divided into two groups. Group I consists of those products that can be related to some structural portion of the carbon skeleton of the parent molecule, 2,2,4-trimethylpentane. There are ten of these products, with *G*-values ranging from 1.6 to 0.04, *viz.*, in order of decreasing yield: isobutane, isobutylene, methane, 4,4-dimethyl-*cis*-pentene-2, propylene, neopentane, 2,2- and/or 2,4-dimethylpentane, propane, 4,4-dimethyl-*trans*-pentene-2, and 4,4-dimethylpentene-1. Group II consists of those products that cannot be related to the carbon skeleton of the parent molecule. There are seven of these products, all with low yields, with *G*-values ranging from 0.05 to 0.003, *viz.*, in order of decreasing yield: ethane, isopentane, ethylene, neohexane, 2-methylpentane (probable), 4-methyl-*trans*-pentene-2 (probable), and 4-methylpentene-1 (probable).

Inspection of the structure of 2,2,4-trimethylpentane shows that there are 13 possible products that can be formed directly by cleavage of the carbon-carbon bonds, assuming the formation of alkanes or alkenes through either uptake or elimination of hydrogen. Two of the possible products of cleavage were not found in this investigation, *viz.*, 2,4-dimethylpentene-1 and -2.

The hydrogen and methane yields are linear up to a total dose of 10²¹ e.v./g. The yields of propane, propylene, isobutane, isobutylene, neopentane, 4,4-dimethyl-*trans*-pentene-2, 4,4-dimethyl-*cis*-pentene-2, and 2,2- and/or 2,4-dimethylpentane are linear up to a total dose of 3.5 × 10²¹ e.v./g. The yield of the terminal olefin, 4,4-dimethylpentene-1, is linear up to a total dose of 2 × 10²¹ e.v./g. and then decreases.

Acknowledgment.—This work was supported in part by the United States Atomic Energy Commission, Division of Research, Contract No. AT (40-1)-2490.

(5) C. S. Schoepfle and C. H. Fellows, *Ind. Eng. Chem.*, **23**, 1396 (1931).

ON POLAROGRAPHIC AND COULOMETRIC INVESTIGATIONS OF THE REDUCTION RATE OF COBALT IONS IN THE PRESENCE OF SOME AMINO ACIDS AND PROTEINS

By E. B. WERONSKI

Department of Chemistry, University of Warszawa, Warszawa, Poland
Received May 8, 1961

In a recently published paper by Shinagawa, *et al.*,¹ the authors reported results obtained by

comparing the radioactivity-potential curves of cobalt Co⁶⁰, in the presence of cystine and histidine in Brdicka's electrolyte, with corresponding current-potential curves. In the case of histidine they came to the conclusion that the enhancement of current is due to an increase in the reduction rate of cobalt(II) ions rather than to the catalytic reduction of hydrogen. This conclusion is identical with that reported in our previous paper² concerning the reaction in the presence of cystine. However, in the case of cystine the results¹ lead to a different conclusion. In our experiments we compared two decreases in currents of cobalt(II) in Brdicka's electrolyte, measured polarographically in the presence of cystine. One decrease was measured at -1.35 v. after coulometric electrolysis carried out at the same potential (at which the curve of cobalt was assumed to be undistorted by the amino acid). The second decrease was measured under similar conditions at -1.65 v. (*i.e.*, at the top of the catalytic maximum of the current-potential curve). Although the half-wave potentials of the current-potential curves of cobalt presented by Shinagawa and co-workers were not in all cases identical with those of the radioactivity-potential curves (the reason has not been elucidated by the authors), the radioactivity-potential curves should be compatible with our results provided that the possible influence of ionizing action of cobalt-Co⁶⁰ on the electrode reaction may be neglected.

To explain the discrepancy we examined their and our results in different ways. It was found that if the coulometric electrolysis of Brdicka's electrolyte is carried out during the same period of time and under identical conditions in the absence or in the presence of cystine at -1.35 v., the decrease in the current in the absence of cystine is several times greater than in the presence. These results suggest, despite the previously made assumption, that during the electrolysis at -1.35 v. the current-potential curve is increasingly affected by cystine. To avoid errors in explaining the results of similar measurements in the presence of other amino acids or proteins, the changes of current after coulometric electrolysis should be compared both in the absence and in the presence of amino acids or proteins using the previously described techniques.² Then the results obtained with the radiometric and coulometric methods are and should be compatible also in other cases provided that the influence of the ionizing action of cobalt-Co⁶⁰ on the electrode reaction may be neglected.

(1) M. Shinagawa, H. Nezu, H. Sunahara, F. Nakashima, H. Okashita and T. Yamada, Proc. II. Intern. Congr. Cambridge 1959, in "Advances in Polarography" (Ed. by I. S. Longmuir), Pergamon Press, London, 1960, Vol. 3, p. 1142.

(2) E. B. Weronki, *J. Phys. Chem.*, **65**, 564 (1961).

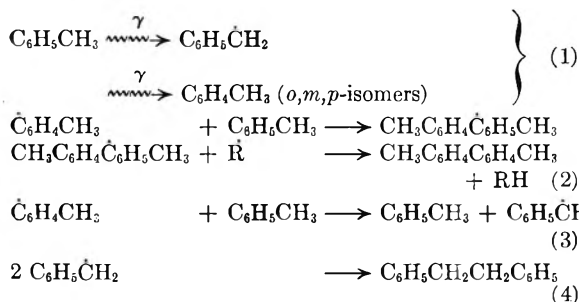
COMMUNICATIONS TO THE EDITOR

ON A POSSIBLE TRACK REACTION IN THE RADIOLYSIS OF TOLUENE¹

Sir:

The dimeric products which are formed on gamma irradiation of liquid toluene may largely be explained by reactions of radiolytically produced benzyl or tolyl radicals. Less important are the methylhexatrienyl biradicals and the phenyl radical.

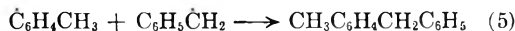
The main reactions yielding dimers are



Step 2 is formulated in analogy to reactions observed in irradiated benzene² or when dibenzoyl peroxide is decomposed in this solvent.³ The tolyl radicals are scavenged rapidly by toluene.⁴

It was possible to reproduce steps 2, 3 and 4 by decomposing the toluoyl peroxides in toluene. In this system the benzyl radicals are formed only by the radical transfer reaction (3). The fact that there is formed about half as much bibenzyl as the sum of the isomeric bitolylys shows that this reaction is important.

In the radiolytic products we find as the main additional products the phenyltolylmethanes, amounting to 20% of all the dimer products. For their formation we suppose the reaction



This reaction still takes place in solutions containing iodine, in a system where the benzyl radicals become scavenged (no formation of bibenzyl). Therefore we are forced to assume that this special reaction takes place only in the spur⁵ of the ionizing electrons.

A similar disagreement between the reactions induced by the decomposition of peroxides and those induced by radiation is found in benzene-toluene mixtures. Only the second treatment yields diphenylmethane. Thereby the maximum

(1) Work supported by the Swiss Kommission für Atomwissenschaft.

(2) T. Gäumann, *Helv. Chim. Acta*, **44**, 1337 (1961).

(3) D. F. DeTar and R. A. J. Long, *J. Am. Chem. Soc.*, **80**, 4742 (1958).

(4) G. H. Williams, "Homolytic Aromatic Substitution," Pergamon Press, London, 1960, p. 45.

(5) C. J. Hochanadel, in "Comparative Effects of Radiation" by M. Burton, J. S. Kirby-Smith and J. L. Magee, John Wiley and Sons, Inc., New York, N. Y., 1960, p. 159.

for the formation of this compound is obtained in about an equimolar mixture.

A strong linear energy transfer effect has been reported for the yields of gases and dimers in aromatic liquids.^{6,7} The direct demonstration of a dimolecular spur reaction now may give a clue in explaining those facts.

Details of the radiation effects in toluene and toluene-benzene mixtures will be published elsewhere.⁸

EIDGENÖSSISCHE TECHNISCHE
HOCHSCHULE
ZÜRICH, SWITZERLAND

JÜRIG HOIGNÉ
TINO GÄUMANN

RECEIVED JULY 20, 1961

(6) W. G. Burns, "VI Rassegna Internazionale Elettronica e Nucleare," **3**, 99, Rome (1959); W. G. Burns, W. Wild and T. F. Williams, *Proc. 2nd Geneva Conf. on Peaceful uses of Atomic Energy*, **29**, 266 (1958).

(7) T. Gäumann and R. H. Schuler, *J. Phys. Chem.*, **65**, 703 (1961).

(8) J. Hoigné and T. Gäumann, *Helv. Chim. Acta*, **44**, 2141 (1961).

HEAT OF DISSOCIATION OF BORON PHOSPHIDE, BP(s)

Sir:

Williams and Ruehrwein¹ have made semi-quantitative studies of the vaporization of BP by a gas saturation method. Their phosphorus dissociation pressure data are given in the first two lines of Table I and are expressed by the equation

$$\log P_{\text{P}_2}(\text{mm.})_{\text{diss.}} = (-13.7 \times 10^3)/T + 10.1$$

which corresponds to a heat of dissociation of 62.6 kcal. mole⁻¹ at 1523°K. and an entropy of dissociation of 46.2 cal. deg.⁻¹ per mole of P₂(g). Since the entropy² of P₂(g) is 65.92 cal. deg.⁻¹ at 1523°K., this entropy change would require the contribution of phosphorus atoms to the entropy of BP at 298°K. to be near zero, assuming reasonable values for the entropy contribution of boron and the heat capacity of BP. Inasmuch as such a low entropy contribution on the part of phosphorus is unlikely, it was believed that a "third law" calculation would provide a more reliable heat of dissociation.

For the purposes of this calculation, the contribution of boron to the free energy function of a boron phosphide was assumed to be the same as for elemental boron. The change in the free energy function upon dissociation is then the difference between the free energy function for P₂(g) and that for two gram atoms of phosphorus in BP(s). The values of the free energy function for bound phosphorus were estimated by taking the atomic

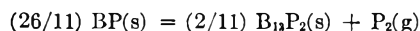
(1) F. V. Williams and R. A. Ruehrwein, *J. Am. Chem. Soc.*, **82**, 1332 (1960).

(2) D. R. Stull and G. C. Sinke, "Thermodynamic Properties of the Elements," American Chemical Society, Washington, D. C., 1956, p. 148.

TABLE I
HEAT OF DISSOCIATION OF BP

T , °K.	1473	1523	1573
P_{P_2} , mm.	6.3	12.6	24.2
$\Delta F/T$, cal. mole ⁻¹ deg. ⁻¹	9.52	8.15	6.85
$-\Delta(F - H_{298,16})/T$, cal. mole ⁻¹ deg. ⁻¹	40.3	39.9	39.6
$\Delta H_{298,16}/T$, cal. mole ⁻¹ deg. ⁻¹	49.8	48.0	46.4
$\Delta H_{298,16}$, kcal. mole ⁻¹	73.4	73.1	73.0
Average $\Delta H_{298,16} = 73.2$ kcal. mole ⁻¹			

heat of phosphorus in a phosphide to be 6 cal. per degree³ and the contribution of phosphorus to the entropy of a phosphide to be 5 cal. deg.⁻¹ per gram atom. The values of the free energy function for $P_2(g)$ were taken from the tabulation of Stull and Sinke.² The results of the calculation are presented in Table I. In view of the findings of Matkovich,⁴ the dissociation reaction is presumed to be



STATE UNIVERSITY OF NEW YORK
COLLEGE OF CERAMICS AT
ALFRED UNIVERSITY
ALFRED, N. Y.

CLIFFORD E. MYERS

RECEIVED SEPTEMBER 23, 1961

(3) O. Kubaschewski and J. A. Caterall, "Thermochemical Data of Alloys," Pergamon Press, New York, N. Y., 1956, p. 135.

(4) V. I. Matkovich, *Acta Cryst.*, **14**, 53 (1961).

ON THE MORRIS MECHANISM OF HYDROLYSIS OF CHLORINE

Sir:

In a recent paper Lifshitz and Perlmutter-Hayman¹ discuss the mechanism of the hydrolysis of chlorine and demonstrate the inadequacy of Morris's scheme² suggesting hydroxyl ion is the active agent of chlorine hydrolysis even in acid solutions.

This demonstration is entirely correct, but we wish to mention that we criticized Morris's reaction scheme already in 1947,³ since it does not fit the kinetic results obtained by us in 1945. Apparently our paper of 1947 was overlooked by Lifshitz and Perlmutter-Hayman.

The value of k of the rate of the hydrolysis of chlorine given in the article of Lifshitz and Perlmutter-Hayman is 5.60 sec.⁻¹ at 9.5°. We determined $k = 1.75$ sec.⁻¹ at 0° and 8.97 at 17.6°.⁴ The Arrhenius plot gives the value $k = 4.3$ at 9.5°. The comparison of the two results, not made by Lifshitz and Perlmutter-Hayman, means good agreement of the old and new data on the rate of chlorine hydrolysis.

INSTITUTE OF ORGANIC CHEMISTRY EUGENE SHILOV
ACADEMY OF SCIENCES OF THE UKRAINIAN SSR
KIEV 30, U.S.S.R. S. SOLODUSENKOV

RECEIVED AUGUST 21, 1961

(1) A. Lifshitz and B. Perlmutter-Hayman, *J. Phys. Chem.*, **64**, 1663 (1960).

(2) J. C. Morris, *J. Am. Chem. Soc.*, **68**, 1692 (1946).

(3) E. A. Shilov and S. Solodushenkov, *J. Phys. Chem. (Russ.)*, **21**, 1159 (1947); *Chem. Abstr.*, **42**, 2945 (1948).

(4) E. Shilov and S. Solodushenkov, *Acta Physicochimica U.R.S.S.* **20**, 667 (1945).

- Increasingly, authors are asked to prepare abstracts of their papers to accompany the complete papers when published in primary journals.
- Scientists must frequently index their own books.
- Industrial organizations routinely build collections of abstracts and indexes with emphasis on their own special interests.

CA TODAY

This informative 130 page clothbound volume describes for the reader the interworkings of the world's largest and most successful abstracting undertaking.

All scientists and organizations interested in producing abstracts and/or indexes will find this book on the production of CHEMICAL ABSTRACTS an invaluable aid.

CA Today tells how source material is gathered, explains the assignment of abstracts, and the problems of recording, editing, and classifying abstracts. Indexing procedures are explained, methods of printing are discussed, and research, administration, housing and equipment, nomenclature, and records are amply described in separate chapters. The total concept behind the development of successful abstracting is presented for the first time in one reference.

Clothbound 130 pages \$3.50

order from

Special Issues Sales

AMERICAN CHEMICAL SOCIETY

1155 16th Street, N. W.
Washington, D. C.

analytical & metallurgical services

Analytical Services:

- Analyses of gasses in metals
- BET surface area measurements
- Rare earth analyses
- Optical emission, X-ray fluorescence, X-ray diffraction spectroscopy
- Uranium isotopic assays
- Wet chemical analyses
- Powder characterization
- Thermogravimetric analyses

Metallurgical Services:

- Metallography
- Tensile, fatigue, hardness, impact and burst testing
- Leak detection
- Corrosion testing

Other NUMEC SERVICES include: Vacuum and inert atmospheric arc and induction melting. Recovery of precious metals. Consulting and R&D services. Unirradiated nuclear fuel scrap recovery.

For information and prices contact:

NUMEC

NUCLEAR MATERIALS AND EQUIPMENT CORPORATION
APOLLO, P. A. PHONE GR 2-8411
TWX: APD 276 CABLE NUMEC

INDEXES

PUBLISHED BY THE

AMERICAN CHEMICAL SOCIETY

27-Year Collective Formula Index to Chemical Abstracts

Over half a million organic and inorganic compounds listed and thoroughly cross referenced for 1920-1946. In 2 volumes of about 1000 pages each.

Paper bound \$100.00 Cloth bound \$120.00

10-Year Numerical Patent Index to Chemical Abstracts

Over 143,000 entries classified by countries in numerical order with volume and page references to Chemical Abstracts for 1937-1946. Contains 182 pages.

Cloth bound \$10.00

Decennial Indexes to Chemical Abstracts

Complete subject and author indexes to Chemical Abstracts for the 10-year periods of 1917-1926, 1927-1936 and 1937-1946.

2nd Decennial Index (1917-1926). Paper bound..\$125.00

3rd Decennial Index (1927-1936). Paper bound..\$175.00

4th Decennial Index (1937-1946). Paper bound..\$200.00
(Foreign postage on the Decennial Indexes is extra.)

Order from:

Special Issues Sales

American Chemical Society

1155 16th St., N.W. Washington 6, D.C.

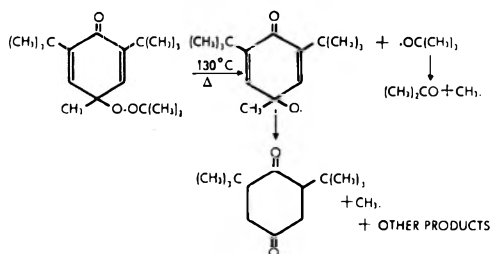
STUDY OF A CHEMICAL REACTION MECHANISM WITH EPR

(ELECTRON PARAMAGNETIC RESONANCE)

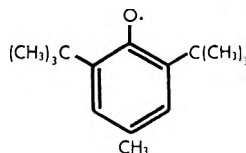
EPR Spectroscopy can often provide valuable information about the mechanism of a chemical reaction because it permits the observer to follow the reaction as it is taking place. By the detection and identification of any radical intermediates present during the reaction, it is often possible to determine the details of the reaction mechanism.

EXAMPLE

In a recent experiment, it was desired to confirm the presence of free radicals in the thermal decomposition of 2,6-di-*tert*-butyl-4-methyl-4-*tert*-butyl peroxycyclohexa-2,5-diene-1-one. The decomposition can be carried out at 130°C in toluene solution. The reaction scheme which had been envisaged was:



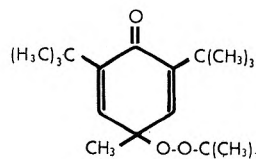
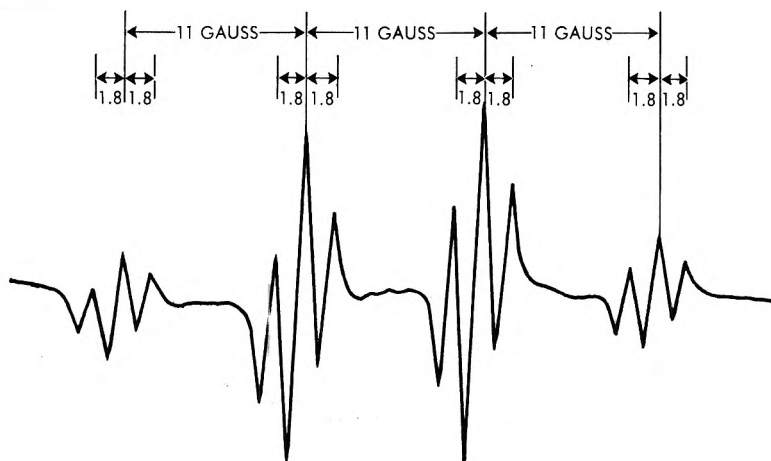
As shown in the figure, a free radical signal was, indeed, detected when this compound was decomposed at 130°C in the EPR cavity. The spectrum obtained, however, was identical to that obtained by other workers⁽¹⁾ for the 2,6-di-*tert*-butyl-4-methylphenoxy radical:



It was therefore suggested that this radical, rather than the one proposed, was the principal radical intermediate. Later chemical evidence, including the discovery of *t*-butyl hydroperoxide and other products consistent with the 2,6-di-*tert*-butyl-4-methylphenyl radical supported the suggestion that the thermal decomposition involved a C-O cleavage.⁽²⁾

(1) J. K. Becconsall, S. Clough and G. Scott, *Trans. Farad. Soc.* 56, 459 (1960).

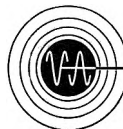
(2) We wish to thank Dr. J. M. Turner of Canadian Industries, Ltd., McMasterville, Quebec, for permission to use these results.



TEMP. = 130°C

IN XYLENE

For literature which fully explains the 100 kc EPR Spectrometer and its application to basic and applied research in physics, chemistry, biology and medicine, write the Instrument Division.



VARIAN associates
PALO ALTO 52, CALIFORNIA